UNIVERSITY OF GRANADA

DEPARTMENT OF CHEMICAL ENGINEERING

Doctoral Programme in Chemistry

DOCTORAL THESIS

DEVELOPMENT OF PRODUCTION AND STABILIZATION PROCESSES FOR ANTIDIABETIC PEPTIDES

CARMEN BERRAQUERO GARCÍA

2025

Thesis supervisors:
Dr. Emilia M. Guadix Escobar
Dr. Pedro Jesús García Moreno

Editor: Universidad de Granada. Tesis Doctorales
Autor: Carmen Berraquero García
ISBN: 978-84-1195-814-1
URI: https://hdl.handle.net/10481/104901

Acknowledgments

En primer lugar, me gustaría agradecer a mis directores, Emilia M. Guadix y Pedro J. García Moreno, no solo por haberme dado la oportunidad de realizar esta tesis doctoral, si no también por haberme guiado pacientemente y por ayudarme a crecer como investigadora. Habéis sido un ejemplo a seguir y una fuente constante de aprendizaje.

I would also like to thank Simon Gregersen, my "supervisor away from home," who helped me overcome many difficulties during my research stay at Aalborg. Thank you for always being a friendly face and a source of calmness and wisdom.

A mis compañeros y compañeras del Departamento de Ingeniería Química, gracias por haber compartido este camino. En especial, a Raúl y Maricarmen, por haberme acompañado en mis primeros pasos en la ciencia, allá por 2017. Gracias a Enrique, estar siempre ahí para solucionarlo todo, y por saber ofrecer un buen consejo en el momento justo.

Sobre todo, quiero dar las gracias a mis amigas y compañeras. A Lizeth, Cristina, Julia, Álvaro, María, Ainara y Alba, por todos los momentos compartidos, dentro y fuera del laboratorio. Me habéis acompañado en un proceso tan complicado cómo único y, gracias a vosotras, también maravilloso. Habéis sido y seréis siempre una parte inseparable de todo este trabajo. Muchas gracias por todas las risas, por los consejos y (especialmente) por los cafés. A Liza, Ariana, Nana, Sandra, Marta y MJ, por haber sido mi soporte fuera del laboratorio, por escucharme cuándo ni siquiera sabíais de qué hablaba. Gracias por haber estado ahí cuando más lo he necesitado, ya fuera para desahogarme, ir al veterinario o hacerme la comida. Me habéis enseñado la importancia del apoyo mutuo y, sin vosotras, no habría llegado hasta aquí. Desde el fondo de mi corazón, os agradezco a todas y cada una de vosotras, porque habéis tejido la red que me ha sostenido estos años. Gracias por haberme hecho sentir capaz de seguir adelante.

Gracias a mi familia: a mi padre, Manuel, y a mi madre, María del Carmen, por haberme escuchado una y otra vez, por haber entendido cuando no he podido estar. Gracias, María, por ser la mejor hermana que se podría pedir, estoy muy orgullosa de ti.

Finalmente, gracias a Jesús, por estar siempre ahí, incluso en la distancia. Gracias por cuidarme y quererme todos estos años (y los que quedan). Sobre todo, gracias por ser mi hogar.

Table of contents

RESUMEN 19

SUMMARY 25

1. INTRODUCTION 27

1.1. Proteins, protein hydrolysates and bioactive peptides 29

1.1.1. Selection of protein sources. 30

1.1.2. Selection of enzymes 33

1.1.3. Use of Computer-Based Techniques in Peptide Research 35

1.2. Antidiabetic potential of bioactive peptides 36

1.2.1. α-Amylase and α-glucosidase inhibitors 37

1.2.2. Incretin mimetics 38

1.2.3. DPP-IV inhibitors 39

1.3. Bioaccessibility and bioavailability of antidiabetic peptides 40

1.4. Encapsulation of bioactive peptides 42

1.4.1. Spray-drying 43

1.4.2. Electrospraying 44

1.5. Peptidomics analysis in peptide encapsulation 46

2. OBJECTIVES 49

3. MATERIALS AND METHODS 53

3.1. Materials 55

3.2. Methodology 55

3.2.1. Protein content determination 57

3.2.2. Enzymatic hydrolysis and degree of hydrolysis 57

3.2.3. Meal solubilization 58

3.2.4. Molecular weight distribution 58

3.2.5. DPP-IV inhibitory activity assay 59

3.2.6. *In vitro* digestion (INFOGEST) 60

3.2.7. Electrospraying encapsulation 60

3.2.8. Spray-drying encapsulation 60

3.2.9. Peptidomics analysis and data processing 61

3.2.10. *In silico* analysis 63

4. RESULTS AND DISCUSSION 65

4.1. Study of the processing conditions for the targeted production of DPP-IV Inhibitory peptides 67

4.1.1. Identification of bioactive sequences and their susceptibility to degradation during gastrointestinal digestion 67

4.1.2. Identification of bioactive sequences in alternative sustainable sources 69

4.2. Investigation of enzymatic hydrolysis for producing DPP-IV inhibitory hydrolysates from sustainable sources: characterization and digestive stability 70

4.3. Study of the state of the art in bioactive peptides stabilization using spray drying and electrospraying techniques 73

4.4. Optimization and evaluation of encapsulation processes for the stabilization of protein hydrolysates with DPP-IV inhibitory activity 76

4.4.1. Monoaxial electrospraying and spray-drying 76

4.4.2. Coaxial spray-drying 78

4.5. Investigation of the encapsulation effect for the stabilization of DPP-IV inhibitory protein hydrolysates during gastrointestinal digestion 80

5. REFERENCES 85

CHAPTERS 99

I. ACTIVITY, STRUCTURAL FEATURES AND *IN SILICO* DIGESTION OF ANTIDIABETIC PEPTIDES 101

1. Introduction 103

2. α-Amylase inhibitory peptides 104

3. α-Glucosidase inhibitory peptides 110

4. DPP-IV inhibitory peptides 117

5. Activity prediction *in silico* for antidiabetic peptides 124

6. Evidence of antidiabetic activity of peptides in cell models and *in vivo* studies 125

7. Potential degradation of active peptides during digestion 127

8. Conclusions 129

9. References 129

10. Supplementary material 137

II. GASTROINTESTINAL STABILITY OF DIPEPTIDYL PEPTIDASE IV (DPP-IV)-INHIBITORY PEPTIDES IDENTIFIED IN *TENEBRIO MOLITOR* **169**

1. Introduction **171**

2. Materials and methods **173**

2.1. Materials and reagents 173

2.2. Screening of DPP-IV inhibitory peptides and *in silico* gastrointestinal digestion 173

2.3. Presence of selected DPP-IV inhibitory peptides in *Tenebrio molitor* 173

2.4. *In silico* assessment of bioaccessibility and bioavailability 173

2.5. Targeted hydrolysis for potential production of DPP-IV inhibitory peptides found in *Tenebrio molitor* 174

2.6. *In vitro* measurement of DPP-IV inhibitory activity 174

2.7. Determination of DPP-IV inhibition mechanism for selected peptides 174

3. Results and discussion **175**

3.1. Screening of DPP-IV inhibitory peptides and *in silico* gastrointestinal digestion 175

3.2. Presence of selected DPP-IV inhibitory peptides in *Tenebrio molitor* 178

3.3. *In silico* bioaccesibility and bioavailability 179

3.4. Production of DPP-IV inhibitory peptides by targeted enzymatic hydrolysis. 181

3.5. DPP-IV inhibitory activity and inhibition mechanism of peptides 183

3.6. DPP-IV inhibitory activity of peptide fragments originated during digestion. 186

4. Conclusions **188**

5. References **188**

6. Supplementary material **195**

III. ANTIDIABETIC ACTIVITY OF *TENEBRIO MOLITOR* AND *OLEA EUROPAEA* PROTEIN HYDROLYSATES AFTER SIMULATED GASTROINTESTINAL DIGESTION: *IN VITRO* AND *EX VIVO* STUDY **199**

1. Introduction **201**

2. Materials and methods **203**

2.1. Materials 203

2.2. Enzymatic hydrolysis 203

2.3. Amino acid composition 204

2.4. *In vitro* DPP-IV inhibitory activity 205

2.5. *In vitro* simulated gastrointestinal digestion (SGIC) 205

2.6. Size exclusion chromatography (SEC) 205

2.7. Peptidomic analysis by LC–MS/MS 206

2.8. LC-MS/MS data processing 206
2.9. Crypt Isolation and Organoid 206
2.10. Reverse transcription quantitative real-time PCR (RT-qPCR) analysis 207
2.11. Statistical analysis 207
3. Results and discussion 208
3.1. Hydrolysis curves, meal solubilization and protein content of *T. molitor* and *O. europaea* seed hydrolysates 208
3.2. DPP-IV inhibitory activity of the *T. molitor* and *O. europaea* hydrolysates 210
3.3. Gastrointestinal digestion of *T. molitor* and *O. europaea* seed hydrolysates 214
3.4. Peptide identification by mass spectrometry 216
3.5. Anti-diabetic effect on mouse jejunum organoids 218
4. Conclusions 220
5. References 220
6. Supplementary material 225

IV. ENCAPSULATION OF BIOACTIVE PEPTIDES BY SPRAY-DRYING AND ELECTROSPRAYING 231
1. Introduction 233
2. Literature Search 235
3. Encapsulation of Protein-Based Bioactives by Spray-Drying 236
3.1. Fundamentals of Spray-Drying 236
3.2. Encapsulation by Monoaxial Spray-Drying 238
3.2.1. Formulation of the Feed Stream 238
3.2.2. Processing Conditions 246
3.3. Encapsulation by Coaxial Spray-Drying 248
4. Encapsulation of Protein-Based Bioactives by Electrospraying 249
4.1. Fundamentals of Electrospraying 249
4.2. Encapsulation by Monoaxial Electrospraying 252
4.2.1. Formulation of the Feed Stream 252
4.2.2. Processing Conditions 256
4.3. Encapsulation by Coaxial Electrospraying 257
5. Activity Retention and Release of the Encapsulated Protein-Based Bioactives 261
6. Bioaccessibility of Encapsulated Protein-Based Bioactives and Enrichment of Food Matrices 263
7. Conclusions and Future Perspectives 265
8. References 266

V. ENCAPSULATION OF *TENEBRIO MOLITOR* HYDROLYSATE WITH DPP-IV INHIBITORY ACTIVITY BY ELECTROSPRAYING AND SPRAY-DRYING 275

1. Introduction 276

2. Materials and Methods 278

2.1. Materials 278

2.2. Production of the *Tenebrio molitor* protein hydrolysate 279

2.3. Production of electrosprayed capsules 279

2.4. Production of the spray-dried capsules 280

2.5. Characterization of the capsules 280

2.5.1. Morphology and particle size distribution 280

2.5.2. X-ray Photoelectron Spectroscopy (XPS) 280

2.5.3. DPP-IV inhibitory activity 280

2.5.4. Statistical analysis 281

3. Results 281

3.1. Optimization of the formulation for electrospraying 281

3.2. Surface nitrogen of the capsules 285

3.3. DPP-IV inhibitory activity 287

4. Conclusions 289

5. References 289

VI. OPTIMIZATION OF COAXIAL SPRAY-DRYING FOR THE ENCAPSULATION OF *TENEBRIO MOLITOR* PROTEIN HYDROLYSATE EXHIBITING DPP-IV INHIBITORY ACTIVITY 295

1. Introduction 297

2. Materials and methods 298

2.1. Materials 298

2.2. Protein hydrolysate 299

2.3. Encapsulation of *Tenebrio molitor* hydrolysate by coaxial spray-drying 299

2.4. Characterization of the capsules 300

2.4.1. Morphology and particle size distribution 300

2.4.2. Structure of the microcapsules 301

2.4.3. Protein content 301

2.4.4. X-ray Photoelectron Spectroscopy (XPS) 301

2.4.5. DPP-IV inhibitory activity 301

2.4.6. Statistical analysis 302

3. Results and discussion 302
3.1. Characterization of microcapsules 302
3.1.1. Morphology and structure of the microcapsules 302
3.1.2. Particle size and size distribution 303
3.2. Statistical modeling 307
3.2.1. Yield 307
3.2.2. Protein load and surface composition of the microcapsules 308
3.2.3. DPP-IV inhibitory activity 310
3.2.4. Optimization 311
4. Conclusions 315
5. References 315
6. Supplementary material 319

VII. IMPACT OF ENCAPSULATION ON DPP-IV INHIBITORY ACTIVITY AND GASTROINTESTINAL STABILITY OF *TENEBRIO MOLITOR* AND *OLEA EUROPAEA* PROTEIN HYDROLYSATES 321
1. Introduction 323
2. Materials and methods 325
2.1. Materials 325
2.2. Encapsulation by monoaxial spray-drying 325
2.3. Characterization of the capsules 327
2.3.1. Morphology and particle size distribution 327
2.3.2. Core-shell structure of the coaxial microcapsules 327
2.3.3. Protein content 327
2.3.4. Surface nitrogen 327
2.4. *In vitro* simulated gastrointestinal digestion (SGIC) 328
2.5. DPP-IV inhibitory activity 328
2.6. Size exclusion chromatography (SEC) 328
2.7. Peptidomics analysis by LC–MS/MS 329
2.8. LC-MS/MS data processing 329
2.9. Statistical analysis 329
3. Results and discussion 330
3.1. Characterization of the capsules 330
3.1.1. Morphology, structure and particle size distribution 330
3.1.2. Yield, protein load and surface composition 332

3.2. Effect of gastrointestinal digestion on microcapsules properties 334
3.2.1. DPP-IV inhibitory activity 334
3.2.2. Peptide size distribution analysis 336
3.3. Peptidomics analysis 339
3.3.1. Impact of encapsulation on peptides retention 339
3.3.2. Identification of bioactive peptides 345
4. Conclusions 349
5. References 349
6. Supplementary material 354

FINAL CONCLUSSIONS 355
364

RESUMEN

Los péptidos bioactivos derivados de hidrolizados proteicos han ganado atención en los últimos años debido a sus beneficios para la salud, particularmente en la regulación de los niveles de glucosa posprandial. En este contexto, los péptidos inhibidores de la enzima dipeptidil peptidasa-IV (DPP-IV) destacan por su capacidad para prolongar la vida media de las hormonas incretinas, como el péptido-1 similar al glucagón (GLP-1) y el polipéptido inhibidor gástrico (GIP), resultando en una mejora de la secreción de insulina y del control glicémico. Consecuentemente, se han dedicado importantes esfuerzos a la identificación y obtención de estos péptidos, con un énfasis en el uso de fuentes alternativas de proteínas, en línea con la tendencia global a la producción de alimentos sostenibles y la revalorización de residuos agroalimentarios.

No obstante, la inclusión de estos péptidos en alimentos funcionales presenta diversas limitaciones técnicas. Por una parte, el procesado para su inclusión en matrices alimentarias puede afectar a su estabilidad y, además, son altamente susceptibles a ser degradados durante la digestión gastrointestinal, resultando en pérdida de bioactividad y biodisponibilidad. Ante estas limitaciones, la encapsulación ha surgido como una estrategia altamente eficiente para proteger estos péptidos. Diversas técnicas de encapsulación han sido desarrolladas, siendo el secado por atomización la más utilizada a escala industrial gracias a una baja degradación de compuestos termolábiles y a su alta productividad. Por otra parte, la encapsulación por electroesprayado ha surgido como una alternativa de encapsulación a temperatura ambiente. Además, ambas tecnologías pueden aplicarse en configuración coaxial, utilizando dos flujos concéntricos que generan encapsulados con una estructura núcleo-carcasa, lo que podría aportar una protección adicional. Sin embargo, la aplicación de esta tecnología coaxial en el ámbito alimentario aún está poco desarrollada.

En base a lo expuesto, el objetivo de esta Tesis Doctoral ha sido investigar el proceso de producción de péptidos inhibidores de la enzima dipeptidil peptidasa-IV (DPP-IV) y su estabilización durante la digestión gastrointestinal mediante encapsulación, empleando tanto técnicas de encapsulación térmica, como el secado por atomización en monoaxial y coaxial, así como técnicas electrohidrodinámicas, como el electroesprayado en configuración monoaxial. Para ello, se estudiaron dos fuentes de proteína alternativas: *Tenebrio molitor,* un insecto recientemente aprobado para el consumo humano y que requiere un uso menor de recursos frente a proteínas de origen animal tradicionales, y la semilla de olivo (*Olea europaea*) un subproducto de la industria del aceite de oliva susceptible de ser revalorizado.

Con la finalidad de identificar las características de los péptidos bioactivos a producir se realizó la caracterización estructural de secuencias peptídicas con actividad inhibidora de α-amilasa, α-glucosidasa y DPP-IV medidas experimentalmente en bibliografía. En el caso de los péptidos inhibidores de DPP-IV, destacó la importancia del contenido en aminoácidos hidrofóbicos (alanina, valina, isoleucina, leucina, metionina, fenilalanina, tirosina, y triptófano), la longitud de la cadena (3-13 aminoácidos) y la presencia de prolina en las dos primeras posiciones del extremo N-terminal. La obtención de estos péptidos a partir de la proteína de *Tenebrio*

molitor fue investigada mediante homología de secuencias *in silico* para su posterior hidrólisis dirigida empleando proteasas comerciales, como Alcalasa (subtilisina, EC 3.4.21.62) y tripsina (EC 3.4.21.4) Esta aproximación resaltó la importancia de la metodología tradicional mediante diseño experimental para la obtención de hidrolizados con distintas combinaciones enzimáticas y grados de hidrólisis (DH). De esta forma se obtuvieron 10 hidrolizados para cada sustrato a grados de hidrólisis entre 10 y 20%, con combinaciones de proteasas (Alcalasa EC 3.4.21.62, tripsina EC 3.4.21.4 y Flavourzyme EC 3.4.11.1). Esta estrategia permitió optimizar las condiciones de obtención de péptidos inhibidores de DPP-IV, destacando el tratamiento combinado de Alcalasa y Flavourzyme a DH 20%, que resultó en la mejor bioactividad para el hidrolizado de *Tenebrio molitor* (IC_{50} = 0.87 mg proteína/mL) y semilla de *Olea europaea* (IC_{30} = 1.23 mg proteína/mL).

Mediante herramientas de peptidómica, se identificaron 7,565 secuencias en el hidrolizado más bioactivo de *Tenebrio molitor* y 1,079 en el de semilla de *Olea europaea*, de las cuales más del 50% presentaron características compatibles con la inhibición de la enzima DPP-IV al ser analizadas *in silico* con la herramienta StackDPPIV. Adicionalmente, estos hidrolizados fueron evaluados *ex vivo*, empleando organoides de yeyuno de ratón, determinándose que el hidrolizado de semilla de *O. europaea* podría modular positivamente la expresión de genes involucrados en el metabolismo de los carbohidratos (PYY y GLP-1). Finalmente, se estudió el impacto de la digestión gastrointestinal en todos estos hidrolizados empleando el protocolo estandarizado INFOGEST. Esto confirmó una degradación significativa de los péptidos durante la digestión, encontrando distribuciones de peso molecular que indicaban la formación de secuencias de menor tamaño, y una subsecuente pérdida de bioactividad *in vitro*.

Con objeto de mejorar la estabilidad y preservar estas secuencias bioactivas durante el proceso gastrointestinal, se exploró la encapsulación mediante secado por atomización y electroesprayado. En primer lugar, se realizó una revisión de la literatura científica para identificar las formulaciones y las condiciones óptimas de procesamiento en configuración tanto monoaxial como coaxial. Este análisis mostró una carencia de estudios sobre la encapsulación de compuestos proteicos antidiabéticos empleando estas técnicas, así como en el uso de las configuraciones coaxiales. Debido a esta falta de información, fue necesario realizar una optimización de las condiciones de encapsulación para electroesprayado monoaxial y secado por atomización en coaxial, empleando el secado por atomización en monoaxial como referencia.

La optimización del proceso de encapsulación mediante secado por atomización en coaxial de un hidrolizado de *Tenebrio molitor* demostró que una alta concentración de sólidos tanto en la solución interna (40%) como en la externa (30%) se relacionaba con una mejora en la retención de la bioactividad y en la protección de los péptidos. Sin embargo, estos parámetros afectaban negativamente a la productividad del proceso y la carga de proteína de las cápsulas. Por otro lado, la aplicación de un ratio elevado de flujo externo/interno (67%) mejoraba la protección de los péptidos, reflejándose en los valores de nitrógeno superficial (relacionado con la rentención del hidrolizado en el interior de las cápsulas) y en la capacidad de inhibición

de la enzima DPP-IV *in vitro*. Esta mejora en la bioactividad se atribuyó a la formación de una carcasa más estructurada y uniforme.

La encapsulación mediante electroesprayado permitió la producción de cápsulas de menor tamaño, y con una distribución más estrecha (1.2 ± 0.5 μm) comparada con el secado por atomización monoaxial (11.3 ± 5.8 μm, 12.4 ± 8.7 μm con aditivos) y coaxial (5.5–8.7 μm). Por otra parte, la adición de estabilizantes como Tween 20 y pululano en el secado por atomización monoaxial mejoraba la eficiencia de la encapsulación. Además, las cápsulas obtenidas por secado por atomización monoaxial, electroesprayado monoaxial y secado por atomización coaxial mostraron valores significativamente similares en cuanto al contenido en nitrógeno superficial y la actividad inhibidora de la enzima DPP-IV. Cabe destacar que, aunque la encapsulación por electroesprayado demostró una alta estabilización y retención de bioactividad, su baja productividad representó una limitación importante para su aplicación en estudios posteriores.

Se evaluó la eficacia de la encapsulación para la protección de los pépidos durante el proceso de digestión gastrointestinal, empleándose secado por atomización en monoaxial y coaxial para encapsular los hidrolizados con mayor actividad, previamente descritos. La determinación de los perfiles de masa molecular y las medidas de bioactividad *in vitro* demostraron una mejora de la resistencia a la digestión para todos los encapsulados, en comparación con los hidrolizados libres. En particular, se observó una mayor retención de la inhibición de la enzima DPP-IV tras la digestión en los encapsulados obtenidos por secado por atomización monoaxial con aditivos (86-97%) y por secado por atomización coaxial (91-96%). Mediante un análisis de peptidómica se exploró el efecto de la encapsulación en la conservación de secuencias peptídicas tras la digestión, examinando el solapamiento de péptidos identificados entre las diferentes muestras. Sin embargo, la complejidad de las matrices usadas, la adición de los numerosos reactivos requeridos para el protocolo de digestión, y las potenciales interacciones entre los péptidos y los agentes encapsulantes, dificultaron una verificación exhaustiva. No obstante, se observó que las muestras encapsuladas retuvieron un porcentaje ligeramente mayor de péptidos tras la digestión (12.7% y 11.1% en cápsulas monoaxiales y coaxiales de *Tenebrio molitor*, respectivamente) en comparación con los hidrolizados libres (8.9%). Los encapsulados de hidrolizado de *Olea europaea* mostraron resultados similares. Adicionalmente, se identificaron 11 secuencias peptídicas con actividad inhibidora de la enzima dipeptidil peptidasa-IV previamente reportadas en la literatura, siendo LPR, VPF, LPLF, VPW, y ELPF resistentes a la digestión tras la encapsulación de los hidrolizados.

Por tanto, los resultados de esta tesis contribuyen al avance en la producción y estabilización de péptidos inhibidores de DPP-IV mediante el uso de técnicas de encapsulación, especialmente el secado por atomización en coaxial, que permitirá una mejora en la producción de alimentos funcionales con péptidos bioactivos.

SUMMARY

1. INTRODUCTION

1.1. Proteins, protein hydrolysates and bioactive peptides

Proteins are highly complex biopolymers with diverse roles in biological and food systems. They are composed of chains of amino acids that assemble through amide bonds known as peptide links. The unique properties of each amino acid are determined by their side-chain group or R-group. This linear sequence of amino acids, known as the primary structure, is read from the amino-terminal (N) to the carboxyl-terminal (C). There are 20 naturally occurring amino acids which can be nutritionally classified into three categories: (i) essential, which must be obtained from the diet (His, Ile, Leu, Lys, Met, Phe, Thr, Trp, Val); (ii) nonessential, synthesized by the body (Ala, Asn, Asp, Glu) and (iii) semi-essential, which are synthesized by the body but are designated essential during periods of stress (Arg, Cys, Gln, Gly, Pro, Ser and Tyr) (Lopez & Mohiuddin, 2024).

Protein structure is organized into four hierarchical levels. The secondary structure refers to the local arrangements of the chain in space, held by hydrogen bonds. This level includes alpha helices, spiral structures favored by the presence of Ala, Glu, Leu and Met, and beta strands, nearly linear chains forming beta sheets in parallel, antiparallel or mixed orientations (Pollock, 2007). Further compact folding results in the formation of the tertiary structure, a three-dimensional shape configuration stabilized by hydrogen bonds, electrostatic forces, disulfide linkages, and Vander Waals forces. Proteins composed of multiple polypeptide chains exhibit a quaternary structure, maintained by covalent (i.e., disulfide bonds) or noncovalent forces. (Pollock, 2007).

During digestion, the peptide bonds in intact proteins are hydrolyzed, leading to the liberation of a complex mixture of oligopeptides, peptides, and free amino acids (Figure 1A). This process produces smaller peptide fragments, which improve digestibility and reduce antigenicity (Rieder et al., 2021). Similarly, bioactive protein hydrolysates can be generated from protein sources using *in vitro* processes such as chemical hydrolysis, enzymatic hydrolysis by proteolytic enzymes, or microbial fermentation with proteolytic bacteria. According to the literature, *in vitro* hydrolysis of protein substrates using appropriate proteolytic enzymes is the most widely method utilized due to its ability to produce protein hydrolysates with desirable biological and techno-functional properties (Cruz-Casas et al., 2021). Protein hydrolysates derived from various food sources have been extensively studied over the past few decades. Beyond their nutritional value, they exhibit numerous biological activities, including antioxidant, antimicrobial, hypotensive, anticoagulant, hypoglycemic, and antitumoral effects. These functions are primarily associated to the biopeptides contained in the hydrolysates, typically composed of 2–20 amino acid residues (Figure 1B) (Nasri, 2017).

Compared to chemical methods, enzymatic processes operate under milder conditions (pH 6.0–8.0; temperature 40–60°C) allowing a better control of the hydrolysis process and preserving the amino acid composition of the original protein substrate. While slight modifications in peptide composition may occur depending on the proteolytic enzymes used, the nutraceutical value of the resulting hydrolysates remains intact (Vogelsang-O'dwyer et al., 2022). Furthermore, enzymatic hydrolysis avoids the use of organic solvents or toxic chemicals, making it more suitable for applications in the food and pharmaceutical industries (Nasri, 2017). Additionally, enzymatic hydrolysis can be tailored using specific proteases to produce reproducible bioactive protein hydrolysates with defined properties.

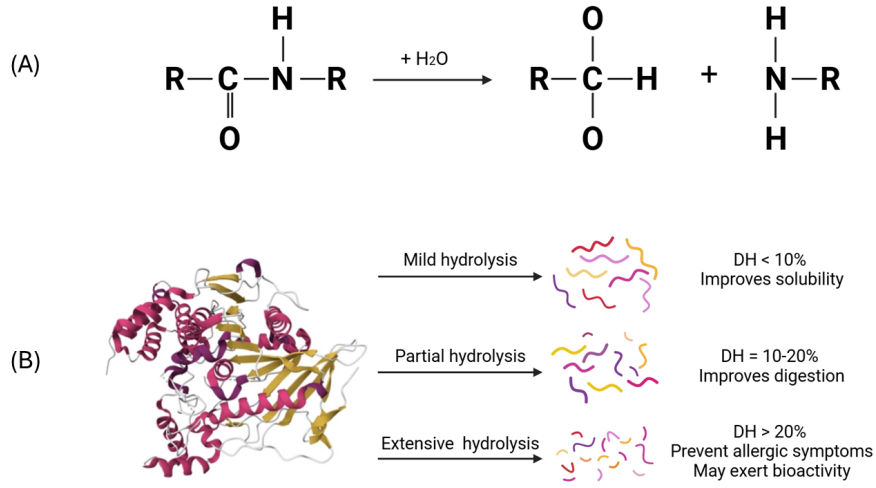

Figure 1. The process of protein hydrolysis and its products. (A) chemical reaction of protein hydrolysis; (B) different hydrolysates serve different purposes.

1.1.1. Selection of protein sources.

Protein hydrolysates and peptides can be derived from a wide range of animal and plant sources, as well as their by-products. The choice of protein source is influenced by the feasibility of the protein source to produce peptides in sufficiently high quantities to ensure economic and practical viability (Akbarian et al., 2022a). To date, animal-based proteins such as dairy proteins are known to be the best source of food-derived bioactive peptides due to their high-quality protein content (Ali et al., 2021). Additionally, proteins obtained from fish (Rivero-Pino et al., 2020; Zu et al., 2022) and meat by-products, such as collagen (Banerjee & Shanthi, 2012; Cao et al., 2020) or blood (Catiau et al., 2011) are also considered valuable sources of bioactive peptides.

Plant-based foods, such as cereals and legumes, are also rich in bioactive peptides with a diverse array of health benefits (Esfandi et al., 2019; Ospina-Quiroga et al., 2022; Zou et al., 2020). While these products have traditionally received less attention than animal proteins, they offer significant advantages. In fact, over 70% of global dietary protein needs are met by plant-based foods (Görgüç et al., 2020). Although plant proteins are often incomplete due to missing essential amino acids, exceptions like wheat germ protein provide a complete amino acid profile, comparable to animal proteins (Salas et al., 2015). Legumes, soybean in particular, has gained popularity as a high-quality protein source and is often used to replace animal proteins in diets (Luigia, 2019). Additionally, some protein can be obtained from the most widely consumed crops globally, such as cereals like rice, wheat or maize (Görgüç et al., 2020), and by-products of oil crops, generated in high quantities during oil extraction (Gullón et al., 2020). These by-products can be transformed into high nutritional value meals, suitable both for animal and human consumption. In this sense, olive (*Olea europaea*) oil production generates substantial amounts of by-products, which poses a significant environmental challenge, especially in the Mediterranean region, where Spain is the global leader in olive oil production. Particularly, Andalusia accounts for 80% of the national production (Ministerio de Agricultura, 2024). Recent research has explored the potential of olive by-products, such as leaves, exhausted pomace, and a residual fraction from olive pit cleaning, as sources of bioactive compounds (Gullón et al., 2020). Among these residues, olive seeds are an abundant and cost-effective by-product. Although they are commonly used as an energy source, their high protein content (17.2%) makes them a valuable material to repurpose as a rich bioactive protein substrate (Maestri et al., 2019a).

Insect proteins have emerged as a promising protein source due to their nutritional profile and environmental benefits. Unlike traditional protein sources, insects boast minimal environmental footprints due to their short reproductive cycles, high fecundity, low cost, low greenhouse gas emissions, and high feed conversion efficiency, which makes them sustainable and affordable with a high feed conversion efficiency (Oonincx & Finke, 2023). Research on insect-derived bioactive peptides has only been actively pursued in recent years. Specifically, the European Food Safety Authority (EFSA) has authorized four different insects for consumption as novel foods in the European Union: frozen, dried and powder forms of *Tenebrio molitor* larva (yellow mealworm); frozen, dried and powder forms of *Locusta migratoria* (migratory locust); frozen, dried and powder forms of *Acheta domesticus* (house cricket) and *Alphitobius diaperinus* (lesser mealworm) (Weimers, 2023). This has catapulted the investigation on insect-derived protein and there are numerous studies on the antihypertensive, antidiabetic, and antioxidant properties of insect-derived peptides already (Öztürk & Oraç, 2024). However, challenges such as consumer acceptance and potential allergenicity (e.g., tropomyosin) remain significant barriers (Hall et al., 2018). Among these edible insects, *Tenebrio molitor*, commonly known as mealworm, is one of the most studied

insects in the scientific community. Although traditionally considered a pest due to its damage to cereal crops and flours, *T. molitor* possess excelent nutritional value, such as protein and fat content, digestibility, favorable flavor and functional properties. These insects are easy to breed and maintain a stable protein content regardless of their diet, making their produced highly reliable. Furthermore, *T. molitor* has a significantly higher feed conversion ratio compared to traditional livestock. Unlike cattle (40%), pigs, and chickens (55%), the edible fraction of *T. molitor* larvae is almost 100% (Errico et al., 2022). *T. molitor* larvae are mainly fed on cereal bran or flour (ie., wheat, oats, or maize), making them an inexpensive protein source. As the interest in *T. molitor* larvae as a sustainable food and feed source grows, its commercial production has also expanded. Spain has been leading effort in the production of *T. molitor*, with the construction of the world's largest insect farm in Salamanca (International Pet Food, 2025). Currently, *T. molitor* is used for feeding animals, such as birds, fish, and pets in general, and is gaining attention as a potential ingredient in human diets. Compared to other edible insects, it is also recognized as one of the most consumer-accepted species for human consumption, particularly in Europe (Zunzunegui et al., 2024). A strategy adopted to reduce neophobia associated with insect consumption is to incorporate the *T. molitor* either as a meal or protein isolate into familiar food products, such as bakery items, biscuits, pasta, chocolates or other snacks. However, the high-fat content (Table 1) of *T. molitor* larvae complicates the pulverization process, leading to agglomeration and can reduce protein solubility due to lipid-protein interactions. Therefore, defatting is a crucial step in producing high-quality insect protein meals, as it improves both protein content (Table 1) and functionality (Errico et al., 2022). *T. molitor* also demonstrates health benefits as a source of bioactive peptides, including antioxidant and antimicrobial effects, making it suitable for sustainable and nutritious foods. Nonetheless, to fully benefit from its nutritional potential, particularly its high protein and bioactive peptide content, it is essential to use methods that optimize its functional properties (Guiné et al., 2025).

Table 1. Nutritional composition (% in dry matter) of *Tenebrio molitor* meals.

	Defatted commercial *T. molitor* meal	Commercial *T. molitor* meal
Protein	67.85 ± 0.75	56.95 ± 0.24
Fat	7.27± 0.01	14.35 ± 0.09
Carbohydrate	14.64± 0.78	14.69 ± 0.84
Minerals (ash)	4.92 ± 0.03	4.05 ± 0.01
Energy (kcal/100g)	395.38	415.69

1.1.2. Selection of enzymes

Regarding the selection of the proteases, the enzymes responsible for breaking peptide bonds, they are broadly classified into (i) endopeptidases, which target internal peptide bonds, and (ii) exopeptidases (aminopeptidases and carboxypeptidases), which cleave peptide bonds at the NH_2 and COOH termini, respectively (López-Otín & Bond, 2008). Typically, these enzymes, such as pepsin, bromelain, trypsin, chymotrypsin, and papain, are used at their optimum pH and temperature conditions. The choice of protease is critical, as its specificity and working conditions directly influence the number and type of peptide bonds hydrolyzed, ultimately determining the characteristics of the resulting bioactive peptides (Sbroggio et al., 2016). As a result, different proteases and enzyme-to-substrate ratios can be used to tailor hydrolysis for specific applications (Figure 1B). For example, mildly hydrolyzed proteins are commonly used in clinical and sports nutrition to enhance digestibility, while extensively hydrolyzed proteins are suitable for infant formulas as hypoallergenic alternatives to intact cow's milk proteins (Kiewiet et al., 2018). Furthermore, the addition of exopeptidases can hydrolyze hydrophobic, bitter peptides, reducing bitterness and even creating pleasant flavor compounds, which is highly beneficial in food formulation (Raksakulthai & Haard, 2003).

Numerous proteolytic enzymes are employed for producing bioactive peptides from food sources, with Alcalse and Flavourzyme being some of the most used in research (Mora & Toldrá, 2022). Alcalase, a broad-spectrum alkaline endopeptidase derived from *Bacillus licheniformis,* cleaves peptide bonds preferentially adjacent to hydrophobic amino acids such as Glu, Met, Leu, Tyr, Lys, and Gln (Tacias-Pascacio et al., 2020). Hence Alcalase can be used to obtain peptides with general hydrophobic characteristics, making it especially interesting for the obtention of multifunctional peptides, mainly antioxidant, ACE-inhibitory or DPP-IV inhibitory. On the other hand, Flavourzyme is a mixture of exo- and endo-peptidases, which hydrolyses both internal and terminal peptide bonds, generating free amino acids and bioactive peptide fractions. It is particularly effective to produce antioxidant and antimicrobial peptides. Nonetheless, it requires pairing with a broad-expectrum endopeptidase, like Alcalase, for efficient hydrolysis (Alahmad et al., 2023). The use of enzymes with digestive activities such as pepsin, trypsin and chymotrypsin is also common. Pepsin, typically of porcin origin, cleaves preferably after bulky hydrophobic amino acid residues (i.e., Phe, Leu) (Ahn et al., 2012). Nonetheless, it is much less specific than other proteases. Trypsin targets basic amino acids (Arg and Lys), while chymotrypsin hydrolyzes bonds adjacent to aromatic amino acids (Tyr, Phe, and Trp) (Akbarian et al., 2022b). Trypsin is particularly used due to its high specificity, favoring the obtention of ACE-inhibitory peptides and calcium-binding phosphopeptides (Akbarian et al., 2022b).

The combination of different enzymes improves hydrolysis, yielding smaller fragments with high bioactive potential. Enzymes can be added simultaneously or sequentially, depending on their working conditions. For example, the combination of Trypsin and Alcalase has demonstrated superior efficiency in producing bioactive peptides compared to using either enzyme alone, highlighting the synergistic effect of their specificities (Chen et al., 2018; Xu et al., 2019).

1.1.3. Use of Computer-Based Techniques in Peptide Research

The traditional method for identifying and processing bioactive peptides involves *in vitro* enzymatic hydrolysis followed by chromatographic purification of the hydrolysates. After evaluating the bioactivity of the peptides, their sequences are identified, and, in most cases, the biological activity of the chemically synthesized peptide is subsequently confirmed. Indeed, over the past several years, significant research efforts have focused following this methodology, resulting in the identification of numerous peptide sequences with various bioactivities (Qin et al., 2022). However, this conventional methodology is labor-intensive, time-consuming, and expensive. To address these challenges, researchers are increasingly adopting *in silico* approaches, which combine the study of pre-identified bioactive sequences with computational tools (Figure 2). These *in silico* methodologies streamline the research process by enabling more targeted selection of enzymes and protein sources, simulating proteolysis, predicting biological activities, and assessing allergenicity and toxicity. Additionally, molecular docking techniques are employed to explore the action mechanisms of the peptides (Peredo-Lovillo et al., 2022). In general, the *in silico* approach adopts the following targeted workflow:

- Protein substrate selection based on economic and sustainable considerations. Protein sequences are retrieved from specialized databases such as UniProt Knowledgebase (Consortium et al., 2025).
- Simulated proteolysis employing tools such as the Enzyme Action tool in the BIOPEP database (http://www.uwm.edu.pl/biochemia/index.php/en/biopep, Mooney et al., 2012) or PeptideCutter (Maillet, 2020).
- Sequence analysis of the resulting peptides to determine their abundance within the protein and their potential bioactivity (Öztürk & Oraç, 2024). Among the most relevant tools for bioactivity prediction, PeptideRanker has been frequently utilized. It utilizes machine learning trained on known bioactive sequences to assign a bioactivity score (0–1), where higher values indicate greater potential. However, it lacks specificity regarding the type of bioactivity (Mooney et al., 2012). Hence, BIOPEP-UWM has overcome this limitation by offering a categorized database of bioactive peptides and allowing to simulate hydrolysis *in silico* hydrolysis predict the generation of bioactive

fragments from protein sources. Regarding the prediction of DPP-IV inhibitory peptides, the tools iDPPIV-SCM and StackDPPIV can be highlighted. The first computational model developed was iDPPIV-SCM, which is based on the Scoring Card Method (SCM), analyzing the amino acid sequence without requiring structural information (Shoombuatong et al., 2020). More recently, StackDPPIV has been developed to improve prediction accuracy by combining five machine learning algorithms with ten feature encodings. It employes a genetic algorithm to optimize probabilistic features, reporting a score (0–1) on whether the sequence would exhibit inhibitory activity (Charoenkwan et al., 2022).

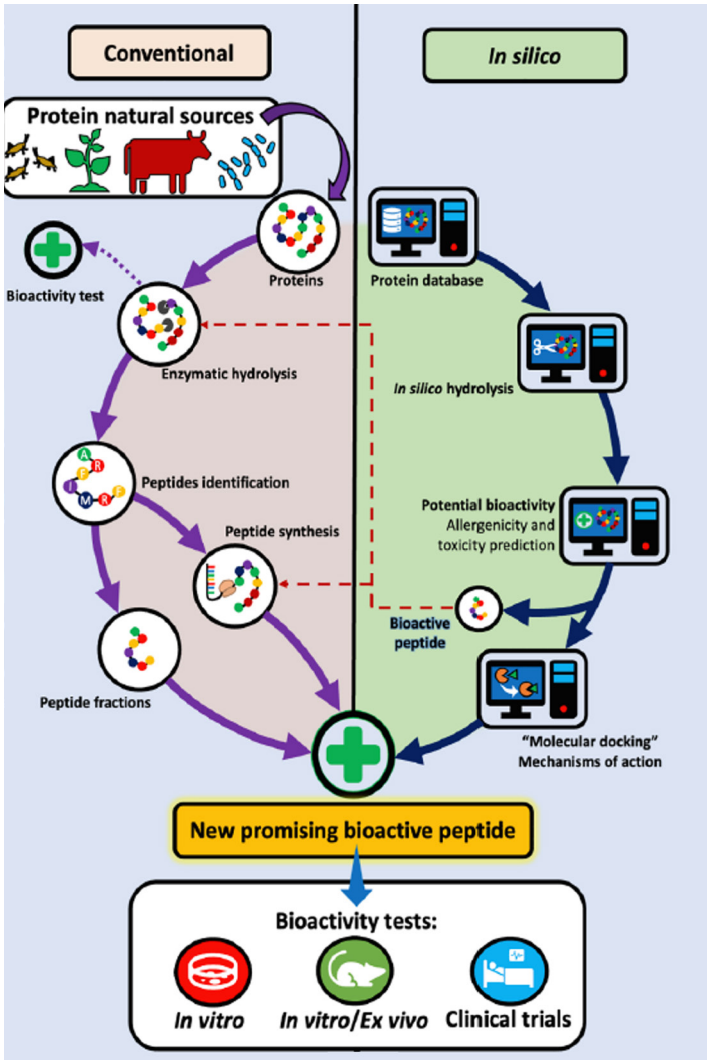

Figure 2. Hybrid approach for the generation of new bioactive peptides from food-derived proteins. Modified from (Peredo-Lovillo et al., 2022).

This novel methodology has successfully resulted in the identification of bioactive peptides derived from various protein sources, such as oilseed (Han et al., 2019), flaxseed (Langyan et al., 2021), or potato (Bjørlie et al., 2023). Nonetheless, this approach presents limitations such as being restricted to the information available in existing databases and requires validation through *in vitro* and *in vivo* studies to confirm the biological activity of the identified peptides (Peredo-Lovillo et al., 2022).

Although *in silico* evaluations contribute to a better understanding of peptide nature and function, they may not be sufficient to solve these problems. Therefore, there is a need for strategies using combined approaches where *in silico* and *in vitro* methods are used together to obtain new and potential bioactive peptides in a cost-effective way. For instance, antioxidant peptides derived from chicken protein were successfully identified using this hybrid approach (Xiao et al., 2022).

1.2. Antidiabetic potential of bioactive peptides

Food-derived peptides exhibit a broad spectrum of bioactivities, including significant potential in regulating the glycemic index. Glycemic dysregulation and persistent hyperglycemia are the main characteristics of diabetes mellitus (DM), a chronic condition that significantly impacts global health. Indeed, the prevalence of adult diabetes is estimated to reach 578 million by 2030 (Saeedi et al., 2019). DM is categorized into type 1 diabetes (T1DM), characterized by inadequate insulin production due to genetic or autoimmune responses (Reed et al., 2021). Type 2 diabetes (T2DM), which accounts for 90% of cases, originates with insulin resistance and progresses to β-cell dysfunction, with additional influences such as sedentary lifestyles, weight gain, and stress. This disease also exhibits significant heterogeneity, as it can manifest at any age, with or without chronic complications, and while it is more commonly associated with obesity, it can also occur in lean individuals. Additionally, a large number of genes are implicated in its progression (Mijares, 2010). Current treatments for T2DM aim to manage or delay its long-term complications employing insulin and various synthetic oral hypoglycemic agents, such as metformin. However, insulin therapy is limited by the need for non-oral administration, and synthetic oral drugs often come with serious side effects and potential toxicity.

Recent studies have highlighted the importance of early intervention and the integration of glucose-lowering medications with alternative approaches that enhance treatment adherence (Davies et al., 2018). In this context, food-derived bioactive peptides present a promising complementary strategy, acting through key mechanisms such as the inhibition of α-amylase, α-glucosidase, and dipeptidyl peptidase IV (DPP-IV), as well as functioning as incretin agonists (Jahandideh et al., 2022).

1.2.1. α-Amylase and α-glucosidase inhibitors

Alpha-Amylase (EC 3.2.1.1) and α-glucosidase (EC 3.2.1.20) are key enzymes in carbohydrate digestion. Alpha-Amylase, a digestive enzyme secreted from the salivary and pancreatin glands, hydrolyzes complex carbohydrates into oligosaccharides. These oligosaccharides are further broken down by α-glucosidase, an enzyme located on the brush border of enterocytes lining the intestinal villi, into absorbable monosaccharides. Inhibiting these enzymes slows carbohydrate digestion and reduces postprandial blood glucose levels (Jahandideh et al., 2022). Synthetic inhibitors of α-glucosidase, such as acarbose and miglitol, are effective in the regulation of hyperglycemia, but are associated with undesirable gastrointestinal side-effects, including bloating and diarrhea. These inhibitors also require frequent dosing and precise adjustments to prevent renal complications. Notably, there have been no significant advancements in these medications in recent years (Davies et al., 2018). Thus, efforts have been directed to the development of natural inhibitors, which are believed to offer comparable efficacy with fewer adverse effects.

Bioactive peptides with inhibitory effects on these enzymes represent a promising natural alternative. These peptides can bind to the catalytic sites of α-amylase and α-glucosidase, preventing the enzymes from interacting with or hydrolyzing carbohydrate substrates. Their effectiveness is often attributed to key characteristics such as short peptide chain length, high hydrophobicity and the presence of aromatic (Phe, Tyr and Trp) or hydroxyl-containing residues (Ser, Thr, Tyr), which can contribute to binding affinity and specificity by interacting with the active site of the enzyme through hydrogen bonding (Berraquero-García, Rivero-Pino, et al., 2023). Additionally, some α-amylase inhibitory peptides can attach to starch molecules, further hindering their digestion (Evaristus et al., 2018). Numerous food sources have been explored for α-amylase and α-glucosidase inhibitory peptides, as reviewed elsewhere (Berraquero-García, Rivero-Pino, et al., 2023). For instance, FFRSKLLSDGAAAAKGALLPQYW, a potent α-amylase inhibitor (IC_{50} of 0.02 μM), derived from cumin seed protein (Siow & Gan, 2016), and FDPFPK, inhibiting α -glucosidase with IC_{50} of 7.93 μM, obtained from the simulated digestion of Desert locus (*Schistocerca gregaria*) (Zielińska et al., 2020). Nonetheless, the literature on α-amylase and α-glucosidase inhibitory peptides indicate that little effort has been dedicated to validating their activity through cellular or animal model studies.

1.2.2. Incretin mimetics

Patients with type 2 diabetes mellitus (T2DM) exhibit an inability to suppress postprandial glucagon release, alongside impaired insulin secretion. This failure to regulate glucagon makes incretin-based therapies particularly effective in addressing the condition. Incretins are peptide hormones, primarily glucagon-like peptide 1 (GLP-1) and glucose-dependent insulinotropic polypeptide (GIP), which regulate postprandial insulin secretion. These hormones are secreted by intestinal L and K cells, respectively, in response to food ingestion (Jahandideh et al., 2022).

GLP-1 has mainly garnered significant attention due to its fundamental role enhancing insulin secretion, suppressing glucagon production, delaying gastric emptying, and promoting satiety. However, GLP-1 has an extremely short half-life (<2 min) as it is rapidly degraded by DPP-IV (Mijares, 2009). To overcome this limitation, two therapeutic strategies have been developed: GLP-1 receptor agonists (GLP-1 RA) resistant to DPP-IV degradation and DPP-IV inhibitors. Common GLP-1 RA include exenatide, liraglutide and semaglutide. These medications are administered via injection, and offer several advantages, such as excellent postprandial glucose control, a low risk of hypoglycemia when used as monotherapy, and cardiovascular risk reduction. Notably, Ozempic®, which employs semaglutide as its active ingredient, has demonstrated superior efficacy compared to other antihyperglycemic agents in controlling glucose levels, reducing body weight, and mitigating cardiovascular risks. However, while Ozempic® was initially developed for glycemic management in T2DM, its role in weight loss is gaining prominence among individuals without T2DM (Zaazouee et al., 2022). Additionally, Rybelsus®, an oral semaglutide formulation approved by the FDA in 2019, offers a convenient alternative to injectable GLP-1 RA (Meisel, 2004). Although these treatments present significant benefits and increased adherence due to additional effects (i.e., weight loss), they also include severe disadvantages like GI side effects, increased heart rate and, in rare cases, acute pancreatitis. Injectable formulations also require patient training, which may limit their accessibility (Davies et al., 2018).

Diverse peptides have been identified with capacity to increase incretin secretion and regulation of blood glucose. For example, wheat protein hydrolyzed by bacterial proteases yields a glutamine-rich, low-molecular-weight fraction that stimulates GLP-1 secretion (Kato et al., 2017). Similarly, peptides LGG and GF have also been reported to enhance GLP-1 release in murine primary L cells (Diakogiannaki et al., 2013). Other peptides, such as LIVTQTM and VAWRNRCKGTD, derived from β-lactoglobulin and β-casein, respectively, have demonstrated the ability to increase GLP-1 release. In general, these peptides are characterized by significant hydrophobicity and the presence of serine (S) and tryptophan (W) at their N-terminus, which appear to enhance their bioactivity (Santos-Hernández et al., 2023).

1.2.3. DPP-IV inhibitors

During regular metabolism, incretins GLP-1 and GIP would be rapidly cleaved and inactivated after release into circulation by the action of DPP-IV (EC 3.4.14.5). This enzyme is a serine protease widely distributed across tissues, including the intestinal brush border, renal membranes, vascular endothelium, and pancreas (Deacon, 2019). However, since T2DM patients have insufficient insulin level in the bloodstream, the inhibition of DPP-IV leading to an increase of the half-life of these incretins, would cause insulin secretion to be stimulated and subsequently, the blood glucose level would be adequately regulated (Nongonierma & FitzGerald, 2019). Consequently, DPP-IV inhibitors have become a well-established class of oral antihyperglycemic agents, recommended for T2DM patients without atherosclerotic cardiovascular disease (Deacon, 2019). Common commercial DPP-IV inhibitors include sitagliptin, vildagliptin, saxagliptin, linagliptin, and alogliptin. These oral agents are generally well-tolerated, do not induce hypoglycemia, and have a neutral effect on body weight. However, adverse effects such as nasopharyngitis, dermatitis, urinary infections, and headaches have been reported. The efficacy of these drugs is maximized when used as adjunctive therapy rather than as monotherapy (Mijares, 2009).

DPP-IV inhibitory peptides are among the most extensively studied bioactive peptides. These peptides are characterized by high hydrophobicity, the presence of proline (P) in the last two N-terminal positions, and aromatic residues such as phenylalanine (F) and tryptophan (W) in the catalytic domains. These features enable peptides to interact with the S2 sub-pocket of DPP-IV via hydrophobic interactions and hydrogen bonds. The most potent DPP-IV inhibitory peptides identified to date are GPAGPQGPR (IC_{50} = 0.51 μM), and PPGLPGSPGQ (IC_{50} = 0.55 μM) and LPQPPQE (IC_{50} = 0.97 μM), all derived from the simulated digestion of deer antler velvet. Although these peptides are relatively long, most DPP-IV inhibitory peptides are short peptides containing 3–6 residues (Nongonierma & FitzGerald, 2019).

Most of the works reported in literature are focused on *in vitro* or *in silico* evaluations, however, *In vivo* evaluation is specially needed considering the bioavailability of the peptides. Some of the studies in the literature used cell models such as Caco-2 and HepG2 cells to analyze the inhibition by peptides of DPP-IV, and to a lesser extent of α-amylase and α-glucosidase(Harnedy-Rothwell et al., 2020) (S. Hu et al., 2019). However, *in vivo* data remains scarce, and further work should be carried out testing this activity (J. Hu et al., 2023; Lin et al., 2016).

1.3. Bioaccessibility and bioavailability of antidiabetic peptides

An important consideration for the application of bioactive peptides in functional foods is their bioaccessibility and bioavailability. Understanding their stability, digestion, and absorption throughout the gastrointestinal tract (GIT) is fundamental. When bioactive peptides are ingested orally, they must undergo digestion by gastric and intestinal proteases and withstand variations in pH. Due to the complexity of the digestive process, several *in vitro* simulation mechanisms have been developed, with the INFOGEST protocol being the most prominent (Brodkorb et al., 2019). Although *in vitro* methods cannot fully replicate the intricacies of *in vivo* digestion, the INFOGEST protocol serves as a reliable alternative to animal models, which are often criticized for their limited relevance to human digestion (Sousa et al., 2020). Digestion can be divided into three distinct phases:

- Oral: In the mouth, ingested nutrients are fragmented by mastication and are mixed with saliva to form a food bolus that can easily be swallowed. In addition, enzymatic digestion by salivary enzymes also starts within the oral cavity, primarily through the action of salivary α-amylase, which targets starches.
- Gastric: in the stomach, gastric secretions facilitate the full or partial digestion of protein through acid denaturation and enzymatic hydrolysis by pepsins. The acidic environment of the stomach, with a pH ranging from 1.5 to 3, is crucial for enzyme activation and optimal activity. Pepsins, which are endopeptidases, cleave internal peptide bonds, particularly those adjacent to hydrophobic amino acids (Ala, Val, Ile, Leu, Met, Tyr, Trp, Glu and Pro) (Keller, 2013).
- Intestinal: the chyme formed in the stomach enters the small intestine, where pancreatic and biliary secretions neutralize the acidic pH, maintaining it between 6 and 7, a prerequisite for efficient protein digestion. Pancreatic enzymes (i.e., *α*-amylase, trypsin and chymotrypsin, lipase, and colipase), play a central role in breaking down proteins, carbohydrates, and lipids into absorbable monomers. The small intestine is the main site of macronutrient digestion and absorption (Keller, 2013).

While some drugs and potential constituents of human food, for example, urea and ethanol, may already be absorbed via the oral or gastric mucosa, the vast majority of nutrients are absorbed in the upper small intestine (Keller, 2013).Hence, for bioactive peptides to exert their postprandial effects, such as DPP-IV inhibition, they must reach the small intestine in their active form. The intestinal epithelium is critical in this process, as it not only facilitates peptide absorption but, as previously mentioned, it also regulates glucose metabolism through incretin hormone production (Ezcurra et al., 2013). Intestinal cell lines, such as Caco-2, have been widely used to assess the effects of food components on the intestinal epithelium. These models allow for the study of peptide transport mechanisms, including (Figure 3):

1. Paracellular: Involves the passage of peptides through tight junctions between intestinal epithelial cells. Although this pathway has low permeability under normal conditions, it may increase in specific scenarios.

2. Passive diffusion: Highly lipid-soluble, small peptides can diffuse through the epithelial membrane. However, larger peptides (>600 Da) are generally excluded.

3. Transcytosis: Large polar peptides (>600 Da) interact with the apical lipid bilayer of intestinal epithelium through hydrophobic interaction, are internalized into vesicles, and transported across the cell (Sun et al., 2020).

4. PepT1-mediated permeation: The proton-dependent transporter PepT1 is a high-capacity and low-affinity carrier that actively transports small peptides (di-tripeptides) with neutral charge and high hydrophobicity from the gastrointestinal lumen into the intestinal epithelium. This is based upon a proton gradient that is maintained by the H^+/Na^+ exchanger (Sun et al., 2020).

Although Caco-2 cells have provided valuable insights into peptide transport, they have limitations, such as their lack of tissue complexity and stem cells, limiting their physiological relevance, and understanding of the function of the mucus layer that covers the intestinal epithelium (Sun et al., 2020). Additionally, intestinal organoid models are emerging as a superior alternative, offering greater physiological relevance by incorporating stem cells and multiple epithelial cell types, partially recapitulating the complexity of the intestinal tissue (Aquino et al., 2024). Moreover, organoids can offer insights as well into carbohydrate metabolism, as the intestinal epithelium is responsible for carbohydrate absorption and incretin production. Therefore, organoids represent a suitable model to investigate the regulation of gene expression related to carbohydrate metabolism in the intestinal epithelium (Takahashi et al., 2022; Zietek et al., 2020). Indeed, recent work on organoid models has demonstrated their potential for studying the effects of bioactive peptides on carbohydrate metabolism at the molecular level. Gene expression analysis has revealed that peptides derived from brewer's spent yeast can modulate key metabolic pathways by regulating the expression of

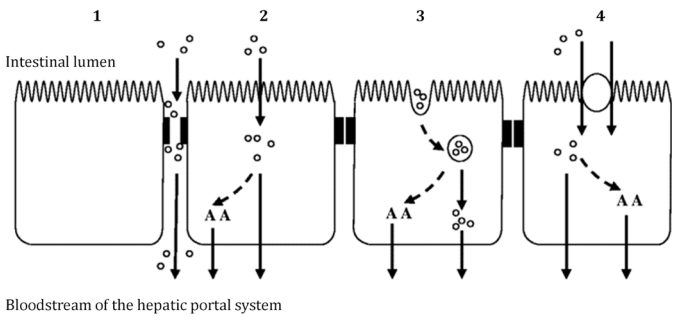

Figure 3. Potential mechanisms of small-intestinal epithelium movement of peptides: 1, paracellular; 2, passive diffusion; 3, transcytosis; 4, carrier mediated transport (Miner-Williams et al., 2014).

enzymes involved in carbohydrate digestion, incretin hormones, and glucose transporters (Aquino et al., 2024).

In addition to retaining structural integrity and biological activity during digestion and absorption, bioactive peptides must be incorporated into systemic circulation. However, several factors are challenging, such as their incorporation into food matrices for the development of functional food, which may cause structural alterations or loss of function during processing or storage (Kamdem & Tsopmo, 2019), or degradation by intestinal brush border membrane peptidases, as shown in studies of DPP-IV inhibitory peptides (Lacroix et al., 2017). Hence, while understanding the transport mechanisms and bioavailability of bioactive peptides is crucial, current knowledge is incomplete. Future approaches must integrate *in silico*, *in vitro*, and *in vivo* studies to fully account for degradation pathways, including those influenced by food matrices and the mucus layer. Advanced techniques, such as organoid-based models, hold promise for overcoming the limitations of traditional cell lines and providing deeper insights into peptide absorption and activity. Additionally, strategies to enhance peptide stability and maintain bioactivity in functional foods will be essential to unlock their full potential as regulators of glycemic response and metabolic health.

1.4. Encapsulation of bioactive peptides

To minimize the degradation and loss of bioactivity of peptides during processing, storage and digestion, various encapsulation methods have been developed. Encapsulation involves enclosing active materials within a matrix of encapsulating materials. Encapsulates are generally classified into two categories based on their size: microencapsulation, which produces particles in the range of 1–800 μm, and nanoencapsulation, which produces particles between 1 nm and 1 μm (Yan et al., 2022). The active ingredient typically serves as the core material, while the carrier, or encapsulating materials, form a barrier between the core and the external environment. This prevents the degradation of active ingredients, enhances their stability during processing, extends their shelf life, mask undesirable flavors and tastes, and improves the bioavailability of the final product (Gibbs et al., 1999). For applications in functional foods, it is crucial that the encapsulation materials are food-grade and exhibit minimal reactivity (Singh, 2016).

A variety of microencapsulation technologies have been employed in the food industry, including coacervation, fluidized-bed coating, extrusion, molecular encapsulation, and spray drying (Aguilar-Toala et al., 2022). Alternative techniques, such as aerogelation and electrospraying, have also been explored. While the latter methods show promise in preserving active food ingredients, they face challenges in scaling up and remain financially restrictive for widespread commercial use (Yan et al., 2022).

1.4.1. Spray-drying

Spray drying is one of the most used and cost-effective techniques for producing dry powders and can be employed to enhance the stability of peptides during gastrointestinal digestion. This method involves dispersing the active ingredients into a wall or shell material before pumping the mixture into a drying chamber, where it is atomized using an atomizer. A high-temperature gas stream (140–220 °C) concurrently enters the drying chamber, driving the drying process (Jacobs, 2014). During the first drying stage, water evaporates from the surface of the droplets while the temperature is maintained at the wet-bulb temperature (Figure 4). As drying continues, a crust forms on the droplet surface, limiting further evaporation and causing the particle temperature to rise until it is fully dried (Woo & Bhandari, 2013). This quick drying process (15–30 s) results in the formation of micron-sized capsules (5–80 μm) (Yan et al., 2022), which are then separated from the air stream in the cyclone (Figure 4).

For the successful encapsulation of bioactive peptides, both the formulation of the feed stream and the processing conditions are crucial in determining encapsulation efficiency and target properties. While polysaccharides such as maltodextrin (MD) are common carriers due to their stability and functional properties (Akbarbaglu et al., 2021), their digestion releases glucose, which is undesirable in the production of functional foods with antidiabetic activity (Hofman et al., 2016). Therefore, alternative encapsulants, such as Arabic gum or chitosan, should be considered. Additionally, systems like nanoliposomes or nanoemulsions offer enhanced stability but may face issues such as lipid oxidation (Mehta et al., 2023). Processing conditions, such as inlet/outlet temperature of drying air and feed flow rate, influence particle size, stability, and encapsulation efficiency, highlighting the importance of optimizing these parameters.

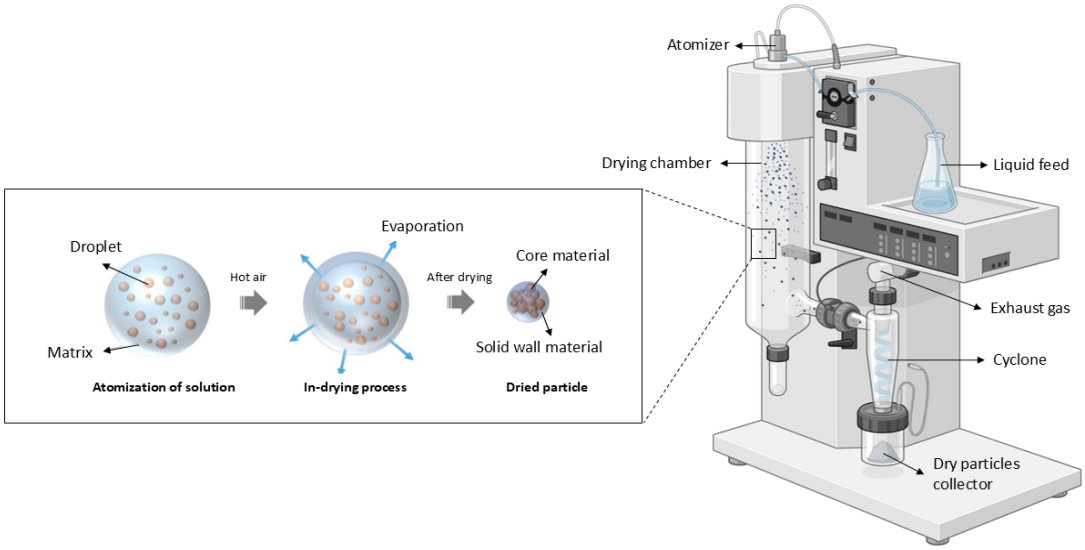

Figure 4. Schematic diagram of the droplet drying process in the spray dryer. Modified from (Yan et al., 2022) in BioRender.com.

The nozzle type also plays a significant role in determining the characteristics of the final product. A two-fluid nozzle, or monoaxial encapsulation, results in standard capsule formation. Alternatively, using a three-fluid nozzle, or coaxial spray-drying, allows the simultaneous atomization of two separate liquid feeds. Monoaxial spray-drying leads to solubilized peptides being randomly distributed within the encapsulating matrix, potentially resulting in protein exposure on the capsule surface, making them more susceptible to degradation by external stressors (Figure 5A). In contrast, coaxial spray-drying results in the production of core-shell microcapsules since, during the drying process, the shell material solidifies around the core, resulting in a distinct core-shell microcapsule morphology (Figure 5B). This method offers key advantages compared to monoaxial spray-drying, such as enhanced protection of the peptides included in the core feed, since the shell can act as an additional barrier against oxidation, hydrolysis, pH variations, and enzymatic degradation. Other advantages include a more controlled release of bioactives compared with monoaxial spray-drying, or the ability to encapsulate both hydrophobic and hydrophilic compounds simultaneously by employing different solvents in the shell and core feeds. Despite its success in encapsulating other compounds with a tendency to degrade in harsh conditions (i.e., carotenoids and organosulfur molecules), its application for protein hydrolysates and peptides remains largely unexplored (Berraquero-García, Pérez-Gálvez, et al., 2023).

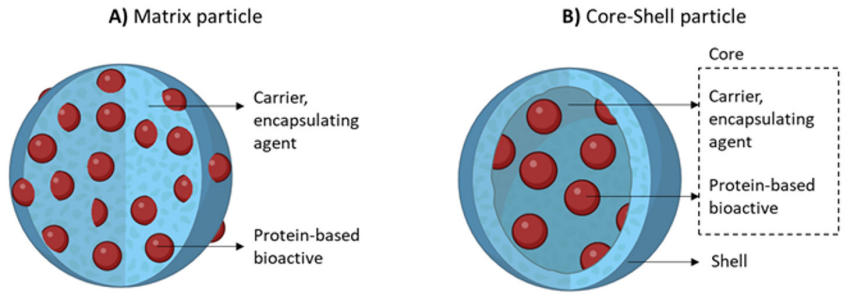

Figure 5. Different types of microcapsules (A) matrix particles, obtained through monoaxial spray-drying; (B) bore-shell particles, obtained through coaxial spray-drying. Created in BioRender.com.

1.4.2. Electrospraying

Electrospraying, also known as electrohydrodynamic atomization, is a technique used to obtain micro/nanocapsules at room temperature by applying a high-voltage (5–30 kV) electric field to a liquid solution. The process involves pumping a solution that contains the sample through a conductive needle, with a grounded collector placed at a specified distance. When the electric field is applied between the injector and the collector, the electrostatic forces polarize the liquid at the air-liquid interface, causing it to deform into a cone-like

structure known as a Taylor cone. As the voltage increases, the surface tension can no longer contain the liquid, and a charged jet is ejected from the cone's tip. This jet breaks into a spray of charged droplets driven by the electrostatic repulsion and low viscoelasticity of the solution. As the droplets travel to the collector, the solvent evaporates, leaving behind dry nano- or microparticles (Figure 6) (Ghorani & Tucker, 2015). This process allows for the encapsulation of sensitive biomolecules while maintaining their properties (García-Moreno et al., 2018). Particle size and morphology are affected by various parameters, including solution properties (conductivity, surface tension, viscoelasticity), processing conditions (electric field, feed flow-rate, distance injector to collector), and environmental conditions (temperature and humidity). In particular, high voltage typically reduces particle size, which enhances solubility. Feed flow rate also impacts particle size, with lower flow rates providing smaller particles, generally with high encapsulation efficiency but limiting productivity (Berraquero-García, Pérez-Gálvez, et al., 2023). Similarly to spray drying, electrospraying can be carried out in either monoaxial or coaxial configurations. Coaxial electrospraying differs from the monoaxial configuration by incorporating a coaxial emitter with two concentric needles. This approach offers a key advantage over monoaxial electrospraying, since it allows for a centralized distribution of the peptide solution. As a result, the produced capsules report higher encapsulation efficiency (Berraquero-García, Pérez-Gálvez, et al., 2023).

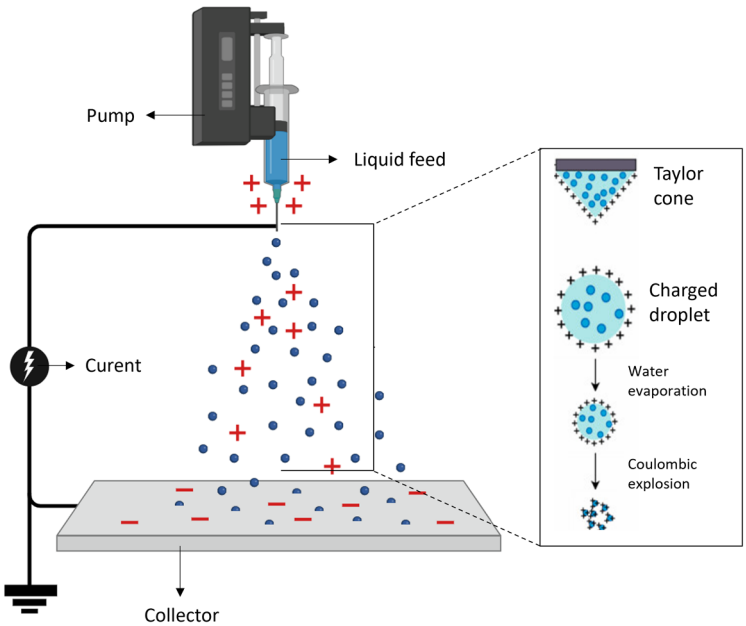

Figure 6. Schematic diagram of the electrospraying technique. Modified from (Jayaprakash et al., 2023) in BioRender.com.

Electrospraying has gained attention for the encapsulation of bioactive peptides and proteins due to its ability to produce nano- and microparticle, improving stability and controlled release. For instance, peptides such as α-calcitonin gene-related peptide (Kumar et al., 2021) and pp65489–503 (Furtmann et al., 2017) have been encapsulated for their use as vasodilator and immune stimulatory treatments, respectively. However, most research on electrospraying encapsulation has focused on pharmaceuticals applications, with food-related applications primarily dedicated to the optimization of polymeric carriers, solution properties, and processing conditions (Bock et al., 2014; Musaei et al., 2017). A key limitation of this technology in the food industry is its low production capacity. To overcome this challenge, recent advancements have emerged, such as multi-needle systems (Moreira et al., 2021), or electrospraying assisted by pressurized gas. The latter combines the benefits of electrohydrodynamic atomization with the increased flow rate favored by compressed air or gas. This technique accelerates solvent evaporation by facilitating the breakup of liquid streams into finer droplets within the high electric field, at room temperature, which allows a more viable large-scale application (Busolo et al., 2019).

1.5. Peptidomics analysis in peptide encapsulation

The use of peptidomics has emerged as a potent analytical approach for verifying the success of encapsulation of bioactive peptides, as well as assessing the stability of the encapsulated peptides after gastrointestinal digestion. In contrast to conventional techniques that commonly depend on indirect measures like molecular weight distribution and bioactivity retention, peptidomics offer detailed molecular profiles, enabling direct comparison and validation of encapsulation effectiveness (Chauhan et al., 2021). Employing this approach facilitates the understanding of the protective mechanism of encapsulation and its impact on peptide stability.

Recent studies have reported successful encapsulation of bioactive peptides employing well-known techniques. Monoaxial spray-drying has been applied to encapsulate antidiabetic and antihypertensive peptides derived from *Phaseolus lunatus* and Brewers' spent grain protein hydrolysates. In these cases, bioactivity retention and peptide identification post-digestion were used to confirm successful encapsulation (Cian et al., 2019, 2020, 2022; Ferreira et al., 2022; Garzón et al., 2023). Moreover, Fourier Transform Infrared (FTIR) spectroscopy has also been employed to assess structural stability within encapsulation matrices (Akbarbaglu et al., 2019). Comparison of the chromatographic profiles of encapsulated samples before and after digestion, have also been employed as a robust method for confirming encapsulation success (Garzón et al., 2023). However, a peptidomic approach would go beyond these methods by allowing precise peptide identification through what has been named "untargeted" workflows. This approach aims to identify and characterize all detectable peptides in a sample, without prior knowledge or selection of specific target peptides (Fan et al., 2023).

Traditional proteomics, commonly referred to as bottom-up proteomics, focuses on identifying complete proteins present in the original sample based on unique peptide identification. In contrast, the objective for food applications and digestion studies is to characterize the peptides formed when the proteins in the original sample are known (Vreeke et al., 2022). Peptidomics targets peptides generated through enzymatic hydrolysis or digestion. This distinction is particularly significant in encapsulation studies, where the goal is to preserve specific peptide sequences despite gastrointestinal conditions (Dallas et al., 2015). Encapsulation systems must protect these peptide sequences from degradation, requiring analytical techniques capable of accurately detecting short peptides within the intricate mixtures of the samples. Peptidomics workflows generally begin with sample pretreatment to remove interfering components and concentrate peptides for improved detection. This is followed by mass spectrometry (MS) data acquisition, where fragmentation spectra are used to deduce peptide sequences.

The identification of small peptides, such as dipeptides and tripeptides, presents a significant challenge due to limited fragmentation patterns and spectral library coverage. This is due to current search algorithms often being limited to peptides containing 4 or more amino acids and di/tripeptides usually not producing enough unique fragment ions for unambiguous sequence identification (Tang et al., 2014). Studies have shown that dipeptides and tripeptides often lack sufficient unique fragment ions for unambiguous identification, making their resolution particularly difficult. Additionally, advanced scoring algorithms like MASCOT or Andromeda are frequently used to annotate peptides based on MS/MS spectra, but the lack of standardized protocols often complicates cross-study comparisons (Vreeke et al., 2022). In addition, only a list of the identified peptide sequences is reported for most papers, without any parameters describing the completeness of the analysis and no way to ensure reproducibility.

The complexity of the hydrolysates or digests adds another layer of difficulty. These samples often result in a large number of peptides identified in studied samples, which require rigorous pretreatments to remove interfering components and to concentrate in peptides. High-performance liquid chromatography (HPLC), in its various modes, has become the preferred technique for separating peptides due to its efficiency and automation capabilities (Sánchez-Rivera et al., 2014). For this untargeted approach, all detected mass-to-charge (m/z) signals should be included in the analysis and converted into peptide sequences. This involves separating noise from true peptide signals and subsequently assigning sequences to these signals. A critical step is determining the threshold for identifying peptide-related signals versus non-peptide noise. Setting a high noise threshold risks excluding low-intensity peptides, while a low threshold may include unrelated signals (Zhang et al., 2013). The confirmation of peptide identities requires analyzing fragmentation

spectrum, however there is no general consensus on the number of fragments required for reliable identification, leading to inconsistencies in literature reporting.

Despite the challenges, peptidomics offer potential for evaluating encapsulation effect and optimization. Beyond encapsulation verification, advanced analytical techniques such as reversed-phase HPLC (RP-HPLC) and matrix-assisted laser desorption/ionization time-of-flight mass spectrometry (MALDI-TOF MS) have already been employed as well to monitor bioactivity retention during food processing. For instance, this methodology has been used to track peptides with antimicrobial and antihypertensive activities in the presence of yogurt starter cultures, facilitating insights into how bioactive peptides interact with food components (Paul & Somkuti, 2009).

Up to date and, to apply this approach to encapsulation and digestion studies, research has been focused on a limited set of longer peptides to confirm the success of the encapsulation process. This approach minimizes the risk of potentially generating the same sequences during gastrointestinal digestion, ensuring the verification of peptide integrity (Alvarado et al., 2019; Jiménez-Munoz et al., 2024). Moreover, other studies have simplified the analytical process by directly encapsulating synthetic peptides. This creates a less complex matrix for analysis, making it easier to confirm encapsulation success and evaluate peptide stability (Atma et al., 2024).

2. OBJECTIVES

The objective of this Ph.D. Thesis was to investigate the production process of dipeptidyl peptidase IV (DPP-IV) inhibitory peptides and their stabilization during gastrointestinal digestion by encapsulation. Both thermal encapsulation techniques, such as monoaxial and coaxial spray-drying, and electrohydrodynamic techniques, such as electrospraying, were evaluated. To this end, the research carried out was divided into the following specific goals:

1. To study the processing conditions for potential targeted production of DPP-IV inhibitory peptides. To determine, using *in silico* tools, the most bioactive sequences, their susceptibility to degradation during the digestive process, and their presence in alternative sustainable protein sources (**Chapter I and Chapter II**).

2. To investigate the production of hydrolysates containing the identified DPP-IV inhibitory peptides through enzymatic hydrolysis of sustainable proteins. To assess their inhibitory activity through *in vitro* and *ex vivo* assays and the effect of the digestive process (**Chapter III**).

3. To study the state of the art of bioactive peptides stabilization using spray-drying and electrospraying techniques in mono- and co-axial configurations (**Chapter IV**).

4. To optimize the formulation and evaluate the processing variables of the encapsulation processes, investigating their effect on the physicochemical properties and DPP-IV inhibitory activity of the hydrolysates:

    4.1. Encapsulation by electrospraying and spray-drying in monoaxial configuration (**Chapter V**).

    4.2. Encapsulation by spray-drying in coaxial configuration (**Chapter VI**)

5. To investigate the effect of the encapsulation process on the stabilization of DPP-IV inhibitory protein hydrolysates during gastrointestinal digestion (**Chapter VII**)

3. MATERIALS & METHODS

In this section, the main materials and the methodology used to produce and stabilize the protein hydrolysates rich in antidiabetic peptides are briefly described.

For further details, please refer to the respective Chapters as specified in the text and Table 2.

3.1. Materials

In this Ph.D. Thesis, two different protein sources have been studied to produce hydrolysates rich in DPP-IV inhibitory peptides. These sources were selected based on their sustainability: mealworm, *Tenebrio molitor,* defatted meal (68.01 ± 0.76% protein) was selected as a novel and sustainable protein source, and olive (*Olea europaea)* seed meal (23.28 ± 0.11% protein) as a revalorized by-product from the agri-food industry. Both meals were kindly donated by Tebrio (Salamanca, Spain) and Q'omer (Valencia, Spain), respectively. To maintain quality, these meals were stored at -20 °C until use.

The hydrolysis experiments were carried out using the proteolytic enzymes Alcalase 2.4L (subtilisin, EC 3.4.21.62), PTN 6.0S (trypsin, EC 3.4.21.4) and Flavourzyme 1000L (endo- and exopeptidase mix, EC 3.4.11.1), all provided by Novozymes (Bagsvaerd, Denmark). Synthetic peptides with a purity >95% were purchased from pepMic Co., Ltd (Jiangsu, China). Enzymes and substrates for the DPP-IV inhibitory activity assays, as well as the reagents for the gastrointestinal digestion assays, were purchased from Sigma-Aldrich (St Louis, US).

The encapsulation studies involved the use of whey protein hydrolysate (84 % protein) as model protein for the optimization of the formulation, provided by Abbott Laboratories S.A (Granada, Spain). Arabic gum, used as an encapsulating agent, was kindly donated by Nexira (Serqueux, France). Pullulan was used as thickening agent to increase the viscoelasticity of the solutions, supplied by Hayashibara Co., Ltd. (Okayama, Japan; molecular weight = 200kDa). Alginic acid sodium salt, used as an encapsulating agent, Tween 20, used as a surfactant, and 5(6)- carboxyfluorescein, a marker for confocal microscopy, were purchased from Sigma Aldrich (Darmstadt, Germany).

3.2. Methodology

Table 2 shows the main methodology employed throughout this thesis. The basic principles of the main methodology used in the Ph.D. Thesis are described next.

Table 2. Methodology used in the Ph.D. Thesis.

Analysis	Description	Chapter
Protein Content	Quantified using the Dumas method	III, V VI, VII
Enzymatic Hydrolysis	Enzymatic hydrolysis of *Tenebrio molitor* and *Olea europaea* seed meals performed in an automatic titrator 718 Stat Titrino using the pH-stat-method	III, V, VI
Meal solubilization	Gravimetric assay	V
DPP-IV Enzyme Inhibitory Activity	DPP-IV inhibition measured through the enzymatic degradation of Gly-Pro-p-nitroanilide, assessed spectrophotometrically	II, III, V, VI, VII
In Vitro Digestion	Simulated protein digestion conducted according to the INFOGEST protocol	III, VII
Amino Acid Composition	Analyzed using strong cation exchange chromatography	III
Molecular Weight Distribution	Determined by size-exclusion chromatography (SEC) using fast protein liquid chromatography (FPLC)	III, VII
Antidiabetic Analysis on Mouse Jejunum Organoids	Mouse jejunum organoids were cultured, dissociated, and seeded to generate intestinal epithelial monolayers. Followed by RNA extraction and RT-qPCR analysis to quantify target gene expression using normalization with reference genes	III
Electrospraying Encapsulation	Monoaxial encapsulation using a SpinBox Electrospinning equipment	V
Spray-Drying Encapsulation	Monoaxial encapsulation conducted using a Büchi B-190 spray-drier with a 2-fluids nozzle	V, VII
	Coaxial encapsulation conducted using a Büchi B-190 spray-drier with a 3-fluids nozzle	VI, VII
Capsule Microstructure	Capsule morphology analyzed through scanning electron microscopy (SEM), and particle size distribution calculated using ImageJ software	V, VI, VII
	Microstructure of the coaxial spray-dried capsules determined by confocal microscopy	VI, VII
Surface Nitrogen Determination	Capsule surface composition by X-ray photoelectron spectroscopy (XPS)	V, VI, VII
Proteomic Analysis	Samples purified and analyzed using an EASY-nLC system coupled with a Q Exactive HF mass spectrometer	VII
In Silico Analysis	Characterization of the peptide sequences properties using PepCalc	I
	Probability of peptides acting as DPP-IV inhibitors predicted using iDPPIV-SCM and StackDPP-IV	I, VII
	Susceptibility of peptides to gastrointestinal digestion assessed using PeptideCutter	I, II
	Alignment analysis with the proteome conducted to identify proteins containing the selected peptides, using the Basic Local Alignment Search Tool (BLASTp)	I, II
	Bioavailability predictions of peptides using ADMETLab3.0	II

3.2.1. Protein content determination

The protein content in the meals, hydrolysates, subsequent digests, and encapsulated products were determined through elemental analysis. A Flash 2000 CHNS/O elemental analyzer (Thermo Scientific, MA, USA) was utilized to quantify the nitrogen content of the samples. Initially, the samples were carefully weighed and loaded into small containers, then introduced into a combustion reactor where complete combustion occurred. The resulting gases were transported via a helium flow to a copper layer for further processing. The gases subsequently passed through a gas chromatography column (GC), facilitating the separation of the combustion products. Finally, a thermal conductivity detector identified the combustion products (CO_2, H_2O, N_2, and SO_2) by detecting an electrical signal proportional to the concentration of each element (C, H, N, and S) (Liliana Krotz et al., n.d.). The protein content of the samples was then calculated using nitrogen-to-protein conversion factors. A conversion factor of 5.6 was applied for the samples containing *T. molitor* (Janssen et al., 2017), while a factor of 5.3 was used for the samples containing *O. europaea* seed meal (Maestri et al., 2019b).

3.2.2. Enzymatic hydrolysis and degree of hydrolysis

Enzymatic hydrolysis of *Tenebrio molitor* and *Olea europaea* meals was performed in a 250 mL jacketed reactor equipped with magnetic stirring for homogenous mixing. Temperature control was achieved by circulating water from a thermostatic bath, and pH adjustments were performed automatically using a Metrohm titrator (Metrohm AG, Herisau, Switzerland) (Figure 7).

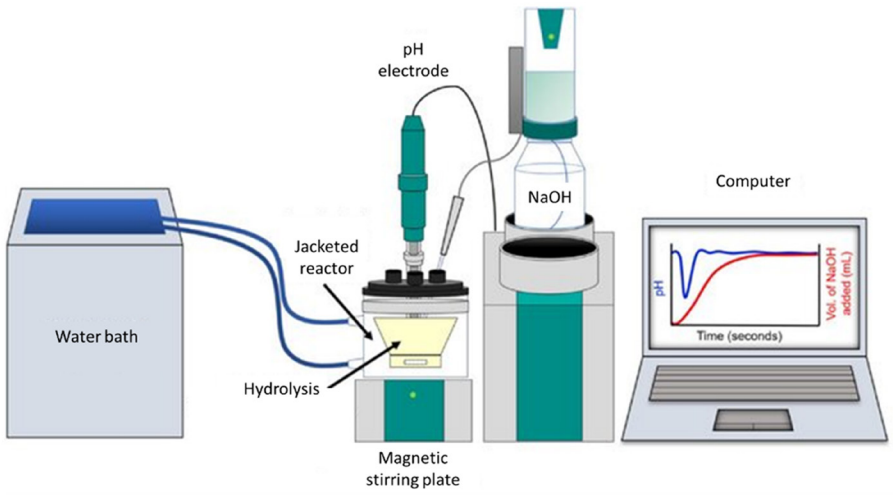

Figure 7. Schematic diagram of the pH-stat apparatus for enzymatic hydrolysis. Modified from (Pham et al., 2021).

The meals were solubilized in distilled water, with protein concentrations of 50 g/L for *T. molitor* and 30 g/L for *O. europaea* seed meal. Hydrolysis was conducted at 50 °C and an initial pH of 8.0. The pH was maintained using 1 M NaOH, and the enzymes Alcalase 2.4L (subtilisine, EC 3.4.21.62), PTN 6.0S (trypsin, EC 3.4.21.4), and Flavourzyme 1000L(endo- and exopeptidase mix, EC 3.4.11.1) were added at varying enzyme-to-substrate (E/S) ratios to achieve the desired degrees of hydrolysis (DH). The DH, defined as the percentage of peptide bonds cleaved relative to the total bonds present in the substrate, was determined using the pH-Stat method. This approach allows to monitor in real-time the DH through the correlation between the volume of base (1 M NaOH) added to maintain the pH constant and the number of peptide bonds hydrolyzed. The DH can be calculated as defined in the equation (Adler-Nissen, 1986): $DH = \frac{V_b \cdot N_b}{\alpha \cdot m_p \cdot H_{tot}} \cdot 100$

Where V_b represents the volume of NaOH consumed, and its normality is N_b. The average degree of dissociation of the α-NH_2 amino groups released during hydrolysis is represented by α, calculated using the equilibrium constant p_K (temperature-dependent). Additionally, m_p represents the mass of protein in the substrate, and H_{tot} is the total milliequivalents of peptide bonds per gram of protein. Further details on the protein solutions and the operating conditions can be found in Chapters III, V and VI.

3.2.3. Meal solubilization

The solubilization of the meals employed in water after the enzymatic treatment was calculated according to: $$Solubilization\left(\%\right) = \left(1 - \frac{M_g}{M_0}\right) \cdot 100$$

Where MR (g) represents the mass of dried solids retained on the filter paper, and M0 (g) is the mass of the meal dissolved in water at the beginning of the hydrolysis.

3.2.4. Molecular weight distribution

The molecular size distribution of the hydrolysate samples was determined using size exclusion chromatography (SEC) on an ÄKTA Purifier 10 fast protein liquid chromatography (FPLC) system equipped with a Superdex Peptide 10/300 GL size-exclusion column (GE Healthcare, Uppsala, Sweden). This technique separates and purifies biomolecules such as peptides and proteins based on their size, making it particularly useful for analyzing complex hydrolysates, which typically contain a wide range of peptide and protein fragments (Sheehan & O'Sullivan, 2004). Milli-Q water was used as the mobile phase, with a flow rate of either 0.5 mL/min or 0.8 mL/min. The absorbance of the eluted samples was measured at 280 nm. To calibrate the system, a standard curve was constructed using molecular weight markers prepared in Milli-Q water (Figure 8): L-tyrosine (0.22 kDa), Vitamin B12 (1.36 kDa), Insulin (5.73 kDa) and Aprotinin (6.51 kDa).

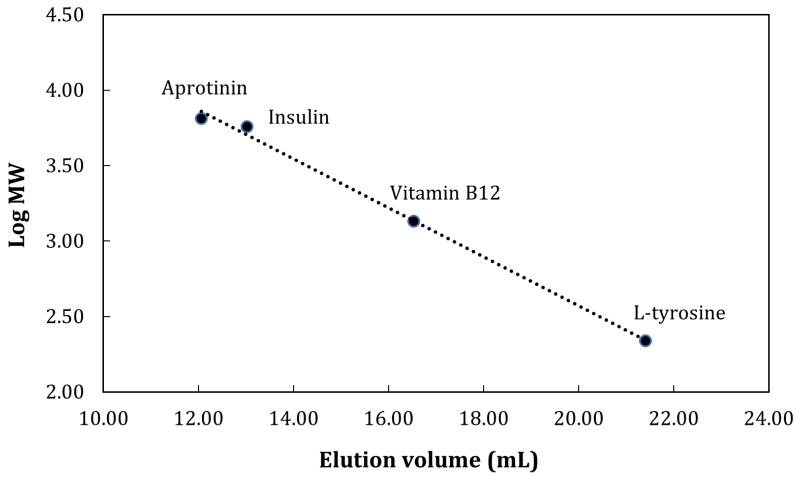

Figure 8. Standard curve employed for size exclussion chromatography (SEC).

3.2.5. DPP-IV inhibitory activity assay

The dipeptidyl peptidase IV (DPP-IV) inhibitory activity of the samples was evaluated using a spectrophotometrically assay adapted from the method derived of (Lacroix & Li-Chan, 2012). This assay quantifies the enzymatic activity of the DPP-IV enzyme by measuring its ability to cleave Gly-Pro-p-nitroanilide (GPPN), a chromogenic substrate (Figure 9). The cleavage of GPPN releases p-nitroaniline, which is detected colorimetrically at 405 nm. The presence of an inhibitor (sample) in the reaction mixture reduces the release of p-nitroaniline by interfering with the DPP-IV activity. By comparing the colorimetric changes in the reactions, conducted at the conditions described in Chapters II, III, V, VI, VII, with and without the inhibitor, over the 2-hour assay, the percentage of inhibition can be calculated at different sample concentrations. To ensure accuracy, all measurements were performed in triplicate and included color control, to correct any intrinsic color of the samples.

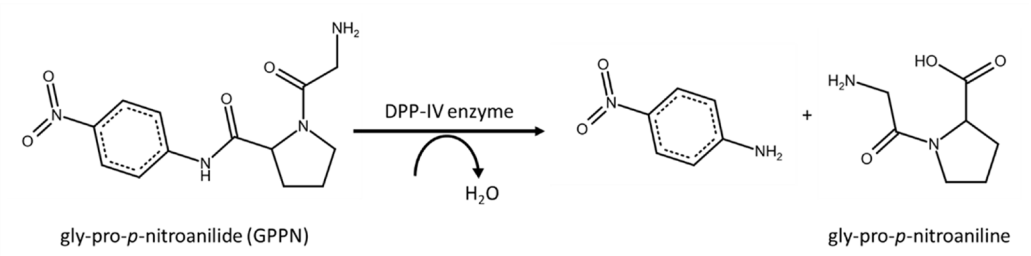

Figure 9. Scheme of the operation of the spectrophotometric analysis for the detection of the inhibitory activity of DDP-IV

3.2.6. *In vitro* digestion (INFOGEST)

The *in vitro* digestion of the samples was carried out following the INFOGEST Protocol (Brodkorb et al., 2019), a standardized method designed to unify the different digestion procedures already being used by the scientific community and improve the comparability of the research. The enzyme activities and bile concentration were measured prior to the digestion experiment per the assays described in the harmonized protocol (Brodkorb et al., 2019). All assays were carried out in duplicate/triplicate in a temperature-controlled shaker (Heidolph, Germany) at 37°C with 250 rpm shaking. Inactivation of the enzymes was performed by heating the mixture at 85 ^{0}C for 15 min (Gallo et al., 2022). Further details on the conditions can be found in Chapters III and VII.

3.2.7. Electrospraying encapsulation

For the encapsulation of the *T. molitor* hydrolysate, Arabic gum and pullulan were used as encapsulating agents and Tween 20 was employed as surfactant. All these compounds were dissolved in distilled water and stirred overnight at room temperature to ensure complete homogenization of the feed solution. The electrospraying system consisted of a drying chamber equipped with a high-voltage power supply (up to 30 kV), a syringe pump, and a grounded stainless steel collector plate (15 × 15 cm, stainless steel) (SpinBox Electrospinning; Bioinicia, Valencia, Spain). A syringe containing the feed solution was mounted on the syringe pump, and 16G needles (Proto Advantage, Hamilton, ON, Canada) were used. Different emitters were employed based on the application. Further details on the technique and the specific operating conditions can be found in Chapters IV and V, respectively.

3.2.8. Spray-drying encapsulation

Spray-drying was performed using a Büchi B-190 spray-drier (Büchi Labortechnik, Flawill, Switzerland) and Arabic gum served as the primary encapsulating agent. Further details on the technique can be found in Chapter IV. In this Ph.D. Thesis two different nozzles were employed: a 2-fluid nozzle (monoaxial) and a 3-fluid nozzle (coaxial) (Figure 10). For monoaxial spray-drying various formulations were tested to evaluate the effects of additional additives, as detailed in Chapters V and VII. Coaxial spray-drying was used to produce encapsulates with core-shell structure, where the hydrolysate is encapsulated in the core, potentially increasing its stability. This process employed a 3-fluid nozzle (Büchi, Flawill, Switzerland) with core and shell tip diameters of 0.7 mm and 2.0 mm, respectively. The process conditions were optimized for key parameters, including yield, protein content, protein migration, and DPP-IV inhibitory activity. These parameters and the final optimized formulations are further discussed in Chapters VI-VII.

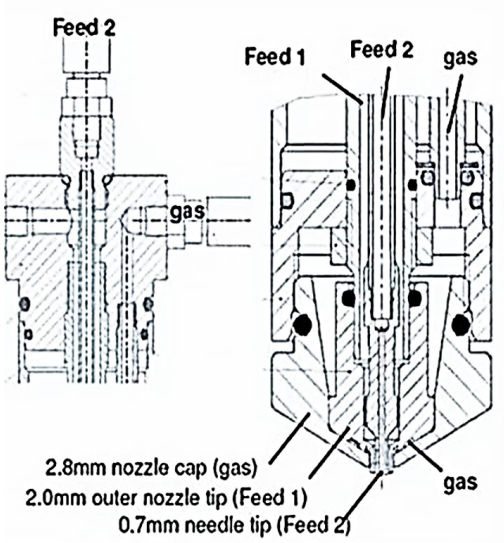

Figure 10. Scheme of the three fluids nozzle employed for coaxial spray-drying encapsulation (Büchi Labortechnik).

3.2.9. Peptidomics analysis and data processing

Quantitative proteomics was performed by liquid chromatography with tandem mass spectrometry (LC-MS-MS), a powerful analytical technique that combines the separation ability of liquid chromatography (LC) with selective mass analysis by mass spectrometry (MS). Samples analyses were performed at the Department of Chemistry and Bioscience, Aalborg University.

Samples were solubilized in ammonium bicarbonate buffer (50 mM), reduced with Tris(2-carboxyethyl) phosphine (2.5 µg/ µL) 1:25 (w/w) during 30 min at 37 °C, and alkylated with iodoacetamide (2.5 µg/ µL) 1:10 (w/w) during 20 min at 37 °C in the dark. Purification was carried out with in-house prepared C-18 StageTips, followed by drying and resuspension in buffer of 2% acetonitrile (ACN) with 0.1% formic acid (FA) for subsequent analysis. Peptide concentrations were determined by employing UV spectroscopy (DS-11 FX, DeNovix, Wilmington, USA) at standard settings (1 Abs = 1 mg/mL) and diluted accordingly.

Samples were loaded onto a 96-well microplate (Thermo Fisher Scientific, Waltham, Massachusetts, USA), using the 2%ACN 0.1%FA buffer as a blank. The microplate was sealed and loaded into an EASY-nLC 1200 system (Thermo Fisher Scientific, Waltham, MA, USA) with ESI coupled to a Q Exactive HF Orbitrap mass spectrometer (Thermo Fisher Scientific, Waltham, MA, USA). Peptides were first retained on a PepMap precolumn (C18, 100 Å, 100 µm x 2 cm), followed by a Pepmap analytical Column (C18, 100 Å, 74 µm x 50 cm). Separation was performed over a 90 min gradient using mobile phase A (MPA, water) and mobile phase B (MPB, 95% acetonitrile). The elution profile consisted of an initial increase from 0 to 10%

MPB over 5 min, followed by a linear gradient to 40% MPB over 59 min, a further increase to 50% MPB within 5 min, and a final wash at 100% MPB for 15 min.

The analysis was performed in a full MS/ddMS2 data-dependent mode, with an MS1 scan range of 75–1125 m/z, positive polarity, and a default charge state of +2. The MS1 and dd-MS2 resolutions were set to 60,000 and 15,000, respectively. The ddMS2 was operated in Top20 mode, with an AGC target of 1e5 and a Maximum Injection Time (IT) of 45 ms. The isolation window, (N)CE, and dynamic exclusion window were configured to 1.2 m/z, 28 eV, and 20.0 s, respectively. Peptide match was preferred, and "exclude isotopes" was enabled.

Raw data was processed using the MaxQuant v.2.2.0.0 software (Tyanova et al., 2016), employing the built-in Andromeda search engine (Cox et al., 2011). The protein databases were obtained from UniProt (Consortium et al., 2025), including *Tenebrio molitor* (Taxon ID 7067) with 15,916 entries and *Olea europaea* (Taxon ID 4146) with 79,666 entries (downloaded October 4th, 2024). Due to the diversity of produced hydrolysates, data was analysed as unspecific *in silico* digest as previously described (Gregersen Echers et al., 2023), but with minor modifications. Briefly, peptide length range was set to 3-30 amino acids. False discovery rate (FDR) was defined as 100% on both protein and peptide level to allow as high initial data throughput as possible using reverted sequences and minimum peptide score defined as zero. All quality-based data filtering was performed downstream. Common contaminants were included and match between runs and dependent peptides (1% FDR) enabled. Carbamidomethylation of Cys was defined as a fixed modification while Met oxidation protein N-term alkylation were included as variable modifications.

Following removal of peptides from common contaminants and false positive, identified peptides were filtered based on quality criteria. The Andromeda score, a metric of spectral match quality within the MaxQuant search engine, was employed to refine the identification of peptides. This score assesses the concordance between experimental and theoretical peptide fragmentation spectra, with higher scores denoting greater reliability (Cox et al., 2011). To ensure robustness, only peptide sequences exhibiting an Andromeda score of at least 40 were retained. While an alternative threshold of posterior error probability (PEP) < 0.1 was also tested, the resulting peptide distribution did not resemble the unfiltered distribution of the sequences. Additionally, reproducibility filter was included, requiring at least two out of three replicates to exhibit intensity values over zero, assuring this way that potential false-positive and low confidence identifications were removed.

3.2.10. *In silico* analysis

- Databases

The Universal Protein database UniProt (https://www.uniprot.org/) was used to retrieve protein sequences and IDs, and other searches of protein information (Consortium et al., 2025).

- Sequence management

Multiple sequence alignment was performed using the tool Basic Local Alignment Search Tool (BLASTp) (https://blast.ncbi.nlm.nih.gov/) by the National Institutes of Health (NIH) (Ye et al., 2006).

Simulated gastrointestinal digestion was assessed using the tool PeptideCutter (https://web.expasy.org/peptide_cutter/) by the Swiss Institute of Bioinformatics (SIB) (Duvaud et al., 2021). The cleavage enzymes selected were pepsin (pH: 1.3), chymotrypsin (low and high specificity) and trypsin, as recommended in the literature (Barati et al., 2020).

- Sequence analysis

The solubility and net charge of the peptide sequences were estimated using PepCalc (https://pepcalc.com/) by Innovagen AB. This tool calculates physicochemical properties based on amino acid composition and sequence-specific parameters (Lear & Cobb, 2016).

Potential DPP-IV inhibitory activity of peptide sequences reported in the literature was evaluated using iDPPIV-SCM (http://camt.pythonanywhere.com/iDPPIV-SCM) and StackDPPIV (https://stackdppiv.bb.ku.ac.th/) by Kasetsart University (Charoenkwan et al., 2022; Shoombuatong et al., 2020). Other potential bioactivities were evaluated employing the BIOPEP-UWM™ database (www.uwm.edu.pl/biochemia, Minkiewicz et al., 2019)

The Simplified Molecular Input Line-Entry System (SMILES) of the peptides was obtained using PepSMI Novopro (https://www.novoprolabs.com/tools/). Bioavailability was predicted using ADMETLab3.0 (https://admetlab3.scbdd.com/), an advanced computational platform for absorption, distribution, metabolism, excretion, and toxicity (ADMET) analysis, which integrates a high-quality database of 0.37 million entries and a Directed Message Passing Neural Network framework (Fu et al., 2024). Pharmacokinetic parameters analyzed included Caco-2 permeability, Parallel Artificial Membrane Permeability Assay (PAMPA), P-glycoprotein substrate status (P-gp), Human Intestinal Absorption (HIA), Oral Bioavailability (F20, F30, F50), Plasma Protein Binding, and Blood-Brain Barrier Penetration (BBB).

4. RESULTS & DISCUSSION

4.1. Study of the processing conditions for the targeted production of DPP-IV Inhibitory peptides

4.1.1. Identification of bioactive sequences and their susceptibility to degradation during gastrointestinal digestion

Given the growing interest in natural alternatives for managing postprandial glucose regulation, the study of enzyme-inhibitory peptides has increased. Understanding the characteristics that provide bioactivity to these peptides is essential for their generation and application in therapeutic and functional food formulations.

In Chapter I of this PhD Thesis, an extensive literature review was conducted in order to identify inhibitory sequences for α-amylase, α-glucosidase, and DPP-IV, considering only those peptides with experimentally determined IC_{50}. This approach ensured the elaboration of a reliable database, filtering out sequences predicted solely though in silico methodology. A significant challenge when compiling this database was the lack of harmonization in the methodology employed across studies, leading to wide variations in the reported IC_{50} values for acarbose (used as standard), which ranged from 3.34 to 2338.9 μM. Therefore, this highlights the need for the development of standardized methods to measure *in vitro* inhibition of peptides.

Regarding α-amylase inhibitory peptides, only 18 peptide sequences were found in the literature, with 15 derived from plant proteins, highlighting a trend towards sustainable protein sources. The choice of proteases employed for their obtention played a significant role in peptide production, with Protamex (a broad-spectrum endoprotease with a preference for cleaving hydrophobic and aromatic residues (Ustunol, 2014)) being the most frequently used. Many of these peptides reported the presence of Leu in the last two positions of the N-terminus and exhibited high hydrophobic amino acid content (>40%), which contributed to their poor solubility in water. Since net charge at pH 7 influences peptide absorption via transcytosis (Amigo & Hernández-Ledesma, 2020), it was noteworthy that many peptides exhibited positive net charge, suggesting potential bioavailability. However, due to the limited number of sequences available in the literature, establishing a reliable structure-activity relationship was not feasible.

For α-glucosidase inhibitory peptides, 39 peptide sequences were found in the literature, equally derived from plant and animal proteins. Notably, 12 derived from insect proteins (i.e., *Tenebrio molitor* and *Schistocerca gregaria*) reinforcing the trend of utilizing novel, sustainable protein sources. Enzymatic hydrolysis with digestive proteases (e.g., pepsin, trypsin, chymotrypsin) was frequently employed, potentially enhancing peptide stability post-ingestion by reducing susceptibility to further degradation. Over 70% of these peptides contained at least 40% hydrophobic amino acids, yet key structural features previously reported in the literature

(González-Montoya et al., 2018) (mainly Ser, Thr, and Tyr) at the N-terminus or the presence of Pro, Ala or Met at the C-terminus, were rarely observed. Indeed, the most conserved feature was the Pro at the N-terminal, present in only 7 of the 39 peptides. Additionally, these peptides exhibited limited bioavailability, as indicated by their predominantly negative net charge at pH 7, suggesting the need for stabilization strategies to enhance absorption.

For both α-amylase and α-glucosidase inhibitors, peptide chain length (PCL) varied widely (3–23 amino acids for α-amylase and 2–16 for α-glucosidase), yet no correlation between PCL and bioactivity was observed, emphasizing the predominant role of peptide structure in functionality.

Regarding DPP-IV inhibitory peptides, 230 sequences were identified, highlighting the growing interest in the inhibition of this enzyme as a potential approach for regulating the glycemic index. The 40 most bioactive sequences were selected, with IC_{50} values between 0.51 and 69.84 μM. Unlike α-amylase and α-glucosidase inhibitors, DPP-IV inhibitory peptides predominantly were derived from traditional sources, such as fish (13 peptides), revealing a gap in research on novel, sustainable protein sources. Enzymatic hydrolysis was primarily conducted with Alcalase (a broad-spectrum endoprotease), either alone or combined with Flavourzyme (a mix of endo- and exo-proteases), as well as digestive enzymes. The identified peptides had PCLs of 3–13 amino acids, with 70% being under 6 residues long. Notably, all peptides contained over 50% hydrophobic amino acids, supporting previous findings that hydrophobic N-terminal residues interact with DPP-IV's active site inhibiting its function (Acquah et al., 2018). Moreover, 80% of these sequences presented Pro in the first two positions of the N-terminus, suggesting a strong structural preference for DPP-IV inhibition. However, their predominantly negative net charge at pH 7 indicated limited bioavailability. Comparison of IC_{50} values with two *in silico* DPP-IV inhibitory predictors (iDPPIV-SCM and StackDPPIV) demonstrated that StackDPPIV provided superior accuracy and interpretability. The model predicted 164 inhibitory sequences out of 230, compared to 154 identified by iDPPIV-SCM. These findings confirmed that while *in silico* predictors can offer preliminary qualitative insights, experimental validation remains essential.

Finally, the assessment *in silico* of gastrointestinal stability revealed that a significant proportion of identified sequences were prone to degradation: 15 out of 18 for α-amylase inhibitors, 27 out of 39 for α-glucosidase inhibitors, and 14 out of 40 for DPP-IV inhibitors. These estimations did not account for additional factors affecting peptide integrity, such as gastric pH fluctuations, further reinforcing the need for stabilization strategies. Notably, peptide degradation could either diminish or enhance bioactivity, necessitating further investigation into the digestive effects.

4.1.2. Identification of bioactive sequences in alternative sustainable sources

Given the promising potential DPP-IV inhibition for glycemic control and the better-characterized nature of DPP-IV inhibitory peptides, this PhD thesis focused on obtaining such peptides from novel, sustainable sources. In particular, *T. molitor* was selected due to its sustainability and recent approval for human consumption by the EFSA (Liguori et al., 2022).

In Chapter II, the 40 most bioactive DPP-IV inhibitory sequences identified in Chapter I were used as the parting point, and the 14 most susceptible to degradation during digestion were selected for further analysis in *T. molitor*. Using BLASTp homology alignment (J. Ye et al., 2006), three intact matches were identified: ILAP, FLQP, and APVAH. The limited number of matches was likely due to the incomplete characterization of the *T. molitor* proteome at the time of this study.

The bioaccessibility and bioavailability of these peptides were analyzed *in silico*. It was already determined in Chapter I that both ILAP and FLQP were degraded through gastrointestinal digestion, while APVAH was kept intact. Bioavailability assessment *in silico* (Fu et al., 2024) predicted low bioavailability for these peptides in CaCo-2 cell models, contradicting expectations for short peptide absorption. However, the PAMPA model (Sun et al., 2017) assays suggested high passive diffusion potential. Further pharmacokinetic assessments (i.e., Human Intestinal Absorption, Plasma Protein Binding and Estimated percentage of the compound bioavailable at 50% threshold after oral administration), indicated that ILAP had the highest potential, followed by APVAH and the digested IL fragment.

Once the potential pharmacokinetic properties for oral application were confirmed, we investigated the feasibility of obtaining these sequences through enzymatic targeted hydrolysis. Instead of conducting a comprehensive hydrolysis battery, which would be time-consuming and resource-intensive, the objective was to identify the locations of these sequences within the *T. molitor* proteome and optimize their release using specific proteases. This type of analysis had previously proven successful in obtaining longer sequences with emulsifying functionality (Gregersen Echers et al., 2023). However, when applied in this study, where the sequences were shorter and more specific, the results indicated that a simple release method would not be feasible for any of the sequences when using the commercially available proteases (e.g., Alcalase and trypsin). Consequently, it was determined that bioactive peptides would need to be obtained through the classical hydrolysis mechanism of trial-and-error.

Finally, the DPP-IV inhibitory activity of the identified sequences and their digested fractions were assessed *in vitro* by using synthetic peptides. This experimental validation confirmed a significant loss of activity after digestion, particularly for FLQP, with IC_{50} increasing from 0.13 mg/mL to 0.61 mg/mL for its FL fragment and complete loss of activity

for its QP fragment. In contrast, APVAH exhibited the highest bioactivity (IC_{50} = 0.013 mg/mL), functioning via a mixed competitive and noncompetitive mechanism. Additionally, APVAH remained intact during *in silico* digestion.

Altogether, this chapter tried to establish a novel workflow employing an in silico approach to optimize hydrolysis, aiming to minimize resources. However, findings emphasized that hydrolysis optimizations through traditional methods and *in vitro* assays using synthetic peptides remain indispensable for confirming peptide bioactivity and stability.

4.2. Investigation of enzymatic hydrolysis for producing DPP-IV inhibitory hydrolysates from sustainable sources: characterization and digestive stability

Based on the findings presented in Chapter II, it was determined as necessary to investigate the production of DPP-IV inhibitory hydrolysates through traditional enzymatic hydrolysis of trial-and-error. To this end, two alternative protein sources were selected: *T. molitor* and olive (*Olea europaea*) seed meal, the latter representing a plant-derived alternative obtained from the reutilization of agricultural waste generated in olive oil production.

In Chapter III, enzymatic hydrolysis experiments were performed to characterize and optimize the production of DPP-IV inhibitory hydrolysates. A total of 10 hydrolysates were generated for each substrate using Alcalase (EC 3.4.21.62.), Trypsin (EC 3.4.21.4.), and Flavourzyme, either individually or in combination (A, T, A+T, A+F, and A+T+F). Given that DPP-IV inhibitory peptides typically range from 3 to 13 amino acids in length, hydrolysis was conducted at degrees of hydrolysis (DH) of 10%, 15%, and 20%, aiming to obtain peptides with an average peptide chain length (PCL) of 5–10 amino acids.

The protein content of the raw materials was 68% for *T. molitor* and 23% for *O. europaea* seed meal. After hydrolysis, the protein content of the resulting hydrolysates remained relatively stable (66.9–69.6 % for *T. molitor* and 22.6–26.8 for *O. europaea* seed), indicating homogeneous solubilization of the proteins alongside other components. Protein solubilization ranged from 35–41% for *T. molitor* hydrolysates and 9–13% for olive seed, reflecting the inherent challenges of solubilizing plant-based proteins. These findings are consistent with previous literature, which reports that plant proteins are generally less soluble, limiting their industrial applications (Yu et al., 2021). Notably, Flavourzyme played a key role in enhancing protein solubility, an effect attributed to its exoprotease activity (Segura-Campos et al., 2012).

The inhibitory activity of all 20 hydrolysates was assessed *in vitro*, revealing a strong correlation between DH and bioactivity. Higher DH values consistently led to greater DPP-IV inhibition for the same enzymatic combination, an effect particularly pronounced in olive seed hydrolysates, which exhibited IC_{30} values ranging from 1.23 to 2.67 mg protein/mL. Due to the intense coloration of olive seed hydrolysates, IC_{30} was used instead of IC_{50}, as

high concentrations interfered with the colorimetric assay used for measuring bioactivity. Conversely, *T. molitor* hydrolysates displayed IC_{50} values in the range of 0.87 – 2.33 mg protein/mL. The selection of enzymatic treatments also significantly influenced bioactivity. Specifically, the combination of Alcalase and Flavourzyme at DH 20% yielded the highest inhibitory activity for both substrates. These results align with previous studies on *T. molitor* hydrolysates prepared under similar conditions (Dávalos Terán et al., 2020). The observed trends underscore the importance of optimizing hydrolysate production, particularly given the substantial impact of enzymes such as Flavourzyme, whose activity is difficult to replicate *in silico*.

To elucidate the structural features responsible for DPP-IV inhibitory activity, the amino acid composition of the hydrolysates was analyzed. The results confirmed homogeneous protein solubilization across all samples, with *T. molitor* and olive seed hydrolysates containing 50% and 45% hydrophobic amino acids, respectively, and moderate levels of aromatic amino acids (9% for *T. molitor* and 6% for olive seed). Notably, Pro content was higher in *T. molitor* hydrolysates (8%) than in olive seed (5%). As established in Chapter I, the presence of Pro at the first two positions of the N-terminus is strongly associated with potent DPP-IV inhibition, suggesting that the elevated Pro content in *T. molitor* hydrolysates may contribute to their superior bioactivity. The molecular weight distribution (MWD) of the hydrolysates was analyzed, revealing the effect of DH on the size of the peptides generated. For the *T. molitor* hydrolysates, higher DH generally produced smaller peptides (1.0–0.2 kDa). Additionally, the choice of enzymes also was influential, with trypsin hydrolysates resulting in larger peptides, likely due to the high specificity of the enzyme, which limited its activity.

Further characterization was obtained via LC-MS/MS analysis of the most bioactive hydrolysates for each substrate: HTAF20 (*T. molitor* hydrolysate) and HOAF20 (olive seed hydrolysate), both produced using Alcalase and Flavourzyme at DH 20%. Peptidomics analysis identified 7,565 sequences in HTAF20 and 1,119 sequences in HOAF20. The disparity in sequence identification is likely due to the lower protein content of olive seed hydrolysates, which contain a higher proportion of non-proteinaceous compounds that may interfere with mass spectrometry analysis (Portmann et al., 2023). Importantly, over 90% of the identified peptides had a PCL below 13 amino acids, aligning with known bioactive peptide characteristics. Using StackDPPIV, approximately 60% of HTAF20 and 50% of HOAF20 sequences were classified as bioactive. These findings were consistent with the *in vitro* assays, which reported greater inhibitory activity for HTAF20 (IC_{50} = 0.87 mg protein/mL) compared to HOAF20 (IC_{30} = 1.23 mg protein/mL). Additionally, the identified peptides ranged between 0.36 and 0.6 kDa, a size range reportedly associated with high bioactivity in *T. molitor* hydrolysates (Rivero-Pino et al., 2021). Key features were investigated according to the characteristics determined in Chapter I. Particularly, the presence of Pro in the N-terminus was found to be highly conserved, appearing in 34% of the HTAF20 sequences

and 16% of the HOAF20 sequences. Additionally, the presence of aromatic amino acids in the C-terminus was also studied, revealing that approximately 15% of the identified sequences exhibited this characteristic. Finally, we sought to confirm whether the sequences identified in Chapter I and studied in Chapter II had been released during hydrolysis, finding 9 of the peptides described in the literature (LPY, VPW, VPF, ELPF, LPVYD, LPQ, LPR, LPLF, LPY) and 2 additional peptides (MPF and LPLPL) documented in the BIOPEP database, all ranging from 3 to 5 amino acids in length. Specifically, the APVAH peptide characterized in Chapter II was identified.

A key objective of this PhD Thesis was the study of the stability of the obtained hydrolysates under simulated gastrointestinal digestion, which was evaluated following the INFOGEST protocol (Brodkorb et al., 2019). Analysis of the MWD after digestion resulted in a significant degradation of peptides, evidenced by the breakdown of larger fractions into smaller ones, which can be attributed to the high content of hydrophobic amino acids, known to be cleaved by pepsin (H. Ye et al., 2022). Furthermore, the lack of substantial differences in degradation profiles, regardless of trypsin use, suggests that gastric pepsin digestion played a primary role in hydrolysate degradation. It is worth highlighting that MWD analysis revealed a shift from larger peptides (1–2.5 kDa) to smaller fragments (0.5–1 kDa and 0.2–0.5 kDa). To assess the impact of digestion on inhibitory potential, post-digestion hydrolysates were tested for DPP-IV-inhibitory activity. A significant loss of bioactivity was observed, with IC_{50} values ranging from 0.73 to 1.45 mg protein/mL for *T. molitor* digests and IC_{30} values between 1.71 and 2.14 mg protein/mL for olive seed digests. The most substantial reduction in activity was detected in HTAF20 and HOAF20, which increased their IC_{50} and IC_{30} values in 58.0 and 50.4 %, respectively.

Finally, the bioactivity of HTAF20 and HOAF20 was evaluated *ex vivo* in mouse jejunum organoids, assessing the expression of genes involved in carbohydrate metabolism, including *Pyy* and *Glp1* (Aquino et al., 2024). Although HTAF20 exhibited higher *in vitro* DPP-IV inhibition, HOAF20 demonstrated additional functional effects by promoting the expression of the incretin GLP-1 and peptide YY (PYY), which are linked to beta-cell regeneration in diabetes mellitus type 2 (Lafferty et al., 2024).

Overall, these findings underscore the necessity of developing strategies to stabilize and protect highly bioactive hydrolysates to ensure their effective application as nutraceuticals or functional food ingredients.

4.3. Study of the state of the art in bioactive peptides stabilization using spray drying and electrospraying techniques

To address the limitations identified in this study, stabilization methods are necessary to enhance physicochemical stability and bioaccessibility of the hydrolysates. Therefore, encapsulation technologies were investigated, with a focus on spray-drying and electrospraying due to their ability to encapsulate thermosensitive compounds and their potential for large-scale application (Jacobsen et al., 2018; Rahmani-Manglano et al., 2022). Both monoaxial and coaxial (only in spray-drying) configurations were studied to determine their feasibility for protein encapsulation. Chapter IV reviewed existing literature on the use of spray-drying and electrospraying for encapsulation of protein-based compounds, evaluating both formulation and processing parameters.

The first step in optimizing monoaxial spray-drying was the formulation of the feed solution, with the choice of encapsulating agent being a critical factor. While proteins can serve as encapsulating agents (Wang et al., 2015), their similarity to the target compounds can hinder stability and bioactivity detection. Consequently, polysaccharides are preferred, with maltodextrin identified as the most frequently used carrier in 19 out of 31 studies. Although it effectively retains bioactivity, maltodextrin poses limitations in antidiabetic applications due to glucose release upon digestion (Hofman et al., 2015). Hence, alternative polysaccharides such as Arabic gum (used in five studies) and chitosan (used in four studies) were proposed as superior options for encapsulating antidiabetic peptides. The addition of surfactants, such as Tween 20 and Tween 80, was also explored in the literature, as these agents mitigate the migration of peptides to the air-water interface during drying (Sarabandi & Jafari, 2020). The carrier-to-protein ratio markedly influenced encapsulation efficiency, with higher ratios improving yield and encapsulation efficiency (Akbarbaglu et al., 2019). Nonetheless, excessive carrier content reduces bioactivity due to a lower protein load.

Since spray-drying relies on atomization and subsequent drying with heated gas, key processing parameters included inlet and outlet temperature, feed flow rate, and drying gas flow rate. The inlet temperature, ranging from 60–200 °C, was found to be a determining factor in drying kinetics. However, temperatures below 100 °C were only feasible with low-boiling-point solvents (Zhu et al., 2015). It was reported that higher temperature values reduced moisture content and increased particle size, these being crucial factors in food formulations, where capsules under 5 μm with tight size distributions are preferred due to improved stability (Piñón-Balderrama et al., 2020). Feed flow rate influenced particle size, with higher rates producing larger particles and increasing wall deposition, though they also improved yield (De Koker et al., 2014). Thus, a balance was considered with flow rates of 300–500 mL/h in lab equipment. Drying air flow rates, rarely reported in the literature, varied between 34–38,000 L/h, with optimal values identified between 350–500 L/h in lab equipment.

Limited research was available on coaxial spray-drying, with only one relevant study identified, which evaluated the encapsulation of lysozyme with trehalose as encapsulating agent in the core and PLGA in the shell (Wan et al., 2014). The use of dual feeds (core and shell) might result in core-shell microcapsules with enhanced stability and protection but also introduces process complexity. Thus, the encapsulation by coaxial systems require optimization to ensure proper coating while avoiding excessive condensation within the drying chamber.

Electrospraying was also examined as an alternative encapsulation technique, with studies related to protein-based bioactives focusing primarily on pharmaceutical applications. In monoaxial electrospraying, maltodextrin was again a widely used carrier, followed by poly(lactic-co-glycolic acid) (PLGA) and alginate, both of which exhibit high bioavailability, making them suitable for oral delivery systems. Since electrospraying applies high voltage to atomize and dry at room temperature, key parameters included voltage and feed flow rate. Reported voltage values ranged from 2–20 kV, with higher voltage producing smaller particles (Musaei et al., 2017). Nonetheless, voltages exceeding 20 kV risked altering protein structure, suggesting an optimal range close to 20 kV (Onyekuru et al., 2021). Regarding feed flow rates, they were typically between 0.1 and 1 mL/h, with higher flow rate increasing particle size and resulting in reduced encapsulation efficiency (Onyekuru et al., 2021).

In coaxial electrospraying, PLGA was the predominant encapsulating agent. However, unlike spray-drying studies, no reports utilized carriers in the core feed, only in the shell feed. Furthermore, most studies were pharmacologically oriented, employing solvents like dimethylformamide (DMF), which pose potential safety concerns for food applications (Hu et al., 2020). The voltage range used in coaxial electrospraying (5–22.5 kV) was similar to monoaxial studies, favoring voltages below 20 kV (Onyekuru et al., 2021). Optimization of feed flow rates was particularly crucial, with core flow rates ranging from 0.02–3.6 mL/h, while shell flow rates varied from 0.5–18 mL/h. The shell-to-core feed ratio was typically between 4:1 and 40:1. Notably, coaxial electrospraying improved encapsulation efficiency for bovine serum albumin (BSA) with PLGA compared to monoaxial approaches (Zamani et al., 2014). In any case, it should be noted that electrospraying operates at significantly lower flow rates compared to spray-drying, resulting in much lower productivity. This limitation is particularly evident in laboratory-scale equipment commonly used in the studies presented in the literature.

The bioaccessibility of encapsulated hydrolysates was assessed based on available studies. Although all reports indicated some degree of bioactivity loss after gastrointestinal digestion, encapsulation consistently enhanced stability compared to the digestion of the free protein or hydrolysate. For instance, P. lunatus hydrolysate encapsulated by spray-drying with maltodextrin and Arabic gum showed a significant retention of bioactivity (i.e., ACE, DPP-IV, and α-amylase inhibition) after simulated digestion (IC_{50} < 200 μg/mL) compared to the free hydrolysates (IC_{50}

≈ 300 μg/mL) (Cian et al., 2019). Similarly, food matrix studies demonstrated increased stability (Gómez-Mascaraque et al., 2016) and improved sensory acceptability when encapsulation of Pink Perch hydrolysates with maltodextrin and Arabic gum was carried out (Murthy et al., 2017).

Table 3 summarizes the gaps found in the literature on the encapsulation of bioactive peptides/hydrolysates by spray-drying and electrospraying technologies.

Table 3. Gaps in the literature on the encapsulation of bioactive peptides/hydrolyates and contributions provided by this PhD Thesis.

Identified research gaps	Contributions of this PhD Thesis
Monoaxial Electrospraying	
No studies on the encapsulation of food protein hydrolysates. No studies on antidiabetic peptides or hydrolysates	Encapsulation of insect protein hydrolysates (*Tenebrio molitor*) with DPP-IV inhibitory activity Optimization of the formulation using Arabic gum and pullulan as encapsulating agents, and Tween 20 as a surfactant.
Monoaxial spray-drying	
No studies on the impact of pullulan and Tween 20, in combination with Arabic gum, in the encapsulation of protein hydrolysates	Evaluation of the influence of these additives on the encapsulation of *T. molitor* and *O. europaea* hydrolysates, their bioactivity and gastrointestinal stability
No systematic research on the retention of bioactive peptide sequences after gastrointestinal digestion	Investigation of the effect of the formulation in the gastrointestinal resistance of encapsulated *T. molitor* and *O. europaea* protein hydrolysates
Coaxial spray-drying	
No studies on the encapsulation of protein hydrolysates by coaxial spray-drying	Optimization of the formulation for coaxial encapsulation of *T. molitor* and *O. europaea* protein hydrolysate, employing Arabic gum as encapsulating agent in the core and the shell. Influence of the incorporation of alginate in the shell.
The effect of coaxial encapsulation on bioactive peptide retention after digestion has not been systematically studied.	Evaluation of the influence of the formulation on the gastrointestinal resistance of encapsulated *T. molitor* and *O. europaea* protein hydrolysates
No comparative studies on monoaxial vs. coaxial encapsulation of protein-based compounds.	Evaluation n of the differences in the encapsulation of *T. molitor* y *O. europaea* hydrolysates, their bioactivity and gastrointestinal stability

4.4. Optimization and evaluation of encapsulation processes for the stabilization of protein hydrolysates with DPP-IV inhibitory activity

4.4.1. Monoaxial electrospraying and spray-drying

Based on the findings in Chapter IV, the encapsulation of a *T. molitor* hydrolysate with previously demonstrated DPP-IV inhibitory activity was selected for further study. This hydrolysate was obtained through Alcalase hydrolysis at DH 20%. Based on the knowledge gained from Chapter IV and the specific requirement for antidiabetic encapsulates, Arabic gum was selected as the encapsulating agent. This choice was driven by its ability to maintain stability without breaking down into glucose and its reported capacity to lower glucose levels by inhibiting intestinal glucose absorption (Bock et al., 2012).

The optimization of monoaxial electrospraying was carried out by selecting the minimum feed flow rate provided by the lab equipment used (0.2 mL/h) and a voltage of 22 kV, as this voltage provided the most stable Taylor cone among the tested range (15–23 kV; data not shown). The concentration of Arabic gum was maintained at 15% in water as solvent, similar to other reported values for other encapsulation agents such as glucose syrup or dextran (García-Moreno et al., 2018). However, this formulation exhibited low viscoelasticity, necessitating the addition of pullulan (0.5–1%). Tween 20 (1%) was also added to reduce surface tension, enhancing the electrospraying process. Morphological analysis revealed that pullulan concentrations exceeding 1% resulted in fiber formation, whereas concentrations below 1% led to significantly lower productivity and decreased stability during electrospraying. This instability was evidenced by an elongated and unstable Taylor cone. Thus, the final formulation selected for the encapsulation of *T. molitor* hydrolysate by electrospraying was 15 wt.% Arabic gum, 1 wt.% Tween 20, and 1 wt.% pullulan. Hydrolysate was included so that the concentration of protein was kept at 20 % in the final capsules.

To compare encapsulation techniques, the same formulation was spray-dried, along with a control solution without Tween 20 and pullulan, as these additives are generally unnecessary for effective spray-drying and, for instance Tween 20 has potential negative connotations in food applications (Consumer Perceptions Unwrapped: Ultra-Processed Foods (UPF), 2024).

Scanning electron microscopy (SEM) revealed that all three treatments produced spherical capsules without agglomerations, displaying wrinkles typically associated with Arabic gum encapsulation (Zaeim et al., 2018). However, significant differences were observed in particle size distribution. Electrosprayed capsules exhibited the smallest average diameter of 1.2 ± 0.5 μm, an advantage of electrospraying as well as its ability to produce narrowly distributed particles. Conversely, spray-dried capsules had average diameters of 11.3 ± 5.8 μm (Arabic gum only) and 12.4 ± 8.7 μm (Arabic gum and additives). Despite being significantly larger, these particle size values remain below 50 μm, ensuring they are not detected by taste buds

(McClements, 2018). Interestingly, the addition of Tween 20 and pullulan resulted in a broader size distribution, which was associated with an increase in the viscosity of the feed leading to larger atomized droplets. Nonetheless, these wider ranges and larger sizes were expected for spray-drying (Berraquero-García et al., 2023). Encapsulation efficiency was evaluated by analyzing protein migration to the capsule surface using X-ray photoelectron spectroscopy (XPS), which measured surface nitrogen content. Electrosprayed capsules contained 7% surface nitrogen, whereas spray-dried capsules exhibited 9.5% (Arabic gum only) and 7.5% (with additives). The latter value was remarkably similar to that of electrosprayed capsules, suggesting comparable levels of hydrolysate encapsulation. This enhanced retention for the formulation spray-dried additives was attributed to Tween 20, which rapidly migrates to the air-liquid interface, preventing protein migration (Sarabandi & Jafari, 2020).

The DPP-IV inhibitory activity of the encapsulated hydrolysate was evaluated *in vitro*. The free hydrolysate exhibited an IC_{50} of 1.29 ± 0.07 mg protein/mL, with electrosprayed and spray-dried capsules with additives displaying similar inhibition levels, with IC_{50} values of 1.50 ± 0.07 and 1.61 ± 0.08 mg protein/mL, respectively. In contrast, spray-dried capsules without additives reported a higher IC_{50} of 1.99 ± 0.03 mg protein/mL. This last result was in line with other studies on spray-drying, which reported IC_{50} values 2-fold higher after encapsulation (Garzón et al., 2023). The observed loss of bioactivity may be attributed to protein denaturation caused by the high voltage used in electrospraying or shear stress during spray-drying atomization and dehydration.

Finally, it is worth highlighting that, despite the favorable results obtained for electrospraying, the reported productivity was notably low (data not shown), representing a significant limitation for further investigation due to insufficient material production. This drawback could be mitigated using alternative configurations, such as multi-needle systems (Moreira et al., 2021), or electrospraying assisted by pressurized gas (Busolo et al., 2019). However, these approaches were not explored within the scope of this PhD thesis. Given the observed results, spray-drying was selected as the primary encapsulation methodology, since this approach provided comparable bioactivity while ensuring higher productivity, making it the most viable option for further applications..

4.4.2. Coaxial spray-drying

Due to the lack of research on coaxial spray-drying for the encapsulation of bioactive protein compounds, no relevant information was available regarding formulation and processing parameters. Hence, the optimization of the composition of the feeds and the process variables was required.

Chapter VI investigated the impact of key input variables, including solid content in the core feed, solid content in the shell feed, and shell/core feed flow-rate ratio. The response variables assessed were yield (%), protein load (%), surface nitrogen (%), and DPP-IV inhibitory activity (IC_{50}, mg protein/mL). For this study, the *T. molitor* hydrolysate obtained using Alcalase and Flavourzyme at DH 20% (HTAF20), previously identified in Chapter III as the most bioactive hydrolysate, was used. Arabic gum was employed as the encapsulating agent due to its favorable encapsulation performance demonstrated in Chapter V. The inlet temperature was set at 190°C. All input variables were analyzed and optimized using a Box-Behnken design with three levels per variable (% core solids: 30–35–40%; % shell solids: 15–25–35%; shell/core feed flow ratio: 50–58.3–66.7%), including a triplicate of the central point. This resulted in the production of 15 different encapsulates.

The 15 encapsulates were characterized by scanning electron microscopy (SEM), revealing a morphology consistent with previous findings in Chapter V. Briefly, the capsules were spherical and wrinkled (Figure 11a). Interestingly, additional larger capsules were observed, which appeared hollow and cracked. These structures were indicative of rapid, unstable crust formation that collapsed under internal vapor pressure accumulation, a phenomenon linked to high temperatures and solid concentrations (Kurozawa et al., 2009). The core-shell structure was confirmed using confocal microscopy, where the formation of an additional shell layer stained with carboxyfluorescein was clearly visible (Figure 11b).

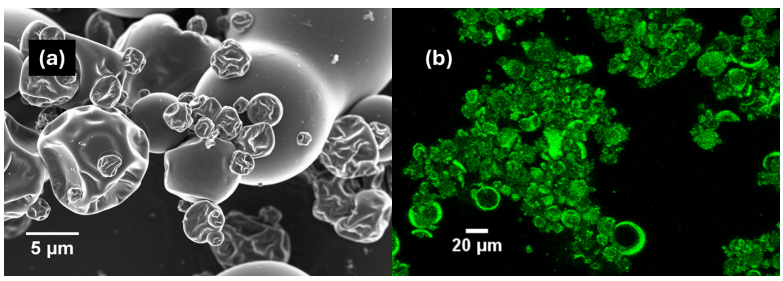

Figure 11. (a) Scanning electron microscopy (SEM) image showing structurally stable capsules with the characteristic wrinkled surface obtained via coaxial spray-drying. (b) Confocal microscopy image confirming the formation of core-shell structures in coaxial spray-dried capsules

Regarding particle size distribution analysis, given the large sample set, the D50 value (mean diameter under which 50% of the particles fall) and span (distribution width) were determined. D50 values ranged between 3 and 6 μm, with span values between 1.4 and 2.6 μm. These results indicated that the particle sizes and distributions were within acceptable ranges for this type of encapsulation mechanism. The primary variable affecting size distribution was the % shell solids, where higher concentrations resulted in broader distributions. This effect was attributed to increased viscosity, which can lead to atomization or larger particles (Teo et al., 2021).

The experimental results were fitted to quadratic models to assess both linear and quadratic effects. For yield, values ranged between 13–31%, which, although low, are typical for lab-scale spray dryers due to reduced size and heat loss, leading to condensation and powder deposition in the chamber (Sosnik & Seremeta, 2015). Even though the yield model presented an R^2 of 0.77, and the lack-of-fit value of 0.08 validated its significance. The most significant variable affecting yield was % shell solids (p-value < 0.05), indicating that increased Arabic gum concentration in the shell improved productivity, consistent with findings in Chapter IV.

Protein load values ranged from 9.5–15.3%. Although a significant difference between expected and actual values was observed, the model exhibited a strong correlation (R^2 = 0.93). All variables had a significant linear effect on protein load (p-value < 0.05). Core and shell solid content influenced protein load inversely, as increasing shell solids reduced proportionally the protein content.

Regarding surface nitrogen, values ranged from 4.5–6.7%, indicating partial migration of protein to the surface. The surface nitrogen model (R^2 = 0.87) identified the shell/core feed flow ratio as the most critical parameter (p-value < 0.05). Interestingly, while the coefficient for this variable suggested a direct effect, global interaction analysis indicated an inverse proportional relationship, meaning higher shell/core ratios reduced surface nitrogen. This finding aligns with the expectation that a thicker and more complete shell layer provides better hydrolysate protection and prevents migration to the surface.

Finally, the inhibitory activity of the 15 encapsulates was evaluated *in vitro*, with IC_{50} values ranging from 0.79 to 1.21 mg protein/mL. Differences in bioactivity could be attributed to shear stress during atomization, denaturation during drying, protein migration to the surface (Akbarbaglu et al., 2019) or interactions between peptides in the hydrolysate and Arabic gum (Alvarado et al., 2019; Comunian et al., 2022). Interestingly, this model predicted particularly well the bioactivity, with the highest correlation at R^2 = 0.97. The linear effect of the shell/core feed flow rate was the most significant effect, similar to its effect on surface nitrogen. This relationship suggests that improved shell formation, enhanced by higher shell/core feed flow ratios, significantly enhanced peptide retention and, consequently, bioactivity.

Considering all results, the coaxial encapsulation process for the *T. molitor* hydrolysate with DPP-IV inhibitory activity was optimized, as summarized in Table 4. The findings indicate the necessity of balancing process variables to maximize bioactivity retention while maintaining acceptable yield.

Table 4 Optimized processing variables for the encapsulation of the DPP-IV inhibitory hydrolysate by coaxial spray-drying. Inlet/outlet air temperature: 190/100-110 °C.

	Yield	Protein load	Surface nitrogen	DPP-IV inhibitory activity
Max/min value	**Maximum: 31.32%**	**Maximum: 16.08%**	**Minimum: 4.63%**	**Minimum: 0.76 mg protein/mL**
%Core solids	30%	30%	40%	38%
%Shell solids	20%	15%	29%	24%
%Shell/core feed flow rate	65%	50%	67%	67%

4.5. Investigation of the encapsulation effect for the stabilization of DPP-IV inhibitory protein hydrolysates during gastrointestinal digestion

Based on the findings from Chapters V and VI, where different encapsulation methods were evaluated in terms of yield and bioactivity retention, monoaxial and coaxial spray drying were selected to further study protection during gastrointestinal digestion. Thus, Chapter VII focused on the encapsulation of the two most bioactive hydrolysates obtained in Chapter III. These hydrolysates, HTAF20 (*T. molitor*) and HOAF20 (olive seed), were obtained through the combination of Alcalase and Flavourzyme at a 20% DH exhibited significant bioactivity *in vitro*, but it was markedly reduced after digestion. Furthermore, their molecular weight distribution (MWD) profiles showed substantial changes post-digestion, highlighting the need for an effective protective strategy.

To formulate the encapsulation solutions, a standardized approach was used, independently of the substrate or encapsulation configuration (i.e., monoaxial or coaxial) (Table 5). Thus, the hydrolysates were incorporated at a concentration ensuring 15% protein content in the final encapsulates. Three monoaxial configurations were tested: the based formulation used in Chapter V, which contained Arabic gum as the carrier (C1), a second formulation including Tween 20 as surfactant (C2), and a third formulation which also included pullulan, the same as in Chapter V (C3). For coaxial spray-drying two formulations were developed, using the optimized data from Chapter VI, containing 40% solids in the core, 30% solids in the shell and a 67% shell/core feed flow rate (C4). A second coaxial formulation was included, with 1% alginate in the shell, based on its reported resistance to gastric conditions (Alvarez et al., 2024).

Table 5. Composition of feed(s) formulations prepared for spray-drying encapsulation.

			Core (40% solids)		Shell (30% solids)
Substrate	**Code**	**Spray-drying configuration**	**Encapsulating material**	**Additives**	**Encapsulating material**
T. molitor meal	CT1	Monoaxial	Arabic gum	–	
	CT2		Arabic gum	Tween 20 (1%)	
	CT3		Arabic gum	Tween 20 (1%) + pullulan (1%)	
	CT4	Coaxial	Arabic gum	–	Arabic gum
	CT5		Arabic gum	–	Arabic gum + alginate (1%)
O. europaea seed meal	CO1	Monoaxial	Arabic gum	–	
	CO2		Arabic gum	Tween 20 (1%)	
	CO3		Arabic gum	Tween 20 (1%) + pullulan (1%)	
	CO4	Coaxial	Arabic gum	–	Arabic gum
	CO5		Arabic gum	–	Arabic gum + alginate (1%)

Scanning electron microscopy confirmed that the morphology of the 10 encapsulated formulations (5 for *T. molitor* and 5 for olive seed hydrolysates), was consistent with those observed in previous chapters. Confocal microscopy further verified the formation of a distinct shell-core structure in the coaxial encapsulations. Regarding the size distribution of the capsules, the addition of Tween 20 and pullulan led to larger sizes within the monoaxial capsules, likely due to the increased viscosity of the solutions. CT1 and CO1 had diameters of 5.4 and 5.5 μm, respectively, while CT3 and CO3 reached 7.8 and 8.5 μm. Interestingly, these sizes were significantly smaller than those obtained in Chapter V (11.3–12.4 μm), a difference attributed to the use of lower flow rates in order to reduce condensation and prevent material loss from adhesion to the drying chamber wall. For coaxial capsules, the optimized formulations (C4) were slightly larger than the monoaxial counterparts, with diameters of 8.7 and 6.6 μm for the *T. molitor* and olive seed-derived encapsulates, respectively. These results aligned with previous data from Chapter VI, were encapsulates reported sizes ranging 5.5–7.6 μm. Contrarily, the capsules with alginate (C5) had a much smaller average size and a narrower size distribution, which could be linked to the stabilizing effect of alginate (Szekalska et al., 2015).

Encapsulation yield varied between the techniques, with monoaxial formulations achieving higher yields (20.6–27.7%) compared to coaxial formulations (12.0–20.6%). These lower results were likely due to increased material deposition on the chamber walls, as the additional liquid feed made drying kinetics and humidity control more complex. Still,

the yield for C4 (19.7–20.6%) was consistent with the optimization results in Chapter VI, which ranged 19.7-20.6%. It is worth highlighting that the addition of alginate in C5 further reduced yield, as its higher viscosity led to frequent clogging of the syringe, requiring system disassembly and leading to material loss.

To assess hydrolysate retention within the capsules, nitrogen content on the surface was measured using XPS. As was expected, nitrogen was detected on all capsules, similarly to Chapters V and VI. Nonetheless, nitrogen levels were relatively low (1.7–6.4% of the total surface), particularly in Tween 20-containing formulations (C2 and C3, <4.5%), likely due to the surfactant's ability to retain peptides within the capsule. Interestingly, C4 capsules exhibited similar nitrogen content (4.3% for CT4 and 3.1% for CO4), though the protein load was lower (11–12%) that those of monoaxial capsules (15–16%). This could be related to the increased deposition on the wall due to humidity buildup.

To evaluate the effectiveness of encapsulation in protecting and retaining the bioactivity of the hydrolysates during gastrointestinal digestion, the *in vitro* DPP-IV inhibitory activity and MWD of the samples were analyzed. The digestive process was divided into partial (gastric) and complete (intestinal) phases, revealing that both stages impacted hydrolysate stability. A significant loss of DPP-IV inhibitory activity was observed after gastric digestion, followed by partial recovery in the intestinal phase. This effect was also observed in the encapsulated samples, demonstrating that the analysis of both phases is crucial, as studying only complete digestion could lead to incorrect conclusions about the protective capabilities of encapsulation. Significant differences were also identified across formulations, with the monoaxial formulation with additives (C3) and coaxial formulations (C4 and C5) providing the highest degree of protection. Indeed, for *T. molitor* samples, C3 and C4 capsules showed no significant differences in IC_{50} values compared to the free hydrolysate after encapsulation, and the bioactivity decreased only by 9–14% after digestion.

Analysis of the MWD revealed that peptides over 7 kDa were significantly degraded during gastric digestion, whereas intestinal digestion primarily affected smaller peptides (1–0.2 kDa). Coaxial C4 capsules revealed the highest protection, as indicated by the identified fractions, highlighting the stabilizing effect of the shell-core structure. However, this benefit was not observed for C5 capsules, suggesting that the addition of alginate might not be advantageous under these conditions. Thus, further optimization of the formulation should be studied, considering its effects on the viscoelastic properties. It is worth noting an increase in the >7 kDa following digestion in most encapsulated samples, suggesting possible aggregation, either among peptides themselves (Pérez-Gálvez et al., 2024) or with encapsulation agents. Indeed, similar interactions have been reported between whey peptides and Arabic gum (Klein et al., 2010).

Peptidomics analysis was performed to further validate the effectiveness of the encapsulation, identifying the retention of peptide sequences before and after digestion. The monoaxial C3 and coaxial C4 capsules, which demonstrated the highest protective potential, were investigated and compared to the free hydrolysate as well as the complete digestive samples. However, several methodological challenges arose due to the complexity of the samples and the presence of non-protein compounds, which hindered the identification of peptides below 0.3 kDa. It is worth noting that this fraction represents over 20% of peptides in *T. molitor*-derived hydrolysates and approximately 10% in olive seed hydrolysates, according to the SEC results. Additionally, as digestion progressed and the sample matrix became more complex (with enzymes and digestion byproducts contributing to the noise), fewer sequences could be confidently identified. For example, while 7,565 sequences were identified in undigested *T. molitor* hydrolysates, only 2,623 were detected post-digestion, consistent with previous reports on *T. molitor* samples (Gonzalez-de la Rosa et al., 2024). Interestingly, even fewer sequences could be identified in olive seed samples, likely due to the higher proportion of non-protein compounds (>70%) and the fact that only the seed stone was analyzed, unlike *T. molitor*, where the entire organism was used.

Regarding sequence overlap, the analysis indicated that coaxial capsules potentially retained peptides more effectively than monoaxial formulations, with 65% peptide retention for *T. molitor* and 55% for olive seed hydrolysates. Since nearly half of the sequences could not be identified, this supports the hypothesis that peptide aggregation or interactions may be occurring, preventing detection. Such interactions have been previously reported for Arabic gum (Comunian et al., 2022) and may be increased in spray drying due to the high processing temperatures (Gómez-Mascaraque et al., 2016).

After digestion, encapsulated samples appeared to retain more peptide sequences than free hydrolysates. However, the differences were relatively small, with 8.9% of peptides remaining in the digested *T. molitor* free hydrolysate, compared to 12.7% in digested monoaxial capsules and 11.1% in digested coaxial capsules. Similar values were also obtained for the olive seed samples. Nonetheless, validating encapsulation efficiency in this context is particularly challenging, as there is no reliable way to determine whether these sequences were genuinely protected by encapsulation or if they were simply regenerated from the degradation of larger parent peptides, as previously observed in whey protein hydrolysates (Alvarado et al., 2019).

Additionally, the retention of peptides previously identified as DPP-IV inhibitors was analyzed (Chapter III) to assess whether encapsulation provided protection. Some of these sequences (i.e., LPR, VPF, LPLF, VPW, and ELPF) were indeed detected after encapsulation and subsequent digestion. However, their identification could not be solely attributed to the encapsulation process, as it may also result from an inherent resistance to enzymatic

degradation. Notably, DPP-IV inhibitory sequences often contain proline at positions P2'-P3', a feature known to limit cleavage by pepsin, the primary gastric enzyme (Keil, 1992).

Given these limitations, it is unsurprising that published research using this methodology remains limited when applied to complex matrices such as hydrolysates. These findings also emphasize the need for further exploration of alternative analytical and purification techniques, particularly to enhance the reliability of LC-MS/MS as a validation method.

5. REFERENCES

Adler-Nissen, Jens. (1986). Enzymic hydrolysis of food proteins. New York: Elsevier Applied Science Publishers. p9-17 and p146-147.

Aguilar-Toala, J. E., Quintanar-Guerrero, D., Liceaga, A. M., & Zambrano- Zaragoza, M. L. (2022). Encapsulation of bioactive peptides: a strategy to improve the stability, protect the nutraceutical bioactivity and support their food applications. *RSC Advances*, 12(11), 6449–6458. https://doi.org/10.1039/D1RA08590E

Ahn, J., Cao, M. J., Yu, Y. Q., & Engen, J. R. (2012). Accessing the Reproducibility and Specificity of Pepsin and other Aspartic Proteases. *Biochimica et Biophysica Acta*, 1834(6), 1222. https://doi.org/10.1016/J.BBAPAP.2012.10.003

Akbarbaglu, Z., Mahdi Jafari, S., Sarabandi, K., Mohammadi, M., Khakbaz Heshmati, M., & Pezeshki, A. (2019). Influence of spray drying encapsulation on the retention of antioxidant properties and microstructure of flaxseed protein hydrolysates. *Colloids and Surfaces B: Biointerfaces*, 178, 421–429. https://doi.org/10.1016/J.COLSURFB.2019.03.038

Akbarbaglu, Z., Peighambardoust, S. H., Sarabandi, K., & Jafari, S. M. (2021). Spray drying encapsulation of bioactive compounds within protein-based carriers; different options and applications. *Food Chemistry*, 359, 129965. https://doi.org/10.1016/J.FOODCHEM.2021.129965

Akbarian, M., Khani, A., Eghbalpour, S., & Uversky, V. N. (2022b). Bioactive Peptides: Synthesis, Sources, Applications, and Proposed Mechanisms of Action. *International Journal of Molecular Sciences*, 23(3), 1445. https://doi.org/10.3390/IJMS23031445

Alahmad, K., Noman, A., Xia, W., Jiang, Q., & Xu, Y. (2023). Influence of the Enzymatic Hydrolysis Using Flavourzyme Enzyme on Functional, Secondary Structure, and Antioxidant Characteristics of Protein Hydrolysates Produced from Bighead Carp (*Hypophthalmichthys nobilis*). *Molecules* 2023, Vol. 28, Page 519, 28(2), 519. https://doi.org/10.3390/MOLECULES28020519

Ali, M. A., Kamal, M. M., Rahman, M. H., Siddiqui, M. N., Haque, M. A., Saha, K. K., & Rahman, M. A. (2021). Functional dairy products as a source of bioactive peptides and probiotics: current trends and future prospectives. *Journal of Food Science and Technology* 2021 59:4, 59(4), 1263–1279. https://doi.org/10.1007/S13197-021-05091-8

Alvarado, Y., Muro, C., Illescas, J., Díaz, M. del C., & Riera, F. (2019). Encapsulation of Antihypertensive Peptides from Whey Proteins and Their Releasing in Gastrointestinal Conditions. *Biomolecules* 2019, Vol. 9, Page 164, 9(5), 164. https://doi.org/10.3390/BIOM9050164

Alvarez, R., Robert, P., Quintriqueo, A., Oyarzún-Ampuero, F., Mackie, A., & Torcello-Gómez, A. (2024). Characterization and *in vitro* bioaccessability of optimized chia oil-Capsul-sodium alginate microparticles obtained by 3 nozzle spray-drying. *Food and Bioproducts Processing*, 148, 240–246. https://doi.org/10.1016/J.FBP.2024.09.012

Amigo, L., & Hernández-Ledesma, B. (2020). Current Evidence on the Bioavailability of Food Bioactive Peptides. *Molecules* 2020, Vol. 25, Page 4479, 25(19), 4479. https://doi.org/10.3390/MOLECULES25194479

Aquino, M. E., Drago, S. R., Sánchez de Medina, F., Martínez-Augustin, O., & Cian, R. E. (2024). Anti-diabetic properties of brewer's spent yeast peptides. *In vitro*, *in silico* and *ex vivo* study after simulated gastrointestinal digestion. *Food & Function*, 15(7), 3778–3790. https://doi.org/10.1039/D3FO04040B

Atma, Y., Murray, B. S., Sadeghpour, A., & Goycoolea, F. M. (2024). Encapsulation of short-chain bioactive peptides (BAPs) for gastrointestinal delivery: a review. *Food & Function*, 15(8), 3959–3979. https://doi.org/10.1039/D3FO04195F

Banerjee, P., & Shanthi, C. (2012). Isolation of novel bioactive regions from bovine Achilles tendon collagen having angiotensin I-converting enzyme-inhibitory properties. *Process Biochemistry*, 47(12), 2335–2346. https://doi.org/10.1016/J.PROCBIO.2012.09.012

Barati, M., Javanmardi, F., Jabbari, M., Mokari-Yamchi, A., Farahmand, F., Eş, I., Farhadnejad, H., Davoodi, S. H., & Mousavi Khaneghah, A. (2020). An *in silico* model to predict and estimate digestion-resistant and bioactive peptide content of dairy products: A primarily study of a time-saving and affordable method for practical research purposes. *LWT*, 130, 109616. https://doi.org/10.1016/J.LWT.2020.109616

Berraquero-García, C., Pérez-Gálvez, R., Espejo-Carpio, F. J., Guadix, A., Guadix, E. M., & García-Moreno, P. J. (2023). Encapsulation of Bioactive Peptides by Spray-Drying and Electrospraying. *Foods*, 12(10), 2005. ***https://doi.org/10.3390/foods12102005***

Berraquero-García, C., Rivero-Pino, F., Ospina, J. L., Pérez-Gálvez, R., Espejo-Carpio, F. J., Guadix, A., García-Moreno, P. J., & Guadix, E. M. (2023). Activity, structural features and *in silico* digestion of antidiabetic peptides. *Food Bioscience*, 55, 102954. https://doi.org/10.1016/J.FBIO.2023.102954

Bjørlie, M., Yesiltas, B., García-Moreno, P. J., Espejo-Carpio, F. J., Rahmani-Manglano, N. E., Guadix, E. M., Jafarpour, A., Hansen, E. B., Marcatili, P., Overgaard, M. T., Gregersen Echers, S., & Jacobsen, C. (2023). Bioinformatically predicted emulsifying peptides and potato protein hydrolysate improves the oxidative stability of microencapsulated fish oil. *Food Chemistry Advances*, 3, 100441. https://doi.org/10.1016/J.FOCHA.2023.100441

Bock, N., Dargaville, T. R., & Woodruff, M. A. (2012). Electrospraying of polymers with therapeutic molecules: State of the art. *Progress in Polymer Science*, 37(11), 1510–1551. https://doi.org/10.1016/J.PROGPOLYMSCI.2012.03.002

Bock, N., Dargaville, T. R., & Woodruff, M. A. (2014). Controlling microencapsulation and release of micronized proteins using poly(ethylene glycol) and electrospraying. *European Journal of Pharmaceutics and Biopharmaceutics*, 87(2), 366–377. https://doi.org/10.1016/J.EJPB.2014.03.008

Brodkorb, A., Egger, L., Alminger, M., Alvito, P., Assunção, R., Ballance, S., Bohn, T., Bourlieu-Lacanal, C., Boutrou, R., Carrière, F., Clemente, A., Corredig, M., Dupont, D., Dufour, C., Edwards, C., Golding, M., Karakaya, S., Kirkhus, B., Le Feunteun, S., … Recio, I. (2019). INFOGEST static *in vitro* simulation of gastrointestinal food digestion. *Nature Protocols* 2019 14:4, 14(4), 991–1014. https://doi.org/10.1038/s41596-018-0119-1

Busolo, M. A., Torres-Giner, S., Prieto, C., & Lagaron, J. M. (2019). Electrospraying assisted by pressurized gas as an innovative high-throughput process for the microencapsulation and stabilization of docosahexaenoic acid-enriched fish oil in zein prolamine. *Innovative Food Science & Emerging Technologies*, 51, 12–19. https://doi.org/10.1016/J.IFSET.2018.04.007

Cao, S., Wang, Y., Hao, Y., Zhang, W., & Zhou, G. (2020). Antihypertensive Effects *in Vitro* and *in Vivo* of Novel Angiotensin-Converting Enzyme Inhibitory Peptides from Bovine Bone Gelatin Hydrolysate. *Journal of Agricultural and Food Chemistry*, 68(3), 759–768. https://doi.org/10.1021/ACS.JAFC.9B05618

Catiau, L., Traisnel, J., Delval-Dubois, V., Chihib, N. E., Guillochon, D., & Nedjar-Arroume, N. (2011). Minimal antimicrobial peptidic sequence from hemoglobin alpha-chain: KYR. *Peptides*, 32(4), 633–638. https://doi.org/10.1016/J.PEPTIDES.2010.12.016

Charoenkwan, P., Nantasenamat, C., Hasan, M. M., Moni, M. A., Lio', P., Manavalan, B., & Shoombuatong, W. (2022). StackDPPIV: A novel computational approach for accurate prediction of dipeptidyl peptidase IV (DPP-IV) inhibitory peptides. *Methods*, 204, 189–198. https://doi.org/10.1016/J.YMETH.2021.12.001

Chauhan, S., O'Callaghan, S., Wall, A., Pawlak, T., Doyle, B., Adelfio, A., Trajkovic, S., Gaffney, M., & Khaldi, N. (2021). Using Peptidomics and Machine Learning to Assess Effects of Drying Processes on the Peptide Profile within a Functional Ingredient. *Processes*, Vol. 9, Page 425, 9(3), 425. https://doi.org/10.3390/PR9030425

Chen, L., Wang, J., Shu, G., & Chen, H. (2018). Production of Angiotensin-I-Converting Enzyme inhibitory peptide from goat milk casein: optimization conditions of complex protease hydrolysate by response surface methodology and purification. *Emirates Journal of Food and Agriculture*, 30(9), 742–749. https://doi.org/10.9755/EJFA.2018.V30.I9.1795

Cian, R. E., Campos-Soldini, A., Chel-Guerrero, L., Drago, S. R., & Betancur-Ancona, D. (2019). Bioactive *Phaseolus lunatus* peptides release from maltodextrin/gum arabic microcapsules obtained by spray drying after simulated gastrointestinal digestion. *International Journal of Food Science & Technology*, 54(6), 2002–2009. https://doi.org/10.1111/IJFS.14031

Cian, R. E., Oliva, M. E., Garzón, A. G., Ferreira, M. del R., D´Alessandro, M. E., & Drago, S. R. (2022). *In vitro* and *in vivo* antithrombotic and antioxidant properties of microencapsulated brewers' spent grain peptides. *International Journal of Food Science & Technology*, 57(6), 3872–3879.

https://doi.org/10.1111/IJFS.15717

Cian, R. E., Salgado, P. R., Mauri, A. N., & Drago, S. R. (2020). *Pyropia columbina* phycocolloids as microencapsulating material improve bioaccessibility of brewers' spent grain peptides with ACE-I inhibitory activity. *International Journal of Food Science & Technology*, 55(3), 1311–1317. https://doi.org/10.1111/IJFS.14397

Comunian, T. A., Archut, A., Gomez-Mascaraque, L. G., Brodkorb, A., & Drusch, S. (2022). The type of gum arabic affects interactions with soluble pea protein in complex coacervation. *Carbohydrate Polymers*, 295, 119851. https://doi.org/10.1016/J.CARBPOL.2022.119851

Consortium, T. U., Bateman, A., Martin, M.-J., Orchard, S., Magrane, M., Adesina, A., Ahmad, S., Bowler-Barnett, E. H., Bye-A-Jee, H., Carpentier, D., Denny, P., Fan, J., Garmiri, P., Gonzales, L. J. da C., Hussein, A., Ignatchenko, A., Insana, G., Ishtiaq, R., Joshi, V., … Zhang, J. (2025). UniProt: the Universal Protein Knowledgebase in 2025. *Nucleic Acids Research*, 53(D1), D609–D617. https://doi.org/10.1093/NAR/GKAE1010

Consumer perceptions unwrapped: ultra-processed foods (UPF). (2024).

Cox, J., Neuhauser, N., Michalski, A., Scheltema, R. A., Olsen, J. V., & Mann, M. (2011). Andromeda: A peptide search engine integrated into the MaxQuant environment. *Journal of Proteome Research*, 10(4), 1794–1805. https://doi.org/10.1021/PR101065J/SUPPL_FILE/PR101065J_SI_002.ZIP

Cruz-Casas, D. E., Aguilar, C. N., Ascacio-Valdés, J. A., Rodríguez-Herrera, R., Chávez-González, M. L., & Flores-Gallegos, A. C. (2021). Enzymatic hydrolysis and microbial fermentation: The most favorable biotechnological methods for the release of bioactive peptides. *Food Chemistry: Molecular Sciences*, 3, 100047. https://doi.org/10.1016/J.FOCHMS.2021.100047

Dallas, D. C., Guerrero, A., Parker, E. A., Robinson, R. C., Gan, J., German, J. B., Barile, D., & Lebrilla, C. B. (2015). Current peptidomics: Applications, purification, identification, quantification, and functional analysis. *Proteomics*, 15(5–6), 1026–1038. https://doi.org/10.1002/PMIC.201400310

Dávalos Terán, I., Imai, K., Lacroix, I. M. E., Fogliano, V., & Udenigwe, C. C. (2020). Bioinformatics of edible yellow mealworm (*Tenebrio molitor*) proteome reveal the cuticular proteins as promising precursors of dipeptidyl peptidase-IV inhibitors. *Journal of Food Biochemistry*, 44(2), e13121. https://doi.org/10.1111/JFBC.13121

Davies, M. J., D'Alessio, D. A., Fradkin, J., Kernan, W. N., Mathieu, C., Mingrone, G., Rossing, P., Tsapas, A., Wexler, D. J., & Buse, J. B. (2018). Management of Hyperglycemia in Type 2 Diabetes, 2018. A Consensus Report by the American Diabetes Association (ADA) and the European Association for the Study of Diabetes (EASD). *Diabetes Care*, 41(12), 2669–2701. https://doi.org/10.2337/DCI18-0033

De Koker, S., Fierens, K., Dierendonck, M., De Rycke, R., Lambrecht, B. N., Grooten, J., Remon, J. P., & De Geest, B. G. (2014). Nanoporous polyelectrolyte vaccine microcarriers. A formulation platform for enhancing humoral and cellular immune responses. *Journal of Controlled Release*, 195, 99–109. https://doi.org/10.1016/J.JCONREL.2014.07.043

Deacon, C. F. (2019). Physiology and Pharmacology of DPP-4 in Glucose Homeostasis and the Treatment of Type 2 Diabetes. *Frontiers in Endocrinology*, 10, 440649. https://doi.org/10.3389/FENDO.2019.00080

Diakogiannaki, E., Pais, R., Tolhurst, G., Parker, H. E., Horscroft, J., Rauscher, B., Zietek, T., Daniel, H., Gribble, F. M., & Reimann, F. (2013). Oligopeptides stimulate glucagon-like peptide-1 secretion in mice through proton-coupled uptake and the calcium-sensing receptor. *Diabetologia*, 56(12), 2688–2696. https://doi.org/10.1007/S00125-013-3037-3

Duvaud, S., Gabella, C., Lisacek, F., Stockinger, H., Ioannidis, V., & Durinx, C. (2021). Expasy, the Swiss Bioinformatics Resource Portal, as designed by its users. *Nucleic Acids Research*, 49(W1), W216–W227. https://doi.org/10.1093/NAR/GKAB225

Errico, S., Spagnoletta, A., Verardi, A., Moliterni, S., Dimatteo, S., & Sangiorgio, P. (2022). *Tenebrio molitor* as a source of interesting natural compounds, their recovery processes, biological effects, and safety aspects. *Comprehensive Reviews in Food Science and Food Safety*, 21(1), 148–197. https://doi.org/10.1111/1541-4337.12863

Esfandi, R., Willmore, W. G., & Tsopmo, A. (2019). Peptidomic analysis of hydrolyzed oat bran

proteins, and their *in vitro* antioxidant and metal chelating properties. *Food Chemistry*, 279, 49–57. https://doi.org/10.1016/J.FOODCHEM.2018.11.110

Evaristus, N. A., Wan Abdullah, W. N., & Gan, C. Y. (2018). Extraction and identification of α-amylase inhibitor peptides from *Nephelium lappacheum* and *Nephelium mutabile* seed protein using gastro-digestive enzymes. *Peptides*, 102, 61–67. https://doi.org/10.1016/J.PEPTIDES.2018.03.001

Ezcurra, M., Reimann, F., Gribble, F. M., & Emery, E. (2013). Molecular mechanisms of incretin hormone secretion. *Current Opinion in Pharmacology*, 13(6), 922–927. https://doi.org/10.1016/J.COPH.2013.08.013

Fan, K. T., Hsu, C. W., & Chen, Y. R. (2023). Mass spectrometry in the discovery of peptides involved in intercellular communication: From targeted to untargeted peptidomics approaches. *Mass Spectrometry Reviews*, 42(6), 2404–2425. https://doi.org/10.1002/MAS.21789

Ferreira, M. R., Garzón, A. G., Oliva, M. E., Cian, R. E., Drago, S. R., & D'Alessandro, M. E. (2022). Lipid-lowering effect of microencapsulated peptides from brewer's spent grain in high-sucrose diet-fed rats. *Food Bioscience*, 49, 101981. https://doi.org/10.1016/J.FBIO.2022.101981

Fu, L., Shi, S., Yi, J., Wang, N., He, Y., Wu, Z., Peng, J., Deng, Y., Wang, W., Wu, C., Lyu, A., Zeng, X., Zhao, W., Hou, T., & Cao, D. (2024). ADMETlab 3.0: an updated comprehensive online ADMET prediction platform enhanced with broader coverage, improved performance, API functionality and decision support. *Nucleic Acids Research*, 52(W1), W422–W431. https://doi.org/10.1093/NAR/GKAE236

Furtmann, B., Tang, J., Kramer, S., Eickner, T., Luderer, F., Fricker, G., Gomez, A., Heemskerk, B., & Jähn, P. S. (2017). Electrospray Synthesis of Poly(lactide-co-glycolide) Nanoparticles Encapsulating Peptides to Enhance Proliferation of Antigen-Specific CD8+ T Cells. *Journal of Pharmaceutical Sciences*, 106(11), 3316–3327. https://doi.org/10.1016/J.XPHS.2017.06.013

Gallo, V., Romano, A., Miralles, B., Ferranti, P., Masi, P., Santos-Hernández, M., & Recio, I. (2022). Physicochemical properties, structure and digestibility in simulated gastrointestinal environment of bread added with green lentil flour. *LWT*, 154, 112713. https://doi.org/10.1016/J.LWT.2021.112713

García-Moreno, P. J., Mendes, A. C., Jacobsen, C., & Chronakis, I. S. (2018). Biopolymers for the nanomicroencapsulation of bioactive ingredients by electrohydrodynamic processing. *Polymers for Food Applications*, 447–479. https://doi.org/10.1007/978-3-319-94625-2_17

García-Moreno, P. J., Pelayo, A., Yu, S., Busolo, M., Lagaron, J. M., Chronakis, I. S., & Jacobsen, C. (2018). Physicochemical characterization and oxidative stability of fish oil-loaded electrosprayed capsules: Combined use of whey protein and carbohydrates as wall materials. *Journal of Food Engineering*, 231, 42–53. https://doi.org/10.1016/J.JFOODENG.2018.03.005

Garzón, A. G., Cian, R. E., & Drago, S. R. (2023). Effects of agar-carrageenan wall materials and core-to-wall material ratio on physicochemical properties and *in vitro* bioaccessibility of microencapsulated bioactive peptides. *Food Hydrocolloids*, 139, 108570. https://doi.org/10.1016/J.FOODHYD.2023.108570

Ghorani, B., & Tucker, N. (2015). Fundamentals of electrospinning as a novel delivery vehicle for bioactive compounds in food nanotechnology. *Food Hydrocolloids*, 51, 227–240. https://doi.org/10.1016/J.FOODHYD.2015.05.024

Gibbs, B. F., Kermasha, S., Alli, I., & Mulligan, C. N. (1999). Encapsulation in the food industry: a review. *International Journal of Food Sciences and Nutrition*, 50(3), 213–224. https://doi.org/10.1080/096374899101256

Gómez-Mascaraque, L. G., Miralles, B., Recio, I., & López-Rubio, A. (2016). Microencapsulation of a whey protein hydrolysate within micro-hydrogels: Impact on gastrointestinal stability and potential for functional yoghurt development. *Journal of Functional Foods*, 26, 290–300. https://doi.org/10.1016/J.JFF.2016.08.006

Gonzalez-de la Rosa, T., Montserrat-de la Paz, S., & Rivero-Pino, F. (2024). Production, characterisation, and biological properties of *Tenebrio molitor*-derived oligopeptides. *Food Chemistry*, 450, 139400. https://doi.org/10.1016/J.FOODCHEM.2024.139400

González-Montoya, M., Hernández-Ledesma, B., Mora-Escobedo, R., & Martínez-Villaluenga, C. (2018). Bioactive Peptides from Germinated Soybean with Anti-Diabetic Potential by Inhibition of

Dipeptidyl Peptidase-IV, α-Amylase, and α-Glucosidase Enzymes. *International Journal of Molecular Sciences* 2018, Vol. 19, Page 2883, 19(10), 2883. https://doi.org/10.3390/IJMS19102883

Görgüç, A., Gençdağ, E., & Yılmaz, F. M. (2020). Bioactive peptides derived from plant origin by-products: Biological activities and techno-functional utilizations in food developments – A review. *Food Research International*, 136, 109504. https://doi.org/10.1016/J.FOODRES.2020.109504

Gregersen Echers, S., Jafarpour, A., Yesiltas, B., García-Moreno, P. J., Greve-Poulsen, M., Hansen, D. K., Jacobsen, C., Overgaard, M. T., & Hansen, E. B. (2023). Targeted hydrolysis of native potato protein: A novel workflow for obtaining hydrolysates with improved interfacial properties. *Food Hydrocolloids*, 137, 108299. https://doi.org/10.1016/J.FOODHYD.2022.108299

Guiné, R. P. F., Barroca, M. J., Maciejewska, M., Abrowska, A. D. ˛, & Cano-Lamadrid, M. (2025). Sustainable Protein Sources: Functional Analysis of *Tenebrio molitor* Hydrolysates and Attitudes of Consumers in Poland and Spain Toward Insect-Based Foods. *Foods*, Vol. 14, Page 333, 14(2), 333. https://doi.org/10.3390/FOODS14020333

Gullón, P., Gullón, B., Astray, G., Carpena, M., Fraga-Corral, M., Prieto, M. A., & Simal-Gandara, J. (2020). Valorization of by-products from olive oil industry and added-value applications for innovative functional foods. *Food Research International*, 137, 109683. https://doi.org/10.1016/J.FOODRES.2020.109683

Hall, F., Johnson, P. E., & Liceaga, A. (2018). Effect of enzymatic hydrolysis on bioactive properties and allergenicity of cricket (*Gryllodes sigillatus*) protein. *Food Chemistry*, 262, 39–47. https://doi.org/10.1016/J.FOODCHEM.2018.04.058

Han, R., Maycock, J., Murray, B. S., & Boesch, C. (2019). Identification of angiotensin converting enzyme and dipeptidyl peptidase-IV inhibitory peptides derived from oilseed proteins using two integrated bioinformatic approaches. *Food Research International*, 115, 283–291. https://doi.org/10.1016/J.FOODRES.2018.12.015

Harnedy-Rothwell, P. A., McLaughlin, C. M., O'Keeffe, M. B., Le Gouic, A. V., Allsopp, P. J., McSorley, E. M., Sharkey, S., Whooley, J., McGovern, B., O'Harte, F. P. M., & FitzGerald, R. J. (2020). Identification and characterisation of peptides from a boarfish (Capros aper) protein hydrolysate displaying *in vitro* dipeptidyl peptidase-IV (DPP-IV) inhibitory and insulinotropic activity. *Food Research International*, 131, 108989. https://doi.org/10.1016/J.FOODRES.2020.108989

Hofman, D. L., van Buul, V. J., & Brouns, F. J. P. H. (2016). Nutrition, Health, and Regulatory Aspects of Digestible Maltodextrins. *Critical Reviews in Food Science and Nutrition*, 56(12), 2091–2100. https://doi.org/10.1080/10408398.2014.940415

Hu, J., Lai, X., Wu, X., Wang, H., Weng, N., Lu, J., Lyu, M., & Wang, S. (2023). Isolation of a Novel Anti-Diabetic α-Glucosidase Oligo-Peptide Inhibitor from Fermented Rice Bran. *Foods*, 12(1), 183. https://doi.org/10.3390/FOODS12010183/S1

Hu, S., Fan, X., Qi, P., & Zhang, X. (2019). Identification of anti-diabetes peptides from *Spirulina platensis. Journal of Functional Foods*, 56, 333–341. https://doi.org/10.1016/J.JFF.2019.03.024

Hu, Z. Y., Chang, J., Guo, F. F., Deng, H. Y., Pan, G. T., Li, B. Y., Zhang, Z. L., & Wang, J. (2020). The effects of dimethylformamide exposure on liver and kidney function in the elderly population: A cross-sectional study. *Medicine*, 99(27), e20749. https://doi.org/10.1097/MD.0000000000020749

International Pet Food. (2025, January 17). Tebrio breaks ground on world's largest insect farm in Spain. https://internationalpetfood.com/tebrio-breaks-ground-on-worlds-largest-insect-farm-in-spain/

Jacobs, I. C. (2014). Atomization and Spray-Drying Processes. *Microencapsulation in the Food Industry: A Practical Implementation Guide*, 47–56. https://doi.org/10.1016/B978-0-12-404568-2.00005-4

Jacobsen, C., García-Moreno, P. J., Mendes, A. C., Mateiu, R. V., & Chronakis, I. S. (2018). Use of Electrohydrodynamic Processing for Encapsulation of Sensitive Bioactive Compounds and Applications in Food, *Annual Review of Food Science and Technology,* 9, 525–549. https://doi.org/10.1146/ANNUREV-FOOD-030117-012348

Jahandideh, F., Bourque, S. L., & Wu, J. (2022). A comprehensive review on the glucoregulatory properties of food-derived bioactive peptides. *Food Chemistry: X*, 13, 100222.

https://doi.org/10.1016/J.FOCHX.2022.100222

Janssen, R. H., Vincken, J. P., Van Den Broek, L. A. M., Fogliano, V., & Lakemond, C. M. M. (2017). Nitrogen-to-Protein Conversion Factors for Three Edible Insects: *Tenebrio molitor, Alphitobius diaperinus*, and *Hermetia illucens*. *Journal of Agricultural and Food Chemistry*, 65(11), 2275–2278. https://doi.org/10.1021/ACS.JAFC.7B00471

Jayaprakash, P., Maudhuit, A., Gaiani, C., & Desobry, S. (2023). Encapsulation of bioactive compounds using competitive emerging techniques: Electrospraying, nano spray drying, and electrostatic spray drying. *Journal of Food Engineering*, 339, 111260. https://doi.org/10.1016/J.JFOODENG.2022.111260

Jiménez-Munoz, L., Nielsen, S. D. H., & Corredig, M. (2024). Changes in potato peptide bioactivity after gastrointestinal digestion. An in silico and *in vitro* study of different patatin-rich potato protein isolate matrices. *Food Chemistry Advances*, 4, 100679. https://doi.org/10.1016/J.FOCHA.2024.100679

Kamdem, J. P., & Tsopmo, A. (2019). Reactivity of peptides within the food matrix. *Journal of Food Biochemistry*, 43(1), e12489. https://doi.org/10.1111/JFBC.12489

Kato, M., Nakanishi, T., Tani, T., & Tsuda, T. (2017). Low-molecular fraction of wheat protein hydrolysate stimulates glucagon-like peptide-1 secretion in an enteroendocrine L cell line and improves glucose tolerance in rats. *Nutrition Research*, 37, 37–45. https://doi.org/10.1016/J.NUTRES.2016.12.002

Keil, B. (1992). Specificity of Proteolysis. *Specificity of Proteolysis*. https://doi.org/10.1007/978-3-642-48380-6

Keller, J. (2013). Gastrointestinal Digestion and Absorption. *Encyclopedia of Biological Chemistry: Second Edition*, 354–359. https://doi.org/10.1016/B978-0-12-378630-2.00106-7

Kiewiet, M. B. G., Faas, M. M., & de Vos, P. (2018). Immunomodulatory Protein Hydrolysates and Their Application. *Nutrients*, 10 (7), 904. https://doi.org/10.3390/NU10070904

Klein, M., Aserin, A., Ishai, P. Ben, & Garti, N. (2010). Interactions between whey protein isolate and gum Arabic. *Colloids and Surfaces B: Biointerfaces*, 79(2), 377–383. https://doi.org/10.1016/J.COLSURFB.2010.04.021

Kumar, A., Belhaj, M., DiPette, D. J., & Potts, J. D. (2021). A Novel Alginate-Based Delivery System for the Prevention and Treatment of Pressure-Overload Induced Heart Failure. *Frontiers in Pharmacology*, 11, 602952. https://doi.org/10.3389/FPHAR.2020.602952

Kurozawa, L. E., Park, K. J., & Hubinger, M. D. (2009). Effect of carrier agents on the physicochemical properties of a spray dried chicken meat protein hydrolysate. *Journal of Food Engineering*, 94(3–4), 326–333. https://doi.org/10.1016/J.JFOODENG.2009.03.025

Lacroix, I. M. E., & Li-Chan, E. C. Y. (2012). Dipeptidyl peptidase-IV inhibitory activity of dairy protein hydrolysates. *International Dairy Journal*, 25(2), 97–102. https://doi.org/10.1016/J.IDAIRYJ.2012.01.003

Lacroix, I. M. E., Chen, X. M., Kitts, D. D., & Li-Chan, E. C. Y. (2017). Investigation into the bioavailability of milk protein-derived peptides with dipeptidyl-peptidase IV inhibitory activity using Caco-2 cell monolayers. *Food & Function*, 8(2), 701–709. https://doi.org/10.1039/C6FO01411A

Lafferty, R. A., Flatt, P. R., & Irwin, N. (2024). NPYR modulation: Potential for the next major advance in obesity and type 2 diabetes management? *Peptides*, 179, 171256. https://doi.org/10.1016/J.PEPTIDES.2024.171256

Langyan, S., Khan, F. N., Yadava, P., Alhazmi, A., Mahmoud, S. F., Saleh, D. I., Zuan, A. T. K., & kumar, A. (2021). In silico proteolysis and analysis of bioactive peptides from sequences of fatty acid desaturase 3 (FAD3) of flaxseed protein. *Saudi Journal of Biological Sciences*, 28(10), 5480–5489. https://doi.org/10.1016/J.SJBS.2021.08.027

Lear, S., & Cobb, S. L. (2016). Pep-Calc.com: A set of web utilities for the calculation of peptide and peptoid properties and automatic mass spectral peak assignment. *Journal of Computer-Aided Molecular Design*, 30(3), 271–277. https://doi.org/10.1007/S10822-016-9902-7

Liguori, B., Sancho, A. I., Poulsen, M., & Lindholm Bøgh, K. (2022). Novel foods: allergenicity assessment of insect proteins. *EFSA Journal*, 20. https://doi.org/10.2903/j.efsa.2022.e200910

Liliana Krotz, A., Leone, F., & Giazzi Thermo Fisher Scientifi, G. (n.d.). Application Note: Elemental Analysis: CHNS/O Determination in Coals.

Lin, Y. S., Han, C. H., Lin, S. Y., & Hou, W. C. (2016). Synthesized Peptides from Yam Dioscorin Hydrolysis in Silico Exhibit Dipeptidyl Peptidase-IV Inhibitory Activities and Oral Glucose Tolerance Improvements in Normal Mice. *Journal of Agricultural and Food Chemistry*, 64(33), 6451–6458. https://doi.org/10.1021/ACS.JAFC.6B02403

Lopez, M. J., & Mohiuddin, S. S. (2024, April 30). Biochemistry, Essential Amino Acids. Treasure Island (FL). *StatPearls Publishing*. https://www.ncbi.nlm.nih.gov/books/NBK557845

López-Otín, C., & Bond, J. S. (2008). Proteases: Multifunctional enzymes in life and disease. *Journal of Biological Chemistry*, 283(45), 30433–30437. https://doi.org/10.1074/jbc.R800035200

Luigia, D. S. (2019). New protein Sources: Novel Foods. *Encyclopedia of Food Security and Sustainability*, 276–279. https://doi.org/10.1016/B978-0-08-100596-5.22129-X

Maestri, D., Barrionuevo, D., Bodoira, R., Zafra, A., Jiménez-López, J., & Alché, J. de D. (2019). Nutritional profile and nutraceutical components of olive (*Olea europaea L.*) seeds. *Journal of Food Science and Technology*, 56(9), 4359–4370. https://doi.org/10.1007/S13197-019-03904-5

Maillet, N. (2020). Rapid Peptides Generator: fast and efficient *in silico* protein digestion. *NAR Genomics and Bioinformatics*, 2(1). https://doi.org/10.1093/NARGAB/LQZ004

McClements, D. J. (2018). Encapsulation, protection, and delivery of bioactive proteins and peptides using nanoparticle and microparticle systems: A review. *Advances in Colloid and Interface Science*, 253, 1–22. https://doi.org/10.1016/J.CIS.2018.02.002

Mehta, M., Bui, T. A., Yang, X., Aksoy, Y., Goldys, E. M., & Deng, W. (2023). Lipid-Based Nanoparticles for Drug/Gene Delivery: An Overview of the Production Techniques and Difficulties Encountered in Their Industrial Development. *ACS Materials* Au, 3(6), 600–619. https://doi.org/10.1021/ACSMATERIALSAU.3C00032

Meisel, H. (2004). Multifunctional peptides encrypted in milk proteins. *BioFactors*, 21(1–4), 55–61. https://doi.org/10.1002/BIOF.552210111

Mijares, A. H. (2009). Inhibidores de la DPP-4 frente a análogos del receptor de GLP-1 tras el fracaso de la monoterapia con metformina en la diabetes tipo 2. *Avances En Diabetología*, 26(3), 200–202. https://doi.org/10.1016/S1134-3230(10)63015-3

Miner-Williams, W. M., Stevens, B. R., & Moughan, P. J. (2014). Are intact peptides absorbed from the healthy gut in the adult human? *Nutrition Research Reviews*, 27(2), 308–329. https://doi.org/10.1017/S0954422414000225

Ministerio de Agricultura. (2024, December). Avances e Informes de Situación de Mercado del Sector del Aceite de Oliva y la Aceituna de Mesa. https://www.mapa.gob.es/es/agricultura/temas/producciones-agricolas/aceite-oliva-y-aceituna-mesa/avances.aspx

Minkiewicz, P., Iwaniak, A., & Darewicz, M. (2019). BIOPEP-UWM Database of Bioactive Peptides: Current Opportunities. *International Journal of Molecular Sciences*, 20(23). https://doi.org/10.3390/IJMS20235978

Mooney, C., Haslam, N. J., Pollastri, G., & Shields, D. C. (2012). Towards the improved discovery and design of functional peptides: common features of diverse classes permit generalized prediction of bioactivity. *PloS One,* 7(10). https://doi.org/10.1371/JOURNAL.PONE.0045012

Mora, L., & Toldrá, F. (2022). Advanced enzymatic hydrolysis of food proteins for the production of bioactive peptides. *Current Opinion in Food Science*, 49. https://doi.org/10.1016/j.cofs.2022.100973

Moreira, A., Lawson, D., Onyekuru, L., Dziemidowicz, K., Angkawinitwong, U., Costa, P. F., Radacsi, N., & Williams, G. R. (2021). Protein encapsulation by electrospinning and electrospraying. *Journal of Controlled Release*, 329, 1172–1197. https://doi.org/10.1016/J.JCONREL.2020.10.046

Murthy, L. N., Phadke, G. G., Mohan, C. O., Chandra, M. V., Annamalai, J., Visnuvinayagam, S., Unnikrishnan, P., & Ravishankar, C. N. (2017). Characterization of Spray-Dried Hydrolyzed Proteins from Pink Perch Meat Added with Maltodextrin and Gum Arabic. *Journal of Aquatic Food Product Technology*, 26(8), 913–928. https://doi.org/10.1080/10498850.2017.1362684

Musaei, M., Mokhtari, J., Nouri, M., & Rad, Z. P. (2017). Fabrication and Characterization of Nanocapsules of PLGA Containing BSA Using Electrospray Technique. *Nanomedicine Research Journal*, 2(3), 158–164. https://doi.org/10.22034/NMRJ.2017.03.003

Nasri, M. (2017). Protein Hydrolysates and Biopeptides: Production, Biological Activities, and Applications in Foods and Health Benefits. A Review. *Advances in Food and Nutrition Research*, 81, 109–159. https://doi.org/10.1016/BS.AFNR.2016.10.003

Nongonierma, A. B., & FitzGerald, R. J. (2019). Features of dipeptidyl peptidase IV (DPP-IV) inhibitory peptides from dietary proteins. *Journal of Food Biochemistry*, 43(1), e12451. https://doi.org/10.1111/JFBC.12451

Onyekuru, L. C., Moreira, A., Zhang, J., Angkawinitwong, U., Costa, P. F., Brocchini, S., & Williams, G. R. (2021). An investigation of alkaline phosphatase enzymatic activity after electrospinning and electrospraying. *Journal of Drug Delivery Science and Technology*, 64, 102592. https://doi.org/10.1016/J.JDDST.2021.102592

Oonincx, D. G. A. B., & Finke, M. D. (2023). Insects as a complete nutritional source. *Journal of Insects as Food and Feed*, 9(5), 541–543. https://doi.org/10.3920/JIFF2023.X002

Ospina-Quiroga, J. L., García-Moreno, P. J., Guadix, A., Guadix, E. M., Almécija-Rodríguez, M. del C., & Pérez-Gálvez, R. (2022). Evaluation of Plant Protein Hydrolysates as Natural Antioxidants in Fish Oil-In-Water Emulsions. *Antioxidants*, 11(8), 1612. https://doi.org/10.3390/ANTIOX11081612/S1

Öztürk, H. İ., & Oraç, A. (2024). Harvesting bioactive peptides from sustainable protein sources: Unveiling technological and functional properties through *in silico* analyses. *Food and Humanity*, 2, 100294. https://doi.org/10.1016/J.FOOHUM.2024.100294

Paul, M., & Somkuti, G. A. (2009). Degradation of milk-based bioactive peptides by yogurt fermentation bacteria. *Letters in Applied Microbiology*, 49(3), 345–350. https://doi.org/10.1111/J.1472-765X.2009.02676.X

Peredo-Lovillo, A., Hernández-Mendoza, A., Vallejo-Cordoba, B., & Romero-Luna, H. E. (2022). Conventional and *in silico* approaches to select promising food-derived bioactive peptides: A review. *Food Chemistry: X*, 13, 100183. https://doi.org/10.1016/J.FOCHX.2021.100183

Pérez-Gálvez, R., Berraquero-García, C., Ospina-Quiroga, J. L., Espejo-Carpio, F. J., Almécija, M. C., Guadix, A., García-Moreno, P. J., & Guadix, E. M. (2024). Influence of *In Vitro* Digestion on Dipeptidyl Peptidase-IV (DPP-IV) Inhibitory Activity of Plant-Protein Hydrolysates Obtained from Agro-Industrial By-Products. *Foods*, Vol. 13, Page 2691, 13(17), 2691. https://doi.org/10.3390/FOODS13172691

Piñón-Balderrama, C. I., Leyva-Porras, C., Terán-Figueroa, Y., Espinosa-Solís, V., Álvarez-Salas, C., & Saavedra-Leos, M. Z. (2020). Encapsulation of Active Ingredients in Food Industry by Spray-Drying and Nano Spray-Drying Technologies. *Processes*, Vol. 8, Page 889, 8(8), 889. https://doi.org/10.3390/PR8080889

Pollock, V. (2007). Proteins. *XPharm: The Comprehensive Pharmacology Reference*, 1–11. https://doi.org/10.1016/B978-008055232-3.60055-8

Portmann, R., Jiménez-Barrios, P., Jardin, J., Abbühl, L., Barile, D., Danielsen, M., Huang, Y. P., Dalsgaard, T. K., Miralles, B., Briard-Bion, V., Cattaneo, S., Chambon, C., Cudennec, B., De Noni, I., Deracinois, B., Dupont, D., Duval, A., Flahaut, C., López-Nicolás, R., … Egger, L. (2023). A multi-centre peptidomics investigation of food digesta: current state of the art in mass spectrometry analysis and data visualisation. *Food Research International*, 169, 112887. https://doi.org/10.1016/J.FOODRES.2023.112887

Qin, D., Bo, W., Zheng, X., Hao, Y., Li, B., Zheng, J., & Liang, G. (2022). DFBP: a comprehensive database of food-derived bioactive peptides for peptidomics research. *Bioinformatics*, 38(12), 3275–3280. https://doi.org/10.1093/BIOINFORMATICS/BTAC323

Rahmani-Manglano, N. E., Jones, N. C., Hoffmann, S. V., Guadix, E. M., Pérez-Gálvez, R., Guadix, A., & García-Moreno, P. J. (2022). Structure of whey protein hydrolysate used as emulsifier in wet and dried oil delivery systems: Effect of pH and drying processing. *Food Chemistry*, 390, 133169. https://doi.org/10.1016/J.FOODCHEM.2022.133169

Raksakulthai, R., & Haard, N. F. (2003). Exopeptidases and Their Application to Reduce Bitterness in Food: A Review. *Critical Reviews in Food Science and Nutrition*, 43(4), 401–445. https://doi.org/10.1080/10408690390826572

Reed, J., Bain, S., & Kanamarlapudi, V. (2021). A Review of Current Trends with Type 2 Diabetes

Epidemiology, Aetiology, Pathogenesis, Treatments and Future Perspectives. *Diabetes, Metabolic Syndrome and Obesity*, 14, 3567–3602. https://doi.org/10.2147/DMSO.S319895

Rieder, A., Afseth, N. K., Böcker, U., Knutsen, S. H., Kirkhus, B., Mæhre, H. K., Ballance, S., & Wubshet, S. G. (2021). Improved estimation of *in vitro* protein digestibility of different foods using size exclusion chromatography. *Food Chemistry*, 358, 129830. https://doi.org/10.1016/J.FOODCHEM.2021.129830

Rivero-Pino, F., Espejo-Carpio, F. J., & Guadix, E. M. (2020). Bioactive fish hydrolysates resistance to food processing. *LWT*, 117, 108670. https://doi.org/10.1016/J.LWT.2019.108670

Rivero-Pino, F., Guadix, A., & Guadix, E. M. (2021). Identification of novel dipeptidyl peptidase IV and α-glucosidase inhibitory peptides from *Tenebrio molitor*. *Food & Function*, 12(2), 873–880. https://doi.org/10.1039/D0FO02696D

Saeedi, P., Petersohn, I., Salpea, P., Malanda, B., Karuranga, S., Unwin, N., Colagiuri, S., Guariguata, L., Motala, A. A., Ogurtsova, K., Shaw, J. E., Bright, D., & Williams, R. (2019). Global and regional diabetes prevalence estimates for 2019 and projections for 2030 and 2045: Results from the International Diabetes Federation Diabetes Atlas, 9th edition. *Diabetes Research and Clinical Practice*, 157, 107843. https://doi.org/10.1016/j.diabres.2019.107843

Salas, C. E., Badillo-Corona, J. A., Ramírez-Sotelo, G., & Oliver-Salvador, C. (2015). Biologically Active and Antimicrobial Peptides from Plants. *BioMed Research International*, 1, 102129. https://doi.org/10.1155/2015/102129

Sánchez-Rivera, L., Martínez-Maqueda, D., Cruz-Huerta, E., Miralles, B., & Recio, I. (2014). Peptidomics for discovery, bioavailability and monitoring of dairy bioactive peptides. *Food Research International*, 63, 170–181. https://doi.org/10.1016/J.FOODRES.2014.01.069

Santos-Hernández, M., Vivanco-Maroto, S. M., Miralles, B., & Recio, I. (2023). Food peptides as inducers of CCK and GLP-1 secretion and GPCRs involved in enteroendocrine cell signalling. *Food Chemistry*, 402, 134225. https://doi.org/10.1016/J.FOODCHEM.2022.134225

Sarabandi, K., & Jafari, S. M. (2020). Improving the antioxidant stability of flaxseed peptide fractions during spray drying encapsulation by surfactants: Physicochemical and morphological features. *Journal of Food Engineering*, 286, 110131. https://doi.org/10.1016/J.JFOODENG.2020.110131

Sbroggio, M. F., Montilha, M. S., Figueiredo, V. R. G. de, Georgetti, S. R., & Kurozawa, L. E. (2016). Influence of the degree of hydrolysis and type of enzyme on antioxidant activity of okara protein hydrolysates. *Food Science and Technology*, 36(2), 375–381. https://doi.org/10.1590/1678-457X.000216

Segura-Campos, M. R., Espinosa-García, L., Chel-Guerrero, L. A., & Betancur-Ancona, D. A. (2012). Effect of Enzymatic Hydrolysis on Solubility, Hydrophobicity, and *In Vivo* Digestibility in Cowpea (*Vigna unguiculata*). *International Journal of Food Properties*, 15(4), 770–780. https://doi.org/10.1080/10942912.2010.501469

Sheehan, D., & O'Sullivan, S. (2004). Fast protein liquid chromatography. *Methods in Molecular Biology* (Clifton, N.J.), 244, 253–258. https://doi.org/10.1385/1-59259-655-X:253

Shoombuatong, W., Charoenkwan, P., Kanthawong, S., Nantasenamat, C., & Hasan, M. M. (2020). IDPPIV-SCM: A sequence-based predictor for identifying and analyzing dipeptidyl peptidase IV (DPP-IV) inhibitory peptides using a scoring card method. *Journal of Proteome Research*, 19(10), 4125–4136. https://doi.org/10.1021/ACS.JPROTEOME.0C00590

Singh, H. (2016). Nanotechnology Applications in Functional Foods; Opportunities and Challenges. *Preventive Nutrition and Food Science*, 21(1), 1. https://doi.org/10.3746/PNF.2016.21.1.1

Siow, H. L., & Gan, C. Y. (2016). Extraction, identification, and structure–activity relationship of antioxidative and α-amylase inhibitory peptides from cumin seeds (*Cuminum cyminum*). *Journal of Functional Foods*, 22, 1–12. https://doi.org/10.1016/J.JFF.2016.01.011

Sosnik, A., & Seremeta, K. P. (2015). Advantages and challenges of the spray-drying technology for the production of pure drug particles and drug-loaded polymeric carriers. *Advances in Colloid and Interface Science*, 223, 40–54. https://doi.org/10.1016/J.CIS.2015.05.003

Sousa, R., Portmann, R., Dubois, S., Recio, I., & Egger, L. (2020). Protein digestion of different protein sources using the INFOGEST static digestion model. *Food Research International*, 130, 108996.

https://doi.org/10.1016/J.FOODRES.2020.108996

Sun, H., Nguyen, K., Kerns, E., Yan, Z., Yu, K. R., Shah, P., Jadhav, A., & Xu, X. (2017). Highly predictive and interpretable models for PAMPA permeability. *Bioorganic & Medicinal Chemistry*, 25(3), 1266–1276. https://doi.org/10.1016/J.BMC.2016.12.049

Sun, X., Acquah, C., Aluko, R. E., & Udenigwe, C. C. (2020). Considering food matrix and gastrointestinal effects in enhancing bioactive peptide absorption and bioavailability. *Journal of Functional Foods*, 64, 103680. https://doi.org/10.1016/J.JFF.2019.103680

Szekalska, M., Amelian, A., & Winnicka, K. (2015). Alginate microspheres obtained by the spray drying technique as mucoadhesive carriers of ranitidine. *Acta Pharm*., 65, 15–27. https://intapi.sciendo.com/pdf/10.1515/acph-2015-0008

Tacias-Pascacio, V. G., Morellon-Sterling, R., Siar, E. H., Tavano, O., Berenguer-Murcia, Á., & Fernandez-Lafuente, R. (2020). Use of Alcalase in the production of bioactive peptides: A review. *International Journal of Biological Macromolecules*, 165, 2143–2196. https://doi.org/10.1016/J.IJBIOMAC.2020.10.060

Takahashi, Y., Noguchi, M., Inoue, Y., Sato, S., Shimizu, M., Kojima, H., Okabe, T., Kiyono, H., Yamauchi, Y., & Sato, R. (2022). Organoid-derived intestinal epithelial cells are a suitable model for preclinical toxicology and pharmacokinetic studies. *IScience*, 25(7), 104542. https://doi.org/10.1016/j.isci.2022.104542

Tang, Y., Li, R., Lin, G., & Li, L. (2014). PEP search in MyCompoundID: Detection and identification of dipeptides and tripeptides using dimethyl labeling and hydrophilic interaction liquid chromatography tandem mass spectrometry. *Analytical Chemistry*, 86(7), 3568–3574. https://doi.org/10.1021/AC500109Y

Teo, A., Lam, Y., Lee, S. J., & Goh, K. K. T. (2021). Spray drying of whey protein stabilized nanoemulsions containing different wall materials – maltodextrin or trehalose. *LWT*, 136, 110344. https://doi.org/10.1016/J.LWT.2020.110344

Tyanova, S., Temu, T., & Cox, J. (2016). The MaxQuant computational platform for mass spectrometry-based shotgun proteomics. *Nature Protocols,* 11:12, 11(12), 2301–2319. https://doi.org/10.1038/nprot.2016.136

Ustunol, Z. (2014). Physical, Chemical, and Processing-Induced Changes in Proteins. *Applied Food Protein Chemistry*, 23–46. https://doi.org/10.1002/9781118860588.CH4

Vogelsang-O'dwyer, M., Sahin, A. W., Arendt, E. K., & Zannini, E. (2022). Enzymatic Hydrolysis of Pulse Proteins as a Tool to Improve Techno-Functional Properties. *Foods*, Vol. 11, Page 1307, 11(9), 1307. https://doi.org/10.3390/FOODS11091307

Vreeke, G. J. C., Lubbers, W., Vincken, J. P., & Wierenga, P. A. (2022). A method to identify and quantify the complete peptide composition in protein hydrolysates. *Analytica Chimica Acta*, 1201, 339616. https://doi.org/10.1016/J.ACA.2022.339616

Wan, F., Maltesen, M. J., Andersen, S. K., Bjerregaard, S., Foged, C., Rantanen, J., & Yang, M. (2014). One-Step Production of Protein-Loaded PLGA Microparticles via Spray Drying Using 3-Fluid Nozzle. *Pharmaceutical Research*, 31(8), 1967–1977. https://doi.org/10.1007/S11095-014-1299-1

Wang, Z., Ju, X., He, R., Yuan, J., & Wang, L. (2015). The Effect of Rapeseed Protein Structural Modification on Microstructural Properties of Peptide Microcapsules. *Food and Bioprocess Technology*, 8(6), 1305–1318. https://doi.org/10.1007/S11947-015-1472-5

Weimers, C. (2023). Insects in food. *Question for written answer E-000581/2023 to the Commission*. In European Parliament.

Woo, M. W., & Bhandari, B. (2013). Spray drying for food powder production. *Handbook of Food Powders: Processes and Properties*, 29–56. https://doi.org/10.1533/9780857098672.1.29

Xiao, C., Toldrá, F., Zhao, M., Zhou, F., Luo, D., Jia, R., & Mora, L. (2022). *In vitro* and *in silico* analysis of potential antioxidant peptides obtained from chicken hydrolysate produced using Alcalase. *Food Research International*, 157, 111253. https://doi.org/10.1016/J.FOODRES.2022.111253

Xu, F., Yao, Y., Xu, X., Wang, M., Pan, M., Ji, S., Wu, J., Jiang, D., Ju, X., & Wang, L. (2019). Identification and Quantification of DPP-IV-Inhibitory Peptides from Hydrolyzed-Rapeseed-Protein-Derived Napin

with Analysis of the Interactions between Key Residues and Protein Domains. *Journal of Agricultural and Food Chemistry*, 67(13), 3679–3690. https://doi.org/10.1021/ACS.JAFC.9B01069

Yan, C., Kim, S. R., Ruiz, D. R., & Farmer, J. R. (2022). Microencapsulation for Food Applications: A Review. *ACS Applied Bio Materials*, 5(12), 5497–5512. https://doi.org/10.1021/ACSABM.2C00673

Ye, H., Tao, X., Zhang, W., Chen, Y., Yu, Q., & Xie, J. (2022). Food-derived bioactive peptides: production, biological activities, opportunities and challenges. *Journal of Future Foods*, 2(4), 294–306. https://doi.org/10.1016/J.JFUTFO.2022.08.002

Ye, J., McGinnis, S., & Madden, T. L. (2006). BLAST: improvements for better sequence analysis. *Nucleic Acids Research*, 34(suppl_2), W6–W9. https://doi.org/10.1093/NAR/GKL164

Yu, X., Oh, E., & Kim, Y. (2021). A comparative study on the functional properties of mealworm (*Tenebrio molitor*) larvae and soybean protein isolates and hydrolysates. *International Food Research Journal*, 28(4), 816–826. https://doi.org/10.47836/IFRJ.28.4.18

Zaazouee, M. S., Hamdallah, A., Helmy, S. K., Hasabo, E. A., Sayed, A. K., Gbreel, M. I., Elmegeed, A. A., Aladwan, H., Elshanbary, A. A., Abdel-Aziz, W., Elshahawy, I. M., Rabie, S., Elkady, S., Ali, A. S., Ragab, K. M., & Nourelden, A. Z. (2022). Semaglutide for the treatment of type 2 Diabetes Mellitus: A systematic review and network meta-analysis of safety and efficacy outcomes. *Diabetes & Metabolic Syndrome: Clinical Research & Reviews*, 16(6), 102511. https://doi.org/10.1016/J.DSX.2022.102511

Zaeim, D., Sarabi-Jamab, M., Ghorani, B., Kadkhodaee, R., & Tromp, R. H. (2018). Electrospray-assisted drying of live probiotics in acacia gum microparticles matrix. *Carbohydrate Polymers*, 183, 183–191. https://doi.org/10.1016/J.CARBPOL.2017.12.001

Zamani, M., Prabhakaran, M. P., Thian, E. S., & Ramakrishna, S. (2014). Protein encapsulated core–shell structured particles prepared by coaxial electrospraying: Investigation on material and processing variables. *International Journal of Pharmaceutics*, 473(1–2), 134–143. https://doi.org/10.1016/J.IJPHARM.2014.07.006

Zhang, Y., Fonslow, B. R., Shan, B., Baek, M. C., & Yates, J. R. (2013). Protein analysis by shotgun/bottom-up proteomics. *Chemical Reviews*, 113(4), 2343–2394. https://doi.org/10.1021/CR3003533

Zhu, C., Huang, Y., Zhang, X., Mei, L., Pan, X., Li, G., & Wu, C. (2015). Comparative studies on exenatide-loaded poly (d,l-lactic-co-glycolic acid) microparticles prepared by a novel ultra-fine particle processing system and spray drying. *Colloids and Surfaces B: Biointerfaces*, 132, 103–110. https://doi.org/10.1016/J.COLSURFB.2015.05.001

Zielińska, E., Karaś, M., Baraniak, B., & Jakubczyk, A. (2020). Evaluation of ACE, α-glucosidase, and lipase inhibitory activities of peptides obtained by *in vitro* digestion of selected species of edible insects. *European Food Research and Technology*, 246(7), 1361–1369. https://doi.org/10.1007/S00217-020-03495-Y

Zietek, T., Giesbertz, P., Ewers, M., Reichart, F., Weinmüller, M., Urbauer, E., Haller, D., Demir, I. E., Ceyhan, G. O., Kessler, H., & Rath, E. (2020). Organoids to Study Intestinal Nutrient Transport, Drug Uptake and Metabolism – Update to the Human Model and Expansion of Applications. *Frontiers in Bioengineering and Biotechnology*, 8, 577656. https://doi.org/10.3389/FBIOE.2020.577656

Zou, Z., Wang, M., Wang, Z., Aluko, R. E., & He, R. (2020). Antihypertensive and antioxidant activities of enzymatic wheat bran protein hydrolysates. *Journal of Food Biochemistry*, 44(1), e13090. https://doi.org/10.1111/JFBC.13090

Zu, X. Y., Zhao, Y. J., Fu, S. M., Liao, T., Li, H. L., & Xiong, G. Q. (2022). Physicochemical Properties and Biological Activities of Silver Carp Scale Peptide and Its Nanofiltration Fractions. *Frontiers in Nutrition*, 8, 812443. https://doi.org/10.3389/FNUT.2021.812443

Zunzunegui, I., Martín-García, J., Santamaría, Ó., & Poveda, J. (2024). Analysis of yellow mealworm (*Tenebrio molitor*) frass as a resource for a sustainable agriculture in the current context of insect farming industry growth. *Journal of Cleaner Production*, 460, 142608. https://doi.org/10.1016/J.JCLEPRO.2024.142608

CHAPTERS

CHAPTER I

Activity, structural features and *in silico* digestion of antidiabetic peptides

ABSTRACT

Food antidiabetic peptides inhibit the enzymes involved in the regulation of the glycemic index (e.g. α-amylase, α-glucosidase and dipeptidyl peptidase-IV (DPP-IV)). This work reviews the antidiabetic peptide sequences reported in the literature, with activity confirmed by using synthetic peptides, and critically discusses their structural features. Moreover, it provides an overview of the potency of *in silico* analysis tools to predict the *in vitro* antidiabetic activity of DPP-IV-inhibitory peptides. In addition, the potential degradation of the most active peptides during digestion was evaluated *in silico*. Therefore, this work advances our understanding on the structure-activity relationship of antidiabetic peptides and provides new insights on their stability during digestion.

JOURNAL PAPER: Berraquero-García, C., Rivero-Pino, F., Ospina, J. L., Pérez-Gálvez, R., Espejo-Carpio, F. J., Guadix, A., García-Moreno, P. J., & Guadix, E. M. (2023). Activity, structural features and *in silico* digestion of antidiabetic peptides. *Food Bioscience*, *55*, 102954. https://doi.org/10.1016/j.fbio.2023.102954 (IF: 4.8; Category: Food Science and Technology; Position: 36/173; Q1)

1. Introduction

Type 2 diabetes mellitus (T2DM) is characterized by the combined effect of insufficient insulin production and insulin resistance (i.e., inability of the organism to react to the insulin action) (Axelsson et al., 2017). Diabetes is the result of a deficient absorption of glucose, which is provoked by both genetic and environmental factors, such as nutritional habits. Insulin administration is the main treatment available to date. However, it is injected subcutaneously and cannot be orally administered since the active compound is degraded by digestive juices, hindering its easy use for patients (Howard-Thompson et al., 2018).

Alternatively, diabetes could be tackled by acting on the enzymes involved in the carbohydrate hydrolysis, such as the α-amylase and α-glucosidase (Mustad et al., 2020). By inhibiting these enzymes, carbohydrate digestion is delayed and blood sugar level lowered (S. et al., 2019). Hence, inhibitors of α-glucosidase and α-amylase, have been considered first-line medications for the management of T2DM. These synthetic inhibitors (i.e., acarbose, miglitol and voglibose) do not cause hypoglycemia and have a high safety profile; but they cause undesired gastrointestinal side-effects, limiting their administration for a long period (Kaur et al., 2021; Scheen, 2003).

Research into the pathophysiology of T2DM has led to the introduction of new medication approaches like those based on the inhibition of dipeptidyl peptidase IV (DPP-IV) (Ahmad & Chowdhury, 2019). DPP-IV regulates the insulin secretion, glucagon synthesis and gastric emptying by rapid degradation of incretins (i.e., Glucagon-like peptide 1, GLP-1, and Gastric Inhibitory Peptide, GIP) (Kazakos, 2011; Lammi et al., 2018; Pais et al., 2016). DPP-IV inhibitors are drugs able to limit the degradation of GLP-1 and GIP, and thus, increasing the half-life of incretins, enabling to achieve an adequate metabolic condition. They have a good general safety and tolerability profile and have demonstrated to be effective in improving glycemic control but may present risk of acute pancreatitis (Deacon, 2020).

Despite the availability of various drugs for diabetes treatment, extensive research is still being conducted in the hopes of discovering useful, naturally derived molecules, free of side effects and toxicity (Park & Jang, 2017). Bioactive peptides derived from animal and plant proteins have recently attracted significant attention due to their multifaceted health benefits (Antony & Vijayan, 2021). The most widely used technologies to produce bioactive peptides are microbial fermentation and enzymatic hydrolysis (Cruz-Casas et al., 2021). Enzymatic hydrolysis might release bioactive peptides and may improve technological aspects of the protein, facilitate the digestibility by increasing the available N-terminal sites and decrease the antigenicity by degrading the allergenic epitopes (Rivero-Pino et al., 2020).

Food-derived peptides have been proven to exert different biological activities (El-Sayed et al., 2019; Karami & Akbari-adergani, 2019). It has been demonstrated that their bioactivity is determined by the specific amino acid sequence and the relative number of certain

residues (e.g., hydrophilic, hydrophobic, or aromatic) (Sánchez & Vázquez, 2017) within the peptide. Besides, they may be free from serious side-effects since they are obtained from food sources that have been safely consumed over the years (Daliri et al., 2017). Bioactive peptide sequences usually range in length from two to twenty amino acids, although longer peptides have also been reported (Korhonen & Pihlanto, 2006). Peptides displaying antidiabetic activity have normally low molecular weight, whose concentration and further isolation from the crude protein hydrolysate is challenging. To this regard, bioinformatic analyses play an essential role in predicting and identifying potentially bioactive compounds in this area. Computer simulation (*in silico*) might be a useful tool to predict the potential of peptide sequences such as DPP-IV inhibitors at a low-cost, which may help identify the relationship between peptide structure and its function. Other *in silico* tools can conduct simulated digestion on protein or peptide sequences, which is useful to design a targeted-hydrolysis process or to ensure that the sequence of a given peptide is not degraded during gastrointestinal digestion (Barati et al., 2020).

Hence, the aim of this review was to critically discuss the activity, structural features and *in silico* digestion of previously reported antidiabetic peptides. Furthermore, the potential of *in silico* tools to predict the *in vitro* antidiabetic activity of peptides was presented.

2. α-Amylase inhibitory peptides

α-Amylase (EC 3.2.1.1) is a digestive enzyme, secreted from the salivary andpancreatin glands, that hydrolyzes α-1,4 glycosidic bonds of complex carbohydrates, both linear and branched, into oligosaccharides (Figure 1A). α-Amylase is responsible for starch digestion, thus inhibiting its activity will reduce the glucose spike in ostprandial hyperglycemia (Kaur et al., 2021).

Therefore, a literature review of the peptide sequences exhibiting α-amylase inhibitory activity by searching in Scopus and Pubmed databases (period between 2015 and March 2022) was carried out. The following keywords were used: "antidiabetic peptide", "α-amylase inhibitory peptide", "synthetic antidiabetic peptide" and "hydrolysis antidiabetic peptide". Only studies reporting experimental IC_{50} value of the peptides identified were selected. Table 1 provides the complete list of α-amylase inhibitory peptides identified recently in literature, which were arranged by protein source and IC_{50} (μM).

The total number of peptide sequences with available *in vitro* values of α-amylase inhibitory activity is limited in the literature, reporting only 18 sequences with experimental IC_{50}. Most of the sequences identified were obtained from plant substrates, reflecting the focus on sustainable protein sources such as plants and algae, which has been a trend in the last years. Although some studies based on animal protein sources were found, they have been disregarded due to their

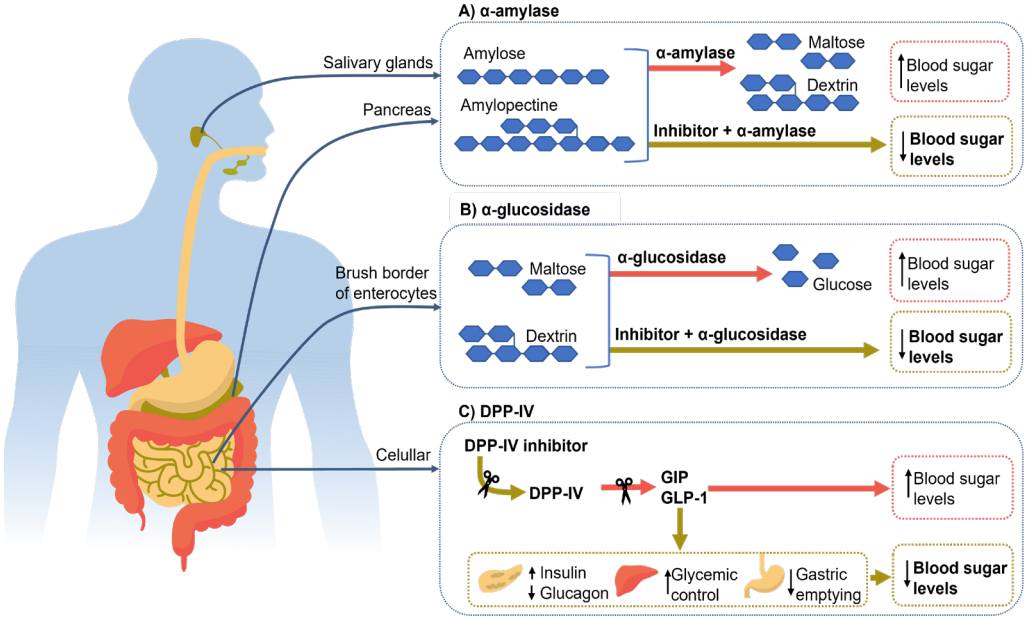

Figure 1. Inhibition mechanisms of A) α-amylase, B) α-glucosidase and C) DPP-IV for the control of T2DM.

antiquity (Z. Yu et al., 2012) or because no sequence identification was carried out (L. Liu et al., 2013; Kumar et al., 2018). Acarbose is the most common positive control referenced, with IC_{50} values ranging from 100 to 774.47 μM (Xiong et al., 2020). This wide difference shows a lack of harmonization of the analysis, implying a possible misrepresentation in the results found and highlighting the need for standard methods.

IC_{50} values for the peptides reported in literature range from 0.02 to 2000 μM (Table 1). Sequences presenting lower IC_{50} values shared common attributes, which could be related to the hydrolysis procedure. The protease employed in the hydrolysis is a key parameter to release antidiabetic peptides. In this regard, most of the sequences reported were obtained with Protamex, individually or in combination with other proteases. Protamex is a broad-spectrum endo-protease which cleaves preferably hydrophobic and aromatic residues (i.e., L, F, and V among others) (Ustunol, 2015).

Peptide FFRSKLLSDGAAAAKGALLPQYW had the lowest IC_{50}. It was obtained by hydrolysis of cumin seed protein with Protamex at pH 8 and 42.6 °C (Siow & Gan, 2016). Other studies (Esfandi et al., 2022, Ngoh & Gan, 2018) hydrolyzed pinto beans and oat meal at pH 7.5 and 50 °C with both Protamex and papain (Esfandi et al., 2022), a cysteine protease which cleaves positively charged amino acids, such as A, K, and residues following F (Vatić et al., 2020) . The remaining proteases reported were both endopeptidases of broad specificity: Alcalase (J.

Wang et al., 2020) and pepsin (Admassu et al., 2018). Alcalase preferences hydrophobic and aromatic residues, while pepsin shows specificity towards the Ct of F and L (Ahn et al., 2013; Tang et al., 2018). Peptides released by these enzymes showed low inhibitory activity (IC_{50} = 2000 - 2620 μM).

Sequences LRSELAAWSR, GVPMPNK and RNPFVFAPTLLTVAAR were extracted from *Spirulina platensis* by ultrasound coupled with subcritical water (USW) technology (S. Hu et al., 2019). Microbial fermentation was used to obtain the tripeptide IPP from Parmigiano-Reggiano Cheese (Martini et al., 2021). These peptides presented IC_{50} values of 264.0 - 763.5 μM. In general, there is little information on the production of α-amylase inhibitory peptides by enzymatic hydrolysis. Further work is needed for the isolation of active sequences by enzymatic processing, employing new proteases of different specificity.

In attempt to gain more insights into the activity of α-amylase inhibitory peptides, the most frequently reported structural features for bioactive peptides were studied and linked to their activity, namely: their average peptide chain length (PCL), number of hydrophobic residues, ratio of hydrophobic to total residues, pI, presence of L and P in the last two positions at the Nt (L in Nt, P in Nt) and estimated solubility (Ngoh & Gan, 2018) (Table 1).

Identified sequences have a wide PCL distribution, 3 - 23 residues, with ~70% of them being 3-10 residues long. Hydrophobic interactions and hydrogen bonds also play a large part in substrate binding to α-amylase (Tysoe et al., 2016). All peptides, except for YFDEQNEQFR (Esfandi et al., 2022), contained over 44% of hydrophobic amino acids. Furthermore, presence of these residues (i.e., P and L) at the Nt of the sequences has been proposed as an important characteristic of α-amylase inhibitors (Ngoh & Gan, 2018). The Nt last two positions were studied, finding that 6 out of the 18 peptides contained L and 7 contained P. Other important identifying factor of these peptides is the presence of F residues at either end (Ngoh & Gan, 2016), however only 2 of the peptides met this characteristic.

The pI, net charge and estimated solubility of the peptides were also calculated. pI values of 5-6 have been reported to lower the degradation rate of the peptides by deamidation (Keservani et al., 2015). Twelve of the peptides identified were estimated *in silico* to have poor solubility in water , adding difficulty to its use as a functional ingredient due to its technological limitations. This low solubility is not only affected by pI but also by the hydrophobic amino acids content (A, V, I, L, M, Y, W, G, and P). Indeed, peptides with poor solubility contained at least 50% of hydrophobic amino acids. Out of 18 peptides, 11 had positive net charge at pH 7 (Table 1), which could positively affect their absorption by transcytosis transport according to previous studies on cell models (Amigo & Hernández-Ledesma, 2020).

The most active peptide identified had a PCL of 23 residues (Siow & Gan, 2016), making it the longest sequence. Its hydrophobic amino acids content was ca. 61% and did not present L or P residues at the Nt. Nonetheless, there are only a few studies evaluating the kinetics and inhibition mode of α-amylase inhibitory peptides. Among the few studies, Admassu et al. (Admassu et al., 2018) investigated the α-amylase inhibition mechanism for red seaweed peptides, using the Lineweaver-Burk double reciprocal of the velocity-substrate plot, observing a near non-competitive mode of inhibition. The authors reported that the peptides bounded to the allosteric site of the enzyme leading to conformation changes in the enzyme, which did not allow the bind of the substrate to the enzyme or inhibited the enzyme activity to convert substrate into product. Using the same approach, Ngoh et al. (Ngoh et al., 2017) studied the α-amylase inhibition mechanism of five Pinto bean peptides, revealing that three of them displayed uncompetitive inhibition when binding to the (α-amylase)-starch complex. This binding altered the α-amylase structure and resulted in the detachment of starch from the complex, thereby preventing its hydrolysis. Interestingly, the remaining two peptides exhibited an unconventional inhibition mechanism, as they required a higher concentration of substrate for binding to either the substrate or the enzyme, which resulted in the inability of starch and enzyme to bind, thus leading to the inhibition. Another study conducted on soybean protein investigated the inhibition mechanism for four peptides (Awosika & Aluko, 2019). Three of them exhibited mixed inhibition, displaying both competitive and uncompetitive modes, indicating that they can bind to both the free enzyme and the enzyme-substrate complex. These two modes of inhibition could act synergistically if two peptides bind simultaneously. Another peptide identified in soybeans was a pure uncompetitive inhibitor, which specifically binds to non-carbohydrate binding sites rather than the active site. Therefore, further analysis identifying and evaluating peptides experimentally is needed to draw conclusions about the structure-activity relationship of α-amylase inhibitory peptides. The lack of research in this area can be explained by the lower physiological relevance of these inhibitors compared to α-glucosidase and DPP-IV inhibitory peptides.

Table 1. Summary and structure analysis of α-amylase inhibiting peptides found in literature.

Type	Source	Sequence	Enzymatic treatment	IC_{50} (μM)	PCL	% HPO AA	L in Nt	P in Nt	pI	Net charge	Estimated solubility	Reference
Plant	Cumin seed (*Cuminum cyminum*)	FFRSKLLSDGAAAAKGALLPQYW	Protamex	0,02	23	60,87			10,20	2	Poor	(Siow & Gan, 2016)
Plant	Cumin seed (*Cuminum cyminum*)	DPAQPNYPWTAVLVFRH	Protamex	0,03	17	52,94		DP	7,78	0.1	Poor	(Siow & Gan, 2016)
Plant	Cumin seed (*Cuminum cyminum*)	RCMAFLLSDGAAAAQQLLPQYW	Protamex	0,04	22	59,09			5,90	-0.1	Poor	(Siow & Gan, 2016)
Plant	Oat meal (*Avena sativa*)	YFDEQNEQFR	Papain & Protamex	37,5	10	0,00			3,69	-2	Good	(Esfandi et al., 2022)
Plant	Oat meal (*Avena sativa*)	NINAHSVVY	Papain & Protamex	67,3	9	44,44			7,38	0.1	Poor	(Esfandi et al., 2022)
Plant	Oat meal (*Avena sativa*)	RALPIDVL	Papain & Protamex	72,8	8	75,00			6,35	0	Good	(Esfandi et al., 2022)
Plant	Spirulina platensis (*Spirulina platensis*)	LRSELAAWSR	No hydrolysis	264,0	10	50,00	LR		10,68	1	Good	(Hu et al., 2019)
Plant	Spirulina platensis (*Spirulina platensis*)	GVPMPNK	No hydrolysis	318,3	7	71,43			10,12	1	Good	(Hu et al., 2019)
Plant	Spirulina platensis (*Spirulina platensis*)	RNPFVFAPTLLTVAAR	No hydrolysis	607,8	16	56,25			12,10	2	Poor	(Hu et al., 2019)
Animal	Parmigiano-Reggiano Cheese	IPP	Ripening at 12-30 months	763,5	3	100,00		IP	13,10	0	Poor	(Martini et al., 2021)

(Continued) **Table 1.** Summary and structure analysis of α-amylase inhibiting peptides found in literature.

Type	Source	Sequence	Enzymatic treatment	IC_{50} (μM)	PCL	% HPO AA	L in Nt	P in Nt	pI	Net charge	Estimated solubility	Reference
Plant	Walnut (*Juglans mandshurica*)	LPLLR	Alcalase	2000	5	80,00%	LP	LP	10.84	1	Poor	(J. Wang et al., 2020)
Seaweed	Red Seaweed (*Porphyra spp*)	GGSK	Pepsin	2580	4	50,00%			10.12	1	Good	(Admassu et al., 2018)
Seaweed	Red Seaweed (*Porphyra spp*)	ELS	Pepsin	2620	3	33,33%	EL		1.01	-1	Good	(Admassu et al., 2018)
Plant	Pinto bean (*Phaseolus vulgaris*)	LSSLEMGSLGALFVCM	Protamex	10030	16	62,50%	LS		1,00	-1.1	Poor	(Ngoh & Gan, 2018)
Plant	Pinto bean (*Phaseolus vulgaris*)	PLPWGAGF	Protamex	15730	8	87,50%	PL	PL	4.15	0	Poor	(Ngoh & Gan, 2018)
Plant	Pinto bean (*Phaseolus vulgaris*)	PLPLHMLP	Protamex	15800	8	87,50%	PL	PL	8.26	0.1	Poor	(Ngoh & Gan, 2018)
Plant	Pinto bean (*Phaseolus vulgaris*)	PPHMGGP	Protamex	19830	7	85,71%		PP	8.26	0.1	Poor	(Ngoh & Gan, 2018)
Plant	Pinto bean (Phaseolus vulgaris)	PPHMLP	Protamex	23330	6	83,33%		PP	8.26	0.1	Poor	(Ngoh & Gan, 2018)

IC_{50} (μM): half maximal inhibitory activity, expressed in μM
PCL: peptide chain length
HPO: Hydrophobic aminoacids
L in Nt: presence of leucine in the last two positions of the N-terminus
P in Nt: presence of proline in the last two positions of the N-terminus
pI: isoelectric point
Net charge was determined at pH 7.

3. α-Glucosidase inhibitory peptides

α-Glucosidase (EC 3.2.1.20), which is found in the epithelial mucosa of the small intestine (brush border of the enterocytes), degrades the oligosaccharides produced by α-amylase, releasing free glucose molecules from terminal, non-reducing (1-4)-linked α-D glucose residues (Figure 1B). Hence, inhibition of α-glucosidase allows reducing the release of glucose from ingested carbohydrates and its absorption, which leads to a decrease of postprandial blood glucose levels (Hossain et al., 2020).

The sequences of α-glucosidase inhibitory peptides identified in the literature were studied, following the search criteria previously mentioned and including "α-glucosidase inhibitory peptide" as keyword (Table 2). According to the literature research, α-glucosidase inhibitory peptides were isolated from both animal and plant sources. It is worth mentioning that, among the animal sources, one of the most used substrates were insects, mainly mealworm and desert locust (Y. Zhang et al., 2016; Zielińska et al., 2020). Interest in insects as a source of bioactive peptides dated back to 2005 (Vercruysse et al., 2005), although their use for antidiabetic peptides has started recently (Nongonierma & FitzGerald, 2017; Rivero Pino et al., 2020).

Acarbose is the reference control most frequently reported in literature but, inconsistencies were identified concerning the IC_{50} values, which ranged from 3.34 μM (Sulistiyani et al., 2016) to 2338.90 μM (Zhao et al., 2020). This is in line with the data found for α-amylase inhibitory peptides. Although the reason for these differences could not be reliably determined, it can be estimated that they are due to the use of different methods to perform the inhibition analysis, sources of acarbose and enzyme/substrate ratios. This non-conformity in the performance of analysis should be considered, since the α-glucosidase inhibitory peptides identified present a wide range of IC_{50}, from 7.93 to 2000 μM (Table 2). This implies a difference of 700-fold between the lowest and the highest value, which might be related not only to real differences in peptides activity but also to lack of harmonization on the methods. Most of the α-glucosidase inhibitory peptides identified so far in the literature were produced enzymatically by digestive proteases (i.e., trypsin, chymotrypsin, and pepsin) (Ibrahim et al., 2018b). Trypsin is a very specific protease, cleaving only R and K residues, whereas chymotrypsin preferentially recognizes bulky aromatic residues such as F, Y, and W (Olsen et al., 2004). Pepsin shows a narrower specificity, cleaving after F and L residues (Ahn et al., 2013). The hydrolysis conditions, including those set for the *in silico* simulations, were physiological conditions. The peptides released presented IC_{50} values of 7.93 - 1215.42 μM. The most active peptide sequence identified–FDPFPK–was obtained by simulating oral, gastric, and intestinal digestion (Zielińska et al., 2020).

Other authors produced α-glucosidase inhibitory peptides employing different commercial proteases. For instance, two recent works report inhibitory peptides obtained with Alcalase

at pH 9 and 50 °C, reporting three peptides from soybean protein with IC_{50} values ranging 162.29 - 237.43 μM (J. Wang et al., 2020; R. Wang et al., 2019), and one peptide from walnut seeds with moderate inhibitory potency, 2000 μM (J. Wang et al., 2020; R. Wang et al., 2019). Other studies hydrolyzed soft-shelled turtle employing a variety of commercial proteases (i.e., Alcalase, Flavourzyme, papain and neutrase) at optimal conditions (Qiu et al., 2021). Papain hydrolysates were fractionated by ultrafiltration and reverse chromatography, allowing the identification of three inhibitory peptides (HNKPEVEVR, ARDASVLK, SGTLLHK), which presented the highest α-glucosidase inhibitory activity with IC_{50} values of 162.29 - 237.43 μM.

Several studies used alternative technologies to produce inhibitory peptides. To this regard, the sequences VVDLVVFFAAAK, TAELLPR, CGKKFVR and AVPANLVDLNVPALLK were obtained from dark tea protein (Zhao et al., 2020) using centrifuge ultrafiltration through 30 kDa and further purification by high-performance liquid chromatography (HPLC). The sequence VVDLVVFFAAAK displayed the highest potency, with IC_{50} = 33.93 μM, while the other peptides presented low inhibition, IC_{50} above 500 μM. As mentioned above, other studies employed subcritical water to extract antidiabetic peptides from *Spirulina platensis* (S. Hu et al., 2019), identifying some bioactive sequences which were tested for their α-glucosidase inhibition (IC_{50} from 92.78 to 204.18 μM). Finally, the IPP peptide obtained by ripening Parmigiano-Reggiano Cheese was also found to have inhibitory capacity for α-glucosidase with IC_{50} 764.50 μM (Martini et al., 2021).

Some previous efforts have been put to study the structure-activity relationship of α-glucosidase inhibitory peptides (Ibrahim et al., 2018b; Mojica & De Mejía, 2016), indicating that the amino acid composition of the peptide, mainly residues containing a hydroxyl group on their sidechain at their Nt, and positive net charge were important characteristics. We found a large deviation in the PCL of α-glucosidase inhibitory peptides, ranging from 2 to 16 amino acids. Nevertheless, 80% of the peptides were found to have PCLs of 2-10 residues (Table 2). The three most active peptides have PCLs of 6 (FDPFPK, IC_{50} = 7.93 μM), and 9 (AAAPVAVAK, IC_{50} = 13.70 μM, AIGVGAIER, IC_{50} = 14.73 μM) residues. Meanwhile, the three least active peptides have a length of 5 (LPLLR, IC_{50} = 2000.00 μM), 11 (YINQMPQKSRE, IC_{50} = 1215.42 μM) and 7 residues (STFQQQMW, IC_{50} = 1190.94 μM), which indicates that peptide size is not the main factor affecting its α-glucosidase inhibitory activity.

The mechanisms involved in the activity of α-glucosidase inhibitory peptides are not yet well elucidated, but previous studies with quantitative structure-activity relationship (QSAR) models have revealed that hydrophobic amino acid residues of peptides predominantly interact with residues in the active site of α-glucosidase (Acquah et al., 2018). Overall, the presence of hydrophobic amino acids was common in the peptides identified and, although we found a large deviation on their relative content in the bioactive sequence, ranging from 0 (GSR, IC_{50}= 20.4 μM) to 100% of content of hydrophobic amino acids (IPP, IC_{50} = 764.5 μM). Despite

this variability, our study concluded that 75% of the peptides analyzed presented 40%-60% of hydrophobic amino acids in their sequences (Table 2).

Furthermore, previous studies have determined that peptides inhibiting α-glucosidase might have diverse molecular features (Ibrahim et al., 2018b; Z. Yu et al., 2011; Zielińska et al., 2020). According to the literature the presence of S, T, and Y residues in the last two positions of the Nt (S in Nt, T in Nt and Y in Nt) and that of P, A and M in the last two positions of the Ct (P in Ct, A in Ct, and M in Ct) affected positively the inhibitory activity of the peptides due to inhibitory peptides binding mostly to the α-glucosidase catalytic domain by hydrogen bonds and electrostatic interactions (González-Montoya et al., 2018). Table 2 shows that only a minority of the peptides met any of these conditions, where the most repeated factor was the presence of P in the last two positions of the Ct.

We determined the pI, net charge, and estimated solubility of the peptides, with 22 out of the 39 peptides listed in Table 2 showing good solubility. As for the pI, we found that only 3 of the 39 peptides presented pI in the range of the intestinal pH (7-8.5), which may negatively affect their solubility. Regarding the net charge, 29 of the 39 peptides identified in literature presented a net charge of either 0 or +1, 7 peptides showed a net positive charge different than 1 and only 3 peptides showed a negative net charge. This agrees with previous studies (González-Montoya et al., 2018), which proposed that negatively charged peptides may exhibit limited α-glucosidase inhibitory activity. The most active peptide (FDPFPK) presented PCL = 6 and 33% content of hydrophobic amino acids. After analyzing the structural characteristics previously mentioned, we only found the presence of P in the second to last position at the Ct. This peptide showed good solubility and a pI of 6.39 (net charge of zero at pH 7).

The Lineweaver-Burk double reciprocal plot has also been employed to determine the mechanisms by which bioactive peptides can inhibit α-glucosidase. Ibrahim et al. (Ibrahim et al., 2018a) investigated computationally designed bioactive peptides and found that the two most active peptides against α-glucosidase exhibited uncompetitive and noncompetitive inhibition modes. Specifically, the peptide SVPA demonstrated uncompetitive inhibition by binding to the substrate-enzyme complex. On the other hand, the peptide SEPA bound to a portion of the active site, but due to the presence of a valine residue, it was unable to fully interact with the active site, resulting in noncompetitive inhibition. A study based on antidiabetic peptides derived from fermented rice bran (J. Hu et al., 2023) demonstrated that the most active sequence against α-glucosidase exhibited a noncompetitive inhibition mechanism. It appears that the mechanism involves reversible bonding with the Asp616 and His674 residues of the enzyme's active site, although the exact mechanism remains unclear. It is worth noting that the current literature on the kinetics and inhibition mode of α-glucosidase inhibitory peptides remains limited. Further work is needed to elucidate the molecular interactions and binding mechanisms of these sequenced peptides with reported activity.

Table 2. Summary and structure analysis of α-glucosidase inhibiting peptides.

Type	Source	Sequence	Enzymatic treatment	IC_{50} (μM)	PCL	% HPOAA	S in Nt	T in Nt	Y in Nt	P in Ct	A in Ct	M in Ct	pI	Net charge	Estimated solubility	Reference
Animal	Desert locus (*Schistocerca gregaria*)	FDPFPK	GI digestion	7,93	6	33,33				PK			6,39	0	Good	(Zielińska et al., 2020)
Animal	Mealworm (*Tenebrio molitor*)	AAAPVAVAK	GI digestion	13,70	9	88,89					AK		10,19	1	Poor	(Zielińska et al., 2020)
Animal	Desert locus (*Schistocerca gregaria*)	AIGVGAIER	GI digestion	14,73	10	50,00							6,93	0	Good	(Zielińska et al., 2020)
Plant	Almond oil manufacture residue (*Prunus dulcis*)	WH	Prote Ax and protease M	17,03	2	50,00							7,69	0.1	Poor	(Gu et al., 2020)
Animal	Silkworm pupae (*Bombyx mori*)	SQSPA	In silico GI digestion	20,00	5	40,00	SQ			PA	PA		3,36	0	Good	(Y. Zhang et al., 2016)
Plant	Soybean protein (*Glycine max*)	GSR	Trypsin	20,40	3	0,00	GS						10,84	1	Good	(Jiang et al., 2018)
Plant	Changium Root (*Changii radix*)	KVIISAPSKDAPMF	Simulated GI digestion	21,28	15	53,33							9,74	1	Good	(L. Liu et al., 2021)
Animal	Desert locus (*Schistocerca gregaria*)	GKDAVIV	GI digestion	22,74	7	57,14							6,63	0	Good	(Zielińska et al., 2020)
Animal	Cricket (*Grylloides sigillatus*)	KVEGDLK	GI digestion	23,31	7	28,57							6,71	0	Good	(Zielińska et al., 2020)
Plant	Almond oil manufacture residue (*Prunus dulcis*)	WS	Prote Ax and protease M	24,71	2	50,00	WS						3,61	0	Poor	(Gu et al., 2020)
Animal	Mealworm (*Tenebrio molitor*)	NYVADGLG	GI digestion	25,21	9	33,33			NY				0,68	-1	Poor	(Zielińska et al., 2020)

(Continued) **Table 2.** Summary and structure analysis of α-glucosidase inhibiting peptides.

Type	Source	Sequence	Enzymatic treatment	IC_{50} (μM)	PCL	% HPOAA	S in Nt	T in Nt	Y in Nt	P in Ct	A in Ct	M in Ct	pI	Net charge	Estimated solubility	Reference
Animal	Mealworm (*Tenebrio molitor*)	AGDDAPR	GI digestion	27,77	7	42,86				PR			3,71	-1	Good	(Zielińska et al., 2020)
Animal	Cricket (*Grylloides sigillatus*)	IIAPPER	GI digestion	28,75	8	62,50							6,87	0	Good	(Zielińska et al., 2020)
Plant	Dark tea protein (*Camellia sinensis*)	VVDLVFFAAAK	No hydrolysis	33,93	11	63,64					AK		6,60	0	Poor	(Zhao et al., 2020)
Animal	Soft-shelled turtle egg (*Pelodiscus sinensis*)	HNKPEVEVR	Papain	56,00	9	33,33							7,56	0.1	Good	(Qiu et al., 2021)
Animal	Cricket (*Grylloides sigillatus*)	LAPSTIK	GI digestion	62,55	7	57,14							10,12	1	Good	(Zielińska et al., 2020)
Animal	Silkworm pupae (*Bombyx mori*)	QPGR	*In silico* digestion	65,80	4	25,00							10,55	1	Good	(Y. Zhang et al., 2016)
Plant	Spirulina platensis (*Spirulina platensis*)	RNPFVFAPTLLTVAAR	No hydrolysis	92,78	17	52,94							12,10	2	Poor	(S. Hu et al., 2019)
Plant	Quinoa (*Chenopodium quinoa*)	IQAEGGLT	Simulated GI digestion	109,48	8	37,50							0,97	-1	Poor	(Vilcacundo et al., 2017)
Plant	Spirulina platensis (*Spirulina platensis*)	LRSELAAWSR	No hydrolysis	112,96	10	50,00							10,68	1	Good	(S. Hu et al., 2019)
Plant	Soybean protein (*Glycine max*)	WLRL	Alkaline proteinase	162,29	4	75,00							10,72	1	Poor	(R. Wang et al., 2019)
Plant	Soybean protein (*Glycine max*)	SWLRL	Alkaline proteinase	182,05	5	60,00	SW						10,57	1	Poor	(R. Wang et al., 2019)

(Continued) **Table 2.** Summary and structure analysis of α-glucosidase inhibiting peptides.

Type	Source	Sequence	Enzymatic treatment	IC_{50} (μM)	PCL	% HPOAA	S in Nt	T in Nt	Y in Nt	P in Ct	A in Ct	M in Ct	pI	Net charge	Estimated solubility	Reference
Animal	Soft shelled turtle egg (*Pelodiscus sinensis*)	ARDASVLK	Papain	195,00	8	50,00							10,18	1	Good	(Qiu et al., 2021)
Plant	Spirulina platensis (*Spirulina platensis*)	GVPMPNK	No hydrolysis	204,18	8	50,00							10,12	1	Good	(S. Hu et al., 2019)
Animal	Silkworm pupae (*Bombyx mori*)	NSPR	*In silico* digestion	205,00	4	25,00	NS			PR			10,42	1	Good	(Y. Zhang et al., 2016)
Plant	Soybean protein (*Glycine max*)	LLPLPVLK	Alkaline proteinase	237,43	8	87,50							10,12	1	Poor	(R. Wang et al., 2019)
Animal	Soft-shelled turtle egg (*Pelodiscus sinensis*)	SGTLLHK	Papain	289,00	7	28,57	SG						9,86	1.1	Good	(Qiu et al., 2021)(
Animal	Eggyolk protein by-product (*Gallus domesticus*)	VTGRFAGHPAAQ	Pepsin	301,73	12	41,67		VT			AQ		10,81	1.1	Poor	(Zambrowicz et al., 2015)
Animal	Eggyolk protein by-product (*Gallus domesticus*)	YINQMPQKSREA	Pepsin	310,31	12	33,33			YI		EA		9,49	1	Good	(Zambrowicz et al., 2015)
Plant	Soybean protein (*Glycine max*)	EAK	Trypsin	520,20	3	33,33					AK		6,85	0	Good	(Jiang et al., 2018)
Plant	Changium Root (*Changii Radix*)	SQHISTAGMEASGTSNMKF	Simulated GI digestion	529,74	20	25,00	SQ						7,54	0.1	Poor	(L. Liu et al., 2021)
Plant	Dark tea protein (*Camellia sinensis*)	TAELLPR	No hydrolysis	538,17	7	57,14		TA		PR			6,55	0	Good	(Zhao et al., 2020))
Animal	Silkworm pupae (*Bombyx mori*)	QPPT	*In silico* digestion	560,00	4	50,00				PT			3,40	0	Poor	(Y. Zhang et al., 2016)

(Continued) **Table 2.** Summary and structure analysis of α-glucosidase inhibiting peptides.

Type	Source	Sequence	Enzymatic treatment	IC_{50} (μM)	PCL	% HPO AA	S in Nt	T in Nt	Y in Nt	P in Ct	A in Ct	M in Ct	pI	Net charge	Estimated solubility	Reference
Plant	Dark tea protein (*Camellia sinensis*)	CGKKFVR	No hydrolysis	621,27	7	14,29							10,82	2.9	Good	(Zhao et al., 2020)
Plant	Dark tea protein (*Camellia sinensis*)	AVPANLVDLNVPALLK	No hydrolysis	625,38	16	75,00							6,69	0	Poor	(Zhao et al., 2020)(
Animal	Parmigiano-Reggiano Cheese	IPP	Ripening at 12-30 months	764,50	3	100,00				PP			3,83	0	Poor	(Martini et al., 2021)
Plant	Changium Root (*Changii Radix*)	STFQQMW	Simulated GI digestion	1190,94	8	25,00	ST	ST					3,34	0	Poor	(L. Liu et al., 2021)
Animal	Eggyolk protein by-product (*Gallus domesticus*)	YINQMPQKSRE	Pepsin	1215,42	11	27,27			YI				9,49	1	Good	(Zambrowicz et al., 2015)
Plant	Walnut (*Juglans mandshurica*)	LPLLR	Alcalase	2000,00	5	80,00							10,84	1	Poor	(J. Wang et al., 2020)

IC_{50} (μM): half maximal inhibitory activity, expressed in μM
PCL: peptide chain length
HPO: Hydrophobic aminoacids
S in Nt: presence of serine in the last two positions of the N-terminus
T in Nt: presence of threonine in the last two positions of the N-terminus
Y in Nt: presence of tyrosine in the last two positions of the N-terminus
T in Ct: presence of proline in the last two positions of the C-terminus
A in Ct: presence of alanine in the last two positions of the C-terminus
M in Ct: presence of methionine in the last two positions of the C-terminus
pI: isoelectric point determined by Innovagen's peptide calculator PepCalc
Net charge was determined at pH 7 by Innovagen's peptide calculator PepCalc
Estimated solubility: solubility is estimated since Innovagen's tool does not take into consideration factors such as peptide concentration.

4. DPP-IV inhibitory peptides

In regular metabolism, food intake results in the liberation of insulin secretion hormones known as incretins (GLP-1 and GIP) that would affect numerous target tissues in the body acting as endocrine signal to the pancreas. Pancreatic β-cells increase insulin concentration in the bloodstream, with suitable insulin secretion being a key-factor to maintain physiological blood glucose level. Furthermore α-pancreatic cells would reduce glucagon concentration, avoiding glucose production in the liver. Then, blood glucose concentration is maintained at healthy levels(Rivero-Pino et al., 2020). The enzyme DPP-IV would degrade incretins in order to regulate its concentration(Kshirsagar et al., 2011). Nonetheless, T2DM patients have insufficient insulin level in the bloodstream, and they end up by developing insulin resistance, leading to an increase in glucose blood level inadequate to the organism. According to this physiological background, the inhibition of DPP-IV leads to an increase of the half-life of these incretins, causing insulin secretion to be stimulated and subsequently, the blood glucose level is adequately regulated (Nongonierma & FitzGerald, 2019). (Figure 1C).

Thus, literature was searched for sequences of DPP-IV inhibitory peptides, by following previously described search criteria and including "dipeptidyl peptidase IV inhibitory peptide" as keyword. The total number of peptide sequences inhibiting DPP-IV was 230 (data not shown). The 40 most active DPP-IV inhibitory peptides were selected based on their higher activity (Table 3), including only those with an IC_{50} value up to 20 times the value of tripeptide IPI, a very well-known DPP-IV inhibitor with IC_{50} = 3.5 μM which was chosen as reference (Nongonierma et al., 2018). The peptide sequences were identified from animal or plant origin, with IC_{50} values varying from 0.51 to 69.84 μM.

In contrast to peptides with α-glucosidase inhibitory activity, potential DPP-IV inhibitory peptides from insects have been identified (Rivero-Pino et al., 2021), although their activity has not been yet confirmed by measuring the DPP-IV inhibitory activity of the synthetic peptides. Moreover, plant sources, although gaining increasing interest, have not been studied so far as sources for DPP-IV inhibitory peptides. Thus, plant proteins, together with other sustainable sources such as insect or food by-products, present a great potential as substrate for antidiabetic peptides.

As for the enzymes used, 40% of the peptides selected were obtained by hydrolysis with Alcalase—a serine endopeptidase primarily consisting of subtilisin—alone or in combination with other proteases. Hydrolysis combining Alcalase with Flavourzyme, an enzyme cocktail mainly containing exo-peptidases (Merz et al., 2015), has been shown to be considerably efficient for obtaining DPP-IV inhibitory peptides. Previous authors employed a combination of Alcalase and Flavourzyme to hydrolyze boarfish flesh at pH 7 and 50 °C (Harnedy-Rothwell et al., 2020) and brewers' spent grain at pH 9 and 50 °C (Cermeño et al., 2019). The former identified 10 peptide sequences with IC_{50} values ranging from 3.49 to 68.13 μM, while brewers' spent grain hydrolysis produced 4 peptides with IC_{50} = 38.67 – 54.69 μM. The active sequence

GPAGPOGFPG (IC_{50} = 67.12 μM) was obtained from sheep skin hydrolysis with Alcalase (B. Wang et al., 2021). Hydrolysis of tilapia skin (T. Y. Wang et al., 2015) and salmon flesh (Li-Chan et al., 2012) with Flavourzyme at pH 7.0, and 50 °C released active sequences with IC_{50} ranging from 41.90 to 65.40 μM (Table 3).

Similarly to α-glucosidase inhibition, digestive enzymes were mostly reported in literature to produce DPP-IV inhibitory peptides. The most active peptides were obtained by hydrolysis of antler velvet from Cervidae employing a mixture of pepsin, trypsin, and chymotrypsin, under physiological conditions (Y. Yu et al., 2017). These peptides displayed high inhibitory potency, with IC_{50} values varying from 0.51 to 1.67 μM. Three active tripeptides (VPV, YPI and VPF) were obtained after simulated digestion of camel whey protein, with IC_{50} of 6.60, 35.0 and 55.10 μM, respectively (Nongonierma, Cadamuro, Le Gouic, et al., 2019).

Regarding the average peptide chain length of the 40 most active DPP-IV inhibitory peptides identified (Table 3), it ranged from 3 to 13 amino acids, with an average value of 6 residues. More precisely, 72% of the peptides presented between 3 to 6 amino acids. The three most active peptides have PCLs of 9 (GPAGPQGPR, IC_{50} = 0.51 μM), 10 (PPGLPGSPGQ, IC_{50} = 0.55 μM) and 7 residues (LPQPPQE, IC_{50} = 0.97 μM) (Y. Yu et al., 2017). Meanwhile, the three least active ones have a length of 13 (TQMVDEEIMEKFR, IC_{50} = 69.84 μM), 4 (GPSL, IC_{50} = 68.13 μM) and 10 residues (GPAGPOGFPG. IC_{50} = 67.12 μM).

Although the mechanisms involved in the activity of DPP-IV inhibitory peptides are not yet well elucidated, recent studies on structure-activity relationship analysis and sequential alignment of inhibitory peptides have demonstrated that the hydrophobicity of the amino acids played an important role in the inhibitory activity. Indeed, inhibitory compounds bind to DPP-IV enzyme through a variety of interactions such as salt bridges, hydrophobic interactions, and hydrogen bonds. The predominant mechanism is the interaction between the charged sub-pocket S2 of the DPP-IV enzyme and the Nt hydrophobic region of the inhibitory peptides (Acquah et al., 2018; González-Montoya et al., 2018). In this study, the presence of hydrophobic residues within the active sequences was quantified, finding that 75% of the peptides had a hydrophobic content over 80%, and only three of the sequences had a content of less than 50% in hydrophobic amino acids (QLRDIVDK, 37.5%; HPF, 33.3%; TQMVDEEIMEKFR, 30.8%).

Moreover, it has been suggested that the presence of amino acids with aromatic rings could improve the potency of DPP-IV inhibitors by forming hydrophobic interactions with the catalytic domain (Ojeda-Montes et al., 2018). After studying the amino acid content of the peptides, it was found that the most present amino acid within the sequences was P—a hydrophobic amino acid with an aromatic chain—appearing in 38 of the 40 peptides (95%). The presence of other aromatic amino acids in the identified peptides is lower, with only 33% of the studied peptides containing one aromatic amino acid different than P. Previous works (González-Montoya et al., 2018; Nongonierma & FitzGerald, 2013) have reported that the position of P in the first, second, third, or

fourth Nt position positively affects the inhibitory activity of the peptides. This is consistent among the peptides studied since we found that 80% of them had P in the last two positions (P in Nt), rising to 93% when considering the last 4 positions (P in Nt, 4 positions). The presence of A in the first or second position of the Nt (A in Nt), as well as the presence of aromatic amino acids in the last two positions of the Ct (F in Ct, W in Ct, and Y in Ct), have also been determined to positively affect their inhibitory activity (Hsieh et al., 2016). We searched for these characteristics but did not observe that they were repeated factors in the identified peptides (Table 3). For instance, 10% of the peptides analyzed presented A in Nt or F in Ct, only 5% presented Y in Ct, and none of the peptides contained W in Ct.

Studies on the pI, solubility, and charge of DPP-IV inhibitory peptides have been carried out with the aim of linking these characteristics with the activity of the peptides, however no clear correlation has been found yet (Kęska et al., 2019; Nongonierma et al., 2014). The peptides reported in this study had very low pI values (Table 3), with only 2 peptides having a pI higher than 7 (GPAGPQGPR, pI = 10.84 and HPF, pI = 7.56). Out of the 40 peptides identified, 13 showed a negative net charge, 29 presented a neutral net charge, and only one of the peptides was positively charged at pH 7. Interestingly and despite the high hydrophobicity of the peptides studied, 14 out of the 40 identified peptides showed good solubility. The most active peptide, GPAGPQGPR, was obtained by simulated gastric-pancreatic digestion of deer antler velvet with an IC_{50} of 0.51 μM. This peptide had a PCL of 9, 78% of hydrophobic amino acids and presented P in the second to last position of the Nt (Y. Yu et al., 2017). Table 4 highlights the main findings on the structure-activity relationship for antidiabetic peptides.

Most of the research dedicated to elucidating the inhibition mechanisms of the presented enzymes has focused on DPP-IV, revealing two clearly different mechanisms depending on peptide size. Peptides smaller than 1 kDa can directly interact with the active site of DPP-IV, resulting in competitive inhibition (Nongonierma & Fitzgerald, 2013b; You et al., 2022). This occurs because small peptides can easily access the enzyme's active site to bind. For example, tripeptides like IPR and VPW from *Chlorella vulgaris* (Zhu et al., 2017) have been shown to form hydrogen bonds with residues in the catalytic center of the enzyme and establish van der Waals interactions with both sockets (S1 and S2). Specifically, the presence of W at the N-terminus has been associated with increased interaction with the S1 socket. Another study on dipeptides derived from milk proteins (Nongonierma & Fitzgerald, 2013a) also demonstrated a competitive inhibition mechanism, with the exception of the dipeptide WV, which acted as a non-competitive inhibitor.

On the other hand, larger peptides can inhibit DPP-IV by interacting with its dimerization sites, leading to more complex mechanisms such as non-competitive or anti-competitive inhibition. This aligns with the findings of a study on 13-long peptides derived from goat milk casein, which demonstrated uncompetitive inhibition (Y. Zhang et al., 2015). However, the mechanisms behind the interaction of these larger peptides are still not fully understood (Nongonierma & FitzGerald, 2019).

Table 3. Summary and structure analysis of DPP-IV inhibiting peptides.

Type	Source	Sequence	Enzymatic treatment	IC_{50} (μM)	PCL	Score (DPP-IVi)	Stack DPPIV	% HPO AA	A in Nt	P in Nt	P in Nt*	F in Ct	W in Ct	Y in Ct	pI	Net charge	Estimated solubility	References
Animal	Velvet aqueous extract (Cervus elaphus)	GPAGPQGPR	Gastric-pancreatic digestion	0,51	9	320,88	0.47	77,78		GP	GPAG				10,84	0	Good	(Y. Yu et al., 2017)
Animal	Velvet aqueous extract (Cervus elaphus)	PPGLPGSPGQ	Gastric-pancreatic digestion	0,55	10	342,78	0.62	80,00		PP	PPGL				4,15	0	Poor	(Y. Yu et al., 2017)
Animal	Velvet aqueous extract (Cervus elaphus)	LPQPPQE	Gastric-pancreatic digestion	0,97	7	439,50	0.92	57,14		LP	LPQP				1,00	-1	Good	(Y. Yu et al., 2017)
Animal	Velvet aqueous extract (Cervus elaphus)	LPPLTAD	Gastric-pancreatic digestion	1,67	7	369,67	0.84	71,43		LP	LPPL				0,88	-1	Poor	(Y. Yu et al., 2017)
Plant	Picrorhiza kurroa (Picrorhiza kurrooa)	ASGLCPEEAVPRR	Trypsin	2,20	14	247,33	0.06	50,00	AS						6,29	-0.1	Good	(Thakur et al., 2021)
Animal	Boarfish (Capros aper)	IPV	Alcalase and Flavourzyme	5.61	3	500,00	1	100,00		IP	IPV				3.66	0	Poor	(Harnedy-Rothwell et al., 2020)(
Animal	Camel whey protein (Camelus dromedarius)	VPV	Trypsin	6,6	3	531,00	1	100,00		VP	VPV				3,63	0	Poor	(Nongonierma, Cadamuro, Le Gouic, et al., 2019)
Plant	Sorghum bicolor seed protein (Sorghum bicolor L.)	QLRDIVDK	In silico GI digestion	8,55	9	229,57	0.27	33,33							6,50	0	Good	(Majid et al., 2022)
Animal	Boarfish (Capros aper)	IPVDM	Alcalase and Flavourzyme	21,72	5	397,25	0.75	80,00		IP	IPVD				0,78	-1	Good	(Harnedy-Rothwell et al., 2020)
Plant	Quinoa (*Chenopodium quinoa*)	HPF	*In silico* bromelain	34,31	3	519,50	0.97	33,33		HP	HPF	PF			7,56	0.1	Poor	(Guo et al., 2020)

(Continued) **Table 3.** Summary and structure analysis of DPP-IV inhibiting peptides.

Type	Source	Sequence	Enzymatic treatment	IC_{50} (μM)	PCL	Score (DPP-IVi)	Stack DPPIV	% HPO AA	A in Nt	P in Nt	P in Nt*	F in Ct	W in Ct	Y in Ct	pI	Net charge	Estimated solubility	References
Animal	Boarfish (*Capros aper*)	APIT	Alcalase and Flavourzyme	34,73	4	401,33	0.95	75,00	AP	AP	APIT				3,76	0	Poor	(Harnedy-Rothwell et al., 2020)
Animal	Camel whey protein (*Camelus dromedarius*)	YPI	Trypsin	35,00	3	493,50	0.91	100,00		YP	YPI				3,37	0	Poor	(Nongonierma, Cadamuro, le Gouic, et al., 2019)
Plant	Brewers' spent grain (*Hordeum vulgare*)	IPVP	Alcalase and Flavourzyme	38,67	4	493,33	0.69	100,00		IP	IPVP				3,83	0	Poor	(Cermeño et al., 2019)
Animal	Boarfish (*Capros aper*)	VPTP	Alcalase and Flavourzyme	38,93	4	510,00	0.93	75,00		VP	VPTP				3,78	0	Poor	(Harnedy-Rothwell et al., 2020)
Animal	Discarded shrimp head (*Penaeus vannamei*)	YPGE	Animal protease	40,9	4	401,00	0.95	75,00		YP	YPGE				1,00	-1	Good	(Xiang et al., 2021)
Animal	Casein	VPYPQ	Neutrase	41,45	6	462,25	0.45	66,67		VP	VPYP				3,62	0	Poor	(Zheng et al., 2019)
Animal	Atlantic salmon (*Salmo salar*)	GPGA	Flavourzyme	41,9	4	344,67	0.81	100,00		GP	GPGA				3,63	0	Poor	(Li-Chan et al., 2012)
Animal	Whey protein isolate	LKPTPEGDLE	Thermoase PC10F	42	10	302,56	0.7	50,00			LKPT				3,69	-2	Good	(Lacroix et al., 2016)
Plant	Dulse (*Palmaria palmata*)	ILAP	Corolase PP	43,4	4	402,00	0.96	100,00			ILAP				3,83	0	Poor	(Harnedy et al., 2015)(
Animal	Whey protein concentrate	IPAVF	Trypsin	44,70	5	371,50	0.8	80,00		IP	IPAV	VF			3,71	0	Poor	(Silveira et al., 2013)
Plant	Brewers' spent grain (*Hordeum vulgare*)	LPIA	Alcalase and Flavourzyme	45,07	4	402,00	1	100,00		LP	LPIA				3,63	0	Poor	(Cermeño et al., 2019)

(Continued) **Table 3.** Summary and structure analysis of DPP-IV inhibiting peptides.

Type	Source	Sequence	Enzymatic treatment	IC_{50} (μM)	PCL	Score (DPP-IVi)	Stack DPPIV	% HPO AA	A in Nt	P in Nt	P in Nt*	F in Ct	W in Ct	Y in Ct	pI	Net charge	Estimated solubility	References
Animal	Boarfish (*Capros aper*)	GPIN	Alcalase and Flavourzyme	48,96	4	391,33	0.52	75,00		GP	GPIN				3,71	0	Poor	(Harnedy-Rothwell et al., 2020)
Animal	Parmigiano-Reggiano Cheese	APFPE	Ripening at different times	49,50	5	430,50	0.87	60,00	AP	AP	APFP				1,00	-1	Good	(Martini et al., 2021)
Animal	Atlantic salmon (*Salmo salar*)	GPAE	Flavourzyme	49,60	4	380,33	0.53	75,00		GP	GPAE				1,00	-1	Good	(Li-Chan et al., 2012)
Animal	Boarfish (*Capros aper*)	LPVYD	Alcalase and Flavourzyme	51,36	5	382,75	0.55	80,00		LP	LPVY			YD	0,88	-1	Poor	(Harnedy-Rothwell et al., 2020)
Plant	Brewers' spent grain (*Hordeum vulgare*)	IPY	Alcalase and Flavourzyme	52,15	3	493,50	0.91	100,00		IP	IPY			PY	3,62	0	Poor	(Cermeño et al., 2019)
Plant	Rapeseed napin (*Brassica napus*)	IPQVS	Alcalase and trypsin	52,16	5	344,25	0.45	60,00		IP	IPQV				3,73	0	Poor	(Xu et al., 2019)(
Animal	Boarfish (*Capros aper*)	LPVDM	Alcalase and Flavourzyme	53,50	5	410,25	0.67	80,00		LP	LPVD				0,78	-1	Good	(Harnedy-Rothwell et al., 2020)
Plant	Dulse (*Palmaria palmata*)	LLAP	Corolase PP	53,74	4	419,33	0.98	100,00			LLAP				3,82	0	Poor	(Harnedy et al., 2015)
Plant	Brewers' spent grain (*Hordeum vulgare*)	VPIP	Alcalase and Flavourzyme	54,69	4	493,33	0.68	100,00		VP	VPIP				3,78	0	Poor	(Cermeño et al., 2019)
Animal	Camel whey protein (*Camelus dromedarius*)	VPF	Trypsin	55,10	3	520,50	0.95	66,67		VP	VPF	PF			3,67	0	Poor	(Nongonierma, Cadamuro, le Gouic, et al., 2019)
Plant	Wheat gluten hydrolysate (*Triticum aestivum*)	LPQ	Ginger protease (Zingibain)	56,70	3	540,50	0.78	66,67		LP	LPQ				3,70	0	Poor	(Taga et al., 2017)

(Continued) **Table 3.** Summary and structure analysis of DPP-IV inhibiting peptides.

Type	Source	Sequence	Enzymatic treatment	IC_{50} (μM)	PCL	Score (DPP-IVi)	Stack DPPIV	% HPO AA	A in Nt	P in Nt	P in Nt*	F in Ct	W in Ct	Y in Ct	pI	Net charge	Estimated solubility	References
Animal	Whey protein isolate	LKPTPEGDLEIL	Thermoase PC10F	57,00	12	293,91	0.49	58,33			LKPT				3,69	-2	Good	(Lacroix et al., 2016)
Animal	Boarfish (*Capros aper*)	APLER	Alcalase and Flavourzyme	63,67	5	334,25	0.24	60,00	AP	AP	APLE				6,93	0	Good	(Harnedy-Rothwell et al., 2020)
Animal	Casein-derived peptides	FLQP	*In silico*	65,30	4	450,33	0.79	50,00			FLQP				3,57	0	Poor	(Nongonierma & FitzGerald, 2013)
Animal	Tilapia skin (*Oreochromis niloticus*)	IPGDPGPPGPPGP	Flavourzyme	65,40	13	372,17	0.45	92,31		IP	IPGD				0,88	-1	Good	(T. Y. Wang et al., 2015)
Animal	Boarfish (*Capros aper*)	IPGA	Alcalase and Flavourzyme	66,37	4	364,67	1	100,00		IP	IPGA				3,63	0	Poor	(Harnedy-Rothwell et al., 2020)
Animal	Sheep skin (*Ovis aries*)	GPAGPOGFPG	Alcalase, Neutrase & Flavourzyme	67,12	10	n. d.	0.86	80,00		GP	GPAG				3,62	0	Poor	(B. Wang et al., 2021)
Animal	Boarfish (*Capros aper*)	GPSL	Alcalase and Flavourzyme	68,13	4	329,00	0.99	75,00		GP	GPSL				3,63	0	Poor	(Harnedy-Rothwell et al., 2020)
Animal	Mare whey protein (*Equus caballus*)	TQMVDEEIMEKFR	Papain	69,84	13	215,67	0.51	30,77				FR			4,04	-2	Good	(Song et al., 2017)

IC_{50} (μM): half maximal inhibitory activity, expressed in μM
PCL: peptide chain length
HPO: Hydrophobic aminoacids
A in Nt: presence of alanine in the last two positions of the N-terminus
P in Nt: presence of proline in the last two positions of the N-terminus
P in Nt*: presence of proline in the last four positions of the N-terminus
F in Ct: presence of phenylalanine in the last two positions of the C-terminus
W in Ct: presence of tryptophan in the last two positions of the C-terminus
Y in Ct: presence of tyrosine in the last two positions of the C-terminus
pI: isoelectric point determined by Innovagen's peptide calculator PepCalc
Net charge was determined at pH 7 by Innovagen's peptide calculator PepCalc
Estimated solubility: solubility is estimated since Innovagen's tool does not take into consideration factors such as peptide concentration

5. Activity prediction *in silico* for antidiabetic peptides

Lately, *in silico* tools have gained attention for the identification and obtaining of bioactive peptides (Barati et al., 2020). To our knowledge, there are no bioinformatic tools available that allow to predict the α-amylase and α-glucosidase inhibitory activities of peptides. Hence, this study aimed to evaluate the correlation between DPP-IV experimental inhibitory activity of the peptide sequences reported in the literature and the theoretical activity predicted by previously developed *in silico* tools as iDPPIV-SCM tool and StackDPPIV. iDPPIV-SCM was the first computational model for predicting and analyzing DPP-IV inhibitory peptides using sequence information. It is based on the Scoring Card Method (SCM), analyzing protein and peptide functions directly from their amino acid sequence without known structural information (Shoombuatong et al., 2020). StackDPPIV has been recently developed and it aims to improve the prediction accuracy of the iDPPIV-SCM by combining five popular machine learning algorithms in conjunction with ten different feature encodings from multiple perspectives in order to generate a pool of various baseline models, as well as using a genetic algorithm based on the self-assessment-report to determine the optimal informative probabilistic features to develop the final meta-predictor (Charoenkwan et al., 2022).

The *in silico* analysis was conducted on the total amount of DPP-IV inhibitory sequences identified (i.e., 230 sequences). Table 3 shows the *in silico* prediction of the inhibition activity for the 40 DPP-IV peptides selected according to the criteria (i.e., IC_{50} up to 20 times higher than the reference value for the tripeptide IPI). The iDPPIV-SCM tool expresses their prediction as a score value, where values over 294 indicate possible DPP-IV inhibitory peptides (Shoombuatong et al., 2020). The StackDPPIV tool expresses the prediction as the probability of inhibition, assigning values 0-1 where only peptides over 0.5 are predicted to inhibit the DPP-IV (Charoenkwan et al., 2022).

The iDPPIV-SCM tool reported that 154 out of the 230 peptides were possible inhibitors of the DPP-IV, while 11 peptides were not detected (i.e., peptides with only one amino acid or peptides with modified amino acids). The peptides with highest activity according to the calculated score were PP (score = 960.00), VPW (score = 596.50) and ER (score = 360.00) with reported IC_{50} values of 4343.48 μM (Neves et al., 2017), 174.78 μM (Xiang et al., 2021) and 4480.00 μM (Lafarga et al., 2016), respectively. Unexpectedly, their reported *in vitro* inhibitory capacities were significantly poorer, compared to their *in silico* scores. This discrepancy was also observed for the peptides with the highest *in vitro* activity reported in the literature review, GPAGPQGPR, PPGLPGSPGQ and LPQPPQE, with IC_{50} values of 0.51, 0.55 and 0.97 μM respectively. According to the *in silico* analysis, their score values were 320.88, 342.78 and 439.50, placing them at rank 130, 118 and 46 respectively within the original list of 230 inhibitory sequences. Indeed, no significant relationship (r^2 = 0.0102) can be found between the IC_{50} values of the 40 most active peptides reported in the literature and the

score values calculated *in silico*. This leads to conclude that, although the DPP-IVi tool is very promising, it still has limitations because it mainly predicts bioactivity only based on the propensity scores of 20 amino acids. It is also worth mentioning that 60% of the peptides used for the DPP-IVi tool database were composed of 5 or less amino acids, which differs from the PCL range of DPP-IV inhibitory peptides reported in the literature.

Regarding the data obtained with the StackDPPIV, 164 out of the 230 peptides identified in literature were possible inhibitors of DPP-IV, while 6 peptides were not detected (i.e., peptides with only one amino acid or peptides with modified amino acids). From these 164 peptides, 24 of them were assigned with the highest probability value, while their reported IC_{50} values ranged from 5.61 μM (Harnedy-Rothwell et al., 2020) to 9690 μM (Gallego et al., 2014). Considering the 40 selected peptides (Table 3), 4 of them were assigned the maximum probability of 1: IPV, VPV, LPIA and IPGA with reported IC_{50} values of 5.61 μM (Harnedy-Rothwell et al., 2020), 6.6 μM (Nongonierma, Cadamuro, Le Gouic, et al., 2019), 45.07 μM (Cermeño et al., 2019) and 66.37 μM (Harnedy-Rothwell et al., 2020), respectively. Up to 20% of the peptides were predicted to not be inhibitors of the enzyme DPP-IV. The peptide with the least probability estimated was ASGLCPEEAVPRR with 0.06 value and an IC_{50} of 2.2 μM (Thakur et al., 2021). As for iDPPIV-SCM, there was no correlation between the probability value calculated by the StackDPPIV and the *in vitro* activity reported in literature (r^2 = 0.0041). Moreover, the correlation between the predicted results obtained from both tools was also compared but a poor correlation was found (r^2 = 0.270). This lack of correlation between the experimental data and the predictors shows that *in vitro* analyses by conventional enzymatic means are still necessary to assay the activity of these peptides. However, both the iDPPIV-SCM and the StackDPPIV could be used as a preliminary guidance tool to estimate in a qualitative way (yes/no) whether the peptides could express inhibitory activities.

6. Evidence of antidiabetic activity of peptides in cell models and *in vivo* studies

Despite the importance of *in vivo* studies investigating the physiological effects of antidiabetic peptides, most of the recent studies focus on *in vitro* or *in silico* evaluations. *In vivo* evaluation is specially needed considering that the bioavailability of the peptides can be greatly affected both by hydrolysis of peptidases in the stomach and by intestinal brush border membrane enzymes (R. Liu et al., 2019).

Some of the literature found used cell models to analyze the inhibition of DPP-IV, and to a lesser extent of α-amylase and α-glucosidase, in cells. Harnedy-Rothwell et al. studied the DPP-IV inhibitory activity of boarfish peptides in Caco-2 cells (Harnedy-Rothwell et al., 2020). This cell model simulates intestinal mucosal conditions to analyze the ability of the peptides to pass through human intestinal cell membranes and resist degradation by brush border

enzymes. In general, they found that all peptides were able to exert antidiabetic activity, albeit to a lesser extent. Similar results were obtained with peptides obtained from sorghum bicolor seed (Majid et al., 2022) and silver carp swim bladder hydrolysates (Hong et al., 2020). No significant difference was found in the DPP-IV inhibitory activity of sheep skin peptides both *in vitro* and in the cell model (B. Wang et al., 2021).

Another frequently used model is HepG2 cell, which show deficient glycogen synthesis and failure to suppress glucose production. This model was used to measure the antidiabetic activity of *Spirulina platensis* peptides, which had previously showed α-amylase, α-glucosidase, and DPP-IV inhibition (S. Hu et al., 2019). The peptides significantly increased the glycogen content and glucose metabolism enzymes activities, lowering blood sugar and improving insulin resistance. HepG2 cells were also used to demonstrate the antidiabetic activity of common carp roe peptides (C. Zhang et al., 2020).

Regarding *in vivo* assays, very little information was found in the literature. Rats and mice were the most commonly used animals, since they are easy to handle and cost-effective. High-fat diet/streptozotocin-treated (HFD/STZ) rats were used to determine the *in vivo* activity of tilapia skin gelatin peptides, which had inhibited DPP-IV activity *in vitro* (T. Y. Wang et al., 2015).This study demonstrated that fish skin gelatin hydrolysates had dual actions of DPP-IV inhibition and GLP-1 secretion enhancement, improving glycemic control in the rats after only 30 days. Other studies have also demonstrated the *in vivo* ability of fish-derived peptides to regulate the glycemic index. The glucose-lowering and insulin releasing properties of blue whiting muscle protein hydrolysates was studied using the Oral Glucose Tolerance Test (OGTT) in NIH Swiss mice (Harnedy et al., 2018). This test consists of administering a preload of the bioactive peptides followed by a glucose load and measuring the blood glucose levels at different times. They found that the hydrolysates mediated insulin and glucagon-like peptide-1 (GLP-1) release, increasing its secretion. Furthermore, they produced glucose-lowering effects both acutely (at 90-120 min after glucose load) and persistently (at 4h after glucose load). The antidiabetic effect of sturgeon collagen hydrolysates by *in vitro* analysis of α-glucosidase and DPP-IV and by OGTT in Institute of Cancer Research (ICR) mice was analyzed, obtaining positive results (Sasaoka et al., 2021).

The most frequent method of administration was via oral, an easier to perform and safer method compared to intraperitoneal administration (Nong & Hsu., 2021). Some studies tested the OGTT on ICR mice fed with Yam tuber peptides (Lin et al., 2016) and casein-derived peptides (Zheng et al., 2019). They found that postprandial blood glucose levels were reduced. The *in vitro* activity of brewer's spent grain hydrolysates was studied *in vivo* (Cermeño et al., 2019), where wistar rats were supplemented via oral with encapsulated brewer's spent grain hydrolysates and found that the activity of α-amylase, α-glucosidase and DPP-IV was reduced, and serum glucose levels decreased (Garzón et al., 2022). Only

Table 4. Main relationships between structural features and activity for antidiabetic peptides

Enzyme inhibited	PCL	AA in Nt	AA in Ct	Hydrophobicity	Aromatic AAs	Solubility	Net charge
α-amylase	~70% between 3-10 AAs	> 50% present L or P in first 2 positions	10% present F in last 2 positions	>44% hydrophobic AAs	-	>65% low	~60% positive
α -glucosidase	~80% between 2-10 AAs	~35% present S, T or Y in first 2 positions	30% present P or A in last 2 positions	75% contain ~50% hydrophobic AAs	-	>55% good	~75% neutral or positive
DPP-IV	>70% between 3-6 AAs	>90% present P in first 4 positions	-	75% contain >80% hydrophobic AAs	95% contain P	65% low	>70% neutral

PCL: peptide chain length
AA in Nt: amino acids in N-terminal
AA in Ct: amino acids in C-terminal
Net charge at pH 7

one study used the via intraperitoneal to treat the tested NIH Swiss mice. They went on to investigate *Palmaria palmata* peptides which had previously shown DPP-IV inhibitory activity *in vitro* (Harnedy et al., 2015), testing the effect of injecting glucose alone or in combination with the bioactive peptides. They found that these peptides were able to act as glucose-dependent insulinotropic polypeptide (GIP) secretagogues and could therefore be used in combination with drugs to aid in the prevention and management of diabetes (Harnedy-Rothwell et al., 2021). Finally, the effect of oral and intraperitoneal supplementation was studied, using soybean-derived peptides in alloxan-induced diabetes Kunming mice, finding stronger results via oral (Jiang et al., 2018).

7. Potential degradation of active peptides during digestion

One of the most effective approaches to ingest bioactive peptides is by using them as bioactive ingredients in functional foods (Tadesse & Emire, 2020). Nonetheless, there is a risk that these peptides are degraded by the effect of gastrointestinal proteases and serum peptidases during the digestion process (Sun et al., 2020). Although not all peptides are equally susceptible to this enzymatic degradation, those that are altered can reduce their activity or could enhance it in case the new released peptides are more active compared to the parent peptide. In this regard, the use of *in silico* tools is useful to simulate digestion and predict which of the identified peptides can be degraded and at which specific point they are attacked by the native enzymes present. PeptideCutter (Maillet, 2020) was used to perform an *in silico* gastrointestinal digestion of the peptides identified by entering the peptide sequences and predicting the potential sites cleaved by pepsin (pH: 1.3), chymotrypsin (low

and high specificity) and trypsin (Barati et al., 2020). This tool allowed us to predict the potential new species produced after digestive degradation.

It was found that longer peptides are more susceptible to being digested, as they have more possible cleavage sites. This is confirmed by data shown in Tables S1-3 (supplementary material), where 15 of the 18 α-amylase inhibitory peptides (average PCL = 10) undergo at least one modification, 27 of the 39 α-glucosidase inhibitory peptides (average PLC = 8) are modified, and only 19 of the 40 DPP-IV inhibitory peptides (average PLC = 6) are modified. The peptides with α-amylase inhibitory activity can be highly hydrolyzed by digestion, finding that the most active sequence (FFRSKLLSDGAAAAKGALLPQYW) can be attacked by the different enzymes at up to 11 different cleavage sites. For α-glucosidase and DPP-IV inhibitory peptides, this rate of degradation is much lower, where the most inhibitory sequences of each enzyme (FDPFPK and GPAGPQGPR) have only one cleavage site where they can be cleaved.

To study the potential effect of peptide degradation on their activity iDPPIV-SCM was used to predict the bioactivity of the new released peptides. Although iDPPIV-SCM computational tool did not present a good correlation with the inhibitory activity obtained *in vitro*, it was selected as qualitative predictor of inhibitory activity of the released peptides (score>294.0 for active peptides). iDPPIV-SCM was selected over StackDPPIV tool, due to the much extended use of the former in the literature. From the 40 DPP-IV inhibitory peptides digested, 47 peptide fractions were obtained, 30 of which would maintain their activity according to the computational tool, and 17 would lose their inhibitory activity or were not able to be detected (Table S3).

In any case, it is worth noting that the results obtained are indicative, considering the wide limitations shown by both computational predictors and the PeptideCutter tool. Although PeptideCutter tool allows us to estimate the alteration that peptides would undergo during gastrointestinal digestion, it should be taken into account that hydrolysis could not be performed at 100%, and not all the bonds susceptible to attack would actually be broken. Hence, it would be necessary to study experimentally the real effect of digestion, since this *in silico* analysis can only serve as an approximation of the digestive effect, as it does not consider other factors affecting peptide stability, such as pH. For instance, the acid pH found in the stomach can modify the structure, charge, and interaction capacity of the peptides, thus limiting their activity (Marcolini et al., 2015). Thus, it would be advisable to carry out *in vitro* studies using the INFOGEST method (Brodkorb et al., 2019) to investigate how gastrointestinal digestion can affect the degradation and activity of antidiabetic peptides. To our knowledge, only one work has been reported regarding the effect of *in vitro* gastrointestinal digestion of synthetic antidiabetic peptides (Rendón-Rosales et al., 2022), which resulted in degradation of most of the peptides after digestion and increased inhibition of DPP-IV for 7 out of the 12 peptides. This lack of literature highlights the need

to focus research on the effect of gastric digestion on the bioactivity of antidiabetic peptides.

8. Conclusions

In vitro analyses to determine the inhibitory activity of α-amylase, α-glucosidase and DPP-IV by peptides serve as initial assessment to establish if these food-derived molecules obtained by enzymatic hydrolysis can have potential bioactivity to prevent or pre-treat diabetes. Peptides identified from different sources, with an experimentally determined IC_{50} to inhibit α-amylase, α-glucosidase, and DPP-IV were reviewed. A critical assessment of the data suggests that the methodology employed among authors is not consistent in some cases (e.g., for α-amylase and α-glucosidase), as the IC_{50} for the positive control (acarbose) varies among authors. This hinders the complete comparison of results. Nevertheless, for DPP-IV inhibitory peptides, the methodology is highly identical among authors. Although *in silico* tools are gaining attention to identify antidiabetic peptides, no correlation was found between the experimental DPP-IV inhibitory activity of the peptides and the one predicted by the iDPPIV-SCM and StackDPPIV tools. Thus, further development of the bioinformatic tools is required. Although the number of α-amylase and α-glucosidase inhibitory peptides identified so far is low, the relationship between the structural features of the reported peptides and their activity has been discussed. For DPP-IV inhibitory peptides, the presence of P at the Nt is found to be a highly conserved feature. It was found that α-amylase inhibitory peptides have the longest PCLs (11 amino acids average), whereas DPP-IV inhibitors are the shortest (6 amino acids average), which would justify that their sequences are much less degraded during gastrointestinal digestion *in silico*.

9. References

Acquah, C., Stefano, E. D., & Udenigwe, C. C. (2018). Role of hydrophobicity in food peptide functionality and bioactivity. *Journal of Food Bioactives*, *4*. https://doi.org/10.31665/jfb.2018.4164

Admassu, H., Gasmalla, M. A. A., Yang, R., & Zhao, W. (2018). Identification of bioactive peptides with α-amylase inhibitory potential from enzymatic protein hydrolysates of red seaweed (*Porphyra spp*). *Journal of Agricultural and Food Chemistry, 66*(19), 4872–4882. https://doi.org/10.1021/acs.jafc.8b00960

Ahmad, H., & Chowdhury, M. A. N. (2019). A short review on anti-diabetics for uncontrolled type 2 diabetes mellitus. *Medicine Today*, *31*(2), 120–127. https://doi.org/10.3329/medtoday.v31i2.41966

Ahn, J., Cao, M.-J., Yu, Y. Q., & Engen, J. R. (2013). Accessing the reproducibility and specificity of pepsin and other aspartic proteases. *Biochimica et Biophysica Acta (BBA) - Proteins and Proteomics*, *1834*(6), 1222–1229. https://doi.org/10.1016/j.bbapap.2012.10.003

Amigo, L., & Hernández-Ledesma, B. (2020). Current evidence on the bioavailability of food bioactive peptides. *Molecules*, *25*(19), 4479. https://doi.org/10.3390/molecules25194479

Antony, P., & Vijayan, R. (2021). Bioactive peptides as potential nutraceuticals for diabetes therapy: a comprehensive review. *International Journal of Molecular Sciences*, *22*(16), 9059. https://doi.org/10.3390/ijms22169059

Awosika, T. O., & Aluko, R. E. (2019). Inhibition of the *in vitro* activities of α-amylase, α-glucosidase and pancreatic lipase by yellow field pea (*Pisum sativum L.*) protein hydrolysates. *International Journal of Food Science & Technology*, *54*(6), 2021–2034. https://doi.org/10.1111/ijfs.14087

Axelsson, A. S., Mahdi, T., Nenonen, H. A., Singh, T., Hänzelmann, S., Wendt, A., Bagge, A., Reinbothe, T. M., Millstein, J., & Yang, X. (2017). SOX5 regulates beta-cell phenotype and is reduced in type 2 diabetes. *Nature Communications*, *8*(1). https://doi.org/10.1038/ncomms15652

Barati, M., Javanmardi, F., Jabbari, M., Mokari-Yamchi, A., Farahmand, F., Eş, I., Farhadnejad, H., Davoodi, S. H., & Mousavi Khaneghah, A. (2020). An *in silico* model to predict and estimate digestion-resistant and bioactive peptide content of dairy products: A primarily study of a time-saving and affordable method for practical research purposes. *LWT*, *130*, 109616. https://doi.org/10.1016/j.lwt.2020.109616

Brodkorb, A., Egger, L., Alminger, M., Alvito, P., Assunção, R., Ballance, S., Bohn, T., Bourlieu-Lacanal, C., Boutrou, R., & Carrière, F. (2019). INFOGEST static *in vitro* simulation of gastrointestinal food digestion. *Nature Protocols*, *14*, 991–1014. https://doi.org/10.1038/s41596-018-0119-1

Cermeño, M., Connolly, A., O'Keeffe, M. B., Flynn, C., Alashi, A. M., Aluko, R. E., & FitzGerald, R. J. (2019). Identification of bioactive peptides from brewers' spent grain and contribution of Leu/Ile to bioactive potency. *Journal of Functional Foods*, *60*, 103455. https://doi.org/10.1016/j.jff.2019.103455

Charoenkwan, P., Kanthawong, S., Nantasenamat, C., Hasan, Md. M., & Shoombuatong, W. (2020). iDPPIV-SCM: a sequence-based predictor for identifying and analyzing dipeptidyl peptidase IV (DPP-IV) inhibitory peptides using a scoring card method. *Journal of Proteome Research*, *19*(10), 4125–4136. https://doi.org/10.1021/acs.jproteome.0c00590

Charoenkwan, P., Nantasenamat, C., Hasan, M. M., Moni, M. A., Lio', P., Manavalan, B., & Shoombuatong, W. (2022). StackDPPIV: A novel computational approach for accurate prediction of dipeptidyl peptidase IV (DPP-IV) inhibitory peptides. *Methods*, *204*, 189–198. https://doi.org/10.1016/j.ymeth.2021.12.001

Cruz-Casas, D. E., Aguilar, C. N., Ascacio-Valdés, J. A., Rodríguez-Herrera, R., Chávez-González, M. L., & Flores-Gallegos, A. C. (2021). Enzymatic hydrolysis and microbial fermentation: The most favorable biotechnological methods for the release of bioactive peptides. *Food Chemistry: Molecular Sciences*, *3*, 100047. https://doi.org/10.1016/j.fochms.2021.100047

Daliri, E. B. M., Oh, D. H., & Lee, B. H. (2017). Bioactive peptides. *Foods*, *6*, 32. https://doi.org/10.3390/FOODS6050032

Deacon, C. F. (2020). Dipeptidyl peptidase 4 inhibitors in the treatment of type 2 diabetes mellitus. *Nature Reviews Endocrinology*, *16*(11), 642–653. https://doi.org/10.1038/s41574-020-0399-8

El-Sayed, M., & Awad, S. (2019). Milk bioactive peptides: antioxidant, antimicrobial and anti-diabetic activities. *Advances in Biochemistry*, *7*(1), 22. https://doi.org/10.11648/j.ab.20190701.15

Esfandi, R., Seidu, I., Willmore, W., & Tsopmo, A. (2022). Antioxidant, pancreatic lipase, and α-amylase inhibitory properties of oat bran hydrolyzed proteins and peptides. *Journal of Food Biochemistry*, *46*(4). https://doi.org/10.1111/jfbc.13762

Gallego, M., Aristoy, M.-C., & Toldrá, F. (2014). Dipeptidyl peptidase IV inhibitory peptides generated in Spanish dry-cured ham. *Meat Science*, *96*(2), 757–761. https://doi.org/10.1016/j.meatsci.2013.09.014

Garzón, A. G., Ferreira, M. del R., Cian, R. E., Oliva, M. E., D'Alessandro, M. E., & Drago, S. R. (2022). Microencapsulated bioactive peptides from brewer's spent grain promotes antihypertensive and antidiabetogenic effects on a hypertensive and insulin-resistant rat model. *Journal of Food Biochemistry*, *46*(10). https://doi.org/10.1111/jfbc.14283

González-Montoya, M., Hernández-Ledesma, B., Mora-Escobedo, R., & Martínez-Villaluenga, C. (2018). Bioactive peptides from germinated soybean with anti-diabetic potential by inhibition of dipeptidyl peptidase-IV, α-amylase, and α-glucosidase enzymes. *International Journal of Molecular Sciences*, *19*(10), 2883. https://doi.org/10.3390/ijms19102883

Gu, X., Gao, T., Hou, Y., Li, D., & Fu, L. (2020). Identification and characterization of two novel α-glucosidase inhibitory peptides from almond (*Armeniaca sibirica*) oil manufacture residue. *LWT*, *134*, 110215. https://doi.org/10.1016/j.lwt.2020.110215

Guo, H., Richel, A., Hao, Y., Fan, X., Everaert, N., Yang, X., & Ren, G. (2020). Novel dipeptidyl peptidase-IV and angiotensin-I-converting enzyme inhibitory peptides released from quinoa protein by *in silico*

proteolysis. *Food Science & Nutrition*, *8*(3), 1415–1422. https://doi.org/10.1002/fsn3.1423

Harnedy, P. A., O'Keeffe, M. B., & FitzGerald, R. J. (2015). Purification and identification of dipeptidyl peptidase (DPP) IV inhibitory peptides from the macroalga *Palmaria palmata*. *Food Chemistry*, *172*, 400–406. https://doi.org/10.1016/j.foodchem.2014.09.083

Harnedy, P. A., Parthsarathy, V., McLaughlin, C. M., O'Keeffe, M. B., Allsopp, P. J., McSorley, E. M., O'Harte, F. P. M., & FitzGerald, R. J. (2018). Blue whiting (*Micromesistius poutassou*) muscle protein hydrolysate with *in vitro* and *in vivo* antidiabetic properties. *Journal of Functional Foods*, *40*, 137–145. https://doi.org/10.1016/j.jff.2017.10.045

Harnedy-Rothwell, P. A., McLaughlin, C. M., Le Gouic, A. V., Mullen, C., Parthsarathy, V., Allsopp, P. J., McSorley, E. M., FitzGerald, R. J., & O'Harte, F. P. M. (2021). *In vitro* and *in vivo* effects of *Palmaria palmata* derived peptides on glucose metabolism. *International Journal of Peptide Research and Therapeutics*, *27*(3), 1667–1676. https://doi.org/10.1007/s10989-021-10199-8

Harnedy-Rothwell, P. A., McLaughlin, C. M., O'Keeffe, M. B., Le Gouic, A. V., Allsopp, P. J., McSorley, E. M., Sharkey, S., Whooley, J., McGovern, B., & O'Harte, F. P. M. (2020). Identification and characterisation of peptides from a boarfish (*Capros aper*) protein hydrolysate displaying *in vitro* dipeptidyl peptidase-IV (DPP-IV) inhibitory and insulinotropic activity. *Food Research International*, *131*, 108989. https://doi.org/10.1016/j.foodres.2020.108989

Hong, H., Zheng, Y., Song, S., Zhang, Y., Zhang, C., Liu, J., & Luo, Y. (2020). Identification and characterization of DPP-IV inhibitory peptides from silver carp swim bladder hydrolysates. *Food Bioscience*, *38*, 100748. https://doi.org/10.1016/j.fbio.2020.100748

Hossain, U., Das, A. K., Ghosh, S., & Sil, P. C. (2020). An overview on the role of bioactive α-glucosidase inhibitors in ameliorating diabetic complications. *Food and Chemical Toxicology*, *145*, 111738. https://doi.org/10.1016/j.fct.2020.111738

Howard-Thompson, A., Khan, M., Jones, M., & George, C. M. (2018). Type 2 Diabetes Mellitus: Outpatient Insulin Management. *American Family Physician* , *97(1)*, 29–37.

Hsieh, C.-H., Wang, T.-Y., Hung, C.-C., Jao, C.-L., Hsieh, Y.-L., Wu, S.-X., & Hsu, K.-C. (2016). *In silico*, *in vitro* and *in vivo* analyses of dipeptidyl peptidase IV inhibitory activity and the antidiabetic effect of sodium caseinate hydrolysate. *Food & Function*, *7*(2), 1122–1128. https://doi.org/10.1039/c5fo01324k

Hu, J., Lai, X., Wu, X., Wang, H., Weng, N., Lu, J., Lyu, M., & Wang, S. (2023). Isolation of a novel anti-diabetic α-glucosidase oligo-peptide inhibitor from fermented rice bran. *Foods*, *12*(1), 183. https://doi.org/10.3390/foods12010183

Hu, S., Fan, X., Qi, P., & Zhang, X. (2019). Identification of anti-diabetes peptides from *Spirulina platensis*. *Journal of Functional Foods*, *56*, 333–341. https://doi.org/10.1016/j.jff.2019.03.024

Ibrahim, M. A., Bester, M. J., Neitz, A. W., & Gaspar, A. R. M. (2018a). Rational *in silico* design of novel α-glucosidase inhibitory peptides and *in vitro* evaluation of promising candidates. *Biomedicine & Pharmacotherapy*, *107*, 234–242. https://doi.org/10.1016/j.biopha.2018.07.163

Ibrahim, M. A., Bester, M. J., Neitz, A. W. H., & Gaspar, A. R. M. (2018b). Structural properties of bioactive peptides with α-glucosidase inhibitory activity. *Chemical Biology & Drug Design*, *91*(2), 370–379. https://doi.org/10.1111/cbdd.13105

Jiang, M., Yan, H., He, R., & Ma, Y. (2018). Purification and a molecular docking study of α-glucosidase-inhibitory peptides from a soybean protein hydrolysate with ultrasonic pretreatment. *European Food Research and Technology*, *244*(11), 1995–2005. https://doi.org/10.1007/s00217-018-3111-7

Karami, Z., & Akbari-adergani, B. (2019). Bioactive food derived peptides: a review on correlation between structure of bioactive peptides and their functional properties. *Journal of Food Science and Technology*, *56*(2), 535–547. https://doi.org/10.1007/s13197-018-3549-4

Kaur, N., Kumar, V., Nayak, S. K., Wadhwa, P., Kaur, P., & Sahu, S. K. (2021). Alpha-amylase as molecular target for treatment of diabetes mellitus: A comprehensive review. *Chemical Biology & Drug Design*, *98*(4), 539–560. https://doi.org/10.1111/cbdd.13909

Kazakos, K. (2011). Incretin effect: GLP-1, GIP, DPP4. *Diabetes Research and Clinical Practice*, *93*, S32–S36. https://doi.org/10.1016/s0168-8227(11)70011-0

Keservani, R. K., Sharma, A. K., & Jarouliya, U. (2015). Protein and peptide in drug targeting and its therapeutic approach. *Ars Pharmaceutica (Internet)*, *56*(3), 165–177. https://doi.org/10.4321/s2340-98942015000300006

Kęska, P., Stadnik, J., Bąk, O., & Borowski, P. (2019). Meat proteins as dipeptidyl peptidase iv inhibitors and glucose uptake stimulating peptides for the management of a type 2 diabetes mellitus *in silico* study. *Nutrients*, *11*(10), 2537. https://doi.org/10.3390/nu11102537

Korhonen, H., & Pihlanto, A. (2006). Bioactive peptides: Production and functionality. *International Dairy Journal*, *16*(9), 945–960. https://doi.org/10.1016/j.idairyj.2005.10.012

Kshirsagar, A. D., Aggarwal, A. S., Harle, U. N., & Deshpande, A. D. (2011). DPP IV inhibitors: Successes, failures and future prospects. *Diabetes & Metabolic Syndrome: Clinical Research & Reviews*, *5*(2), 105–112. https://doi.org/10.1016/j.dsx.2012.02.017

Kumar, L. V., Shakila, R. J., & Jeyasekaran, G. (2019). *In vitro* anti-cancer, anti-diabetic, anti-inflammation and wound healing properties of collagen peptides derived from unicorn leatherjacket (*Aluterus Monoceros*) at different hydrolysis. *Turkish Journal of Fisheries and Aquatic Sciences*, *19(7)*, 551–560. http://dx.doi.org/10.4194/1303-2712-v19_7_02

Lacroix, I. M. E., Meng, G., Cheung, I. W. Y., & Li-Chan, E. C. Y. (2016). Do whey protein-derived peptides have dual dipeptidyl-peptidase IV and angiotensin I-converting enzyme inhibitory activities? *Journal of Functional Foods*, *21*, 87–96. https://doi.org/10.1016/j.jff.2015.11.038

Lafarga, T., Aluko, R. E., Rai, D. K., O'Connor, P., & Hayes, M. (2016). Identification of bioactive peptides from a papain hydrolysate of bovine serum albumin and assessment of an antihypertensive effect in spontaneously hypertensive rats. *Food Research International*, *81*, 91–99. https://doi.org/10.1016/j.foodres.2016.01.007

Lammi, C., Bollati, C., Ferruzza, S., Ranaldi, G., Sambuy, Y., & Arnoldi, A. (2018). Soybean- and lupin-derived peptides inhibit DPP-IV activity on *in situ* human intestinal caco-2 cells and *ex vivo* human serum. *Nutrients*, *10*(8), 1082. https://doi.org/10.3390/nu10081082

Li-Chan, E. C. Y., Hunag, S.-L., Jao, C.-L., Ho, K.-P., & Hsu, K.-C. (2012). Peptides derived from atlantic salmon skin gelatin as dipeptidyl-peptidase iv inhibitors. *Journal of Agricultural and Food Chemistry*, *60*(4), 973–978. https://doi.org/10.1021/jf204720q

Lin, Y.-S., Han, C.-H., Lin, S.-Y., & Hou, W.-C. (2016). Synthesized peptides from yam dioscorin hydrolysis *in silico* exhibit dipeptidyl peptidase-iv inhibitory activities and oral glucose tolerance improvements in normal mice. *Journal of Agricultural and Food Chemistry*, *64*(33), 6451–6458. https://doi.org/10.1021/acs.jafc.6b02403

Liu, Lingling, Chen, J., & Li, X. (2021). Novel peptides with α-glucosidase inhibitory activity from *Changii Radix* hydrolysates. *Process Biochemistry*, *111*, 200–206. https://doi.org/10.1016/j.procbio.2021.08.019

Liu, Liyuan, Wang, Y., Peng, C., & Wang, J. (2013). Optimization of the preparation of fish protein anti-obesity hydrolysates using response surface methodology. *International Journal of Molecular Sciences*, *14*(2), 3124–3139. https://doi.org/10.3390/ijms14023124

Liu, R., Cheng, J., & Wu, H. (2019). Discovery of food-derived dipeptidyl peptidase iv inhibitory peptides: a review. *International Journal of Molecular Sciences*, *20*(3), 463. https://doi.org/10.3390/ijms20030463

Maillet, N. (2020). Rapid Peptides Generator: fast and efficient *in silico* protein digestion. *NAR Genomics and Bioinformatics, 2*(1). https://doi.org/10.1093/nargab/lqz004

Majid, A., Lakshmikanth, M., Lokanath, N. K., & Poornima Priyadarshini, C. G. (2022). Generation, characterization and molecular binding mechanism of novel dipeptidyl peptidase-4 inhibitory peptides from sorghum bicolor seed protein. *Food Chemistry*, *369*, 130888. https://doi.org/10.1016/j.foodchem.2021.130888

Marcolini, E., Babini, E., Bordoni, A., Di Nunzio, M., Laghi, L., Maczó, A., Picone, G., Szerdahelyi, E., Valli, V., & Capozzi, F. (2015). Bioaccessibility of the bioactive peptide carnosine during *in vitro* digestion of cured beef meat. *Journal of Agricultural and Food Chemistry, 63*(20), 4973–4978. https://doi.org/10.1021/acs.jafc.5b01157

Martini, S., Solieri, L., Cattivelli, A., Pizzamiglio, V., & Tagliazucchi, D. (2021). An integrated peptidomics and *in silico* approach to identify novel anti-diabetic peptides in parmigiano-reggiano cheese. *Biology*, *10*(6), 563. https://doi.org/10.3390/biology10060563

Merz, M., Eisele, T., Berends, P., Appel, D., Rabe, S., Blank, I., Stressler, T., & Fischer, L. (2015). Flavourzyme, an enzyme preparation with industrial relevance: automated nine-step purification and partial characterization of eight enzymes. *Journal of Agricultural and Food Chemistry, 63*(23), 5682–5693. https://doi.org/10.1021/acs.jafc.5b01665

Mojica, L., & de Mejía, E. G. (2016). Optimization of enzymatic production of anti-diabetic peptides from black bean (*Phaseolus vulgaris L.*) proteins, their characterization and biological potential. *Food & Function*, *7*(2), 713–727. https://doi.org/10.1039/c5fo01204j

Mustad, V. A., Huynh, D. T. T., López-Pedrosa, J. M., Campoy, C., & Rueda, R. (2020). The role of dietary carbohydrates in gestational diabetes. *Nutrients*, *12*(2), 385. https://doi.org/10.3390/nu12020385

Neves, A. C., Harnedy, P. A., O'Keeffe, M. B., Alashi, M. A., Aluko, R. E., & FitzGerald, R. J. (2017). Peptide identification in a salmon gelatin hydrolysate with antihypertensive, dipeptidyl peptidase IV inhibitory and antioxidant activities. *Food Research International*, *100*, 112–120. https://doi.org/10.1016/j.foodres.2017.06.065

Ngoh, Y.-Y., & Gan, C.-Y. (2016). Enzyme-assisted extraction and identification of antioxidative and α-amylase inhibitory peptides from Pinto beans (*Phaseolus vulgaris cv. Pinto*). *Food Chemistry*, *190*, 331–337. https://doi.org/10.1016/j.foodchem.2015.05.120

Ngoh, Y.-Y., & Gan, C.-Y. (2018). Identification of Pinto bean peptides with inhibitory effects on α-amylase and angiotensin converting enzyme (ACE) activities using an integrated bioinformatics-assisted approach. *Food Chemistry*, *267*, 124–131. https://doi.org/10.1016/j.foodchem.2017.04.166

Ngoh, Y.-Y., Tye, G. J., & Gan, C.-Y. (2017). The investigation of α-amylase inhibitory activity of selected Pinto bean peptides via preclinical study using AR42J cell. *Journal of Functional Foods*, *35*, 641–647. https://doi.org/10.1016/j.jff.2017.06.037

Nong, N. T. P., & Hsu, J.-L. (2021). Characteristics of food protein-derived antidiabetic bioactive peptides: a literature update. *International Journal of Molecular Sciences*, *22*(17), 9508. https://doi.org/10.3390/ijms22179508

Nongonierma, A. B., Cadamuro, C., Le Gouic, A., Mudgil, P., Maqsood, S., & FitzGerald, R. J. (2019). Dipeptidyl peptidase IV (DPP-IV) inhibitory properties of a camel whey protein enriched hydrolysate preparation. *Food Chemistry*, *279*, 70–79. https://doi.org/10.1016/j.foodchem.2018.11.142

Nongonierma, A. B., Dellafiora, L., Paolella, S., Galaverna, G., Cozzini, P., & FitzGerald, R. J. (2018). *In silico* approaches applied to the study of peptide analogs of Ile-Pro-Ile in relation to their dipeptidyl peptidase IV inhibitory properties. *Frontiers in Endocrinology*, *9*. https://doi.org/10.3389/fendo.2018.00329

Nongonierma, A. B., & FitzGerald, R. J. (2013a). Dipeptidyl peptidase IV inhibitory and antioxidative properties of milk protein-derived dipeptides and hydrolysates. *Peptides*, *39*, 157–163. https://doi.org/10.1016/j.peptides.2012.11.016

Nongonierma, A. B., & FitzGerald, R. J. (2013b). Inhibition of dipeptidyl peptidase IV (DPP-IV) by proline containing casein-derived peptides. *Journal of Functional Foods*, *5*(4), 1909–1917. https://doi.org/10.1016/j.jff.2013.09.012

Nongonierma, A. B., & FitzGerald, R. J. (2013c). Inhibition of dipeptidyl peptidase IV (DPP-IV) by tryptophan containing dipeptides. *Food & Function*, *4*(12), 1843. https://doi.org/10.1039/c3fo60262a

Nongonierma, A. B., & FitzGerald, R. J. (2017). Unlocking the biological potential of proteins from edible insects through enzymatic hydrolysis: A review. *Innovative Food Science & Emerging Technologies*, *43*, 239–252. https://doi.org/10.1016/j.ifset.2017.08.014

Nongonierma, A. B., & FitzGerald, R. J. (2019). Features of dipeptidyl peptidase IV (DPP-IV) inhibitory peptides from dietary proteins. *Journal of Food Biochemistry*, *43*(1), e12451. https://doi.org/10.1111/jfbc.12451

Nongonierma, A. B., Mooney, C., Shields, D. C., & FitzGerald, R. J. (2014). *In silico* approaches to predict the potential of milk protein-derived peptides as dipeptidyl peptidase IV (DPP-IV) inhibitors.

Peptides, *57*, 43–51. https://doi.org/10.1016/j.peptides.2014.04.018

Ojeda-Montes, M. J., Gimeno, A., Tomas-Hernández, S., Cereto-Massagué, A., Beltrán-Debón, R., Valls, C., Mulero, M., Pujadas, G., & Garcia-Vallvé, S. (2018). Activity and selectivity cliffs for DPP-IV inhibitors: Lessons we can learn from SAR studies and their application to virtual screening. *Medicinal Research Reviews*, *38*(6), 1874–1915. https://doi.org/10.1002/med.21499

Olsen, J. V., Ong, S.-E., & Mann, M. (2004). Trypsin cleaves exclusively C-terminal to arginine and lysine residues. *Molecular & Cellular Proteomics*, *3*(6), 608–614. https://doi.org/10.1074/mcp.t400003-mcp200

Pais, R., Gribble, F. M., & Reimann, F. (2016). Signalling pathways involved in the detection of peptones by murine small intestinal enteroendocrine L-cells. *Peptides*, *77*, 9–15. https://doi.org/10.1016/j.peptides.2015.07.019

Park, J., & Jang, H.-J. (2017). Anti-diabetic effects of natural products an overview of therapeutic strategies. *Molecular & Cellular Toxicology*, *13*(1), 1–20. https://doi.org/10.1007/s13273-017-0001-1

Qiu, L., Deng, Z., Zhao, C., Xiao, T., Weng, C., Li, J., & Zheng, L. (2021). Nutritional composition and proteomic analysis of soft-shelled turtle (*Pelodiscus sinensis*) egg and identification of oligopeptides with alpha-glucosidase inhibitory activity. *Food Research International*, *145*, 110414. https://doi.org/10.1016/j.foodres.2021.110414

Rendón-Rosales, M. Á., Torres-Llanez, M. J., Mazorra-Manzano, M. A., González-Córdova, A. F., Hernández-Mendoza, A., & Vallejo-Cordoba, B. (2022). *In vitro* and *in silico* evaluation of multifunctional properties of bioactive synthetic peptides identified in milk fermented with *Lactococcus lactis* NRRL B-50571 and NRRL B-50572. *LWT*, *154*, 112581. https://doi.org/10.1016/j.lwt.2021.112581

Rivero Pino, F., Pérez Gálvez, R., Espejo Carpio, F. J., & Guadix, E. M. (2020). Evaluation of *Tenebrio molitor* protein as a source of peptides for modulating physiological processes. *Food & Function*, *11*(5), 4376–4386. https://doi.org/10.1039/d0fo00734j

Rivero-Pino, F., Espejo-Carpio, F. J., & Guadix, E. M. (2020). Antidiabetic food-derived peptides for functional feeding: Production, functionality and *in vivo* evidences. *Foods*, *9*(8), 983. https://doi.org/10.3390/foods9080983

Rivero-Pino, F., Guadix, A., & Guadix, E. M. (2021). Identification of novel dipeptidyl peptidase IV and α-glucosidase inhibitory peptides from *Tenebrio molitor*. *Food & Function*, *12*(2), 873–880. https://doi.org/10.1039/d0fo02696d

Sánchez, A., & Vázquez, A. (2017). Bioactive peptides: A review. *Food Quality and Safety*, *1(1)*, 29–46. https://doi.org/10.1093/fqsafe/fyx006

Sasaoka, Y., Takagi, T., Michiba, S., Yamamoto, Y., Kumagai, Y., & Kishimura, H. (2021). Study on the mechanism of the blood-glucose-lowering effect of collagen peptides from sturgeon by-products. *Marine Drugs*, *19*(10), 584. https://doi.org/10.3390/md19100584

Scheen, A. J. (2003). Is there a role for α-glucosidase inhibitors in the prevention of type 2 diabetes mellitus? *Drugs*, *63*(10), 933–951. https://doi.org/10.2165/00003495-200363100-00002

Silveira, S. T., Martínez-Maqueda, D., Recio, I., & Hernández-Ledesma, B. (2013). Dipeptidyl peptidase-IV inhibitory peptides generated by tryptic hydrolysis of a whey protein concentrate rich in β-lactoglobulin. *Food Chemistry*, *141*(2), 1072–1077. https://doi.org/10.1016/j.foodchem.2013.03.056

Siow, H.-L., & Gan, C.-Y. (2016). Extraction, identification, and structure–activity relationship of antioxidative and α-amylase inhibitory peptides from cumin seeds (*Cuminum cyminum*). *Journal of Functional Foods*, *22*, 1–12. https://doi.org/10.1016/j.jff.2016.01.011

Song, J. J., Wang, Q., Du, M., Ji, X. M., & Mao, X. Y. (2017). Identification of dipeptidyl peptidase-IV inhibitory peptides from mare whey protein hydrolysates. *Journal of Dairy Science*, *100*(9), 6885–6894. https://doi.org/10.3168/jds.2016-11828

Sulistiyani, Safithri, M., & Sari, Y. P. (2016). Inhibition of α-glucosidase activity by ethanolic extract of *Melia azedarach L*. leaves. *IOP Conference Series: Earth and Environmental Science*, *31*, 012025. https://doi.org/10.1088/1755-1315/31/1/012025

Sun, X., Acquah, C., Aluko, R. E., & Udenigwe, C. C. (2020). Considering food matrix and gastrointestinal

effects in enhancing bioactive peptide absorption and bioavailability. *Journal of Functional Foods*, *64*, 103680. https://doi.org/10.1016/j.jff.2019.103680

Tadesse, S. A., & Emire, S. A. (2020). Production and processing of antioxidant bioactive peptides: A driving force for the functional food market. *Heliyon*, *6*(8), e04765. https://doi.org/10.1016/j.heliyon.2020.e04765

Taga, Y., Hayashida, O., Kusubata, M., Ogawa-Goto, K., & Hattori, S. (2017). Production of a novel wheat gluten hydrolysate containing dipeptidyl peptidase-IV inhibitory tripeptides using ginger protease. *Bioscience, Biotechnology, and Biochemistry, 81*(9), 1823–1828. https://doi.org/10.1080/09168451.2017.1345615

Tang, Y., Debnath, T., Choi, E.-J., Kim, Y. W., Ryu, J. P., Jang, S., Chung, S. U., Choi, Y.-J., & Kim, E.-K. (2018). Changes in the amino acid profiles and free radical scavenging activities of *Tenebrio molitor* larvae following enzymatic hydrolysis. *PLoS ONE*, *13*(5), e0196218. https://doi.org/10.1371/journal.pone.0196218

Thakur, S., Chhimwal, J., Joshi, R., Kumari, M., Padwad, Y., & Kumar, R. (2021). Evaluating peptides of *picrorhiza kurroa* and their inhibitory potential against ACE, DPP-IV, and oxidative stress. *J. Proteome Res.*, *20*(8), 3798–3813. https://doi.org/10.1021/acs.jproteome.1c00081

Tysoe, C., Williams, L. K., Keyzers, R., Nguyen, N. T., Tarling, C., Wicki, J., Goddard-Borger, E. D., Aguda, A. H., Perry, S., & Foster, L. J. (2016). Potent human α-amylase inhibition by the β-defensin-like protein helianthamide. *ACS Central Science.*, *2*(3), 154–161. https://doi.org/10.1021/acscentsci.5b00399

Ustunol, Z. (2015). Physical, chemical, and processing-induced changes in proteins. In *Applied food protein chemistry.* p. 23–46. https://doi.org/10.1002/9781118860588.ch4

Vatić, S., Mirković, N., Milošević, J. R., Jovčić, B., & Polović, N. Đ. (2020). Broad range of substrate specificities in papain and fig latex enzymes preparations improve enumeration of *Listeria monocytogenes*. *International Journal of Food Microbiology*, *334*, 108851. https://doi.org/10.1016/j.ijfoodmicro.2020.108851

Vercruysse, L., Smagghe, G., Herregods, G., & Van Camp, J. (2005). Ace inhibitory activity in enzymatic hydrolysates of insect protein. *Journal of Agricultural and Food Chemistry*, *53*(13), 5207–5211. https://doi.org/10.1021/jf050337q

Vilcacundo, R., Martínez-Villaluenga, C., & Hernández-Ledesma, B. (2017). Release of dipeptidyl peptidase IV, α-amylase and α-glucosidase inhibitory peptides from quinoa (*Chenopodium quinoa Willd*.) during *in vitro* simulated gastrointestinal digestion. *Journal of Functional Foods*, *35*, 531–539. https://doi.org/10.1016/j.jff.2017.06.024

Wang, B., Yu, Z., Yokoyama, W., Chiou, B.-S., Chen, M., Liu, F., & Zhong, F. (2021). Collagen peptides with DPP-IV inhibitory activity from sheep skin and their stability to *in vitro* gastrointestinal digestion. *Food Bioscience*, *42*, 101161. https://doi.org/10.1016/j.fbio.2021.101161

Wang, J., Wu, T., Fang, L., Liu, C., Liu, X., Li, H., Shi, J., Li, M., & Min, W. (2020). Anti-diabetic effect by walnut (*Juglans mandshurica Maxim*.)-derived peptide LPLLR through inhibiting α-glucosidase and α-amylase, and alleviating insulin resistance of hepatic HepG2 cells. *Journal of Functional Foods*, *69*, 103944. https://doi.org/10.1016/j.jff.2020.103944

Wang, R., Zhao, H., Pan, X., Orfila, C., Lu, W., & Ma, Y. (2019). Preparation of bioactive peptides with antidiabetic, antihypertensive, and antioxidant activities and identification of α-glucosidase inhibitory peptides from soy protein. *Food Science & Nutrition*, *7*(5), 1848–1856. https://doi.org/10.1002/fsn3.1038

Wang, T.-Y., Hsieh, C.-H., Hung, C.-C., Jao, C.-L., Chen, M.-C., & Hsu, K.-C. (2015). Fish skin gelatin hydrolysates as dipeptidyl peptidase IV inhibitors and glucagon-like peptide-1 stimulators improve glycaemic control in diabetic rats: A comparison between warm- and cold-water fish. *Journal of Functional Foods*, *19*, 330–340. https://doi.org/10.1016/j.jff.2015.09.037

Xiang, X., Lang, M., Li, Y., Zhao, X., Sun, H., Jiang, W., Ni, L., & Song, Y. (2021). Purification, identification and molecular mechanism of dipeptidyl peptidase IV inhibitory peptides from discarded shrimp (*Penaeus vannamei*) head. *Journal of Chromatography B*, *1186*, 122990. https://doi.org/10.1016/j.jchromb.2021.122990

Xiong, Y., Ng, K., Zhang, P., Warner, R. D., Shen, S., Tang, H.-Y., Liang, Z., & Fang, Z. (2020). *In vitro* α-glucosidase and α-amylase inhibitory activities of free and bound phenolic extracts from the bran and kernel fractions of five sorghum grain genotypes. *Foods*, *9*(9), 1301. https://doi.org/10.3390/foods9091301

Xu, F., Yao, Y., Xu, X., Wang, M., Pan, M., Ji, S., Wu, J., Jiang, D., Ju, X., & Wang, L. (2019). Identification and quantification of DPP-IV-inhibitory peptides from hydrolyzed-rapeseed-protein-derived napin with analysis of the interactions between key residues and protein domains. *Journal of Agricultural and Food Chemistry*, *67*(13), 3679–3690. https://doi.org/10.1021/acs.jafc.9b01069

You, H., Zhang, Y., Wu, T., Li, J., Wang, L., Yu, Z., Liu, J., Liu, X., & Ding, L. (2022). Identification of dipeptidyl peptidase IV inhibitory peptides from rapeseed proteins. *LWT*, *160*, 113255. https://doi.org/10.1016/j.lwt.2022.113255

Yu, Y., Jin, Y., Wang, F., Yan, J., Qi, Y., & Ye, M. (2017). Protein digestomic analysis reveals the bioactivity of deer antler velvet in simulated gastrointestinal digestion. *Food Research International*, *96*, 182–190. https://doi.org/10.1016/j.foodres.2017.04.002

Yu, Z., Yin, Y., Zhao, W., Liu, J., & Chen, F. (2012). Anti-diabetic activity peptides from albumin against α-glucosidase and α-amylase. *Food Chemistry*, *135*(3), 2078–2085. https://doi.org/10.1016/j.foodchem.2012.06.088

Yu, Z., Yin, Y., Zhao, W., Yu, Y., Liu, B., Liu, J., & Chen, F. (2011). Novel peptides derived from egg white protein inhibiting alpha-glucosidase. *Food Chemistry*, *129*(4), 1376–1382. https://doi.org/10.1016/j.foodchem.2011.05.067

Zambrowicz, A., Pokora, M., Setner, B., Dąbrowska, A., Szołtysik, M., Babij, K., Szewczuk, Z., Trziszka, T., Lubec, G., & Chrzanowska, J. (2015). Multifunctional peptides derived from an egg yolk protein hydrolysate: isolation and characterization. *Amino Acids*, *47*(2), 369–380. https://doi.org/10.1007/s00726-014-1869-x

Zhang, C., Gao, S., Zhang, C., Zhang, Y., Liu, H., Hong, H., & Luo, Y. (2020). Evaluating *in vitro* dipeptidyl peptidase IV inhibition by peptides from common carp (*Cyprinus carpio*) roe in cell culture models. *European Food Research and Technology*, *246*(1), 179–191. https://doi.org/10.1007/s00217-019-03399-6

Zhang, Ying, Chen, R., Ma, H., & Chen, S. (2015). Isolation and identification of dipeptidyl peptidase IV-inhibitory peptides from trypsin/chymotrypsin-treated goat milk casein hydrolysates by 2D-TLC and LC–MS/MS. *Journal of Agricultural and Food Chemistry*, *63*(40), 8819–8828. https://doi.org/10.1021/acs.jafc.5b03062

Zhang, Yu, Wang, N., Wang, W., Wang, J., Zhu, Z., & Li, X. (2016). Molecular mechanisms of novel peptides from silkworm pupae that inhibit α-glucosidase. *Peptides*, *76*, 45–50. https://doi.org/10.1016/j.peptides.2015.12.004

Zhao, B., Su, K., Mao, X., & Zhang, X. (2020). Separation and identification of enzyme inhibition peptides from dark tea protein. *Bioorganic Chemistry*, *99*, 103772. https://doi.org/10.1016/j.bioorg.2020.103772

Zheng, L., Xu, Q., Lin, L., Zeng, X.-A., Sun, B., & Zhao, M. (2019). *In vitro* metabolic stability of a casein-derived dipeptidyl peptidase-IV (DPP-IV) inhibitory peptide VPYPQ and its controlled release from casein by enzymatic hydrolysis. *Journal of Agricultural and Food Chemistry*, *67*(38), 10604–10613. https://doi.org/10.1021/acs.jafc.9b03164

Zhu, Q., Chen, X., Wu, J., Zhou, Y., Qian, Y., Fang, M., Xie, J., & Wei, D. (2017). Dipeptidyl peptidase IV inhibitory peptides from *Chlorella vulgaris*: *in silico* gastrointestinal hydrolysis and molecular mechanism. *European Food Research and Technology*, *243*(10), 1739–1748. https://doi.org/10.1007/s00217-017-2879-1

Zielińska, E., Karaś, M., Baraniak, B., & Jakubczyk, A. (2020). Evaluation of ACE, α-glucosidase, and lipase inhibitory activities of peptides obtained by *in vitro* digestion of selected species of edible insects. *European Food Research and Technology*, *246*(7), 1361–1369. https://doi.org/10.1007/s00217-020-03495-y

Table S1. Simulated digestion of the α-amylase inhibiting peptides.

Source	Sequence	*In silico* digestion	No. of cleavages	Positions of cleavage sites	Digested peptides
Cumin seed (*Cuminum cyminum*)	FFRSKLLSDGAAAAKGALLPQYW	Chymotrypsin-high specificity	3	1, 2, 22	F, FF, FFRSKLLSDGAAAAKGALLPQY
		Chymotrypsin-low specificity	6	1, 2, 6, 7, 18, 22	F, FF, FFRSKL, FFRSKLL, FFRSKLLSDGAAAAKGAL, FFRSKLLSDGAAAAKGALLPQY
		Pepsin (pH1.3)	4	1, 2, 6, 19	F, FF, FFRSKL, FFRSKLLSDGAAAAKGALL
		Trypsin	3	3, 5, 15	FFR, FFRSK, FFRSKLLSDGAAAAK
Cumin seed (*Cuminum cyminum*)	DPAQPNYPWTAVLVFRH	Chymotrypsin-high specificity	2	9, 15	DPAQPNYPW, DPAQPNYPWTAVLVF
		Chymotrypsin-low specificity	3	9, 13, 15	DPAQPNYPW, DPAQPNYPWTAVL, DPAQPNYPWTAVLVF
		Pepsin (pH1.3)	4	12, 13, 14, 15	DPAQPNYPWTAV, DPAQPNYPWTAVL, DPAQPNYPWTAVLV, DPAQPNYPWTAVLVF
		Trypsin	1	16	DPAQPNYPWTAVLVFR
Cumin seed (*Cuminum cyminum*)	RCMAFLLSDGAAAAQQLLPQYW	Chymotrypsin-high specificity	2	5, 21	RCMAF, RCMAFLLSDGAAAAQQLLPQY
		Chymotrypsin-low specificity	6	3, 5, 6, 7, 17, 21	RCM, RCMAF, RCMAFL, RCMAFLL, CMAFLLSDGAAAAQQL, RCMAFLLSDGAAAAQQLLPQY
		Pepsin (pH1.3)	6	4, 5, 6, 7, 16, 18	RCMA, RCMAF, RCMAFL, RCMAFLL, RCMAFLLSDGAAAAQQ, RCMAFLLSDGAAAAQQLL
Oat meal (*Avena sativa*)	YFDEQNEQFR	Trypsin	1	1	R
		Chymotrypsin-high specificity	3	1, 2, 9	Y, YF, YFDEQNEQF
		Chymotrypsin-low specificity	3	1, 2, 9	Y, YF, YFDEQNEQF
		Pepsin (pH1.3)	4	1, 2, 8, 9	Y, YF, YFDEQNEQ, YFDEQNEQF
Oat meal (*Avena sativa*)	NINAHSVVY	Trypsin	-	-	-
		Chymotrypsin-high specificity	-	-	-
		Chymotrypsin-low specificity	1	5	NINAH
		Pepsin (pH1.3)	-	-	-
		Trypsin	-	-	-

(Continued) **Table S1.** Simulated digestion of the α-amylase inhibiting peptides.

Source	Sequence	*In silico* digestion	No. of cleavages	Positions of cleavage sites	Digested peptides
Oat meal (*Avena* sativa)	RALPIDVL	Chymotrypsin-high specificity	-	-	-
		Chymotrypsin-low specificity	-	-	-
		Pepsin (pH1.3)	1	7	RALPIDV
		Trypsin	1	1	R
Spirulina platensis (*Spirulina platensis*)	LRSELAAWSR	Chymotrypsin-high specificity	1	8	LRSELAAW
		Chymotrypsin-low specificity	3	1, 5, 8	L, LRSEL, LRSELAAW
		Pepsin (pH1.3)	2	1, 5	L, LRSEL
		Trypsin	1	2	LR
Spirulina platensis (*Spirulina platensis*)	GVPMPNK	Chymotrypsin-high specificity	-	-	-
		Chymotrypsin-low specificity	-	-	-
		Pepsin (pH1.3)	-	-	-
		Trypsin	-	-	-
Spirulina platensis (*Spirulina platensis*)	RNPFVFAPTLLTVAAR	Chymotrypsin-high specificity	2	4, 6	RNPF, RNPFVF
		Chymotrypsin-low specificity	4	4, 6, 10, 11	RNPF, RNPFVF, RNPFVFAPTL, RNPFVFAPTLL
		Pepsin (pH1.3)	3	5, 10, 11	RNPFV, RNPFVFAPTL, RNPFVFAPTLL
		Trypsin	1	1	R
Parmigiano-Reggiano Cheese	IPP	Chymotrypsin-high specificity	-	-	-
		Chymotrypsin-low specificity	-	-	-
		Pepsin (pH1.3)	-	-	-
		Trypsin	-	-	-
Walnut (*Juglans mandshurica*)	LPLLR	Chymotrypsin-high specificity	-	-	-
		Chymotrypsin-low specificity	2	3, 4	LPL, LPLL
		Pepsin (pH1.3)	3	1, 2, 4	L, LP, LPLL
		Trypsin	1	5	LPLLR

(Continued) **Table S1.** Simulated digestion of the α-amylase inhibiting peptides.

Source	Sequence	*In silico* digestion	No. of cleavages	Positions of cleavage sites	Digested peptides
Red Seaweed (*Porphyra spp*)	GGSK	Chymotrypsin-high specificity	-	-	-
		Chymotrypsin-low specificity	-	-	-
		Pepsin (pH1.3)	-	-	-
		Trypsin	-	-	-
Red Seaweed (*Porphyra spp*)	ELS	Chymotrypsin-high specificity	-	-	-
		Chymotrypsin-low specificity	1	2	EL
		Pepsin (pH1.3)	2	1, 2	E, EL
		Trypsin	-	-	-
Pinto bean (*Phaseolus vulgaris*)	LSSLEMGSLGALFVCM	Chymotrypsin-high specificity	1	13	LSSLEMGSLGALF
		Chymotrypsin-low specificity	6	1, 4, 6, 9, 12, 13	L, LSSL, LSSLEM, LSSLEMGSL, LSSLEMGSLGAL, LSSLEMGSLGALF
		Pepsin (pH1.3)	8	1, 3, 4, 8, 9, 11, 12, 13	L, LSS, LSSL, LSSLEMGS, LSSLEMGSL, LSSLEMGSLGA, LSSLEMGSLGAL, LSSLEMGSLGALF
		Trypsin	-	-	-
Pinto bean (*Phaseolus vulgaris*)	PLPWGAGF	Chymotrypsin-high specificity	1	4	PLPW
		Chymotrypsin-low specificity	1	4	PLPW
		Pepsin (pH1.3)	1	7	PLPWGAG
		Trypsin	-	-	-
Pinto bean (*Phaseolus vulgaris*)	PLPLHMLP	Chymotrypsin-high specificity	-	-	-
		Chymotrypsin-low specificity	2	4, 6	PLPL, PLPLHM
		Pepsin (pH1.3)	1	3	PLP
		Trypsin	-	-	-
Pinto bean (*Phaseolus vulgaris*)	PPHMGGP	Chymotrypsin-high specificity	-	-	-
		Chymotrypsin-low specificity	1	4	PPHM
		Pepsin (pH1.3)	-	-	-
		Trypsin	-	-	-

(Continued) **Table S1.** Simulated digestion of the α-amylase inhibiting peptides.

Source	Sequence	*In silico* digestion	No. of cleavages	Positions of cleavage sites	Digested peptides
Pinto bean (*Phaseolus vulgaris*)	PPHMLP	Chymotrypsin-high specificity	-	-	-
		Chymotrypsin-low specificity	1	4	PPHM
		Pepsin (pH1.3)	-	-	-
		Trypsin	-	-	-

Table S2. Simulated digestion of the α-glucosidase inhibiting peptides.

Source	Sequence	*In silico* digestion	No. of cleavages	Positions of cleavage sites	Digested peptides
Desert locus (*Schistocerca gregaria*)	FDPFPK	Chymotrypsin-high specificity	1	1	F
		Chymotrypsin-low specificity	1	1	F
		Pepsin (pH1.3)	-	-	-
		Trypsin	-	-	-
Mealworm (*Tenebrio molitor*)	AAAPVAVAK	Chymotrypsin-high specificity	-	-	-
		Chymotrypsin-low specificity	-	-	-
		Pepsin (pH1.3)	-	-	-
		Trypsin	-	-	-
Desert locus (*Schistocerca gregaria*)	AIGVGAIER	Chymotrypsin-high specificity	-	-	-
		Chymotrypsin-low specificity	-	-	-
		Pepsin (pH1.3)	-	-	-
		Trypsin	-	-	-
Almond oil manufacture residue (*Prunus dulcis*)	WH	Chymotrypsin-high specificity	1	1	W
		Chymotrypsin-low specificity	1	1	W
		Pepsin (pH1.3)			
		Trypsin	-	-	-
Silkworm pupae (*Bombyx mori*)	SQSPA	Chymotrypsin-high specificity	-	-	-
		Chymotrypsin-low specificity	-	-	-
		Pepsin (pH1.3)	-	-	-
		Trypsin	-	-	-
Soybean protein (*Glycine max*)	GSR	Chymotrypsin-high specificity	-	-	-
		Chymotrypsin-low specificity	-	-	-
		Pepsin (pH1.3)	-	-	-
		Trypsin	-	-	-
Changium Root (*Changii Radix*)	KVIISAPSKDAPMF	Chymotrypsin-high specificity	-	-	-
		Chymotrypsin-low specificity	1	13	KVIISAPSKDAPM
		Pepsin (pH1.3)	-	-	-
		Trypsin	2	1, 9	K, KVIISAPSK

(Continued) **Table S2.** Simulated digestion of the α-glucosidase inhibiting peptides.

Source	Sequence	*In silico* digestion	No. of cleavages	Positions of cleavage sites	Digested peptides
Desert locus (*Schistocerca gregaria*)	GKDAVIV	Chymotrypsin-high specificity	-	-	-
		Chymotrypsin-low specificity	-	-	-
		Pepsin (pH1.3)	-	-	-
		Trypsin	1	2	GK
Criket (*Grylloides sigillatus*)	KVEGDLK	Chymotrypsin-high specificity	-	-	-
		Chymotrypsin-low specificity	1	6	KVEGDL
		Pepsin (pH1.3)	2	5, 6	KVEGD, KVEGDL
		Trypsin	1	1	K
Almond oil manufacture residue (*Prunus dulcis*)	WS	Chymotrypsin-high specificity	1	1	W
		Chymotrypsin-low specificity	1	1	W
		Pepsin (pH1.3)	-	-	-
		Trypsin	-	-	-
Mealworm (*Tenebrio molitor*)	NYVADGLG	Chymotrypsin-high specificity	1	2	NY
		Chymotrypsin-low specificity	2	2, 7	NY, NYVADGL
		Pepsin (pH1.3)	2	6, 7	NYVADG, NYVADGL
		Trypsin	-	-	-
Mealworm (*Tenebrio molitor*)	AGDDAPR	Chymotrypsin-high specificity	-	-	-
		Chymotrypsin-low specificity	-	-	-
		Pepsin (pH1.3)	-	-	-
		Trypsin	-	-	-
Cricket (*Grylloides sigillatus*)	IIAPPER	Chymotrypsin-high specificity	-	-	-
		Chymotrypsin-low specificity	-	-	-
		Pepsin (pH1.3)	-	-	-
		Trypsin	-	-	-
Dark tea protein (*Camellia sinensis*)	VVDLVFFAAAK	Chymotrypsin-high specificity	2	6, 7	VVDLVF, VVDLVFF
		Chymotrypsin-low specificity	3	4, 6, 7	VVDL, VVDLVF, VVDLVFF
		Pepsin (pH1.3)	5	3, 4, 5, 6, 7	VVD, VVDL, VVDLV, VVDLVF, VVDLVFF
		Trypsin	-	-	-

(Continued) **Table S2.** Simulated digestion of the α-glucosidase inhibiting peptides.

Source	Sequence	*In silico* digestion	No. of cleavages	Positions of cleavage sites	Digested peptides
Soft-shelled turtle egg (*Pelodiscus sinensis*)	HNKPEVEVR	Chymotrypsin-high specificity	-	-	-
		Chymotrypsin-low specificity	1	1	H
		Pepsin (pH1.3)	-	-	-
		Trypsin	-	-	-
Cricket (*Grylloides sigillatus*)	LAPSTIK	Chymotrypsin-high specificity	-	-	-
		Chymotrypsin-low specificity	1	1	L
		Pepsin (pH1.3)	-	-	-
		Trypsin	-	-	-
Silkworm pupae (*Bombyx mori*)	QPGR	Chymotrypsin-high specificity	-	-	-
		Chymotrypsin-low specificity	-	-	-
		Pepsin (pH1.3)	-	-	-
		Trypsin	-	-	-
Spirulina platensis (*Spirulina platensis*)	RNPFVFAPTLLTVAAR	Chymotrypsin-high specificity	2	4, 6	RNPF, RNPFAP
		Chymotrypsin-low specificity	4	4, 6, 10, 11	RNPF, RNPFAP, RNPFVFAPTL, RNPFVFAPTLL
		Pepsin (pH1.3)	3	5, 10, 11	RNPFA, RNPFVFAPTL, RNPFVFAPTLL
		Trypsin	1	1	R
Quinoa (*Chenopodium quinoa*)	IQAEGGLT	Chymotrypsin-high specificity	-	-	-
		Chymotrypsin-low specificity	1	7	IQAEGGL
		Pepsin (pH1.3)	2	6, 7	IQAEGG, IQAEGGL
		Trypsin	-	-	-
Spirulina platensis (*Spirulina platensis*)	LRSELAAWSR	Chymotrypsin-high specificity	1	8	LRSELAAW
		Chymotrypsin-low specificity	3	1, 5, 8	L, LRSEL, LRSELAAW
		Pepsin (pH1.3)	2	1, 5	L, LRSEL
		Trypsin	1	2	LR

(Continued) **Table S2.** Simulated digestion of the α-glucosidase inhibiting peptides.

Source	Sequence	*In silico* digestion	No. of cleavages	Positions of cleavage sites	Digested peptides
Soybean protein (*Glycine max*)	WLRL	Chymotrypsin-high specificity	1	1	W
		Chymotrypsin-low specificity	2	1, 2	W, WL
		Pepsin (pH1.3)	2	1, 2	W, WL
		Trypsin	1	3	WLR
Soybean protein (*Glycine max*)	SWLRL	Chymotrypsin-high specificity	1	2	SW
		Chymotrypsin-low specificity	2	2, 3	SW, SWL
		Pepsin (pH1.3)	2	2, 3	SW, SWL
		Trypsin	-	-	-
Soft-shelled turtle egg (*Pelodiscus sinensis*)	ARDASVLK	Chymotrypsin-high specificity	-	-	-
		Chymotrypsin-low specificity	1	7	A
		Pepsin (pH1.3)	2	6, 7	ARDASV, ARDASVL
		Trypsin	1	2	AR
Spirulina platensis (*Spirulina platensis*)	GVPMPNK	Chymotrypsin-high specificity	-	-	-
		Chymotrypsin-low specificity	-	-	-
		Pepsin (pH1.3)	-	-	-
		Trypsin	-	-	-
Silkworm pupae (*Bombyx mori*)	NSPR	Chymotrypsin-high specificity	-	-	-
		Chymotrypsin-low specificity	-	-	-
		Pepsin (pH1.3)	-	-	-
		Trypsin	-	-	-
Soybean protein (*Glycine max*)	LLPLPVLK	Chymotrypsin-high specificity	-	-	-
		Chymotrypsin-low specificity	2	1, 7	L, LLPLPVL
		Pepsin (pH1.3)	2	2, 7	LL, LLPLPVL
		Trypsin	-	-	-
Soft-shelled turtle egg (*Pelodiscus sinensis*)	SGTLLHK	Chymotrypsin-high specificity	-	-	-
		Chymotrypsin-low specificity	3	4, 5, 6	SGTL, SGTLL, SGTLLH
		Pepsin (pH1.3)	3	3, 4, 5	SGT, SGTL, SGTLL
		Trypsin	-	-	-

(Continued) **Table S2.** Simulated digestion of the α-glucosidase inhibiting peptides.

Source	Sequence	*In silico* digestion	No. of cleavages	Positions of cleavage sites	Digested peptides
Eggyolk protein by-product (*Gallus domesticus*)	VTGRFAGHPAAQ	Chymotrypsin-high specificity	1	5	VTGRF
		Chymotrypsin-low specificity	1	5	VTGRF
		Pepsin (pH1.3)	1	5	VTGRF
		Trypsin	1	4	VTGR
Eggyolk protein by-product (*Gallus domesticus*)	YINQMPQKSREA	Chymotrypsin-high specificity	1	1	Y
		Chymotrypsin-low specificity	1	1	Y
		Pepsin (pH1.3)	-	-	-
		Trypsin	2	8, 10	YINQMPQK, YINQMPQKSR
Soybean protein (*Glycine max*)	EAK	Chymotrypsin-high specificity	-	-	-
		Chymotrypsin-low specificity	-	-	-
		Pepsin (pH1.3)	-	-	-
		Trypsin	-	-	-
Changium Root (*Changii Radix*)	SQHISTAGMEASGTSNMKF	Chymotrypsin-high specificity	-	-	-
		Chymotrypsin-low specificity	3	3, 9, 17	SQH, SQHISTAGM, SQHISTAGMEASGTSNM
		Pepsin (pH1.3)	2	18	SQHISTAGMEASGTSNMK
		Trypsin	1	18	SQHISTAGMEASGTSNMK
Dark tea protein (*Camellia sinensis*)	TAELLPR	Chymotrypsin-high specificity	-	-	-
		Chymotrypsin-low specificity	1	4	TAEL
		Pepsin (pH1.3)	2	3, 5	TAE, TAELL
		Trypsin	-	-	-
Silkworm pupae (*Bombyx mori*)	QPPT	Chymotrypsin-high specificity	-	-	-
		Chymotrypsin-low specificity	-	-	-
		Pepsin (pH1.3)	-	-	-
		Trypsin	-	-	-

(Continued) **Table S2.** Simulated digestion of the α-glucosidase inhibiting peptides.

Source	Sequence	*In silico* digestion	No. of cleavages	Positions of cleavage sites	Digested peptides
Dark tea protein (*Camellia sinensis*)	CGKKFVR	Chymotrypsin-high specificity	1	5	CGKKF
		Chymotrypsin-low specificity	1	5	CGKKF
		Pepsin (pH1.3)	1	4	CGKK
		Trypsin	2	3, 4	CGK, CGKK
Dark tea protein (*Camellia sinensis*)	AVPANLVDLNVPALLK	Chymotrypsin-high specificity	-	-	-
		Chymotrypsin-low specificity	4	6, 9, 14, 15	AVPANL, AVPANLVDL, AVPANLVDLNVPAL, AVPANLVDLNVPALL
		Pepsin (pH1.3)	6	5, 6, 8, 9, 14, 15	AVPAN, AVPANL, AVPANLVD, AVPANLVDL, AVPANLVDLNVPAL, AVPANLVDLNVPALL
		Trypsin	-	-	-
Parmigiano-Reggiano Cheese	IPP	Chymotrypsin-high specificity	-	-	-
		Chymotrypsin-low specificity	-	-	-
		Pepsin (pH1.3)	-	-	-
		Trypsin	-	-	-
Changium Root (*Changii Radix*)	STFQQMW	Chymotrypsin-high specificity	1	3	STF
		Chymotrypsin-low specificity	2	3, 6	STF, STFQQM
		Pepsin (pH1.3)	2	2, 3	ST, STF
		Trypsin	-	-	-
Eggyolk protein by-product (*Gallus domesticus*)	YINQMPQKSRE	Chymotrypsin-high specificity	1	1	Y
		Chymotrypsin-low specificity	1	1	Y
		Pepsin (pH1.3)	-	-	-
		Trypsin	2	8, 10	YINQMPQK, YINQMPQKSR
Walnut (*Juglans mandshurica*)	LPLLR	Chymotrypsin-high specificity	-	-	-
		Chymotrypsin-low specificity	2	3, 4	LPL, LPLL
		Pepsin (pH1.3)	3	1, 2, 4	L, LP, LPLL

Table S3. Simulated digestion of the DPP-IV inhibiting peptides.

Source	Sequence	*In silico* digestion	No. of cleavages	Positions of cleavage sites	Digested peptides	Score (iDPPIV-SCM)
Velvet aqueous extract	GPAGPQGPR	Chymotrypsin-high specificity	-	-	-	
		Chymotrypsin-low specificity	-	-	-	
		Pepsin (pH1.3)	-	-	-	
		Trypsin	-	-	-	
Velvet aqueous extract	PPGLPGSPGQ	Chymotrypsin-high specificity	-	-	-	
		Chymotrypsin-low specificity	-	-	-	
		Pepsin (pH1.3)	1	4	PPGL	470
		Trypsin	-	-	-	
Velvet aqueous extract	LPQPPQE	Chymotrypsin-high specificity	-	-	-	
		Chymotrypsin-low specificity	-	-	-	
		Pepsin (pH1.3)	1	1	L	n.d
		Trypsin	-	-	-	
Velvet aqueous extract	LPPLTAD	Chymotrypsin-high specificity	-	-	-	
		Chymotrypsin-low specificity	1	4	LPPL	507.33
		Pepsin (pH1.3)	-	-	-	
		Trypsin	-	-	-	
Picrorhiza kurroa	ASGLCPEEAVPRR	Chymotrypsin-high specificity	-	-	-	
		Chymotrypsin-low specificity	1	4	ASGL	241
		Pepsin (pH1.3)	1	3	ASG	221
		Trypsin	1	12	ASGLCPEEAVPR	262.18
Boarfish	IPI	Chymotrypsin-high specificity	-	-	-	
		Chymotrypsin-low specificity	-	-	-	
-		Pepsin (pH1.3)	-	-	-	
		Trypsin	-	-	-	

(Continued) **Table S3.** Simulated digestion of the DPP-IV inhibiting peptides.

Source	Sequence	*In silico* digestion	No. of cleavages	Positions of cleavage sites	Digested peptides	Score (iDPPIV-SCM)
Camel whey protein	VPV	Chymotrypsin-high specificity	-	-	-	
		Chymotrypsin-low specificity	-	-	-	
		Pepsin (pH1.3)	-	-	-	
		Trypsin	-	-	-	
Sorghum bicolor seed protein	QLRDIVDK	Chymotrypsin-high specificity	-	-	-	
		Chymotrypsin-low specificity	1	2	QL	601
		Pepsin (pH1.3)	2	1	Q	n.d.
		Trypsin	1	2	QL	601
Boarfish	IPVDM	Chymotrypsin-high specificity	-	-	-	
		Chymotrypsin-low specificity	-	-	-	
		Pepsin (pH1.3)	-	-	-	
		Trypsin	-	-	-	
Quinoa	HPF	Chymotrypsin-high specificity	-	-	-	
		Chymotrypsin-low specificity	-	-	-	
		Pepsin (pH1.3)	1	2	HP	519.5
		Trypsin	-	-	-	
Boarfish	APIT	Chymotrypsin-high specificity	-	-	-	
		Chymotrypsin-low specificity	-	-	-	
		Pepsin (pH1.3)	-	-	-	
		Trypsin	-	-	-	
Camel whey protein	YPI	Chymotrypsin-high specificity	-	-	-	
		Chymotrypsin-low specificity	-	-	-	
		Pepsin (pH1.3)	-	-	-	
		Trypsin	-	-	-	

(Continued) **Table S3.** Simulated digestion of the DPP-IV inhibiting peptides.

Source	Sequence	*In silico* digestion	No. of cleavages	Positions of cleavage sites	Digested peptides	Score (iDPPIV-SCM)
Brewers' spent grain	IPVP	Chymotrypsin-high specificity	-	-	-	
		Chymotrypsin-low specificity	-	-	-	
		Pepsin (pH1.3)	-	-	-	
		Trypsin	-	-	-	
Boarfish	VPTP	Chymotrypsin-high specificity	-	-	-	
		Chymotrypsin-low specificity	-	-	-	
		Pepsin (pH1.3)	-	-	-	
		Trypsin	-	-	-	
Discarded shrimp (Penaeus vannamei) head	YPGE	Chymotrypsin-high specificity	-	-	-	
		Chymotrypsin-low specificity	-	-	-	
		Pepsin (pH1.3)	-	-	-	
		Trypsin	-	-	-	
Casein	VPYPQ	Chymotrypsin-high specificity	-	-	-	
		Chymotrypsin-low specificity	-	-	-	
		Pepsin (pH1.3)	-	-	-	
		Trypsin	-	-	-	
Atlantic salmon (Salmo salar)	GPGA	Chymotrypsin-high specificity	-	-	-	
		Chymotrypsin-low specificity	-	-	-	
		Pepsin (pH1.3)	-	-	-	
		Trypsin	-	-	-	
Whey protein isolate	LKPTPEGDLE	Chymotrypsin-high specificity	-	9	LKPTPEGDL	305.88
		Pepsin (pH1.3)	2	8	LKPTPEGD	309.43
		Pepsin (pH1.3)	2	9	LKPTPEGDL	305.88
		Trypsin	-	-	-	

(Continued) **Table S3.** Simulated digestion of the DPP-IV inhibiting peptides.

Source	Sequence	*In silico* digestion	No. of cleavages	Positions of cleavage sites	Digested peptides	Score (iDPPIV-SCM)
Palmaria palmata	ILAP	Chymotrypsin-high specificity	-	-	-	
		Chymotrypsin-low specificity	1	2	IL	510
		Pepsin (pH1.3)	1	1	I	n.d
		Trypsin	-	-	-	
Whey protein concentrate rich in β-lactoglobulin	IPAVF	Chymotrypsin-high specificity	-	-	-	n.d
		Chymotrypsin-low specificity	1	5		
				4	IPAV	405.33
		Pepsin (pH1.3)	2	5		
		Trypsin	-	-	-	
Brewers' spent grain	LPIA	Chymotrypsin-high specificity	-	-	-	
		Chymotrypsin-low specificity	-	-	-	
		Pepsin (pH1.3)	1	1	L	n.d.
		Trypsin	-	-	-	
Boarfish	GPIN	Chymotrypsin-high specificity	-	-	-	
		Chymotrypsin-low specificity	-	-	-	
		Pepsin (pH1.3)	-	-	-	
		Trypsin	-	-	-	
Parmigiano-Reggiano Cheese	APFPE	Chymotrypsin-high specificity	-	-	-	
		Chymotrypsin-low specificity	-	-	-	
		Pepsin (pH1.3)	-	-	-	
		Trypsin	-	-	-	
Atlantic salmon (Salmo salar)	GPAE	Chymotrypsin-high specificity	-	-	-	
		Chymotrypsin-low specificity	-	-	-	
		Pepsin (pH1.3)	-	-	-	

(Continued) **Table S3.** Simulated digestion of the DPP-IV inhibiting peptides.

Source	Sequence	*In silico* digestion	No. of cleavages	Positions of cleavage sites	Digested peptides	Score (iDPPIV-SCM)
Boarfish	LPVYD	Trypsin	-	-	-	
		Chymotrypsin-high specificity	1	4	LPVY	443.33
		Chymotrypsin-low specificity	1	4	LPVY	443.33
		Pepsin (pH1.3)	1	1	L	n.d
Brewers' spent grain	IPY	Trypsin	-	-	-	
		Chymotrypsin-high specificity	-	-	-	
		Chymotrypsin-low specificity	-	-	-	
		Pepsin (pH1.3)	-	-	-	
Rapeseed (Brassica napus) napin	IPQVS	Trypsin	-	-	-	
		Chymotrypsin-high specificity	-	-	-	
		Chymotrypsin-low specificity	-	-	-	
		Pepsin (pH1.3)	-	-	-	
Boarfish	LPVDM	Trypsin	-	-	-	
		Chymotrypsin-high specificity	-	-	-	
		Chymotrypsin-low specificity	-	-	-	
		Pepsin (pH1.3)	1	1	L	n.d
Palmaria palmata	LLAP	Trypsin	-	-	-	
		Chymotrypsin-high specificity	-	-	-	
		Chymotrypsin-low specificity	2	1	L	n.d
		Trypsin	-	2	LL	562
		Pepsin (pH1.3)	1	1	L	n.d
Brewers' spent grain	VPIP	Trypsin	-	-	-	
		Chymotrypsin-high specificity	-	-	-	
		Chymotrypsin-low specificity	-	-	-	

(Continued) **Table S3.** Simulated digestion of the DPP-IV inhibiting peptides.

Source	Sequence	*In silico* digestion	No. of cleavages	Positions of cleavage sites	Digested peptides	Score (iDPPIV-SCM)
Camel whey protein	VPF	Chymotrypsin-high specificity	-	-	-	
		Chymotrypsin-low specificity	-	-	-	
		Pepsin (pH1.3)	1	2	VP	771
		Trypsin	-	-	-	
Wheat gluten hydrolysate	LPQ	Chymotrypsin-high specificity	-	-	-	
		Chymotrypsin-low specificity	-	-	-	
		Pepsin (pH1.3)	1	1	L	n.d.
		Trypsin	-	-	-	
Whey protein isolate	LKPTPEGDLEIL	Chymotrypsin-high specificity	2	1	L	n.d.
		Chymotrypsin-low specificity	1	9	LKPTPEGDL	305.88
		Pepsin (pH1.3)	1			
		Chymotrypsin-low specificity	3	8	LKPTPEGD	309.43
				9	LKPTPEGDL	305.88
				11	LKPTPEGDLEI	295.2
Boarfish	APLER	Pepsin (pH1.3)	-	-	-	
		Trypsin	-	-	-	
		Chymotrypsin-high specificity	-	-	-	
		Chymotrypsin-low specificity	1	3	APL	488.5
		Pepsin (pH1.3)	1	2	AP	696
Casein-derived peptides	FLQP	Trypsin	-	-	-	
		Chymotrypsin-high specificity	1	1	F	n.d
		Chymotrypsin-low specificity	2	1	F	n.d
		Pepsin (pH1.3)	2	2	FL	551
		Pepsin (pH1.3)	1	1	F	n.d

(Continued) **Table S3.** Simulated digestion of the DPP-IV inhibiting peptides.

Source	Sequence	*In silico* digestion	No. of cleavages	Positions of cleavage sites	Digested peptides	Score (iDPPIV-SCM)
Fish skin - tilapia	IPGDPGPPGPPGP	Trypsin	-	-	-	
		Chymotrypsin-high specificity	-	-	-	
		Chymotrypsin-low specificity	-	-	-	
Boarfish	IPGA	Pepsin (pH1.3)	-	-	-	
		Chymotrypsin-high specificity	-	-	-	
		Chymotrypsin-low specificity	-	-	-	
Sheep skin	GPAGPOGFPG	Pepsin (pH1.3)	-	-	-	
		Trypsin	-	-	-	
		Chymotrypsin-high specificity	-	-	-	
		Chymotrypsin-low specificity	-	-	-	
		Pepsin (pH1.3)	1	8	GPAGPOGF	n.d
Boarfish	GPSL	Trypsin	-	-	-	
		Chymotrypsin-high specificity	-	-	-	
		Chymotrypsin-low specificity	-	-	-	
		Pepsin (pH1.3)	-	-	-	
Mare whey protein	TQMVDEEIMEKFR	Trypsin	-	-	-	
		Chymotrypsin-high specificity	1	12	TQMVDEEIMEKF	290.36
				3	TQM	493.5
				9	TQMVDEEIM	331
		Chymotrypsin-low specificity	3	12	TQMVDEEIMEKF	290.36
				11	TQMVDEEIMEK	292.4
		Pepsin (pH1.3)	2	12	TQMVDEEIMEKF	290.36
				11	TQMVDEEIMEK	292.4
		Trypsin	-	-	-	

Table S4. New protein sources of the α-amylase inhibiting peptides.

Source	Sequence	New sources BLASTp *	Hits
Cumin seed (*Cuminum cyminum*)	FFRSKLLSDGAAAAKGALLPQYW	*Lupinus albus*	43
		Cicer arietinum	10
		Helianthus annuus	23
		Olea europaea	21
		Tenebrio molitor	12
Cumin seed (*Cuminum cyminum*)	DPAQPNYPWTAVLVFRH	*Lupinus albus*	22
		Cicer arietinum	16
		Helianthus annuus	51
		Oleaeuropaea	11
		Tenebrio molitor	9
		Sardina pilchardus	4
Cumin seed (*Cuminum cyminum*)	RCMAFLLSDGAAAAQQLLPQYW	*Lupinus albus*	33
		Cicer arietinum	11
		Helianthus annuus	22
		Olea europaea	21
		Tenebrio molitor	11
Oat meal (*Avena sativa*)	YFDEQNEQFR	*Olea europaea*	18
		Helianthus annuus	70
		Cicer arietinum	9
		Lupinus albus	11
		Tenebrio molitor	16
Oat meal (*Avena sativa*)	NINAHSVVY	*Olea europaea*	13
		Helianthus annuus	47
		Lupinus albus	20
		Cicer arietinum	20
		Pisum sativum	19
		Tenebrio molitor	10
Oat meal (*Avena sativa*)	RALPIDVL	*Helianthus annuus*	33
		Olea europaea	19
		Lupinus albus	33
		Cicer arietinum	22
		Tenebrio molitor	12
Spirulina platensis (*Spirulina platensis*)	LRSELAAWSR	*Olea europaea*	32
		Helianthus annuus	37
		Lupinus albus	27
		Cicer arietinum	11
		Tenebrio molitor	8

(Continued) **Table S4.** New protein sources of the α-amylase inhibiting peptides.

Source	Sequence	New sources BLASTp *	Hits
Spirulina platensis (*Spirulina platensis*)	GVPMPNK	*Helianthus annuus*	36
		Olea europaea	30
		Cicer arietinum	13
		Lupinus albus	15
		Pisum sativum	3
		Tenebrio molitor	6
Spirulina platensis (*Spirulina platensis*)	RNPFVFAPTLLTVAAR	*Tenebrio molitor*	22
		Micromesistius poutassou	2
		Lupinus albus	19
		Helianthus annuus	35
		Cicer arietinum	11
		Olea europaea	13
Parmigiano-Reggiano Cheese	IPP	No significant similarity found.	
Walnut (*Juglans mandshurica*)	LPLLR	*Tenebrio molitor*	8
		Helianthus annuus	67
		Cicer arietinum	2
		Lupinus albus	9
		Olea europaea	17
Red Seaweed (*Porphyra spp*)	GGSK	*Tenebrio molitor*	1
		Helianthus annuus	1
		Cicer arietinum	1
		Lupinus albus	1
		Olea europaea	1
Red Seaweed (*Porphyra spp*)	ELS	No significant similarity found.	
Pinto bean (*Phaseolus vulgaris*)	LSSLEMGSLGALFVCM	*Tenebrio molitor*	1
		Helianthus annuus	1
		Cicer arietinum	1
		Lupinus albus	1
		Olea europaea	2
Pinto bean (*Phaseolus vulgaris*)	PLPWGAGF	*Tenebrio molitor*	7
		Helianthus annuus	69
		Cicer arietinum	3
		Lupinus albus	18
		Olea europaea	9
		Sardina pilchardus	2
		Micromesistius poutassou	2
		Trachurus trachurus	3

(Continued) **Table S4.** New protein sources of the α-amylase inhibiting peptides.

Source	Sequence	New sources BLASTp *	Hits
Pinto bean (*Phaseolus vulgaris*)	PLPLHMLP	*Tenebrio molitor*	19
		Helianthus annuus	15
		Cicer arietinum	9
		Lupinus albus	22
		Olea europaea	25
		Micromesistius poutassou	2
Pinto bean (*Phaseolus vulgaris*)	PPHMGGP	*Tenebrio molitor*	22
		Helianthus annuus	50
		Cicer arietinum	6
		Lupinus albus	11
		Olea europaea	14
Pinto bean (*Phaseolus vulgaris*)	PPHMLP	*Tenebrio molitor*	10
		Helianthus annuus	53
		Cicer arietinum	9
		Lupinus albus	16
		Olea europaea	22

Table S5. New protein sources of the α-glucosidase inhibiting peptides

Source	Sequence	New sources BLASTp *	Hits
Desert locus (*Schistocerca gregaria*)	FDPFPK	*Helianthus annuus*	38
		Olea europaea	25
		Lupinus albus	17
		Cicer arietinum	14
		Tenebrio molitor	9
Mealworm (*Tenebrio molitor*)	AAAPVAVAK	*Lupinus albus*	16
		Olea europaea	11
		Helianthus annuus	11
		Cicer arietinum	9
Desert locus (*Schistocerca gregaria*)	AIGVGAIER	*Helianthus annuus*	44
		Lupinus albus	37
		Olea europaea	14
		Cicer arietinum	7
		Tenebrio molitor	5
		Pisum sativum	1
Almond oil manufacture residue (*Prunus dulcis*)	WH	No significant similarity found	
Silkworm pupae (*Bombyx mori*)	SQSPA	*Helianthus annuus*	34
		Lupinus albus	30
		Olea europaea	25
		Tenebrio molitor	12
		Cicer arietinum	6
Soybean protein (*Glycine max*)	GSR	No significant similarity found	
Changium Root (*Changii Radix*)	KVIISAPSKDAPMF	*Olea europaea*	36
		Helianthus annuus	33
		Lupinus albus	24
		Cicer arietinum	8
		Pisum sativum	6
		Tenebrio molitor	2
Desert locus (*Schistocerca gregaria*)	GKDAVIV	*Lupinus albus*	32
		Tenebrio molitor	28
		Olea europaea	17
		Cicer arietinum	14
		Helianthus annuus	16
		Pisum sativum	5

(Continued) **Table S5.** New protein sources of the α-glucosidase inhibiting peptides

Source	Sequence	New sources BLASTp *	Hits
Cricket (*Grylloides sigillatus*)	KVEGDLK	*Helianthus annuus*	32
		Tenebrio molitor	22
		Lupinus albus	20
		Olea europaea	16
		Cicer arietinum	7
Almond oil manufacture residue (*Prunus dulcis*)	WS	No significant similarity found	
Mealworm (*Tenebrio molitor*)	NYVADGLG	*Lupinus albus*	30
		Olea europaea	23
		Helianthus annuus	21
		Olea europaea	18
		Cicer arietinum	14
		Pisum sativum	4
Mealworm (*Tenebrio molitor*)	AGDDAPR	*Lupinus albus*	39
		Helianthus annuus	36
		Olea europaea	28
		Cicer arietinum	12
		Pisum sativum	10
Cricket (*Grylloides sigillatus*)	IIAPPER	*Helianthus annuus*	36
		Lupinus albus	35
		Olea europaea	34
		Pisum sativum	17
		Cicer arietinum	13
		Tenebrio molitor	11
		Sardina pilchardus	1
Dark tea protein (*Camellia sinensis*)	VVDLVFFAAAK	*Helianthus annuus*	34
		Tenebrio molitor	22
		Cicer arietinum	20
		Lupinus albus	19
		Olea europaea	17
Soft-shelled turtle egg (*Trionyx sinensis*)	HNKPEVEVR	*Helianthus annuus*	37
		Olea europaea	26
		Lupinus albus	24
		Tenebrio molitor	17
		Cicer arietinum	10

(Continued) **Table S5.** New protein sources of the α-glucosidase inhibiting peptides

Source	Sequence	New sources BLASTp *	Hits
Cricket (*Grylloides sigillatus*)	LAPSTIK	*Helianthus annuus*	31
		Tenebrio molitor	25
		Lupinus albus	18
		Olea europaea	17
		Cicer arietinum	9
		Sardina pilchardus	1
Silkworm pupae (*Bombyx mori*)	QPGR	*Lupinus albus*	58
		Tenebrio molitor	26
		Olea europaea	6
		Helianthus annuus	5
		Cicer arietinum	4
Spirulina platensis (*Spirulina platensis*)	RNPFVFAPTLLTVAAR	*Helianthus annuus*	35
		Tenebrio molitor	22
		Lupinus albus	19
		Olea europaea	13
		Cicer arietinum	11
		Micromesistius poutassou	2
Quinoa (*Chenopodium quinoa*)	IQAEGGLT	*Helianthus annuus*	45
		Lupinus albus	24
		Tenebrio molitor	18
		Olea europaea	16
		Cicer arietinum	13
Spirulina platensis (*Spirulina platensis*)	LRSELAAWSR	*Helianthus annuus*	37
		Olea europaea	32
		Lupinus albus	27
		Cicer arietinum	11
		Tenebrio molitor	8
Soybean protein (*Glycine max*)	WLRL	*Lupinus albus*	32
		Olea europaea	25
		Tenebrio molitor	17
		Cicer arietinum	16
		Helianthus annuus	13

(Continued) **Table S5.** New protein sources of the α-glucosidase inhibiting peptides

Source	Sequence	New sources BLASTp *	Hits
Soybean protein (*Glycine max*)	SWLRL	*Lupinus albus*	30
		Helianthus annuus	28
		Tenebrio molitor	22
		Cicer arietinum	14
		Olea europaea	9
Soft-shelled turtle egg (*Trionyx sinensis*)	ARDASVLK	*Helianthus annuus*	57
		Lupinus albus	44
		Olea europaea	15
		Cicer arietinum	7
		Tenebrio molitor	6
Spirulina platensis (*Spirulina platensis*)	GVPMPNK	*Helianthus annuus*	36
		Olea europaea	30
		Lupinus albus	15
		Cicer arietinum	13
		Tenebrio molitor	6
		Pisum sativum	3
Silkworm pupae (*Bombyx mori*)	NSPR	*Tenebrio molitor*	50
		Helianthus annuus	19
		Olea europaea	17
		Lupinus albus	10
		Cicer arietinum	6
		Pisum sativum	1
Soybean protein (*Glycine max*)	LLPLPVLK	*Lupinus albus*	32
		Helianthus annuus	32
		Olea europaea	16
		Tenebrio molitor	14
		Cicer arietinum	11
		Pisum sativum	4
Soft-shelled turtle egg (*Trionyx sinensis*)	SGTLLHK	*Helianthus annuus*	32
		Lupinus albus	22
		Tenebrio molitor	19
		Cicer arietinum	16
		Olea europaea	15

(Continued) **Table S5.** New protein sources of the α-glucosidase inhibiting peptides

Source	Sequence	New sources BLASTp *	Hits
Eggyolk protein by-product (*Gallus domesticus*)	VTGRFAGHPAAQ	*Olea europaea*	32
		Lupinus albus	27
		Helianthus annuus	25
		Cicer arietinum	13
		Tenebrio molitor	7
Eggyolk protein by-product (*Gallus domesticus*)	YINQMPQKSREA	*Helianthus annuus*	31
		Lupinus albus	25
		Olea europaea	21
		Tenebrio molitor	17
		Cicer arietinum	7
		Pisum sativum	1
Soybean protein (*Glycine max*)	EAK	No significant similarity found.	
Changium Root (*Changii Radix*)	SQHISTAGMEASGTSNMKF	*Helianthus annuus*	37
		Lupinus albus	30
		Cicer arietinum	23
		Olea europaea	18
		Tenebrio molitor	3
Dark tea protein (*Camellia sinensis*)	TAELLPR	*Helianthus annuus*	44
		Lupinus albus	27
		Cicer arietinum	17
		Tenebrio molitor	16
		Olea europaea	13
Silkworm pupae (*Bombyx mori*)	QPPT	*Tenebrio molitor*	60
		Helianthus annuus	16
		Lupinus albus	12
		Cicer arietinum	7
		Olea europaea	7
Dark tea protein (*Camellia sinensis*)	CGKKFVR	*Tenebrio molitor*	41
		Olea europaea	18
		Helianthus annuus	17
		Cicer arietinum	14
		Lupinus albus	14
		Trachurus trachurus	1

(Continued) **Table S5.** New protein sources of the α-glucosidase inhibiting peptides

Source	Sequence	New sources BLASTp *	Hits
Dark tea protein (*Camellia sinensis*)	AVPANLVDLNVPALLK	*Olea europaea*	29
		Lupinus albus	23
		Helianthus annuus	21
		Tenebrio molitor	16
		Cicer arietinum	5
Parmigiano-Reggiano Cheese	IPP	No significant similarity found.	
Changium Root (*Changii Radix*)	STFQQMW	*Lupinus albus*	35
		Helianthus annuus	34
		Olea europaea	29
		Cicer arietinum	17
		Pisum sativum	16
		Tenebrio molitor	13
		Sardina pilchardus	1
Eggyolk protein by-product (*Gallus domesticus*)	YINQMPQKSRE	*Helianthus annuus*	32
		Lupinus albus	23
		Tenebrio molitor	21
		Olea europaea	18
		Cicer arietinum	8
Walnut (*Juglans mandshurica*)	LPLLR	*Helianthus annuus*	67
		Olea europaea	17
		Lupinus albus	9
		Tenebrio molitor	8
		Cicer arietinum	2

Table S6. New protein sources of the DPP-IV inhibiting peptides.

Source	Sequence	New sources BLASTp *	Hits
Velvet aqueous extract (*Cervus elaphus*)	GPAGPQGPR	*Tenebrio molitor*	32
		Helianthus annuus	35
		Pisum sativum	1
		Cicer arietinum	11
		Lupinus albus	22
		Olea europaea	8
Velvet aqueous extract (*Cervus elaphus*)	PPGLPGSPGQ	*Tenebrio molitor*	39
		Helianthus annuus	31
		Cicer arietinum	12
		Lupinus albus	14
		Olea europaea	13
Velvet aqueous extract (*Cervus elaphus*)	LPQPPQE	*Tenebrio molitor*	9
		Helianthus annuus	17
		Cicer arietinum	4
		Lupinus albus	57
		Olea europaea	13
Velvet aqueous extract (*Cervus elaphus*)	LPPLTAD	*Tenebrio molitor*	13
		Helianthus annuus	25
		Pisum sativum	17
		Cicer arietinum	22
		Lupinus albus	13
		Olea europaea	22
Picrorhiza kurroa (*Picrorhiza kurrooa*)	ASGLCPEEAVPRR	*Tenebrio molitor*	4
		Helianthus annuus	51
		Cicer arietinum	17
		Lupinus albus	30
		Olea europaea	14
Boarfish (*Capros aper*)	IPI	*No significant similarity found.*	
Camel whey *protein (Camelus dromedarius*)	VPV	*No significant similarity found.*	
Sorghum bicolor seed protein (*Sorghum bicolor L.)*	QLRDIVDK	*Tenebrio molitor*	13
		Helianthus annuus	31
		Cicer arietinum	14
		Lupinus albus	24
		Olea europaea	21

(Continued) **Table S6.** New protein sources of the DPP-IV inhibiting peptides.

Source	Sequence	New sources BLASTp *	Hits
Boarfish (*Capros aper*)	IPVDM	*Tenebrio molitor*	10
		Helianthus annuus	47
		Cicer arietinum	7
		Lupinus albus	15
		Olea europaea	19
Quinoa (*Chenopodium quinoa*)	HPF	*No significant similarity found.*	
Boarfish (*Capros aper*)	APIT	*Tenebrio molitor*	37
		Helianthus annuus	24
		Cicer arietinum	8
		Lupinus albus	19
		Olea europaea	15
Camel whey protein *(Camelus dromedarius*)	YPI	*No significant similarity found.*	
Brewers' spent grain (*Hordeum vulgare*)	IPVP	*Tenebrio molitor*	32
		Helianthus annuus	41
		Pisum sativum	1
		Cicer arietinum	5
		Lupinus albus	13
		Olea europaea	11
Boarfish (*Capros aper*)	VPTP	*Tenebrio molitor*	52
		Helianthus annuus	11
		Cicer arietinum	6
		Lupinus albus	11
		Olea europaea	14
Discarded shrimp head (*Penaeus vannamei*)	YPGE	*Tenebrio molitor*	27
		Helianthus annuus	42
		Cicer arietinum	8
		Lupinus albus	14
		Olea europaea	18
Casein	VPYPQ	*Tenebrio molitor*	32
		Helianthus annuus	17
		Cicer arietinum	10
		Lupinus albus	23
		Olea europaea	21
Atlantic salmon (*Salmo salar*)	GPGA	*Tenebrio molitor*	45
		Helianthus annuus	6
		Cicer arietinum	8
		Lupinus albus	39
		Olea europaea	6

(Continued) **Table S6.** New protein sources of the DPP-IV inhibiting peptides.

Source	Sequence	New sources BLASTp *	Hits
Whey protein isolate	LKPTPEGDLE	*Tenebrio molitor*	23
		Helianthus annuus	17
		Pisum sativum	2
		Cicer arietinum	10
		Lupinus albus	27
		Olea europaea	29
Dulse (*Palmaria palmata*)	ILAP	*Tenebrio molitor*	31
		Helianthus annuus	53
		Cicer arietinum	9
		Lupinus albus	7
		Olea europaea	3
Whey protein concentrate rich in β-lactoglobulin	IPAVF	*Tenebrio molitor*	11
		Helianthus annuus	32
		Cicer arietinum	8
		Lupinus albus	21
		Olea europaea	26
Brewers' spent grain (*Hordeum vulgare*)	LPIA	*Tenebrio molitor*	32
		Helianthus annuus	42
		Cicer arietinum	16
		Lupinus albus	13
		Olea europaea	13
Boarfish (*Capros aper*)	GPIN	*Tenebrio molitor*	33
		Helianthus annuus	26
		Cicer arietinum	14
		Lupinus albus	16
		Olea europaea	18
Parmigiano-Reggiano Cheese	APFPE	*Tenebrio molitor*	25
		Helianthus annuus	32
		Cicer arietinum	9
		Lupinus albus	13
		Olea europaea	13
Atlantic salmon (*Salmo salar*)	GPAE	*Tenebrio molitor*	43
		Helianthus annuus	16
		Cicer arietinum	6
		Lupinus albus	18
		Olea europaea	15

(Continued) **Table S6.** New protein sources of the DPP-IV inhibiting peptides.

Source	Sequence	New sources BLASTp *	Hits
Boarfish (*Capros aper*)	LPVYD	*Tenebrio molitor*	17
		Helianthus annuus	51
		Pisum sativum	1
		Cicer arietinum	10
		Lupinus albus	22
		Olea europaea	18
Brewers' spent grain (*Hordeum vulgare*)	IPY	*No significant similarity found.*	
Rapeseed napin (*Brassica napus*)	IPQVS	*Tenebrio molitor*	14
		Helianthus annuus	38
		Cicer arietinum	17
		Lupinus albus	27
		Olea europaea	16
Boarfish (*Capros aper*)	LPVDM	*Tenebrio molitor*	23
		Helianthus annuus	39
		Cicer arietinum	3
		Lupinus albus	12
		Olea europaea	24
Dulse (*Palmaria palmata*)	LLAP	*Tenebrio molitor*	56
		Helianthus annuus	9
		Cicer arietinum	9
		Lupinus albus	19
		Olea europaea	8
Brewers' spent grain (*Hordeum vulgare*)	VPIP	*Tenebrio molitor*	66
		Helianthus annuus	21
		Cicer arietinum	7
		Lupinus albus	9
		Olea europaea	5
Camel whey protein (*Camelus dromedarius*)	VPF	*No significant similarity found.*	
Whey protein isolate	LKPTPEGDLEIL	*Tenebrio molitor*	17
		Helianthus annuus	34
		Pisum sativum	3
		Cicer arietinum	13
		Lupinus albus	20
		Olea europaea	25

(Continued) **Table S6.** New protein sources of the DPP-IV inhibiting peptides.

Source	Sequence	New sources BLASTp *	Hits
Boarfish (*Capros aper*)	APLER	*Tenebrio molitor*	6
		Helianthus annuus	60
		Cicer arietinum	7
		Lupinus albus	17
		Olea europaea	22
Casein-derived peptides	FLQP	*Tenebrio molitor*	26
		Helianthus annuus	27
		Cicer arietinum	20
		Lupinus albus	19
		Olea europaea	16
Tilapia skin (*Oreochromis niloticus*)	IPGDPGPPGPPGP	*Tenebrio molitor*	40
		Helianthus annuus	43
		Cicer arietinum	4
		Lupinus albus	11
		Olea europaea	15
Boarfish (*Capros aper*)	IPGA	*Tenebrio molitor*	28
		Helianthus annuus	33
		Cicer arietinum	4
		Lupinus albus	17
		Olea europaea	16
Sheep skin (*Ovis aries*)	GPAGPOGFPG	*Tenebrio molitor*	36
		Helianthus annuus	14
		Pisum sativum	4
		Cicer arietinum	5
		Lupinus albus	15
		Olea europaea	25
Boarfish (*Capros aper*)	GPSL	*Tenebrio molitor*	38
		Helianthus annuus	12
		Cicer arietinum	19
		Lupinus albus	14
		Olea europaea	12
Mare whey protein (*Equus caballus*)	TQMVDEEIMEKFR	*Tenebrio molitor*	13
		Helianthus annuus	31
		Cicer arietinum	6
		Lupinus albus	11
		Olea europaea	39

CHAPTER II

Gastrointestinal stability of Dipeptidyl peptidase IV (DPP-IV)-inhibitory peptides identified in *Tenebrio molitor*

ABSTRACT

The use of insects recently emerged as an alternative source of high-quality protein for the obtention of peptides with a wide range of bioactivities, such as antidiabetic, while offering a more environmentally sustainable approach. However, antidiabetic DPP-IV inhibitory peptides are often rich in leucine, making them susceptible to degradation by pepsin and chymotrypsin during gastrointestinal digestion. This study uses bioinformatic prediction and *in vitro* activity assays to identify DPP-IV inhibitory peptides within the *Tenebrio molitor* proteome and assess their bioavailability. Conducting homology analysis, three peptides—ILAP, FLQP, and APVAH— were identified as complete matches, but efficient release of the sequences through targeted hydrolysis remains a significant challenge. Notably, a substantial decline in the DDP-IV inhibitory activity was found for the peptide fragments generated after digestion, compared to the original parent peptides. The inhibitory mechanisms of all three peptides were examined, revealing that mixed inhibition was associated with enhanced activity. Insect-derived peptides, such as APVAH with an IC_{50} of 0.013±0.001 mg peptide/mL, may serve as effective DPP-IV inhibitors for diabetes management. However, protecting these peptides from gastrointestinal proteases is essential due to observed activity loss in digested fragments.

JOURNAL PAPER: Berraquero-García, C., García-Moreno, P. J., Pérez-Gálvez, R., Espejo-Carpio, F. J., & Guadix, E. M. (2025). Gastrointestinal stability of Dipeptidyl peptidase IV (DPP-IV)-inhibitory peptides identified in *Tenebrio molitor*. *Journal of Insects as Food and Feed*. https://doi.org/10.1163/23524588-00001304 (IF: 4.7 (2023); Category: Food Science and Technology; Position: 37/173; Q1)

1. Introduction

In recent years, there has been an increasing interest in exploring protein sources that not only contain high quality bioactive peptides but also address sustainability concerns. Among these, insects have emerged as a promising alternative due to their nutritional profile and environmentally friendly production methods (Oonincx & Finke, 2023). Unlike traditional protein sources, such as dairy, fish, or plant proteins, insects boast minimal environmental footprints, requiring less land and water while having a low ecological impact (Smetana et al., 2023). Particularly, *Tenebrio molitor* is gaining recognition for its potential in functional food applications due to its rich content in bioactive peptides and has been approved by regulatory bodies like the European Food Safety Authority (EFSA) (Liguori et al., 2022) as a novel food. Studies have highlighted the potential therapeutic value of *T. molitor* derived peptides, such as managing conditions like Type 2 diabetes by inhibiting key metabolic enzymes like peptidyl-peptidase IV (DPP-IV) (Rivero-Pino et al., 2021; Zielińska et al., 2018, 2020). DPP-IV has the capacity to break down and inactivate glucagon-like peptide-1 (GLP-1) and glucose-dependent insulinotropic polypeptide (GIP). These incretins stimulate the secretion of insulin in response to food intake during the post-prandial phase (Nongonierma & FitzGerald, 2019). Thus, the inhibition of DPP-IV has been demonstrated to effectively control blood glucose levels. As a result, the search for DPP-IV inhibitors has gained attention, however synthetic inhibitors (e.g., gliptins) can exhibit adverse side-effects (Richter, 2008).

Nevertheless, current research on the production of DPP-IV inhibitory peptides from *T. molitor* and other sources, have used a non-specific trial-and-error approach where numerous enzymatic hydrolysis experiments were carried out (e.g. varying the hydrolysis conditions such as type of enzyme, degree of hydrolysis, pH, temperature and others) and then the bioactivity of the obtained hydrolysates was tested (Cermeño et al., 2019; Nongonierma et al., 2018; Tan et al., 2022; Thakur et al., 2021; B. Wang et al., 2021). As an alternative, this study aims to propose an approach that combines the prior study of bioactive sequences and the use of bioinformatic tools to identify the structural characteristics of sequences that define bioactivity (Peredo-Lovillo et al., 2022). This *in silico* methodology allows for a more targeted study and optimizes the search for new protein sources. Thus, once the specific sequences are identified and their presence in a protein matrix is ensured, it is possible to proceed with the hydrolysis, purification, and analysis of peptide activity.

The use of bioactive peptides to produce functional food is limited, since they are susceptible to undergo proteolysis during digestion, often resulting in a decrease or complete loss of their activity (Daliri et al., 2017). Hence, it is crucial that these bioactive peptides reach intact the small intestine to exert their physiological effects. However, the bioaccessibility and bioavailability

of peptides have not been yet thoroughly studied. Bioaccessibility refers to the fraction of peptides released from the food matrix during gastrointestinal digestion that are available for absorption, while bioavailability describes the fraction that enters the bloodstream and reaches the target organ to exert a specific effect (Barba et al., 2017). Different *in vitro* and *in silico* models have been developed to determine the bioaccessibility and bioavailability of other peptides, with simulated gastrointestinal digestion (SGD) models being mostly used to assess the bioaccessibility and stability of bioactive peptides (Álvarez-Olguín et al., 2023). To establish the bioavailability of peptides, the Caco-2 cell monolayer model is the most widely used (Sun et al., 2008). Additionally, several *in silico* models have been developed to simulate physiological processes involved in nutrient bioavailability (Moda et al., 2007; Yoshida & Topliss, 2000), and they may offer a promising tool for initial assessments of bioavailability, serving as a filter before conducting more complex and costly cell-based analyses. Existing studies present conflicting findings regarding the bioaccessibility of DPP-IV-inhibitory peptides. While some research, such as that involving cricket protein hydrolysates, indicates an improvement in DPP-IV inhibition following simulated gastrointestinal digestion (Nongonierma et al., 2018), other investigations demonstrate the potential loss of bioactivity during the gastrointestinal process. For instance, salmon skin gelatine hydrolysate, sericin-derived peptides, and Bambara bean hydrolysates exhibited notably reduced DPP-IV inhibitory activity after undergoing gastrointestinal digestion (Mune Mune et al., 2018; Sangsawad et al., 2022; T.-Y. Wang et al., 2015). Thus, further research is required to evaluate the impact of gastrointestinal digestion on DPP-IV inhibitory sequences, allowing to predict their potential bioactivity when absorbed in the small intestine. In our previous work (Berraquero-García et al., 2023), we conducted *in silico* examinations of the digestion of synthetic DPP-IV inhibitory peptides to investigate the potential degradation of these peptides when undergoing gastrointestinal digestion. We found that several peptides are susceptible to be further hydrolysed by gastrointestinal proteases, although the activity of the resultant peptide fragments has not been yet investigated.

As we progress towards a more sustainable and health-conscious future, the unexplored potential of insects as an alternative source of bioactive peptides warrants further investigation. Therefore, this study aims to explore the capacity of insect-derived peptides to manage Type 2 diabetes by examining the production of selected peptides through targeted enzymatic hydrolysis of *T. molitor* proteins. Additionally, we evaluated the *in vitro* DPP-IV inhibitory activity and mechanism of action of the selected peptides. Finally, we assessed the impact of gastrointestinal digestion on these peptides by analysing the DPP-IV inhibitory activity of the resulting peptide fragments, as well as analysing their bioaccesibility and bioavailability *in silico*.

2. Materials and methods

2.1. Materials and reagents

Human DPP-IV enzyme and Gly-Pro-p-nitroanilide were purchased from Sigma-Aldrich (Spain). Synthetic peptides with a purity >95% were purchased from pepMic Co., Ltd (Jiangsu, China).

2.2. Screening of DPP-IV inhibitory peptides and *in silico* gastrointestinal digestion

In previous work, 40 peptides, from different protein sources and reported DPP-IV inhibitory activity were identified in the literature (Berraquero-García et al., 2023). Among these, 14 peptides derived from *Tenebrio* which showed high probability of being degraded by gastrointestinal proteases during *in silico* digestion were selected. This allowed to predict the potential sites cleaved by pepsin and chymotrypsin and thus the peptide fragments obtained after digestion. Additionally, the peptide sequence APVAH, which was identified in a *Tenebrio molitor* protein hydrolysate with high DPP-IV-inhibitory activity (Rivero-Pino et al., 2021), was also included in this research study, since the authors did not synthesise the peptide APVAH, nor they determined its DPP-IV inhibitory activity or inhibition mechanism. Therefore, APVAH was considered in this study as a potential positive control (e.g., peptide from *Tenebrio molitor* potentially exhibiting high DPP-IV-inhibitory activity).

2.3. Presence of selected DPP-IV inhibitory peptides in *Tenebrio molitor*

To evaluate the potential of *Tenebrio molitor* meal as a source of the 15 peptides previously selected, their sequences were cross-referenced with the proteins found in *Tenebrio molitor* larvae (Table S1 in Supplementary Material). These larvae are the primary constituents of commercially available *Tenebrio* meal (Barre et al., 2019; Yi et al., 2016). We retrieved the protein sequences from the UniProt database (Soudy et al., 2020) and conducted comparisons using BLASTp (Basic Local Alignment Search Tool)(Ye et al., 2006).

2.4. *In silico* assessment of bioaccessibility and bioavailability

The Simplified Molecular Input Line-Entry System (SMILE) of the selected peptides was obtained from the PepSMI Novopro tool (https://www.novoprolabs.com/tools/). The bioaccessibility of the peptide sequences was determined using PeptideCutter (Maillet, 2020) to perform an *in silico* gastrointestinal digestion with pepsin, chymotrypsin, and trypsin (Barati et al., 2020). Then, the bioavailability was evaluated using ADMETLab3.0 (https://admetlab3.scbdd.com/), a platform for *in silico* prediction of absorption, distribution, metabolism, excretion, and toxicity (ADMET)

properties. This platform utilizes a high-quality database of 0.37M entries spanning 77 endpoints and a Directed Message Passing Neural Network framework (L. Fu et al., 2024). The following parameters were used to assess the peptides' pharmacokinetic profiles: Caco-2 Permeability, Parallel Artificial Membrane Permeability Assay (PAMPA), P-glycoprotein substrate status (P-gp), Human Intestinal Absorption (HIA), Oral Bioavailability prediction (F20, F30, F50), Plasma Protein Binding, and Blood-Brain Barrier Penetration (BBB).

2.5. Targeted hydrolysis for potential production of DPP-IV inhibitory peptides found in *Tenebrio molitor*

The potential release of the identified peptides by targeted enzymatic hydrolysis of the most abundant proteins in *Tenebrio molitor* was evaluated using commercial proteases (e.g., Alcalase, trypsin) commonly reported to produce protein hydrolysates with DPP-IV-inhibitory activity. A wide region of the parent protein was extracted with the UniProt tool (https://www.uniprot.org/), containing the target peptide sequence and enlarged down- and upstream by 15 amino acid residues. Cleavage specificity of the proteases was used to manually analyse potential hydrolysis of the protein region following the methodology proposed by (Gregersen Echers et al., 2023). Particularly, Alcalase is known for its broad specificity, but for this *in silico* analysis, preference for cleaving after Leu/Phe/Tyr/Gln residues was considered, as reported by the supplier (Novozymes A/S). Trypsin specificity is well-documented, cleaving after Lys/Arg (Olsen et al., 2004).

2.6. *In vitro* measurement of DPP-IV inhibitory activity

The *in vitro* DPP-IV inhibition assay for synthetic peptides, including the full sequences of the identified peptides and their digested fragments, was conducted following a modified method based on (Lacroix & Li-Chan, 2012). Briefly, 25 µL of DPP-IV enzyme at 0.02 U/mL were incubated at 37 °C with 100 µL of peptide solutions at varying concentrations (1-0.01 mg/mL) for 10 min. The reaction was then initiated by adding 50 µL of 1 mM Gly-Pro-p-nitroanilide. The release of the reaction product (p-nitroanilide) was monitored by measuring the absorbance at 405 nm every 2 min over 2 h at 37 °C using a Multiskan FC microplate photometer (Thermo Scientific, Vantaa, Finland). Each sample was analysed in triplicate, and the half maximal inhibitory concentration (IC_{50}) values were calculated. Results are expressed in mg of peptide/mL, as mean ± standard deviation.

2.7. Determination of DPP-IV inhibition mechanism for selected peptides

The mechanism of DPP-IV inhibition was assessed using the Lineweaver-Burk double reciprocal representation. The peptides were evaluated at two concentrations, namely their IC_{50} and $IC_{50}/2$ values. The concentration of the substrate Gly-Pro-p-nitroanilide ranged from 0.5 to 1.75 mM. The reaction was carried out as described in the previous section.

3. Results and discussion

3.1. Screening of DPP-IV inhibitory peptides and *in silico* gastrointestinal digestion

In a previous study, we investigated the impact of gastrointestinal digestion on 40 peptide sequences of known DPP-IV inhibitory activity, using the *in silico* tool PeptideCutter (Berraquero-García et al., 2023). In the *in silico* study, we included pepsin (pH: 1.3), chymotrypsin (both low and high specificity), and trypsin, as described in Barati et al. (2020), resulting in alterations in 14 out of the 40 peptide sequences due to their hydrolysis by the digestive proteases. The peptide sequences, as well as the peptide fragments derived from their digestion, are listed in Table 1.

The peptides subjected to digestion exhibited an average peptide chain length (PCL) of 8 ± 3 amino acids, which make them more susceptible to digestive enzymes attack due to their longer sequences compared to the short-chain peptides reported as DPP-IV inhibitors (Agustia et al., 2023; Gao et al., 2020; Nongonierma & FitzGerald, 2019). Nevertheless, it should be noted that short peptides (e.g., tetrapeptides) are similarly degraded by digestive proteases (Table 1). In fact, the susceptibility of proteolytic enzymes to hydrolyse peptide bonds within polypeptide substrates depends on the specific residues forming the peptide bond, as well as on those amino acids positioned before (P1) and/or after the cleavage site (P1') (Ahmed et al., 2022). According to the analysis of the peptide composition shown in Table 1, of the most abundant amino acid was Pro, with 86% of the sequences containing at least one Pro residue, followed by Leu at 79% and Ala at 50%.

Pepsin, an aspartate protease active under acidic conditions, is a main compound present in the human gastric juice (Castañeda-Valbuena et al., 2022). Pepsin has a relatively broad specificity, but primarily cleaves when bulky hydrophobic amino acid residues are on the P_1 position (Figure 1A), notably Phe, Tyr, Trp, or Leu (Ahn et al., 2013), which was the case for 10 out of the 17 pairs of the pepsin-derived peptide fragments.

Table 1. Peptide sequences and peptide fragments derived from their digestion. Retrieved from (Berraquero-García et al., 2023).

Protein Source	Sequence	IC_{50} (μM)	Peptide fragments after digestion	Digestive enzymes	Reference
Velvet aqueous extract	PPGLPGSPGQ	0.55	PPGL / PGSPGQ	Pepsin (pH1.3)	(Yu et al., 2017)
Velvet aqueous extract	LPPLTAD	1.67	LPPL / TAD	Chymotrypsin-low specificity	(Yu et al., 2017)
Picrorhiza kurroa	ASGLCPEEAVPRR	2.20	ASG / LCPEEAVPRR ASGL / CPEEAVPRR ASGLCPEEAVPR / R	Pepsin (pH1.3) Chymotrypsin-low specificity Trypsin	(Thakur et al., 2021)
Sorghum bicolor seed protein	QLRDIVDK	8.55	QLR / DIVDK QL / RDIVDK Q / LRDIVDK	Pepsin (pH1.3) Pepsin (pH1.3) Chymotrypsin-low specificity	(Majid et al., 2022)
Whey protein isolate	LKPTPEGDLE	42.00	LKPTPEGDL / E LKPTPEGD / LE L / KPTPEGDLE	Pepsin (pH1.3) Chymotrypsin-low specificity Chymotrypsin-high specificity	(Lacroix et al., 2016)
Palmaria palmata	ILAP	43.45	IL / AP I / LAP	Pepsin (pH1.3) Chymotrypsin-low specificity	(Harnedy et al., 2015)
Whey protein concentrate	IPAVF	44.70	IPAV / F	Chymotrypsin-low specificity	(Silveira et al., 2013)
Boarfish	LPVYD	51.36	LPVY / D L / PVYD	Chymotrypsin-low and high specificity Pepsin (pH1.3)	(Harnedy-Rothwell et al., 2020)
Palmaria palmata	LLAP	53.74	LL / AP L / LAP	Chymotrypsin-low specificity Pepsin (pH1.3)	(Harnedy et al., 2015)
Whey protein isolate	LKPTPEGDLEIL	57.00	LKPTPEGDLEI / L LKPTPEGDL / EIL L / KPTPEGDLEIL	Chymotrypsin-low specificity Chymotrypsin-low and high specificity Chymotrypsin- high specificity	(Lacroix et al., 2016)
Boarfish	APLER	63.67	APL / ER AP / LER	Chymotrypsin-low specificity Pepsin (pH1.3)	(Harnedy-Rothwell et al., 2020)
Casein-derived peptides	FLQP	65.30	FL / QP F / LQP	Chymotrypsin-low specificity Chymotrypsin-low and high specificity and Pepsin (pH1.3)	(Nongonierma & FitzGerald, 2013)
Sheep skin	GPAGPOGFPG	67.12	GPAGPOGF/ PG	Pepsin (pH1.3)	(B. Wang et al., 2021)
Mare whey protein	TQMVDEEIMEKFR	69.84	TQMVDEEIMEKF / R TQMVDEEIMEK / FR TQMVDEEIM / EKFR TQM / VDEEIMEKFR	Chymotrypsin-low specificity and Pepsin (pH1.3) Chymotrypsin- high specificity Chymotrypsin- high specificity	(Song et al., 2017)

Similarly, chymotrypsin, combining both low and high specificity variants, produced 17 pairs of fragments from peptides in Table 1. Chymotrypsin, a key constituent of pancreatic juice, feature an uncharged hydrophobic pocket (known as S_1 pocket) that favours the cleavage after large hydrophobic and aromatic amino acids like Tyr, Phe, Trp, and Leu (Figure 1B) (Leiros et al., 2004). Additionally, chymotrypsin can hydrolyse bonds formed by other amino acids such as Asn, Cys, Gly, or His, depending on the adjacent residue (Chen et al., 2017; Hill & Schmidt, 1962). For instance, the presence of Pro in position P_2 has been identified as favouring chymotrypsin cleavage, as observed in the peptides LPPLTAD and APLER (Gráf et al., 2013). Among the 17 pairs of fragments generated by chymotrypsin, 12 resulted from cleavage after Leu (Table 1). In contrast, trypsin exhibited the least impact on the digestion of DPP-IV inhibitory peptides shown in Table 1. Trypsin, a pancreatic serine protease renowned for its well-defined binding sites, primarily cleaves longer peptide sequences, particularly those containing Arg and Lys (Leiros et al., 2004). Given that the content of these amino acids in the peptides was only 14% for Arg and 21% for Lys (Table 1), it was expectable that only two peptides (QLRDIVDK and TQMVDEEIMEKFR) were susceptible to trypsin cleavage..

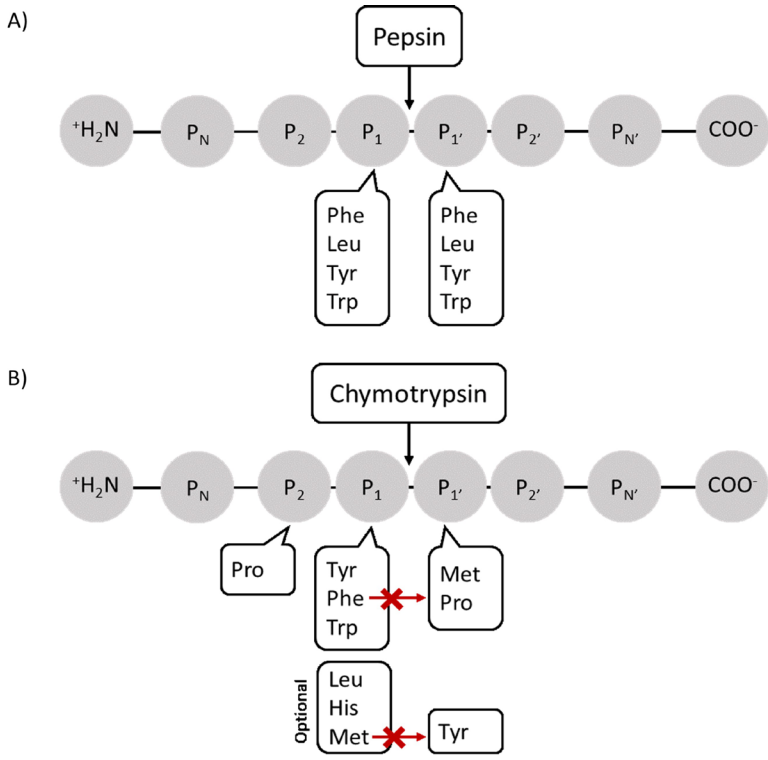

Figure 1. Cleavage preference by A) Pepsin and B) Chymotrypsin.

3.2. Presence of selected DPP-IV inhibitory peptides in *Tenebrio molitor*

The potential generation of the 14 peptide sequences listed in Table 1 after hydrolysis of *Tenebrio molitor* meal was investigated by determining their presence within the most abundant proteins of *Tenebrio molitor*. First, we established a database containing the principal proteins identified in *Tenebrio molitor* meal (Barre et al., 2019) using UniProt (Table 1S in Supplementary Material). Secondly, the peptide sequences were compared against the protein database through a BLASTp analysis.

BLASTp is currently the most widely used tool for conducting homology studies between peptides and proteins. Through the alignment of these sequences, it enables the identification of peptide uniqueness and/or potential protein sources (sources from which these peptides may originate) (Bianco et al., 2022; Di Renzo et al., 2023; Hou et al., 2023; Kim et al., 2023). Additionally, the 'Peptide Search' web-tool (https://www.uniprot.org/peptidesearch/) within UniProtKB (Bateman et al., 2021) allows retrieving sequences that precisely match the query sequence (Jia et al., 2022; Yesiltas et al., 2022). However, these sequences must be at least 7 amino acids long, which excluded all our selected peptides. While BLASTp acknowledges sequences with slight discrepancies (e.g., amino acid substitutions, gaps) as matches, only sequences with a 100% sequence coverage were considered in this study. Consequently, we observed only two peptide sequences exhibiting complete matches with *Tenebrio molitor* proteins: 1) ILAP, identified in the Myosin heavy chain protein (A0A8J6HQ90_TENMO) (Figure S1A in Supplementary Material), and 2) FLQP, identified in the alpha-amylase protein (AMY_TENMO) (Figure S1B in Supplementary Material). The presence of the peptide APVAH, with reported DPP-IV inhibitory activity and previously identified in *Tenebrio molitor* protein hydrolysate, was also confirmed within the sequence of the cuticular protein (O18508_TENMO) (Figure S1C in Supplementary Material).

It is worth noting that the *Tenebrio molitor* proteome is not fully characterised and the UniProt proteome database only encompasses 31 reviewed sequences, while the remaining 19,482 identified proteins are unreviewed (accessed on 02/12/2024). For the peptide APVAH, we could identify a reviewed protein (O18508_TENMO - Cuticular protein) in this search. Therefore, our findings suggest that while we identified complete matches for some of the sequences, the full extent of their presence within the *Tenebrio molitor* proteome remains still uncertain. Further research and characterization of the proteome are essential for a more comprehensive understanding of the peptide composition in *Tenebrio molitor*.

3.3. *In silico* bioaccesibility and bioavailability

The peptides ILAP, FLQP, and APVAH exhibit varying degrees of bioaccessibility and bioavailability, which are critical for their potential as antidiabetic agents. Regarding bioaccessibility, peptides were found to undergo degradation during gastrointestinal digestion, as discussed in the criteria for sequence selection. Specifically, ILAP and FLQP were degraded by chymotrypsin-low specificity and pepsin, whereas APVAH demonstrated higher bioaccessibility, showing resistance to digestive enzymatic degradation. Previous work on edible insects has focused on mineral bioaccessibility, reporting negative impacts of gastrointestinal digestion on nutrient bioaccessibility (Manditsera et al., 2019). However, the digestibility of insect proteins, closely linked to bioaccessibility, has also been explored, reporting high digestibility for *Tenebrio molitor* protein (Lampová et al., 2024). Furthermore, bioaccessibility improvements have been observed in *T. molitor* protein when used to supplement bread, with cooking enhancing nutrient availability (Igual et al., 2021). Regarding bioavailability, *in silico* analysis using ADMETLab3.0 facilitated a comprehensive comparison of several key parameters. The Caco-2 permeability model, a widely employed method for assessing bioavailability, predicts the ability of a compound to pass through intestinal cells via passive diffusion (Panse & Gerk, 2022). Previous research using Caco-2 models has indicated that the mineral bioavailability of *T. molitor* and grasshoppers is comparable to that of sirloin beef (Panse & Gerk, 2022). However, data on the bioavailability of edible insect proteins/peptides using Caco-2 or similar models remain limited. In this study, ADMETLab3.0 predicted low Caco-2 permeability for all peptides and their digested fractions (> -5.15 log unit) (Table 2), yet it is well stablished within the scientific community that small peptides are able to cross the gut-wall and be absorbed (Miner-Williams et al., 2014). Furthermore, while this model offers valuable insights, it oversimplifies the complexities of peptide absorption by omitting active transport mechanisms (Sun et al., 2008). Therefore, the PAMPA model was also employed to measure passive diffusion across a lipophilic membrane, simulating permeability under simplified conditions (Sun et al., 2017). All peptides and their fractions reported the highest permeability classification (+++) (Table 2). These results were complemented by the HIA model, which directly predicts a compound's absorption in the gastrointestinal system (Wessel et al., 1998). Among the peptides, ILAP exhibited the most promising profile with strong PAMPA permeability, high HIA, and superior bioavailability in the F20%, F30%, and F50% ranges (Table 2). Similarly, APVAH reported high PAMPA permeability, moderate HIA, and excellent bioavailability. In contrast, FLQP, despite showing strong PAMPA permeability, reported very low HIA and moderate bioavailability at F20% and F30%. .

Table 2. Bioavailability parameters of the selected peptides and their digested fractions. Obtained from ADMETLab3.0.

Peptide	Caco-2 Permeability	PAMPA[a]	HIA[b]	Bioavailability (F20, F30, F50%)[c]	Pgp substrate[d]	PPB[e]	BBB[f]
ILAP	-5.817	+++	+++	+++, +++, +++	++	47.3%	---
IL	-5.438	+++	+	+++, +++, +++	---	60.0%	---
AP	-5.641	+++	-	--, ---, --	+	13.5%	---
FLQP	-5.812	+++	---	+, +, +++	+++	37.5%	---
FL	-6.034	+++	---	--, --, +	+++	52.6%	---
QP	-5.949	+++	---	---, ---, --	+	9.0%	---
APVAH	-6.071	+++	+	+++, +++, +++	---	15.3%	---

[a] PAMPA: Parallel Artificial Membrane Permeability Assay

[b] HIA: Human Intestinal Absorption

[c] Estimated percentage of the compound bioavailable at 20% (F20), 30% (F30), and 50% (F50) thresholds after oral administration

[d] P-glycoprotein (P-gp) substrate

[e] PPB: Plasma Protein Binding

[f] BBB: Blood-Brain Barrier Penetration

The P-glycoprotein test is important for understanding protein bioavailability. This test identifies whether a peptide will be actively pumped out by the P-gp pump, which can reduce its absorption and bioavailability (Fromm, 2000). While the peptides APVAH and ILAP are not P-gp substrates, FLQP could present limited absorption (Table 2). Hence, FLQP may need strategies to overcome P-gp efflux, such as employing P-gp inhibitors or encapsulation. Another key factor is plasma protein binding (PPB), which affects how much of the peptide is available to interact with its targets (Wanat, 2020). The PPB of the studied peptides was in an acceptable range (<90%), meaning most of the peptide would remain unbound and active in the blood. Finally, none of the peptides are predicted to cross the blood-brain barrier (BBB). This could be beneficial, as it may prevent unwanted effects in the nervous system.

In summary, the studied peptides exhibit promising pharmacokinetic properties. Particularly, APVAH and ILAP show strong potential as pharmacological compounds for antidiabetic therapies. However, FLQP, while moderately permeable, could be limited due to P-gp efflux. Furthermore, when combining the information on the bioaccessibility and bioavailability of the studied peptides, it would be necessary to explore innovative drug delivery systems to enhance their stability. Specifically, encapsulation strategies such as nano-microparticle-based delivery systems or lipid formulations can protect peptides from degradation, enhance intestinal permeability, and potentially mitigate P-gp efflux (Mohan et al., 2015).

Finally, despite the promising *in silico* profiles, it is essential to recognize the limitations of these models, as they cannot fully replicate the complexities of *in vivo* conditions. While the *in silico* results provide valuable preliminary insights, the next critical step in optimizing these peptides for clinical use would be to validate these findings through *in vitro* studies, such as Caco-2 assays, which can more accurately simulate peptide transport and absorption behaviour within the human gastrointestinal system.

3.4. Production of DPP-IV inhibitory peptides by targeted enzymatic hydrolysis.

The production of the selected DPP-IV inhibitory peptides present in *Tenebrio molitor* proteins was further investigated by targeted enzymatic hydrolysis using commercial proteases such as Alcalase and trypsin. Therefore, this *in silico* analysis relied on th specificities of these enzymes and employed a 15-amino acid N- and C-terminal cleavage window as previously reported by (Gregersen Echers et al., 2023) (Figure 2).

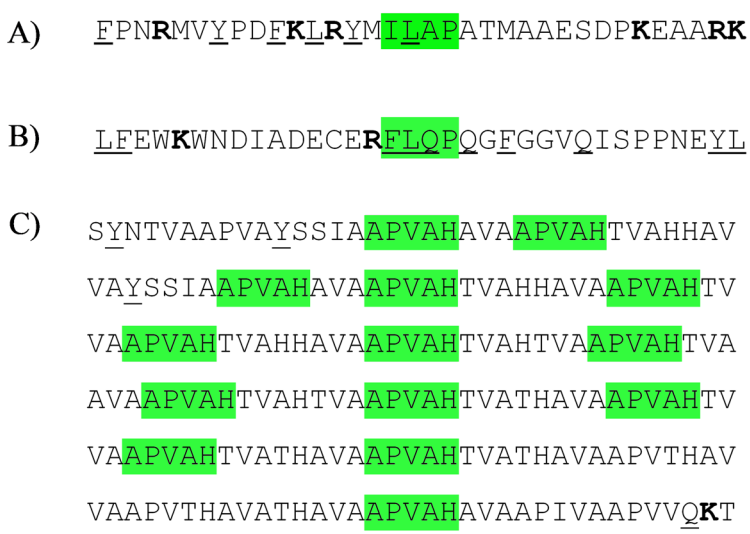

Figure 2. *In silico* potential release following targeted enzymatic hydrolysis for A) ILAP,B) FLQP and C) APVAH. Peptides are highlighted in gray, cleavage sites for trypsin (cleavage after R/K) are **bold** and cleavage sites for Alcalase (cleavage after L/F/Y/Q) are underlined

Figure 2 shows that nor Alcalase neither trypsin allowed the direct release of the target peptides. For instance, the peptide ILAP (Figure 2A), would not be released after hydrolysis with Alcalase, considering the cleavage site in the Leu residue. Hydrolysis with trypsin could potentially yield a 16-amino acid sequence, YMILAPATMAAESDPK, which comprises the target ILAP sequence. Notably, this peptide exhibits the potential for robust DPP-IV inhibitory activity, attributed to the presence of Pro in the second position at the C-terminal end, a well-recognised favourable characteristic (Nongonierma & FitzGerald, 2019). Nevertheless, the DPP-IV inhibitory activity of YMILAPATMAAESDPK might markedly differ from the targeted peptide.

The release of the peptide FLQP using Alcalase presents a challenge due to the susceptibility of three out of its four constituent residues to cleavage by this enzyme (Figure 2B). A feasible alternative involves the generation of peptide LQPQ, which contains nearly the entire target peptide sequence. This alternative peptide also features a Pro in the second position at the C-terminal end, favouring DPP-IV inhibitory activity. The combination of Alcalase and trypsin might facilitate the release of the peptide FLQPQ by cleaving trypsin after the Arg residue. In both cases, the target amino acids for Alcalase are abundant within the peptide sequences ILAP and FLQP, making the release of the peptides less likely. Furthermore, while the presence of target amino acids for both Alcalase and trypsin exists within both proteins, achieving a controlled and reproducible release of target peptides remains improbable. Similarly, the production of the peptide APVAH through targeted hydrolysis with Alcalase and trypsin is unfavourable, as only one cleavage site was identified for trypsin and none for Alcalase (Figure 2C). Considering that this peptide was experimentally obtained through conventional hydrolysis using a combination of Alcalase and Flavourzyme (a mix of endo- and exopeptidases) (Rivero-Pino et al., 2021), we assume that its release through other enzymatic combinations might be valid. However, we cannot include Flavourzyme's cleavage sites in this *in silico* study due to its broad specificity.

It should be noted that, while there is existing research on the targeted release of larger, emulsifying peptides (Bjørlie et al., 2023; Gregersen Echers et al., 2023), successful targeted hydrolysis of protein substrates has primarily focused on well-characterised proteins such as potato, some algae, grains, or collagen proteins (Amin et al., 2022; Nuñez et al., 2020; Valenzuela Zamudio et al., 2022; Yesiltas et al., 2022). Nevertheless, the targeted enzymatic release of the ILAP, FLQP and APVAH peptides is limited by the used commercial proteases, although it may be possible that these peptides exist in other yet-to-be-identified *Tenebrio molitor* proteins. Thus, a better understanding of the *Tenebrio molitor* proteome would be needed. It is worth mentioning that targeted hydrolysis can be beneficial for enhancing hydrolysis efficiency when employed as an initial *in silico* analysis aimed at optimizing specific factors, such as enzyme selection (Nongonierma et al., 2016). Nevertheless, executing targeted hydrolysis

with the goal of efficiently releasing specific sequences remains a significant challenge. In this sense, further efforts are required for the development of novel enzymes with the desired specificity (García-Moreno et al., 2023).

3.5. DPP-IV inhibitory activity and inhibition mechanism of peptides

The selected peptides identified in *Tenebrio molitor*, which were found to be degraded during gastrointestinal digestion presented potent DPP-IV inhibition showing a IC_{50} value of 0.079±0.002 mg/mL for ILAP 0.129±0.003 mg/mL for FLQP. It was observed that the peptide APVAH included with the purpose of comparison since it has been previously identified in a *Tenebrio molitor* protein hydrolysate exhibited higher DPP-IV inhibition (IC_{50} = 0.013±0.001 mg/mL,) All these peptides share many of the common features associated with DPP-IV inhibitory peptides, as all of them contain at least 75% hydrophobic amino acids (Liu et al., 2019). The highest inhibitory activity of APVAH might be attributed to the presence of Pro at the second position of N-terminus. This is consistent with previous studies which have reported a link between peptides containing this characteristic playing an important role in glycaemic control (Du et al., 2023). In addition, the presence of Pro at the first position of C-terminus is a highly conserved characteristic for DPP-IV inhibitory peptides (Nongonierma & FitzGerald, 2019), which might explain the DPP-IV inhibitory activity obtained for ILAP and FLQP. (Dávalos Terán et al., 2020) previously conducted studies on DPP-IV inhibition by different proteins from *Tenebrio* using bioinformatics tools, and they determined that cuticular proteins exhibit stronger DPP-IV inhibition compared to non-cuticular proteins. This fact could be linked to the higher activity demonstrated by APVAH. Furthermore, APVAH displayed notable inhibitory activity compared to other DPP-IV inhibitory peptides also identified in *Tenebrio molitor*, such as LPDQWDWR and APPDGGFWEWGD, with IC_{50} values of 0.15 and 1.03 mg/mL, respectively (Tan et al., 2022).

The mechanism of DPP-IV inhibition (e.g., competitive, acompetitive, noncompetitive) of the peptides was further investigated by using the Lineweaver-Burk plot (Figure 3). Traditionally, DPP-IV inhibitory peptides are reported to follow a competitive mechanism (Nongonierma et al., 2018; Zhu et al., 2017). Similarly, our findings confirmed a competitive inhibition pattern for the peptide FLQP (Figure 3B), as evidenced by the significant difference between the estimated values for the apparent Michaelis-Menten constant K_{app} (in the presence of inhibitor) and those calculated in absence of inhibitor K_m, as listed in Table 3. The hypothesis of competitive inhibition for the peptide FLQP is consistent with the presence of Pro at the C-terminus. This feature is reported to favour its binding to the active site of DPP-IV, forming an enzyme-inhibitor complex (Nongonierma & FitzGerald, 2013).

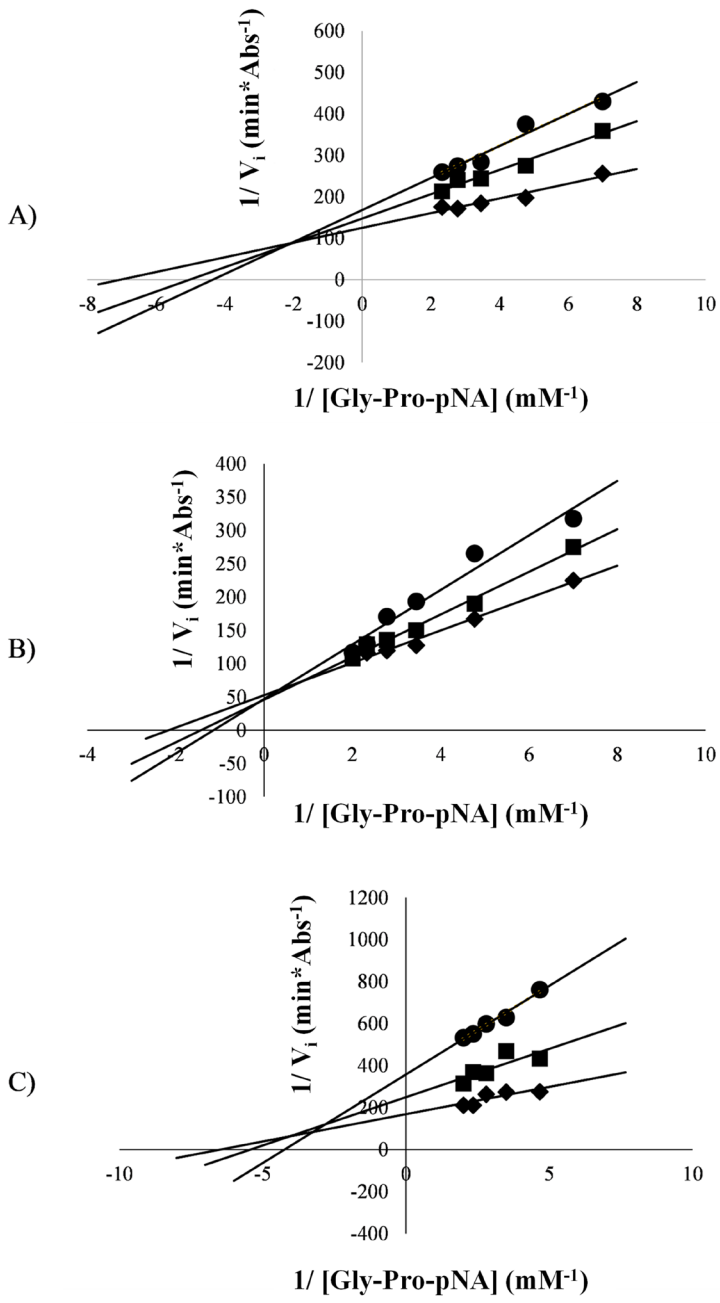

Figure 3. Lineweaver-Burk plots of DPP-IV inhibition by selected peptides: A) ILAP (mixed-type), B) FLQP (competitive), and C) APVAH (mixed-type). Filled diamond control, filled circle IC_{50} (mM), filled square $IC_{50}/2$ (mM).

Table 3. Kinetic parameters of DPP-IV inhibition in the presence of inhibitory peptides.

	ILAP			FLQP			APVAH		
	Control	IC_{50} (mM)	$IC_{50}/2$ (mM)	Control	IC_{50} (mM)	$IC_{50}/2$ (mM)	Control	IC_{50} (mM)	$IC_{50}/2$ (mM)
Inhibition type	**Mixed competitive – noncompetitive**			**Competitive**			**Mixed competitive – noncompetitive**		
K_m or K_{app} (mM)	0.142	0.199	0.231	0.462	0.672	0.699	0.155	0.184	0.236
V_{max} or V_{app}	0.008	0.007	0.006	0.0190	0.021	0.018	0.006	0.004	0.003
K_i (mM)	0.095			0.416			0.006		
K_{is} (mM)	0.319						0.013		

Moreover, there is emerging evidence from molecular docking studies suggesting that certain DPP-IV inhibitors may bind to regions different to the enzyme's active site (Lorey et al., 2003). Notably, this phenomenon was observed with peptides like FAGDDAPR, FAGDDAPRA, and FLMESH derived from *Ruditapes philippinarum* hydrolysates, exhibiting mixed inhibition patterns (Liu et al., 2017). Likewise, we observed mixed inhibition mechanisms for ILAP and APVAH peptides in this work (Figure 3A and C). The Lineweaver-Burk plots for APVAH and ILAP exhibited a mixed competitive–noncompetitive inhibition mechanism (with $K_I<K_{IS}$), which implies that the inhibitory peptide can bind either to the catalytic active site of DPP-IV or to auxiliary sites external to the catalytic centre, although the competitive inhibition was more favourable. The inhibition constant (K_I) values for ILAP and APVAH were estimated to 0.095 and 0.006 mM, respectively. The lower value of K_I for APVAH implies a stronger affinity to the active site of DPP-IV compared to ILAP (Y. Fu et al., 2017). The mixed inhibition behaviour found for APVAH can be attributed to the presence of Ala at the N-terminal end, potentially limiting the binding to the S_2 pocket of DPP-IV and impeding hydrogen bond formation between Pro in the penultimate N-terminal position and the enzyme, as suggested by (Liu et al., 2017). Simultaneously, the presence of Pro in the second position of the peptide favours its competitive inhibition of DPP-IV, contributing to this mixed inhibition pattern (Zhang et al., 2016). Interestingly, both peptides APVAH and ILAP, exhibiting mixed inhibition patterns, showed enhanced DPP-IV inhibition when compared to FLQP (Table 3).

Table 4. DPP-IV inhibitory activity of the selected peptides and their fragments originated from digestion.

Peptide	IC_{50} (mg peptide/mL)
ILAP	0.079 ± 0.002[a]
IL	0.411 ± 0.041[b]
AP	0.896 ± 0.026[c]
FLQP	0.129 ± 0.003[a]
FL	0.612 ± 0.021[d]
QP	-
APVAH	0.013 ± 0.001[f]

IC_{50} refers to half maximal inhibitory concentration value of DPP-IV in mg of peptide/mL. Different letters indicate significant differences among substrates (n = 3).

3.6. DPP-IV inhibitory activity of peptide fragments originated during digestion.

The stability of the selected peptides against gastrointestinal proteases was analysed by comparing the IC_{50} values obtained *in vitro* for the parent peptides and their fragments originated during *in silico* digestion (Table 4). It should be noted that APVAH did not result in any peptide fragment during *in silico* gastrointestinal digestion. Among the four fragments analysed, the DPP-IV inhibitory activity decreased for three of them when compared to their parent peptide, while the fragment QP exhibited no inhibition (Table 4). This suggests that the original peptides may not withstand the digestive process, resulting in the loss of their DPP-IV inhibitory activity. In fact, the activity of the peptide fragment FL, derived from the digestion of the peptide FLQP, had previously been reported at significantly lower activity compared to the parent peptide (Nongonierma et al., 2018).

Dipeptides and tripeptides are often investigated for their potential to inhibit various biological mechanisms due to their small size, which can make them more resistant to enzymatic degradation during gastrointestinal digestion, facilitating their transport to target organs (Heres et al., 2022). Specifically, numerous studies have focused on identifying dipeptides for DPP-IV inhibition (Nongonierma & FitzGerald, 2013; Nongonierma & Fitzgerald, 2013). Nevertheless, it is important to note that many of these sequences with predicted DPP-IV inhibitory activity exhibited lower inhibition than longer sequences containing them. Furthermore, previous studies evaluating the digestion of DPP-IV inhibitory peptides have reported that it can result in reduced inhibitory activity, both *in vitro* and *in vivo* (B.

Wang et al., 2021). In contrast, other studies have reported that DPP-IV inhibitory peptides derived from *Chlorella vulgaris,* and Black Soldier Fly Prepupae could withstand simulated gastrointestinal digestion (Zhu et al., 2017). However, it is essential to consider that the peptides reported in this previous study were generated through simulated gastrointestinal digestion, suggesting that the sequences produced were inherently resistant to protease attack; otherwise, they would not have been generated in the first place.

The reduction in activity observed for ILAP and FLQP is attributed to the sequence and size alterations of their fragments. Previous studies have highlighted the importance of specific features in DPP-IV inhibitory peptides to exert their activity (Nongonierma & FitzGerald, 2019; Rodhi et al., 2023). Notably, none of the four obtained fragments presented any of these features, and even IL and FL, which contained Leu in the second position, displayed significantly higher IC_{50} values compared to the value of the parent peptides. Regarding the parent peptide ILAP, all its amino acids align with the favourable structural characteristics found for DPP-IV inhibitory tetrapeptides. Specifically, the presence of Ile at the N-terminal position has been identified as one of the top reactive residues in short peptides (Rodhi et al., 2023), as well as Leu at the second position and Pro at the C-terminal position (Nongonierma & FitzGerald, 2019). Similarly, both IL and AP showed DPP-IV inhibitory capabilities, possibly due to their complete composition of hydrophobic amino acids with aliphatic chains, capable of interacting with the hydrophobic pockets within the S_1 pocket of DPP-IV (Nongonierma & FitzGerald, 2019). Moreover, studies investigating the Structure-Activity relationship of DPP-IV inhibitory dipeptides have highlighted the significant role of the N-terminal position. They observed that the hydrophobicity, bulkiness, and polarity of the amino acid contribute to improve inhibition (Kęska & Stadnik, 2020). Specifically, the presence of Trp at the N-terminal position was favoured compared to other hydrophobic amino acids (Kęska & Stadnik, 2020; Nongonierma & FitzGerald, 2019). For the FLQP peptide, the presence of Pro at the C-terminal position also facilitates its interaction with DPP-IV through hydrophobic bonds. However, this positive factor is absent in the QP digestion fragment, showing no *in vitro* activity. On the other hand, although the FL peptide exhibits more than a fourfold reduction in activity compared to its parent peptide, it still inhibits DPP-IV. This activity could be attributed to the presence of Phe at the N-terminal position, which has been identified as an important amino acid interacting and inhibiting DPP-IV via the formation of hydrophobic interactions (Rodhi et al., 2023).

4. Conclusions

This work aimed at evaluating the antidiabetic potential of identified peptides *in Tenebrio molitor* as well as their resistance to gastrointestinal digestion and bioavailability. Out of fourteen DPP-IV inhibitory peptides, identified from various protein sources and degraded *in silico* by digestive enzymes, only peptides ILAP, FLQP, and APVAH were found to have complete matches in the *Tenebrio molitor* proteome, as revealed by BLASTp analysis. The three selected peptides, as well as their digested fractions, were analysed *in silico* to predict their bioavailability. The results indicated that ILAP and APVAH demonstrated the highest potential for effective absorption and bioavailability, while FLQP could face limitations due to P-gp efflux. The peptides were specifically targeted for production from *Tenebrio molitor* proteins by using Alcalase or trypsin. However, these commonly used commercial proteases did not allow the targeted release of the selected peptides and trial-and-error hydrolysis remains as the current method for obtaining these DPP-IV inhibitory peptides. The three studied peptides showed DPP-IV inhibitory activity, with the most potent being APVAH. This peptide showed a mixed inhibition mechanism, with competitive predominance. The peptides fragments of ILAP and FLQP formed during digestion (IL, AP, FL, and QP), exhibited a significant lower activity compared to the original parent peptides. This decline was attributed to the alteration of structural properties post-cleavage by digestive enzymes (i.e., the presence of Pro at the C-terminal of tetrapeptides), thus leading to the loss of their original antidiabetic characteristics. Thus, this study highlights the importance of protecting peptides during gastrointestinal digestion to preserve their antidiabetic potential (e.g., by encapsulation), which is required for the development of functional foods containing DPP-IV inhibitory peptides.

5. References

Agustia, F. C., Murdiati, A., Supriyadi, & Indrati, R. (2023). Production of Dipeptidyl Peptidase-IV Inhibitory Peptides from Germinated Jack Bean [Canavalia ensiformis (L.) DC.] Flour. *Preventive Nutrition and Food Science*, *28*(2), 149–159. https://doi.org/10.3746/PNF.2023.28.2.149

Ahmed, T., Sun, X., & Udenigwe, C. C. (2022). Role of structural properties of bioactive peptides in their stability during simulated gastrointestinal digestion: A systematic review. *Trends in Food Science & Technology*, *120*, 265–273. https://doi.org/10.1016/J.TIFS.2022.01.008

Ahn, J., Cao, M. J., Yu, Y. Q., & Engen, J. R. (2013). Accessing the reproducibility and specificity of pepsin and other aspartic proteases. *Biochimica et Biophysica Acta (BBA) - Proteins and Proteomics*, *1834*(6), 1222–1229. https://doi.org/10.1016/J.BBAPAP.2012.10.003

Álvarez-Olguín, M. A., González-Córdova, A. F., Hernandez-Mendoza, A., Beltrán-Barrientos, L. M., Sotelo Mundo, R. R., Torres-Llanez, M. J., & Vallejo-Cordoba, B. (2023). Bioaccessibility and Bioavailability of ACE Inhibitory Peptides from Fermented Milk with Lactococcus lactis NRRL B-50571 after an Ex Vivo Absorption Model. *ACS Food Science and Technology*, *3*(7), 1269–1277. https://doi.org/10.1021/ACSFOODSCITECH.3C00148

Amin, M. A., Chondra, U., Mostafa, E., & Alam, M. M. (2022). Green seaweed Ulva lactuca, a potential source of bioactive peptides revealed by in silico analysis. *Informatics in Medicine Unlocked*, *33*,

101099. https://doi.org/10.1016/J.IMU.2022.101099

Barati, M., Javanmardi, F., Jabbari, M., Mokari-Yamchi, A., Farahmand, F., Eş, I., Farhadnejad, H., Davoodi, S. H., & Mousavi Khaneghah, A. (2020). An in silico model to predict and estimate digestion-resistant and bioactive peptide content of dairy products: A primarily study of a time-saving and affordable method for practical research purposes. *LWT*, *130*, 109616. https://doi.org/10.1016/J.LWT.2020.109616

Barba, F. J., Mariutti, L. R. B., Bragagnolo, N., Mercadante, A. Z., Barbosa-Cánovas, G. V., & Orlien, V. (2017). Bioaccessibility of bioactive compounds from fruits and vegetables after thermal and nonthermal processing. *Trends in Food Science & Technology*, *67*, 195–206. https://doi.org/10.1016/J.TIFS.2017.07.006

Barre, A., Pichereaux, C., Velazquez, E., Maudouit, A., Simplicien, M., Garnier, L., Bienvenu, F., Bienvenu, J., Burlet-Schiltz, O., Auriol, C., Benoist, H., & Rougé, P. (2019). Insights into the Allergenic Potential of the Edible Yellow Mealworm (Tenebrio molitor). *Foods 2019, Vol. 8, Page 515*, *8*(10), 515. https://doi.org/10.3390/FOODS8100515

Bateman, A., Martin, M. J., Orchard, S., Magrane, M., Agivetova, R., Ahmad, S., Alpi, E., Bowler-Barnett, E. H., Britto, R., Bursteinas, B., Bye-A-Jee, H., Coetzee, R., Cukura, A., da Silva, A., Denny, P., Dogan, T., Ebenezer, T. G., Fan, J., Castro, L. G., … Teodoro, D. (2021). UniProt: the universal protein knowledgebase in 2021. *Nucleic Acids Research*, *49*(D1), D480–D489. https://doi.org/10.1093/NAR/GKAA1100

Berraquero-García, C., Rivero-Pino, F., Ospina, J. L., Pérez-Gálvez, R., Espejo-Carpio, F. J., Guadix, A., García-Moreno, P. J., & Guadix, E. M. (2023). Activity, structural features and in silico digestion of antidiabetic peptides. *Food Bioscience*, *55*, 102954. https://doi.org/10.1016/j.fbio.2023.102954

Bianco, M., Ventura, G., Calvano, C. D., Losito, I., & Cataldi, T. R. I. (2022). Discovery of marker peptides of spirulina microalga proteins for allergen detection in processed foodstuffs. *Food Chemistry*, *393*, 133319. https://doi.org/10.1016/J.FOODCHEM.2022.133319

Bjørlie, M., Yesiltas, B., García-Moreno, P. J., Espejo-Carpio, F. J., Rahmani-Manglano, N. E., Guadix, E. M., Jafarpour, A., Hansen, E. B., Marcatili, P., Overgaard, M. T., Gregersen Echers, S., & Jacobsen, C. (2023). Bioinformatically predicted emulsifying peptides and potato protein hydrolysate improves the oxidative stability of microencapsulated fish oil. *Food Chemistry Advances*, *3*, 100441. https://doi.org/10.1016/J.FOCHA.2023.100441

Castañeda-Valbuena, D., Berenguer-Murcia, Á., Fernandez-Lafuente, R., Morellon-Sterling, R., & Tacias-Pascacio, V. G. (2022). Biological activities of peptides obtained by pepsin hydrolysis of fishery products. *Process Biochemistry*, *120*, 53–63. https://doi.org/10.1016/J.PROCBIO.2022.05.029

Cermeño, M., Connolly, A., O'Keeffe, M. B., Flynn, C., Alashi, A. M., Aluko, R. E., & FitzGerald, R. J. (2019). Identification of bioactive peptides from brewers' spent grain and contribution of Leu/Ile to bioactive potency. *Journal of Functional Foods*, *60*, 103455. https://doi.org/10.1016/J.JFF.2019.103455

Chen, Y., Li, T., Li, J., Cheng, S., Wang, J., Verma, C., Zhao, Y., & Wu, C. (2017). Stabilization of peptides against proteolysis through disulfide-bridged conjugation with synthetic aromatics. *Organic & Biomolecular Chemistry*, *15*(8), 1921–1929. https://doi.org/10.1039/C6OB02786E

Daliri, E. B. M., Oh, D. H., & Lee, B. H. (2017). Bioactive Peptides. *Foods 2017, Vol. 6, Page 32*, *6*(5), 32. https://doi.org/10.3390/FOODS6050032

Dávalos Terán, I., Imai, K., Lacroix, I. M. E., Fogliano, V., & Udenigwe, C. C. (2020). Bioinformatics of edible yellow mealworm (Tenebrio molitor) proteome reveal the cuticular proteins as promising precursors of dipeptidyl peptidase-IV inhibitors. *Journal of Food Biochemistry*, *44*(2), e13121. https://doi.org/10.1111/JFBC.13121

Di Renzo, T., Reale, A., Nazzaro, S., Siano, F., Addeo, F., & Picariello, G. (2023). Shotgun proteomics for the identification of yeasts responsible for pink/red discoloration in commercial dairy products. *Food Research International*, *169*, 112945. https://doi.org/10.1016/J.FOODRES.2023.112945

Du, X., Jiang, C., Wang, S., Jing, H., Mo, L., Ma, C., & Wang, H. (2023). Preparation, identification, and inhibitory mechanism of dipeptidyl peptidase IV inhibitory peptides from goat milk whey protein. *Journal of Food Science*, *88*(8), 3577–3593. https://doi.org/10.1111/1750-3841.16694

Fromm, M. F. (2000). P-glycoprotein: A defense mechanism limiting oral bioavailability and CNS accumulation of drugs. *International Journal of Clinical Pharmacology and Therapeutics*, *38*(2), 69–74. https://doi.org/10.5414/CPP38069

Fu, L., Shi, S., Yi, J., Wang, N., He, Y., Wu, Z., Peng, J., Deng, Y., Wang, W., Wu, C., Lyu, A., Zeng, X., Zhao, W., Hou, T., & Cao, D. (2024). ADMETlab 3.0: an updated comprehensive online ADMET prediction platform enhanced with broader coverage, improved performance, API functionality and decision support. *Nucleic Acids Research*, *52*(W1), W422–W431. https://doi.org/10.1093/NAR/GKAE236

Fu, Y., Alashi, A. M., Young, J. F., Therkildsen, M., & Aluko, R. E. (2017). Enzyme inhibition kinetics and molecular interactions of patatin peptides with angiotensin I-converting enzyme and renin. *International Journal of Biological Macromolecules*, *101*, 207–213. https://doi.org/10.1016/J.IJBIOMAC.2017.03.054

Gao, J., Gong, H., & Mao, X. (2020). Dipeptidyl Peptidase-IV Inhibitory Activity and Related Molecular Mechanism of Bovine α-Lactalbumin-Derived Peptides. *Molecules 2020, Vol. 25, Page 3009*, *25*(13), 3009. https://doi.org/10.3390/MOLECULES25133009

García-Moreno, P. J., Yesiltas, B., Gregersen Echers, S., Marcatili, P., Overgaard, M. T., Hansen, E. B., & Jacobsen, C. (2023). Recent advances in the production of emulsifying peptides with the aid of proteomics and bioinformatics. *Current Opinion in Food Science*, *51*, 101039. https://doi.org/10.1016/J.COFS.2023.101039

Gráf, L. A., Szilágyi, L. A., & Venekei, I. A. (2013). Chymotrypsin. *Handbook of Proteolytic Enzymes*, *3*, 2626–2633. https://doi.org/10.1016/B978-0-12-382219-2.00582-2

Gregersen Echers, S., Jafarpour, A., Yesiltas, B., García-Moreno, P. J., Greve-Poulsen, M., Hansen, D. K., Jacobsen, C., Overgaard, M. T., & Hansen, E. B. (2023). Targeted hydrolysis of native potato protein: A novel workflow for obtaining hydrolysates with improved interfacial properties. *Food Hydrocolloids*, *137*, 108299. https://doi.org/10.1016/J.FOODHYD.2022.108299

Harnedy, P. A., O'Keeffe, M. B., & Fitzgerald, R. J. (2015). Purification and identification of dipeptidyl peptidase (DPP) IV inhibitory peptides from the macroalga Palmaria palmata. *Food Chemistry*, *172*, 400–406. https://doi.org/10.1016/J.FOODCHEM.2014.09.083

Harnedy-Rothwell, P. A., McLaughlin, C. M., O'Keeffe, M. B., Le Gouic, A. V., Allsopp, P. J., McSorley, E. M., Sharkey, S., Whooley, J., McGovern, B., O'Harte, F. P. M., & FitzGerald, R. J. (2020). Identification and characterisation of peptides from a boarfish (Capros aper) protein hydrolysate displaying in vitro dipeptidyl peptidase-IV (DPP-IV) inhibitory and insulinotropic activity. *Food Research International*, *131*, 108989. https://doi.org/10.1016/j.foodres.2020.108989

Heres, A., Gallego, M., Mora, L., & Toldrá, F. (2022). Identification and Quantitation of Bioactive and Taste-Related Dipeptides in Low-Salt Dry-Cured Ham. *International Journal of Molecular Sciences*, *23*(5), 2507. https://doi.org/10.3390/IJMS23052507

HILL, R. L., & SCHMIDT, W. R. (1962). The Complete Enzymic Hydrolysis of Proteins. *Journal of Biological Chemistry*, *237*(2), 389–396. https://doi.org/10.1016/S0021-9258(18)93931-1

Hou, Y., Chitrakar, B., Mao, K., Wang, K., Gu, X., Gao, J., Zhang, Q., Bekhit, A. E. D. A., & Sang, Y. (2023). Bioactivity of collagen peptides derived from commercial animals: In silico investigation. *LWT*, *187*, 115381. https://doi.org/10.1016/J.LWT.2023.115381

Igual, M., García-Segovia, P., & Martínez-Monzó, J. (2021). Amino acids and proteinin vitro bio-accessibility from edible insect and pea protein enriched bread. *Journal of Insects as Food and Feed*, *7*(6), 1001–1010. https://doi.org/10.3920/JIFF2020.0122

Jia, W., Du, A., Dong, X., Fan, Z., Zhang, D., Wang, R., & Shi, L. (2022). Physicochemical and molecular transformation of novel functional peptides from Baijiu. *Food Chemistry*, *375*, 131894. https://doi.org/10.1016/J.FOODCHEM.2021.131894

Kęska, P., & Stadnik, J. (2020). Structure–activity relationships study on biological activity of peptides as dipeptidyl peptidase IV inhibitors by chemometric modeling. *Chemical Biology & Drug Design*, *95*(2), 291–301. https://doi.org/10.1111/CBDD.13643

Kim, K., Kim, Y., Lee, H., Lee, C., Kim, S., Oh, S., & Park, Z. Y. (2023). Discovery, verification, and validation of walnut protein marker peptides using LC-MS approaches. *Food Chemistry*, *429*, 136889.

https://doi.org/10.1016/J.FOODCHEM.2023.136889

Lacroix, I. M. E., & Li-Chan, E. C. Y. (2012). Dipeptidyl peptidase-IV inhibitory activity of dairy protein hydrolysates. *International Dairy Journal*, *25*(2), 97–102. https://doi.org/10.1016/J.IDAIRYJ.2012.01.003

Lacroix, I. M. E., Meng, G., Cheung, I. W. Y., & Li-Chan, E. C. Y. (2016). Do whey protein-derived peptides have dual dipeptidyl-peptidase IV and angiotensin I-converting enzyme inhibitory activities? *Journal of Functional Foods*, *21*, 87–96. https://doi.org/10.1016/j.jff.2015.11.038

Lampová, B., Doskočil, I., Kulma, M., Kurečka, M., & Kouřimská, L. (2024). Culinary treatments impact the digestibility and protein quality of edible insects: a case study with Tenebrio molitor and Gryllus assimilis. *Frontiers in Nutrition*, *11*, 1399827. https://doi.org/10.3389/FNUT.2024.1399827

Leiros, H.-K. S., Brandsdal, B. O., Andersen, O. A., Os, V., Leiros, I., Helland, R., Otlewski, J., Willassen, N. P., & Smalås, A. O. (2004). Trypsin specificity as elucidated by LIE calculations, X-ray structures, and association constant measurements. *Protein Science*, *13*(4), 1056–1070. https://doi.org/10.1110/PS.03498604

Liguori, B., Sancho, A. I., Poulsen, M., & Lindholm Bøgh, K. (2022). Novel foods: allergenicity assessment of insect proteins. *EFSA Journal*, *20*. https://doi.org/10.2903/j.efsa.2022.e200910

Liu, R., Cheng, J., & Wu, H. (2019). Discovery of Food-Derived Dipeptidyl Peptidase IV Inhibitory Peptides: A Review. *International Journal of Molecular Sciences 2019, Vol. 20, Page 463*, *20*(3), 463. https://doi.org/10.3390/IJMS20030463

Liu, R., Zhou, L., Zhang, Y., Sheng, N. J., Wang, Z. K., Wu, T. Z., Wang, X. Z., & Wu, H. (2017). Rapid Identification of Dipeptidyl Peptidase-IV (DPP-IV) Inhibitory Peptides from Ruditapes philippinarum Hydrolysate. *Molecules 2017, Vol. 22, Page 1714*, *22*(10), 1714. https://doi.org/10.3390/MOLECULES22101714

Lorey, S., Stöckel-Maschek, A., Faust, J., Brandt, W., Stiebitz, B., Gorrell, M. D., Kähne, T., Mrestani-Klaus, C., Wrenger, S., Reinhold, D., Ansorge, S., & Neubert, K. (2003). Different modes of dipeptidyl peptidase IV (CD26) inhibition by oligopeptides derived from the N-terminus of HIV-1 Tat indicate at least two inhibitor binding sites. *European Journal of Biochemistry*, *270*(10), 2147–2156. https://doi.org/10.1046/J.1432-1033.2003.03568.X

Maillet, N. (2020). Rapid Peptides Generator: fast and efficient in silico protein digestion. *NAR Genomics and Bioinformatics*, *2*(1). https://doi.org/10.1093/NARGAB/LQZ004

Majid, A., Lakshmikanth, M., Lokanath, N. K., & Poornima Priyadarshini, C. G. (2022). Generation, characterization and molecular binding mechanism of novel dipeptidyl peptidase-4 inhibitory peptides from sorghum bicolor seed protein. *Food Chemistry*, *369*, 130888. https://doi.org/10.1016/j.foodchem.2021.130888

Manditsera, F. A., Luning, P. A., Fogliano, V., & Lakemond, C. M. M. (2019). Effect of domestic cooking methods on protein digestibility and mineral bioaccessibility of wild harvested adult edible insects. *Food Research International*, *121*, 404–411. https://doi.org/10.1016/J.FOODRES.2019.03.052

Miner-Williams, W. M., Stevens, B. R., & Moughan, P. J. (2014). Are intact peptides absorbed from the healthy gut in the adult human? *Nutrition Research Reviews*, *27*(2), 308–329. https://doi.org/10.1017/S0954422414000225

Moda, T. L., Montanari, C. A., & Andricopulo, A. D. (2007). Hologram QSAR model for the prediction of human oral bioavailability. *Bioorganic & Medicinal Chemistry*, *15*(24), 7738–7745. https://doi.org/10.1016/J.BMC.2007.08.060

Mohan, A., Rajendran, S. R. C. K., He, Q. S., Bazinet, L., & Udenigwe, C. C. (2015). Encapsulation of food protein hydrolysates and peptides: a review. *RSC Advances*, *5*(97), 79270–79278. https://doi.org/10.1039/C5RA13419F

Mune Mune, M. A., Minka, S. R., & Henle, T. (2018). Investigation on antioxidant, angiotensin converting enzyme and dipeptidyl peptidase IV inhibitory activity of Bambara bean protein hydrolysates. *Food Chemistry*, *250*, 162–169. https://doi.org/10.1016/j.foodchem.2018.01.001

Nongonierma, A. B., & Fitzgerald, R. J. (2013). Dipeptidyl peptidase IV inhibitory and antioxidative properties of milk protein-derived dipeptides and hydrolysates. *Peptides*, *39*(1), 157–163. https://doi.

org/10.1016/J.PEPTIDES.2012.11.016

Nongonierma, A. B., & FitzGerald, R. J. (2013). Inhibition of dipeptidyl peptidase IV (DPP-IV) by proline containing casein-derived peptides. *Journal of Functional Foods*, *5*(4), 1909–1917. https://doi.org/10.1016/J.JFF.2013.09.012

Nongonierma, A. B., & FitzGerald, R. J. (2019). Features of dipeptidyl peptidase IV (DPP-IV) inhibitory peptides from dietary proteins. *Journal of Food Biochemistry*, *43*(1), e12451. https://doi.org/10.1111/JFBC.12451

Nongonierma, A. B., Lamoureux, C., & FitzGerald, R. J. (2018). Generation of dipeptidyl peptidase IV (DPP-IV) inhibitory peptides during the enzymatic hydrolysis of tropical banded cricket (Gryllodes sigillatus) proteins. *Food & Function*, *9*(1), 407–416. https://doi.org/10.1039/C7FO01568B

Nongonierma, A. B., Le Maux, S., Hamayon, J., & FitzGerald, R. J. (2016). Strategies for the release of dipeptidyl peptidase IV (DPP-IV) inhibitory peptides in an enzymatic hydrolyzate of α-lactalbumin. *Food & Function*, *7*(8), 3437–3443. https://doi.org/10.1039/C6FO00239K

Nuñez, S. M., Guzmán, F., Valencia, P., Almonacid, S., & Cárdenas, C. (2020). Collagen as a source of bioactive peptides: A bioinformatics approach. *Electronic Journal of Biotechnology*, *48*, 101–108. https://doi.org/10.1016/J.EJBT.2020.09.009

Olsen, J. V., Ong, S. E., & Mann, M. (2004). Trypsin cleaves exclusively C-terminal to arginine and lysine residues. *Molecular and Cellular Proteomics*, *3*(6), 608–614. https://doi.org/10.1074/mcp.T400003-MCP200

Oonincx, D. G. A. B., & Finke, M. D. (2023). Insects as a complete nutritional source. *Journal of Insects as Food and Feed*, *9*(5), 541–543. https://doi.org/10.3920/JIFF2023.X002

Panse, N., & Gerk, P. M. (2022). The Caco-2 Model: Modifications and enhancements to improve efficiency and predictive performance. *International Journal of Pharmaceutics*, *624*, 122004. https://doi.org/10.1016/J.IJPHARM.2022.122004

Peredo-Lovillo, A., Hernández-Mendoza, A., Vallejo-Cordoba, B., & Romero-Luna, H. E. (2022). Conventional and in silico approaches to select promising food-derived bioactive peptides: A review. *Food Chemistry: X*, *13*, 100183. https://doi.org/10.1016/J.FOCHX.2021.100183

Richter, B. (2008). Emerging role of dipeptidyl peptidase-4 inhibitors in the management of type 2 diabetes. *Vascular Health and Risk Management*, *Volume 4*, 753–768. https://doi.org/10.2147/VHRM.S1707

Rivero-Pino, F., Guadix, A., & Guadix, E. M. (2021). Identification of novel dipeptidyl peptidase IV and α-glucosidase inhibitory peptides from Tenebrio molitor. *Food & Function*, *12*(2), 873–880. https://doi.org/10.1039/D0FO02696D

Rodhi, A. M., Yap, P.-G., Abayomi, O. O., & Gan, C.-Y. (2023). A review on the types of amino acid at ultimate, penultimate and antepenultimate position in some dipeptidyl-peptidase IV inhibitory peptides based on molecular docking analysis. *Food Chemistry Advances*, *2*, 100244. https://doi.org/10.1016/J.FOCHA.2023.100244

Sangsawad, P., Katemala, S., Pao, D., Suwanangul, S., Jeencham, R., & Sutheerawattananonda, M. (2022). Integrated Evaluation of Dual-Functional DPP-IV and ACE Inhibitory Effects of Peptides Derived from Sericin Hydrolysis and Their Stabilities during In Vitro-Simulated Gastrointestinal and Plasmin Digestions. *Foods*, *11*(23), 3931. https://doi.org/10.3390/foods11233931

Silveira, S. T., Martínez-Maqueda, D., Recio, I., & Hernández-Ledesma, B. (2013). Dipeptidyl peptidase-IV inhibitory peptides generated by tryptic hydrolysis of a whey protein concentrate rich in β-lactoglobulin. *Food Chemistry*, *141*(2), 1072–1077. https://doi.org/10.1016/J.FOODCHEM.2013.03.056

Smetana, S., Bhatia, A., Batta, U., Mouhrim, N., & Tonda, A. (2023). Environmental impact potential of insect production chains for food and feed in Europe. *Animal Frontiers*, *13*(4), 112–120. https://doi.org/10.1093/AF/VFAD033

Song, J. J., Wang, Q., Du, M., Ji, X. M., & Mao, X. Y. (2017). Identification of dipeptidyl peptidase-IV inhibitory peptides from mare whey protein hydrolysates. *Journal of Dairy Science*, *100*(9), 6885–6894. https://doi.org/10.3168/JDS.2016-11828

Soudy, M., Anwar, A. M., Ahmed, E. A., Osama, A., Ezzeldin, S., Mahgoub, S., & Magdeldin, S. (2020). UniprotR: Retrieving and visualizing protein sequence and functional information from Universal Protein Resource (UniProt knowledgebase). *Journal of Proteomics*, *213*, 103613. https://doi.org/10.1016/J.JPROT.2019.103613

Sun, H., Chow, E. C. Y., Liu, S., Du, Y., & Pang, K. S. (2008). The Caco-2 cell monolayer: usefulness and limitations. *Expert Opinion on Drug Metabolism & Toxicology*, *4*(4), 395–411. https://doi.org/10.1517/17425255.4.4.395

Sun, H., Nguyen, K., Kerns, E., Yan, Z., Yu, K. R., Shah, P., Jadhav, A., & Xu, X. (2017). Highly predictive and interpretable models for PAMPA permeability. *Bioorganic & Medicinal Chemistry*, *25*(3), 1266–1276. https://doi.org/10.1016/J.BMC.2016.12.049

Tan, J., Yang, J., Zhou, X., Hamdy, A. M., Zhang, X., Suo, H., Zhang, Y., Li, N., & Song, J. (2022). Tenebrio molitor Proteins-Derived DPP-4 Inhibitory Peptides: Preparation, Identification, and Molecular Binding Mechanism. *Foods 2022, Vol. 11, Page 3626*, *11*(22), 3626. https://doi.org/10.3390/FOODS11223626

Thakur, S., Chhimwal, J., Joshi, R., Kumari, M., Padwad, Y., & Kumar, R. (2021). Evaluating Peptides of Picrorhiza kurroa and Their Inhibitory Potential against ACE, DPP-IV, and Oxidative Stress. *Journal of Proteome Research*, *20*(8), 3798–3813. https://doi.org/10.1021/ACS.JPROTEOME.1C00081

Valenzuela Zamudio, F., Hidalgo-Figueroa, S. N., Ortíz Andrade, R. R., Hernández Álvarez, A. J., & Segura Campos, M. R. (2022). Identification of antidiabetic peptides derived from in silico hydrolysis of three ancient grains: Amaranth, Quinoa and Chia. *Food Chemistry*, *394*, 133479. https://doi.org/10.1016/J.FOODCHEM.2022.133479

Wanat, K. (2020). Biological barriers, and the influence of protein binding on the passage of drugs across them. *Molecular Biology Reports*, *47*(4), 3221–3231. https://doi.org/10.1007/S11033-020-05361-2

Wang, B., Yu, Z., Yokoyama, W., Chiou, B. Sen, Chen, M., Liu, F., & Zhong, F. (2021). Collagen peptides with DPP-IV inhibitory activity from sheep skin and their stability to in vitro gastrointestinal digestion. *Food Bioscience*, *42*, 101161. https://doi.org/10.1016/J.FBIO.2021.101161

Wang, T.-Y., Hsieh, C.-H., Hung, C.-C., Jao, C.-L., Chen, M.-C., & Hsu, K.-C. (2015). Fish skin gelatin hydrolysates as dipeptidyl peptidase IV inhibitors and glucagon-like peptide-1 stimulators improve glycaemic control in diabetic rats: A comparison between warm- and cold-water fish. *Journal of Functional Foods*, *19*, 330–340. https://doi.org/10.1016/j.jff.2015.09.037

Wessel, M. D., Jurs, P. C., Tolan, J. W., & Muskal, S. M. (1998). Prediction of Human Intestinal Absorption of Drug Compounds from Molecular Structure. *Journal of Chemical Information and Computer Sciences*, *38*(4), 726–735. https://doi.org/10.1021/CI980029A

Ye, J., McGinnis, S., & Madden, T. L. (2006). BLAST: improvements for better sequence analysis. *Nucleic Acids Research*, *34*(suppl_2), W6–W9. https://doi.org/10.1093/NAR/GKL164

Yesiltas, B., García-Moreno, P. J., Gregersen, S., Olsen, T. H., Jones, N. C., Hoffmann, S. V., Marcatili, P., Overgaard, M. T., Hansen, E. B., & Jacobsen, C. (2022). Antioxidant peptides derived from potato, seaweed, microbial and spinach proteins: Oxidative stability of 5% fish oil-in-water emulsions. *Food Chemistry*, *385*, 132699. https://doi.org/10.1016/J.FOODCHEM.2022.132699

Yi, L., Van Boekel, M. A. J. S., Boeren, S., & Lakemond, C. M. M. (2016). Protein identification and in vitro digestion of fractions from Tenebrio molitor. *European Food Research and Technology*, *242*(8), 1285–1297. https://doi.org/10.1007/s00217-015-2632-6

Yoshida, F., & Topliss, J. G. (2000). QSAR model for drug human oral bioavailability. *Journal of Medicinal Chemistry*, *43*(13), 2575–2585. https://doi.org/10.1021/JM0000564

Yu, Y., Jin, Y., Wang, F., Yan, J., Qi, Y., & Ye, M. (2017). Protein digestomic analysis reveals the bioactivity of deer antler velvet in simulated gastrointestinal digestion. *Food Research International*, *96*, 182–190. https://doi.org/10.1016/J.FOODRES.2017.04.002

Zhang, Y., Chen, R., Chen, X., Zeng, Z., Ma, H., & Chen, S. (2016). Dipeptidyl Peptidase IV-Inhibitory Peptides Derived from Silver Carp (Hypophthalmichthys molitrix Val.) Proteins. *Journal of Agricultural and Food Chemistry*, *64*(4), 831–839. https://doi.org/10.1021/ACS.JAFC.5B05429

Zhu, Q., Chen, X., Wu, J., Zhou, Y., Qian, Y., Fang, M., Xie, J., & Wei, D. (2017). Dipeptidyl peptidase

IV inhibitory peptides from Chlorella vulgaris: in silico gastrointestinal hydrolysis and molecular mechanism. *European Food Research and Technology*, *243*(10), 1739–1748. https://doi.org/10.1007/S00217-017-2879-1

Zielińska, E., Baraniak, B., & Karaś, M. (2018). Identification of antioxidant and anti-inflammatory peptides obtained by simulated gastrointestinal digestion of three edible insects species (*Gryllodes sigillatus* , *Tenebrio molitor* , *Schistocerca gragaria*). *International Journal of Food Science & Technology*, *53*(11), 2542–2551. https://doi.org/10.1111/ijfs.13848

Zielińska, E., Karaś, M., Baraniak, B., & Jakubczyk, A. (2020). Evaluation of ACE, α-glucosidase, and lipase inhibitory activities of peptides obtained by in vitro digestion of selected species of edible insects. *European Food Research and Technology*, *246*(7), 1361–1369. https://doi.org/10.1007/s00217-020-03495-y

6. Supplementary material

Table S1. Database containing the principal proteins identified in *Tenebrio molitor* meal, extracted from Barre et al. (2019).

Protein	Accession Number
Aldehyde oxidase	A0A0K1YW91_TENMO A0A0K1YWY0_TENMO
Ca-transporting ATPase	A0A8J6HQ19_TENMO A0A8J6HVY2_TENMO A0A8J6LHH4_TENMO
Tropomyosin 2	A0A4P8D346_TENMO
Actin 5C	A0A8J6HX45_TENMO A0A8J6HUX7_TENMO
Tubulin beta	A0A8J6H6I7_TENMO A0A8J6L3C0_TENMO A0A8J6LNB4_TENMO A0A8J6HDJ6_TENMO A0A8J6HV89_TENMO
Prophenoloxidase	L7UVJ1_TENMO O97047_TENMO L7US91_TENMO
Tropomyosin 1	A0A4P8D332_TENMO
ATP synthase subunit beta	A0A8J6HHL0_TENMO
Alpha-Amylase	AMY_TENMO (P56634)
Tubulin	A0A8J6HG40_TENMO A0A8J6LDL6_TENMO
Apolipophorin-III	X5J679_TENMO
Arginine kinase	A0A8J6LH90_TENMO
HSP 70	A0A8J6LFF6_TENMO A0A8J6LPK5_TENMO A0A8J6LID5_TENMO A0A8J6HJW4_TENMO A0A8J6LGH1_TENMO
Filamin-A	A0A8J6HGC2_TENMO A0A8J6HDC3_TENMO
12 kDa hemolymph protein a	Q27011_TENMO
Cockroach allergen-like protein	Q7YZB8_TENMO
Serpin 1	D1MYQ7_TENMO
ATP synthase subunit	A0A075CAJ2_TENMO
Hexamerin 2	A0A288EPS5_TENMO Q95PI7_TENMO
Glyceraldehyde-3-phosphate	A0A8J6HIR4_TENMO
Paramyosin long form	A0A8J6L7Z8_TENMO
Serpin 93 kDa	G3XGC4_TENMO
Larval cuticle protein A1A	CUA1A_TENMO (P80681)
Serpin 40	D1MYQ4_TENMO
Cathepsin F10	A0A0B5ITV2_TENMO
alpha-1,4-glucan phosphorylase	A0A8J6LAH5_TENMO
Larval cuticle protein A2B	CUA2B_TENMO (P80682)
Troponin T	A0A8J6HTK8_TENMO
Melanization-related protein	Q9NDN7_TENMO

(Continued) **Table S1.** Database containing the principal proteins identified in *Tenebrio molitor* meal, extracted from Barre et al. (2019).

Protein	Accession Number
Paramyosin short form	A0A8J6L7Z8_TENMO
Peptidyl-prolyl cis-trans isomerase	A0A8J6HPE8_TENMO
Myosin heavy chain, muscle	A0A8J6HQ90_TENMO
HSP 60	A0A8J6LIB0_TENMO
Pyruvate kinase	A0A8J6H905_TENMO
Melanin-inhibiting protein	Q4LE89_TENMO
Serpin 48	D1MYQ6_TENMO
Superoxide dismutase (Cu-Zn)	A0A076G467_TENMO
12 kDa hemolymph protein b	Q7YWD7_TENMO
13 kDa hemolymph protein d	Q7YWC9_TENMO
Larval cuticle protein A3A	CUA3A_TENMO (P80683)
12 kDa hemolymph protein c	Q7YWD6_TENMO
Myosin light chain alkali	A0A8J6HUF1_TENMO
Serine proteinase	A1XG67_TENMO
13 kDa hemolymph protein b	Q7YWD1_TENMO
Vitellogenin receptor	A0A8J6HIS2_TENMO
Troponin C	A0A8J6H161_TENMO
Cytochrome c2	A0A075CDH3_TENMO
Muscle LIM protein Mlp84B	A0A8J6L7Q2_TENMO
Protein disulfide-isomerase	A0A8J6HBC0_TENMO
13 kDa hemolymph protein c	Q7YWD0_TENMO
Phosphoglycerate kinase	A0A8J6HLK6_TENMO
Chemosensory protein CSP12	A0A0C5DAQ4_TENMO
Alpha-Spectrin	A0A8J6HEM6_TENMO
1.1.1. Zeta	A0A0D3RLR7_TENMO
Glycogenin-1-like protein	A0A8J6HH77_TENMO
Phosphoglycerate kinase	A0A8J6HLK6_TENMO
Ferritin	A0A8J6LE89_TENMO
Calumenin	A0A8J6L2S1_TENMO
Cathepsin L11	A0A0B5IZ56_TENMO
Ribosomal protein S3	A0A8J6LKL1_TENMO
G protein-coupled receptor kinase 1	A0A8J6LGB3_TENMO
THP isoform 84aa-XY	Q308N7_TENMO
Cuticular protein	CUH1C_TENMO (P80686) CUF1_TENMO (Q9TXD9)
Glucose-6-phosphate isomerase	A0A8J6HI63_TENMO
Multiple coagulation factor deficiency protein 2	A0A8J6HSB2_TENMO
ATP carrier protein	A0A8J6H6Z1_TENMO
Aspartate aminotransferase	A0A8J6HDC4_TENMO
Adenosylhomocysteinase	A0A8J6HP41_TENMO
Reticulon-like protein	A0A8J6HIL7_TENMO

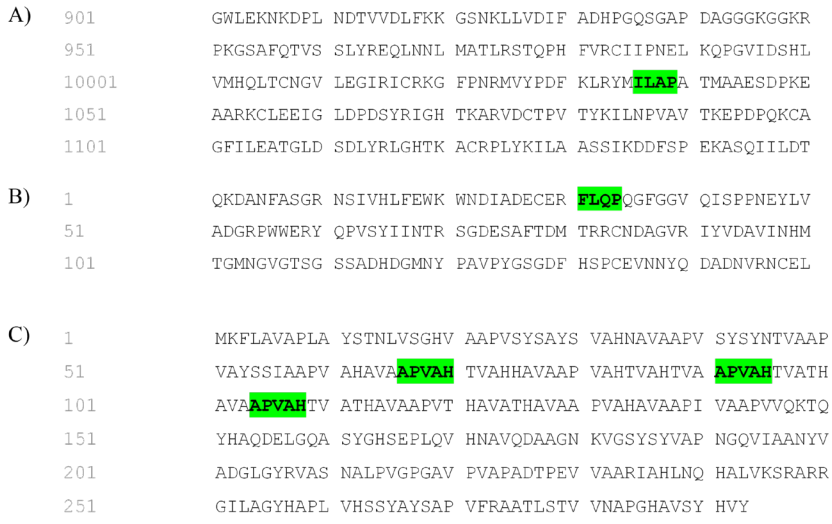

Figure S1. Presence of DPP-IV inhibitory peptides in *Tenebrio molitor* proteome. Identified peptides are highlighted in green:A) ILAP identified in Myosin heavy chain protein (A0A8J6HQ90_TENMO), B) FLQP identified in the alpha-amylase protein (AMY_TENMO), C) APVAH identified in the alpha-amylase protein (AMY_TENMO).

CHAPTER III

Antidiabetic activity of *Tenebrio molitor* and *Olea europaea* protein hydrolysates after simulated gastrointestinal digestion: *in vitro* and *ex vivo* study

ABSTRACT

This study evaluated the antidiabetic potential of protein hydrolysates derived from *Tenebrio molitor* and *Olea europaea* seed, using *in vitro* and *ex vivo* models. Enzymatic hydrolysis was conducted, employing various endo- and exoproteases with diverse specificities to obtain hydrolysates with degrees of hydrolysis ranging from 10 to 20%. Analysis of the DPP-IV inhibitory activity of all the hydrolysates revealed that treatment with a combination of a broad-spectrum endoprotease and a mix of endo- and exoproteases at the highest degree of hydrolysis produced the greatest DPP-IV inhibition for both types of hydrolysates. In fact, the mealworm hydrolysate produced under these conditions exhibited the highest inhibition (IC_{50} = 0.87 ± 0.02 mg protein/mL). The bioactivity of all hydrolysates was studied after simulated digestion, resulting in a significant loss of activity. The two most active hydrolysates were characterized using LC-MS/MS, revealing a significant prevalence of N-terminal proline and resulting in the identification of 12 peptides with predicted DPP-IV inhibitory activity. The *ex vivo* bioactivity of the hydrolysates was evaluated using a mouse intestinal organoid model. The results show that the selected olive hydrolysate influenced the expression of the GLP-1 gene, suggesting its potential to regulate glycemic response. These findings highlight the promise of these sustainable protein hydrolysates as bioactive food ingredients for diabetes management..

1. Introduction

Bioactive peptides derived from food proteins have emerged as promising health-promoting ingredients for the formulation of functional foods and nutraceuticals. Biotechnological processes, such as enzymatic protein hydrolysis, have facilitated the production of peptides with a wide range of bioactivities, including antioxidant, anti-inflammatory, and antihypertensive effects (Aluko, 2015; Galland et al., 2022; Lorenzo et al., 2018). More recently, these peptides have garnered attention for their potential in managing diabetes, particularly through the inhibition of the enzyme dipeptidyl peptidase IV (Liu et al., 2019), which degrades the incretins glucagon-like peptide-1 (GLP-1) and gastric inhibitory polypeptide (GIP), thereby suppressing insulin secretion and increasing glucagon secretion. There has been growing interest in utilizing alternative protein sources, such as insects and plant by-products, as these sources not only offer a pool of high-quality protein but also align with the principles of sustainability and circular economy by promoting resource efficiency and reducing environmental impact (Henchion et al., 2017). Insects, particularly *Tenebrio molitor*, are increasingly investigated as a sustainable protein source due to their minimal resource requirements and have demonstrated high potential for producing DPP-IV inhibitory peptides (Dávalos Terán et al., 2020; Rivero Pino et al., 2020; Rivero-Pino, Guadix, et al., 2021; Tan et al., 2022). Additionally, agri-food industry wastes and by-products possess highly valuable components that can be utilized to produce low-cost bioactive compounds (Ben-Othman et al., 2020). In this context, by-products from vegetable oil production, such as olive seeds, have been revalorized through protein hydrolysis, yielding bioactive peptides with antioxidant and DPP-IV inhibitory activities (Bartolomei et al., 2022; Ospina-Quiroga et al., 2022). This approach not only adds value to agricultural waste, but also reduces overall waste in agricultural processes, thus enhancing both environmental and nutritional sustainability. However, it is important to emphasize that research in this field is still emerging, and additional efforts are necessary to fully understand and optimize these methods for broader industrial application.

Several studies have indicated that the biological properties of DPP-IV inhibitory peptides are closely linked to their size and sequence (Berraquero-García et al., 2023; Nongonierma & Fitzgerald, 2016). Previous research on highly bioactive peptide sequences for different protein sources has shown that DPP-IV inhibitory peptides typically range in length from 3 to 14 amino acids (Berraquero-García et al., 2023). The amino acid composition and sequence are fundamental in binding to and inhibiting the DPP-IV enzyme, for instance, a high proportion of hydrophobic amino acids (i.e., Gly, Ala, Val, Leu, Ile, Pro, Phe, Met, and Trp) is associated with increased bioactivity. More specifically, a high content of Pro, particularly in the first two positions, has been identified as crucial for DPP-IV inhibition (Berraquero-García et al., 2023; Nongonierma & FitzGerald, 2019). This diversity highlights the importance of exploring a wide range of enzyme combinations and hydrolysis conditions to uncover the full spectrum

of bioactive peptides, considering their diverse structures and lengths, and optimizing the potential for developing effective interventions in diabetes management.

While peptides constitute a major class of clinical drug compounds, their stability during gastrointestinal digestion can be limited (Lacroix et al., 2017; B. Wang et al., 2021). Upon ingestion, peptides are exposed to various proteolytic enzymes present in the gastrointestinal tract. The action of these digestive enzymes can maintain, decrease, or enhance the biological properties of protein hydrolysates (Mudgil et al., 2021). Bioactive peptides are typically short, composed of 2–20 amino acids, which generally enhances their gastrointestinal stability (Majura et al., 2022). However, their stability also depends on factors such as amino acid sequence, and charge (Amigo & Hernández-Ledesma, 2020). Consequently, additional research is required to investigate the impact of simulated gastrointestinal digestion on the bioactive characteristics of these type of hydrolysates prior to asserting any health advantages or considering their incorporation as functional food ingredients.

Intestinal cell lines have mostly been studied to assess the effects of food components on the intestinal epithelium. However, these models present several limitations as they are often restricted to two-dimensional cultures, which lack tissue complexity and stem cells, limiting their physiological relevance. In contrast, organoid systems provide a more complex and detailed evaluation of hydrolysate activity, including the presence of stem cells and their niche, as well as multiple intestinal epithelial cell types, partially recapitulating the heterogeneity and cellular behaviour of the original tissue. Moreover, organoids can offer insights as well into carbohydrate metabolism, as the intestinal epithelium is responsible for carbohydrate absorption and incretin production (Aquino et al., 2024). Therefore, organoids represent a suitable model to investigate the regulation of gene expression related to carbohydrate metabolism in the intestinal epithelium. To the best our knowledge, the effect of *T. molitor* or *O. europaea* seed protein hydrolysates on the intestinal epithelium, a key component of the glucose absorption and incretin hormone production, has not been yet described.

The aim of this study was to explore the potential of bioactive protein hydrolysates derived from sustainable sources, such as *Tenebrio molitor* and *Olea europaea* seed, as inhibitors of the enzyme dipeptidyl peptidase IV (DPP-IV), which is a key target in diabetes management. To achieve this, we produced a series of hydrolysates using various well-established food-grade proteolytic enzymes (i.e., Alcalase, Flavourzyme, and trypsin), obtaining different degrees of hydrolysis to generate diverse peptide profiles. The effect of simulated gastrointestinal digestion was evaluated by changes in molecular weight distribution (MWD) and bioactivity of the hydrolysates, giving insight into their stability during digestion, while peptide composition of the most bioactive hydrolysates was characterized by liquid chromatography-tandem mass spectrometry (HPLC–MS/MS). Moreover, hydrolysates were assessed for their *ex vivo* antidiabetic activity. Specifically, their capacity to induce the expression of genes regulating

the glycemic response (i.e., *Pyy* and *Glp1*) in an epithelial monolayer model was investigated. These genes have been positively correlated with weight loss (Andersen et al., 2018; Lafferty et al., 2024) and insulin biosynthesis and pancreatic secretion stimulation (Andersen et al., 2018). Therefore, the induction of *Pyy* and *Glp1* expressions *in vitro* could yield beneficial effects. Thus, this work evaluated the production/characterization, gastrointestinal stability, and DPP-IV inhibitory activity (*in vitro* and *ex vivo*) of protein hydrolysates produced from *T. molitor* and *O. europaea* seed flours. Therefore, this study contributes to the development of therapeutic applications for diabetes management using sustainable protein sources.

2. Materials and methods

2.1. Materials

T. molitor meal was kindly donated by Tebrio (Salamanca, Spain). *Olea europae* seed (OS) meal was provided by Q'omer (Valencia, Spain). Both meals were stored at −16 °C until further use. Alcalase 2.4L (subtilisin, EC 3.4.21.62), PTN 6.0S (trypsin EC 3.4.21.4) and Flavourzyme 1000L (3.4.11.1) were all provided by Novozymes (Bagsvaerd, Denmark). Enzyme and substrates for the DPP-IV inhibitory activity assays, as well as the reagents for digestion were purchased from Sigma-Aldrich (St Louis, US). The digestive enzymes employed were pepsin (Merck, Germany) and pancreatin (Sigma-Aldrich, US).

2.2. Enzymatic hydrolysis

T. molitor and *O. europaea* seed meals were employed. Protein content was analyzed by Dumas method, assuming a nitrogen-to-protein factor of 5.6 for the *T. molitor* (Janssen et al., 2017) and 5.3 for *O. europaea* seed (Maestri et al., 2019). Hydrolysis was conducted at 50 °C and pH 8, either 50 g/L of *T. molitor* meal or 30 g/L of *O. europaea* seed meal protein was dissolved in distilled water, and enzymes Alcalase 2.4L (A), PTN 6.0 (P) and Flavourzyme 1000L™ (F) were employed at different enzyme-to-substrate ratio for the obtention of the corresponding degrees of hydrolysis (DH) (Table 1). The reaction was monitored by pH-stat method, using a 902 Titrando (Metrohm AG, Herisau, Switzerland) which keeps the pH constant. The DH is measured by correlation with the amount of 1M sodium hydroxide added, as defined in the equation:

$$DH = (V_b \cdot N_b)/(m_p \cdot \alpha \cdot H_{tot}).$$

Where the volume of NaOH consumed is represented by V_b, and its normality is N_b. The average degree of dissociation of the α-NH_2 amino groups released during hydrolysis is represented by α, which depends on the temperature and pH. Additionally, m_p represents the mass of protein in the substrate, and H_{tot} is the number of equivalents of peptide bonds per gram of protein. Given the reaction conditions and substrates used, the value

of *1/α* was set to 1.13. H_{tot} was assumed to be 8.6 for *T. molitor*, as reported in the literature (Adler-Nissen, 1986) and was calculated to be 7.72 for *O. europaea* (Maestri et al., 2019).

The obtained hydrolysates were subsequently deactivated via heat treatment at 100 °C for 15 min and vacuum-filtered through an 8 µm cellulose membrane to remove insoluble residues. This pore size was selected to retain a large particulate matter while allowing the soluble protein hydrolysates to pass through. Although finer membranes could remove non-protein components, they were not used due to potential loss of peptides or

Table 1. Enzymatic treatment for the hydrolysis of *T. molitor* and *O. euroapea* seed meals.

Code	Substrate	DH (%)	E/S (%)	Enzyme treatment	Code	Substrate	DH (%)	E/S (%)	Enzyme treatment
HTA10	*T. molitor* meal (50 g/L)	10	1	A	**HOA10**	*O. europaea* seed meal (30 g/L)	10	1	A
HTP10				P	**HOP10**				P
HTAP10				AP	**HOAP10**				AP
HTA15		15	3	A	**HOA15**		15	1	A
HTP15				P	**HOP15**				P
HTAP15				AP	**HOAP15**				AP
HTA20		20	6	A	**HOA20**		20	3	A
HTAP20				AP	**HOAP20**				AP
HTAF20				AF	**HOAF20**				AF
HTAFP20				AFP	**HOAFP20**				AFP

DH: Degree of hydrolysis
E/S: Enzyme/substrate ratio
A: Alcalase 2.4 L
P: PTN 6.0
F: Flavourzyme 1000L™

partial clogging during filtration. Samples were then lyophilized (LyoMicron, Coolvacuum Technologies S.L., Barcelona, Spain). The resulting powdered product was stored at -20 °C until further analysis.

2.3. Amino acid composition

The amino acid composition of the hydrolysates was determined through ion exchange chromatography using an automated amino acid analyzer, Biochrom 30 (Biochrom, Cambridge, UK), following the methodology by Spackman et al. (1958). The process used to analyze the amino acid composition consisted of strong cation exchange chromatography, followed by the ninhydrin color reaction and photometric detection at 570 nm, apart from proline, which was detected at 440 nm. Prior to analysis, the samples underwent acid hydrolysis in 6M HCl at 110°C for 21 h. Subsequently, the samples were dissolved in loading

buffer and then analyzed. The amino acids were identified and quantified by comparing their retention times and signal to those of standard amino acids calibration curves. The analysis was carried out in duplicate, and the results were expressed as molar percentage.

2.4. *In vitro* DPP-IV inhibitory activity

The DPP-IV inhibitory activity of the hydrolysates and their digests was assessed *in vitro,* as previously described (Lacroix & Li-Chan, 2012). Briefly, 100 µL of sample solutions (1.5–5 mg protein/mL) were incubated with 25 µL of DPP-IV enzyme (0.02 U/mL) at 37 °C for 10 min, followed by the addition of 50 µL of 1 mM Gly-Pro-p-nitroanilide. The reaction kinetic was measured at 405 nm (37 °C) over 2 hours at 2 min intervals using a Multiskan FC microplate photometer (Thermo Scientific, Vantaa, Finland). All samples were tested in triplicate and a color control was included to avoid potential interference from the sample coloration. The activity was determined as the half-maximal inhibitory concentration (IC_{50}) by plotting the progress of the reactions compared to the blank (distilled water). Results are indicated in mg protein/mL as mean ± standard deviation.

2.5. *In vitro* simulated gastrointestinal digestion (SGIC)

The digestion simulation was carried out following the INFOGEST Protocol (Brodkorb et al., 2019). *In vitro* the oral, gastric, and intestinal digestion were divided into three stages, and carried out in duplicate in a temperature-controlled shaker (Heidolph, Germany) at 37°C with 250 rpm shaking. The hydrolysates were first dissolved in distilled water to the concentration of 50 mg/mL, and then 7.5 mL of this solution was mixed with 7.5 mL of simulated salivary solution (SSF). After pH adjustment, they were incubated for 2 min with salivary amylase (75 U/mL). After the incubation, the same volume of simulated gastric fluid was added to the bolus and pH was adjusted to 3. Pepsin (2000 U/mL) was added, and the mixtures were incubated for 2 h. Finally, the simulated intestinal solution was added at the same ratio and pH was adjusted to 7. Pancreatin (100 U/ml) was added, and the digests were further incubated for 2 h. Inactivation after the intestinal phase was performed by heating the mixture at 85 ^{0}C for 15 min (Gallo et al., 2022). After enzyme inactivation, the digested samples were centrifuged at 5000 g for 20 min and stored at -20 ^{0}C until further analysis.

2.6. Size exclusion chromatography (SEC)

Size exclusion chromatography was employed to study the molecular weight distribution (MWD) of the different hydrolysates and their digests. SEC analysis was conducted as described in Ospina-Quiroga et al. (2022). The hydrolysate samples were solubilized in distilled water at a concentration of 5 mg/mL, and 500 µL aliquots were injected into a Superdex Peptide 10/300 GL size-exclusion column (GE Health-care, Uppsala, Sweden). Elution was carried out using distilled water as the mobile phase at a flow rate of 0.5 mL/min, and the absorbance of the eluted fractions was monitored at 280 nm. The molecular weight distribution of the samples was related to

a calibration curve prepared with glycine (75.1 Da), peptide LPSDATPVLD (1027.1 Da), peptide VSKDSPETYEEALKR (1751.9 Da), peptide LLVQVGENLLKKPVSKDNPE (2220.6 Da), peptide GVKGIIPGTILEFLEGQLQKMDNNADAR (3028.44 Da), peptide SSQLGYNLLYCPVTSSSDDQFCSK (3810.08) and aprotinin (6511.5 Da) as standards.

2.7. Peptidomic analysis by LC–MS/MS

The detailed proteomics protocol has been previously described in the Materials and Methods section in the summary of this Ph.D thesis. Briefly, samples were solubilized, reduced, alkylated, and purified using C-18 StageTips. Peptides were resuspended in buffer of 2% acetonitrile (ACN) with 0.1% formic acid (FA) and analyzed via EASY-nLC 1200 system (Thermo Fisher Scientific, Waltham, MA, USA) with ESI coupled to a Q Exactive HF Orbitrap mass spectrometer (Thermo Fisher Scientific, Waltham, MA, USA). Peptides were first retained on a PepMap precolumn (C18, 100 Å, 100 μm x 2 cm), followed by a Pepmap analytical Column (C18, 100 Å, 74 μm x 50 cm). A 90-minute gradient was applied using mobile phase A (MPA, water) and mobile phase B (MPB, 95% acetonitrile). Mass spectrometry analysis was performed in full MS/ddMS2 data-dependent mode, as detailed earlier. Peptide match was preferred, and "exclude isotopes" was enabled.

2.8. LC-MS/MS data processing

Raw data processing was conducted as previously detailed in the Materials and Methods section in the summary of this Ph.D thesis. Briefly, data were analyzed using MaxQuant v.2.2.0.0 software and the Andromeda search engine against UniProt databases for *Tenebrio molitor* and *Olea europaea*. An unspecific *in silico* digestion approach was applied, with peptides filtered based on quality criteria: Andromeda score ≥40 and reproducibility in at least two out of three replicates. Peptide characteristics such as sequence length, molecular weight, hydrophobicity, key amino acid presence, and predicted bioactivity using StackDPPIV were assessed. Findings were validated against the BIOPEP database (Minkiewicz et al., 2019) and existing literature (Berraquero-García et al., 2023).

2.9. Crypt Isolation and Organoid

Culture from Mouse Jejunum intestinal organoids were obtained as previously described (González et al., 2024; Romero-Calvo et al., 2018). Briefly, jejunum intestinal organoids from wild-type (WT) mice were dissected and incubated for30 min at 4 ◦ C in PBS with 2 mM EDTA. After shaking, dissociated fragments were passed through 70μm filter and

crypts were counted and centrifuged for seeding. The pellet was resuspended in Corning-Matrigel®(Fisher Scientific, Madrid, Spain) and IntestiCultTM (StemCell, Grenoble, France) with a 1:1 ratio. Domes were cultured in 24 well plates with IntestiCultTM supplemented with penicillin-streptomycin (Sigma-Aldrich)

To generate organoid-derived intestinal epithelial monolayers, matrigel drops containing jejunum organoids were disrupted using TrypLE Express1x (Thermo Fisher Scientific). Cell suspension was incubated for 5 minutes at 37°C and then centrifuged at 2000 g, for 30 seconds. Cells were cultured in Human IntestiCult™ in plates coated with diluted Matrige (1:30) and incubated for 24 hours with HTAF20 or HOAF20 (1mg/mL of protein). Then cells were processed for RNA extraction.

2.10. Reverse transcription quantitative real-time PCR (RT-qPCR) analysis

Total RNA was isolated using the RNeasy Mini Kit (Qiagen, Barcelona, Spain). An amount of 1 mg was retro-transcribed, and specific RNA sequences were amplified with a Bio-RadCFX

Table 2. Genes purchased by Sigma Aldrich, San Luis, Missouri. EE. UU

Gene	Forward Sequence	Reverse Sequence
18s	ACACGGACAGGATTGACAGATTG	GCCAGAGTCTCGTTCGTTATCG
Hprt	AGGGATTTGAATCACGTTTG	TTTACTGGCAACATCAACAG
Glp1	AGCGTGTTAGGCGACATG	CTATCCTCGGCCTTTCACC
Pyy	GGTATGGAAAAAGAGATGTCC	GTGTAGTTAACACATCTCGC
Lrh11	TTGAGTGGGCCAGGAGTAGT	ACGCGACTTCTGTGTGTGAG
Lct	TTCCTATCAGGTTGAAGGTG	GTCATTCCCAATCTTCAGTG
Sis	GAAGATAACTCTGGCAAGTC	GTCCAATGAGCTCTTGATATTG
Slc2a2	TTGTGCTGCTGGATAAATTC	AAATTCAGCAACCATGAACC

Connect real-time PCR device (Bio-Rad Hercules, CA, USA). The $2^{-\Delta\Delta CT}$ method was used for the relative quantification Hprt and 18s were used as reference genes. Table 2 details the primers used for qPCR analysis. Please note that GLP-1 protein is generated by post-translational processing of proglucagon; for clarity we refer to Glp1 to the PCR amplification product.

2.11. Statistical analysis

Significant differences were analyzed by means of Statgraphics 5.1 by the Tukey's test at a *p*-value ≤ 0.05. Data is shown as average ± standard deviation. For the RT-qPCR data a one-way analysis of variance (ANOVA) test was carried out followed by a Dunnett's multiple comparison test in which treated groups were compared to the control group.

3. Results and discussion

3.1. Hydrolysis curves, meal solubilization and protein content of *T. molitor* and *O. europaea* seed hydrolysates

T. molitor meal with a 68.0 ± 0.8% protein content and *O. europaea* seed meal with 23.3 ± 0.1% protein content were used as substrates to produce the hydrolysates. Ten different hydrolysates were obtained from each substrate: HT for *T. molitor* hydrolysates and HO for *O. europaea* seed hydrolysates, as described in Table 1. For each substrate, three degrees of hydrolysis (i.e., 10, 15 and 20%) were studied, since this is a critical parameter that directly influences the MWD of the hydrolysate and thus the bioactive properties of the generated peptides. Three different enzymes were used to study their effect on the properties of the hydrolysates. Specifically, a broad-spectrum endoprotease composed primarily of subtilisin (Alcalase), a specific endopeptidase that cleaves after Arg or Lys, unless followed by Pro (trypsin, coded as PTN), and a mixture of endo- and exoproteases (Flavourzyme). The combination of these enzymes, alone or in combination, were investigated since the type of enzyme and the substrate involved in the hydrolysis process play a crucial role in determining the production of bioactive DPP-IV inhibitory peptides (Cruz-Casas et al., 2021). The hydrolysis curves indicated that both *T. molitor* and *O. europaea* seed proteins are effectively broken down by enzymatic treatments, exhibiting a rapid initial phase followed by a plateau (See Supplementary Figure S1), which could result from enzyme inhibition by the hydrolysis byproducts (Al-Mardeai et al., 2022). Similar hydrolysis patterns have been observed in previous studies using various substrates (Berraquero-García et al., 2022; García-Moreno et al., 2015; J. Wang et al., 2013).

Meal solubilization, referring to the fraction of the meal (including proteins, carbohydrates, and lipids) dissolved during hydrolysis, was measured. A significant portion of meal solubility can be linked to increased protein solubility as a result of hydrolysis; however, the extended stirring time required to achieve higher degrees of hydrolysis may secondarily increase the solubility of other meal components. This is especially notable for the *O. europaea* seed meal solubilization, since it included many other non-protein components (See Supplementary Table S1). Both meal and protein solubility were analyzed (Table 3), showing a clear increase with higher degrees of hydrolysis. This is consistent with the known relationship between hydrolysis progression and improved protein solubility due to the cleavage of peptide bonds and the generation of smaller peptides with enhanced solubility compared to the original proteins (Bao et al., 2017; Klost & Drusch, 2019).

Regarding the effect of the enzymatic treatment, data showed that hydrolysis with PTN alone resulted in the lowest protein (and meal) solubility regardless of the degree of hydrolysis in both substrates, which is attributed to the high specificity of PTN, exclusively

Table 3. Percentage solubilization and protein content of the *T. molitor* and *O. europaea* seed protein hydrolysates. Sample ID referring to Table 1.

***T. molitor* hydrolysates**	**Meal solubility (%)**	**Protein solubility (%)**	**Protein content (%)**	***O. europaea* hydrolysates**	**Meal solubility (%)**	**Protein solubility (%)**	**Protein content (%)**
HTA10	52.6	35.19	66.9 ± 0.91	HOA10	43.2	9.78	22.64 ± 0.01
HTP10	51.6	35.14	68.10 ± 0.06	HOP10	37.2	8.57	23.05 ± 0.01
HTAP10	53.4	37.17	69.61 ± 0.37	HOAP10	43.4	11.11	25.61 ± 0.07
HTA15	56.7	38.91	68.64 ± 0.20	HOA15	44.1	10.65	24.15 ± 0.04
HTP15	56.3	38.72	68.77 ± 0.00	HOP15	44.2	11.86	26.83 ± 0.07
HTAP15	57.1	39.15	68.56 ± 0.65	HOAP15	45.3	11.64	25.69 ± 0.02
HTA20	60.3	41.29	68.47 ± 0.39	HOA20	48.0	11.96	24.92 ± 0.08
HTAP20	61.3	41.79	68.18 ± 0.41	HOAP20	47.5	12.0	25.24 ± 0.06
HTAF20	63.5	43.0	67.70 ± 0.26	HOAF20	52.2	13.40	25.68 ± 0.02
HTAFP20	63.9	43.62	68.26 ± 0.17	HOAFP20	50.8	13.28	26.14 ± 0.03

cleaving after Lys and Arg (Olsen et al., 2004). Contrarily, the use of Flavourzyme resulted in enhanced solubilization. This is likely because Flavourzyme, a mix of endo- and exo-proteases, can break the protein at different sites and in various ways compared to Alcalase and PTN (Segura-Campos et al., 2012), increasing the release of short peptides and free amino acids. However, strong differences were identified between the two substrates when comparing protein solubility. *T. molitor* hydrolysates (HT) achieved over 40% protein solubility, whereas *O. europaea* seed hydrolysates (HO) only reached a maximum of 13.4%. Previous studies comparing the solubility of hydrolysates from *T. molitor* and plant-based protein (i.e., soybean isolates) using 2% E/S Alcalase found that *T. molitor* exhibited much higher solubility, consistent with our findings, suggesting its protein would be suitable for various food applications (Yu et al., 2021). Plant proteins are notoriously challenging to solubilize, posing a significant obstacle for industrial applications. Although optimized treatments exist to improve solubility, these methods can be aggressive and may alter the bioactive properties of the peptides (Gao et al., 2024). Recent studies on the solubility of hydrolysates from different plant protein isolates (e.g., pea, rice, oat, and hemp) using 4% E/S Alcalase demonstrated that

the degree of hydrolysis is crucial for enhancing protein solubility, with up to 100% solubility achieved at DH = 30% (Shahbal et al., 2023). In our study, working with flours rather than isolated proteins introduces various compounds that may have limited protein solubility due to interactions leading to aggregation (Pérez-Gálvez et al., 2024).

Finally, HTAP10 showed the highest protein content for HT at 69.61 ± 0.37%, compared to 68.01 ± 0.76% in the original meal. Similarly, HOP15 exhibited the highest protein content for HO at 26.83 ± 0.07%, exceeding the original meal at 23.28 ± 0.11%. Incomplete solubilization can be due to the separation method used since, unlike centrifugation, filtration might allow small insoluble particles to pass through.

3.2. DPP-IV inhibitory activity of the *T. molitor* and *O. europaea* hydrolysates

The antidiabetic activity of the hydrolysates was evaluated by assessing their DPP-IV inhibitory activity *in vitro*. Figure 1 presents the inhibition values, with HT expressed as IC_{50} (mg protein/mL) and HO as IC_{30}(mg protein/mL). This difference in units was due to the colorimetric nature of the *in vitro* DPP-IV inhibition assay used in this study.

The results reveal two distinct trends regarding the DPP-IV inhibitory activity of the hydrolysates, dependent on the substrate. For the HO hydrolysates, there was a significant positive correlation between the degree of hydrolysis and the inhibitory potency, as indicated by the decreasing IC_{30} values with increasing degree of hydrolysis. A similar, though less pronounced, trend was also observed for the HT hydrolysates. Notably, at the highest degrees of hydrolysis, the IC_{30} values of the HO hydrolysates did not differ significantly. This is consistent with the understanding that smaller peptides, typically below 4 amino acids in length, tend to exhibit greater DPP-IV inhibitory activity, as observed in previous studies (Nongonierma & FitzGerald, 2019; Xu et al., 2022). The HO hydrolysates demonstrated IC_{30} values ranging from 2.67 ± 0.31 to 1.23 ± 0.09 mg protein/mL, with the HOAF20 being the most bioactive. While previous research has investigated *O. europaea* seed protein hydrolysates, specific IC_{50} values have not been published. However, previous studies have exhibited inhibition percentages of up to 72% at concentrations of 1.5 mg protein/mL (Bartolomei et al., 2022), a slightly higher inhibitory activity compared to the values observed for the hydrolysates in this study. The variation identified in DPP-IV inhibitory activities may be due to the use of different experimental methods, as we have previously noted the lack of standardized analysis protocols (Berraquero-García et al., 2023). This suggests a potential misrepresentation in the findings and underscores the need for establishing standard methodologies. It is also important to note that the hydrolysate HOP10 did not show any measurable inhibition of DPP-IV *in vitro*.

HT hydrolysates exhibited IC_{50} values ranging from 2.33 ± 0.08 to 0.87 ± 0.02 mg protein/mL, with the degree of hydrolysis and the specific enzymes used significantly influencing these values. The incorporation of Flavourzyme at 20% DH resulted in a marked increase in DPP-IV inhibitory activity, a phenomenon previously described for *T. molitor* hydrolysates (Rivero Pino et al., 2020). This enhancement is attributed to the synergistic effect between Flavourzyme and Alcalase, where the latter releases peptide fragments that are subsequently cleaved by Flavourzyme near the carboxyl terminus. However, when PTN was combined with these two enzymes, a reduction in inhibitory activity was observed. Although PTN (trypsin) has specificity for cleaving peptide bonds at the carboxyl side of Arg and Lys, which can typically yield potent DPP-IV inhibitory peptides (Nongonierma et al., 2017), the combined use of PTN with Alcalase and Flavourzyme could alter the peptidic profile in a manner that reduced the

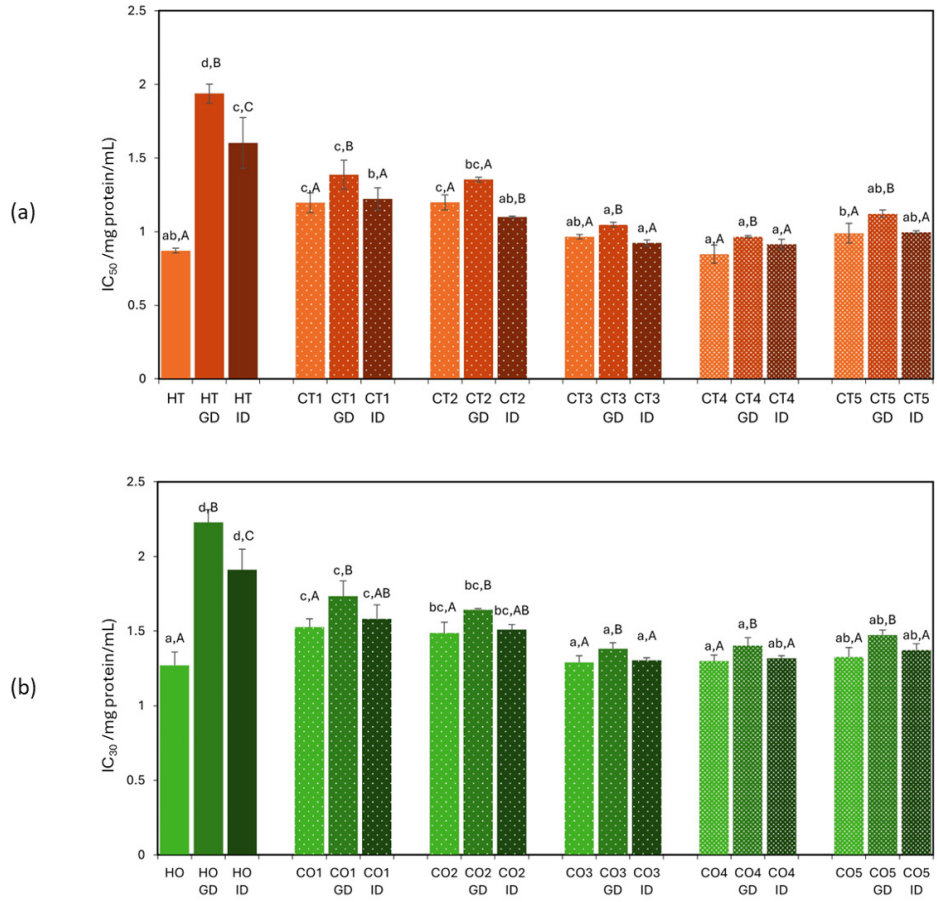

Figure 1. DPP-IV inhibitory activity of *T. molitor* (a) and *O. europaea* seed (b) hydrolysates before and after simulated gastrointestinal digestion. Results represent the mean ± SD (n= 3). Samples with different letters are significantly different (p < 0.05). Sample ID referring to Table 1.

overall bioactivity. Notably, the HTAF20 hydrolysate exhibited the highest DPP-IV inhibition, with an IC_{50} value of 0.87 ± 0.02 mg protein/mL, categorizing it as a potent inhibitor according to Nongonierma and FitzGerald's classification (Nongonierma & FitzGerald, 2019). This potency is comparable to a previously identified *T. molitor* hydrolysate generated using papain, with an IC_{50} of 0.82 mg protein/mL (Dávalos Terán et al., 2020), as well as specific peptide sequences, such as LPDQWDWR, that have demonstrated IC_{50} values below 1 mg/mL (Tan et al., 2022).

The significant variations in DPP-IV inhibitory potency among the samples emphasize the importance of optimizing hydrolysis parameters to generate potent DPP-IV inhibitory peptides. Interestingly, the amino acid profiles of the hydrolysates were observed to be relatively consistent across the different degrees of hydrolysis (DH) and enzymatic treatments (See Supplementary Table S2), suggesting that the solubilization of the original protein was uniform across the various conditions. This finding has been previously demonstrated in other studies on anchovy hydrolysates using a mixture of Alcalase, papain, and pancreatin (Zhao et al., 2017), as well as with Grass Turtle hydrolysates produced using papain (Islam et al., 2021).

The major amino acids present in the HT hydrolysates were Asp, Glu, Gly, Ala, Leu, and Pro, collectively accounting for approximately 57% of the hydrolysates (Figure 2). In contrast, the HO hydrolysates were predominantly composed of Asp, Ser, Glu, and Gly, which made up to 63% of the hydrolysates. A significant difference in Pro content was observed between the hydrolysates of the two substrates, with HT containing 8.02 ± 0.01% and HO containing 5.44 ± 0.15% Pro. This amino acid has been widely associated to DPP-IV inhibition, particularly when present at the peptide C-terminus (Nongonierma & FitzGerald, 2013a), which may add to the stronger inhibitory activity of the *T. molitor* hydrolysates. Furthermore, another amino acid identified as highly frequent in DPP-IV inhibitory sequences is Ala (Leiting et al., 2003), which also appears in significantly higher concentrations in HT at 11.83 ± 0.03% compared to 7.32 ± 0.04% in HO.

The MWD of the HO and HT hydrolysates was analysed using SEC (Figure 3). For HT hydrolysates, two main fractions were identified: over 7 kDa and 2.5–1 kDa. Higher degrees of hydrolysis were generally linked to an increase in the 1.0–0.5 kDa and 0.5–0.2 kDa fractions, except for HTAFP20. In contrast, hydrolysates obtained using PTN alone did not exhibit this increase in lower molecular weight fractions, likely due to the specificity of trypsin, as previously discussed. Regarding Alcalase treatment, even at 10% DH, a large fraction of small peptides was generated. At 20% DH, the HTA20 and HTAF20 treatments showed a significant increase in the 1.0–0.5 kDa fraction. This aligns with previous findings by Chewaka et al., who described that *T. molitor* hydrolysis with Alcalase resulted in the highest content of peptides > 1 kDa, attributed to the greater generation of soluble peptides from the endo-protease activity of Alcalase (Chewaka et al., 2023).

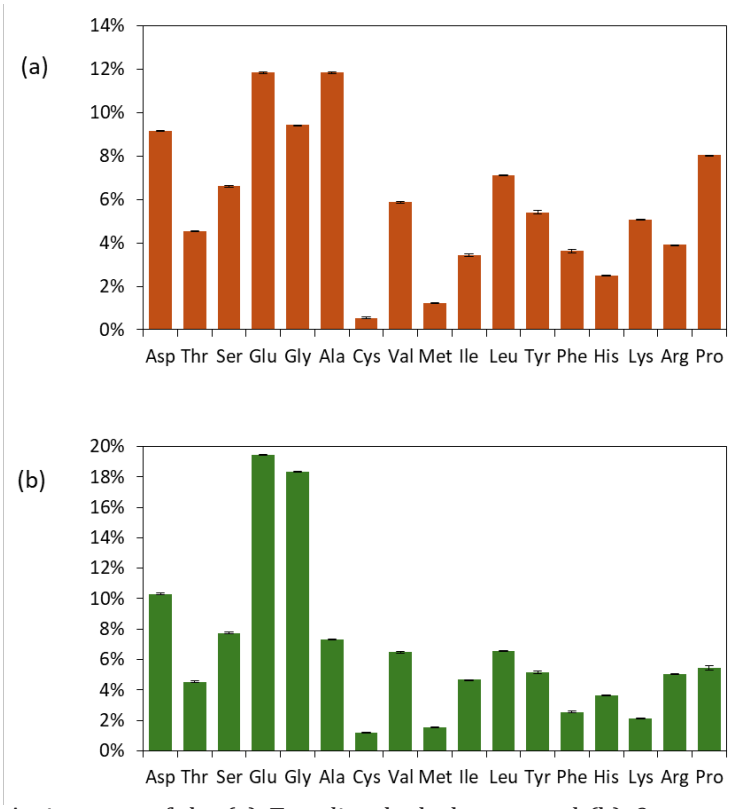

Figure 2. Aminogram of the (a) *T. molitor* hydrolysates and (b) *O. europaea* seed protein hydrolysates. Results represent the mean ± SD (n = 3).

For HO hydrolysates, significant changes in MWD were also observed, particularly influenced by the degree of hydrolysis. HO predominantly featured fractions larger than 7 kDa, comprising over 60% of the sample composition in all cases. However, at 20% DH and with the combined enzymatic treatment AF, the fraction smaller than 7 kDa increased to 40%. While this is consistent with previous studies on the molecular weight distribution of different plant protein hydrolysates (Ospina-Quiroga et al., 2022), the observed MWD suggests a complexity that limits the clear identification of trends based on enzyme effect and DH. Furthermore, at 20% DH, a significant portion of the peptides would be expected to fall below 1 kDa. These discrepancies could suggest the presence of larger, non-peptide components that remain largely unaffected by proteolysis. This is supported by the low protein content of the *O. europaea* hydrolysates (22.64 ± 0.01 - 26.83 ± 0.07 %).

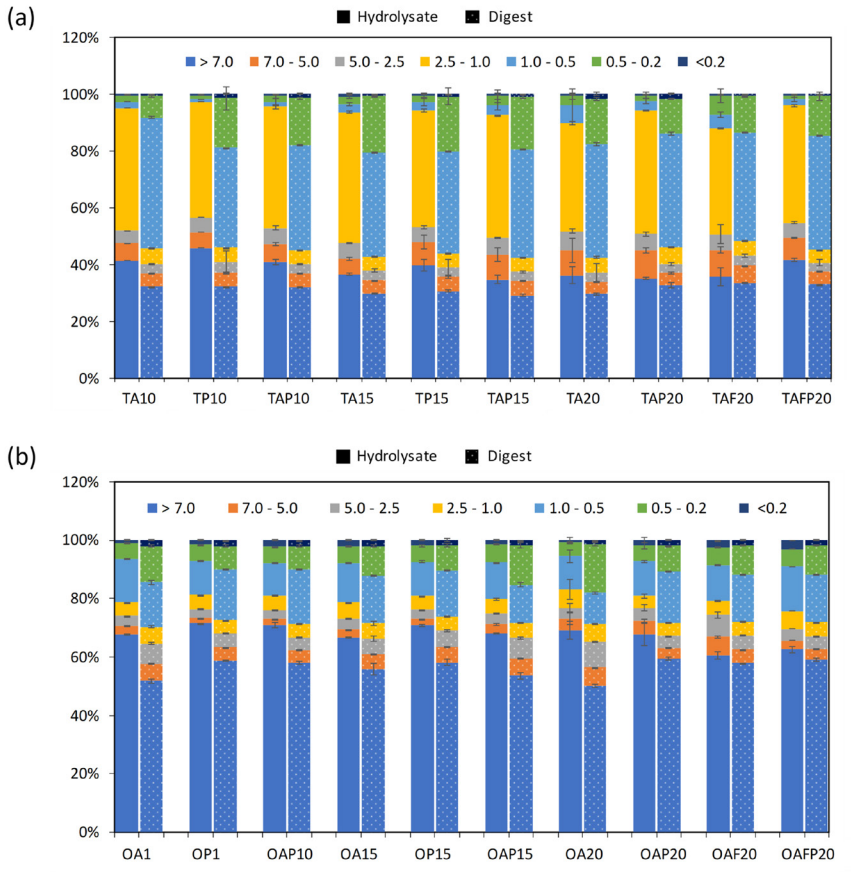

Figure 3. Molecular weight distribution of the *T. molitor* (a) and *O. europaea* seed (b) hydrolysates (filled) and their digests (dotted). Results represent the mean ± SD (n = 3). Sample ID referring to Table 1.

3.3. Gastrointestinal digestion of *T. molitor* and *O. europaea* seed hydrolysates

The development of functional foods containing bioactive protein hydrolysates, require that the bioactive peptides are not degraded during gastrointestinal digestion. Hence, the HT and HO hydrolysates were subjected to *in vitro* simulated gastrointestinal digestion using the INFOGEST protocol (Brodkorb et al., 2019), and the DPP-IV inhibitory activity of the digests was assessed (Figure 1).

The *in vitro* bioactivity assessment of the different *T. molitor* samples after digestion revealed that the *T. molitor* digests exhibited IC_{50} values ranging from 3.43 ± 0.71 to 1.32 ± 0.13 mg protein/mL. Compared to the original hydrolysates, a significant reduction in bioactivity was observed for most samples, except for the digest of HTA15, which showed

improved bioactivity, and the digest of HTAP15, which showed no significant difference. The highest loss of inhibitory activity was found in the hydrolysates with DH of 20%, where the IC_{50} values nearly doubled after the digestion process (i.e., HTAF20 presented IC_{50} of 0.87 ± 0.02 mg protein/mL, while its digest had an IC_{50} of 1.69 ± 0.17 mg protein/mL, $p<0.05$).

In contrast, *O. europaea* seed protein hydrolysates with a DH under 20%, improved DPP-IV inhibitory activity after simulated gastrointestinal digestion, while those at DH 20% experienced a marked decrease. Similar results were reported on investigations on pea protein for the inhibition of ACE, showing that the bioactive peptide identified was degraded after pancreatic digestion, but some of the newly formed peptides exhibited comparable activity to the parent peptide (Liao et al., 2019). Conversely, the already low-molecular-weight peptides in hydrolysates with DH 20% may have been completely degraded, leading to a loss of bioactivity, or formed new sequences with a mixed bioactivity profile, resulting in a lower inhibitory concentration (IC_{30}) value. Previous studies have demonstrated that the biological activity of plant-derived peptides can decrease following gastrointestinal digestion. For instance, the effect of pepsin and pancreatin digestion was studied on the retention of ACE inhibitory activity of different peptides obtained from soybean protein isolates, finding that two out of the three obtained peptides lost all bioactivity (Daliri et al., 2018). However, no studies have yet been found on the gastrointestinal digestion of *O. europaea* seed hydrolysates.

Gastrointestinal stability of the hydrolysates is related with changes in the MWD of the hydrolysates after simulated gastrointestinal digestion. The comparison of HT and their digested samples revealed that the digestive process reduced the peptide size, leading to a higher proportion of lower molecular weight peptides (Figure 3a). Particularly, the 2.5–1 kDa fraction was substantially diminished by the digestive enzymes, with the 1.0–0.5 kDa fraction becoming predominant in the digests. Similarly, the 0.5–0.2 kDa fraction increased in the digests compared to the original hydrolysates. Notably, the 1.0–0.5 kDa fraction has been previously identified as a highly bioactive fraction of *T. molitor* derived peptides for the inhibition of DPP-IV (Rivero-Pino, Guadix, et al., 2021). However, it is important to acknowledge that while peptide size is relevant, the amino acid composition and specific peptide sequences play critical roles in determining the extent and nature of bioactivity (Nongonierma & Fitzgerald, 2016; Nongonierma & FitzGerald, 2019). For HO and the corresponding digested samples (Figure 3b), differences between the MWD were less pronounced. Nonetheless, the degradation of the 1.0–0.5 kDa fraction led to the formation of peptides in the 0.5–0.2 kDa range and the emergence of a small fraction <0.2 kDa, which could be linked to the reported loss of bioactivity due to the formation of new sequences with a mixed bioactivity profile.

3.4. Peptide identification by mass spectrometry

An in-depth analysis was performed using LC-MS/MS to characterize the peptide sequences from the hydrolysates with highest DPP-IV inhibitory activity (HTAF20 and HOAF20). The peptide length distribution for these samples was determined (Fig. 4), finding a total of 7,565 sequences for HTAF20 and 1,119 for HOAF20 (Supplementary Table S3:). Regarding peptide mass, sequences ranged from 285.15 to 3,166.83 Da in HTAF20 and 287.18 to 3,212.68 Da in HOAF20, placing most peptides within the 400–3,000 Da range previously associated with strong DPP-IV inhibitory activity (Rivero-Pino, Espejo-Carpio, et al., 2021). It is worth noting the disparity in the number of identified sequences between both hydrolysates, which may be attributed to differences in the compositions of the matrices. Indeed, *O. europaea* seed hydrolysates are expected to differ in their protein content and peptide profiles compared to whole-organism hydrolysates, such as those derived from *T. molitor*, primarily due to the use of seed material alone.

A filtering step was applied, based on the predicted DPP-IV inhibitory potential reported by the predictor StackDPPIV, and peptides with a score over 0.5 were selected. The peptide length distribution of these peptides (HTAF20_*p* and HOAF20_ *p*) was represented (Fig. 4), revealing a shift towards shorter lengths, suggesting that shorter sequences might exhibit increased inhibitory activity. While this partly reflects a biological reality, since smaller peptides have improved accessibility to the enzymes active sites (Mora & Toldrá, 2023), it may also result from a bias in literature, as most studies focus on short bioactive peptides due to their bioaccessibility and bioavailability (Berraquero-García et al., 2023; Nongonierma & FitzGerald, 2019).

After analyzing the potential bioactivity of the sequences, 59.21% of HTAF20 and 50.94% of HOAF20 peptides were classified as potentially DPP-IV inhibitory. This suggests a higher inhibitory potential in *T. molitor* hydrolysates, which is consistent with the in vitro IC_{50} values previously presented. To understand the bioactive potential of the sequences, a structural analysis was performed. One of the most significant observations was the higher occurrence of Pro at the N-terminal position in HTAF20 (33.63%) compared to HOAF20 (15.64%), with this characteristic being strongly linked to DPP-IV inhibition (Nongonierma & FitzGerald, 2013b, 2019). Furthermore, when considering only peptides predicted as DPP-IV inhibitors by StackDPPIV, the proportion of N-terminal proline increased to 40.63% in HTAF20 compared to 21.7% in HOAF20, reinforcing its relevance. Apart from Pro, other hydrophobic amino acids, such as Ala and Val, were also detected at the N-terminus, particularly in HTAF20. This is consistent with previous studies on brewer's spent grain hydrolysates, where similar amino acid composition was linked to DPP-IV inhibition (Garzón et al., 2023).

Table 4. Identified peptides with previously reported DPP-IV inhibitory activity.

Sample (ID referring to Table 1)	Sequence	Length (amino acids)	Mass (Da)	P at Nt *	A in Nt	F in Ct	W in Ct	Y in Ct	Predicted Bioactivity[a]	Biopep Reported Activity [b]	IC_{50} (μM) [c]
HTAF20	LPY	3	391.21	Y				Y	0.83		87.15
HTAF20	VPW	3	400.21	Y			Y		0.93	Antioxidant	174.78
HTAF20	VPF	3	361.20	Y		Y			0.95		55.10
HTAF20	MPF	3	393.17	Y		Y			0.97	DPP-IV inhibitor	N/A
HTAF20	ELPF	4	504.26			Y			0.80		9920.00
HTAF20	LPVYD	5	605.31	Y					0.55	DPP-IV inhibitor	51.36
HTAF20	LPLPL	5	551.37	Y					0.86	DPP-IV inhibitor	N/A
HOAF20	LPQ	3	356.21	Y					0.78	DPP-IV inhibitor	56.70
HOAF20	LPR	3	384.25	Y					0.82		1430.00
HOAF20	LPLF	4	488.30	Y		Y			1.00		463.60
HTAF20	LPY	3	391.21	Y				Y	0.83		87.15

* First two positions

[a] Values obtained from https://pmlabstack.pythonanywhere.com/StackDPPIV. Values over 0.5 indicate potential bioactivity.

[b] Bioactivity reported in BIOPEP-UWM (https://biochemia.uwm.edu.pl/biopep/peptide_data.php).

[c] IC_{50} reported in the literature (Berraquero-García et al., 2023). N/A indicates not analyzed.

Another key structural feature observed in both hydrolysates was the presence of aromatic and hydrophobic residues at the C-terminus, particularly Phe, Trp and Tyr (Nongonierma & Fitzgerald, 2013). Particularly, 14.50% of the peptides in HTAF20, and 15.10% in HOAF20, presented Phe in their sequence. Several peptides with these motifs, such as VPF, LPY, and VPW, were identified in both hydrolysateshighlighting the crucial role of hydrophobic interactions in their bioactivity. These hydrophobic interactions, alongside potential hydrogen bonds, have been identified as key factors in the bonding process and inhibition of the DPP-IV enzyme (Nongonierma et al., 2013).

To further validate the findings, a database search was conducted to identify peptides with previously reported DPP-IV inhibitory activity. Interestingly, only 11 peptides from the dataset had been previously found in scientific literature or databases (Table 4). This highlights a significant knowledge gap in peptide research, particularly regarding longer sequences. It is significant that 10 out of the 11 peptides presented Pro in the first two positions at the N-terminus and almost all of them were also attributed a high potential bioactivity. Nonetheless, APVAH, identified in HTAF20, was predicted to have low bioactivity (0.18) but

exhibited significant DPP-IV inhibition *in vitro*, with an IC_{50} of 26 μM (Chapter III), highlighting the limitations of *in silico* prediction tools and the necessity of experimental validation.

The observed reduction in bioactivity of the hydrolysates after simulated gastrointestinal digestion highlights the critical need for protective strategies against enzymatic degradation. Ensuring the preservation of the bioactivity of these hydrolysates during digestion is fundamental for their effective application in functional foods and nutraceutical formulations. Future research should be focused on the development of innovative delivery systems, such as nano-microencapsulates, to shield these bioactive peptides from the harsh conditions of the gastrointestinal tract (Amigo & Hernández-Ledesma, 2020).

3.5. Anti-diabetic effect on mouse jejunum organoids

As previously described, the HTAF20 and HOAF20 hydrolysates exhibited the highest *in vitro* DPP-IV inhibition for each protein substrate. Consequently, these hydrolysates were selected to investigate their potential antidiabetic effects using mouse jejunum organoids. Organoid systems provide a more complex and detailed assessment of hydrolysate activity compared to cell line studies. Furthermore, the intestinal epithelium is responsible for carbohydrate absorption and produces hormones like incretins that are involved in carbohydrate metabolism. Therefore, organoids represent a suitable *in vitro* model to study the regulation of gene expression in the intestinal epithelium related to carbohydrate metabolism (Aquino et al., 2024). Thus, we utilized mouse jejunum organoids to investigate how peptides derived from the *in vitro* digestion of hydrolysates affect the expression of carbohydrate-digesting enzymes (Lct and Sis), the hepatic glucose uptake (LRH-1), the glucose transporter GLUT2 (encoded by Slc2a2), and incretin expression (GLP-1).

The expression of *Pyy* and *Glp1* by intestinal epithelial monolayers was studied, finding that HOAF20 induced the expression of these genes (Figure 4). Peptides derived from these genes are produced by small intestine L cells in response to food ingestion and exert effects on glucose metabolism and weight management. Glucagon Like Peptide-1 (GLP-1) main role is the regulation plasma glucose concentration, inducing insulin biosynthesis and pancreatic secretion (Andersen et al., 2018). It also delays gastric emptying and inhibits food intake. In fact, GLP1 is a therapeutic target in diabetes and several drugs are currently commercialized based on modifications of GLP-1 to increase its half-life. Peptide tyrosine-tyrosine (PYY) has been positively related to weight loss and has been proposed as a possible therapeutic option to halt or reverse beta-cell loss in type 2 diabetes mellitus (Andersen et al., 2018; Lafferty et al., 2024). Nevertheless, products exploiting these effects of PYY have not yet reached the clinical stage. Interestingly, after entering the general circulation, both GLP-1 and PYY have a short half-life due to degradation by the enzyme DPP-IV. Our data indicate that HOAF20 not only induced GLP-1 and PYY production but also potentially controlled DPP-IV inhibition, albeit to a lesser extent than the HTAF20 hydrolysate. This could result in an increased half-life of these peptides, thereby enhancing

the concentration of circulating peptides and yielding beneficial effects in the management of diabetes mellitus and weight. Similar results have been obtained for hydrolysates derived from brewer's spent yeast that had been previously digested *in vitro* (Aquino et al., 2024).

Effects of HOAF20 on *Glp1* and *Pyy* in intestinal organoid monolayers were specific, and not derived from protein addition to the culture medium. In fact, HTAF20 did not have effects on the expression of these genes. In contrast, HTAF20 significantly induced the expression of Lct and Sis, genes that codify the disaccharidases lactase and sucrase isomaltase, respectively. No effects were observed on Slc2a2, that codifies the glucose transporter Glut2. The induction on disaccharidases expression would increase available monosaccharides in the intestinal lumen to be absorbed, while the lack of significant effect on Slc2a2 would indicate not changed absorption of glucose. More experiments would be needed to evaluate the final effect of HTAF20 on glucose availability and absorption. Therefore, while the effects of HOAF20 on the intestinal epithelium clearly indicate an antidiabetic effect, the effects of HTAF20 in relation to diabetes are more challenging to interpret, despite its demonstrated high DPP-IV inhibitory activity *in vitro.*

HTAF20 induced Lrh1 expression. The former codifies a nuclear factor named Liver Receptor Homolog-1 (LRH-1), highly expressed in the stem cells localized in the intestinal crypts, where it promotes intestine cell proliferation and renewal (Bayrer et al., 2018; Zerlotin et al., 2021). LRH-1 is known to repress inflammation in digestive organs. In addition, LRH-1 protects pancreatic islets against apoptosis. In fact, a small LRH-1 agonist called BL001 has been shown to impede hyperglycemia progression and immune-dependent inflammation in murine models of type one diabetes mellitus (Cobo-Vuilleumier, Lorenzo, & Gauthier, 2018; Cobo-Vuilleumier, Lorenzo, Rodríguez, et al., 2018). It also increases beta cell mass and insulin secretion, suggesting that LRH-1 agonist promotes a dialogue between immune and islet cells, potentially protecting against diabetes. Nevertheless, relation of LRH-1 with type 2 diabetes remains to be fully studied and understood.

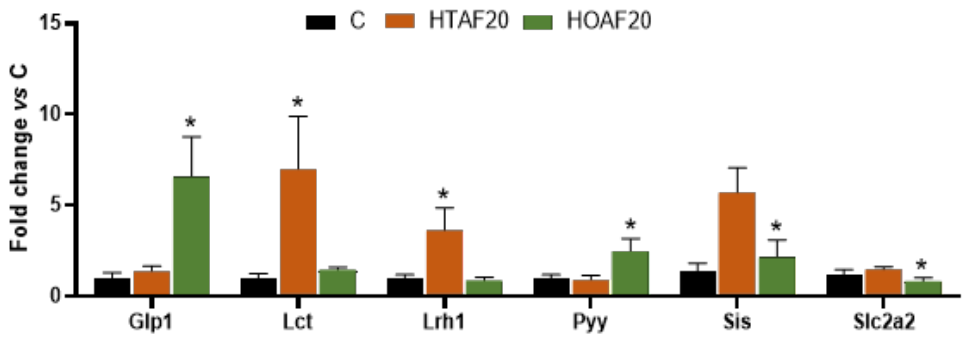

Figure 4. Effect of hydrolysates on the expression of selected genes in intestinal epithelial monolayers of mouse jejunum, derived from organoids. *: $p<0.05$ vs C. C: control group. n= 6-8 from 2 different experiments.

4. Conclusions

This study demonstrates that the enzymatic hydrolysis of *T. molitor* and *O. europaea* seed meals produced hydrolysates with varying degrees of hydrolysis and DPP-IV inhibition activity *in vitro*. The variation in bioactivity highlights the importance of optimizing hydrolysis parameters to enhance peptide bioactivity and stability. Hydrolysates obtained using Alcalase and Flavourzyme with a DH = 20% (HTAF20 and HOAF20) showed the highest inhibition for both substrates. Notably, the HTAF20 hydrolysate exhibited the highest DPP-IV inhibition, with an IC_{50} value of 0.87 ± 0.02 mg protein/mL, categorizing it as a potent inhibitor. However, these hydrolysates also experienced a significant loss of bioactivity after simulated gastrointestinal digestion. Analysis of the MWD before and after digestion revealed a shift towards lower molecular weight peptides in both *T. molitor* and *O. europaea* digests, indicating effective breakdown into smaller fragments. Peptidomics analysis revealed that the presence of Pro at the first two positions at the N-terminus was significantly more prevalent in HTAF20 (33.63%) than in HOAF20 (15.64%), a key structural feature enhancing DPP-IV inhibition. Other hydrophobic/aromatic residues at the C-terminus were also common. Only 11 of the 8,616 identified peptides have previously been reported, emphasizing a knowledge gap in bioactive peptides research. Furthermore, the HTAF20 and HOAF20 hydrolysates were analyzed *ex vivo* using mouse jejunum organoids, revealing that HOAF20 induced the production of GLP-1 and PYY, providing deeper insights into the potential antidiabetic mechanisms. In summary, this study provides compelling evidence for the antidiabetic properties of *T. molitor* and *O. europaea* seed protein hydrolysates, highlighting their role in DPP-IV inhibition and incretin regulation. These sustainable protein sources offer a promising avenue for developing functional foods aimed for diabetes management, aligning with global efforts towards sustainable and health-promoting dietary solutions.

5. References

Adler-Nissen, Jens. (1986). *Enzymic hydrolysis of food proteins. New York: Elsevier Applied Science Publishers*. p9-17 and p146-147.

Al-Mardeai, S., Elnajjar, E., Hashaikeh, R., Kruczek, B., Van der Bruggen, B., & Al-Zuhair, S. (2022). Simultaneous Enzymatic Cellulose Hydrolysis and Product Separation in a Radial-Flow Membrane Bioreactor. *Molecules 2022, Vol. 27, Page 288*, *27*(1), 288. https://doi.org/10.3390/MOLECULES27010288

Aluko, R. E. (2015). Antihypertensive peptides from food proteins. *Annual Review of Food Science and Technology*, *6*(Volume 6, 2015), 235–262. https://doi.org/10.1146/ANNUREV-FOOD-022814-015520

Amigo, L., & Hernández-Ledesma, B. (2020). Current Evidence on the Bioavailability of Food Bioactive Peptides. *Molecules 2020, Vol. 25, Page 4479*, *25*(19), 4479. https://doi.org/10.3390/MOLECULES25194479

Andersen, A., Lund, A., Knop, F. K., & Vilsbøll, T. (2018). Glucagon-like peptide 1 in health and disease. *Nature Reviews Endocrinology 2018 14:7*, *14*(7), 390–403. https://doi.org/10.1038/s41574-018-0016-2

Aquino, M. E., Drago, S. R., Sánchez de Medina, F., Martínez-Augustin, O., & Cian, R. E. (2024). Anti-diabetic properties of brewer's spent yeast peptides. In vitro, in silico and ex vivo study after simulated gastrointestinal digestion. *Food & Function*, *15*(7), 3778–3790. https://doi.org/10.1039/D3FO04040B

Bao, Z. jie, Zhao, Y., Wang, X. ying, & Chi, Y. J. (2017). Effects of degree of hydrolysis (DH) on the functional properties of egg yolk hydrolysate with alcalase. *Journal of Food Science and Technology*, *54*(3), 669–678. https://doi.org/10.1007/S13197-017-2504-0

Bartolomei, M., Capriotti, A. L., Li, Y., Bollati, C., Li, J., Cerrato, A., Cecchi, L., Pugliese, R., Bellumori, M., Mulinacci, N., Laganà, A., Arnoldi, A., & Lammi, C. (2022). Exploitation of Olive (Olea europaea L.) Seed Proteins as Upgraded Source of Bioactive Peptides with Multifunctional Properties: Focus on Antioxidant and Dipeptidyl-Dipeptidase—IV Inhibitory Activities, and Glucagon-like Peptide 1 Improved Modulation. *Antioxidants*, *11*(9), 1730. https://doi.org/10.3390/ANTIOX11091730

Bayrer, J. R., Wang, H., Nattiv, R., Suzawa, M., Escusa, H. S., Fletterick, R. J., Klein, O. D., Moore, D. D., & Ingraham, H. A. (2018). LRH-1 mitigates intestinal inflammatory disease by maintaining epithelial homeostasis and cell survival. *Nature Communications 2018 9:1*, *9*(1), 1–10. https://doi.org/10.1038/s41467-018-06137-w

Ben-Othman, S., Jõudu, I., Bhat, R., Beatriz, M., Oliveira, P., & Alves, R. C. (2020). Bioactives from Agri-Food Wastes: Present Insights and Future Challenges. *Molecules 2020, Vol. 25, Page 510*, *25*(3), 510. https://doi.org/10.3390/MOLECULES25030510

Berraquero-García, C., Almécija, M. C., Guadix, E. M., & Pérez-Gálvez, R. (2022). Valorisation of blood protein from livestock to produce haem iron-fortified hydrolysates with antioxidant activity. *International Journal of Food Science & Technology*, *57*(4), 2479–2486. https://doi.org/10.1111/IJFS.15616

Berraquero-García, C., Rivero-Pino, F., Ospina, J. L., Pérez-Gálvez, R., Espejo-Carpio, F. J., Guadix, A., García-Moreno, P. J., & Guadix, E. M. (2023). Activity, structural features and in silico digestion of antidiabetic peptides. *Food Bioscience*, *55*, 102954. https://doi.org/10.1016/J.FBIO.2023.102954

Brodkorb, A., Egger, L., Alminger, M., Alvito, P., Assunção, R., Ballance, S., Bohn, T., Bourlieu-Lacanal, C., Boutrou, R., Carrière, F., Clemente, A., Corredig, M., Dupont, D., Dufour, C., Edwards, C., Golding, M., Karakaya, S., Kirkhus, B., Le Feunteun, S., … Recio, I. (2019). INFOGEST static in vitro simulation of gastrointestinal food digestion. *Nature Protocols 2019 14:4*, *14*(4), 991–1014. https://doi.org/10.1038/s41596-018-0119-1

Chewaka, L. S., Park, C. S., Cha, Y. S., Desta, K. T., & Park, B. R. (2023). Enzymatic Hydrolysis of Tenebrio molitor (Mealworm) Using Nuruk Extract Concentrate and an Evaluation of Its Nutritional, Functional, and Sensory Properties. *Foods*, *12*(11), 2188. https://doi.org/10.3390/FOODS12112188

Cobo-Vuilleumier, N., Lorenzo, P. I., & Gauthier, B. R. (2018). Targeting LRH-1/NR5A2 to treat type 1 diabetes mellitus. *Cell Stress*, *2*(6), 141. https://doi.org/10.15698/CST2018.06.140

Cobo-Vuilleumier, N., Lorenzo, P. I., Rodríguez, N. G., Herrera Gómez, I. D. G., Fuente-Martin, E., López-Noriega, L., Mellado-Gil, J. M., Romero-Zerbo, S. Y., Baquié, M., Lachaud, C. C., Stifter, K., Perdomo, G., Bugliani, M., De Tata, V., Bosco, D., Parnaud, G., Pozo, D., Hmadcha, A., Florido, J. P., … Gauthier, B. R. (2018). LRH-1 agonism favours an immune-islet dialogue which protects against diabetes mellitus. *Nature Communications 2018 9:1*, *9*(1), 1–15. https://doi.org/10.1038/s41467-018-03943-0

Cruz-Casas, D. E., Aguilar, C. N., Ascacio-Valdés, J. A., Rodríguez-Herrera, R., Chávez-González, M. L., & Flores-Gallegos, A. C. (2021). Enzymatic hydrolysis and microbial fermentation: The most favorable biotechnological methods for the release of bioactive peptides. *Food Chemistry: Molecular Sciences*, *3*, 100047. https://doi.org/10.1016/J.FOCHMS.2021.100047

Daliri, E. B. M., Lee, B. H., Kim, J. H., & Oh, D. H. (2018). Novel angiotensin I-converting enzyme inhibitory peptides from soybean protein isolates fermented by Pediococcus pentosaceus SDL1409. *LWT*, *93*, 88–93. https://doi.org/10.1016/J.LWT.2018.03.026

Dávalos Terán, I., Imai, K., Lacroix, I. M. E., Fogliano, V., & Udenigwe, C. C. (2020). Bioinformatics of edible yellow mealworm (Tenebrio molitor) proteome reveal the cuticular proteins as promising precursors of dipeptidyl peptidase-IV inhibitors. *Journal of Food Biochemistry*, *44*(2), e13121. https://doi.org/10.1111/JFBC.13121

Galland, F., de Espindola, J. S., Lopes, D. S., Taccola, M. F., & Pacheco, M. T. B. (2022). Food-derived bioactive peptides: Mechanisms of action underlying inflammation and oxidative stress in the central nervous system. *Food Chemistry Advances*, *1*, 100087. https://doi.org/10.1016/J.FOCHA.2022.100087

Gallo, V., Romano, A., Miralles, B., Ferranti, P., Masi, P., Santos-Hernández, M., & Recio, I. (2022). Physicochemical properties, structure and digestibility in simulated gastrointestinal environment of bread added with green lentil flour. *LWT*, *154*, 112713. https://doi.org/10.1016/J.LWT.2021.112713

Gao, K., Rao, J., & Chen, B. (2024). Plant protein solubility: A challenge or insurmountable obstacle. *Advances in Colloid and Interface Science*, *324*, 103074. https://doi.org/10.1016/J.CIS.2023.103074

García-Moreno, P. J., Espejo-Carpio, F. J., Guadix, A., & Guadix, E. M. (2015). Production and identification of angiotensin I-converting enzyme (ACE) inhibitory peptides from Mediterranean fish discards. *Journal of Functional Foods*, *18*, 95–105. https://doi.org/10.1016/J.JFF.2015.06.062

Garzón, A. G., Cian, R. E., & Drago, S. R. (2023). Effects of agar-carrageenan wall materials and core-to-wall material ratio on physicochemical properties and in vitro bioaccessibility of microencapsulated bioactive peptides. *Food Hydrocolloids*, *139*, 108570. https://doi.org/10.1016/J.FOODHYD.2023.108570

González, R., Ceacero-Heras, D., Tena-Garitaonaindia, M., Álvarez-Mercado, A., Gámez-Belmonte, R., Chazin, W. J., Sánchez de Medina, F., & Martínez-Augustin, O. (2024). Intestinal inflammation marker calprotectin regulates epithelial intestinal zinc metabolism and proliferation in mouse jejunal organoids. *Biomedicine & Pharmacotherapy*, *174*, 116555. https://doi.org/10.1016/J.BIOPHA.2024.116555

Henchion, M., Hayes, M., Mullen, A. M., Fenelon, M., & Tiwari, B. (2017). Future Protein Supply and Demand: Strategies and Factors Influencing a Sustainable Equilibrium. *Foods 2017, Vol. 6, Page 53*, *6*(7), 53. https://doi.org/10.3390/FOODS6070053

Islam, M. S., Hongxin, W., Admassu, H., Noman, A., Ma, C., & An wei, F. (2021). Degree of hydrolysis, functional and antioxidant properties of protein hydrolysates from Grass Turtle (Chinemys reevesii) as influenced by enzymatic hydrolysis conditions. *Food Science & Nutrition*, *9*(8), 4031–4047. https://doi.org/10.1002/FSN3.1903

Janssen, R. H., Vincken, J. P., Van Den Broek, L. A. M., Fogliano, V., & Lakemond, C. M. M. (2017). Nitrogen-to-Protein Conversion Factors for Three Edible Insects: Tenebrio molitor, Alphitobius diaperinus, and Hermetia illucens. *Journal of Agricultural and Food Chemistry*, *65*(11), 2275–2278. https://doi.org/10.1021/ACS.JAFC.7B00471

Klost, M., & Drusch, S. (2019). Functionalisation of pea protein by tryptic hydrolysis – Characterisation of interfacial and functional properties. *Food Hydrocolloids*, *86*, 134–140. https://doi.org/10.1016/J.FOODHYD.2018.03.013

Lacroix, I. M. E., Chen, X. M., Kitts, D. D., & Li-Chan, E. C. Y. (2017). Investigation into the bioavailability of milk protein-derived peptides with dipeptidyl-peptidase IV inhibitory activity using Caco-2 cell monolayers. *Food & Function*, *8*(2), 701–709. https://doi.org/10.1039/C6FO01411A

Lacroix, I. M. E., & Li-Chan, E. C. Y. (2012). Dipeptidyl peptidase-IV inhibitory activity of dairy protein hydrolysates. *International Dairy Journal*, *25*(2), 97–102. https://doi.org/10.1016/J.IDAIRYJ.2012.01.003

Lafferty, R. A., Flatt, P. R., & Irwin, N. (2024). NPYR modulation: Potential for the next major advance in obesity and type 2 diabetes management? *Peptides*, *179*, 171256. https://doi.org/10.1016/J.PEPTIDES.2024.171256

Leiting, B., Pryor, K. A. D., Wu, J. K., Marsilio, F., Patel, R. A., Craik, C. S., Ellman, J. A., Cummings, R. T., & Thornberry, N. A. (2003). Catalytic properties and inhibition of proline-specific dipeptidyl peptidases II, IV and VII. *Biochemical Journal*, *371*(2), 525–532. https://doi.org/10.1042/BJ20021643

Liao, W., Fan, H., Liu, P., & Wu, J. (2019). Identification of angiotensin converting enzyme 2 (ACE2) up-regulating peptides from pea protein hydrolysate. *Journal of Functional Foods*, *60*, 103395. https://doi.org/10.1016/J.JFF.2019.05.051

Liu, R., Cheng, J., & Wu, H. (2019). Discovery of Food-Derived Dipeptidyl Peptidase IV Inhibitory Peptides: A Review. *International Journal of Molecular Sciences 2019, Vol. 20, Page 463*, *20*(3), 463.

https://doi.org/10.3390/IJMS20030463

Lorenzo, J. M., Munekata, P. E. S., Gómez, B., Barba, F. J., Mora, L., Pérez-Santaescolástica, C., & Toldrá, F. (2018). Bioactive peptides as natural antioxidants in food products – A review. *Trends in Food Science & Technology*, *79*, 136–147. https://doi.org/10.1016/J.TIFS.2018.07.003

Maestri, D., Barrionuevo, D., Bodoira, R., Zafra, A., Jiménez-López, J., & Alché, J. de D. (2019). Nutritional profile and nutraceutical components of olive (Olea europaea L.) seeds. *Journal of Food Science and Technology*, *56*(9), 4359–4370. https://doi.org/10.1007/S13197-019-03904-5

Majura, J. J., Cao, W., Chen, Z., Htwe, K. K., Li, W., Du, R., Zhang, P., Zheng, H., & Gao, J. (2022). The current research status and strategies employed to modify food-derived bioactive peptides. *Frontiers in Nutrition*, *9*, 950823. https://doi.org/10.3389/FNUT.2022.950823

Minkiewicz, P., Iwaniak, A., & Darewicz, M. (2019). BIOPEP-UWM Database of Bioactive Peptides: Current Opportunities. *International Journal of Molecular Sciences*, *20*(23). https://doi.org/10.3390/IJMS20235978

Mora, L., & Toldrá, F. (2023). Advanced enzymatic hydrolysis of food proteins for the production of bioactive peptides. *Current Opinion in Food Science*, *49*, 100973. https://doi.org/10.1016/J.COFS.2022.100973

Mudgil, P., Kamal, H., Priya Kilari, B., Mohd Salim, M. A. S., Gan, C. Y., & Maqsood, S. (2021). Simulated gastrointestinal digestion of camel and bovine casein hydrolysates: Identification and characterization of novel anti-diabetic bioactive peptides. *Food Chemistry*, *353*, 129374. https://doi.org/10.1016/J.FOODCHEM.2021.129374

Nongonierma, A. B., & FitzGerald, R. J. (2013). Inhibition of dipeptidyl peptidase IV (DPP-IV) by proline containing casein-derived peptides. *Journal of Functional Foods*, *5*(4), 1909–1917. https://doi.org/10.1016/J.JFF.2013.09.012

Nongonierma, A. B., & Fitzgerald, R. J. (2013). Inhibition of dipeptidyl peptidase IV (DPP-IV) by tryptophan containing dipeptides. *Food & Function*, *4*(12), 1843–1849. https://doi.org/10.1039/C3FO60262A

Nongonierma, A. B., & Fitzgerald, R. J. (2016). Structure activity relationship modelling of milk protein-derived peptides with dipeptidyl peptidase IV (DPP-IV) inhibitory activity. *Peptides*, *79*, 1–7. https://doi.org/10.1016/J.PEPTIDES.2016.03.005

Nongonierma, A. B., & FitzGerald, R. J. (2019). Features of dipeptidyl peptidase IV (DPP-IV) inhibitory peptides from dietary proteins. *Journal of Food Biochemistry*, *43*(1), e12451. https://doi.org/10.1111/JFBC.12451

Nongonierma, A. B., Mooney, C., Shields, D. C., & FitzGerald, R. J. (2013). Inhibition of dipeptidyl peptidase IV and xanthine oxidase by amino acids and dipeptides. *Food Chemistry*, *141*(1), 644–653. https://doi.org/10.1016/J.FOODCHEM.2013.02.115

Nongonierma, A. B., Paolella, S., Mudgil, P., Maqsood, S., & FitzGerald, R. J. (2017). Dipeptidyl peptidase IV (DPP-IV) inhibitory properties of camel milk protein hydrolysates generated with trypsin. *Journal of Functional Foods*, *34*, 49–58. https://doi.org/10.1016/J.JFF.2017.04.016

Olsen, J. V., Ong, S. E., & Mann, M. (2004). Trypsin cleaves exclusively C-terminal to arginine and lysine residues. *Molecular and Cellular Proteomics*, *3*(6), 608–614. https://doi.org/10.1074/mcp.T400003-MCP200

Ospina-Quiroga, J. L., García-Moreno, P. J., Guadix, A., Guadix, E. M., Almécija-Rodríguez, M. del C., & Pérez-Gálvez, R. (2022). Evaluation of Plant Protein Hydrolysates as Natural Antioxidants in Fish Oil-In-Water Emulsions. *Antioxidants*, *11*(8), 1612. https://doi.org/10.3390/ANTIOX11081612

Pérez-Gálvez, R., Berraquero-García, C., Ospina-Quiroga, J. L., Espejo-Carpio, F. J., Almécija, M. C., Guadix, A., García-Moreno, P. J., & Guadix, E. M. (2024). Influence of In Vitro Digestion on Dipeptidyl Peptidase-IV (DPP-IV) Inhibitory Activity of Plant-Protein Hydrolysates Obtained from Agro-Industrial By-Products. *Foods 2024, Vol. 13, Page 2691*, *13*(17), 2691. https://doi.org/10.3390/FOODS13172691

Rivero Pino, F., Pérez Gálvez, R., Espejo Carpio, F. J., & Guadix, E. M. (2020). Evaluation of Tenebrio molitor protein as a source of peptides for modulating physiological processes. *Food & Function*, *11*(5), 4376–4386. https://doi.org/10.1039/D0FO00734J

Rivero-Pino, F., Espejo-Carpio, F. J., & Guadix, E. M. (2021). Identification of dipeptidyl peptidase IV (DPP-IV) inhibitory peptides from vegetable protein sources. *Food Chemistry*, *354*, 129473. https://doi.org/10.1016/J.FOODCHEM.2021.129473

Rivero-Pino, F., Guadix, A., & Guadix, E. M. (2021). Identification of novel dipeptidyl peptidase IV and α-glucosidase inhibitory peptides from Tenebrio molitor. *Food & Function*, *12*(2), 873–880. https://doi.org/10.1039/D0FO02696D

Romero-Calvo, I., Ocón, B., Gámez-Belmonte, R., Hernández-Chirlaque, C., de Jonge, H. R., Bijvelds, M. J., Martínez-Augustin, O., & Sánchez de Medina, F. (2018). Adenylyl cyclase 6 is involved in the hyposecretory status of experimental colitis. *Pflugers Archiv European Journal of Physiology*, *470*(11), 1705–1717. https://doi.org/10.1007/S00424-018-2187-Z

Segura-Campos, M. R., Espinosa-García, L., Chel-Guerrero, L. A., & Betancur-Ancona, D. A. (2012). Effect of Enzymatic Hydrolysis on Solubility, Hydrophobicity, and In Vivo Digestibility in Cowpea (Vigna unguiculata). *International Journal of Food Properties*, *15*(4), 770–780. https://doi.org/10.1080/10942912.2010.501469

Shahbal, N., Jing, X., Bhandari, B., Dayananda, B., & Prakash, S. (2023). Effect of enzymatic hydrolysis on solubility and surface properties of pea, rice, hemp, and oat proteins: Implication on high protein concentrations. *Food Bioscience*, *53*, 102515. https://doi.org/10.1016/J.FBIO.2023.102515

Spackman, D. H., Stein, W. H., & Moore, S. (1958). Automatic Recording Apparatus for Use in the Chromatography of Amino Acids. *Analytical Chemistry*, *30*(7), 1190–1206. https://doi.org/10.1021/AC60139A006

Tan, J., Yang, J., Zhou, X., Hamdy, A. M., Zhang, X., Suo, H., Zhang, Y., Li, N., & Song, J. (2022). Tenebrio molitor Proteins-Derived DPP-4 Inhibitory Peptides: Preparation, Identification, and Molecular Binding Mechanism. *Foods 2022, Vol. 11, Page 3626*, *11*(22), 3626. https://doi.org/10.3390/FOODS11223626

Wang, B., Yu, Z., Yokoyama, W., Chiou, B. Sen, Chen, M., Liu, F., & Zhong, F. (2021). Collagen peptides with DPP-IV inhibitory activity from sheep skin and their stability to in vitro gastrointestinal digestion. *Food Bioscience*, *42*, 101161. https://doi.org/10.1016/J.FBIO.2021.101161

Wang, J., Su, Y., Jia, F., & Jin, H. (2013). Characterization of casein hydrolysates derived from enzymatic hydrolysis. *Chemistry Central Journal*, *7*(1), 1–8. https://doi.org/10.1186/1752-153X-7-62

Xu, Q., Zheng, L., Huang, M., & Zhao, M. (2022). Exploring structural features of potent dipeptidyl peptidase IV (DPP-IV) inhibitory peptides derived from tilapia (Oreochromis niloticus) skin gelatin by an integrated approach of multivariate analysis and Gly-Pro-based peptide library. *Food Chemistry*, *397*, 133821. https://doi.org/10.1016/J.FOODCHEM.2022.133821

Yu, X., Oh, E., & Kim, Y. (2021). A comparative study on the functional properties of mealworm (Tenebrio molitor) larvae and soybean protein isolates and hydrolysates. *International Food Research Journal*, *28*(4), 816–826. https://doi.org/10.47836/IFRJ.28.4.18

Zerlotin, R., Arconzo, M., Piccinin, E., & Moschetta, A. (2021). Another One Bites the Gut: Nuclear Receptor LRH-1 in Intestinal Regeneration and Cancer. *Cancers 2021, Vol. 13, Page 896*, *13*(4), 896. https://doi.org/10.3390/CANCERS13040896

Zhao, T., Xu, J., Zhao, H., Jiang, W., Guo, X., Zhao, M., Sun-Waterhouse, D., Zhao, Q., & Su, G. (2017). Antioxidant and anti-acetylcholinesterase activities of anchovy (Coilia mystus) protein hydrolysates and their memory-improving effects on scopolamine-induced amnesia mice. *International Journal of Food Science & Technology*, *52*(2), 504–510. https://doi.org/10.1111/IJFS.13306

6. Supplementary material

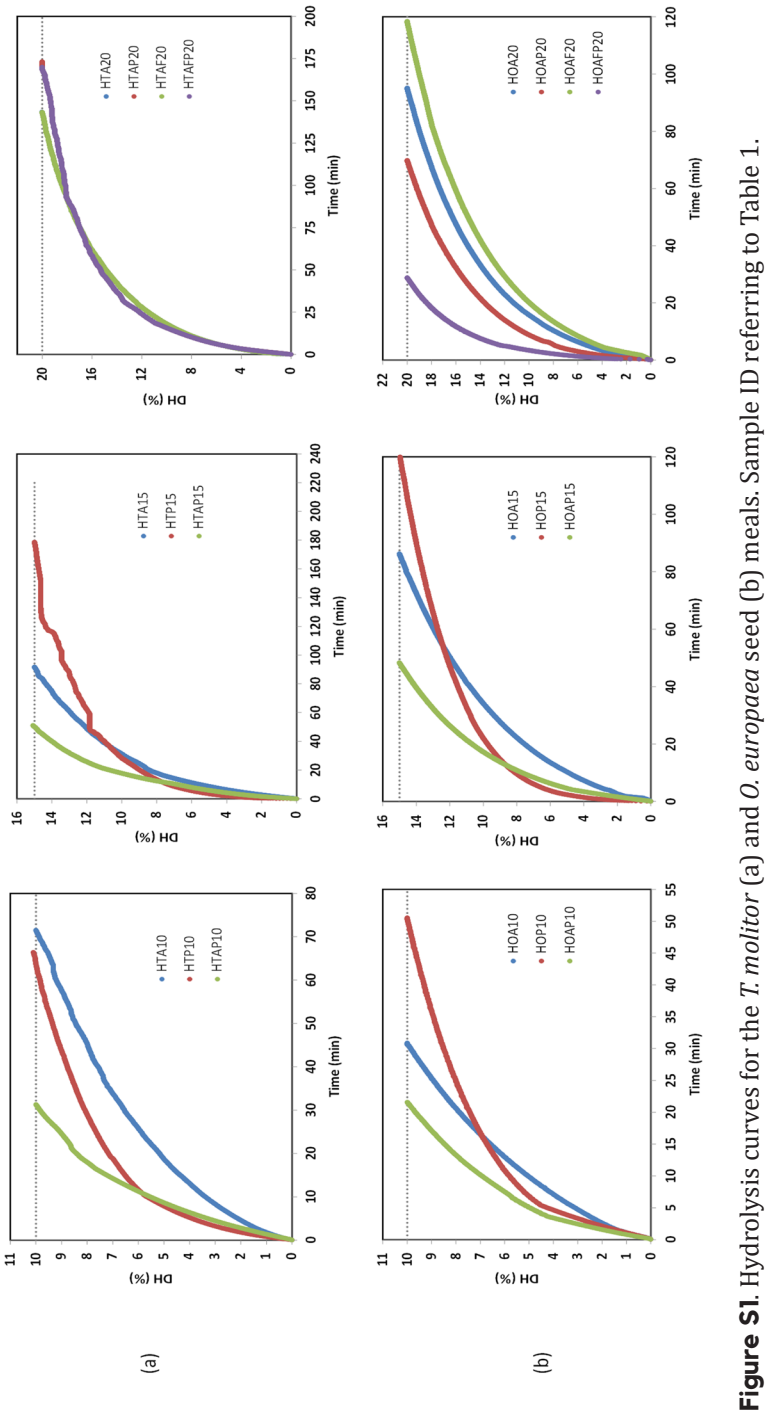

Figure S1. Hydrolysis curves for the *T. molitor* (a) and *O. europaea* seed (b) meals. Sample ID referring to Table 1.

Table S1. Physicochemical analysis of the meals, determined through proximate analysis for *T. molitor* meal and provided by the supplier Q'omer for *O. europaea* seed meal.

Physicochemical composition	***T. molitor***	***O. europaea* seed**
Protein (%)	68	20-25
Fat (%)	7	8-14
Dietary fibre (%)	5	53-61
Carbohydrates (%)	14	2-3
Moisture (%)	5	6-9

Table S2. Amino acid composition (mol %) of *T. molitor* and olive seed hydrolysates

Amino acids	*T. molitor* hydrolysates									
	HTA10	**HTP10**	**HTAP10**	**HTA15**	**HTP15**	**HTAP15**	**HTA20**	**HTAP20**	**HTAF20**	**HTAFP20**
Asp	8.84±0.01	8.98±0.03	9.27±0.03	9.14±0.1	9.07±0.19	9.12±0.05	9.05±0.05	9.54±0.22	8.84±0.03	9.52±0.12
Thr	4.84±0.01	4.76±0.03	4.97±0.00	4.59±0.06	4.75±0.15	4.68±0.08	4.74±0.07	3.8±0.29	4.40±0.00	3.85±0.11
Ser	6.35±0.03	6.44±0.03	6.23±0.02	6.69±0.01	6.83±0.25	6.53±0.03	6.68±0.19	6.77±0.17	6.70±0.01	6.69±0.07
Glu	11.51±0.03	11.56±0.05	12.39±0.08	11.7±0.05	12.11±0.51	11.60±0.08	11.77±0.35	11.98±0.01	11.59±0.08	12.01±0.21
Pro	8.27±0.09	8.09±0.01	8.28±0.51	7.93±0.05	7.90±0.25	7.96±0.06	8.03±0.17	8.14±0.31	7.04±0.13	8.55±0.09
Gly	9.01±0.06	9.21±0.05	8.80±0.03	9.42±0.05	9.25±0.21	9.40±0.04	9.47±0.08	10.22±0.01	9.44±0.16	9.87±0.11
Ala	11.34±0.05	11.61±0.01	10.61±0.04	11.77±0.13	11.72±0.37	11.87±0.09	12.01±0.17	12.64±0.13	12.25±0.04	12.39±0.04
Cys	0.38±0.16	0.47±0.08	0.64±0.01	0.53±0.02	0.49±0.02	0.57±0.01	0.50±0.02	0.58±0.06	0.62±0.08	0.63±0.06
Val	6.87±0.22	6.30±0.05	6.61±0.04	5.75±0.13	5.77±0.30	5.74±0.10	5.80±0.06	4.69±0.16	6.31±0.17	4.71±0.03
Met	1.06±0.18	1.21±0.01	1.21±0.01	1.23±0.02	1.24±0.09	1.35±0.15	1.23±0.02	1.17±0.06	1.21±0.01	1.35±0.04
Ile	4.19±0.17	3.77±0.09	4.01±0.03	3.31±0.12	3.39±0.15	3.37±0.02	3.27±0.06	2.62±0.1	3.40±0.05	2.78±0.13
Leu	7.33±0.04	7.27±0.02	7.22±0.00	7.07±0.05	7.17±0.06	7.22±0.01	7.18±0.03	6.58±0.01	7.25±0.01	6.81±0.04
Tyr	5.19±0.08	5.42±0.07	5.05±0.72	5.58±0.01	5.47±0.00	5.53±0.04	5.63±0.04	5.48±0.27	5.09±0.11	5.51±0.01
Phe	3.06±0.16	3.31±0.14	3.28±0.24	3.54±0.06	3.34±0.09	3.46±0.00	3.48±0.08	4.13±0.45	4.30±0.03	4.28±0.05
His	2.57±0.02	2.48±0.05	2.50±0.00	2.49±0.01	2.45±0.01	2.48±0.02	2.51±0.02	2.46±0.04	2.55±0.01	2.48±0.01
Lys	5.21±0.03	5.10±0.05	5.25±0.18	5.19±0.01	5.04±0.03	5.08±0.05	4.82±0.01	5.11±0.01	5.11±0.02	4.69±0.08
Arg	3.91±0.07	3.96±0.01	3.92±0.07	3.99±0.01	3.93±0.03	3.96±0.01	3.75±0.00	4.01±0.17	3.83±0.06	3.81±0.17

Table S2. Amino acid composition (mol %) of *T. molitor* and olive seed hydrolysates

Amino acids	*O. europaea* hydrolysates									
	HOA10	**HOP10**	**HOAP10**	**HOA15**	**HOP15**	**HOAP15**	**HOA20**	**HOAP20**	**HOAF20**	**HOAFP20**
Asp	10.49±0.01	10.17±0.14	10.23±0.04	10.24±0.01	9.98±0.19	10.26±0.14	10.47±0.05	10.21±0.07	10.5±0.09	10.48±0.02
Thr	4.74±0.04	4.44±0.04	4.24±0.04	4.57±0.07	4.54±0.19	4.31±0.30	4.52±0.02	4.55±0.01	4.47±0.01	4.66±0.02
Ser	7.80±0.02	7.60±0.04	7.76±0.04	7.91±0.28	7.75±0.37	7.57±0.26	7.85±0.01	7.71±0.07	7.72±0.07	7.81±0.08
Glu	20.21±0.05	18.97±0.02	18.97±0.05	19.69±0.16	18.64±0.07	19.62±0.09	20.24±0.01	18.97±0.15	20.05±0.02	19.28±0.12
Pro	4.56±0.08	5.37±0.75	6.35±0.63	4.75±0.06	5.40±0.81	7.71±1.28	5.07±0.05	4.93±0.06	5.08±0.16	5.10±0.09
Gly	9.16±0.08	9.65±0.02	9.65±0.01	9.43±0.18	9.36±0.12	8.99±0.03	9.34±0.01	9.42±0.09	9.30±0.03	9.08±0.05
Ala	6.86±0.01	7.48±0.12	7.48±0.02	7.16±0.15	7.30±0.08	7.12±0.12	7.42±0.02	7.47±0.14	7.43±0.03	7.40±0.08
Cys	1.11±0.03	1.20±0.00	1.20±0.01	1.22±0.35	1.12±0.08	1.16±0.07	1.20±0.01	1.26±0.29	1.36±0.15	1.03±0.30
Val	6.38±0.09	6.50±0.15	6.51±0.10	6.52±0.17	6.73±0.12	6.10±0.02	6.51±0.00	6.44±0.21	6.46±0.04	6.79±0.11
Met	1.76±0.06	1.46±0.13	1.42±0.11	1.68±0.08	1.79±0.25	1.32±0.02	1.47±0.02	1.57±0.11	1.54±0.05	1.36±0.34
Ile	4.64±0.04	4.76±0.16	4.74±0.12	4.63±0.07	5.07±0.06	4.45±0.01	4.43±0.01	4.62±0.22	4.48±0.04	4.76±0.13
Leu	6.22±0.03	6.79±0.06	6.73±0.01	6.30±0.03	6.92±0.03	6.15±0.10	6.50±0.01	6.94±0.04	6.55±0.04	6.63±0.04
Tyr	2.81±0.05	2.41±0.03	2.32±0.16	2.65±0.03	2.46±0.11	2.21±0.02	2.28±0.08	2.51±0.12	2.41±0.01	2.66±0.10
Phe	3.59±0.04	3.88±0.13	3.87±0.15	4.02±0.27	3.73±0.08	3.70±0.08	3.93±0.05	3.97±0.12	3.79±0.14	3.70±0.01
His	1.92±0.01	2.02±0.03	2.15±0.21	1.96±0.01	1.97±0.11	2.08±0.31	1.98±0.01	1.99±0.02	1.92±0.02	1.91±0.01
Lys	2.01±0.09	2.11±0.06	2.19±0.17	1.97±0.21	2.11±0.07	2.19±0.17	2.05±0.04	2.25±0.06	2.02±0.02	2.24±0.03
Arg	5.67±0.03	4.98±0.02	5.00±0.06	5.22±0.04	5.05±0.07	4.99±0.08	4.68±0.08	5.10±0.14	4.82±0.01	5.02±0.01

Table S3:

- https://docs.google.com/spreadsheets/d/1NZ6OQtVnH5iGxafRkppebR-p9iMCrScQ/edit?usp=sharing&ouid=117129379747364115172&rtpof=true&sd=true

CHAPTER IV

Encapsulation of Bioactive Peptides by Spray-Drying and Electrospraying

ABSTRACT

This study evaluated the antidiabetic potential of protein hydrolysates derived from *Tenebrio molitor* and *Olea europaea* seed, using *in vitro* and *ex vivo* models. A screening of enzymatic hydrolysis was conducted, employing various endo- and exoproteases with diverse specificities to achieve degrees of hydrolysis ranging 10-20%. Analysis of the DPP-IV inhibitory activity of all the hydrolysates revealed that treatment with a combination of a broad-spectrum endoprotease and a mix of endo- and exoproteases at the highest degree of hydrolysis produced the greatest DPP-IV inhibition for both types of hydrolysates. In fact, the mealworm hydrolysate produced in these conditions exhibited the highest inhibition (IC_{50}=0.87±0.02 mg protein/mL). The bioactivity of all hydrolysates was studied after simulated digestion, finding a significant loss of activity and high peptide degradation. The two most bioactive hydrolysates were evaluated using a mouse intestinal organoid model. This study demonstrated that the selected olive hydrolysate influenced the expression of the GLP-1 gene, suggesting its potential to regulate glycemic response. The findings highlight the promise of these sustainable protein hydrolysates as bioactive food ingredients for diabetes management..

JOURNAL PAPER: Berraquero-García, C., Pérez-Gálvez, R., Espejo-Carpio, F. J., Guadix, A., Guadix, E. M. & García-Moreno, P. J. (2023). Encapsulation of Bioactive Peptides by Spray-Drying and Electrospraying. *Foods*, *12*. https://doi.org/10.3390/foods12102005 (IF: 4.7 (2023); Category: Food Science and Technology; Position: 38/173; Q1)

1. Introduction

Bioactive peptides have received increasing interest in the last few decades due to the wide range of biological activities they can exert. Multiple studies have demonstrated their antioxidant, antihypertensive, antimicrobial or anti-inflammatory activities, among others, as well as their high potential for the treatment of various diseases, such as diabetes and different types of cancers (Jakubczyk et al., 2020). This has boosted the research on the use of biopeptides as therapeutic agents, especially for the treatment of certain chronic conditions, through their incorporation in supplements, pharmaceutical compounds, or functional foods (Chakrabarti et al., 2018). In addition to the properties previously mentioned, biopeptides have other advantages such as their low production cost, low allergenicity, high nutritional value and high digestibility (Figure 1)(Sarabandi, Gharehbeglou, et al., 2019).

Enzymatic hydrolysis is commonly used to produce bioactive peptides (Cruz-Casas et al., 2021). This technology releases the peptides encrypted in the original protein by means of breaking the peptide bonds with proteases, improving the technological and bioactive properties of the hydrolysates, enhancing their digestibility, and decreasing their antigenicity by degrading the allergenic epitopes (Rivero-Pino et al., 2020). Bioactive peptides are usually of 2-20 amino acids in length, and their activity is determined by the specific amino acid sequence and the relative abundance of certain residues (e.g., hydrophilic, hydrophobic, or aromatic) within the peptide (Sánchez & Vázquez, 2017).

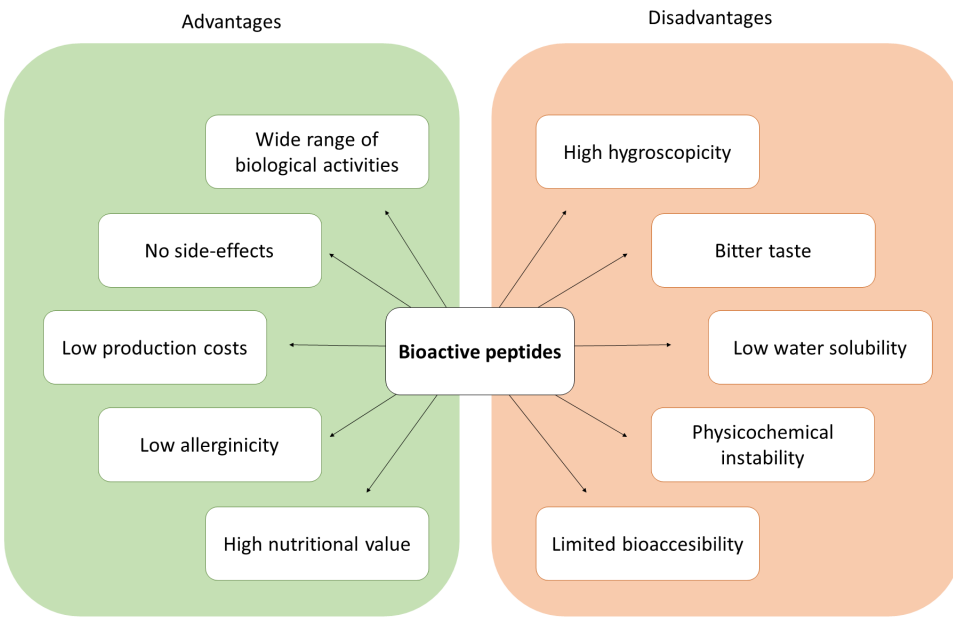

Figure 1. Advantages and disadvantages of using peptides as bioactive ingredients in food.

Clinical application of bioactive peptides is severely limited by the difficulty to find an effective method of administration (L. Wang et al., 2022). In the pharmacological field, most protein-based treatments are administered via parenteral injection. However, this administration approach presents several drawbacks, mainly i) difficulty in self-administration, ii) short half-life of the proteins, and iii) proteins can be easily degraded in the bloodstream (Moreira et al., 2021). Although oral administration of bioactive peptides is a much easier and more practical approach to implement for consumers, there are multiple challenges in its use that must be overcome (Figure 1):

- High hygroscopicity, which may result in physicochemical instability and bioactivity loss (Aguilar-Toala et al., 2022).
- Bitterness due to the exposure to taste receptors of hydrophobic amino acid residues generated from hydrolysis. It has a negative impact on consumer's acceptance (Iwaniak et al., 2019).
- Low water-solubility, limiting the introduction of hydrolysates or peptides into food matrices, which requires generating dispersed systems (Karami & Akbari-adergani, 2019).
- Physicochemical instability during storage, processing, and digestion, due to the exposure of peptides to environmental conditions (e.g., oxygen, heat) or their interaction with the digestive proteases and other compounds present in the food matrix (Pei et al., 2022).
- Limited bioaccessibility. Once ingested, peptides must be able to remain intact until they are absorbed in the intestine in order to exert their bioactivity. This is challenging due to the harsh conditions found in the gastrointestinal tract, such as the strongly acidic pH in the stomach and the enzymatically active gastric and intestinal fluids (Perry & McClements, 2020).

To overcome these limitations, great efforts are focused on increasing the physicochemical stability and bioaccessibility of peptides. Indeed, stabilization of bioactive peptides is an essential process to ensure that their *in vitro* activity properly translates to *in vivo* animal and human models after processing, storage, and digestion (Mohan et al., 2015). Encapsulation of bioactive peptides, consisting in entrapping the peptides within a matrix or layer(s) of encapsulating agent(s), reduces hygroscopicity, masks bitterness and protects the biopeptides from degradation during processing, storage and digestion while maintaining their bioaccessibility (Sun et al., 2021). The pharmaceutical industry has extensively used encapsulation techniques for the stabilization and controlled release of active compounds. Encapsulation processes have attracted much attention from the food industry, especially due to the growing interest during recent decades in the fortification of food with bioactive ingredients, including peptides, to produce functional food products (Mohan et al., 2015). Although significant research has been carried out on the encapsulation of lipids (e.g., omega-3 fatty acids),

probiotics, vitamins and antioxidants (e.g. polyphenols), there are considerably fewer studies on the encapsulation of bioactive peptides (Aguilar-Toala et al., 2022; Mohan et al., 2015; Sarabandi, Gharehbeglou, et al., 2019).

Several techniques are available for the entrapment of food bioactives (i.e., peptides) within a biopolymer matrix (i.e., spray-drying, spray-cooling, fluid-bed coating, extrusion, electrospraying and complex coacervation followed by drying) (Sobel et al., 2014). Nevertheless, spray-drying is the most commonly used technique for the encapsulation of thermosensitivethermo-sensitive compounds, which permits obtainingto obtain dry microparticles at an industrial scale without peptide degradation (e.g., changes in secondary structure) (Sarabandi et al., 2021 , Rahmani-Manglano et al., 2022). In recent years, electrospraying has emerged as a promising technique to encapsulate bioactive ingredients at room temperature, obtaining nano/microcapsules with narrow size distribution, low cost, and potential to be scaled-up (Jacobsen et al., 2018). In any case, it should be noted that the potential degradation of peptides due to electrostatic stresses during electrospraying might need further investigation (Rahmani-Manglano et al., 2022). Furthermore, both spray-drying and electrospraying can work in coaxial configuration, resulting in capsules with a double layer of encapsulating wall(s), which might enhance the protection and delivery of the bioactives (Wan et al., 2014a). Contrarily to coaxial spray-drying and electrospraying, other encapsulating techniques such as fluidized-bed and spray-chilling processes require an additional production stage to provide a second coating of the encapsulates which can result in double-layered capsules (Stone et al., 2015).

In the light of the above, this work presents a systematic review on the encapsulation of bioactive peptides and protein hydrolysates by spray-drying and electrospraying. This review focuses on the various factors affecting the properties of the encapsulates (e.g., morphology, size, encapsulation efficiency), such as the formulation of the feed solution including the type of carrier and solvent. The specific processing conditions used for both encapsulation techniques (i.e., inlet and outlet air temperature for spray-drying and voltage and flow rate for electrospraying, among others) were reviewed. The use of mono- or coaxial encapsulation methods for both spray-drying and electrospraying are discussed. Finally, this review focuses on release, bioactivity and stability after digestion of the encapsulated peptides.

2. Literature Search

A literature search of the papers reporting the encapsulation of peptides, protein hydrolysates and proteins via spray-drying and electrospraying, both monoaxial and coaxial, published in the period between 2012 and November 2022 was carried out using Scopus (https://www.scopus.com/(accessed on 25 November 2022)). Research papers containing the keywords “peptide & encapsulation & spray drying,” “hydrolysate

& encapsulation & spray drying," "protein & encapsulation & spray drying," "peptide & encapsulation & electrospraying," "hydrolysate & encapsulation & electrospraying," "protein & encapsulation & electrospraying," "coaxial & encapsulation & electrospraying" and "coaxial & encapsulation & spray drying" were searched. Consequently, the literature search yielded 444 references that were manually screened. From all the works, 397 were excluded because: (a) the paper was published before 2012 (n = 87), (b) the reference was not a research paper (n = 71), (c) the reference was repeated in different searches (n = 105), (d) peptides, protein hydrolysates or protein were not the active ingredient encapsulated (n = 71), (e) spray-drying or electrospraying was not used to dry the formulations (n = 46), and (f) no information about process or formulation was available (n = 17). Additionally, three works not found in the Scopus literature research were deemed adequate to be added. A total of 50 experimental research papers were considered for the evaluation.

3. Encapsulation of Protein-Based Bioactives by Spray-Drying

3.1. Fundamentals of Spray-Drying

Spray-drying is an encapsulation technique based on the atomization of a solution into droplets and their subsequent drying within a gas (e.g., air or nitrogen) at high temperature, producing dry particles (Jacobs, 2014). More specifically, the encapsulation of bioactives by spray-drying consists in the dispersion/mixing of the bioactive together with a carrier (encapsulating agent) in the selected solvent. The solution is pumped and atomized at the entrance of the drying chamber using an atomizer. The atomizer type (i.e., rotary atomizer, pressure nozzle, or sonic nozzle) is selected depending on the characteristics and desired particle size of the final product. The pressure nozzle is the most used at laboratory scale (Figure 2A) (Woo & Bhandari, 2013).

A gas stream at high temperature is concurrently fed to the chamber, providing the driving force to the drying process (e.g., difference in temperature and relative humidity between the droplet and the inlet air). Most of the water is removed during the first drying stage, where the droplet surface is saturated with water. The evaporation of the solvent provides the cooling needed to maintain the surface temperature at a constant value (i.e., wet-bulb temperature). The second drying stage, known as the falling rate period, begins when the surface of the droplet is no longer saturated with water, resulting in the formation of a thin crust. This crust limits water diffusion to the surface, reducing the evaporation rate and causing an increase in the temperature of the dried particle. The dry particles are separated from the outlet drying gas in a cyclone (Figure 2A) (Woo & Bhandari, 2013). Contrarily to other drying processes (e.g., freeze-drying), spray-drying is normally operated in continuous mode at industrial scale, resulting in high encapsulation efficiency (EE) and minimal degradation of thermolabile

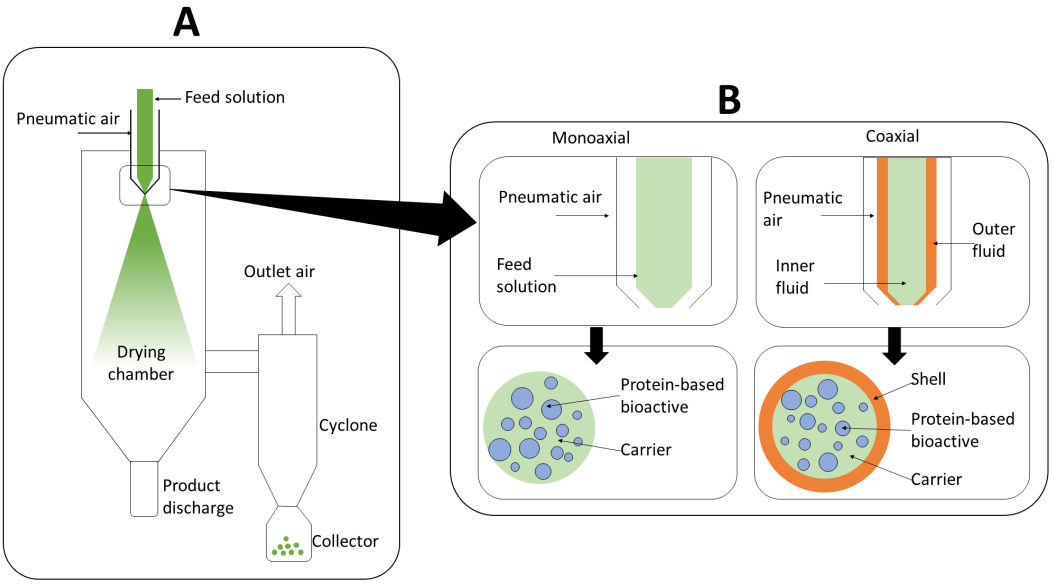

Figure 2. (A) Scheme of spray-drying process. (B) Nozzle configuration and cross section of the microcapsules obtained for monoaxial and coaxial spray-drying for the encapsulation of protein-based bioactives.

bioactive ingredients (Pinto et al., 2021; Sosnik & Seremeta, 2015). During spray-drying, multiple parameters must be optimized to achieve high encapsulation efficiency and reduced heat damage. The parameters to be taken into account are based on the formulation of the solution/dispersion/emulsions, i.e., the carrier type, the ratio between the mass of peptide and that of the carrier (core:wall), and the pretreatments needed, such as the formation of nanoliposomes or nanoemulsions (Akbarbaglu et al., 2021; Y. Wang & Selomulya, 2020). Moreover, drying kinetics are governed by heat and mass transport. Processing variables of the drying process influencing these transport mechanisms are temperature and humidity of the inlet gas, feed flow rate or flow rate of the drying gas (Piñón-Balderrama et al., 2020; Woo & Bhandari, 2013):

- Inlet gas temperature is a key parameter that provides the driving force for the solvent evaporation. The temperature should be set at a level that is sufficiently high to promote water evaporation and ensure complete drying, without leading to agglomeration or deposition of wet particles on the chamber wall. Additionally, an increase in the temperature of the inlet air leads to a decrease in its relative humidity, which promotes water transport. However, excessively high inlet temperatures can lead to prompt crust formation, which limits water diffusion and subsequent evaporation. Therefore, careful control of the temperature of the inlet gas is necessary to ensure effective microencapsulation (Schwarz & Amft, 2021).

- Feed flow rate determines the size of the atomized droplets as well as the amount of water to be evaporated, which influences the temperature of the outlet gas and of the resulting particles.
- Drying-gas flow rate determines the amount of water evaporated and the residence time of the particles in the drying chamber. Too low a flow rate results in higher water condensation, as well as agglomeration or deposition of particles in the drying chamber. On the other hand, too high a flow rate could lead to degradation of the particles by shear stress.

The type of nozzle employed for atomization allows us to process: (1) only one liquid solution in a two-fluid nozzle, known as monoaxial spray-drying, or (2) two concentric liquid solutions in a three-fluid nozzle, known as coaxial spray-drying (Fig. 2B). The type of process carried out (e.g., mono- or coaxial) affects the distribution of the bioactive compound within the matrix of encapsulating agent(s) (Figure 2B). For instance, in monoaxial spray-drying, the bioactive is dispersed within the carrier matrix. On the contrary, the encapsulation by coaxial spray-drying forms two layers of encapsulating agent(s), making it possible to disperse the bioactive within the core matrix of the carrier and forming an additional layer of encapsulating agent (Figure 2B). Nevertheless, it should be noted that both monoaxial and coaxial spray drying have some disadvantages, such as the wide size range (5–100 μm) and particle size distribution of the obtained powder. The latter might lead to capsules with different performance in terms of protection and delivery of the bioactive ingredient (Rahmani-Manglano et al., 2023; Woo & Bhandari, 2013).

3.2. Encapsulation by Monoaxial Spray-Drying

3.2.1. Formulation of the Feed Stream

Different methods are currently available to formulate the feed stream containing both the bioactive and the encapsulating agent. Blending is commonly reported in the literature, with 20 of the 29 papers found (69%) using it (Table 1). This method consists in mixing/dispersing the bioactive protein or peptide with the selected carrier, typically protein- or polysaccharide-based, in a selected solvent.

The use of proteins as carriers is widely used for the encapsulation of other bioactive compounds such as fatty acids or vitamins (Locali Pereira et al., 2019; Moeller et al., 2018; Talón et al., 2019; Yan et al., 2021), due to their functional properties, such as emulsifying, water holding, gelling, and film-forming capacities (Akbarbaglu et al., 2021). However, their use for the encapsulation of protein-based bioactives is still very limited, being reported in only two of the articles found in the literature (Table 1). This is mainly explained by the fact that the use of a carrier with a biochemical composition considerably similar to the bioactive compound to be encapsulated can lead to limitations in stability or expected bioactivity (Molina Ortiz

et al., 2009). Among the few studies using proteins as carrier, Wang et al. (H. Wang et al., 2020) used soy protein isolate and maltodextrin (MD) (1:1) for the encapsulation of antioxidant soy protein hydrolysates at two different core:wall ratios (1.2:1 and 0.8:1). Similarly, Wang et al. used rapeseed protein isolates modified by acylation and high pressure for the encapsulation of rapeseed peptides (Z. Wang et al., 2015b, 2015a). These studies reported particle sizes and encapsulation efficiencies consistent with those achieved using different carriers (Table 1).

Polysaccharides are the most used carriers for encapsulation of protein-based bioactives by spray-drying using a blend feed (Table 1). These biopolymers are abundant and inexpensive, as well as chemically stable (K. Wang et al., 2020). Maltodextrin (MD), a derivative from starch with a dextrose equivalent ranging from 3 to 20, is commonly cited in the literature for the encapsulation of both protein hydrolysates and peptides. MD shows good water solubility, high glass transition temperature and no flavor or odor (Largo Avila et al., 2015). Salleh et al. (2022) studied the use of MD for the encapsulation of edible bird's nest hydrolysates, as well as its combined use with other polysaccharide-based carriers such as carboxymethyl cellulose (CMC) and xanthan gum (XG), demonstrating that the encapsulates produced with MD-XG combination exhibited the best characteristics, with lower water activity, high solubility, and highest retention of the bioactivity.

Another polysaccharide-based carrier found in the literature is chitosan (CS) (Table 1). CS is characterized by being nontoxic, biocompatible, and biodegradable (K. Wang et al., 2020), which makes it very interesting as biomaterials for protein encapsulation. In addition, its mucoadhesive and intestinal epithelium-penetrating properties make it an ideal carrier for the oral delivery of proteins (K. Wang et al., 2020). Despite these advantages, its use is notably limited. Aquino et al. (2020) combined CS and mannitol for the oral delivery of *spirulina* bioactive peptide extracts. Gómez-Mascaraque et al. (2016) compared the effect of encapsulating whey protein hydrolysate with both gelatin and CS, determining that CS was more effective at stabilizing the peptide while not affecting the profile of the peptides after digestion.

An alternative approach for the generation of the feed solution involves the development of nanoliposomes. Nanoliposomes are lipid-based systems composed of a single or multiple concentric bilayers made of phospholipids constituting a vesicle, which allows the storage of the bioactive peptides both in the aqueous core or in the interior of the bilayer (Zarrabi et al., 2020). Sarabandi et al. (2019) studied the encapsulation of flaxseed protein hydrolysates dissolved in a phosphate-buffered solution (PBS) via nanoliposome formation using cholesterol, as well as lecithin and Tween 80 as surfactants. A MD solution was added to the nanoliposomes in a 1:1 (*v*/*v*) ratio before spray-drying. The effect of CS coating of the flaxseed protein hydrolysate–MD nanoliposomes was further studied, showing

improvement in the physical properties of the particles (e.g., smaller particles after reconstitution, improved solubility, higher encapsulation efficiency) (Sarabandi & Jafari, 2020a). Other works studied the effect of adding a CS coating to encapsulated *spirulina platensis* nanoliposomes, finding that it effectively improved the physical stability of the vesicles during storage by reducing particle aggregation. (Mohammadi et al., 2021) Similarly to nanoliposomes, nanoemulsions also use lipidic carriers. Oil-in-water nanoemulsions are colloidal systems with a hydrophobic liquid core composed of the oily/organic phase dispersed in the aqueous phase (El-Messery et al., 2020). De Figueiredo Furtado et al. (2021) produced single emulsions dispersing whey protein isolate and a mix of MD and lactose in an aqueous phase, while the oily phase was composed of a blend of high oleic sunflower oil, coconut oil and caprylic/capric triglyceride. They concluded that using oil blends with medium-chain triacylglycerols favors the formation of smaller spray-dried particles. Thus, the use of CS coating and medium-chain triglycerides can improve the physical properties of the particles. Zhu et al. (2015) obtained emulsified droplets loaded with exenatide, which is a synthetic incretin used in the treatment of diabetes mellitus type 2. In this case, the protein-based bioactive was dispersed in the aqueous phase and poly(lactic-co-glycolic acid) (PLGA) in the organic phase composed of dichloromethane (DCM) and dimethyl carbonate (DMC) (1:1), resulting in particles with higher release and degradation compared to an alternative encapsulation method, such as ultrafine particle processing, which is based on disk rotation principles.

Double-emulsion systems have also been developed for the encapsulation of protein-based bioactives by monoaxial spray-drying. Ying et al. (2021) produced a double emulsion ($W_1/O/W_2$) of soy peptides using different emulsifiers (i.e., polyglycerol polyricinoleate, lecithin and Span 60). To this end, a primary (W_1/O) emulsion was obtained combining the soy peptides and different emulsifiers in the aqueous phase, whereas medium-chain triglycerides composed the oily phase. This primary emulsion was mixed with the W_2 phase, which contained OSA modified starch and MD. The final double emulsion was spray-dried to produce peptide-loaded microcapsules; however, the authors reported that during drying, the double emulsion was ruptured, resulting in low encapsulation efficiency. Calderón-Oliver et al. (2017) compared the use of blend and emulsion methods for the encapsulation of nisin, an antimicrobial peptide, using either pectin or alginate as carrier. They produced a double $W_1/O/W_2$ emulsion by combining the aqueous phase (nisin and avocado peel extract as an antioxidant) and the oily phase (soybean oil with monoglycerides as emulsifier) to produce the primary emulsion (W_1/O). The final $W_1/O/W_2$ was obtained by mixing the primary emulsion with a collagen solution and the carrier (pectin or alginate) solution. This emulsion method resulted in improved encapsulation efficiency.

In summary, when it comes to selecting the optimal formulation method for the encapsulation of bioactive peptides by spray-drying, it is important to consider the advantages and disadvantages of each approach. While feeds obtained by blending the peptides and carriers are simply prepared, leading to high encapsulation efficiency (Table 1), preparation of emulsion-based feeds can lead to degradation of the peptides due to their exposure to oil–water interfaces and the mechanical stress to which they are subjected during the emulsification process (Aquino et al., 2020). Moreover, the production of nanoliposomes has the disadvantage that the particles can suffer lipid oxidation during production and storage, limiting their shelf life (Mohan et al., 2015). Therefore, careful consideration should be given to the specific properties of the bioactive peptides and the intended application of the encapsulated product when selecting a formulation method.

In addition to the method of preparation of the feed solution and the type of carrier used, there are other characteristics of the solution that affect the encapsulation process, as well as the morphology and release of the capsules produced. The peptide:carrier or core:wall ratios greatly affect the encapsulation efficiency, which decreases when increasing the load of peptide (Mohan et al., 2015). Akbarbaglu et al. (2019) studied the effect that core:wall ratios of 1:1, 1:2 and 1:3 (w/w) had on the encapsulation of flaxseed protein hydrolysates using MD as carrier. They found that increasing the concentration of carrier resulted in a higher production yield while the moisture content and water activity decreased. Likewise, Palamutoğlu & Sariçoban (2019) encapsulated fish collagen hydrolysates with MD at 1:4 and 1:9 (w/w) core:wall ratios and found that moisture content and water activity decreased with increasing concentration of MD. Similar results were also obtained by encapsulation of rapeseed peptides using rapeseed protein isolates as wall materials at different core:wall ratios (1:1, 1:2 and 2:1 *w*/*w*), and the production yield increased when more carrier was used (Z. Wang et al., 2015b). Taken together, the core:wall ratio is an important factor that affects the encapsulation efficiency of bioactive peptides. Increasing the concentration of carrier can improve the production yield while reducing the moisture content and water activity of the encapsulates, leading to better entrapment of the bioactive peptides.

Table 1. Studies on the encapsulation of protein-based bioactives by monoaxial spray-drying

	Formulation					Process variables						Capsule characteristics		
	Hydrolysate/ peptide	Bioactivity	Carrier	Solvent	Peptide : Carrier ratio (w/w)	Method	T inlet (°C)	T outlet (°C)	Drying air flow-rate (L/h)	Feed flow-rate (mL/h)	Nozzle diam. (µm)	Size (µm)	EE (%)	Reference
Hydrolysate	Buffalo whey proteins hydrolysate	–	GA + MD	Water	1:10 1:15	Blend	105	90	9000	160	700	2.0 and 20.0	> 95%	(Giroldi et al., 2022)
	Collagen hydrolysate	Organ formation	GA + MD	Water	1:4	Blend	150 – 170	50 – 60	–	–	–	0.4 – 50	86±7 – 85±4 %	(Peres et al., 2012)
	Edible Bird's Nest hydrolysate	AOX	MD MD + CMC MD + XG	Water	1:3.33	Blend	180 ± 2	90 ± 2	–	600	700	–	85.97(MD) 81.15 (MD + CMC) 86.58 (MD+XG)	(Salleh et al., 2022)
	Fish collagen hydrolysate	AOX	MD	Water	1:9 1:4	Blend	140 ± 1	80 ± 0.5	–	–	700	< 425 µm	–	(Palamutoğlu & Sarıçoban, 2019)
	Fish Protein Hydrolysates	AOX	MD	Imidazole-acetate buffer	1:200	Blend	180	90	–	500	500	61.5 ± 1.7 – 183 ± 2.8	–	(Camargo et al., 2021)
	Flaxseed peptide fractions	AOX	MD	Water	1:3	Blend	110 ± 1	60 ± 2	540	300	500	9 – 11	–	(Sarabandi & Jafari, 2020b)
	Flaxseed protein hydrolysate	AOX	MD	Water	1:1, 2:1 3:1	Blend	130 ± 1	75 ± 2	–	300	700	~ 5	–	(Akbarbaglu et al., 2019)
	Flaxseed protein hydrolysate	AOX	MD	Water	1:1	NL	130 ± 1	75 ± 2	–	300	500	0.326 – 0.353	72.12 – 84.99	(Sarabandi, Jafari, et al., 2019)
	Flaxseed protein hydrolysates	AOX	MD	Water	1:1 (v/v)	NL	130 ± 1	73 ± 2	540	300	500	0.132 ± 0.015 – 0.86 ± 0.012	84.0 ± 1.9 – 90.7 ± 1.6	(Sarabandi & Jafari, 2020a)

(Continued) **Table 1**. Studies on the encapsulation of protein-based bioactives by monoaxial spray-drying

Formulation				Process variables							Capsule characteristics		
Hydrolysate/ peptide	Bioactivity	Carrier	Solvent	Peptide : Carrier ratio (w/w)	Method	T inlet (°C)	T outlet (°C)	Drying air flow-rate (L/h)	Feed flow-rate (mL/h)	Nozzle diam. (µm)	Size (µm)	EE (%)	Reference
Mushroom protein hydrolysate	Food flavouring	GA	Water	1:2	Blend	150	95	–	300 g/h	500	–	–	(Lotfy et al., 2015)
Oyster protein hydrolysate	AOX	MD	Water	1:1	NL	170	–	–	300	–	0.392 – 0.719	71.43 – 82.36	(Ma et al., 2022)
P. lunatus hydrolysate	Antidiabetic	MD + GA	Water	1:25 1:10	Blend	160 ± 4	88 ± 2	33.6	1380	–	3.3 – 6.8	59.9 – 82.0	(Cian et al., 2019)
Red tilapia viscera hydrolysate	AOX and anti-hypertensive	Soy-rapeseed lecithin	Phosphate buffer	1:5	NL	130	62	–	630.5	700	0.25 – 0.31	80 – 81	(Sepúlveda et al., 2021)
Watermelon seed hydrolyzed protein	AOX	MD + sucrose	Water	–	Blend	150 – 180	80	–	200	–	10 – 12.9	–	(Cao et al., 2020)
Soy protein hydrolysates	AOX	Soy protein isolate + MD	Water	1:1.2 1:0.8	Blend	180	80 – 90	–	900	700	–	–	(H. Wang et al., 2020)
Spirulina platensis hydrolysate	Hepatoprotective, anti-inflammatory, IMi, AOX, and anticancer	Mannitol + CS	Water (mannitol) and acidified water (CS)	1:10 (w/w)	Blend	120	70	500 600	300	500	14.24 ± 2.66	~ 100	(Aquino et al., 2020)
Spirulina platensis hydrolysate	AOX	MD + CS	Water and acetic acid	60:40	NL	130	75	–	–	–	1-3	88.0 – 89.0	(Mohammadi et al., 2021)
Stripped Weakfish (*Cynoscion guatucupa*) hydrolysate	AOX and ACE inhibitor	MD	Water	60:40	Blend	130	70 ± 2	–	–	–	–	–	(Lima et al., 2021)

(Continued) **Table 1**. Studies on the encapsulation of protein-based bioactives by monoaxial spray-drying

	Formulation				Process variables							Capsule characteristics		
	Hydrolysate/ peptide	**Bioactivity**	**Carrier**	**Solvent**	**Peptide : Carrier ratio (w/w)**	**Method**	**T inlet (°C)**	**T outlet (°C)**	**Drying air flow-rate (L/h)**	**Feed flow-rate (mL/h)**	**Nozzle diam. (µm)**	**Size (µm)**	**EE (%)**	**Reference**
	Whey protein hydrolysate	–	CS gelatin	Acetic acid 20%	3:1 (gelatin) 15:1 (CS)	Blend	90	50 ± 5	9000	–	–	0.6 ± 0.6 (G) 0.6 ± 0.4 (C)	–	(Gómez-Mascaraque et al., 2016)
	Whey protein hydrolysate	Physiological functionality	MD MD + β-CD	Water	30 : 70	Blend	200	90 ± 5	-	1000	–	2.5– 3.3	–	(Yang et al., 2012)
	Whey protein hydrolysate	Infant formulas	MD	HOSO (O) Water (W)	1:2 1:4	O/W emulsion	170	95 ± 3	38000	360	700	10	84.8–97.2	(de Figueiredo Furtado et al., 2021)
	Pink perch meat protein hydrolysate	AOX	None MD + GA	Water		Blend	160	80	–	900-1200	500	4.0 – 17.3 (no carrier) 5.1 – 15.0 (with carrier)	–	(Murthy et al., 2017)
Peptide	Brewers' spent grain digested peptides	ACE-I inhibitor	LBG + MD LBG, PG + MD PG + MD	Water	1:6	Blend	180 ± 2	96 ± 8	357	180	700	5 – 7	> 90%	(Cian et al., 2020)
	Exenatide	Antidiabetic	Mannitol + PLGA	DCM and DMC (O) and water (W)	20:1 (v/v)	W/O emulsion	60	–	–	180	–	4.8±1.8	84.65±2.93	(Zhu et al., 2015)
	Glutathione	AOX	CS β-CD	Water (β-CD) Acetic acid + water (CS)	1:3.5 (β-CD) 1:2.5 (CS)	Blend	200 (β-C) 130 (C)	72 (β-C) 47 (C)	–	600	–	β-CD< CS	62.4(β-CD) 25(CS)	(Webber et al., 2018)
	Nisin	Antimicrobial	Pectin Alginate	Water (Blend) / Soybean oil (O) + water (W_1, W_2)	1:2.5 (pectin) 1:125 (alginate)	Blend / $W_1/O/W_2$ Emulsion	140 ± 5	70 ± 5	–	900	700	17.9-18.7 (B) 44.9-66.6 (E)	63.7 – 69.9(B) 72.80– 84.7(E)	(Calderón-Oliver et al., 2017)

(Continued) **Table 1**. Studies on the encapsulation of protein-based bioactives by monoaxial spray-drying

	Formulation					Process variables						Capsule characteristics		
	Hydrolysate/ peptide	Bioactivity	Carrier	Solvent	Peptide : Carrier ratio (w/w)	Method	T inlet (°C)	T outlet (°C)	Drying air flow-rate (L/h)	Feed flow-rate (mL/h)	Nozzle diam. (µm)	Size (µm)	EE (%)	Reference
	Rapeseed peptides	Dietary protein source	Rapeseed protein isolates	Water	1:2	Blend	135 ± 2	74 ± 2	450	350	–	6.2±0.1 – 8.5±0.2	87.1±1.2 – 94.7±1.8	(Z. Wang et al., 2015a)
	Rapeseed peptides	Dietary protein source	Rapeseed protein isolate	Water	1:1, 1:2 y 2:1	Blend	135 ± 2	74 ± 2	450	350	–	5.8±0.0 – 16.3±0.1	60±0.9 – 72±1.1	(Z. Wang et al., 2015b)
	Soy peptides	Anti-hypertensive	Modified starch + MD (W_2)	MCT oil (O) + water (W_1, W_2)	1:1 (w/w)	W/O/W emulsion	150	–	–	900 – 1200	–	1.4±0.0 – 8.4±0.2	29.51±0.89 – 45.83±0.47	(Ying et al., 2021)
Protein	Ovalbumin (OVA)	Vaccine antigen	Dextran sulphate, mannitol and P_LARG	Water	1:9	Blend	120	–	–	60 – 600	700	1 – 10	99 –110	(De Koker et al., 2014)
	Capreomycin oleate	Anti tuberculosis	Hyaluronic acid + DPPC	Water (DPPC) Ethanol (Hyaluronic acid)	75:25 (v/v)	Blend	110	60 – 65	500	1020	700	2.06 – 9.14	56	(Cambronero-Rojas et al., 2015)

T inlet (°C) : inlet temperature of the drying air in °C; T outlet (°C): outlet temperature of the drying air in °C; EE (%): Encapsulation efficiency in %; O/W: oil-in-water; W/O: water-in-oil; GA: gum Arabic; MD: Maltodextrin; CMC: carboxymethyl cellulose; XG: Xanthan gum; CS: Chitosan; HOSO: High oleic sunflower oil; LBG: Locust bean gum; PG: P. columbina phycocolloids; PLGA: poly(lactic-co-glycolic acid; PLARG: poly-l-arginine; DPPC: 1,2-dipalmitoyl-sn-glycero-3-phosphocholine; IMi: Immunomodulatory, AOX: antioxidant; CD: cyclodextrin.

3.2.2. Processing Conditions

Apart from the formulation of the feed stream, the processing conditions also influence the properties of the encapsulates obtained. The inlet temperature of the drying gas is a key variable determining the drying kinetics. The works reported in the literature on the encapsulation of protein-based bioactives use temperature values in the range of 60–200 °C (Table 1). The lowest inlet temperature was employed by Zhu et al. (2015), who carried out the encapsulation of exenatide by spray-drying using inlet air at 60 °C. This low temperature, out of the norm for spray drying, was due to the use of organic solvents (DMC and DCM) instead of water, as these evaporate at lower temperatures. The highest inlet temperature was 200 °C, which was used for the encapsulation of whey protein hydrolysate (Yang et al., 2012) and glutathione (Webber et al., 2018)] employing β-cyclodextrin (β-CD) or CS as encapsulating agents (Table 1). Yang et al. (2012) reported outlet temperatures of 90 ± 5 °C, while Webber et al. (2018) reported 72 °C. This difference could be due to the joint effect of other parameters such as feed flow rate, drying air flow rate and solid concentration of the feed solution. Cao et al. (2020) studied the effect of inlet temperature on the encapsulation of watermelon seed hydrolyzed protein with MD. They compared inlet temperatures of 150, 160, 170, and 180 °C, finding that increasing temperature led to lower moisture content and solubility of the capsules. Likewise, particle size slightly increased with increasing temperature, varying from an average particle diameter of 10 μm at 150–160 °C to 12.9 μm at 170 °C. These results agree with a previous study on the encapsulation of whey protein concentrates, reporting larger particles with increasing inlet temperature (Park et al., 2014). This was attributed to elevated inlet temperatures increasing the moisture removal rate, forming a crust more quickly and limiting the shrinking time of the particle. Thus, the inlet temperature must be selected based on the nature of the solvent and the bioactive to be encapsulated, as well as other parameters like feed flow rate, drying air flow rate, and solid concentration of the feed solution. While high inlet temperatures increase the moisture removal rate, which can lead rapid crust formation and then larger particles, it also increases the risk of thermal degradation of bioactives. Therefore, it seems reasonable to use inlet temperatures between 130 and 190 °C and to avoid outlet temperatures above 100 °C to obtain encapsulates with minimal thermal degradation.

Feed flow rates reported in the literature range from 160 to 1380 mL/h (Table 1). This variable affects the size of the atomized droplets and consequently the size of the dried particle (Chegini & Ghobadian, 2005). The lowest feed flow rate (160 mL/h) value was applied to encapsulate buffalo whey protein hydrolysates, with gum arabic (GA) and MD as encapsulating agents, obtaining particles of average diameter between 2 and 20 μm when using a two-fluid nozzle with 700 μm inner diameter (Giroldi et al., 2022). The highest feed flow rate was 1380 mL/h and was used for the encapsulation of *P. lunatus* hydrolysates with

GA and MD, forming particles with diameter of 3.3–6.8 μm when using a two-fluid nozzle for atomization with diameter of 500 μm (Cian et al., 2019). Although it is accepted that a higher feed flow rate results in larger particles due to collision and subsequent fusion of small drops (W. Wang et al., 2015), the combined effect of the other processing variables could justify that the particles obtained in the latter study being smaller. Although high feed flow rates are desired for higher production rates, they can also result in condensation on the walls or wet particles in the chamber or cyclone due to higher humidity increasing stickiness and agglomeration, leading to a decrease in particle recovery attributed to wall deposition (de Koker et al., 2014). Thus, ratios of 300–500 mL/h are the most preferred. Curiously, there was a wide difference between the pneumatic air pressures used (40 and 1 bar), which has been proven to affect the particle size during the atomization process (W. Wang et al., 2015).

Regarding the correlation between the nozzle diameter and the morphology of the particles obtained, Keogh et al. (2004) studied the effect of the nozzle diameter in the processing of milk powders and observed that the particle diameter of the spray-dried powders increased when increasing the nozzle diameter. However, the literature in this regard is very limited. Only two nozzle sizes were used in the literature found (500 and 700 μm), making it not possible to establish a correlation between these values and the particle size results.

It is noteworthy that both the solubility and shelf stability of the powdered product is affected by the physicochemical properties of the encapsulates, such as morphology, particle size distribution, moisture content, or encapsulation efficiency. Smallness (under 5 μm) and a tight distribution of particles is desired to improve shelf stability (Piñón-Balderrama et al., 2020). Regarding the morphology of the particles, it was found that the size of the encapsulates produced by monoaxial spray-drying ranged from 0.132 μm (Sarabandi & Jafari, 2020a) to 183 μm (Camargo et al., 2021), with 21 of 24 articles reporting diameter values from 0.25 to 50 μm. These results are consistent with previous studies reporting typical dry particle diameter in laboratory scale spray-dryers of 0.5 to 50 μm (Vehring, 2008). It is also worth highlighting that four out of the five studies reporting average size below 1 μm were obtained via formation of nanoliposomes and similar conditions were used for three of the works found, with inlet air temperature of 130–170 °C and feed flow rate of 300 mL/h (Ma et al., 2022; Sarabandi, Jafari, et al., 2019; Sarabandi & Jafari, 2020a).

Encapsulation efficiency (EE) is one of the main parameters determining shelf-life stability. EE can be defined as the percentage of bioactive compound, whether peptide, hydrolysate, or protein, that is trapped inside the carrier matrix with respect to the amount initially added. Lower EE values lead to more exposed bioactive on the surface of the capsules, which is more easily degraded, resulting in reduced bioactivity (Mohan et al., 2015). All studies reported in the literature on the encapsulation of protein-based bioactives by monoaxial spray-drying obtained EE values over 50%, except for Ying et al. (2021),

who reported EE values in the range 29.51–45.83% for the encapsulation of soy peptides via $W_1/O/W_2$ due to the emulsion not being physically stable (Table 1). The highest EE (~100%) was reached by Koker et al. (2014), where ovalbumin was encapsulated using dextran sulfate and poly-l-arginine as carrier for the elaboration of vaccine antigens. EE of peptide-loaded encapsulates can be improved by the addition of surfactants. For instance, Tween 80 was used to reduce flaxseed peptide migration to the air–water interface in spray-drying when using MD as carrier (Sarabandi & Jafari, 2020b). The authors reported reduced degradation by shear stress and dehydration, leading as well to higher bioactivity (i.e., antioxidant activity), indicating that the addition of surfactants should be considered in the future to improve encapsulation of peptides by spray-drying.

Altogether, processing conditions play a significant role in determining the properties of the encapsulates obtained. The inlet temperature of the drying gas is a crucial variable that affects drying kinetics, particle size, and morphology. Inlet temperatures between 130 and 190 °C are found to obtain desirable encapsulates with minimal thermal degradation. Feed flow rate also affects the size of the atomized droplets, and consequently the size of the dried particles. It was observed that particle size under 5 μm and a narrow distribution of particles improve shelf stability of the encapsulates. Finally, feed flow rate ratios of 300–500 mL/h are preferred to avoid the formation of wet particles or wall deposition in lab spray-dryers.

3.3. Encapsulation by Coaxial Spray-Drying

Lately, several works have been reported on the coaxial encapsulation of food bioactives by spray-drying using a three-fluid nozzle. This configuration (Figure 2B) allows feeding two different solutions through two concentric channels in the nozzle while the pneumatic air responsible for the atomization flows in the external channel (Sunderland et al., 2015). In this way, the bioactive compound dissolved in a solution of carrier (core solution) can be pumped through the inner channel, and a solution containing the same or a different carrier (shell solution) is pumped through the outer channel. Both the shell and core solutions meet concentrically at the tip of the nozzle being atomized and dried in the chamber to form microcapsules with a core–shell structure. Therefore, this method might offer greater protection and better control for the release of the bioactive compound when compared to the monoaxial process (two-fluid nozzle) (Lee, 2022.).

Despite the advantages of this method and its widespread use in the encapsulation of bioactive compounds such as carotenoids, triglycerides or organosulfur compounds (Pérez-Masiá et al., 2015; Shi & Lee, 2020; Tavares & Zapata Noreña, 2019) the literature on the encapsulation of bioactive protein hydrolysates and peptides by coaxial spray-drying is very limited. To the authors' knowledge, only one paper has been published regarding the production of protein-loaded microparticles via spray-drying using a three-fluid nozzle (Wan et al., 2014b). In this work, the authors encapsulated lysozymes employing an aqueous

solution of trehalose as core solution and a shell solution consisting in PLGA dissolved in a mixture of solvents (acetonitrile, DCM, and acetone). The effect of the core:shell flow rate ratio (4:1 or 10:1) was studied. The operating conditions selected were (i) inlet temperature = 60 °C, (ii) outlet temperature = 40–45 °C, and (iii) drying air flow rate = 37500 L/h. The study concluded that solvent selection did not affect particle size, while it did affect EE. On the other hand, the feed flow rate ratio did affect the particle size, which ranged from 1.07 to 1.60 μm. Hence, the coaxial encapsulation by spray-drying of bioactive protein hydrolysates and peptides deserves further research.

4. Encapsulation of Protein-Based Bioactives by Electrospraying

4.1. Fundamentals of Electrospraying

Electrospraying or electrohydrodynamic atomization is a drying and encapsulation technique based on the application of an electric field to a solution to obtain dried nano/microstructures at room temperature (Ghorani & Tucker, 2015). Electrospraying consists of pumping a solution, dispersion, or emulsion that contains the protein-based bioactive through a capillary injector/needle of a conductive material (Lim et al., 2019). A grounded collector is placed opposite the needle at a given distance, and an electric field is applied between the injector and the collector. The solution is pumped through the needle at a regulated flow rate, and if no voltage is applied, as the drop of solution emerges from the needle a meniscus is formed. When the electrostatic field is sufficiently high, the air–liquid interface of the meniscus is polarized, causing it to deform into a conical shape, known as a Taylor cone (Ghorani & Tucker, 2015). As the voltage continues to increase, it reaches a point at which the surface tension is no longer able to hold the liquid in the droplet, resulting in the emission of a jet from the tip of the cone directed towards the collector. The jet breaks into a spray of charged particles due to the low viscoelasticity of the solution and the electrostatic repulsion forces that take place. In the travel of the droplets towards the collector, the solvent(s) used is evaporated and dry nano/microparticles are obtained (Figure 3) (García-Moreno et al., 2018).

Depending on the properties of the solution and the processing parameters used, two different methodologies can be applied, mainly (i) electrospraying, where the intermolecular cohesion of the fluid is low enough that the electrostatic forces break the jet emitted from the solution into small droplets that result in the formation of nano/microparticles after solvent evaporation, or (ii) electrospinning, where the high molecular cohesion avoids jet fragmentation, and after the evaporation of the solvent, it gives rise to the formation of ultrafine fibres (Lim et al., 2019). Electrospraying is the preferred process for obtaining food ingredients, since electrospun fibers, contrarily to nano/microcapsules, result in continuous mats that are difficult to disperse in any food matrix without prior breakage (Jacobsen et al., 2018).

Electrospraying, as spray-drying, also allows working in both mono- and coaxial configurations. Monoaxial electrospraying typically results in the formation of amorphous solid dispersions containing the protein-based bioactives dispersed within the carrier matrix (Figure 3). Alternatively, coaxial electrospraying is a customized version of electrospraying, in which two different liquids are separately delivered through individual coaxial capillary needles (Figure 4). The solution containing the bioactive compound and potentially the encapsulating agent is pumped through the inner needle (core), while a second solution containing the same or a different encapsulating agent is delivered through an outer concentrical needle (shell) (Loscertales et al., 2002). Therefore, a concentric Taylor cone of both solutions is formed at the tip of the needles, and when the solution and processing parameters are appropriately selected, it results in the formation of nano/microcapsules with a core–shell structure (García-Moreno et al., 2021a; López-Herrera et al., 2003) (Figure 4). Coaxial electrospraying combines the advantages of monoaxial electrospraying, adding the ability to precisely control the core–shell shape, as well as better protecting the bioactive peptides from process-induced denaturation and aggregation (Zhang et al., 2014).

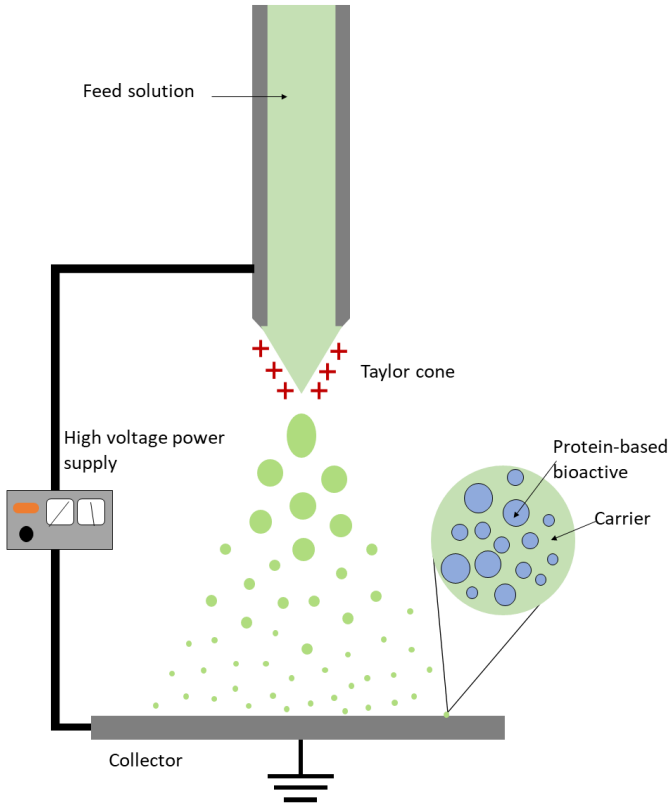

Figure 3. Scheme of monoaxial electrospraying process and theoretical cross section of the nano/microcapsules obtained.

Electrospraying parameters such as solution properties, processing variables and environmental conditions can affect the morphology, particle size and EE (Tapia-Hernández et al., 2017). A high concentration of encapsulating agent leading to high viscosity and density of the solution can derive in the formation of larger particles, while increasing electrical conductivity of the solution results in particles with smaller diameter. Regarding the processing variables, a high electric potential between injector and collector results in smaller particle diameter, whereas increasing solution flow rate increases particle size. Long injector–collector distances allow for better evaporation of the solvent, while short distances may result in wet and collapsed particles. Environmental conditions such as temperature and humidity also affect the drying kinetics, since they determine the driving forces for the drying process. In addition, other factors should be considered when encapsulating protein-based bioactives by electrospraying: (1) proteins lead to highly conductive solutions that prevent charge formation, which reduces the stability of the Taylor cone, and (2) the use of food-grade solvents such as water leads to solutions with high surface tension that hinder jetting (García-Moreno et al., 2021b).

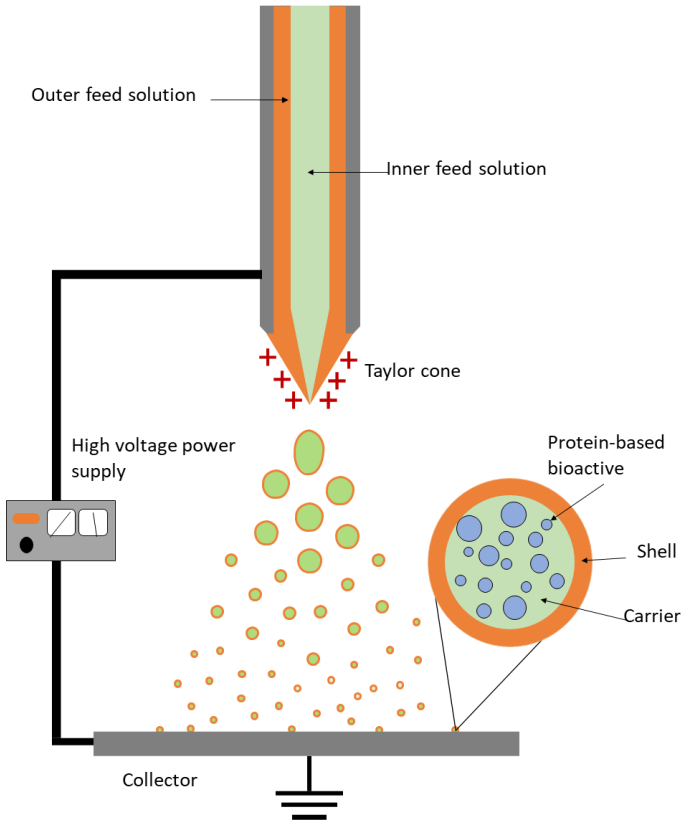

Figure 4. Scheme of coaxial electrospraying process and theoretical cross section of the nano/microcapsules obtained.

Electrospraying encapsulation has been widely used in the pharmacological field due to its low cost, easy operation and improved bioaccessibility of the nano/microcapsules obtained (Moreira et al., 2021). However, its use in food applications is still limited due to its low production capacity. To solve this limitation, several modifications have been reported, including: (i) multineedle electrospraying systems (Parhizkar et al., 2017), (ii) free surface electrospraying systems (Kang et al., 2013), or (iii) pressurized-gas-assisted electrospraying (Busolo et al., 2019). However, this absence of application to the food industry is reflected in a lack of literature on the subject. The available information is mainly oriented to oral pharmacological supplementation, and no data were found on bioactive protein hydrolysates. Thus, further research should be carried out on the application of electrospraying encapsulation in foods.

4.2. Encapsulation by Monoaxial Electrospraying

4.2.1. Formulation of the Feed Stream

The encapsulation of protein-based bioactives by monoaxial electrospraying requires the drying of only one solution containing the bioactive. The most common method to produce this feed stream is blending (e.g., dissolving the bioactive in a solution containing the carrier). Nine of the eleven works found in the literature used this approach (Table 2). Bock et al. (2014) encapsulated bovine serum albumin (BSA) by electrospraying a blend feed stream where BSA was dissolved in chloroform or DCM using poly(ethylene glycol) (PEG) and poly(ε-caprolactone)(PCL)/PLGA as carrier. Similarly, Musaei et al. (Musaei et al., 2017) prepared a blend feed stream using an ethanol–acetic acid mixture to encapsulate BSA using PLGA as encapsulating agent. Blend electrospraying has also been used to encapsulate larger molecules, such as the hormone angiotensin II using N-octyl-O-sulfate chitosan (NOSC) as a carrier (Rasekh et al., 2015), or the enzymes alkaline phosphatase with poly(ethylene oxide) (PEO) (Onyekuru et al., 2021) and streptokinase with PLGA (Yaghoobi et al., 2017).

Although electrospraying is carried out at room temperature, which avoids thermal degradation of thermosensitive ingredients, the use of specific solvents may induce protein denaturation and loss of activity when exposure is prolonged (Moreira et al., 2021). Hence, an alternative approach to a blend for producing the feed stream is to obtain emulsions that prevent contact between specific solvents and the bioactives (Moreira et al., 2021). According to previous studies, encapsulation by emulsion electrospraying allows the formation of particles with core–shell structures similar to those that could be obtained by coaxial electrospraying (Van & Lee, 2018). This process is often used to mix two immiscible fluids, typically through a single W/O or double $W_1/O/W_2$ emulsion (Moreira et al., 2021). The two articles found in the literature using emulsion electrospraying were based on the drying of water-in-water (W/W) emulsions. Yao et al. (2016) used this approach to encapsulate BSA in PLGA. For that, two immiscible solutions were prepared: the organic phase was composed

of PLGA in chloroform and the aqueous phase was composed of the BSA dissolved in water. Similarly, Y. Song et al. (2015) produced a W/W emulsion by dissolving β-amylase in the aqueous phase composed of dextran and sodium alginate, which was electrosprayed into a water solution containing CaCl2 and PEG, forming a calcium alginate shell containing the amylase core. As mentioned in Section 3.2.1., it should be noted that emulsion feed preparation is less used, as it presents difficulties in producing stable emulsions and the shear stress of mechanical mixing required for emulsion preparation could modify the protein-based bioactives (Moreira et al., 2021).

The type of carrier and solvent used determine the main properties of the feed stream influencing the electrospraying process, such as viscoelasticity, conductivity, and surface tension (García-Moreno et al., 2021b). A wide variety of natural and synthetic polymers are used as encapsulating agents in electrospraying, including biocompatible and biodegradable polymers such as gelatin, MD, pullulan, glucose syrup, dextran, hyaluronan, CS, PCL, poly lactic acid (PLA), PEG, PLGA, alginate, PEO, and NOSC, among many others. Carriers commonly used were alginate, PEO and NOSC, all of which are particularly used for the formulation of oral delivery drugs since they are all safe and present high biocompatibility. Alginate was used to encapsulate α-calcitonin gene-related peptide (α-CGRP) (Kumar et al., 2021) and BSA/porcine interleukin-1β (pIL-1β) (Ho et al., 2022), both by blend electrospraying and resulting in particles with widely differing sizes, ranging from 194.23 ± 10.08 to 20 μm, respectively. PEO is a synthetic semicrystalline polymer mostly used for electrospinning due to its rheological characteristics, and thus only one work used it for electrospraying the enzyme alkaline phosphatase (Onyekuru et al., 2021; Romano et al., 2016). Likewise, NOSC was only used for the encapsulation of the hormone angiotensin II (Rasekh et al., 2015). The most reported polymer carrier in the literature for the encapsulation of protein-based bioactives was PLGA (Table 2), a US Food and Drug Administration (FDA)-approved biocompatible copolymer that has been extensively used in biomedical devices with excellent application records in vivo (Yao et al., 2016). Interestingly, Musaei et al. (2017) found that increasing PLGA concentration did indeed affect the particle size of the capsules, increasing the size of the nanocapsules from 120 nm to 225 nm, which is related to increasing EE. Although all these biopolymers have shown good encapsulating capacity, studies have focused on drug release formulation and research on food application is very limited. Only PLGA has been studied for application in food fortification, with good results (J. Song et al., 2022). Polysaccharide and protein-based carriers are commonly employed as encapsulating agents for encapsulation of protein-based bioactives by spray-drying; however their use for the encapsulation of these bioactives by electrospraying was not reported in the literature. These kinds of carriers are especially suitable for the food industry since they are food-grade and soluble in water, which avoids the use of non-food-grade solvents (J. Song et al., 2022). Therefore, further research on the use of food-grade, low-cost biopolymers for the encapsulation of protein-based bioactives by electrospraying is required.

Table 2. Studies on the encapsulation of protein-based bioactives by monoaxial electrospraying

	Formulation						Process variables				Capsule characteristics		
	Hydrolysate/ peptide	**Bioactivity**	**Carrier**	**Solvent**	**Peptide : Carrier ratio (w/w)**	**Method**	**Voltage (kV)**	**Feed flow-rate (mL/h)**	**Distance N-C (cm)**	**Nozzle diam. (µm)**	**Size (µm)**	**EE (%)**	**Reference**
Hydrolysate	Alpha-calcitonin gene related peptide	Vasodilator	Alginate	Water	1:2 (w/v)	Blend	6	60	$7x10^{-3}$	-	194.23 ± 10.08	-	
	Peptide pp65489-503 CMV 4-peptide-mix	Immune stimulatory	PLGA	TFE DMSO	1:22 (w/w)	Blend	10	0.01	14	30	200	84-85	
	SA	-	PCL + PEG PLGA + PEG	Chloroform (PCL + PEG) DCM (PLGA + PEG)	10:90, 5:95, 15:85	Blend	10	0.5 - 3	13 or 25	450 - 800	5.6 ± 0.8 (PLGA) 12.0 ± 4.0 (PCL)	20 - 40	
	BSA	-	PLGA	Acetone (PLGA) Ethanol and acetic acid (BSA)	1:1, 1:4, 1:9	Blend	10, 15 and 20	$36x10^{-3}$ $72x10^{-3}$	10, 15 and 20	-	0.08 - 0.26	-	
	BSA	-	PLGA	Chloroform (O) and water (W)	-	W/O emulsion	6	1	20	-	9.6 ± 1.4 – 7.2 ± 2.4	92 – 80	
	BSA or pIL-1β	Vaccine adjuvant	Alginate	Water	2:1, 4:1, 6:1	Blend	12	0.1	20	511	20	50 (BSA)	
	Bone morphogenetic protein 2	Bone regeneration	PLGA BSA	DMF (PLGA) water (BSA)	1:100 (v/v)	Blend	9-12	0.5	30	900	1.0 ± 0.6	39	
	Alkaline phosphatase	Anti-inflammatory	PEO	Ethanol Water	1:7 (v/v)	Blend	9-15	0.5-1	12-22.5	610	0.73 ± 0.16	85.0 ± 4.0	

(Continued) **Table 2.** Studies on the encapsulation of protein-based bioactives by monoaxial electrospraying

Formulation					Process variables				Capsule characteristics		
Hydrolysate/ peptide	**Bioactivity**	**Carrier**	**Solvent**	**Peptide : Carrier ratio (w/w)**	**Method**	**Voltage (kV)**	**Feed flow-rate (mL/h)**	**Distance N-C (cm)**	**Nozzle diam. (µm)**	**Size (µm)**	**EE (%)**	**Reference**
Amylase	Enzyme	Dextran Sodium alginate	Water	-	Water-in-water (W/W) emulsion	2.67 – 2.85	0.5	$1x10^{-3}$	40 – 320	< 1000	47 ± 3	
Streptokinase	Thrombotic disease treatment	PLGA	Water DCM	1:100 (v/v)	Blend	13	0.1	10	180	0.037 ± 0.012	90	
Angiotensin II	Anti-hypertensive	NOSC	DMSO Water DCm	1:1 (w/w)	Blend	15-19	1.08	0.1	508	1.057 ± $4x10^{-3}$	70-90	

Distance N-C (cm): distance between the nozzle and the collerctor, in cm; EE (%):Encapsulation efficiency in %; W/O: water-in-oil; SA: Serum albumin; PCL: polycaprolactone; PEG: poly(ethylene glycol); PLGA: poly(lactic-co-glycolic acid); DCM: dichloromethane; BSA: Bovine serum albumin; DMF: N,N-dimethylformamide; PEO: poly(ethylene oxide); NOSC: N-octyl-O-sulphate chitosan; DMSO: dimethyl sulfoxide.

4.2.2. Processing Conditions

Processing variables (voltage, injector-to-collector distance and feed flow rate), together with feed solution properties, affect the characteristics of the nano/microcapsules obtained (e.g., morphology, size). The applied voltage for all the studies reported in the literature was kept between 2 and 20 kV (Table 2). The effect of voltage was assessed for the encapsulation of BSA by electrospraying using PLGA as carrier (Musaei et al., 2017). The authors compared three different voltages (10, 15 and 20 kV) and found that increasing voltage from 10 kV to 20 kV resulted in decreasing average diameter from 0.185 μm to 0.085 μm, which is desired to increase surface area and thus improve solubility and permeability. This effect was also found in electrosprayed amylase particles with PEG and dextran as carrier, where the applied voltages were adjusted from 2.6 kV to 2.85 kV to produce particles of different diameters (Y. Song et al., 2015). However, applied voltages over 20 kV were found to alter protein-based bioactives. For instance, a study on the encapsulation of angiotensin II by electrospraying using NOSC as encapsulating agent showed that its stability was significantly reduced at 20 kV. Since the electric field strength is determined by both applied voltage and distance between nozzle and collector (N-C), changes in both parameters affect the stability of the bioactive compounds during processing.

Increasing feed flow rate is desired to increase productivity; however, it is linked to higher particle diameter. Low feed flow rate results in better encapsulation as well, and thus a compromise between productivity and quality of the capsules must be reached. Onyekuru et al. (Onyekuru et al., 2021) studied the effect of feed flow rates ranging from 0.3 to 1.5 mL/h on the encapsulation of alkaline phosphatase with PEO, determining that although low flow rates produced better encapsulation, the optimum flow rate was 0.6 mL/h. Different feed flow rates were also compared for the encapsulation of serum albumin (SA) by electrospraying using PEG and PCL/PLGA as encapsulating agents (Bock et al., 2014). It was reported that increasing the feed flow rate from 0.5 mL/h to 1 mL/h resulted in average diameters increasing from 5.6 ± 0.8 μm to 7.1 ± 1.7 μm. However, higher flow rates also resulted in uneven spread of the solution at the nozzle and an uncontrolled electrospraying of large droplets. This work also utilized different nozzle diameters (450–800 μm), but no effect on particle size was reported. On the other hand, Y. Song et al. (Y. Song et al., 2015) determined that the size of the particles could be reduced by using nozzles with a smaller diameter after comparing three different diameters (40, 170 and 320 μm). The consensus seems to be working at a low feed flow rate, but process productivity must not be compromised to be cost-effective.

The studies shown in Table 2 reported EE values for the nano/microcapsules loaded with protein-based bioactives ranging from 20% to 92%. The lowest EE was obtained for encapsulation of SA using PEG and PCL/PLGA as carriers (Bock et al., 2014). Since higher

EE has been linked to larger particles and lower protein loading (Bock et al., 2012), these parameters were studied. Indeed, the authors confirmed that increased particle diameter corresponded with higher EE values, with a critical size allowing optimum encapsulation. In the same study, lower protein loading also resulted in improved EE, but the extraction method used to measure EE presented limitations due to protein aggregation and the lack of use of surfactants. The highest EE was achieved by encapsulating BSA by emulsion electrospraying using PLGA as encapsulating agent (Yao et al., 2016). This work showed that increasing the aqueous phase volume ratio (e.g., increasing bioactive load) resulted in decreased EE, varying from 92% at 5 μL/mL to 80% at 100 μL/mL. It was explained as being due to increased density of emulsion droplets in the feed solution, and thus increasing migration of the aqueous phase containing the BSA to the surface of the particle.

4.3. Encapsulation by Coaxial Electrospraying

The literature found regarding the encapsulation by coaxial electrospraying of protein-based bioactives was focused exclusively on the pharmacological/medical field. No works on the encapsulation by coaxial electrospraying of bioactive protein hydrolysates or peptides have been reported in the literature.

Only four works studying the coaxial electrospraying of proteins were found (Table 3). None of them used carrier in the formulation of the inner solution (core). For the outer solution (shell) PLGA was the most used encapsulating agent, appearing in two studies. This follows the trend established in monoaxial electrospraying, since, as previously mentioned, all the literature found was mainly focused on oral drug delivery, where PLGA was the most frequently used biopolymer. One study focused on the encapsulation of a water solution of BSA using an outer solution of PLGA dissolved in either DCM or a combination of DCM and DMF (Zamani et al., 2014). The other work encapsulated ranibizumab, a protein drug used for the treatment of age-related macular degeneration, using PLGA dissolved in a combination of DCM and acetonitrile as the outer solution (Zhang et al., 2015). Regarding the use of solvents, six of eight works used organic solvents, mainly for the outer feed. This is because the use of two immiscible solutions provides better core–shell separation by minimizing interdiffusion between layers (Han & Steckl, 2019). A solution of ethyl acetate and n-butanol, along with acetylated dextran as carrier, was used as the outer feed for the encapsulation of anthrax protective antigens dissolved in the inner water solution (Gallovic et al., 2016). Rasekh et al. (Rasekh et al., 2015) coaxially electrosprayed angiotensin II using NOSC as carrier for the inner solution and tristearin dissolved in DCM as outer solution. Since the literature found was focused on the production of oral delivered drugs, it would be necessary to take into consideration the need to apply two completely immiscible food-grade solvents to produce encapsulates oriented for food fortification.

Table 3. Studies on the encapsulation of protein-based bioactives by coaxial electrospraying

	Formulation					Process Variables				Capsule Characteristics		Ref
	Hydrolysate/ Peptide	Bioactivity	Carrier	Solvent	Peptide: Carrier ratio	Voltage (kV)	Feed Flow Rate (mL/h)	Distance N-C (cm)	Nozzle Diameter (µm)	Size (µm)	EE (%)	
Protein	BSA)	–	PLGA (outer)	Water (inner) DCM and DMF (outer)	–	9–11	0.1–0.2 (inner) 1–2 (outer)	–	300 (inner) 840 (outer)	5.4 ± 1.56– 2.90 ± 0.76	46.7 ± 4.3– 74.6 ± 2.9	(Zamani et al., 2014)
	Bovine hemoglobin	Oxygen carrier	–	Ethanol	–	20	0.08 (inner) 0.48 (outer)	10	–	0.37	–	(Liu et al., 2020)
	Anthrax protective antigen	Antibacterial	Acetylated dextran (outer)	Ethanol, ethyl acetate and n-butanol	1:1.85	10–12	0.02 (inner) 0.85 (outer)	14	210 (inner) 603 (outer)	~ 1	–	(Gallovic et al., 2016)
	Ranibizumab	Age-related macular degeneration	PLGA (outer)	Water and EG (inner) DCM and acetonitrile (outer)	1:6	5	0.5 (inner)	16.95	–	1–2	70	(Zhang et al., 2015)

Distance N-C: distance between the nozzle and the collector; EE: encapsulation efficiency; PLGA: poly(lactic-co-glycolic acid); DCM: dichloromethane; DMF: N,N-dimethyl-formamide; EG: ethylene glycol; CMC: carboxymethyl cellulose; PEGDA: poly(ethylene glycol) diacrylate; PEO: poly(ethylene oxide); PBS: phosphate-buffered saline NOSC: N-octyl-O-sulfate chitosan; MBA: maize bran arabinoxylans; MWA: maize wastewater arabinoxylans.

(Continued) **Table 3.** Studies on the encapsulation of protein-based bioactives by coaxial electrospraying

	Formulation					Process Variables				Capsule Characteristics		Ref
	Hydrolysate/ Peptide	Bioactivity	Carrier	Solvent	Peptide: Carrier ratio	Voltage (kV)	Feed Flow Rate (mL/h)	Distance N-C (cm)	Nozzle Diameter (μm)	Size (μm)	EE (%)	
Enzyme	Alkaline phosphatase	Detoxifying	CMC (inner) Alginate and PEGDA (outer)	Water	–	12.5	3.6 (inner) 18 (outer)	5	–	440	84	(Zhao et al., 2021)
	Alkaline phosphatase	Anti-inflammatory	PEO (outer)	PBS (inner) Ethanol and water (outer)	1:2	22.5	0.02 (inner) 0.3 (outer)	15–20	1000 (inner) 2000 (outer)	1.29 ± 0.24	99	(Onyekuru et al., 2021)
Hormone	Angiotensin II	Anti-hypertensive	NOSC and tristearin	Water (inner) DCM (outer)	1:1 (inner)	15–17.9	1.8 (inner) 3.96 (outer)	5–2.5	900 (inner) 1900 (outer)	0.17–0.26	92	(Rasekh et al., 2015)
	Insulin	Antidiabetic	MBA (inner) MWA (outer)	Water	4:1 (inner) 6.67:1 (outer)	16	1	5	184 (inner) 1194 (outer)	290	72	(Paz-Samaniego et al., 2018)

Distance N-C: distance between the nozzle and the collector; EE: encapsulation efficiency; PLGA: poly(lactic-co-glycolic acid); DCM: dichloromethane; DMF: N,N-dimethyl-formamide; EG: ethylene glycol; CMC: carboxymethyl cellulose; PEGDA: poly(ethylene glycol) diacrylate; PEO: poly(ethylene oxide); PBS: phosphate-buffered saline NOSC: N-octyl-O-sulfate chitosan; MBA: maize bran arabinoxylans; MWA: maize wastewater arabinoxylans.

Voltages applied ranged from 5 to 22.5 kV, similar to the values used for monoaxial electrospraying (2.67–20 kV). The effect of voltage was studied for the encapsulation of angiotensin II using tristearin and NOSC as carriers inner and outer carriers, respectively (Rasekh et al., 2015). They applied voltage values were 20 and 30 kV, and the authors compared the stability of the enzyme using an ELISA, finding that at 30 kV the concentration of angiotensin II in the microparticles was reduced by approximately 20%. For the encapsulation of alkaline phosphatase with PEO as outer carrier (Onyekuru et al., 2021), the voltage was optimized to 22.5 kV. Similarly, these authors found that this high voltage resulted in a loss of activity of the enzyme up to 40% compared to the activity obtained by monoaxial electrospraying at 15.5 kV.

Other parameters affecting particle characteristics are feed flow rates (inner and outer) and nozzle diameters. For the inner solutions (core), feed flow rates of 0.02–3.6 mL/h were used, while for the outer solutions (shell), 0.1–18 mL/h was used. Regarding the nozzle diameters, they ranged from 184 to 1000 μm for inner capillary and 603 to 2000 μm for the outer capillary. As previously mentioned in the previous section, increasing feed flow rate and nozzle diameters typically results in larger particles. This agreed with the data obtained by Zhao et al. (Zhao et al., 2021), where alkaline phosphatase was encapsulated using CMC as inner carrier and alginate and PEGDA as outer carriers. They reported the highest feed flow rates (1.8 mL/h for the core and 3.96 mL/h for the shell) in the literature and obtained the largest particles at 440 μm. However, the opposite conclusion was obtained after comparing the encapsulation of angiotensin II (using NOSC as inner carrier and tristearin outer carriers) (Rasekh et al., 2015) and the encapsulation of alkaline phosphatase with PEO as carrier (Onyekuru et al., 2021). Both studies used similar nozzle diameters (1000 μm (inner)–2000 μm (outer), and 900 μm (inner)–1900 μm (outer), respectively), but the first study used feed flow rates 10 times higher. Even though larger particles would be expected for the angiotensin II encapsulation, due to the higher flow rates, their size was up to 86% smaller. In fact, they obtained the smallest particles, which could be due to the nozzle–collector distance, the highest reported in the literature at 20 cm, and the slightly higher voltage used. Coaxial electrospraying of bovine hemoglobin also resulted in small particles of 0.37 μm, as it was particularly important to obtain nano/microcapsules in the range of 0.1 to 3 μm to effectively avoid extravasation through the blood vessel wall and act as oxygen carriers (Liu et al., 2020).

High EE values were obtained for all the studies reported in the literature (Table 3), ranging from 70% to 99%. These values are higher than the ones obtained for monoaxial electrospraying, where four of the nine reported EE values were under 50%. Zamani et al. (Zamani et al., 2014) reported ranges of EE from 46.7 ± 4.3% to 74.6 ± 2.9%, which were linked to incomplete encapsulation due to inner feed flow rates being too high as

well as high concentrations of BSA in the core. The highest EE found was obtained for the encapsulation of alkaline phosphatase with PEO as outer carrier (Onyekuru et al., 2021). They also compared the effect of monoaxial and coaxial electrospraying, confirming that the EE was increased in core–shell structures.

Although coaxial electrospraying has exhibited promising outcomes, the encapsulation of bioactive protein hydrolysates or peptides has only been minimally investigated. Thus, further studies are required to fully evaluate the feasibility of this technology for the encapsulation of bioactive peptides. Particularly, there is a need to investigate the use of food-grade solvents and to optimize processing conditions that lead to encapsulates with potential use in food fortification.

5. Activity Retention and Release of the Encapsulated Protein-Based Bioactives

Spray-drying and electrospraying techniques are viable encapsulation methods of protein-based bioactives. After encapsulation, it is fundamental that these bioactive compounds maintain their original activity. Moreover, they should remain active until reaching the target organ, where they will exert their activity (Amigo & Hernández-Ledesma, 2020). However, research studying the factors that affect the preservation of activity and release of encapsulated protein-based bioactives is scarce.

Maintaining activity after encapsulation is one of the most important challenges facing protein delivery, as this can be limited by protein aggregation or denaturation in the particles (Dai et al., 2005). Regarding the works in the literature studying the retention of activity, it is striking that 7 out of 12 deal with antioxidant activity (i.e., DPPH free radical scavenging activity, ferric reducing antioxidant power, metal-chelating activity). This trend might be due to the increasing focus on the use of natural antioxidants as both bioactives in humans and functional ingredients in food products to avoid lipid oxidation (Lorenzo et al., 2018; Ospina-Quiroga et al., 2022; Z. Wang et al., 2022). Fish collagen hydrolysates exhibiting 2,2-diphenyl-1-picrylhydrazyl (DPPH)-inhibitory activity were spray-dried using MD as carrier at different ratios. Antioxidant activity was lost when MD was used as carrier, with a decrease in activity from 78.36 ± 12.29% when free collagen was spray-dried to 33.59 ± 6.47 % when 80% of MD with 10–12 dextrose equivalent was used (Palamutoğlu & Sariçoban, 2019). Other studies spray-dried fish hydrolysates with MD and GA, reporting that the presence of carbohydrates from the carriers decreased antioxidant activity (Murthy et al., 2017). High retention of activity (>60%) was found by two studies analyzing the antioxidant activity of spray-dried flaxseed protein hydrolysates with MD by different methods (i.e., DPPH free radical scavenging, ABTS free radical scavenging, hydroxyl radical scavenging, reducing power, nitric oxide scavenging) (Akbarbaglu et al., 2019; Sarabandi & Jafari, 2020b). On the

other hand, spray-drying of oyster protein hydrolysate included in emulsions, with MD as carrier and cholesterol for the oily phase, resulted in reduced free radical scavenging activity (Ma et al., 2022). This was related to the high inlet temperature (170 °C) altering the lipid membrane and partially degrading the bioactive compound.

The activity retention capacity of different encapsulated enzymes by electrospraying was also measured. Alkaline phosphatase with PEO was encapsulated both by monoaxial and coaxial electrospraying, retaining ~100% activity when monoaxially electrosprayed. However, when coaxial electrospraying was applied, only 60% of the activity was retained, which was attributed to the high voltage (22.5 kV) applied compared with monoaxial spraying (15.5 kV) (Onyekuru et al., 2021). Amylase included in emulsions using dextran and sodium alginate as carriers was encapsulated by electrospraying; however, the high activity observed for amylase (96%) was related to a low EE, indicating that the substrate had better access to the enzyme due to the location of the enzyme at the surface of the particle (Y. Song et al., 2015).

In addition to the efficient encapsulation of protein-based bioactives, it is essential for the application of these methods that these compounds can be released from the carrier matrix while maintaining their activity. Despite the importance of studying these parameters, literature on release kinetics or tailored release approaches for the encapsulation of protein-based bioactives is limited. In general, the release of nano/microencapsulated bioactive compounds occurs in three stages: i) surface release, which may be caused by inadequate entrapment (low EE) in the carrier matrix, ii) diffusion via swelling of the carrier matrix, and iii) erosion of the carrier matrix (Unagolla & Jayasuriya, 2018). It is usually desired to avoid burst release as much as possible. For that, it is necessary to take into consideration the characteristics of the carrier, which should not totally solubilize in the release medium, not interact with protein-based bioactives, and be protective against external factors, such as acid pH during gastric digestion (Zabot et al., 2022). The most common method to measure protein release from the delivery systems found in the literature is by agitation in PBS release buffer. Bock et al. (Bock et al., 2014) studied the release during 81 days of SA electrosprayed using PEG as carrier. The initial burst release was dependent on the protein load, PEG load and PEG molecular weight (MW). Higher SA load resulted in a strong burst release, up to 60% in the first 24 h. A burst-free release of the SA with sustained release up to 84 days was achieved combining low protein loading (1%) and low MW PEG (6 kDA). These results agreed with the data obtained for the electrospraying of BSA emulsions using PLGA as the carrier (Yao et al., 2016). In order to compare the release profile obtained by coaxial electrospraying versus emulsion monoaxial electrospraying, Zamani et al. encapsulated BSA using PLGA as carrier (Zamani et al., 2014), finding that although coaxial electrospraying enhanced the EE, it also resulted in a stronger burst release (24–27%) than emulsion electrospraying (8–12%). This was due to the centralized distribution of the bioactive in the coaxially produced

encapsulates allowing fast release once the solvent reached the bioactive, contrary to the compartmentalized distribution of the bioactive in the encapsulates produced by emulsion electrospraying (Figure 4). Although this method does not take into consideration the gastrointestinal conditions to which the capsules would be subjected during digestion, it allows us to estimate the stability of the capsules.

6. Bioaccessibility of Encapsulated Protein-Based Bioactives and Enrichment of Food Matrices

Bioactive peptides and proteins must be bioaccessible for their potential use in oral delivery systems for the development of supplements and functional foods. Bioaccessibility refers to the fraction of the biocomponent that, after digestion, becomes accessible for absorption through the epithelial layer of the gastrointestinal tract (Dima et al., 2020). Bioaccesibility can be determined with good results using in vitro methods that simulate the biochemical and mechanical conditions of the gastrointestinal digestion.

The effect of gastrointestinal digestion of spray-dried nanoliposomes of red tilapia viscera hydrolysates over antioxidant and ACE-inhibitory activities were studied (Sepúlveda et al., 2021). Gastric digestion with pepsin induced degradation of the peptides, resulting in loss of antioxidant activity, while increasing ACE-inhibitory activity. For both bioactivities, the intestinal digestion resulted in enhanced inhibition, up to 10% compared to the original hydrolysates. This was attributed to the release of new oligopeptides after digestion with pancreatin, as bile salts in the intestinal phase promoted swelling and disruption of the vesicles, thus leading to leakage of bioactive peptides. Spray-dried peptides derived from spent brewer's grain were encapsulated with locust bean gum, *P. columbina* phycocolloids, or DM as carriers, and their bioaccessibility was measured by analysis of the size distribution of the peptides and the retention of their ACE-inhibitory activity (Lima et al., 2021a). They found that carrier selection affected greatly to the protection of the peptides during digestion, achieving highest protection when P. columbine phycocolloids were used as wall material. Regarding ACE-inhibitory activity, encapsulated peptides showed higher activity than free peptides after digestion, demonstrating that partial protection of bioactive peptides against digestive enzymes was possible. Similar results were obtained by spray-drying *P. lunatus* hydrolysates encapsulated by spray-drying with MD and GA as carriers (Cian et al., 2019), where the ACE-inhibitory activity, as well the DPP-IV and α-amylase activity, of free hydrolysates was severely affected by simulated gastrointestinal digestion ($IC_{50} \approx 300$ μg/mL) compared to the retained activity of encapsulated hydrolysates ($IC_{50} < 200$ μg/mL). Coaxial electrospraying of alkaline phosphatase, with CMC as core carrier and a mixture of alginate and poly(ethylene glycol) diacrylate (PEGDA) as a carrier in the shell, was able to protect the enzyme from potential degradation during simulated gastrointestinal digestion (Zhao et al., 2021).

Gómez-Mascaraque et al. (Gómez-Mascaraque et al., 2016) evaluated the changes in the profile of peptides obtained from whey protein hydrolysate, which was spray-dried using gelatin and CS as encapsulating agents, after digestion. After comparing the chromatograms of the original hydrolysate and the digested capsules, they found that simulated digestion of the free hydrolysate resulted in a "remarkable change" in the identified peptides, compromising bioaccessibility, whereas digestion of CS microcapsules retained the highest number of identified peptides. The higher digestion of the hydrolysate-loaded gelatin capsules was linked to the proteinaceous origin of the carrier, possibly also digested during the assay. Another work studied the release kinetics of bioactive compounds during and after in vitro digestion by measuring changes in absorbance of spray-dried rapeseed peptides (Z. Wang et al., 2015a). This study found that microparticles did not produce an initial burst during gastric digestion, but rather a slow release of encapsulated peptides during the intestinal stage, which would increase bioaccessibility. Paz-Samaniego et al. (Paz-Samaniego et al., 2018) performed a simulation of gastrointestinal digestion with a complex Simulator of the Human Gastrointestinal Tract (Simgi). Insulin-loaded microcapsules obtained by coaxial electrospraying with maize bran arabinoxylans (core) and maize wastewater arabinoxylans (shell) as encapsulating agents were passed through five different reactors, simulating the stomach, small intestine, and the three regions of the colon: ascending, transverse, and descending. In this way, they found that 76% of the encapsulated insulin reached the colon without being degraded in the stomach.

In addition to potential degradation during gastrointestinal digestion, protein-based biocompounds can easily react with complex food matrices, leading to alterations in their bioactivity. These matrices, such as soups or baked goods, can undergo thermal and high-pressure conditions that would make it difficult to maintain peptide stability (Udenigwe & Fogliano, 2017). Thus, encapsulation of bioactive peptides and proteins could potentially benefit their stability when incorporated into food matrices. Only three studies regarding the inclusion in food matrices of protein-based bioactives encapsulated by spray-drying or electrospraying were found in the literature. Yogurt was fortified with spray-dried weakfish hydrolysates exerting antioxidant and ACE-inhibitory activities using MD as carrier (Lima et al., 2021a). After a week of storage, not only were antioxidant and ACE-inhibitory activities maintained, but greater rheological stability was provided by the encapsulated hydrolysates. Whey protein hydrolysate-loaded gelatin or CS capsules were used to enrich yogurt produced by lactic acid fermentation (Gómez-Mascaraque et al., 2016). During the fermentation process, a large part of the peptides present in the hydrolysate was lost due to susceptibility to the living starter cultures. After fermentation, the peptide profile of the yogurt enriched with free hydrolysate, encapsulation with CS or encapsulation with gelatin was analyzed. Enrichment with free hydrolysates resulted in the protection of 30 of the 58 peptides initially identified. The same amount was protected in hydrolysate-loaded CS capsules, but five

different peptides were found. When hydrolysates were encapsulated with gelatin, only 21 peptides were protected; however, it is difficult to determine with certainty the protective effect of gelatin, since its proteinaceous nature resulted in very complex chromatograms that did not allow conclusive conclusions. Spray-dried hydrolysates from pink perch meat were used to fortify a sweet-corn vegetable soup (Murthy et al., 2017). Both particles with and without encapsulating agents (MD and GA) were used, and although higher activity was retained when no carrier was used, their use improved sensory acceptability. The activity loss on MD/GA hydrolysate particles was linked to interaction between the encapsulating agents and the hydrolysates.

7. Conclusions and Future Perspectives

Bioactive peptides and protein hydrolysates are interesting ingredients for the production of functional foods and nutraceuticals due to their high bioactive potential and nutritional value. However, their physicochemical properties (e.g., bitter taste) and potential degradation during digestion have been shown to hinder their use. This work addresses the application of encapsulation technologies such as spray-drying and electrospraying for encapsulation, protection, and release of bioactive peptides and protein hydrolysates. For each encapsulation technology, both monoaxial and coaxial configurations were considered. Various parameters that may affect particle morphology and encapsulation efficiency (e.g., formulation processing method or carrier) were investigated, as well as the specific process parameters for both technologies (e.g., inlet and outlet temperature of the drying air, electrical potential, feed flow, injector–collector distance). It is worth noting that while there has been a significant effort to produce new bioactive peptide sequences, there has been a lack of attention towards their stabilization. Additionally, research on encapsulating protein-based bioactives using monoaxial spray-drying is scarce, and practically nonexistent for coaxial spray-drying. Although some research has been conducted on the encapsulation of bioactive peptides by both monoaxial and coaxial electrospraying, it has mainly been focused on pharmaceutical applications and parenteral supplementation. As a result, there is a significant gap in research regarding food application and oral supplementation. Altogether, encapsulation has an important role in maintaining the efficacy of functional foods containing bioactive peptides and proteins. However, the current widely used spray-drying method has only been studied in monoaxial configuration and the potential of the coaxial mode remains to be investigated. Although advanced methods such as electrospraying encapsulation have shown promise in pharmaceutical development, there is a need to explore their applications in the food industry. As research in this field continues, we can expect to see advances in the nano/microencapsulation of bioactive peptides for their application in functional foods.

Finally, works focusing on release studies, retention of activity, and bioaccessibility are limited, especially regarding the study of monoaxial electrospraying. Overall, there is a lack of research concerning the bioaccessibility of protein-based bioactives encapsulated by spray-drying or electrospraying, as well as their stability in food matrices. To the authors' knowledge, no work has been directed towards the bioaccessibility analysis of monoaxial electrospraying of protein-based bioactives, nor has any study yet compared the effect of monoaxial versus coaxial electrospraying of these biocompounds in their bioaccessibility or use for food matrix enrichment. Hence, future research should prioritize two aspects for activity retention of bioactive peptides: (i) exploring the possibilities of coaxial encapsulation techniques that can improve the entrapment of bioactive peptides, and (ii) investigating the effects of nano/microencapsulation on the stability and release of peptides in the gastrointestinal environment to enhance bioavailability.

8. References

Aguilar-Toala, J. E., Quintanar-Guerrero, D., Liceaga, A. M., & Zambrano- Zaragoza, M. L. (2022). Encapsulation of bioactive peptides: a strategy to improve the stability, protect the nutraceutical bioactivity and support their food applications. *RSC Advances*, *12*(11), 6449–6458. https://doi.org/10.1039/D1RA08590E

Akbarbaglu, Z., Mahdi Jafari, S., Sarabandi, K., Mohammadi, M., Khakbaz Heshmati, M., & Pezeshki, A. (2019). Influence of spray drying encapsulation on the retention of antioxidant properties and microstructure of flaxseed protein hydrolysates. *Colloids and Surfaces B: Biointerfaces*, *178*, 421–429. https://doi.org/10.1016/J.COLSURFB.2019.03.038

Akbarbaglu, Z., Peighambardoust, S. H., Sarabandi, K., & Jafari, S. M. (2021). Spray drying encapsulation of bioactive compounds within protein-based carriers; different options and applications. *Food Chemistry*, *359*, 129965. https://doi.org/10.1016/J.FOODCHEM.2021.129965

Amigo, L., & Hernández-Ledesma, B. (2020). Current Evidence on the Bioavailability of Food Bioactive Peptides. *Molecules 2020, Vol. 25, Page 4479*, *25*(19), 4479. https://doi.org/10.3390/MOLECULES25194479

Aquino, R. P., Auriemma, G., Conte, G. M., Esposito, T., Sommella, E., Campiglia, P., & Sansone, F. (2020). Development of Chitosan/Mannitol Microparticles as Delivery System for the Oral Administration of a Spirulina Bioactive Peptide Extract. *Molecules 2020, Vol. 25, Page 2086*, *25*(9), 2086. https://doi.org/10.3390/MOLECULES25092086

Aragón, J., Salerno, S., De Bartolo, L., Irusta, S., & Mendoza, G. (2018). Polymeric electrospun scaffolds for bone morphogenetic protein 2 delivery in bone tissue engineering. *Journal of Colloid and Interface Science*, *531*, 126–137. https://doi.org/10.1016/J.JCIS.2018.07.029

Bock, N., Dargaville, T. R., & Woodruff, M. A. (2012). Electrospraying of polymers with therapeutic molecules: State of the art. *Progress in Polymer Science*, *37*(11), 1510–1551. https://doi.org/10.1016/J.PROGPOLYMSCI.2012.03.002

Bock, N., Dargaville, T. R., & Woodruff, M. A. (2014). Controlling microencapsulation and release of micronized proteins using poly(ethylene glycol) and electrospraying. *European Journal of Pharmaceutics and Biopharmaceutics*, *87*(2), 366–377. https://doi.org/10.1016/J.EJPB.2014.03.008

Busolo, M. A., Torres-Giner, S., Prieto, C., & Lagaron, J. M. (2019). Electrospraying assisted by pressurized gas as an innovative high-throughput process for the microencapsulation and stabilization of docosahexaenoic acid-enriched fish oil in zein prolamine. *Innovative Food Science & Emerging Technologies*, *51*, 12–19. https://doi.org/10.1016/J.IFSET.2018.04.007

Calderón-Oliver, M., Pedroza-Islas, R., Escalona-Buendía, H. B., Pedraza-Chaverri, J., & Ponce-

Alquicira, E. (2017). Comparative study of the microencapsulation by complex coacervation of nisin in combination with an avocado antioxidant extract. *Food Hydrocolloids*, *62*, 49–57. https://doi.org/10.1016/J.FOODHYD.2016.07.028

Camargo, T. R., Khelissa, S., Chihib, N. E., Dumas, E., Wang, J., Valenti, W. C., & Gharsallaoui, A. (2021). Preparation and Characterization of Microcapsules Containing Antioxidant Fish Protein Hydrolysates: a New Use of Bycatch in Brazil. *Marine Biotechnology*, *23*(2), 321–330. https://doi.org/10.1007/S10126-021-10026-7

Cambronero-Rojas, A., Torres-Vergara, P., Godoy, R., Von Plessing, C., Sepúlveda, J., & Gómez-Gaete, C. (2015). Capreomycin oleate microparticles for intramuscular administration: Preparation, in vitro release and preliminary in vivo evaluation. *Journal of Controlled Release*, *209*, 229–237. https://doi.org/10.1016/J.JCONREL.2015.05.001

Cao, C., Zhao, X., Zhang, C., Ding, Z., Sun, F., & Zhao, C. (2020). Effect of inlet temperature on the physicochemical properties of spray-dried seed-watermelon seed protein powder. *Journal of Food Science*, *85*(10), 3442–3449. https://doi.org/10.1111/1750-3841.15432

Chakrabarti, S., Guha, S., & Majumder, K. (2018). Food-Derived Bioactive Peptides in Human Health: Challenges and Opportunities. *Nutrients 2018, Vol. 10, Page 1738*, *10*(11), 1738. https://doi.org/10.3390/NU10111738

Chegini, G. R., & Ghobadian, B. (2005). Effect of spray-drying conditions on physical properties of orange juice powder. *Drying Technology*, *23*(3), 657–668. https://doi.org/10.1081/DRT-200054161

Cian, R. E., Campos-Soldini, A., Chel-Guerrero, L., Drago, S. R., & Betancur-Ancona, D. (2019). Bioactive Phaseolus lunatus peptides release from maltodextrin/gum arabic microcapsules obtained by spray drying after simulated gastrointestinal digestion. *International Journal of Food Science & Technology*, *54*(6), 2002–2009. https://doi.org/10.1111/IJFS.14031

Cian, R. E., Salgado, P. R., Mauri, A. N., & Drago, S. R. (2020). Pyropia columbina phycocolloids as microencapsulating material improve bioaccessibility of brewers' spent grain peptides with ACE-I inhibitory activity. *International Journal of Food Science & Technology*, *55*(3), 1311–1317. https://doi.org/10.1111/IJFS.14397

Cruz-Casas, D. E., Aguilar, C. N., Ascacio-Valdés, J. A., Rodríguez-Herrera, R., Chávez-González, M. L., & Flores-Gallegos, A. C. (2021). Enzymatic hydrolysis and microbial fermentation: The most favorable biotechnological methods for the release of bioactive peptides. *Food Chemistry: Molecular Sciences*, *3*, 100047. https://doi.org/10.1016/J.FOCHMS.2021.100047

Dai, C., Wang, B., & Zhao, H. (2005). Microencapsulation peptide and protein drugs delivery system. *Colloids and Surfaces B: Biointerfaces*, *41*(2–3), 117–120. https://doi.org/10.1016/J.COLSURFB.2004.10.032

de Figueiredo Furtado, G., da Silva Carvalho, A. G., & Hubinger, M. D. (2021). Model infant formulas: Influence of types of whey proteins and oil composition on emulsion and powder properties. *Journal of Food Engineering*, *292*, 110256. https://doi.org/10.1016/J.JFOODENG.2020.110256

De Koker, S., Fierens, K., Dierendonck, M., De Rycke, R., Lambrecht, B. N., Grooten, J., Remon, J. P., & De Geest, B. G. (2014). Nanoporous polyelectrolyte vaccine microcarriers. A formulation platform for enhancing humoral and cellular immune responses. *Journal of Controlled Release*, *195*, 99–109. https://doi.org/10.1016/J.JCONREL.2014.07.043

Dima, C., Assadpour, E., Dima, S., & Jafari, S. M. (2020). Bioavailability and bioaccessibility of food bioactive compounds; overview and assessment by in vitro methods. *Comprehensive Reviews in Food Science and Food Safety*, *19*(6), 2862–2884. https://doi.org/10.1111/1541-4337.12623

El-Messery, T. M., Altuntas, U., Altin, G., & Özçelik, B. (2020). The effect of spray-drying and freeze-drying on encapsulation efficiency, in vitro bioaccessibility and oxidative stability of krill oil nanoemulsion system. *Food Hydrocolloids*, *106*, 105890. https://doi.org/10.1016/J.FOODHYD.2020.105890

Furtmann, B., Tang, J., Kramer, S., Eickner, T., Luderer, F., Fricker, G., Gomez, A., Heemskerk, B., & Jähn, P. S. (2017). Electrospray Synthesis of Poly(lactide-co-glycolide) Nanoparticles Encapsulating Peptides to Enhance Proliferation of Antigen-Specific CD8+ T Cells. *Journal of Pharmaceutical Sciences*, *106*(11), 3316–3327. https://doi.org/10.1016/J.XPHS.2017.06.013

Gallovic, M. D., Schully, K. L., Bell, M. G., Elberson, M. A., Palmer, J. R., Darko, C. A., Bachelder, E. M., Wyslouzil, B. E., Keane-Myers, A. M., Ainslie, K. M., Gallovic, M. D., Wyslouzil, B. E., Bachelder, E. M., Ainslie, K. M., Schully, K. L., Bell, M. G., Elberson, M. A., Palmer, J. R., Darko, C. A., & Keane-Myers, A. M. (2016). Acetalated Dextran Microparticulate Vaccine Formulated via Coaxial Electrospray Preserves Toxin Neutralization and Enhances Murine Survival Following Inhalational Bacillus Anthracis Exposure. *Advanced Healthcare Materials*, *5*(20), 2617–2627. https://doi.org/10.1002/ADHM.201600642

García-Moreno, P. J., Mendes, A. C., Jacobsen, C., & Chronakis, I. S. (2018). Biopolymers for the nanomicroencapsulation of bioactive ingredients by electrohydrodynamic processing. *Polymers for Food Applications*, 447–479. https://doi.org/10.1007/978-3-319-94625-2_17

García-Moreno, P. J., Rahmani-Manglano, N. E., Chronakis, I. S., Guadix, E. M., Yesiltas, B., Sørensen, A. D. M., & Jacobsen, C. (2021). Omega-3 nano-microencapsulates produced by electrohydrodynamic processing. *Omega-3 Delivery Systems: Production, Physical Characterization and Oxidative Stability*, 345–370. https://doi.org/10.1016/B978-0-12-821391-9.00017-X

Ghorani, B., & Tucker, N. (2015). Fundamentals of electrospinning as a novel delivery vehicle for bioactive compounds in food nanotechnology. *Food Hydrocolloids*, *51*, 227–240. https://doi.org/10.1016/J.FOODHYD.2015.05.024

Giroldi, M., Grambusch, I. M., Schlabitz, C., Kuhn, D., Lehn, D. N., & Volken de Souza, C. F. (2022). Encapsulation of protein hydrolysates by spray drying: feasibility of using buffalo whey proteins. *International Journal of Food Science & Technology*, *57*(6), 3419–3427. https://doi.org/10.1111/IJFS.15665

Gómez-Mascaraque, L. G., Miralles, B., Recio, I., & López-Rubio, A. (2016). Microencapsulation of a whey protein hydrolysate within micro-hydrogels: Impact on gastrointestinal stability and potential for functional yoghurt development. *Journal of Functional Foods*, *26*, 290–300. https://doi.org/10.1016/J.JFF.2016.08.006

Han, D., & Steckl, A. J. (2019). Coaxial Electrospinning Formation of Complex Polymer Fibers and their Applications. In *ChemPlusChem* (Vol. 84, Issue 10, pp. 1453–1497). Wiley-VCH Verlag. https://doi.org/10.1002/cplu.201900281

Ho, W. X., Chen, W. T., Lien, C. H., Yang, H. Y., Chen, K. H., Wei, Y. F., Wang, M. H., Ko, I. T., Tseng, F. G., & Yin, H. S. (2022). Physical, Chemical, and Biological Properties of Chitosan-Coated Alginate Microparticles Loaded with Porcine Interleukin-1β: A Potential Protein Adjuvant Delivery System. *International Journal of Molecular Sciences 2022, Vol. 23, Page 9959*, *23*(17), 9959. https://doi.org/10.3390/IJMS23179959

Iwaniak, A., Hrynkiewicz, M., Bucholska, J., Minkiewicz, P., & Darewicz, M. (2019). Understanding the nature of bitter-taste di- and tripeptides derived from food proteins based on chemometric analysis. *Journal of Food Biochemistry*, *43*(1), e12500. https://doi.org/10.1111/JFBC.12500

Jacobs, I. C. (2014). Atomization and Spray-Drying Processes. *Microencapsulation in the Food Industry: A Practical Implementation Guide*, 47–56. https://doi.org/10.1016/B978-0-12-404568-2.00005-4

Jacobsen, C., García-Moreno, P. J., Mendes, A. C., Mateiu, R. V., & Chronakis, I. S. (2018). Use of Electrohydrodynamic Processing for Encapsulation of Sensitive Bioactive Compounds and Applications in Food. *Annual Review of Food Science and Technology*, *9*, 525–549. https:/doi.org/10.1146/ANNUREV-FOOD-030117-012348

Jakubczyk, A., Karas, M., Rybczynska-Tkaczyk, K., Zielinska, E., & Zielinski, D. (2020). Current Trends of Bioactive Peptides—New Sources and Therapeutic Effect. *Foods 2020, Vol. 9, Page 846*, *9*(7), 846. https://doi.org/10.3390/FOODS9070846

Kang, J. S., Park, I., Jung, J. H., & Kim, S. S. (2013). Free-surface electrospray technique using a multi-hole array. *Journal of Aerosol Science*, *55*, 25–30. https://doi.org/10.1016/J.JAEROSCI.2012.07.010

Karami, Z., & Akbari-adergani, B. (2019). Bioactive food derived peptides: a review on correlation between structure of bioactive peptides and their functional properties. *Journal of Food Science and Technology*, *56*(2), 535–547. https://doi.org/10.1007/S13197-018-3549-4

Keogh, K., Murray, C., Kelly, J., & O'kennedy, B. (2004). Effect of the particle size of spray-dried

milk powder on some properties of chocolate. *Le Lait*, *84*(4), 375–384. https://doi.org/10.1051/lait:2004013

Kumar, A., Belhaj, M., DiPette, D. J., & Potts, J. D. (2021). A Novel Alginate-Based Delivery System for the Prevention and Treatment of Pressure-Overload Induced Heart Failure. *Frontiers in Pharmacology*, *11*, 2227. https://doi.org/10.3389/FPHAR.2020.602952

Largo Avila, E., Cortes Rodríguez, M., & Ciro Velásquez, H. J. (2015). Influence of Maltodextrin and Spray Drying Process Conditions on Sugarcane Juice Powder Quality. *Revista Facultad Nacional de Agronomía Medellín*, *68*(1), 7509–7520. https://doi.org/10.15446/RFNAM.V68N1.47839

Lee, Y. (n.d.). *MICROENCAPSULATION TECHNOLOGY USING A THREE FLUID NOZZLE AND SPRAY DRYING - UNIVERSITY OF ILLINOIS*. Retrieved February 23, 2023, from https://portal.nifa.usda.gov/web/crisprojectpages/1013950-microencapsulation-technology-using-a-three-fluid-nozzle-and-spray-drying.html

Lim, L. T., Mendes, A. C., & Chronakis, I. S. (2019). Electrospinning and electrospraying technologies for food applications. *Advances in Food and Nutrition Research*, *88*, 167–234. https://doi.org/10.1016/BS.AFNR.2019.02.005

Lima, K. O., da Rocha, M., Alemán, A., López-Caballero, M. E., Tovar, C. A., Gómez-Guillén, M. C., Montero, P., & Prentice, C. (2021). Yogurt Fortification by the Addition of Microencapsulated Stripped Weakfish (Cynoscion guatucupa) Protein Hydrolysate. *Antioxidants 2021, Vol. 10, Page 1567*, *10*(10), 1567. https://doi.org/10.3390/ANTIOX10101567

Liu, X., T Jansman, M. M., Thulstrup, P. W., Mendes, A. C., Chronakis, I. S., Hosta-Rigau, L., Liu, X., T Jansman, M. M., Hosta-Rigau, L., Thulstrup, P. W., Mendes, A. C., & Chronakis, I. S. (2020). Low-Fouling Electrosprayed Hemoglobin Nanoparticles with Antioxidant Protection as Promising Oxygen Carriers. *Macromolecular Bioscience*, *20*(2), 1900293. https://doi.org/10.1002/MABI.201900293

Locali Pereira, A. R., Gonçalves Cattelan, M., & Nicoletti, V. R. (2019). Microencapsulation of pink pepper essential oil: Properties of spray-dried pectin/SPI double-layer versus SPI single-layer stabilized emulsions. *Colloids and Surfaces A: Physicochemical and Engineering Aspects*, *581*, 123806. https://doi.org/10.1016/J.COLSURFA.2019.123806

López-Herrera, J. M., Barrero, A., López, A., Loscertales, I. G., & Márquez, M. (2003). Coaxial jets generated from electrified Taylor cones. Scaling laws. *Journal of Aerosol Science*, *34*(5), 535–552. https://doi.org/10.1016/S0021-8502(03)00021-1

Lorenzo, J. M., Munekata, P. E. S., Gómez, B., Barba, F. J., Mora, L., Pérez-Santaescolástica, C., & Toldrá, F. (2018). Bioactive peptides as natural antioxidants in food products – A review. *Trends in Food Science & Technology*, *79*, 136–147. https://doi.org/10.1016/J.TIFS.2018.07.003

Loscertales, I. G., Barrero, A., Guerrero, I., Cortijo, R., Marquez, M., & Gañán-Calvo, A. M. (2002). Micro/nano encapsulation via electrified coaxial liquid jets. *Science (New York, N.Y.)*, *295*(5560), 1695–1698. https://doi.org/10.1126/SCIENCE.1067595

Lotfy, S. N., Fadel, H. H. M., El-Ghorab, A. H., & Shaheen, M. S. (2015). Stability of encapsulated beef-like flavourings prepared from enzymatically hydrolysed mushroom proteins with other precursors under conventional and microwave heating. *Food Chemistry*, *187*, 7–13. https://doi.org/10.1016/J.FOODCHEM.2015.04.027

Ma, Y., Xu, J., Jiang, S., & Zeng, M. (2022). Effect of chitosan coating on the properties of nanoliposomes loaded with oyster protein hydrolysates: Stability during spray-drying and freeze-drying. *Food Chemistry*, *385*, 132603. https://doi.org/10.1016/J.FOODCHEM.2022.132603

Moeller, H., Martin, D., Schrader, K., Hoffmann, W., & Lorenzen, P. C. (2018). Spray- or freeze-drying of casein micelles loaded with Vitamin D2: Studies on storage stability and in vitro digestibility. *LWT*, *97*, 87–93. https://doi.org/10.1016/J.LWT.2018.04.003

Mohammadi, M., Hamishehkar, H., Ghorbani, M., Shahvalizadeh, R., Pateiro, M., & Lorenzo, J. M. (2021). Engineering of Liposome Structure to Enhance Physicochemical Properties of Spirulina plantensis Protein Hydrolysate: Stability during Spray-Drying. *Antioxidants 2021, Vol. 10, Page 1953*, *10*(12), 1953. https://doi.org/10.3390/ANTIOX10121953

Mohan, A., Rajendran, S. R. C. K., He, Q. S., Bazinet, L., & Udenigwe, C. C. (2015). Encapsulation of

food protein hydrolysates and peptides: a review. *RSC Advances*, *5*(97), 79270–79278. https://doi.org/10.1039/C5RA13419F

Molina Ortiz, S. E., Mauri, A., Monterrey-Quintero, E. S., Trindade, M. A., Santana, A. S., & Favaro-Trindade, C. S. (2009). Production and properties of casein hydrolysate microencapsulated by spray drying with soybean protein isolate. *LWT - Food Science and Technology*, *42*(5), 919–923. https://doi.org/10.1016/J.LWT.2008.12.004

Moreira, A., Lawson, D., Onyekuru, L., Dziemidowicz, K., Angkawinitwong, U., Costa, P. F., Radacsi, N., & Williams, G. R. (2021). Protein encapsulation by electrospinning and electrospraying. *Journal of Controlled Release*, *329*, 1172–1197. https://doi.org/10.1016/J.JCONREL.2020.10.046

Murthy, L. N., Phadke, G. G., Mohan, C. O., Chandra, M. V., Annamalai, J., Visnuvinayagam, S., Unnikrishnan, P., & Ravishankar, C. N. (2017). Characterization of Spray-Dried Hydrolyzed Proteins from Pink Perch Meat Added with Maltodextrin and Gum Arabic. *Journal of Aquatic Food Product Technology*, *26*(8), 913–928. https://doi.org/10.1080/10498850.2017.1362684

Musaei, M., Mokhtari, J., Nouri, M., & Rad, Z. P. (2017). Fabrication and Characterization of Nanocapsules of PLGA Containing BSA Using Electrospray Technique. *Nanomedicine Research Journal*, *2*(3), 158–164. https://doi.org/10.22034/NMRJ.2017.03.003

Onyekuru, L. C., Moreira, A., Zhang, J., Angkawinitwong, U., Costa, P. F., Brocchini, S., & Williams, G. R. (2021). An investigation of alkaline phosphatase enzymatic activity after electrospinning and electrospraying. *Journal of Drug Delivery Science and Technology*, *64*, 102592. https://doi.org/10.1016/J.JDDST.2021.102592

Ospina-Quiroga, J. L., García-Moreno, P. J., Guadix, A., Guadix, E. M., Almécija-Rodríguez, M. del C., & Pérez-Gálvez, R. (2022). Evaluation of Plant Protein Hydrolysates as Natural Antioxidants in Fish Oil-In-Water Emulsions. *Antioxidants*, *11*(8), 1612. https://doi.org/10.3390/ANTIOX11081612

Palamutoğlu, R., & Sarıçoban, C. (2019). *PHYSICO-CHEMICAL INVESTIGATION AND ANTIOXIDANT ACTIVITY OF ENCAPSULATED FISH COLLAGEN HYDROLYZATES WITH MALTODEXTRIN*. *43*(1), 94–105. https://doi.org/10.35219/foodtechnology.2019.1.07

Parhizkar, M., Reardon, P. J. T., Knowles, J. C., Browning, R. J., Stride, E., Pedley, R. B., Grego, T., & Edirisinghe, M. (2017). Performance of novel high throughput multi electrospray systems for forming of polymeric micro/nanoparticles. *Materials & Design*, *126*, 73–84. https://doi.org/10.1016/J.MATDES.2017.04.029

Park, C. W., Bastian, E., Farkas, B., & Drake, M. (2014). The Effect of Feed Solids Concentration and Inlet Temperature on the Flavor of Spray Dried Whey Protein Concentrate. *Journal of Food Science*, *79*(1), C19–C24. https://doi.org/10.1111/1750-3841.12279

Paz-Samaniego, R., Rascón-Chu, A., Brown-Bojorquez, F., Carvajal-Millan, E., Pedroza-Montero, M., Silva-Campa, E., Sotelo-Cruz, N., López-Franco, Y. L., & Lizardi-Mendoza, J. (2018). Electrospray-assisted fabrication of core-shell arabinoxylan gel particles for insulin and probiotics entrapment. *Journal of Applied Polymer Science*, *135*(26), 46411. https://doi.org/10.1002/APP.46411

Pei, J., Gao, X., Pan, D., Hua, Y., He, J., Liu, Z., & Dang, Y. (2022). Advances in the stability challenges of bioactive peptides and improvement strategies. *Current Research in Food Science*, *5*, 2162–2170. https://doi.org/10.1016/J.CRFS.2022.10.031

Peres, I., Rocha, S., Loureiro, J. A., Do Carmo Pereira, M., Ivanova, G., & Coelho, M. (2012). Carbohydrate particles as protein carriers and scaffolds: Physico-chemical characterization and collagen stability. *Journal of Nanoparticle Research*, *14*(9), 1–11. https://doi.org/10.1007/S11051-012-1144-6

Pérez-Masiá, R., Lagaron, J. M., & Lopez-Rubio, A. (2015). Morphology and Stability of Edible Lycopene-Containing Micro- and Nanocapsules Produced Through Electrospraying and Spray Drying. *Food and Bioprocess Technology*, *8*(2), 459–470. https://doi.org/10.1007/S11947-014-1422-7

Perry, S. L., & McClements, D. J. (2020). Recent Advances in Encapsulation, Protection, and Oral Delivery of Bioactive Proteins and Peptides using Colloidal Systems. *Molecules 2020, Vol. 25, Page 1161*, *25*(5), 1161. https://doi.org/10.3390/MOLECULES25051161

Piñón-Balderrama, C. I., Leyva-Porras, C., Terán-Figueroa, Y., Espinosa-Solís, V., Álvarez-Salas, C., & Saavedra-Leos, M. Z. (2020). Encapsulation of Active Ingredients in Food Industry by Spray-Drying and

Nano Spray-Drying Technologies. *Processes 2020, Vol. 8, Page 889*, *8*(8), 889. https://doi.org/10.3390/PR8080889

Pinto, J. T., Faulhammer, E., Dieplinger, J., Dekner, M., Makert, C., Nieder, M., & Paudel, A. (2021). Progress in spray-drying of protein pharmaceuticals: Literature analysis of trends in formulation and process attributes. *Drying Technology*, *39*(11), 1415–1446. https://doi.org/10.1080/07373937.2021.1903032

Rahmani-Manglano, N. E., Guadix, E. M., Jacobsen, C., & García-Moreno, P. J. (2023). Comparative Study on the Oxidative Stability of Encapsulated Fish Oil by Monoaxial or Coaxial Electrospraying and Spray-Drying. *Antioxidants*, *12*(2), 266. https://doi.org/10.3390/ANTIOX12020266

Rahmani-Manglano, N. E., Jones, N. C., Hoffmann, S. V., Guadix, E. M., Pérez-Gálvez, R., Guadix, A., & García-Moreno, P. J. (2022). Structure of whey protein hydrolysate used as emulsifier in wet and dried oil delivery systems: Effect of pH and drying processing. *Food Chemistry*, *390*, 133169. https://doi.org/10.1016/J.FOODCHEM.2022.133169

Rasekh, M., Young, C., Roldo, M., Lancien, F., Le Mével, J. C., Hafizi, S., Ahmad, Z., Barbu, E., & Gorecki, D. (2015). Hollow-layered nanoparticles for therapeutic delivery of peptide prepared using electrospraying. *Journal of Materials Science: Materials in Medicine*, *26*(11), 1–12. https://doi.org/10.1007/S10856-015-5588-Y

Rivero-Pino, F., Espejo-Carpio, F. J., & Guadix, E. M. (2020). Antidiabetic Food-Derived Peptides for Functional Feeding: Production, Functionality and In Vivo Evidences. *Foods 2020, Vol. 9, Page 983*, *9*(8), 983. https://doi.org/10.3390/FOODS9080983

Romano, L., Camposeo, A., Manco, R., Moffa, M., & Pisignano, D. (2016). Core-Shell Electrospun Fibers Encapsulating Chromophores or Luminescent Proteins for Microscopically Controlled Molecular Release. *Molecular Pharmaceutics*, *13*(3), 729–736. https://doi.org/10.1021/ACS.MOLPHARMACEUT.5B00560

Salleh, N. H., Jusoh, Y. M. M., Zaidel, D. N. A., & Hashim, Z. (2022). The scavenging activity of encapsulated EBN hydrolysates using different combinations of polysaccharides as wall material by spray drying. *Biocatalysis and Agricultural Biotechnology*, *45*, 102503. https://doi.org/10.1016/J.BCAB.2022.102503

Sánchez, A., & Vázquez, A. (2017). Bioactive peptides: A review. *Food Quality and Safety*, *1*(1), 29–46. https://doi.org/10.1093/FQSAFE/FYX006

Sarabandi, K., Gharehbeglou, P., & Jafari, S. M. (2019). Spray-drying encapsulation of protein hydrolysates and bioactive peptides: Opportunities and challenges. *Drying Technology*, *38*(5–6), 577–595. https://doi.org/10.1080/07373937.2019.1689399

Sarabandi, K., Gharehbeglou, P., Jafari, S. M., & Akbarbaglu, Z. (2021). Spray Drying Encapsulation of Proteins and Bioactive Peptides. *Spray Drying Encapsulation of Bioactive Materials*, 241–270. https://doi.org/10.1201/9780429355462-10

Sarabandi, K., & Jafari, S. M. (2020a). Effect of chitosan coating on the properties of nanoliposomes loaded with flaxseed-peptide fractions: Stability during spray-drying. *Food Chemistry*, *310*, 125951. https://doi.org/10.1016/J.FOODCHEM.2019.125951

Sarabandi, K., & Jafari, S. M. (2020b). Improving the antioxidant stability of flaxseed peptide fractions during spray drying encapsulation by surfactants: Physicochemical and morphological features. *Journal of Food Engineering*, *286*, 110131. https://doi.org/10.1016/J.JFOODENG.2020.110131

Sarabandi, K., Jafari, S. M., Mohammadi, M., Akbarbaglu, Z., Pezeshki, A., & Khakbaz Heshmati, M. (2019). Production of reconstitutable nanoliposomes loaded with flaxseed protein hydrolysates: Stability and characterization. *Food Hydrocolloids*, *96*, 442–450. https://doi.org/10.1016/J.FOODHYD.2019.05.047

Schwarz, K., & Amft, J. (2021). Spray-dried capsules and extrudates as omega-3 lipids delivery systems. *Omega-3 Delivery Systems: Production, Physical Characterization and Oxidative Stability*, 321–343. https://doi.org/10.1016/B978-0-12-821391-9.00007-7

Sepúlveda, C. T., Alemán, A., Zapata, J. E., Montero, M. P., & Gómez-Guillén, M. C. (2021). Characterization and storage stability of spray dried soy-rapeseed lecithin/trehalose liposomes

loaded with a tilapia viscera hydrolysate. *Innovative Food Science & Emerging Technologies*, *71*, 102708. https://doi.org/10.1016/J.IFSET.2021.102708

Shi, X., & Lee, Y. (2020). Encapsulation of tributyrin with whey protein isolate (WPI) by spray-drying with a three-fluid nozzle. *Journal of Food Engineering*, *281*, 109992. https://doi.org/10.1016/J.JFOODENG.2020.109992

Sobel, R., Versic, R., & Gaonkar, A. G. (2014). Introduction to Microencapsulation and Controlled Delivery in Foods. *Microencapsulation in the Food Industry: A Practical Implementation Guide*, 3–12. https://doi.org/10.1016/B978-0-12-404568-2.00001-7

Song, J., Yu, Y., Chen, M., Ren, Z., Chen, L., Fu, C., Ma, Z. feei, & Li, Z. (2022). Advancement of Protein- and Polysaccharide-Based Biopolymers for Anthocyanin Encapsulation. *Frontiers in Nutrition*, *9*, 1323. https://doi.org/10.3389/FNUT.2022.938829

Song, Y., Chan, Y. K., Ma, Q., Liu, Z., & Shum, H. C. (2015). All-Aqueous Electrosprayed Emulsion for Templated Fabrication of Cytocompatible Microcapsules. *ACS Applied Materials and Interfaces*, *7*(25), 13925–13933. https://doi.org/10.1021/ACSAMI.5B02708

Sosnik, A., & Seremeta, K. P. (2015). Advantages and challenges of the spray-drying technology for the production of pure drug particles and drug-loaded polymeric carriers. *Advances in Colloid and Interface Science*, *223*, 40–54. https://doi.org/10.1016/J.CIS.2015.05.003

Stone, A. K., Karalash, A., Tyler, R. T., Warkentin, T. D., & Nickerson, M. T. (2015). Functional attributes of pea protein isolates prepared using different extraction methods and cultivars. *Food Research International*, *76*(P1), 31–38. https://doi.org/10.1016/J.FOODRES.2014.11.017

Sun, X., Okagu, O. D., & Udenigwe, C. C. (2021). Encapsulation technology for protection and delivery of bioactive peptides. In *Biologically Active Peptides: From Basic Science to Applications for Human Health* (pp. 331–356). Academic Press. https://doi.org/10.1016/B978-0-12-821389-6.00028-5

Sunderland, T., Kelly, J. G., & Ramtoola, Z. (2015). Application of a novel 3-fluid nozzle spray drying process for the microencapsulation of therapeutic agents using incompatible drug-polymer solutions. *Archives of Pharmacal Research*, *38*(4), 566–573. https://doi.org/10.1007/S12272-013-0261-9

Talón, E., Lampi, A. M., Vargas, M., Chiralt, A., Jouppila, K., & González-Martínez, C. (2019). Encapsulation of eugenol by spray-drying using whey protein isolate or lecithin: Release kinetics, antioxidant and antimicrobial properties. *Food Chemistry*, *295*, 588–598. https://doi.org/10.1016/J.FOODCHEM.2019.05.115

Tapia-Hernández, J. A., Rodríguez-Félix, F., & Katouzian, I. (2017). Nanocapsule formation by electrospraying. *Nanoencapsulation Technologies for the Food and Nutraceutical Industries*, 320–345. https://doi.org/10.1016/B978-0-12-809436-5.00009-4

Tavares, L., & Zapata Noreña, C. P. (2019). Encapsulation of garlic extract using complex coacervation with whey protein isolate and chitosan as wall materials followed by spray drying. *Food Hydrocolloids*, *89*, 360–369. https://doi.org/10.1016/J.FOODHYD.2018.10.052

Udenigwe, C. C., & Fogliano, V. (2017). Food matrix interaction and bioavailability of bioactive peptides: Two faces of the same coin? *Journal of Functional Foods*, *35*, 9–12. https://doi.org/10.1016/J.JFF.2017.05.029

Unagolla, J. M., & Jayasuriya, A. C. (2018). Drug transport mechanisms and in vitro release kinetics of vancomycin encapsulated chitosan-alginate polyelectrolyte microparticles as a controlled drug delivery system. *European Journal of Pharmaceutical Sciences*, *114*, 199–209. https://doi.org/10.1016/J.EJPS.2017.12.012

Van, V., & Lee, T.-C. (2018). Electrospray technique for preparation of core-shell materials : A mini-review. *Online) Particle and Aerosol Research Part. Aerosol Res*, *14*(3), 49–63. https://doi.org/10.11629/jpaar.2018.14.3.049

Vehring, R. (2008). Pharmaceutical particle engineering via spray drying. *Pharmaceutical Research*, *25*(5), 999–1022. https://doi.org/10.1007/S11095-007-9475-1

Wan, F., Maltesen, M. J., Andersen, S. K., Bjerregaard, S., Foged, C., Rantanen, J., & Yang, M. (2014). One-Step Production of Protein-Loaded PLGA Microparticles via Spray Drying Using 3-Fluid Nozzle.

Pharmaceutical Research, *31*(8), 1967–1977. https://doi.org/10.1007/S11095-014-1299-1

Wang, H., Tong, X., Yuan, Y., Peng, X., Zhang, Q., Zhang, S., Xie, C., Zhang, X., Yan, S., Xu, J., Jiang, L., Qi, B., & Li, Y. (2020). Effect of Spray-Drying and Freeze-Drying on the Properties of Soybean Hydrolysates. *Journal of Chemistry*, *2020*. https://doi.org/10.1155/2020/9201457

Wang, K., Liu, M., & Mo, R. (2020). Polysaccharide-Based Biomaterials for Protein Delivery. *Medicine in Drug Discovery*, *7*, 100031. https://doi.org/10.1016/J.MEDIDD.2020.100031

Wang, L., Wang, N., Zhang, W., Cheng, X., Yan, Z., Shao, G., Wang, X., Wang, R., & Fu, C. (2022). Therapeutic peptides: current applications and future directions. *Signal Transduction and Targeted Therapy 2022 7:1*, *7*(1), 1–27. https://doi.org/10.1038/s41392-022-00904-4

Wang, W., Dufour, C., & Zhou, W. (2015). *CyTA-Journal of Food Impacts of spray-drying conditions on the physicochemical properties of soy sauce powders using maltodextrin as auxiliary drying carrier*. https://doi.org/10.1080/19476337.2015.1014430

Wang, Y., & Selomulya, C. (2020). Spray drying strategy for encapsulation of bioactive peptide powders for food applications. *Advanced Powder Technology*, *31*(1), 409–415. https://doi.org/10.1016/J.APT.2019.10.034

Wang, Z., Ju, X., He, R., Yuan, J., & Aluko, R. E. (2015a). Effect of high pressure treatment on rapeseed protein microparticle properties and gastrointestinal release behavior of the encapsulated peptides. *Food Research International*, *77*, 549–555. https://doi.org/10.1016/J.FOODRES.2015.09.023

Wang, Z., Ju, X., He, R., Yuan, J., & Wang, L. (2015b). The Effect of Rapeseed Protein Structural Modification on Microstructural Properties of Peptide Microcapsules. *Food and Bioprocess Technology*, *8*(6), 1305–1318. https://doi.org/10.1007/S11947-015-1472-5

Wang, Z., Ma, Y., Chen, H., Deng, Y., Wei, Z., Zhang, Y., Tang, X., Li, P., Zhao, Z., Zhou, P., Liu, G., & Zhang, M. (2022). Rice bran-modified wheat gluten nanoparticles effectively stabilized pickering emulsion: An interfacial antioxidant inhibiting lipid oxidation. *Food Chemistry*, *387*, 132874. https://doi.org/10.1016/J.FOODCHEM.2022.132874

Webber, V., de Siqueira Ferreira, D., Barreto, P. L. M., Weiss-Angeli, V., & Vanderlinde, R. (2018). Preparation and characterization of microparticles of β-cyclodextrin/glutathione and chitosan/glutathione obtained by spray-drying. *Food Research International*, *105*, 432–439. https://doi.org/10.1016/J.FOODRES.2017.11.035

Woo, M. W., & Bhandari, B. (2013). Spray drying for food powder production. *Handbook of Food Powders: Processes and Properties*, 29–56. https://doi.org/10.1533/9780857098672.1.29

Yaghoobi, N., Faridi Majidi, R., Faramarzi, M. A., Baharifar, H., & Amani, A. (2017). Preparation, Optimization and Activity Evaluation of PLGA/Streptokinase Nanoparticles Using Electrospray. *Advanced Pharmaceutical Bulletin*, *7*(1), 131–139. https://doi.org/10.15171/apb.2017.017

Yan, B., Davachi, S. M., Ravanfar, R., Dadmohammadi, Y., Deisenroth, T. W., Pho, T. Van, Odorisio, P. A., Darji, R. H., & Abbaspourrad, A. (2021). Improvement of vitamin C stability in vitamin gummies by encapsulation in casein gel. *Food Hydrocolloids*, *113*, 106414. https://doi.org/10.1016/J.FOODHYD.2020.106414

Yang, S., Mao, X. Y., Li, F. F., Zhang, D., Leng, X. J., Ren, F. Z., & Teng, G. X. (2012). The improving effect of spray-drying encapsulation process on the bitter taste and stability of whey protein hydrolysate. *European Food Research and Technology*, *235*(1), 91–97. https://doi.org/10.1007/S00217-012-1735-6

Yao, S., Liu, H., Yu, S., Li, Y., Wang, X., & Wang, L. (2016). Drug-nanoencapsulated PLGA microspheres prepared by emulsion electrospray with controlled release behavior. *Regenerative Biomaterials*, *3*(5), 309–317. https://doi.org/10.1093/RB/RBW033

Ying, X., Gao, J., Lu, J., Ma, C., Lv, J., Adhikari, B., & Wang, B. (2021). Preparation and drying of water-in-oil-in-water (W/O/W) double emulsion to encapsulate soy peptides. *Food Research International*,

141, 110148. https://doi.org/10.1016/J.FOODRES.2021.110148

Zabot, G. L., Schaefer Rodrigues, F., Polano Ody, L., Vinícius Tres, M., Herrera, E., Palacin, H., Córdova-Ramos, J. S., Best, I., & Olivera-Montenegro, L. (2022). Encapsulation of Bioactive Compounds for Food and Agricultural Applications. *Polymers 2022, Vol. 14, Page 4194*, *14*(19), 4194. https://doi.org/10.3390/POLYM14194194

Zamani, M., Prabhakaran, M. P., Thian, E. S., & Ramakrishna, S. (2014). Protein encapsulated core–shell structured particles prepared by coaxial electrospraying: Investigation on material and processing variables. *International Journal of Pharmaceutics*, *473*(1–2), 134–143. https://doi.org/10.1016/J.IJPHARM.2014.07.006

Zarrabi, A., Abadi, M. A. A., Khorasani, S., Reza Mohammadabadi, M., Jamshidi, A., Torkaman, S., Taghavi, E., Mozafari, M. R., & Rasti, B. (2020). Nanoliposomes and Tocosomes as Multifunctional Nanocarriers for the Encapsulation of Nutraceutical and Dietary Molecules. *Molecules 2020, Vol. 25, Page 638*, *25*(3), 638. https://doi.org/10.3390/MOLECULES25030638

Zhang, L., Huang, J., Si, T., & Xu, R. X. (2014). Coaxial electrospray of microparticles and nanoparticles for biomedical applications. *Expert Review of Medical Devices*, *9*(6), 595–612. https://doi.org/10.1586/ERD.12.58

Zhang, L., Si, T., Fischer, A. J., Letson, A., Yuan, S., Roberts, C. J., & Xu, R. X. (2015). Coaxial Electrospray of Ranibizumab-Loaded Microparticles for Sustained Release of Anti-VEGF Therapies. *PLOS ONE*, *10*(8), e0135608. https://doi.org/10.1371/JOURNAL.PONE.0135608

Zhao, C., Chen, G., Wang, H., Zhao, Y., & Chai, R. (2021). Bio-inspired intestinal scavenger from microfluidic electrospray for detoxifying lipopolysaccharide. *Bioactive Materials*, *6*(6), 1653–1662. https://doi.org/10.1016/J.BIOACTMAT.2020.11.017

Zhu, C., Huang, Y., Zhang, X., Mei, L., Pan, X., Li, G., & Wu, C. (2015). Comparative studies on exenatide-loaded poly (d,l-lactic-co-glycolic acid) microparticles prepared by a novel ultra-fine particle processing system and spray drying. *Colloids and Surfaces B: Biointerfaces*, *132*, 103–110. https://doi.org/10.1016/J.COLSURFB.2015.05.001

CHAPTER V

Encapsulation of *Tenebrio molitor* hydrolysate with DPP-IV inhibitory activity by electrospraying and spray-drying

ABSTRACT

This study investigates the encapsulation of *Tenebrio molitor* hydrolysate exhibiting DPP-IV inhibitory activity by spray-drying and electrospraying techniques. First, we optimized the feed formulation and processing conditions required to obtain nano-microcapsules by electrospraying when using Arabic gum as encapsulating agent and pullulan and Tween 20 as additives. The optimum formulation was also dried by using spray-drying, where the removal of the additives was also assayed. Morphology analysis reveals that electrosprayed capsules have smaller size (1.2±0.5 μm vs. 12.4±8.7 μm μm) and greater uniformity compared to those obtained by spray-drying. Regarding surface nitrogen content and DPP-IV inhibitory activity, our results show no significant difference between electrosprayed capsules and spray-dried capsules containing additives (IC_{50} of ~1.5mg protein/mL). Therefore, it was concluded that adding additives during spray-drying allows for similar encapsulation efficiency, and reduced degradation during processing, as achieved by electrospraying technique but providing higher productivity. On the other hand, spray-dried capsules without additives displayed a higher surface nitrogen content percentage, which was mainly due to the absence of Tween 20 in the feed formulation. Consequently, these capsules presented a higher IC_{50} value (IC_{50} of 1.99 ± 0.03 mg protein/mL) due to the potential degradation of surface-exposed peptides.

JOURNAL PAPER: Berraquero-García, C., Martínez-Sánchez, L., Guadix, E. M., & García-Moreno, P. J. (2024). Encapsulation of Tenebrio molitor Hydrolysate with DPP-IV Inhibitory Activity by Electrospraying and Spray-Drying. *Nanomaterials*, Vol. 14, Page 840, 14(10), 840. https://doi.org/10.3390/NANO14100840 (IF: 4.4 (2023); category: Chemistry, multidisciplinary; position: 70/231; Q2)

1. Introduction

According to the International Diabetes Federation, 537 million people have diabetes, with type 2 diabetes mellitus (T2DM) being the most common, accounting for around 90% of all cases. This number is expected to increase to 643 million by 2030 (*IDF Diabetes Atlas 2021 | IDF Diabetes Atlas*, n.d.). T2DM is a metabolic disorder characterized by chronic high blood sugar levels due to insulin resistance and insufficient insulin secretion (Galicia-Garcia et al., 2020). Insulin administration remains the primary treatment available; however, subcutaneous injection, which is undesirable for patients, is required as oral administration is impractical (Howard-Thompson et al., 2018). Hence, there is an increased interest in the development of alternative therapies. In particular, the inhibition of the enzyme dipeptidyl-peptidase IV (DPP-IV) has become a promising approach for controlling glycemic levels (Drucker, 2006), leading to the development of oral antihyperglycemic drugs known as gliptins (Krentz et al., 2012; Makrilakis, 2019). However, these drugs present significant risks (Ahrén, 2007), and increasing efforts have been destined to the use of bioactive peptides due to their potential to serve as antidiabetic agents without exhibiting side-effects (Antony & Vijayan, 2021).

Bioactive peptides are mainly derived from enzymatic hydrolysis of animal proteins (i.e., milk, fish, and others)(Berraquero-García, Rivero-Pino, et al., 2023; Masood & Khosravi-Darani, 2015; Rizzello et al., 2016). Yet, the increasing global population requires novel sustainable protein sources to meet higher demands while minimizing environmental effects (Rivero-Pino et al., 2021). Insects have emerged as a new sustainable protein source in recent years (Gravel & Doyen, 2020). Particularly, *Tenebrio molitor* larvae (mealworms) have been recognized as a novel food by the European Food Safety Agency and are known for their high nutritional value in terms of protein and fat content (De Marco et al., 2015; Nowak et al., 2016), digestibility (Cho et al., 2019; Yoo et al., 2018), and functional ability (Benzertiha et al., 2019, 2020). Additionally, several studies have highlighted the capacity of *T. molitor* to produce DPP-IV inhibitors through enzymatic hydrolysis (Errico et al., 2022; Rivero-Pino et al., 2021).

The oral administration of bioactive peptides, for instance in the form of functional food, is a simple and convenient approach for patients to counteract T2DM. However, biopeptides present some drawbacks that need to be addressed: high hygroscopicity leading to instability and decreased bioactivity (Aguilar-Toala et al., 2022), bitterness from hydrophobic amino acid residues (Iwaniak et al., 2019), low water solubility of highly hydrophobic peptides hindering incorporation into food formulation (Karami & Akbari-adergani, 2019), physicochemical instability during storage and digestion (Pei et al., 2022), and limited bioaccessibility in the intestine (Perry & McClements, 2020). A common strategy employed to overcome these drawbacks is the encapsulation of the protein hydrolysates/peptides used as food bioactive ingredients.

Encapsulation consists in the entrapment of the peptides within a matrix of one or more encapsulating agents (Sun et al., 2021). Despite extensive research on the encapsulation of various substances such as lipids (e.g., omega-3 fatty acids) (Hosseini et al., 2021), vitamins (Azevedo et al., 2023), polyphenols (Li et al., 2023), and other drugs (Talarico et al., 2024; Yang et al., 2024) there have been relatively fewer studies conducted on the encapsulation of bioactive peptides. Furthermore, most of the research on encapsulating bioactive peptides has employed methods like coacervation, freeze-drying and spray-drying (Alu'datt et al., 2022). While coacervation offers benefits such as high efficiency for flavorings and protection against oxidation at mild temperature conditions with potential for controlled release; it also has limited application in the food industry due to its sensitivity to pH and ionic strength between the wall and core material (Giroldi et al., 2021). Freeze drying can ensure physicochemical and bioactive stability but requires a significant amount of time-labor-cost resources compared to previous findings that favor spray-drying (Ma et al., 2014). Spray-drying is widely used in the food industry for encapsulating bioactive components because of its versatility in terms of solvents and encapsulating agents, as well as its cost-effective benefits and high productivity (Abdul Mudalip et al., 2021). This technique is based on the dehydration of finely atomized droplets due to their contact with a hot gas, such as air or, less commonly, an inert gas (e.g., nitrogen), resulting in dry particles (Gharsallaoui et al., 2007; Woo & Bhandari, 2013). The encapsulation of bioactive protein hydrolysates/peptides with antidiabetic activity by this technique has been investigated in various studies using diverse encapsulating agents, such as trehalose, mannitol and sorbitol (Kaur et al., 2015), and maltodextrin combined with gum Arabic (Cian et al., 2019) and with agar and carrageenan (Garzón et al., 2023). Nevertheless, the digestion of trehalose and maltodextrin releases glucose, which is not desirable when producing functional food with antidiabetic activity, and carrageenan has been linked to glucose intolerance (Bhattacharyya et al., 2015; Feferman et al., 2020) thus alternative encapsulating agents should be used instead. In this regard, Arabic gum is a polysaccharide frequently used as encapsulating agent due to its high solubility in water leading to low viscous solution, as well as its stabilizing and emulsifying properties (Daoub et al., 2018). Furthermore, Arabic gum does not provide glucose during digestion as it is not mostly digestible, making it suitable for encapsulating antidiabetic peptides (Phillips, 1998). In addition, studies have shown that Arabic gum may lower blood glucose levels by inhibiting the absorption of glucose in the intestine (Subtil et al., 2014).

On the other hand, electrospraying is an alternative drying technique (Bock et al., 2012) consisting in the application of a high-voltage electric field between the tip of a needle and a grounded collector to induce the ejection of the solution. Upon reaching a high electrostatic field, the meniscus interface polarizes and forms a conical shape known as a Taylor cone. With increasing voltage, the electric force overcomes the surface tension, and a jet is released towards

the collector (Xue et al., 2019). Under sufficiently low solution viscoelasticity conditions, the jet destabilizes to form small, charged droplets that disperse due to electrostatic forces (Xue et al., 2019). Meanwhile, solvent evaporation occurs in the travel of the droplets to the collector, leading to the obtaining of nano-microcapsules in powdered form (García-Moreno et al., 2021). Although this method has been previously used for the encapsulation of diverse bioactive protein hydrolysates/peptides (Furtmann et al., 2017; Kumar et al., 2021), to the best of our knowledge, there are no previous studies on the encapsulation of peptides exhibiting antidiabetic activity.

Therefore, this study aimed at investigating the encapsulation by electrospraying of a *Tenebrio molitor* protein hydrolysate containing bioactive peptides which exhibit antidiabetic activity. For the sake of comparison between encapsulation technologies, the encapsulation of the hydrolysate by spray-drying was also evaluated. Thus, this work specifically examines the efficacy of electrospraying and spray-drying techniques in protecting these bioactive peptides. Initially, the formulation of the feed solution was optimized to obtain a stable electrospraying process and encapsulates with adequate morphology. Subsequently, encapsulates where produced using the optimal formulation by electrospraying and also by spray-drying. The obtained encapsulates were characterized based on their morphology and particle size distribution. Moreover, their surface nitrogen content was evaluated to determine the encapsulation efficiency. Finally, the *in vitro* retention of DPP-IV-inhibitory activity by the encapsulated hydrolysate was investigated.

2. Materials and Methods

2.1. Materials

Whey protein hydrolysate (84 wt.% protein content), which was used as model protein in the optimization of the formulation, and the Arabic gum were kindly donated by Abbott Laboratories S.A (Granada, Spain) and Nexira (Serqueux, France), respectively. Pullulan was supplied by Hayashibara Co., Ltd. (Okayama, Japan). Tween 20 was purchased from Sigma Aldrich (Darmstadt, Germany). *Tenebrio molitor* meal (68.01 wt.% protein) was kindly provided by Tebrio (Salamanca, Spain), which was ground to powder. Alcalase (subtilisin, EC 3.4.21.62) was purchased from Novozymes (Bagsvaerd, Denmark). DPP-IV enzyme (EC 3.4.14.5) and the substrate Gly-pro-p-nitroanilide were supplied by Sigma Aldrich (St. Louis, US) and stored at -20 °C until use.

2.2. Production of the *Tenebrio molitor* protein hydrolysate

The enzymatic hydrolysis of *Tenebrio molitor* meal was conducted in a jacketed reactor connected to an automatic titrator (718 Stat Titrino, Metrohm, Herisau, Switzerland). Briefly, the *T. molitor* hydrolysis was conducted at 50 °C and pH 8. Thirty g/L protein was dissolved in distilled water and Alcalase 2.4 L (EC 3.4.21.62) was added at the beginning of the reaction at a 3% enzyme-to-substrate (protein) ratio. The reaction continued until the degree of hydrolysis (DH), measured by the pH-stat method (Musaei et al., 2017), was 20%. The resulting hydrolysate was then deactivated by heating the solution at 100 °C for 15 min, centrifuged at 5,300 g for 15 min and vacuum filtered through an 8 μm cellulose filter. The supernatant was lyophilized (LyoMicron, Coolvacuum Technologies S.L., Barcelona, Spain) and the powdered product was stored at −20 °C. Nitrogen content the obtained hydrolysate powder was determined in triplicate according to the Dumas method using a Flash 2000 CHNS/O elemental analyzer (Thermo Scientific, Waltham, MA, USA). Protein content was calculated assuming a nitrogen-to-protein factor of 5.6 (Adler-Nissen, 1986), resulting in 68.47 ± 0.39 wt.%.

2.3. Production of electrosprayed capsules

To encapsulate the *T. molitor* hydrolysate, Arabic gum and pullulan were used as encapsulating material and Tween 20 was employed as surfactant. These compounds were dissolved in distilled water and stirred overnight (350 rpm) at room temperature. The concentration of protein was kept at 20 wt.% in the final capsule, whereas Arabic gum at 15 wt.% and pullulan at 1-4 wt.% were referred to the feed formulation. Tween 20 at 1 wt.% (referred to Arabic gum and pullulan) was also used. The solution was electrosprayed utilizing a system comprising a drying chamber, equipped with a high voltage power supply (adjustable up to 30 kV), a syringe pump, and a collector plate (15 x 15 cm, made of stainless steel) (SpinBox Electrospinning; Bioinicia, Valencia, Spain). A 5 mL syringe containing the solutions was mounted onto the syringe pump and 16G needles (Proto Advantage, Hamilton, ON, Canada) were used. A monoaxial single-phase emitter (one needle) was used for the optimization of the formulation, while a monoaxial multi-emitter consisting of five parallel needles was used for increasing productivity of the optimum formulation. The emitter was positioned 15 cm away from the collector plate in a horizontal configuration. The flow rate and voltage were kept at 0.2 mL/h and 22 kV, respectively. The electrospraying process was carried out at room temperature and relative humidity conditions (21–27 °C, 36–51 %RH) in batches of 1 h. The powder collected from the different batches was gently mixed and stored in plastic Eppendorf tubes at 4 °C until further use.

2.4. Production of the spray-dried capsules

The obtained optimum feed solution containing the *T. molitor* solution was prepared as previously described to produce electrosprayed capsules, with and without pullulan and Tween 20. The spray-drying process was carried out in a laboratory-scale spray-drier (Büchi B-190; Büchi Labortechnik, Flawill, Switzerland) using a nozzle with 0.7 mm diameter (Büchi, Flawill, Switzerland). The temperature of inlet air was set at 190 °C and the temperature of the outlet air was kept at 95-97 °C. The drying airflow was fixed at 25 Nm3/h. Once the different microcapsules were collected, they were stored at −20 °C in the dark until analysis.

2.5. Characterization of the capsules

2.5.1. Morphology and particle size distribution

The morphology of the capsules was examined using scanning electron microscopy (SEM) on a FESEM microscope (LEO 1500 GEMINI, Zeiss, Germany). Depending on the employed encapsulation technique, a slender layer of microcapsules (via spray-drying) or a segment of aluminum foil measuring approximately 0.5 x 0.5 cm enclosing the sample (via electrospraying) was affixed onto a carbon tape on a pin and carbon-coated using an EMITECH K975X Turbo-Pumped Thermal Evaporator (Quorum Technologies, UK). SEM images were captured in the range of 2K×-20K× in case of electrosprayed capsules and 200×-2K× in case of spray-dried capsules with a 3 kV accelerating voltage and 30 μm aperture. The particle size distributions and mean diameters were determined by measuring 200 randomly selected particles using the ImageJ software (National Institute of Health, USA).

2.5.2. X-ray Photoelectron Spectroscopy (XPS)

The presence of *T. molitor* hydrolysate on the surface of the microparticles was analyzed by determining the nitrogen surface using X-ray photoelectron spectroscopy (XPS). The microparticles were transferred to a glass slide and analyzed using a Kratos Axis Ultra-DLD (Kratos Analytical, Manchester, UK) The samples were subjected to both an overall spectrum analysis (under conditions of 75 W power and 160 eV pass energy) and a quantification of carbon, oxygen, and nitrogen. Charge neutralization was activated, and the penetration depth was maintained at less than 10 nm.

2.5.3. DPP-IV inhibitory activity

The DPP-IV-inhibitory activity of the produced *T. molitor* hydrolysate and the microcapsules loaded with the hydrolysate was measured following a modified protocol based on Lacroix and Li-Chan (2012) (Janssen et al., 2017). Briefly, 25 μL of DPP-IV enzyme at 0.02 U/mL were incubated at 37 °C with 100 μL of *T. molitor* hydrolysate or capsules aqueous solutions at

varying concentrations (0.25-5 mg/mL) for 10 min. Subsequently, the reaction was initiated by the addition of 50 µL of 1 mM Gly-Pro-p-nitroanilide. The release of the reaction product (p-nitroanilide) was monitored by measuring absorbance at 405 nm every 2 min for 2 h at 37 °C using a Multiskan FC microplate photometer (Thermo Scientific, Vantaa, Finland). Each sample was analyzed in triplicate and a color control was added. The inhibition activity was calculated by comparing the reaction progress to a control (distilled water) as follows:

$$DPP-IV \quad inhibitory \quad activity \quad \left(\%\right) = \frac{1-p_i}{p_0} \cdot 100$$

Where p_i is the slope in the presence of inhibitor (peptide) and p_0 is the slope obtained in the absence of inhibitor (control). The half-maximal inhibitory concentration (IC_{50}) of each sample was calculated. Results are expressed in mg protein/mL as the mean ± standard deviation.

2.5.4. Statistical analysis

The dataset underwent analysis of variance (ANOVA) using Statgraphics version 5.1 (Statistical Graphics Corp., Rockville, MD, USA). Tukey's Honest Significant Difference (HSD) multiple range test was employed at the 95% confidence level ($p < 0.05$) to discern significant variations among mean values.

3. Results

3.1. Optimization of the formulation for electrospraying

Arabic gum was employed as the main encapsulating agent due to its excellent encapsulating properties such as water solubility, stabilizing and emulsifying properties and low viscosity of its aqueous solutions (Lacroix & Li-Chan, 2012). Additionally, Tween 20, a non-ionic surfactant, was used to improve solution properties by reducing surface tension and enhancing viscoelastic properties (Daoub et al., 2018; Lin et al., 2004). Finally, to enhance the stability of the Taylor cone and, thus, the electrospraying process, the addition of pullulan as secondary encapsulating agent was tested. The addition of pullulan leads to an increase in the viscoelasticity of the feed solution due to the interactions and entanglements that occur between the pullulan chains and between the chains of Arabic gum and pullulan (García-Moreno et al., 2021). The latter enhances the stability of the Taylor cone when working at higher flowrate, which increases productivity (Perez-Masia et al., 2014). Nevertheless, pullulan exhibits a high electrospinning capacity in water-based solutions, which is not beneficial for the aimed application, as electrospun fibers, unlike nano/microcapsules, result in continuous mats that are challenging to disperse in any food matrix (García-Moreno et al., 2018).

First, the optimization of the Arabic gum content in the feed was investigated. We observed that using Arabic gum in the range 15-40 wt.% did not properly electrosprayed

(results not shown). Therefore, and based in previous studies using glucose syrup and dextran (Perez-Masia et al., 2014), we fixed the Arabic gum concentration in the feed to 15 wt.%, which will lead to low viscoelasticity and reduced capsule size and added a low content of pullulan and 1 wt.% of Tween 20 (with respect of the total biopolymer). Therefore, the solution comprised of 20 wt.% (in the final capsule) of whey protein, which was used as model protein, 15 wt.% Arabic gum and 1 wt.% Tween 20 (referred to pullulan and Arabic gum concentrations) was electrosprayed, varying the concentration of pullulan in the range 0.5-4 wt.%. Samples were characterized using SEM (Figure 1). As expected, in capsules with lower amounts of pullulan (i.e., 0.5, 0.75 and 1 wt.%), there was only a faint hint of any strands emerging from the capsules, while for concentrations of above 1 wt.%, a greater number and longer strands could be observed. When pullulan concentrations reached 2 wt.%, a notable change in the morphology of the capsules became apparent, transitioning from spheres to interwoven and thick fibers, which turned especially visible at 3 and 4 wt.%. This was attributed, as mentioned before, to the high electrospinning capability exhibited by pullulan (García-Moreno et al., 2018). It should be noted that solutions with both 0.5 wt.% and 0.75 wt.% pullulan concentrations manifested a marginally superior capsule morphology in comparison to the encapsulates with a 1 wt.% concentration. Nevertheless, the observed productivity was much lower for the first two formulations, when pullulan concentration was kept under 1 wt.%. These two formulations (those with 0.5 and 0.75 wt.%) also presented a higher instability in achieving and maintaining a stable Taylor cone during the electrospraying process, which was manifested as an elongated shape of the cone as well as reduced productivity of the process. Taking all these aspects into consideration, the formulation composed of 1 wt.% pullulan was deemed as the optimum.

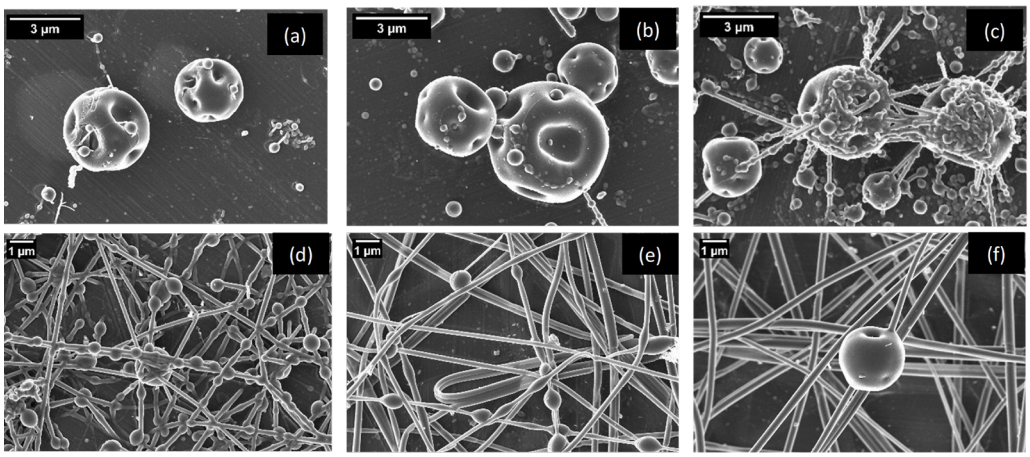

Figure 1. Morphology of the capsules obtained when using 20 wt.% whey protein (in the final capsule), 15 wt.% Arabic gum, 1wt.% Tween 20 (with respect to the total biopolymers) and pullulan 0.5 wt.% (a), 0.75 wt.% (b), 1 wt.% (c), 2 wt.% (d), 3 wt.% (e) and 4 wt.% (f).

SEM micrographs of the resulting T. molitor encapsulates from electrospraying (a) and spray-drying (b-c) processes are presented in Figure 2. The same formulation containing T. molitor hydrolysate, Arabic gum, Tween 20 and pullulan was both electrosprayed (Figure 2a) and spray-dried (Figure 2b). Figure 2c shows the SEM image of the capsules obtained by spray-drying, where the feed solution dried only contains Arabic gum and hydrolysate (e.g. without the additives pullulan and Tween 20). It can be observed in the three SEM images that most of the capsules were non-agglomerated, exhibiting a spherical shape with a wrinkled surface and concavities. The loss of spherical shape exhibited by various capsules might be attributed to an incomplete solvent evaporation and the unraveling of biopolymer chains, causing the unsolidified particles to be prone to deformation upon contacting the collector/walls of the equipment (Jacobsen et al., 2018). Regarding the wrinkles and concavities present on the surface of the capsules, these are characteristic of Arabic gum and could be attributed to the non-uniform distribution of this biopolymer within the droplets (Jacobsen et al., 2018; Zaeim et al., 2018) and the slow formation of this encapsulating agent film/crust during the drying process (Subtil et al., 2014). In the case of spray-dried capsules, several authors also suggest that this phenomenon may be related to the contraction experienced by the particles during drying and cooling (Ré, 1998). Comparing Figure 2b-c, it was noticeable that capsules containing pullulan and Tween 20 showed a moderately smoother surface. This reduction in wrinkles and indentations on the surface of the capsules was associated with the surfactant, owing to the preferential migration of Tween 20 molecules onto the surface of droplets/particles during atomization and drying (Adler et al., 2000; Kurozawa et al., 2009).

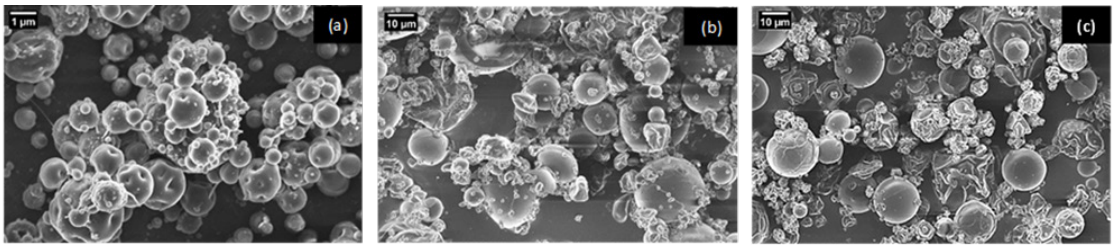

Figure 2. SEM images of capsules loaded with *Tenebrio molitor* hydrolysate formulated with pullulan and Tween 20, either electrosprayed (a) or spray-dried (b) and formulated without pullulan and Tween 20 and spray-dried (c).

The particle size distribution of the electrosprayed and spray-dried capsules is depicted in Figure 3. Particle size distribution of nano-microcapsules obtained by electrospraying was significantly narrower (ranging from 0.5 to 3.1 μm) compared to that of the microcapsules produced by spray-drying (ranging from 4.6-3.4 to 39-36 μm with/without the presence of additives, respectively). For electrospraying technique, capsules with an average size of 1.2 ± 0.5 μm were produced, with 91% of them having a diameter below 2 μm. This smaller particle size obtained employing electrospraying method is attributed to the breakup of droplets through Coulombic repulsion forces during the process, promoting the formation of ultrafine encapsulates with a narrow diameter distribution at the high voltage used (22 kV) (Abdul Mudalip et al., 2021). This is also facilitated by the presence of Tween 20 as surfactant, as it reduces surface tension and aids in the disintegration of droplets, leading to the formation of finer and smaller particles (Adhikari et al., 2009; Ghaeb et al., 2015).

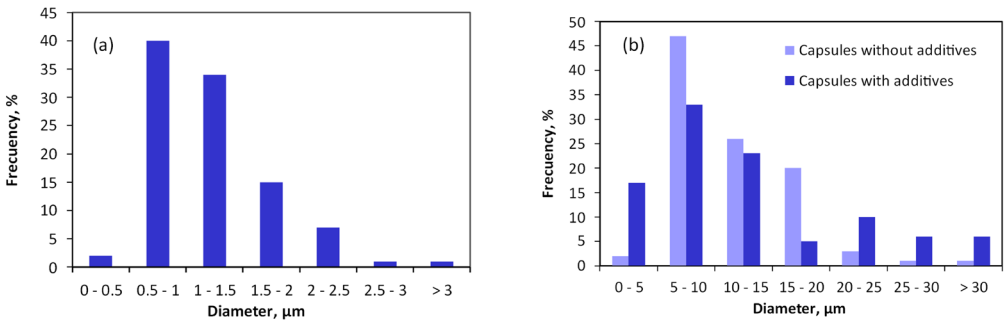

Figure 3. Particle size distribution of the capsules produced by (a) electrospraying and (b) spray-drying.

Microcapsules obtained by spray-drying which contain additives had an average size of 12.4 ± 8.7 μm, while those without additives showed an average size of 11.3 ± 5.76 μm. It is worth noting that there was a higher number of microcapsules of larger size when pullulan and Tween 20 were present. Specifically, only 78% of the capsules were under 20 μm in the presence of additives compared to 95% when no additives were included. This was most likely due to the higher solids content and thus increased viscosity of the solution provided when adding pullulan and Tween 20, bringing about larger droplets after atomization and, consequently, larger particles (García-Moreno et al., 2021; Gharsallaoui et al., 2007). Despite the larger size of the spray-dried capsules compared to the electrosprayed ones, it can be considered sufficiently small, as it is on the order of tens of microns. In fact, according to previous studies, particles with sizes below 50 μm are not capable of being detected as individual entities in the human mouth (Hogan et al., 2001). Therefore, these microcapsules obtained by spray-drying could be employed to enrich food matrices without the capsules

being perceptible on the taste buds. Moreover, a high surface area to volume ratio (small capsules) results in a quicker release, as fluids can penetrate the particles more easily, facilitating enhanced bioactive diffusion and accelerated degradation of the polymeric matrix (McClements, 2018). Nevertheless, it should be highlighted that through spray-drying process, it is common to obtain a broad size range and particle size distribution for the produced encapsulates (Bock et al., 2012). This variation could result in capsules exhibiting diverse performance concerning the protection and administration of bioactive peptides (Berraquero-García, Pérez-Gálvez, et al., 2023; Woo & Bhandari, 2013).

3.2. Surface nitrogen of the capsules

To assess the effectiveness of the encapsulation of *T. molitor* hydrolysate, the mass concentration of nitrogen on the surface of the capsules was determined. The surface nitrogen concentration of the hydrolysate and the encapsulating agents, namely, Arabic gum and pullulan, was also determined. Nevertheless, that of Tween 20, being a fluid, could not be evaluated, although nitrogen is not present in the molecule of Tween 20. The XPS spectra of the samples are illustrated in Figure 4. The various peaks correspond to the identification of carbon at 283.0 eV, nitrogen at 398.0 eV, and oxygen at 530.0 eV. While the peaks corresponding to carbon and oxygen can be observed for all the samples, the carbon peak is particularly intense for the protein hydrolysate as expected from its composition (Figure 4c). The peak corresponding to nitrogen is only significantly present in the *Tenebrio molitor* hydrolysate (Figure 4c) and the corresponding capsules (Figure 4d-f). Therefore, the presence of nitrogen in the surface of the encapsulates indicates that some of the peptides must have migrated to the surface of the capsules during the drying processes.

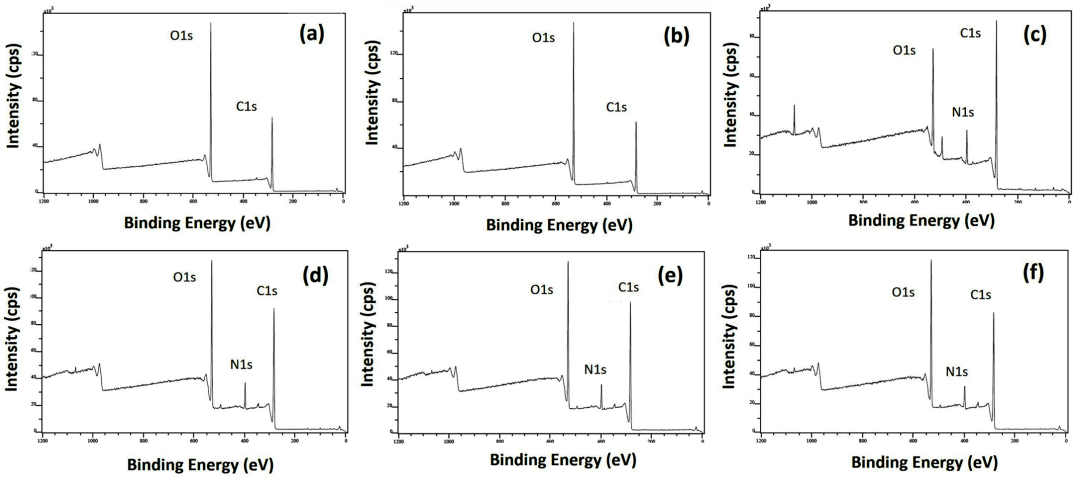

Figure 4. XPS spectra of Arabic gum (a), pullulan (b), *Tenebrio molitor* hydrolysate (c) and electrosprayed capsules (d) and spray-dried capsules with (e) and without additives (f).

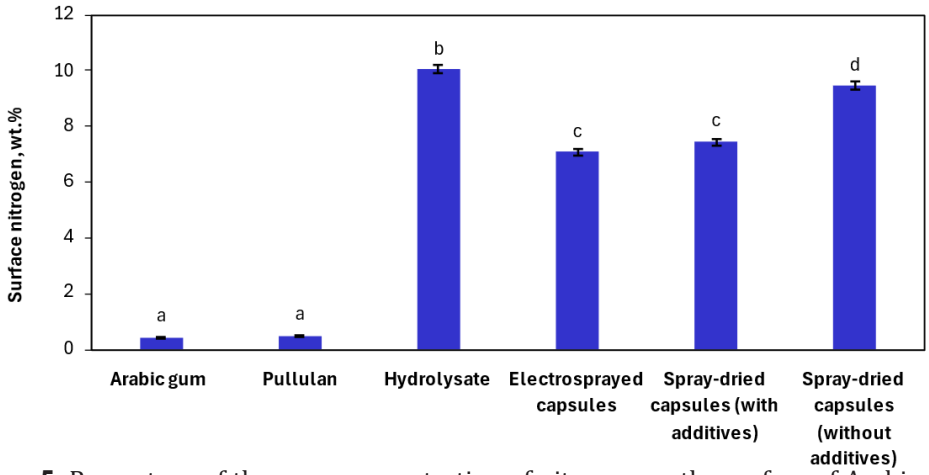

Figure 5. Percentage of the mass concentration of nitrogen on the surface of Arabic gum, pullulan, *Tenebrio molitor* hydrolysate, and the produced nano-microcapsules. Different letters denote significant differences between samples ($p \leq 0.05$).

The quantification of the amount of each material at the surface of the samples is shown in Figure 5 in terms of peak intensities. As can be observed, a small concentration of nitrogen, specifically 0.44 wt.%, was found on the Arabic gum sample. This compound is primarily constituted of polysaccharides, but it also contains a small protein fraction (< 2 wt.%) in its composition (Rahmani-Manglano et al., 2023), which could justify the presence of nitrogen on its surface (small peak shown in Figure 4a). Although pullulan is a polysaccharide and, therefore, should not contain nitrogen in its composition, the XPS revealed a nitrogen concentration on its surface of 0.49 wt.%, which could be attributed to sample contamination during its preparation or measurement. Regarding the hydrolysate, a concentration of nitrogen of 10 wt.% was found when using XPS.

In comparison, all capsules presented lower surface nitrogen values than the hydrolysate, which implies that encapsulation was achieved. Electrosprayed capsules exhibited 7 wt.% of surface nitrogen, spray-dried capsules containing additives had 7.4 wt.% of surface nitrogen and spray-dried capsules without additives 9.5 wt.%. Thus, capsules produced by electrospraying and spray-drying with additives presented a similar concentration of nitrogen on the surface, whereas the highest content of surface nitrogen was obtained for the spray-dried capsules without additives. This was most likely due to the absence of surfactant, as Tween 20 molecules migrate more readily to the air-liquid interface than peptides because of their higher surface activity. Tween 20 is also capable of forming networks with the peptides and, consequently, restricting their movement to the interface (Sanchez et al., 2002). Therefore, both the preferential migration and capability to form networks of Tween 20 reduce the aggregation/localization of the peptides at the interface during spray-drying and electrospraying processes. Nonetheless, it is normal to find diffusion of the protein to the surface due to drying kinetics, as the surface activity

of peptides could result in their adsorption onto the droplet surface, inducing a diffusional flux towards it. Additionally, as the evaporating droplet diminishes, its receding surface contributes to a rise in solute concentrations at the surface (Sarabandi & Jafari, 2020).

3.3. DPP-IV inhibitory activity

After encapsulation, it is crucial that the bioactive peptides comprising the hydrolysate maintain their original bioactivity. Hence, the DPP-IV-inhibitory activity of the non-encapsulated *T. molitor* hydrolysate was compared to that of the encapsulated hydrolysate. The results were expressed as the concentration of protein either in the non- or encapsulated forms at which 50% inhibition of the enzyme was achieved (IC_{50}), which are presented in Figure 6. The IC_{50} value for the initial *T. molitor* hydrolysate was 1.29 ± 0.07 mg protein/mL. Garzón et al. (2023) reported a similar value, approximately 1.5 mg protein/mL, for the brewer's spent grain hydrolysate, employing Neutral protease-Purazyme and Flavourzyme enzymes for the hydrolysis procedure (Garzón et al., 2023). The inhibitory activity of the hydrolysates depends on several factors regarding their peptide composition, among which their peptide chain length (PCL), their content of hydrophobic amino acids and the position of said amino acids play significant roles (Ojeda-Montes et al., 2018; Vehring, 2008). Particularly, short peptides (< 7 amino acids) with the presence of proline between the first and fourth positions relative to N-terminal, and alanine in the first or second position relative to the N-terminal have been determined as favorable (González-Montoya et al., 2018; Y. Yu et al., 2017). Concerning this, numerous studies indicate that *T. molitor* larvae meal exhibits a composition rich in leucine, valine, alanine, and proline (Nongonierma et al., 2018; X. Yu et al., 2021). This composition could explain the high DPP-IV inhibitory activity observed on *T. molitor* hydrolysates by various studies, reporting IC_{50} values of 0.83 and 0.91 mg protein/mL using Papain (Azagoh et al., 2016), and Flavourzyme (Dávalos Terán et al., 2020) enzymes for the hydrolysis, which aligns with our results.

In comparison, the electrosprayed encapsulates as well as the spray-dried encapsulates containing additives showed a similar percentage of DPP-IV inhibition when compared to the free hydrolysate, with an IC_{50} value of 1.50 ± 0.07 mg protein/mL 1.61 ± 0.08 mg protein/mL, respectively. On the other hand, the spray-dried capsules without additives presented a significantly higher IC_{50} value (1.99 ± 0.03 mg protein/mL) when compared to those of the electrosprayed and spray-dried (with additives) capsules. Therefore, the DPP-IV inhibitory activity decreased by 16.16%, 24.13%, and 53.60%, respectively for the electrospraying, spray-drying with additives or spray-drying without additives encapsulation processes. It is worth noting that Garzón et al. (2023) reported higher values, around 3.5 mg protein/mL, for the encapsulates obtained by spray-drying using agar and/or carrageenan together with maltodextrin as carriers when encapsulating a hydrolysate with an initial IC_{50} value around 1.5 mg protein/mL (Garzón et al., 2023).

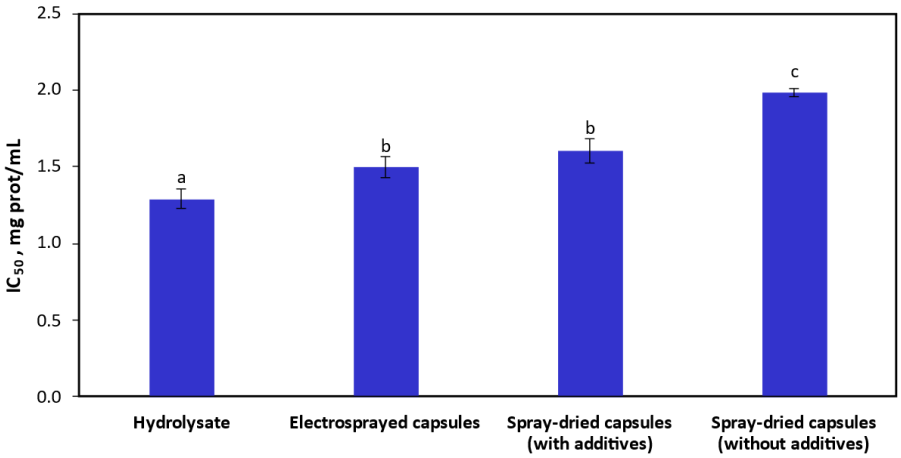

Figure 6. DPP-IV inhibitory activity represented by the IC_{50} values for the *Tenebrio molitor* hydrolysate and the different encapsulates. Values are presented as the mean of three replicates ± standard deviation. Different letters denote significant differences between samples ($p \leq 0.05$).

Regarding the loss of bioactivity in electrosprayed capsules, this might be attributed to a slight denaturation of the peptides due to the high voltage used or a potential detrimental interaction of peptides and the biopolymers used. Nevertheless, electrospraying process is conducted at room temperature, thus, there is no significant loss of their activity. Onyekuru et al. (2021b) found that, for the encapsulation of alkaline phosphatase with PEO as encapsulating agent, employing a voltage of 22.5 kV led to a minor loss of enzyme activity (Tan et al., 2022). With respect to the spray-dried capsules, the decrease in the inhibitory activity of the DPP-IV enzyme was most likely due to the high temperature involved in the process, leading to the thermal degradation of the hydrolysate, although this degradation should be minimal for inlet temperatures ranging from 130 to 190 °C and outlet temperatures below 100 °C, as reported in literature (Cao et al., 2020; Onyekuru et al., 2021; Webber et al., 2018). The loss of inhibitory activity in spray-dried capsules without additives was noticeably higher and could be related to the absence of Tween 20. This surfactant tends to migrate to the surface of the capsule and form networks with the peptides, preventing them from moving towards it and avoiding further degradation due to exposure to heat at the surface of the particle. This reduced migration of peptides to the interface also results in minimized damage caused by shear tension and dehydration stress during drying of droplets, enhancing the bioactivity of the peptides (Sarabandi & Jafari, 2020). Hence, a lower nitrogen concentration on the surface implies that peptides have remained inside the capsule, where they are better protected. In fact, after conducting a correlation comparative between the surface nitrogen and the DPP-IV enzyme inhibition, it was found that the coefficient of determination (R^2) was 0.99. In addition to the process conditions and the incorporation of Tween 20, another

factor that may have affected the bioactivity is the secondary encapsulating agent. No studies have been found in literature employing pullulan as a carrier of compounds with antidiabetic activity. Nevertheless, Rahmani-Manglano et al. (2023) reported that the addition of pullulan improved the oxidative stability of omega-3 encapsulates due to its inherently impermeability to oxygen (Rahmani-Manglano et al., 2023). Hence, it would be interesting to investigate in future studies whether pullulan influences antidiabetic activity.

4. Conclusions

In this study, the encapsulation of *Tenebrio molitor* hydrolysate was studied using electrospraying and spray-drying processes with Arabic gum as the primary encapsulating agent. The addition of pullulan to improve viscoelasticity was studied, and the concentration was optimized at 1 wt% together with the use of Tween 20 to obtain a stable electrospraying process. Electrospraying yielded better results in terms of size and particle distribution compared to spray-drying, producing smaller and more uniform capsules. There was no significant difference observed between electrosprayed capsules and spray-dried capsules containing additives regarding nitrogen content on their surface or DPP-IV inhibitory activity. Conversely, spray-dried capsules without additives showed lower bioactivity and encapsulation efficiency with a higher mass concentration of nitrogen on the surface. This was attributed to the absence of surfactant, which acts reducing the migration of peptides to the liquid/air interface during drying. Overall, it could be noted that microcapsules obtained by spray-drying when adding additives (pullulan and Tween 20) to the feed resulted in similar encapsulation efficiency and antidiabetic activity as achieved for the capsules obtained by electrospraying. Nevertheless, it is worth noting that spray-drying provides higher productivity than electrospraying due to its superior scalability.

5. References

Abdul Mudalip, S. K., Khatiman, M. N., Hashim, N. A., Che Man, R., & Arshad, Z. I. M. (2021). A short review on encapsulation of bioactive compounds using different drying techniques. *Materials Today: Proceedings*, *42*, 288–296. https://doi.org/10.1016/J.MATPR.2021.01.543

Adhikari, B., Howes, T., Wood, B. J., & Bhandari, B. R. (2009). The effect of low molecular weight surfactants and proteins on surface stickiness of sucrose during powder formation through spray drying. *Journal of Food Engineering*, *94*(2), 135–143. https://doi.org/10.1016/J.JFOODENG.2009.01.022

Adler, M., Unger, M., & Lee, G. (2000). Surface composition of spray-dried particles of bovine serum albumin/trehalose/surfactant. *Pharmaceutical Research*, *17*(7), 863–870. https://doi.org/10.1023/A:1007568511399

Adler-Nissen, Jens. (1986). *Enzymic hydrolysis of food proteins. New York: Elsevier Applied Science Publishers*. p9-17 and p146-147.

Aguilar-Toala, J. E., Quintanar-Guerrero, D., Liceaga, A. M., & Zambrano- Zaragoza, M. L. (2022). Encapsulation of bioactive peptides: a strategy to improve the stability, protect the nutraceutical bioactivity and support their food applications. *RSC Advances*, *12*(11), 6449–6458. https://doi.

org/10.1039/D1RA08590E

Ahrén, B. (2007). DPP-4 inhibitors. *Best Practice & Research Clinical Endocrinology & Metabolism*, *21*(4), 517–533. https://doi.org/10.1016/J.BEEM.2007.07.005

Alu'datt, M. H., Alrosan, M., Gammoh, S., Tranchant, C. C., Alhamad, M. N., Rababah, T., Zghoul, R., Alzoubi, H., Ghatasheh, S., Ghozlan, K., & Tan, T. C. (2022). Encapsulation-based technologies for bioactive compounds and their application in the food industry: A roadmap for food-derived functional and health-promoting ingredients. *Food Bioscience*, *50*, 101971. https://doi.org/10.1016/J.FBIO.2022.101971

Antony, P., & Vijayan, R. (2021). Bioactive Peptides as Potential Nutraceuticals for Diabetes Therapy: A Comprehensive Review. *International Journal of Molecular Sciences*, *22*(16), 9059. https://doi.org/10.3390/IJMS22169059

Azagoh, C., Ducept, F., Garcia, R., Rakotozafy, L., Cuvelier, M. E., Keller, S., Lewandowski, R., & Mezdour, S. (2016). Extraction and physicochemical characterization of Tenebrio molitor proteins. *Food Research International*, *88*, 24–31. https://doi.org/10.1016/J.FOODRES.2016.06.010

Azevedo, M. A., Cerqueira, M. A., Gonçalves, C., Amado, I. R., Teixeira, J. A., & Pastrana, L. (2023). Encapsulation of vitamin D3 using rhamnolipids-based nanostructured lipid carriers. *Food Chemistry*, *427*, 136654. https://doi.org/10.1016/J.FOODCHEM.2023.136654

Benzertiha, A., Kierończyk, B., Kołodziejski, P., Pruszyńska–Oszmałek, E., Rawski, M., Józefiak, D., & Józefiak, A. (2020). Tenebrio molitor and Zophobas morio full-fat meals as functional feed additives affect broiler chickens' growth performance and immune system traits. *Poultry Science*, *99*(1), 196–206. https://doi.org/10.3382/PS/PEZ450

Benzertiha, A., Kierończyk, B., Rawski, M., Józefiak, A., Kozłowski, K., Jankowski, J., & Józefiak, D. (2019). Tenebrio molitor and Zophobas morio Full-Fat Meals in Broiler Chicken Diets: Effects on Nutrients Digestibility, Digestive Enzyme Activities, and Cecal Microbiome. *Animals 2019, Vol. 9, Page 1128*, *9*(12), 1128. https://doi.org/10.3390/ANI9121128

Berraquero-García, C., Pérez-Gálvez, R., Espejo-Carpio, F. J., Guadix, A., Guadix, E. M., & García-Moreno, P. J. (2023). Encapsulation of Bioactive Peptides by Spray-Drying and Electrospraying. *Foods*, *12*(10), 2005. https://doi.org/10.3390/foods12102005

Berraquero-García, C., Rivero-Pino, F., Ospina, J. L., Pérez-Gálvez, R., Espejo-Carpio, F. J., Guadix, A., García-Moreno, P. J., & Guadix, E. M. (2023). Activity, structural features and in silico digestion of antidiabetic peptides. *Food Bioscience*, *55*, 102954. https://doi.org/10.1016/J.FBIO.2023.102954

Bhattacharyya, S., Feferman, L., Unterman, T., & Tobacman, J. K. (2015). Exposure to Common Food Additive Carrageenan Alone Leads to Fasting Hyperglycemia and in Combination with High Fat Diet Exacerbates Glucose Intolerance and Hyperlipidemia without Effect on Weight. *Journal of Diabetes Research*, *2015*. https://doi.org/10.1155/2015/513429

Bock, N., Dargaville, T. R., & Woodruff, M. A. (2012). Electrospraying of polymers with therapeutic molecules: State of the art. *Progress in Polymer Science*, *37*(11), 1510–1551. https://doi.org/10.1016/J.PROGPOLYMSCI.2012.03.002

Cao, C., Zhao, X., Zhang, C., Ding, Z., Sun, F., & Zhao, C. (2020). Effect of inlet temperature on the physicochemical properties of spray-dried seed-watermelon seed protein powder. *Journal of Food Science*, *85*(10), 3442–3449. https://doi.org/10.1111/1750-3841.15432

Cho, K. H., Kang, S. W., Yoo, J. S., Song, D. K., Chung, Y. H., Kwon, G. T., & Kim, Y. Y. (2019). Effects of mealworm (*Tenebrio molitor*) larvae hydrolysate on nutrient ileal digestibility in growing pigs compared to those of defatted mealworm larvae meal, fermented poultry by-product, and hydrolyzed fish soluble. *Asian-Australasian Journal of Animal Sciences*, *33*(3), 490–500. https://doi.org/10.5713/AJAS.19.0793

Cian, R. E., Campos-Soldini, A., Chel-Guerrero, L., Drago, S. R., & Betancur-Ancona, D. (2019). Bioactive Phaseolus lunatus peptides release from maltodextrin/gum arabic microcapsules obtained by spray drying after simulated gastrointestinal digestion. *International Journal of Food Science & Technology*, *54*(6), 2002–2009. https://doi.org/10.1111/IJFS.14031

Daoub, R. M. A., Elmubarak, A. H., Misran, M., Hassan, E. A., & Osman, M. E. (2018). Characterization

and functional properties of some natural Acacia gums. *Journal of the Saudi Society of Agricultural Sciences*, *17*(3), 241–249. https://doi.org/10.1016/J.JSSAS.2016.05.002

Dávalos Terán, I., Imai, K., Lacroix, I. M. E., Fogliano, V., & Udenigwe, C. C. (2020). Bioinformatics of edible yellow mealworm (Tenebrio molitor) proteome reveal the cuticular proteins as promising precursors of dipeptidyl peptidase-IV inhibitors. *Journal of Food Biochemistry*, *44*(2), e13121. https://doi.org/10.1111/JFBC.13121

De Marco, M., Martínez, S., Hernandez, F., Madrid, J., Gai, F., Rotolo, L., Belforti, M., Bergero, D., Katz, H., Dabbou, S., Kovitvadhi, A., Zoccarato, I., Gasco, L., & Schiavone, A. (2015). Nutritional value of two insect larval meals (Tenebrio molitor and Hermetia illucens) for broiler chickens: Apparent nutrient digestibility, apparent ileal amino acid digestibility and apparent metabolizable energy. *Animal Feed Science and Technology*, *209*, 211–218. https://doi.org/10.1016/J.ANIFEEDSCI.2015.08.006

Drucker, D. J. (2006). Enhancing the Action of Incretin Hormones: A New Whey Forward? *Endocrinology*, *147*(7), 3171–3172. https://doi.org/10.1210/EN.2006-0494

Errico, S., Spagnoletta, A., Verardi, A., Moliterni, S., Dimatteo, S., & Sangiorgio, P. (2022). Tenebrio molitor as a source of interesting natural compounds, their recovery processes, biological effects, and safety aspects. *Comprehensive Reviews in Food Science and Food Safety*, *21*(1), 148–197. https://doi.org/10.1111/1541-4337.12863

Feferman, L., Bhattacharyya, S., Oates, E., Haggerty, N., Wang, T., Varady, K., Tobacman, J. K., & Zhao, R. (2020). Carrageenan-Free Diet Shows Improved Glucose Tolerance and Insulin Signaling in Prediabetes: A Randomized, Pilot Clinical Trial. *Journal of Diabetes Research*, *2020*. https://doi.org/10.1155/2020/8267980

Furtmann, B., Tang, J., Kramer, S., Eickner, T., Luderer, F., Fricker, G., Gomez, A., Heemskerk, B., & Jähn, P. S. (2017). Electrospray Synthesis of Poly(lactide-co-glycolide) Nanoparticles Encapsulating Peptides to Enhance Proliferation of Antigen-Specific CD8+ T Cells. *Journal of Pharmaceutical Sciences*, *106*(11), 3316–3327. https://doi.org/10.1016/J.XPHS.2017.06.013

Galicia-Garcia, U., Benito-Vicente, A., Jebari, S., Larrea-Sebal, A., Siddiqi, H., Uribe, K. B., Ostolaza, H., & Martín, C. (2020). Pathophysiology of Type 2 Diabetes Mellitus. *International Journal of Molecular Sciences 2020, Vol. 21, Page 6275*, *21*(17), 6275. https://doi.org/10.3390/IJMS21176275

García-Moreno, P. J., Pelayo, A., Yu, S., Busolo, M., Lagaron, J. M., Chronakis, I. S., & Jacobsen, C. (2018). Physicochemical characterization and oxidative stability of fish oil-loaded electrosprayed capsules: Combined use of whey protein and carbohydrates as wall materials. *Journal of Food Engineering*, *231*, 42–53. https://doi.org/10.1016/J.JFOODENG.2018.03.005

García-Moreno, P. J., Rahmani-Manglano, N. E., Chronakis, I. S., Guadix, E. M., Yesiltas, B., Sørensen, A. D. M., & Jacobsen, C. (2021). Omega-3 nano-microencapsulates produced by electrohydrodynamic processing. *Omega-3 Delivery Systems: Production, Physical Characterization and Oxidative Stability*, 345–370. https://doi.org/10.1016/B978-0-12-821391-9.00017-X

Garzón, A. G., Cian, R. E., & Drago, S. R. (2023). Effects of agar-carrageenan wall materials and core-to-wall material ratio on physicochemical properties and in vitro bioaccessibility of microencapsulated bioactive peptides. *Food Hydrocolloids*, *139*, 108570. https://doi.org/10.1016/J.FOODHYD.2023.108570

Ghaeb, M., Tavanai, H., & Kadivar, M. (2015). Electrosprayed maize starch and its constituents (amylose and amylopectin) nanoparticles. *Polymers for Advanced Technologies*, *26*(8), 917–923. https://doi.org/10.1002/PAT.3501

Gharsallaoui, A., Roudaut, G., Chambin, O., Voilley, A., & Saurel, R. (2007). Applications of spray-drying in microencapsulation of food ingredients: An overview. *Food Research International*, *40*(9), 1107–1121. https://doi.org/10.1016/J.FOODRES.2007.07.004

Giroldi, M., Grambusch, I. M., Neutzling Lehn, D., & Volken de Souza, C. F. (2021). Encapsulation of dairy protein hydrolysates: Recent trends and future prospects. *Drying Technology*, *39*(11), 1513–1528. https://doi.org/10.1080/07373937.2021.1906695

González-Montoya, M., Hernández-Ledesma, B., Mora-Escobedo, R., & Martínez-Villaluenga, C. (2018). Bioactive Peptides from Germinated Soybean with Anti-Diabetic Potential by Inhibition of Dipeptidyl Peptidase-IV, α-Amylase, and α-Glucosidase Enzymes. *International Journal of Molecular*

Sciences 2018, Vol. 19, Page 2883, *19*(10), 2883. https://doi.org/10.3390/IJMS19102883

Gravel, A., & Doyen, A. (2020). The use of edible insect proteins in food: Challenges and issues related to their functional properties. *Innovative Food Science & Emerging Technologies*, *59*, 102272. https://doi.org/10.1016/J.IFSET.2019.102272

Hogan, S. A., McNamee, B. F., O'Riordan, E. D., & O'Sullivan, M. (2001). Emulsification and microencapsulation properties of sodium caseinate/carbohydrate blends. *International Dairy Journal*, *11*(3), 137–144. https://doi.org/10.1016/S0958-6946(01)00091-7

Hosseini, S. F., Soofi, M., & Rezaei, M. (2021). Enhanced physicochemical stability of ω-3 PUFAs concentrates-loaded nanoliposomes decorated by chitosan/gelatin blend coatings. *Food Chemistry*, *345*, 128865. https://doi.org/10.1016/J.FOODCHEM.2020.128865

Howard-Thompson, A., Khan, M., Jones, M., & George, C. M. (2018). Type 2 Diabetes Mellitus: Outpatient Insulin Management. *American Family Physician*, *97*(1), 29–37. https://www.aafp.org/pubs/afp/issues/2018/0101/p29.html

IDF Diabetes Atlas 2021 | IDF Diabetes Atlas. (n.d.). Retrieved March 11, 2024, from https://diabetesatlas.org/atlas/tenth-edition/

Iwaniak, A., Hrynkiewicz, M., Bucholska, J., Minkiewicz, P., & Darewicz, M. (2019). Understanding the nature of bitter-taste di- and tripeptides derived from food proteins based on chemometric analysis. *Journal of Food Biochemistry*, *43*(1), e12500. https://doi.org/10.1111/JFBC.12500

Jacobsen, C., García-Moreno, P. J., Mendes, A. C., Mateiu, R. V., & Chronakis, I. S. (2018). Use of Electrohydrodynamic Processing for Encapsulation of Sensitive Bioactive Compounds and Applications in Food. *Annual Review of Food Science and Technology*, *9*, 525–549. https://doi.org/10.1146/ANNUREV-FOOD-030117-012348

Janssen, R. H., Vincken, J. P., Van Den Broek, L. A. M., Fogliano, V., & Lakemond, C. M. M. (2017). Nitrogen-to-Protein Conversion Factors for Three Edible Insects: Tenebrio molitor, Alphitobius diaperinus, and Hermetia illucens. *Journal of Agricultural and Food Chemistry*, *65*(11), 2275–2278. https://doi.org/10.1021/ACS.JAFC.7B00471

Karami, Z., & Akbari-adergani, B. (2019). Bioactive food derived peptides: a review on correlation between structure of bioactive peptides and their functional properties. *Journal of Food Science and Technology*, *56*(2), 535–547. https://doi.org/10.1007/S13197-018-3549-4

Kaur, P., Singh, S. K., Garg, V., Gulati, M., & Vaidya, Y. (2015). Optimization of spray drying process for formulation of solid dispersion containing polypeptide-k powder through quality by design approach. *Powder Technology*, *284*, 1–11. https://doi.org/10.1016/J.POWTEC.2015.06.034

Krentz, A. J., Patel, M. B., & Bailey, C. J. (2012). New Drugs for Type 2 Diabetes Mellitus. *Drugs 2008 68:15*, *68*(15), 2131–2162. https://doi.org/10.2165/00003495-200868150-00005

Kumar, A., Belhaj, M., DiPette, D. J., & Potts, J. D. (2021). A Novel Alginate-Based Delivery System for the Prevention and Treatment of Pressure-Overload Induced Heart Failure. *Frontiers in Pharmacology*, *11*, 602952. https://doi.org/10.3389/FPHAR.2020.602952

Kurozawa, L. E., Park, K. J., & Hubinger, M. D. (2009). Effect of carrier agents on the physicochemical properties of a spray dried chicken meat protein hydrolysate. *Journal of Food Engineering*, *94*(3–4), 326–333. https://doi.org/10.1016/J.JFOODENG.2009.03.025

Lacroix, I. M. E., & Li-Chan, E. C. Y. (2012). Dipeptidyl peptidase-IV inhibitory activity of dairy protein hydrolysates. *International Dairy Journal*, *25*(2), 97–102. https://doi.org/10.1016/J.IDAIRYJ.2012.01.003

Li, Q., Hu, X., Perkins, P., & Ren, T. (2023). Antimicrobial film based on poly(lactic acid) and natural halloysite nanotubes for controlled cinnamaldehyde release. *International Journal of Biological Macromolecules*, *224*, 848–857. https://doi.org/10.1016/J.IJBIOMAC.2022.10.171

Lin, T., Wang, H., Wang, H., & Wang, X. (2004). The charge effect of cationic surfactants on the elimination of fibre beads in the electrospinning of polystyrene. *Nanotechnology*, *15*(9), 1375. https://doi.org/10.1088/0957-4484/15/9/044

Ma, J. J., Mao, X. Y., Wang, Q., Yang, S., Zhang, D., Chen, S. W., & Li, Y. H. (2014). Effect of spray drying and freeze drying on the immunomodulatory activity, bitter taste and hygroscopicity of hydrolysate

derived from whey protein concentrate. *LWT - Food Science and Technology*, *56*(2), 296–302. https://doi.org/10.1016/J.LWT.2013.12.019

Makrilakis, K. (2019). The Role of DPP-4 Inhibitors in the Treatment Algorithm of Type 2 Diabetes Mellitus: When to Select, What to Expect. *International Journal of Environmental Research and Public Health 2019, Vol. 16, Page 2720*, *16*(15), 2720. https://doi.org/10.3390/IJERPH16152720

Masood, R., & Khosravi-Darani, K. (2015). Biopeptides in Milk: Opiate and Antithrombotic Effects. *Mini-Reviews in Medicinal Chemistry*, *15*(10), 872–877. https://doi.org/10.2174/1389557515666150519104219

McClements, D. J. (2018). Encapsulation, protection, and delivery of bioactive proteins and peptides using nanoparticle and microparticle systems: A review. *Advances in Colloid and Interface Science*, *253*, 1–22. https://doi.org/10.1016/J.CIS.2018.02.002

Musaei, M., Mokhtari, J., Nouri, M., & Rad, Z. P. (2017). Fabrication and Characterization of Nanocapsules of PLGA Containing BSA Using Electrospray Technique. *Nanomedicine Research Journal*, *2*(3), 158–164. https://doi.org/10.22034/NMRJ.2017.03.003

Nongonierma, A. B., Dellafiora, L., Paolella, S., Galaverna, G., Cozzini, P., & FitzGerald, R. J. (2018). In silico approaches applied to the study of peptide analogs of Ile-Pro-Ile in relation to their dipeptidyl peptidase IV inhibitory properties. *Frontiers in Endocrinology*, *9*(JUN), 377191. https://doi.org/10.3389/FENDO.2018.00329

Nowak, V., Persijn, D., Rittenschober, D., & Charrondiere, U. R. (2016). Review of food composition data for edible insects. *Food Chemistry*, *193*, 39–46. https://doi.org/10.1016/J.FOODCHEM.2014.10.114

Ojeda-Montes, M. J., Gimeno, A., Tomas-Hernández, S., Cereto-Massagué, A., Beltrán-Debón, R., Valls, C., Mulero, M., Pujadas, G., & Garcia-Vallvé, S. (2018). Activity and selectivity cliffs for DPP-IV inhibitors: Lessons we can learn from SAR studies and their application to virtual screening. *Medicinal Research Reviews*, *38*(6), 1874–1915. https://doi.org/10.1002/MED.21499

Onyekuru, L. C., Moreira, A., Zhang, J., Angkawinitwong, U., Costa, P. F., Brocchini, S., & Williams, G. R. (2021). An investigation of alkaline phosphatase enzymatic activity after electrospinning and electrospraying. *Journal of Drug Delivery Science and Technology*, *64*, 102592. https://doi.org/10.1016/J.JDDST.2021.102592

Pei, J., Gao, X., Pan, D., Hua, Y., He, J., Liu, Z., & Dang, Y. (2022). Advances in the stability challenges of bioactive peptides and improvement strategies. *Current Research in Food Science*, *5*, 2162–2170. https://doi.org/10.1016/J.CRFS.2022.10.031

Perez-Masia, R., Lagaron, J. M., & Lopez-Rubio, A. (2014). Surfactant-aided electrospraying of low molecular weight carbohydrate polymers from aqueous solutions. *Carbohydrate Polymers*, *101*(1), 249–255. https://doi.org/10.1016/J.CARBPOL.2013.09.032

Perry, S. L., & McClements, D. J. (2020). Recent Advances in Encapsulation, Protection, and Oral Delivery of Bioactive Proteins and Peptides using Colloidal Systems. *Molecules 2020, Vol. 25, Page 1161*, *25*(5), 1161. https://doi.org/10.3390/MOLECULES25051161

Phillips, G. O. (1998). Acacia gum (Gum Arabic): A nutritional fibre; metabolism and calorific value. *Food Additives & Contaminants*, *15*(3), 251–264. https://doi.org/10.1080/02652039809374639

Rahmani-Manglano, N. E., Guadix, E. M., Jacobsen, C., & García-Moreno, P. J. (2023). Comparative Study on the Oxidative Stability of Encapsulated Fish Oil by Monoaxial or Coaxial Electrospraying and Spray-Drying. *Antioxidants*, *12*(2), 266. https://doi.org/10.3390/ANTIOX12020266

Ré, M. I. (1998). MICROENCAPSULATION BY SPRAY DRYING. *Drying Technology*, *16*(6), 1195–1236. https://doi.org/10.1080/07373939808917460

Rivero-Pino, F., Guadix, A., & Guadix, E. M. (2021). Identification of novel dipeptidyl peptidase IV and α-glucosidase inhibitory peptides from Tenebrio molitor. *Food & Function*, *12*(2), 873–880. https://doi.org/10.1039/D0FO02696D

Rizzello, C. G., Tagliazucchi, D., Babini, E., Sefora Rutella, G., Taneyo Saa, D. L., & Gianotti, A. (2016). Bioactive peptides from vegetable food matrices: Research trends and novel biotechnologies for synthesis and recovery. *Journal of Functional Foods*, *27*, 549–569. https://doi.org/10.1016/J.JFF.2016.09.023

Sanchez, C., Renard, D., Robert, P., Schmitt, C., & Lefebvre, J. (2002). Structure and rheological properties of acacia gum dispersions. *Food Hydrocolloids*, *16*(3), 257–267. https://doi.org/10.1016/S0268-005X(01)00096-0

Sarabandi, K., & Jafari, S. M. (2020). Improving the antioxidant stability of flaxseed peptide fractions during spray drying encapsulation by surfactants: Physicochemical and morphological features. *Journal of Food Engineering*, *286*, 110131. https://doi.org/10.1016/J.JFOODENG.2020.110131

Subtil, S. F., Rocha-Selmi, G. A., Thomazini, M., Trindade, M. A., Netto, F. M., & Favaro-Trindade, C. S. (2014). Effect of spray drying on the sensory and physical properties of hydrolysed casein using gum arabic as the carrier. *Journal of Food Science and Technology*, *51*(9), 2014–2021. https://doi.org/10.1007/S13197-012-0722-Z

Sun, X., Okagu, O. D., & Udenigwe, C. C. (2021). Encapsulation technology for protection and delivery of bioactive peptides. *Biologically Active Peptides: From Basic Science to Applications for Human Health*, 331–356. https://doi.org/10.1016/B978-0-12-821389-6.00028-5

Talarico, L., Clemente, I., Gennari, A., Gabbricci, G., Pepi, S., Leone, G., Bonechi, C., Rossi, C., Mattioli, S. L., Detta, N., & Magnani, A. (2024). Physiochemical Characterization of Lipidic Nanoformulations Encapsulating the Antifungal Drug Natamycin. *Nanomaterials 2024, Vol. 14, Page 726*, *14*(8), 726. https://doi.org/10.3390/NANO14080726

Tan, J., Yang, J., Zhou, X., Hamdy, A. M., Zhang, X., Suo, H., Zhang, Y., Li, N., & Song, J. (2022). Tenebrio molitor Proteins-Derived DPP-4 Inhibitory Peptides: Preparation, Identification, and Molecular Binding Mechanism. *Foods 2022, Vol. 11, Page 3626*, *11*(22), 3626. https://doi.org/10.3390/FOODS11223626

Vehring, R. (2008). Pharmaceutical particle engineering via spray drying. *Pharmaceutical Research*, *25*(5), 999–1022. https://doi.org/10.1007/S11095-007-9475-1

Webber, V., de Siqueira Ferreira, D., Barreto, P. L. M., Weiss-Angeli, V., & Vanderlinde, R. (2018). Preparation and characterization of microparticles of β-cyclodextrin/glutathione and chitosan/glutathione obtained by spray-drying. *Food Research International*, *105*, 432–439. https://doi.org/10.1016/J.FOODRES.2017.11.035

Woo, M. W., & Bhandari, B. (2013). Spray drying for food powder production. *Handbook of Food Powders: Processes and Properties*, 29–56. https://doi.org/10.1533/9780857098672.1.29

Xue, J., Wu, T., Dai, Y., & Xia, Y. (2019). Electrospinning and electrospun nanofibers: Methods, materials, and applications. *Chemical Reviews*, *119*(8), 5298–5415. https://doi.org/10.1021/ACS.CHEMREV.8B00593

Yang, G., Li, F., Zhang, H., Yan, H., Gao, S., Fu, Y., & Ye, F. (2024). Electrospinning for producing antifungal nanofibers consisting of prochloraz/hydroxypropyl-γ-cyclodextrin inclusion complex. *Industrial Crops and Products*, *211*, 118282. https://doi.org/10.1016/J.INDCROP.2024.118282

Yoo, J. S., Cho, K. H., Hong, J. S., Jang, H. S., Chung, Y. H., Kwon, G. T., Shin, D. G., & Kim, Y. Y. (2018). Nutrient ileal digestibility evaluation of dried mealworm (*Tenebrio molitor*) larvae compared to three animal protein by-products in growing pigs. *Asian-Australasian Journal of Animal Sciences*, *32*(3), 387–394. https://doi.org/10.5713/AJAS.18.0647

Yu, X., He, Q., & Wang, D. (2021). Dynamic Analysis of Major Components in the Different Developmental Stages of Tenebrio molitor. *Frontiers in Nutrition*, *8*, 689746. https://doi.org/10.3389/FNUT.2021.689746

Yu, Y., Jin, Y., Wang, F., Yan, J., Qi, Y., & Ye, M. (2017). Protein digestomic analysis reveals the bioactivity of deer antler velvet in simulated gastrointestinal digestion. *Food Research International*, *96*, 182–190. https://doi.org/10.1016/J.FOODRES.2017.04.002

Zaeim, D., Sarabi-Jamab, M., Ghorani, B., Kadkhodaee, R., & Tromp, R. H. (2018). Electrospray-assisted drying of live probiotics in acacia gum microparticles matrix. *Carbohydrate Polymers*, *183*, 183–191. https://doi.org/10.1016/J.CARBPOL.2017.12.001

CHAPTER VI

Optimization of coaxial spray-drying for the encapsulation of *Tenebrio molitor* protein hydrolysate exhibiting DPP-IV inhibitory activity

ABSTRACT

This study aims to optimize the encapsulation of *Tenebrio molitor* protein hydrolysate exhibiting dipeptidyl peptidase-IV (DPP-IV) inhibitory activity using coaxial spray-drying, a novel and sustainable technique that enhances the stability, protection, and efficacy of bioactive compounds for use in functional foods. The variables investigated included the solids content in the core feed, the solids content in the shell feed, and the shell/core flow ratio. The resulting microcapsules were characterized based on their morphology, particle size distribution, yield, surface nitrogen content, and *in vitro* DPP-IV inhibitory activity. These parameters were systematically investigated using a design of experiments and optimized through response surface methodology. The results showed that a maximum yield was achieved with 30% solids in the core and 19.73% solids in the shell. Furthermore, the shell/core flow ratio had the most significant impact on both the surface nitrogen content and the DPP-IV inhibitory activity of the capsules. Optimal conditions for minimum protein migration and maximum bioactivity values were observed at the highest solid concentrations, requiring a compromise between process yield and hydrolysate protection while maintaining a high shell/core ratio.

JOURNAL PAPER: Berraquero-García, C., Coronas-Lozano, C., Guadix, E. M., & García-Moreno, P. J. (2024). Optimization of Coaxial Spray-Drying for the Encapsulation of *Tenebrio molitor* Protein Hydrolysate Exhibiting DPP-IV Inhibitory Activity. *Food and Bioprocess Technology*. https://doi.org/10.1007/S11947-024-03695-4 (IF: 5.3; category: Food Science and Technology; position: 28/173; Q1)

1. Introduction

Type 2 diabetes mellitus (T2DM) is a widely spread disease on a global scale, affecting up to 537 million people, and its prevalence is expected to rise in the coming years. Consequently, significant efforts have been devoted to finding effective therapeutic approaches for its management. In particular, the inhibition of dipeptidyl-peptidase IV (DPP-IV) has emerged as a promising strategy for regulating glycemic levels (Drucker, 2006). As a result, there has been an increasing interest in investigating natural DPP-IV inhibitors due to their lack of adverse side effects compared to synthetic options such as gliptins (Richter et al., 2008). Interestingly, food proteins have gained attention as a rich source of natural DPP-IV inhibitory peptides, which can be employed for the development of functional food (Power et al., 2014). Insect-derived proteins, particularly those derived from *Tenebrio molitor*, have demonstrated high potential for producing DPP-IV inhibitory peptides with low environmental impact (Dávalos Terán et al., 2020; Rivero Pino et al., 2020; Rivero-Pino et al., 2021; Tan et al., 2022).

Multiple studies have indicated that the biological properties of DPP-IV inhibitory peptides are closely linked with their size and sequence (Berraquero-García et al., 2023; Nongonierma & Fitzgerald, 2016). Nevertheless, bioactive peptides may interact with other ingredients in the food matrix, losing bioactivity during processing and storage and may be also vulnerable to degradation by gastrointestinal proteases during digestion (Lacroix et al., 2017; Wang et al., 2021).Particularly, the physiological effects of bioactive peptides largely depend on their ability to withstand digestive processes intact. Peptides that can resist gastrointestinal digestion and reach the intestinal absorption site intact may exert local effects or potentially cross into the bloodstream and target organs systemically (Amigo & Hernández-Ledesma, 2020; Cian et al., 2019).

Encapsulation is an alternative for protecting bioactive peptides during processing, storage, and digestion. Spray-drying is the most used encapsulation technique due to its flexibility in terms of wall-materials and solvents, as well at its economic advantages for high production rates (Jacobs, 2014). Moreover, spray-drying is suitable for the encapsulation of thermo-sensitive compounds since most of the evaporation of the solvent occurs at the wet bulb temperature of the inlet air, without considerable increase of the temperature of the dried particle due to the short residence time (Singh & Heldman, 2014). Spray-drying is normally carried out in monoaxial mode, where a two-fluids nozzle or rotary atomizer is employed to atomize the feed solution containing the bioactive and the encapsulating agents. This allows to obtain dry microcapsules with the bioactive peptides dispersed in a matrix of encapsulating agent (Woo & Bhandari, 2013).

Alternatively, spray-drying can also be utilized in coaxial configuration using a three-fluid nozzle, allowing the simultaneous atomization of two feeds flowing through concentric channels, while pneumatic air responsible for atomization flows externally. Hence, coaxial spray-drying results in core-shell encapsulates which might offer greater protection and more advanced controlled release of the encapsulated bioactive compound when compared to monoaxial configuration (Galogahi et al., 2020). While most of research on encapsulation by coaxial spray-drying has been carried out for drugs in pharma applications (Focaroli et al., 2020; Kondo et al., 2014; Pabari et al., 2012), only a few studies are reported on the encapsulation of food bioactives such as walnut oil (Cáceres et al., 2022) and curcumin (Maria Leena et al., 2020). To the best of our concern, there are only two studies investigating the encapsulation of protein (lysozyme) by coaxial spray-drying, although it reports the use of non-food grade solvents such as acetonitrile, acetone and dichloromethane (Wan et al., 2014). Moreover, the works reported on this topic lack of a systematic optimization of core and shell formulations as well as processing conditions for coaxial spray-drying.

In the light of the above, this study aimed at optimizing the encapsulation of *Tenebrio molitor* protein hydrolysate exhibiting DPP-IV-inhibitory activity by coaxial spray-drying. The processing variables studied included the total solid content of the core and shell feeds as well as the flowrate ratio between core and shell solutions. These variables were selected as they mainly determine the bioactive load in the microcapsules as well as the encapsulation efficiency and retention of bioactivity. The obtained encapsulates were characterized based on their morphology and particle size distribution. Moreover, the yield as well as the protein load and surface nitrogen content of the microcapsules were evaluated to optimize the efficiency of the process. In addition, the theoretical core-shell structure of the encapsulates was determined by confocal microscopy. Finally, the influence of the processing variables studied on the retention of DPP-IV-inhibitory activity for the encapsulated hydrolysate was evaluated *in vitro*. Therefore, this study contributes to increase our understanding on the encapsulation of bioactive protein hydrolysates by coaxial spray-drying, which will advance the protection and delivery of these bioactive ingredients.

2. Materials and methods

2.1. Materials

Tenebrio molitor meal with a protein content of 68.01 wt.% (nitrogen-to-protein conversion factor of 5.6) was kindly donated by Tebrio (Salamanca, Spain). *T. molitor* meal was stored at −16 °C until further use. Alcalase 2.4 L (EC 3.4.21.62) and Flavourzyme 1000 L ™ (3.4.11.1) were provided by Novozymes (Bagsvaerd, Denmark). Arabic gum was kindly donated by Nexira (Serqueux, France). 5(6)- carboxyfluorescein was used as a marker of the shell solution in confocal microscopy and was purchased from Sigma-Aldrich (St Louis, US). Human DPP-IV enzyme and Gly-Pro-p-nitroanilide were purchased from Sigma-Aldrich (Madrid, Spain).

2.2. Protein hydrolysate

T. molitor hydrolysate was obtained according to the conditions reported by Rivero-Pino et al. (Rivero Pino et al., 2020). Briefly, hydrolysis was conducted at 50 °C and pH 8. Thirty g/L of protein was dissolved in distilled water, and Alcalase 2.4 L (EC 3.4.21.62) and Flavourzyme 1000 L ™ (3.4.11.1) were combined at a 1:1 w/w ratio and added simultaneously at the beginning of the reaction at a total 3% enzyme-to-substrate ratio. The reaction was continued until the degree of hydrolysis (DH), measured by the pH-stat method (Adler-Nissen, 1986), was 20%. The resulting hydrolysate was then deactivated by heating the solution at 100 °C for 15 min, centrifuged at 5300 g for 15 min and vacuum filtered through an 8 µm cellulose filter. The supernatant was lyophilized (LyoMicron, Coolvacuum Technologies S.L., Barcelona, Spain) and the powdered product was stored at −20 °C. Nitrogen content of the freeze-dried hydrolysate was determined in triplicate according to the Dumas method using a Flash 2000 CHNS/O elemental analyzer (Thermo Scientific, Waltham, MA, USA). Protein content of the freeze-dried hydrolysate was calculated assuming a nitrogen-to-protein conversion factor of 5.6 (Janssen et al., 2017), resulting in 67.70 ± 0.26 wt%.

2.3. Encapsulation of *Tenebrio molitor* hydrolysate by coaxial spray-drying

To encapsulate the *T. molitor* hydrolysate, Arabic gum (AG) was selected as the encapsulation material due to its proven ability to improve poor glycemic control. Two different formulations were prepared for the core (inner) and shell (outer) feed solutions. Briefly, for the core solution, AG and *T. molitor* hydrolysate were dispersed in distilled water and stirred for 24 h until complete dissolution. The shell solution was prepared by adding AG to distilled water and stirring for 2 h until complete dissolution, and 5(6)-carboxyfluorescein 25mM was added at the moment of spray-drying. A Box-Behnken design with three factors and three replicates of the central point was performed to evaluate the influence of the following processing variables 1) the solids content (GA and hydrolysate) in the core solution (%solids core), 2) the solids content (i.e., GA) in the shell solution (%solids shell), and 3) the feeding rate ratio of the shell feed solution to the core feed solution (flow shell/core). Each factor was set at three levels as follows: 1) for the %solids core, 30, 35, and 40 wt. %, where the *T. molitor* hydrolysate concentration was fixed to 40% of the total solids for all core formulations; 2) for the %solids shell: 15, 25 and 35 wt.%; and 3) for the ratio of the flowrates shell/core, 50 (ratio 1:1), 58.3 (ratio 1.4:1) and 66.7 (ratio 2:1) % of shell flowrate out of the total (core+shell) flowrate (Table 1). All formulations in the study were dried by spray drying using a laboratory-scale spray-drier (Büchi B-190; Büchi, Flawill, Switzerland) and a 3-fluids nozzle with diameter of the core and shell tips of 0.7 and 2.0 mm respectively,

and 2.8 mm for the gas cap (Büchi, Flawill, Switzerland). The temperature of the inlet air was kept fixed at 190 °C, whereas the temperature of the outlet air was kept in the range 100-110 °C. The drying airflow was fixed at 25 Nm^3/h. The yield of the drying process was calculated based on the amount of powder collected and the theoretical solids fed through the core and shell solutions. Once the different microcapsules were obtained, they were stored at −20 °C in the dark until analysis.

Table 1. Experimental design and measured values for the response variables

	Input variables				Output variables		
Exp. #	**Solids core (%)**	**Solids shell (%)**	**Shell/core flow ratio (%)**	**Yield (%)**	**Protein load (%)**	**Surface nitrogen (%)**	**DPP-IV inhibition (IC_{50}, mg/mL)**
S1	40.00	25.00	50.00	24	13.64 ± 0.03	6.32 ± 0.08	1.21 ± 0.05
S2	40.00	15.00	58.35	31	13.92 ± 0.08	6.42 ± 0.16	1.05 ± 0.08
S3	35.00	25.00	58.35	25	12.10 ± 0.21	5.97 ± 0.06	0.85 ± 0.09
S4	30.00	25.00	66.70	29	9.49 ± 0.14	5.35 ± 0.09	0.95 ± 0.07
S5	40.00	25.00	66.70	18	9.72 ± 0.08	4.47 ± 0.02	0.79 ± 0.20
S6	30.00	25.00	50.00	28	14.87 ± 0.14	6.35 ± 0.05	1.01 ± 0.07
S7	35.00	35.00	66.70	19	9.91 ± 0.06	5.47 ± 0.02	0.97 ± 0.04
S8	35.00	35.00	50.00	15	13.44 ± 0.28	6.40 ± 0.09	1.09 ± 0.04
S9	35.00	15.00	50.00	18	15.29 ± 0.45	6.41 ± 0.03	1.18 ± 0.06
S10	30.00	35.00	58.35	20	12.94 ± 0.06	5.80 ± 0.09	1.15 ± 0.02
S11	40.00	35.00	58.35	13	12.24 ± 0.03	5.61 ± 0.14	0.97 ± 0.11
S12	35.00	15.00	66.70	25	13.72 ± 0.06	5.85 ± 0.02	0.86 ± 0.02
S13	35.00	25.00	58.35	23	12.04 ± 0.11	5.60 ± 0.02	0.89 ± 0.11
S14	35.00	25.00	58.35	26	12.32 ± 0.06	5.53 ± 0.05	0.86 ± 0.05
S15	30.00	15.00	58.35	31	14.34 ± 0.22	6.76 ± 0.06	0.03

2.4. Characterization of the capsules

2.4.1. Morphology and particle size distribution

The morphology of the capsules was examined using scanning electron microscopy (SEM) on a FESEM microscope (LEO 1500 GEMINI, Zeiss, Germany). The samples were transferred onto carbon tape and coated with carbon using an EMITECH K975X Turbo-Pumped Thermal Evaporator (Quorum Technologies, UK). SEM images were captured in the range of 500X-5KX magnification with a 3 kV accelerating voltage and 30 μm aperture. The particle size distributions and mean diameters were determined by measuring 200 randomly selected particles using the ImageJ software (National Institute of Health, USA). The size data were expressed as D_{10}, D_{50}, and D_{90}, which are the diameters at 10%, 50%, and 90% cumulative numbers, respectively. The span, which represents the broadness of the size distribution, was calculated as $(D_{90} - D_{10})/D_{50}$.

2.4.2. Structure of the microcapsules

The structure of the microcapsules was evaluated using confocal microscopy (Leica TCS SP5 I, Leica Microsystems Inc., IL, USA). 5(6)-carboxyfluorescein (0.5 mL, 25 mM) was incorporated into 300g of the shell feed. The microparticles were positioned on a microscope slide, covered with a cover glass, and subjected to an excitation wavelength of 5(6)-carboxyfluorescein (488 nm). The fluorescent signal was collected at 509-548 nm, and confocal images were obtained at a magnification of 3X.

2.4.3. Protein content

Nitrogen content of encapsulates was determined in triplicate according to the Dumas method (Liliana Krotz et al., n.d.) using a Flash 2000 CHNS/O elemental analyzer (Thermo Scientific, Waltham, MA, USA). Protein content was calculated assuming a nitrogen-to-protein factor of 5.6 (Janssen et al., 2017).

2.4.4. X-ray Photoelectron Spectroscopy (XPS)

The presence of *T. molitor* hydrolysate on the surface of the microparticles was analyzed by determining the nitrogen surface using X-ray photoelectron spectroscopy (XPS). It should be noted that the Arabic gum used did not present any nitrogen when measured by XPS, which denotes that all the nitrogen measured is due to the hydrolysate. The microparticles were transferred to a glass slide and analyzed using a Kratos Axis Ultra-DLD (Kratos Analytical, Manchester, UK) with Al-Kα radiation at 450 W. Wide-energy survey scans (0 – 1200 eV) were obtained with a pass energy of 160 eV and a step size of 1.0 eV. Charge neutralization was activated, and the penetration depth was maintained at less than 10 nm. The measurements were conducted in triplicate.

2.4.5. DPP-IV inhibitory activity

The DPP-IV-inhibitory activity of the produced *T. molitor* hydrolysate and the microcapsules loaded with the hydrolysate was measured following a modified protocol based on Lacroix and Li-Chan (2012) (Lacroix & Li-Chan, 2012). Briefly, 25 µL of DPP-IV enzyme at 0.02 U/mL were incubated at 37 °C with 100 µL of *T. molitor* hydrolysate or microcapsule aqueous solutions at varying concentrations (1.5-5 mg/mL) for 10 min. Subsequently, the reaction was initiated by the addition of 50 µL of 1 mM Gly-Pro-p-nitroanilide. The release of the reaction product (p-nitroanilide) was monitored by measuring absorbance at 405 nm every 2 min for 2 h at 37 °C using a Multiskan FC microplate photometer (Thermo Scientific, Vantaa, Finland). Each sample was analyzed in triplicate and a color control was added. The inhibition activity was calculated by comparing the reaction progress to a control (distilled water) as follows:

$$DPP-IV \quad inhibitory \quad activity \quad \left(\%\right) = \frac{1-p_i}{p_0} \cdot 100$$

Where p_i is the slope in the presence of inhibitor (peptide) and p_0 is the slope obtained in the absence of inhibitor (control). The half-maximal inhibitory concentration (IC_{50}) of each sample was calculated. Results are expressed in mg protein/mL as the mean ± standard deviation.

2.4.6. Statistical analysis

Multivariate analysis software (StatGraphics 5.1, Statpoint Technologies, Inc., Warrenton, VA, USA) was used to analyze the experimental data. Multiple comparison analysis of variance (ANOVA) followed by the least significant difference (LSD) test was used to analyze the statistically significant differences (*p-value* < 0.05) among the experimental results for selected output variables.

For the statistical modelling, second-degree polynomial equations (Eq. 2) were generated to relate the input variables (X: %solids core, %solids shell, and flow shell/core) to the output variables (Y: yield of drying process, protein content, surface nitrogen, and DPP-IV-inhibitory activity) as follows:

$$Y_i = b_0 + \sum_{i=1}^{3} b_i X_i + \sum_{i=1}^{3} b_{ii} X_i^2 + \sum_{i<j}^{3} b_{ij} X_i X_j$$

where Y_i is the predicted response, X_i and X_j are variables, b_0 is the constant, b_i are the linear coefficients, b_{ii} are the quadratic coefficients, and b_{ij} are the interaction coefficients. The coefficients of these equations were calculated, and the adequacy of the model was verified by calculating the lack-of-fit and coefficient of determination (R^2). Secondly, an ANOVA was performed. The significance of all terms in the models was determined statistically by computing the *P-value* at a confidence level of 95%. The regression coefficients were then used to generate contour maps to determine the optimum values of solids content in the core solution, solids content in the shell solution, and the feeding rate ratio of the shell feed solution to the core feed solution, following response surface methodology.

3. Results and discussion

3.1. Characterization of microcapsules

3.1.1. Morphology and structure of the microcapsules

Figure 1 shows the morphology of the microcapsules obtained. Most of the microcapsules obtained showed a spherical shape with wrinkled surface, small pores, and no apparent cracks. This morphology has been previously observed for spray-dried particles both in monoaxial (Kim et al., 2009) and coaxial configurations (Bhujbal et al., 2021). This was attributed to high Péclet numbers (Pe>1), indicating that water removal is faster than solids diffusion during drying. The latter leads to the formation of a crust on the surface that shrinks after cooling

down, resulting in dimpled shapes (Boel et al., 2020). Additionally, SEM images revealed some larger and hollow microcapsules with noticeable cracks (Figure 1 S2, S6 and S10). It was also indicative of rapid, unstable crust formation at high Péclet numbers, where internal vapor pressure compromises integrity of the particle and fractures the crust (Kurozawa et al., 2009). High Péclet values might result from various factors including temperature adjustments and formulation variances such as solids content. Elevating inlet air temperature over 100°C for aqueous solutions accelerates solute concentration at the liquid/air interface followed by the formation of a thin, instable crust, prone to collapse and wrinkle (Kurozawa et al., 2009). High solids concentration increases the viscosity of the solutions, which also promotes rapid crust formation (Boel et al., 2020; Kim et al., 2009). Furthermore, the use of coaxial spray drying may also lead to elevated Péclet numbers due to the incorporation of a shell solution containing solids, which could facilitate early crust formation. This restricts the diffusion of hydrolysates within the particle, which consequently affects stability during cooling phases (Cai et al., 2023).

Figure 2 shows the confocal microscopy images of the microcapsules. All images revealed green fluorescence from the 5(6)-carboxyfluorescein present in the shell, while no fluorescence was observed in the core, indicating that core-shell microcapsules were obtained for all the formulations and processing conditions evaluated. Core-shell microcapsules with the two described morphologies mentioned above could be also observed in Figure 2, with larger spherical capsules that often appear fractured being prominent alongside the smaller, wrinkled capsules. This finding aligns with previous research on coaxial spray-drying for encapsulating different bioactive ingredients (Cáceres et al., 2020; Cai et al., 2023; Maria Leena et al., 2020), confirming the formation of core-shell microcapsules by using this method. This structure might facilitate the creation of a core rich in bioactive hydrolysate, preventing peptides from diffusing to the capsules surface, and thus playing a crucial role in protecting them from processing stress and heat (Maria Leena et al., 2020).

3.1.2. Particle size and size distribution

Figure 3 shows the results of the particle size analysis (D_{10}, D_{50}, D_{90}) and particle size distribution (Span) for the microcapsules produced. Among these parameters, D_{50} is commonly used to represent particle size by providing a single value that indicates the mean volume diameter and denotes where 50% of the distribution lies below and above this value (Sarrate et al., 2015). The range of D_{50} results was found to be between 3.20 μm and 6.50 μm (Figure 3b), which falls within the low range compared to normal powders obtained through conventional spray drying methods (Piñón-Balderrama et al., 2020). These findings are consistent with previous research on encapsulation of tributyrin with whey protein isolate as encapsulating agent using the same three-fluid nozzle, reporting values of D_{50} between 3.20±0.30 and 4.10±0.26 μm (Shi & Lee, 2020).

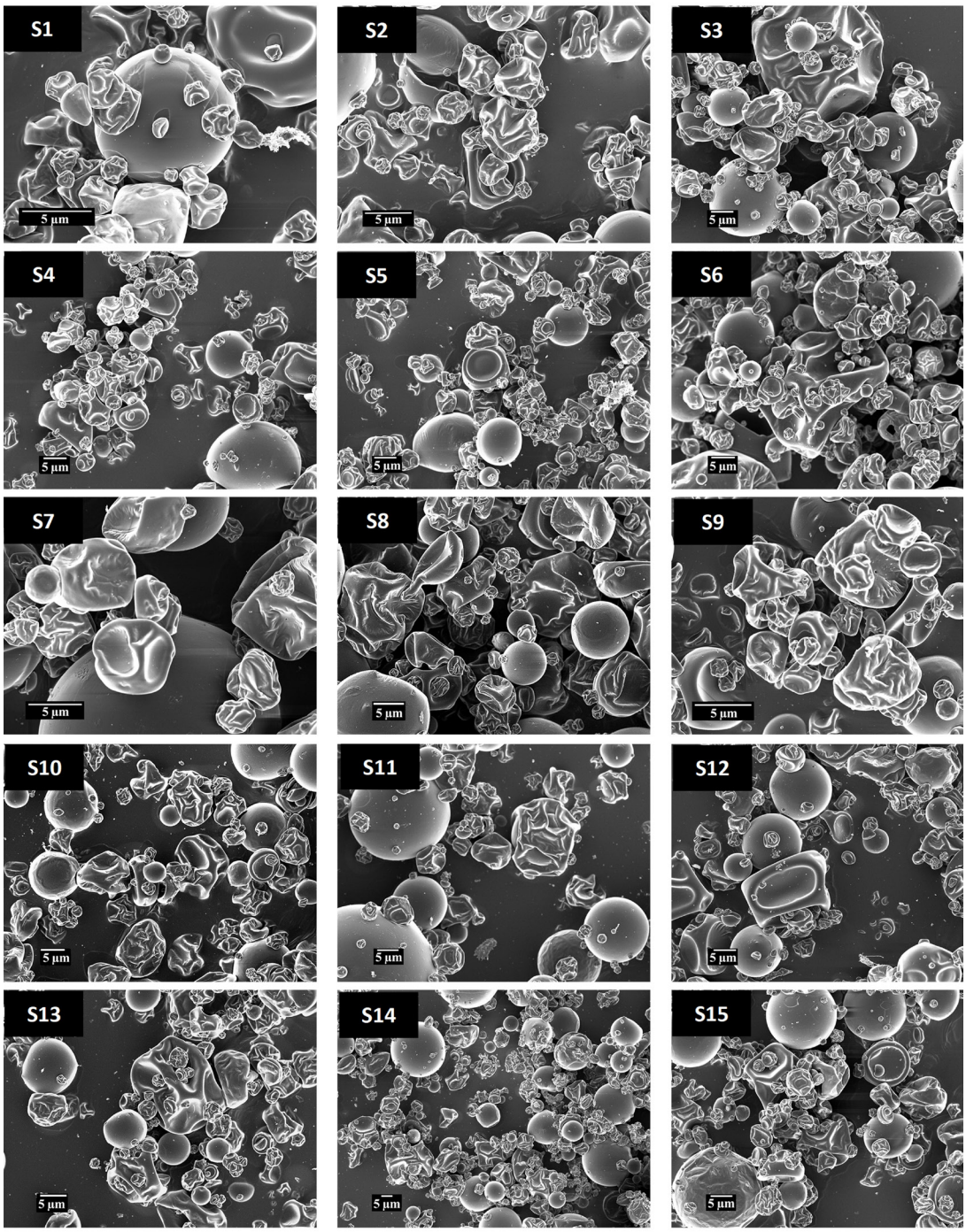

Figure 1. Scanning electron microscopy images of microcapsules loaded with *T. molitor* protein hydrolysate and obtained by coaxial spray-drying. Sample ID referring to Table 1.

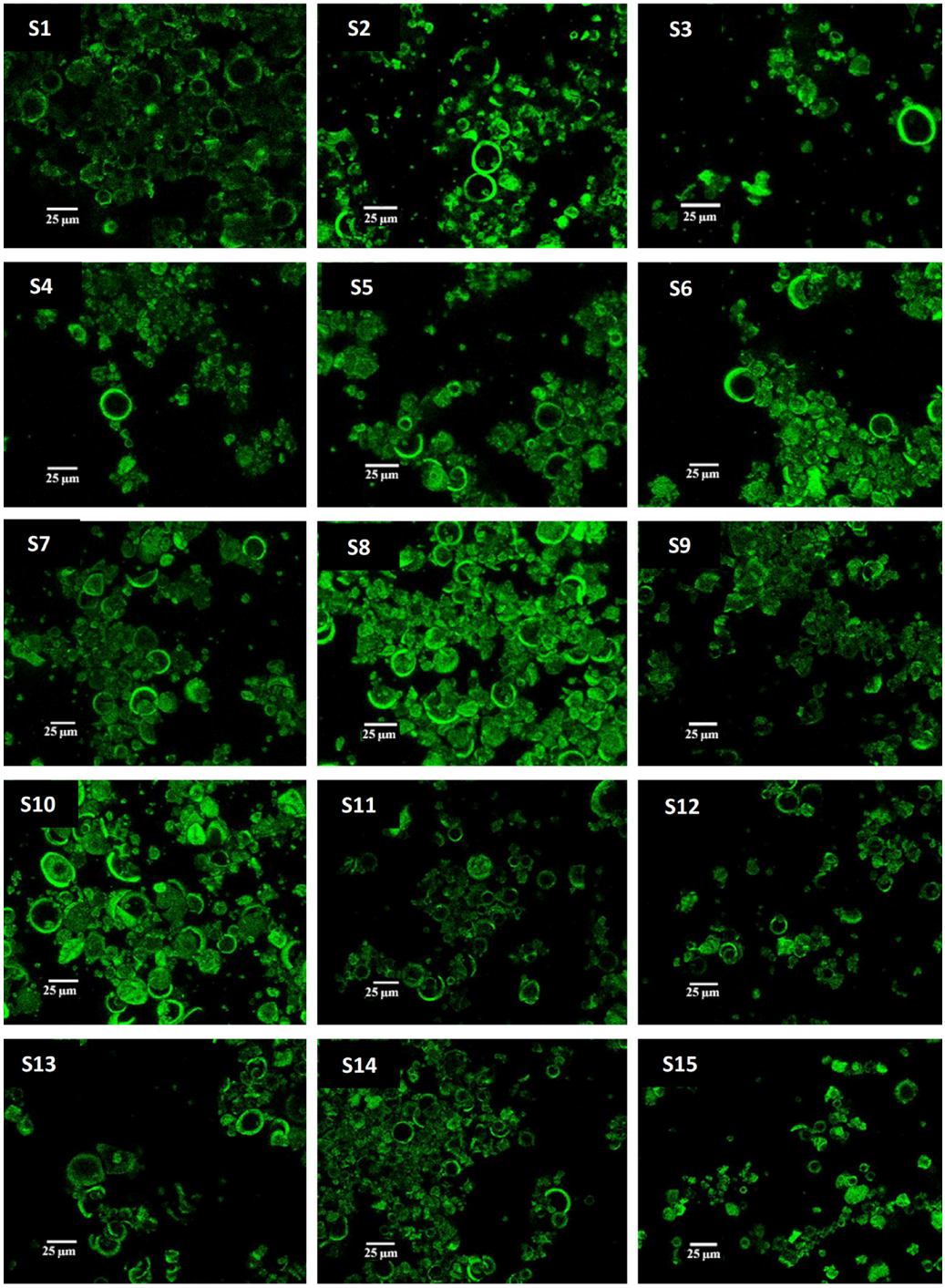

Figure 2. Confocal microscopy images of microcapsules loaded with *T. molitor* protein hydrolysate and obtained by coaxial spray-drying. Sample ID referring to Table 1.

It is quite accepted that a broad particle size distribution is obtained through spray-drying process (Both et al., 2020; Rahmani-Manglano et al., 2023). However, the span values obtained in this study ranged from 1.42 to 2.64 (Figure 3d), which are considered average values for bench spray driers (Woo & Bhandari, 2013). Generally, it was observed that reducing the percentage of solids in the shell feed led to narrower distributions (S2, S12, S15), while higher solids content resulted in broader distributions (S7, S8, S10). This has been attributed to an increase in the viscosity of the shell solutions with increased encapsulating agent concentration leading to the formation of larger droplets at the nozzle tip (Teo et al., 2021).

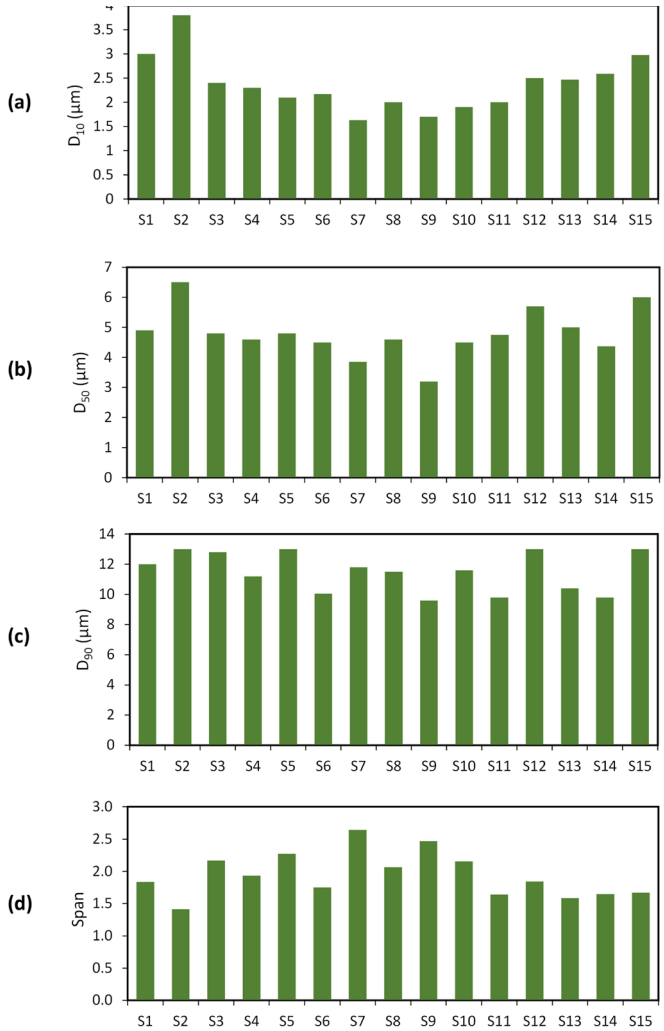

Figure 3. (a) D10, (b) D50, (c) D90 and (d) span of the resulted microcapsules loaded with *T. molitor* protein hydrolysates obtained by coaxial spray-drying. Sample ID referring to Table 1.

3.2. Statistical modeling

3.2.1. Yield

In this study, the influence of the processing variables of the coaxial spray-drying process on the measured response variables was systematically investigated (Table 1). The experimental results were then fitted to quadratic models, capturing both linear and quadratic effects of the input variables. Subsequently, polynomial coefficients for the surface response model were computed and are detailed in Table 2. Additionally, a *p-value* representing associated probability was calculated for each term of the regression model. At a confidence level of 95%, any *p-value* exceeding 0.05 was deemed not statistically significant.

The production yield of the coaxially spray-dried microcapsules is a critical factor to take into consideration, directly impacting the efficiency and economy of the spray drying processes. Table 1 presents the obtained result data, with yields ranging from 13% to 31%, indicating relatively low production yields. Nevertheless, it should be kept in mind that experiments were conducted in lab scale, where the drying chamber used is not isolated, leading to heat loss, and has a reduced size, which normally result in yields below 50% (Sosnik & Seremeta, 2015). In any case, the observed differences in yield can be attributed to differences in the condensation (liquid deposits) within the chamber and the variations in powder stickiness, leading to powder deposits during the different tests.

Table 2 presents the coefficients and the correlation results for the Yield (%) of the coaxial spray-drying process model, indicating a relatively modest value of R^2 = 0.771. Nevertheless, considering the lack-of-fit of 0.085, it can be inferred that the model accurately fits the data. The yield was significantly influenced by the %solids shell (B) (p = 0.016) and had a lower but significant dependence on the %solids core (A), with p = 0.044, both variables affected in an inversely proportional way (Figure S1a). Since protein hydrolysates contain low molecular weight peptides, specially at such high degree of hydrolysis, increasing the incorporation of Arabic gum in the shell, which has a high molecular weight (47,000 to 3000,000 g/mol (Kurozawa et al., 2009)), enhances microcapsule stability by elevating its glass transition temperature (*Tg*), hence reducing powder stickiness and increasing yield. However, in this study, the high outlet air temperature observed (100—110 °C) indicated that the powder reached high temperature, which could overpass the *Tg* of the GA (~57 °C according to Abel and Ghazali (2020)). This can result in a rubbery matrix and increased stickiness leading to powder deposits in the drying chamber and cyclone (Anandharamakrishnan & Padma Ishwarya, 2015). Previous works have shown that maintaining outlet temperatures below 100°C can lead to significantly higher yields, reaching up to 46% for encapsulation of flaxseed protein hydrolysate (Akbarbaglu et al., 2019). However, attempting to further reduce temperature by increasing feed flowrate was not feasible in our study due to the resulting

higher liquid accumulation in the chamber. Indeed, it is worth noting that using coaxial spray drying involves managing two different feeds, which can complicate flow selection and potentially elevate humidity levels within the drying chamber, leading to increased liquid deposits in the drying chamber, as well as resulting in high outlet air temperature (i.e., due to poor drying), which favors stickiness of the powder (Kauppinen et al., 2018).

3.2.2. Protein load and surface composition of the microcapsules

Coaxial spray-drying was aimed to produce microcapsules with a core-shell structure, as previously confirmed through confocal microscopy. Therefore, we used this process to retain the hydrolysate in the core and prevent significant migration to the particle surface. Thus, the efficiency of the coaxial spray-drying for the encapsulation of the bioactive protein hydrolysate was evaluated by determining the protein load and surface composition of the microcapsules (Figure 4 and Figure 5). Furthermore, the surface nitrogen content was validated by studying nitrogen-to-carbon (N/C) ratio to check for good reproducibility of the sample preparation process as proposed by Wang et al. (2014).

The theoretical protein load of the microcapsules was calculated based on the formulations of the core and shell feeds as well as the flowrate ratio between feeds. The actual protein content of the capsules was then measured using the Dumas method, and the protein content was calculated assuming a nitrogen-to-protein factor of 5.6 (Janssen et al., 2017). As a result, the measured protein content ranged from 9.49 ± 0.14 wt.% for S4 to

Table 2. Polynomial coefficients and p-values for the response variables

	Yield (%)		**Protein load (%)**		**Surface nitrogen (%)**		**DPP-IV inhibition (IC_{50}, mg/mL)**	
	Coefficient	***P-value***	**Coefficient**	***P-value***	**Coefficient**	***P-value***	**Coefficient**	***P-value***
Constant	-113.640		33.881		-0.776		3.929	
A: %solids core	-2.815	0.044	-0.593	0.037	0.182	0.162	-0.063	0.187
B: %solids shell	2.989	0.016	-0.309	0.002	-0.202	0.084	-0.052	0.422
C: % flowrate shell/core	5.576	0.273	0.038	0.001	0.298	0.023	-0.030	0.004
AA	0.085	0.143	0.001	0.790	0.001	0.886	0.003	0.019
AB	-0.040	0.146	-0.001	0.442	0.001	0.781	-0.001	0.039
AC	-0.046	0.157	0.009	0.038	-0.005	0.218	-0.002	0.012
BB	-0.031	0.076	0.012	0.004	0.004	0.074	0.001	0.009
BC	-0.009	0.494	-0.006	0.022	-0.001	0.516	0.001	0.043
CC	-0.031	0.139	-0.003	0.085	-0.001	0.521	0.001	0.048
Lack-of-fit	0.085		0.021		0.265		0.178	
R^2	0.771		0.933		0.873		0.970	

15.29 ± 0.45 wt.% for S9, with a significant difference observed between the theoretical and measured value (up to 28%). In fact, the measured values for the protein content indicated that the capsules retained only between 53% and 85% of the theoretical protein load. (Figure 4). Among the different microcapsules, S10 showed the most similarity between the values, while S2 and S9, both with 15% solids in the shell, experienced the greatest difference between theoretical and measured protein load. In fact, the statistical analysis demonstrated that the linear effect of all variables was significant on the protein load (*p-values* < 0.05), with a significant quadratic effect observed for % solids shell as well *(p-value* =0.0042). Considering the significance and the value of the coefficients the %solids shell (B) stands out for its significant influence on the model, with a high coefficient at -0.309 and *p-value*=0.002. The inverse relationship between the %solids shell and the protein load of the capsule makes sense considering that an increase in solids in the shell would imply a decrease in the relative protein load compared to the total solids load. The global effect of the variables is represented in Figure S1b. The proposed quadratic model accounted for this data variability, with a high correlation at R^2 = 0.933, however the lack-of-fit was found significant, mostly due to the center points having extremely small variation (s^2 =0.02).

Surface nitrogen values for the microcapsules ranged from 4.46 ± 0.02 to 6.67 ± 0.06 %, indicating the presence of protein on the surface of the particles, and incomplete encapsulation of the hydrolysate in the core (Figure 5). Table 2 shows that surface nitrogen was significantly influenced by the shell/core flow ratio (C) with a coefficient of 0.2976 and *p-value*=0.0228. Although the coefficient alone expresses a directly proportional relation, the analysis of the global interaction shows an inverse relation (Figure S1c). Hence, increasing the flow ratio from 58.35% to 66.7% resulted in a decrease in the surface nitrogen content, as can be seen for microcapsules S4, S5, and S7. This is easily understood as an increase in this ratio decreased the ratio between the hydrolysate and the encapsulating agent, thereby enhancing

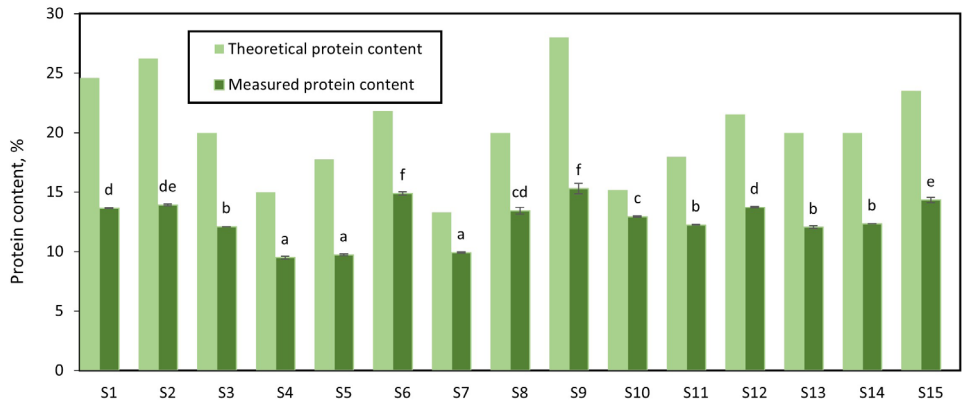

Figure 4. Theoretical and measured protein content of microcapsules loaded with *T. molitor* protein hydrolysate and obtained by coaxial spray-drying (*n*=3 for measured values) Sample ID referring to Table 1.

encapsulation of the hydrolysate. To a lesser but not significant extent, surface nitrogen was also affected by the % solids (Arabic gum) in the shell feed (B) (*p-value* = 0.0840). As a result, microcapsules produced at 15% Arabic gum in the shell tended to have a higher amount of nitrogen in the surface, as can be exemplified by S2, S9 or S15. This could be attributed to diffusional motion affecting component distribution within droplets. For instance, a thinner film, which did not totally cover the core droplet, could be formed when using the low AG content in the shell, which did not reduce the diffusion of the hydrolysate to the liquid/air interface during drying to the same extent than when using 25% AG in the shell. The model accounts for much of the data variability with R^2=0.8734 and *lack-of-fit*>0.05.

A similar trend was also observed for the N/C ratio of the microcapsules, suggesting a good reproducibility of the sample preparation process during XPS analysis and a no significant influence due to potential blank glass area of the different samples (Wan et al., 2014). Other data variability can be accounted for in the proposed quadratic model, with R^2 = 0.8733.

3.2.3. DPP-IV inhibitory activity

Bioactive peptides are prone to degradation during processing, storage, and digestion, making encapsulation a key process for their preservation. Research has shown that monoaxial spray-drying is effective in protecting these bioactive components and preserving their bioactivity (Akbarbaglu et al., 2019; Bowey et al., 2013). However, unlike other bioactive compounds, the amphiphilic and complex structures of peptides can lead to instability and loss of biological activity during spray-drying due to shear tension during atomization, dehydration in the drying phase, and migration of peptides to the surface (Akbarbaglu et al., 2021). Therefore, protecting these compounds throughout the drying process and preserving their activity is crucial.

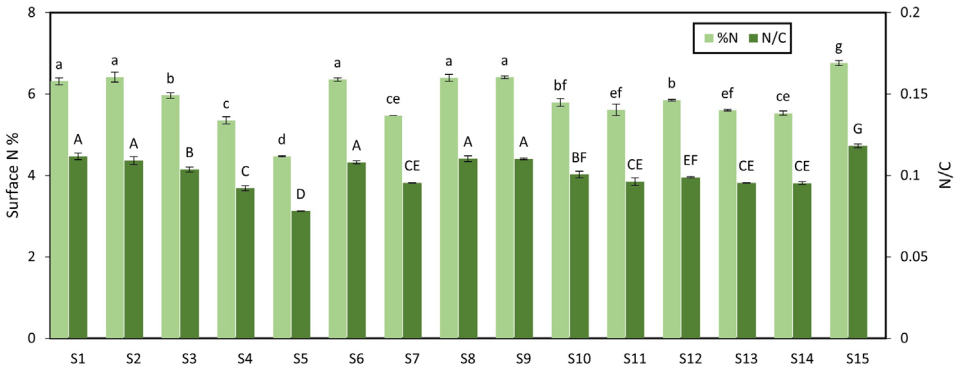

Figure 5. Surface nitrogen content and N/C ratio of the microcapsules loaded with *T. molitor* protein hydrolysate and obtained by coaxial spray-drying (*n*=3 for measured values) Sample ID referring to Table 1.

Figure 6 shows the DPP-IV inhibitory activity, expressed as IC_{50} (half maximal inhibitory concentration) in mg protein/mL. The measured IC_{50} values ranged from 0.791 ± 0.202 to 1.214 ± 0.051 mg protein/mL, indicating that between 53 and 100% of the activity of the original hydrolysate was preserved after encapsulation by coaxial spray-drying. The bioactivity was greatly reduced in S1 and S9, which were obtained with the lowest % shell/core flow ratio. On the other hand, S5 showed the highest level of bioactivity retention, being produced at the highest %solids core content and %shell/core flow ratio. Similarly, previous studies have evaluated the encapsulation of DPP-IV inhibitory hydrolysates using various methods such as double emulsification (W/O/W) with rice bran oil and freeze-drying using maltodextrin (Puri et al., 2023) as well as extrusion employing alginate and chitosan (Thongcumsuk et al., 2023). However, these studies observed a slight decrease in activity following encapsulation and simulated gastrointestinal digestion, suggesting incomplete protection of the bioactive hydrolysate.

Statistical analysis revealed that the DPP-IV inhibitory activity was significantly affected by the shell/core flow ratio (C), with a *p-value* of 0.0040 (Table 2). A significant quadratic impact was also evident for all the processing variables studied. Furthermore, our proposed quadratic model accounts for much of the data variability, demonstrating an impressive coefficient determination (R^2) as high as 0.9702 and a *lack-of-fit*>0.05. This suggests that enhancing the shell/core flow ratio (i.e., increasing the carrier-to-bioactive ratio) resulted in enhanced protection of the hydrolysate and subsequently reduced IC_{50} values. These results were expected since this variable also significantly influences the reduction of surface nitrogen, suggesting that higher shell/core flow ratios increased the protection by forming an outer shell and kept more of the hydrolysate in the interior of the microcapsules, resulting in lower IC_{50} values. These findings are consistent with those from spray-drying encapsulation studies on brewer's spent grain hydrolysate exhibiting DPP-IV inhibitory activity (Garzón et al., 2023), where increased retention of activity was found for higher carrier-to-protein ratio using agar and carrageenan as encapsulating agents.

3.2.4. Optimization

For the optimization of the coaxial spray drying process, the yield was chosen as an important efficiency and economic factor, while protein load, surface nitrogen and DPP-IV inhibition were selected as output indicators reflecting the effectiveness of the encapsulation of the hydrolysate. The goodness of the fit for these three variables was analyzed by plotting measured values against predicted values (Figure 7a-d). Each plot included a regression line correlating the data, along with equations indicating their relation, and dotted lines showing a ±10% deviation between experimental and model values.

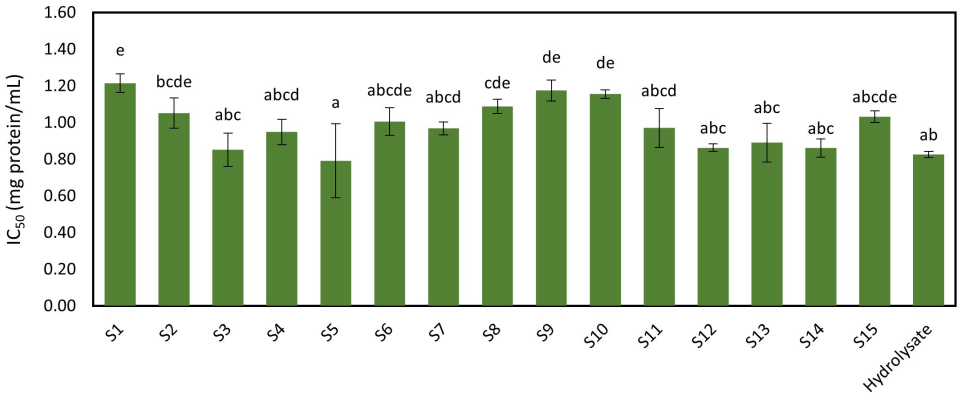

Figure 6. DPP-IV inhibitory activity of the *T. molitor* protein hydrolysate encapsulated by coaxial spray-drying. IC_{50} refers to half the maximal inhibitory concentration value of sample in mg protein/mL (n=3) Sample ID referring to Table 1.

Contour maps were generated by means of the quadratic models obtained and employing response surface methodology (Figure 8). Hence, by optimizing the second-order models, the optimum values for yield, protein load, surface nitrogen and DPP-IV inhibition were found, and they appear marked as circles in the contour plots. For yield (Figure 8a), the shell/core flow ratio was plotted against %solids shell, while keeping the %solids core at the lowest assayed level. To optimize the encapsulation of antidiabetic *T. molitor* hydrolysate a maximum yield is desired. In Figure 7a the optimum yield 31.32 % was found at the lowest %solids core (30%) and low %solids shell (19.73%), along with high shell/core flow ratio (64.59%). High solids content has previously been associated with low yield due to increased stickiness of encapsulating materials under high processing temperatures resulting in powder agglomeration (Lechanteur & Evrard, 2020). Regarding the %solids shell, an increase in the concentration of GA results in a lower process yield due to the feed solution becoming more viscous. This increased viscosity leads to larger atomized particles that are difficult to dry, increasing the likelihood of these particles adhering to dryer chamber walls. Previous studies have observed reduced process yields when using higher AG concentrations for spray-drying juice concentrates and pequi pulp extract (Can Karaca et al., 2016; Santana et al., 2013).

For the protein load, surface nitrogen and DPP-IV inhibition (Figure 8b-d), the %solids shell was plotted against the %solids core, while the shell/core flow ratio was adjusted to the optimum value for the different output variables. In Figure 8b a maximum value of 16.08% was obtained for the protein load. This value was reported for the lowest levels for all variables (30% solids core, 15% solids shell and 50% shell/core ratio). This result is attributed to lower GA being added to these capsules while maintaining the same protein ratio in the core as previously proposed. In Figure 8c, a minimum value of 4.63% was obtained for surface nitrogen.

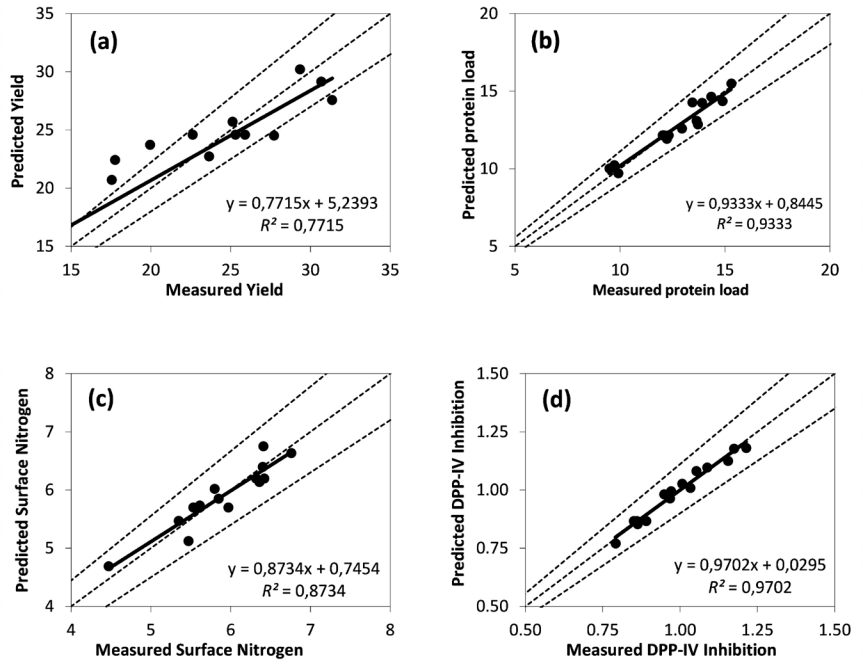

Figure 7. Correlation between predicted and measured values of (a) yield, (b) protein load, (c) surface nitrogen and (d) DPP-IV inhibition

This optimum level was observed at the highest levels for the %solids core (40%) and shell/core flow ratio (66.7%). Regarding the activity retention of the microencapsulates, Figure 8d shows the maximum inhibition of DPP-IV at IC_{50} = 0.76 mg protein/mL. This value was found at the maximum shell/core flow ratio (66.7%), high %solids core (38%) and medium %solids shell (24%). The latter two response variables are closely related, as lower surface nitrogen is associated with better protection of bioactive compounds (Wan et al., 2014), hence leading to enhanced resistance against processing conditions such as high drying temperature and shear stress during atomization (Akbarbaglu et al., 2021). Notably, both responses are significantly influenced by the shell/core flow ratio. This is easily understandable, considering that this suggests a thicker shell would develop in the microcapsules. These results indicate that the optimization of process variables can lead to significant improvements in yield, surface nitrogen content, and DPP-IV inhibition; however, different feed compositions (%solid both in core and shell) are required. Nonetheless, it is observed that high shell/core flow ratios resulted in improved results for all the parameters. Although low solids content in core and shell feeds are required to increase the yield, it is necessary to upkeep the content for maximum protection of the hydrolysate, meaning minimum surface nitrogen and IC_{50} DPP-IV inhibitory value.

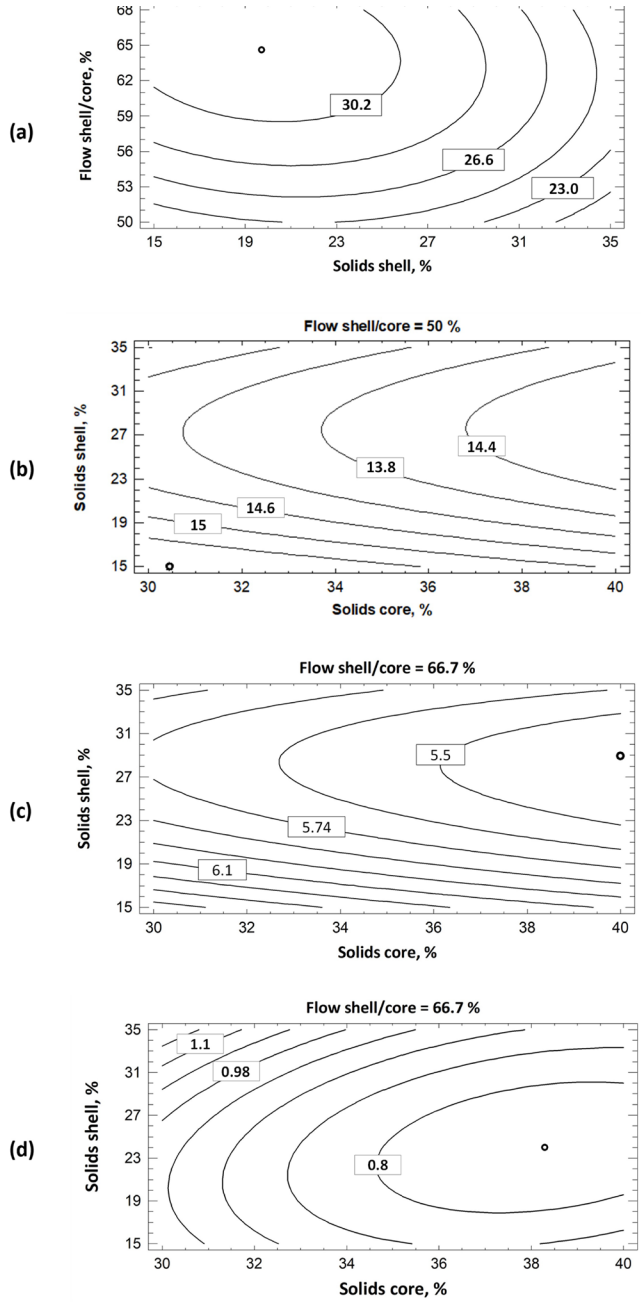

Figure 8. Contour plots for (a) yield, (b) protein load, (c) surface nitrogen and (d) DPP-IV inhibition

4. Conclusions

In this study, coaxial spray drying of a *Tenebrio molitor* protein hydrolysate exhibiting DPP-IV inhibitory activity was optimized and three key processing variables were investigated: solids content in the shell, solids content in the core, and shell/core flow ratio. Our results indicated that *Tenebrio molitor* protein hydrolysate was successfully encapsulated using co-axial spray-drying with gum Arabic as the coating material. The resulting microparticles displayed a spherical shape with a wrinkled surface, narrow size distribution, and D_{50} values ranging from 3.20 μm to 6.50 μm. Moreover, confocal microscopy confirmed the obtaining of microcapsules with a shell-core structure, while statistical modeling identified an optimal combination of processing variables for the encapsulation process. The highest yield was found for the combination of 30% solids in the shell, 19.73% solids in the core and shell/core flowrate in a ratio of 64.59%. However, optimum surface nitrogen content and bioactivity were obtained at higher solids content in the core (38-40%) and in the shell (24-29%), when also using the highest value assayed for shell/core flowrate ratio. Overall, this study not only demonstrated the feasibility of the coaxial encapsulation by spray-drying of *Tenebrio molitor* protein hydrolysate, but also provided information that can be applied to the encapsulation of other peptides or hydrolysates from other sources. The data obtained through model optimization could guide selection of appropriate operational conditions for encapsulation of biopeptides by coaxial spray-drying.

5. References

Abel, R., & Ghazali, M. (2020). Characterisation of physicochemical properties of gum arabic powder at various particle sizes. *Food Research*, *4*, 107–115. https://doi.org/10.26656/fr.2017.4(S1).S32

Adler-Nissen, Jens. (1986). *Enzymic hydrolysis of food proteins. New York: Elsevier Applied Science Publishers*. p9-17 and p146-147.

Akbarbaglu, Z., Mahdi Jafari, S., Sarabandi, K., Mohammadi, M., Khakbaz Heshmati, M., & Pezeshki, A. (2019). Influence of spray drying encapsulation on the retention of antioxidant properties and microstructure of flaxseed protein hydrolysates. *Colloids and Surfaces B: Biointerfaces*, *178*, 421–429. https://doi.org/10.1016/J.COLSURFB.2019.03.038

Akbarbaglu, Z., Peighambardoust, S. H., Sarabandi, K., & Jafari, S. M. (2021). Spray drying encapsulation of bioactive compounds within protein-based carriers; different options and applications. *Food Chemistry*, *359*, 129965. https://doi.org/10.1016/J.FOODCHEM.2021.129965

Amigo, L., & Hernández-Ledesma, B. (2020). Current Evidence on the Bioavailability of Food Bioactive Peptides. *Molecules 2020, Vol. 25, Page 4479*, *25*(19), 4479. https://doi.org/10.3390/MOLECULES25194479

Anandharamakrishnan, C., & Padma Ishwarya, S. (2015). Spray Drying Techniques for Food Ingredient Encapsulation. *Spray Drying Techniques for Food Ingredient Encapsulation*, 1–296. https://doi.org/10.1002/9781118863985

Berraquero-García, C., Rivero-Pino, F., Ospina, J. L., Pérez-Gálvez, R., Espejo-Carpio, F. J., Guadix, A., García-Moreno, P. J., & Guadix, E. M. (2023). Activity, structural features and in silico digestion of antidiabetic peptides. *Food Bioscience*, *55*, 102954. https://doi.org/10.1016/J.FBIO.2023.102954

Bhujbal, S. V., Su, Y., Pathak, V., Zemlyanov, D. Y., Cavallaro, A. A., Munson, E. J., Taylor, L. S., & Zhou,

Q. (2021). Effect of storage humidity on physical stability of spray-dried naproxen amorphous solid dispersions with polyvinylpyrrolidone: Two fluid nozzle vs. three fluid nozzle. *Pharmaceutics*, *13*(7), 1074. https://doi.org/10.3390/PHARMACEUTICS13071074

Boel, E., Koekoekx, R., Dedroog, S., Babkin, I., Vetrano, M. R., Clasen, C., & Van den Mooter, G. (2020). Unraveling Particle Formation: From Single Droplet Drying to Spray Drying and Electrospraying. *Pharmaceutics 2020, Vol. 12, Page 625*, *12*(7), 625. https://doi.org/10.3390/PHARMACEUTICS12070625

Both, E. M., Boom, R. M., & Schutyser, M. A. I. (2020). Particle morphology and powder properties during spray drying of maltodextrin and whey protein mixtures. *Powder Technology*, *363*, 519–524. https://doi.org/10.1016/J.POWTEC.2020.01.001

Bowey, K., Swift, B. E., Flynn, L. E., & Neufeld, R. J. (2013). Characterization of biologically active insulin-loaded alginate microparticles prepared by spray drying. *Drug Development and Industrial Pharmacy*, *39*(3), 457–465. https://doi.org/10.3109/03639045.2012.662985

Cáceres, D., Giménez, B., Márquez-Ruiz, G., Holgado, F., Vergara, C., Romero-Hasler, P., Soto-Bustamante, E., & Robert, P. (2020). Influence of the Location of Ascorbic Acid in Walnut Oil Spray-Dried Microparticles with Outer Layer on the Physical Characteristics and Oxidative Stability. *Antioxidants 2020, Vol. 9, Page 1272*, *9*(12), 1272. https://doi.org/10.3390/ANTIOX9121272

Cáceres, D., Giménez, B., Márquez-Ruiz, G., Holgado, F., Vergara, C., Romero-Hasler, P., Soto-Bustamante, E., & Robert, P. (2022). Incorporation of hydroxytyrosol alkyl esters of different chain length as antioxidant strategy in walnut oil spray-dried microparticles with a sodium alginate outer layer. *Food Chemistry*, *395*, 133595. https://doi.org/10.1016/J.FOODCHEM.2022.133595

Cai, J., Lopez, R., & Lee, Y. (2023). Effect of Feed Material Properties on Microencapsulation by Spray Drying with a Three-Fluid Nozzle: Soybean Oil Encapsulated in Maltodextrin and Sugar Beet Pectin. *Journal of Food Processing and Preservation*, *2023*. https://doi.org/10.1155/2023/4974631

Can Karaca, A., Guzel, O., & Ak, M. M. (2016). Effects of processing conditions and formulation on spray drying of sour cherry juice concentrate. *Journal of the Science of Food and Agriculture*, *96*(2), 449–455. https://doi.org/10.1002/JSFA.7110

Cian, R. E., Campos-Soldini, A., Chel-Guerrero, L., Drago, S. R., & Betancur-Ancona, D. (2019). Bioactive Phaseolus lunatus peptides release from maltodextrin/gum arabic microcapsules obtained by spray drying after simulated gastrointestinal digestion. *International Journal of Food Science & Technology*, *54*(6), 2002–2009. https://doi.org/10.1111/IJFS.14031

Dávalos Terán, I., Imai, K., Lacroix, I. M. E., Fogliano, V., & Udenigwe, C. C. (2020). Bioinformatics of edible yellow mealworm (Tenebrio molitor) proteome reveal the cuticular proteins as promising precursors of dipeptidyl peptidase-IV inhibitors. *Journal of Food Biochemistry*, *44*(2), e13121. https://doi.org/10.1111/JFBC.13121

Drucker, D. J. (2006). Enhancing the Action of Incretin Hormones: A New Whey Forward? *Endocrinology*, *147*(7), 3171–3172. https://doi.org/10.1210/EN.2006-0494

Focaroli, S., Jiang, G., O'connell, P., Fahy, J. V., & Healy, A. M. (2020). The Use of a Three-Fluid Atomising Nozzle in the Production of Spray-Dried Theophylline/Salbutamol Sulphate Powders Intended for Pulmonary Delivery. *Pharmaceutics 2020, Vol. 12, Page 1116*, *12*(11), 1116. https://doi.org/10.3390/PHARMACEUTICS12111116

Galogahi, F. M., Zhu, Y., An, H., & Nguyen, N. T. (2020). Core-shell microparticles: Generation approaches and applications. *Journal of Science: Advanced Materials and Devices*, *5*(4), 417–435. https://doi.org/10.1016/J.JSAMD.2020.09.001

Garzón, A. G., Cian, R. E., & Drago, S. R. (2023). Effects of agar-carrageenan wall materials and core-to-wall material ratio on physicochemical properties and in vitro bioaccessibility of microencapsulated bioactive peptides. *Food Hydrocolloids*, *139*, 108570. https://doi.org/10.1016/J.FOODHYD.2023.108570

Jacobs, I. C. (2014). Atomization and Spray-Drying Processes. *Microencapsulation in the Food Industry: A Practical Implementation Guide*, 47–56. https://doi.org/10.1016/B978-0-12-404568-2.00005-4

Janssen, R. H., Vincken, J. P., Van Den Broek, L. A. M., Fogliano, V., & Lakemond, C. M. M. (2017). Nitrogen-to-Protein Conversion Factors for Three Edible Insects: Tenebrio molitor, Alphitobius diaperinus, and Hermetia illucens. *Journal of Agricultural and Food Chemistry*, *65*(11), 2275–2278. https://doi.org/10.1021/ACS.JAFC.7B00471

Kauppinen, A., Broekhuis, J., Grasmeijer, N., Tonnis, W., Ketolainen, J., Frijlink, H. W., & Hinrichs, W. L. J. (2018). Efficient production of solid dispersions by spray drying solutions of high solid content using a 3-fluid nozzle. *European Journal of Pharmaceutics and Biopharmaceutics*, *123*, 50–58. https://doi.org/10.1016/J.EJPB.2017.11.009

Kim, E. H. J., Chen, X. D., & Pearce, D. (2009). Surface composition of industrial spray-dried milk powders. 2. Effects of spray drying conditions on the surface composition. *Journal of Food Engineering*, *94*(2), 169–181. https://doi.org/10.1016/J.JFOODENG.2008.10.020

Kondo, K., Niwa, T., & Danjo, K. (2014). Preparation of sustained-release coated particles by novel microencapsulation method using three-fluid nozzle spray drying technique. *European Journal of Pharmaceutical Sciences*, *51*(1), 11–19. https://doi.org/10.1016/J.EJPS.2013.09.001

Kurozawa, L. E., Park, K. J., & Hubinger, M. D. (2009). Effect of carrier agents on the physicochemical properties of a spray dried chicken meat protein hydrolysate. *Journal of Food Engineering*, *94*(3–4), 326–333. https://doi.org/10.1016/J.JFOODENG.2009.03.025

Lacroix, I. M. E., Chen, X. M., Kitts, D. D., & Li-Chan, E. C. Y. (2017). Investigation into the bioavailability of milk protein-derived peptides with dipeptidyl-peptidase IV inhibitory activity using Caco-2 cell monolayers. *Food & Function*, *8*(2), 701–709. https://doi.org/10.1039/C6FO01411A

Lacroix, I. M. E., & Li-Chan, E. C. Y. (2012). Dipeptidyl peptidase-IV inhibitory activity of dairy protein hydrolysates. *International Dairy Journal*, *25*(2), 97–102. https://doi.org/10.1016/J.IDAIRYJ.2012.01.003

Lechanteur, A., & Evrard, B. (2020). Influence of Composition and Spray-Drying Process Parameters on Carrier-Free DPI Properties and Behaviors in the Lung: A review. *Pharmaceutics 2020, Vol. 12, Page 55*, *12*(1), 55. https://doi.org/10.3390/PHARMACEUTICS12010055

Liliana Krotz, A., Leone, F., & Giazzi Thermo Fisher Scientifi, G. (n.d.). *Application Note: Elemental Analysis: CHNS/O Determination in Coals*.

Maria Leena, M., Gover Antoniraj, M., Moses, J. A., & Anandharamakrishnan, C. (2020). Three fluid nozzle spray drying for co-encapsulation and controlled release of curcumin and resveratrol. *Journal of Drug Delivery Science and Technology*, *57*, 101678. https://doi.org/10.1016/J.JDDST.2020.101678

Nongonierma, A. B., & Fitzgerald, R. J. (2016). Structure activity relationship modelling of milk protein-derived peptides with dipeptidyl peptidase IV (DPP-IV) inhibitory activity. *Peptides*, *79*, 1–7. https://doi.org/10.1016/J.PEPTIDES.2016.03.005

Pabari, R. M., Sunderland, T., & Ramtoola, Z. (2012). Investigation of a novel 3-fluid nozzle spray drying technology for the engineering of multifunctional layered microparticles. *Expert Opinion on Drug Delivery*, *9*(12), 1463–1474. https://doi.org/10.1517/17425247.2012.734295

Piñón-Balderrama, C. I., Leyva-Porras, C., Terán-Figueroa, Y., Espinosa-Solís, V., Álvarez-Salas, C., & Saavedra-Leos, M. Z. (2020). Encapsulation of Active Ingredients in Food Industry by Spray-Drying and Nano Spray-Drying Technologies. *Processes 2020, Vol. 8, Page 889*, *8*(8), 889. https://doi.org/10.3390/PR8080889

Power, O., Nongonierma, A. B., Jakeman, P., & Fitzgerald, R. J. (2014). Food protein hydrolysates as a source of dipeptidyl peptidase IV inhibitory peptides for the management of type 2 diabetes. *Proceedings of the Nutrition Society*, *73*(1), 34–46. https://doi.org/10.1017/S0029665113003601

Puri, B., Meena, S., Kumar M H, S., Shelke, P. A., Sabikhi, L., & Ashutosh, N. (2023). Encapsulation and Assessment of Antidiabetic Potential of α-Lactalbumin-Derived Hydrolysates. *Journal of Agricultural and Food Chemistry*, *71*(14), 5547–5553. https://doi.org/10.1021/ACS.JAFC.2C08421

Rahmani-Manglano, N. E., Guadix, E. M., Jacobsen, C., & García-Moreno, P. J. (2023). Comparative Study on the Oxidative Stability of Encapsulated Fish Oil by Monoaxial or Coaxial Electrospraying and Spray-Drying. *Antioxidants*, *12*(2), 266. https://doi.org/10.3390/ANTIOX12020266

Richter, B., Bandeira-Echtler, E., Bergerhoff, K., & Lerch, C. (2008). Emerging role of dipeptidyl

peptidase-4 inhibitors in the management of type 2 diabetes. *Vascular Health and Risk Management*, *4*(4), 753–768. https://doi.org/10.2147/VHRM.S1707

Rivero Pino, F., Pérez Gálvez, R., Espejo Carpio, F. J., & Guadix, E. M. (2020). Evaluation of Tenebrio molitor protein as a source of peptides for modulating physiological processes. *Food & Function*, *11*(5), 4376–4386. https://doi.org/10.1039/D0FO00734J

Rivero-Pino, F., Guadix, A., & Guadix, E. M. (2021). Identification of novel dipeptidyl peptidase IV and α-glucosidase inhibitory peptides from *Tenebrio molitor*. *Food & Function*, *12*(2), 873–880. https://doi.org/10.1039/D0FO02696D

Santana, A. A., Kurozawa, L. E., de Oliveira, R. A., & Park, K. J. (2013). Influence of Process Conditions on the Physicochemical Properties of Pequi Powder Produced by Spray Drying. *Drying Technology*, *31*(7), 825–836. https://doi.org/10.1080/07373937.2013.766619

Sarrate, R., Ticó, J. R., Miñarro, M., Carrillo, C., Fàbregas, A., García-Montoya, E., Pérez-Lozano, P., & Suñé-Negre, J. M. (2015). Modification of the morphology and particle size of pharmaceutical excipients by spray drying technique. *Powder Technology*, *270*(Part A), 244–255. https://doi.org/10.1016/J.POWTEC.2014.08.021

Shi, X., & Lee, Y. (2020). Encapsulation of tributyrin with whey protein isolate (WPI) by spray-drying with a three-fluid nozzle. *Journal of Food Engineering*, *281*, 109992. https://doi.org/10.1016/J.JFOODENG.2020.109992

Singh, R. P., & Heldman, D. R. (2014). Dehydration. *Introduction to Food Engineering*, 675–710. https://doi.org/10.1016/B978-0-12-398530-9.00012-7

Sosnik, A., & Seremeta, K. P. (2015). Advantages and challenges of the spray-drying technology for the production of pure drug particles and drug-loaded polymeric carriers. *Advances in Colloid and Interface Science*, *223*, 40–54. https://doi.org/10.1016/J.CIS.2015.05.003

Tan, J., Yang, J., Zhou, X., Hamdy, A. M., Zhang, X., Suo, H., Zhang, Y., Li, N., & Song, J. (2022). *Tenebrio molitor* Proteins-Derived DPP-4 Inhibitory Peptides: Preparation, Identification, and Molecular Binding Mechanism. *Foods 2022, Vol. 11, Page 3626*, *11*(22), 3626. https://doi.org/10.3390/FOODS11223626

Teo, A., Lam, Y., Lee, S. J., & Goh, K. K. T. (2021). Spray drying of whey protein stabilized nanoemulsions containing different wall materials – maltodextrin or trehalose. *LWT*, *136*, 110344. https://doi.org/10.1016/J.LWT.2020.110344

Thongcumsuk, B., Woraprayote, W., Janyaphisan, T., Cheunkar, S., & Oaew, S. (2023). Microencapsulation and Peptide identification of purified bioactive fraction from spirulina protein hydrolysates with dipeptidyl peptidase IV (DPP-IV) inhibitory activity. *Food Bioscience*, *56*, 103438. https://doi.org/10.1016/J.FBIO.2023.103438

Wan, F., Maltesen, M. J., Andersen, S. K., Bjerregaard, S., Foged, C., Rantanen, J., & Yang, M. (2014). One-Step Production of Protein-Loaded PLGA Microparticles via Spray Drying Using 3-Fluid Nozzle. *Pharmaceutical Research*, *31*(8), 1967–1977. https://doi.org/10.1007/S11095-014-1299-1

Wang, B., Yu, Z., Yokoyama, W., Chiou, B. Sen, Chen, M., Liu, F., & Zhong, F. (2021). Collagen peptides with DPP-IV inhibitory activity from sheep skin and their stability to *in vitro* gastrointestinal digestion. *Food Bioscience*, *42*, 101161. https://doi.org/10.1016/J.FBIO.2021.101161

Woo, M. W., & Bhandari, B. (2013). Spray drying for food powder production. *Handbook of Food Powders: Processes and Properties*, 29–56. https://doi.org/10.1533/9780857098672.1.29

6. Supplementary material

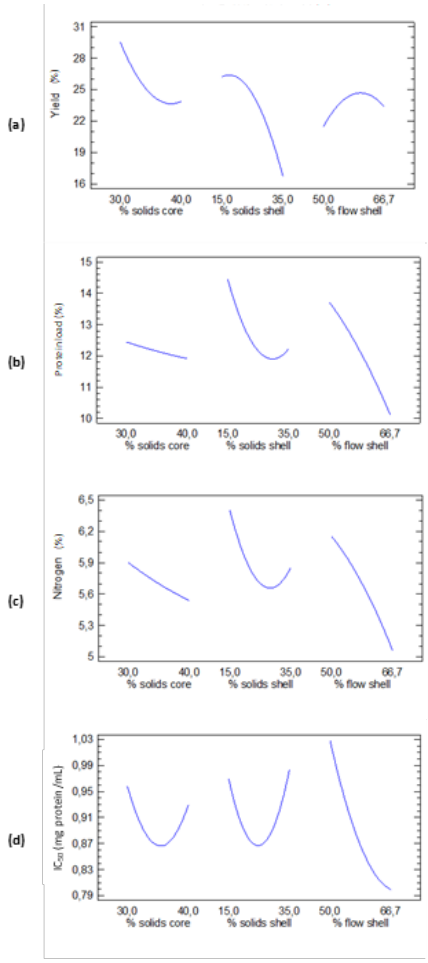

Figure S1. Representation of the global effect of the input variables for (A) yield (%), (B) protein load (%), (C) surface nitrogen, and (D) IC_{50} (mg protein/mL).

CHAPTER VII

Impact of encapsulation on DPP-IV inhibitory activity and gastrointestinal stability of *Tenebrio molitor* and *Olea europaea* protein hydrolysates

ABSTRACT

This study investigated the impact of monoaxial and coaxial spray-drying encapsulation on the stability and bioactivity of antidiabetic protein hydrolysates derived from *Tenebrio molitor* and *Olea europaea* seeds after simulated gastrointestinal digestion. Morphological characterization confirmed the formation of core-shell structures in coaxial encapsulates. Encapsulation significantly improved the retention of DPP-IV inhibitory activity after digestion compared to non-encapsulated hydrolysates, with coaxial spray-drying generally outperforming monoaxial techniques. Notably, formulations containing pullulan in monoaxial encapsulation exhibited comparable protection to coaxial methods, suggesting its role in stabilizing peptide structures. Size-exclusion chromatography revealed that encapsulation helped maintaining the molecular weight distribution of the hydrolysates after digestion, reducing peptide degradation by digestive proteases. Peptidomic analysis using LC-MS/MS identified changes in peptide profiles due to encapsulation and digestion, likely resulting from a combination of protection by the encapsulation but also generation of new peptides during digestion. Challenges in peptide identification were encountered, potentially due to interactions with encapsulating agents and the addition of reagents during simulated digestion. These findings highlight the importance of both encapsulation technique and formulation composition in peptide preservation during gastrointestinal digestion, emphasizing the protective effect of coaxial spray-drying..

1. Introduction

Bioactive peptides derived from food proteins have gained significant attention for their potential in managing diabetes, particularly through the inhibition of dipeptidyl peptidase IV (DPP-IV). This enzyme is responsible for the degradation of glucagon-like peptide-1 (GLP–1) and the gastric inhibitory polypeptide (GIP), resulting in suppressed insulin secretion and increased glucagon levels (Liu et al., 2019). Research has demonstrated that the biological activity of DPP-IV inhibitory peptides is closely linked to their size and sequence. Furthermore, the structural features of these peptides, such as the presence of specific amino acids in specific positions, can influence their ability to bind target enzymes or receptors, thereby affecting their antidiabetic properties (Berraquero–García et al., 2023; Nongonierma & Fitzgerald, 2016).

Although peptides are a major class of therapeutic compounds, their stability during gastrointestinal digestion can be limited (Lacroix & Li–Chan, 2012; Wang et al., 2021). After oral administration, these peptides can be absorbed through the intestinal epithelium and distributed to peripheral tissues via the circulatory system, allowing them to exert their biological effects both locally within the gastrointestinal tract and systemically throughout the body (Garzón et al., 2023). However, without protection from the harsh gastrointestinal environment, these peptides can be hydrolyzed by proteolytic enzymes present in the digestive tract and inactivated before absorption. Although the short length of many bioactive peptides (2–20 amino acid residues) generally improves their gastrointestinal stability (Majura et al., 2022), their stability is also dependent on other factors, such as their amino acid sequence and charge characteristics (Amigo & Hernández–Ledesma, 2020). For instance, we previously reported that simulated gastrointestinal digestion decreased the DPP-IV inhibitory activity of hydrolysates from *Tenebrio molitor* and *Olea europaea* seeds due to degradation of active peptides (Chapter III).

Previous studies have shown that encapsulation can overcome some of these limitations by protecting bioactive molecules and controlling peptide release. However, the effectiveness of encapsulation depends on various factors, such as the type of carrier material, preparation techniques, peptide characteristics, and size (Alvarado et al., 2019). Several encapsulation techniques are available for food bioactives, such as spray drying, spray cooling, spinning disk, fluid–bed coating, extrusion, or multiple emulsions (Sobel et al., 2014). Among these, spray-drying is the most commonly used method for encapsulating thermosensitive compounds in food industry, as it allows the production of dry microparticles at an industrial scale without compromising the integrity of the peptides (Berraquero-García, Pérez-Gálvez, et al., 2023).

Research on the microencapsulation of bioactive peptides by spray-drying has explored the use of various wall materials, including Arabic gum, maltodextrin, alginate, chitosan, concentrated protein isolates, and their combinations (Aquino et al., 2020; Bagheri et al.,

2014; Camargo et al., 2021; Cian et al., 2019). Particularly, Arabic gum has gained interest as the primary encapsulating agent for encapsulation of antidiabetic peptides due to its resistance to digestion and its potential to lower blood glucose levels by inhibiting glucose absorption in the intestine (Phillips, 1998). Interestingly, it was previously reported that the combined used of Arabic gum with Tween 20 and pullulan as encapsulating material enhanced the retention of DPP-IV-inhibitory activity of *T. molitor* hydrolysate encapsulated by monoaxial spray-drying (Berraquero-García, Martínez-Sánchez, et al., 2024). Nevertheless, the presence of synthetic additives such as Tween 20 in food products is often perceived negatively by consumers (Consumer Perceptions Unwrapped: Ultra-Processed Foods (UPF), 2024). As an alternative, coaxial spray-drying can produce advanced capsules with a core-shell structure, potentially improving the protection of bioactive compounds without the need to incorporate additives, or by creating a layer of different wall materials. In this sense, sodium alginate is a valuable shell material due to its resistance to gastric digestion, although its high viscosity at low concentrations limits its use in traditional spray-drying. Coaxial spray drying has successfully incorporated sodium alginate as a shell layer, improving stability and targeted release of bioactive compounds (Alvarez et al., 2024). Although this technique presents significant advantages, the application of coaxial spray-drying for the encapsulation of protein-based bioactive compounds remains relatively unexplored in the literature, with only three published studies on this topic (Berraquero-García, Coronas-Lozano, et al., 2024; Shi & Lee, 2020; Wan et al., 2014).

Mass spectrometry (MS) is a powerful tool for monitoring peptide stability through processing stages (e.g., heat treatment, storage, drying etc.) (Contreras et al., 2008), which can provide both qualitative and quantitative data on encapsulation efficiency and the impact of digestion. However, its application to complex matrices presents significant challenges, particularly due to the presence of multiple interacting components that can interfere with peptide identification. Notably, most of existing studies do not assess whether the encapsulated peptides are retained after digestion using peptidomics. When proteomic analysis is employed, research largely relies on simplified systems, such as synthetic peptides (Atma et al., 2024), or focusing exclusively on longer peptides to avoid digestion-induced generation, which complicates identification (Alvarado et al., 2019; Jiménez-Munoz et al., 2024).

This research focuses on developing an oral delivery system for protein hydrolysates with demonstrated antidiabetic properties, using various encapsulation techniques and formulations. Specifically, *Tenebrio molitor* and olive seed protein hydrolysates, which have previously exhibited antidiabetic effects, were employed for this purpose (Chapter VI). The study evaluates the impact of monoaxial and coaxial spray-drying encapsulation on the preservation of antidiabetic activity and the stability of bioactive peptides under simulated gastrointestinal digestion conditions. Therefore, this work provides new insights into the encapsulation of bioactive peptides which will facilitate the incorporation of these bioactive compounds into diverse food products.

2. Materials and methods

2.1. Materials

Tenebrio molitor (TM) and *Olea europae* seed (OS) meals were kindly donated by Tebrio (Salamanca, Spain) and by Q'omer (Valencia, Spain), respectively. Both meals were stored at −16 °C until further use. Alcalase 2.4L (subtilisin, EC 3.4.21.62) and Flavourzyme 1000L (3.4.11.1) were provided by Novozymes (Bagsvaerd, Denmark). The *T. molitor* hydrolysate (TH, 67.7 ± 0.3% protein) and olive seed hydrolysate (OH, 25.7 ± 0.1% protein) were produced using a 1:1 mix of the enzymes Alcalase® (subtilisine, EC 3.4.21.62) and Flavourzyme® (mix of endo and exo-proteases) at a 6 E/S ratio until a degree of hydrolysis (DH) of 20% was achieved, according to Chapter VI.Nexira (Serqueux, France) generously provided the Arabic gum. Pullulan was kindly donated by Hayashibara Co., Ltd. (Okayama, Japan), while Tween 20 was sourced from Sigma Aldrich (Darmstadt, Germany). Enzyme and substrates for the DPP-IV inhibitory activity assays, as well as the reagents for digestion were purchased from Sigma–Aldrich (St Louis, US). The digestive enzymes employed were pepsin (Merck, Germany) and pancreatin (Sigma–Aldrich, US).

2.2. Encapsulation by monoaxial spray-drying

Table 1 shows the three different formulations prepared for each hydrolysate which were used as feed for the monoaxial spray-drying process. The feed solution was prepared by dispersing the respective hydrolysate and the Arabic gum in distilled water and stirring for 24 h until complete dissolution, followed by the incorporation and dissolution of Tween 20 and/or pullulan for additional 2 h, as described by Berraquero-García, Martínez-Sánchez, et al. (2024). The different formulations were adapted to include 15 % protein (w/w) in the final capsules.

All formulations were spray dryed in monaxial mode, using a laboratory-scale spray dryer (Büchi B–190; Büchi, Flawil, Switzerland) equipped with a 0.7 mm diameter 2- fluids nozzle (Büchi, Flawil, Switzerland). The inlet air temperature was adjusted to 190 °C, with the outlet air temperature controlled between 100 and 110 °C. The drying airflow was fixed at 25 Nm^3/h. The yield of the drying process was calculated based on the amount of powder collected and the theoretical solids fed. After production, the microcapsules were stored at −20 °C in the dark until further analysis. Encapsulation by coaxial spray-drying

Two different formulations were prepared for the shell feed solution while keeping the same core feed solution (Table 1). Arabic gum was maintained as the main encapsulating material for the core and shell feed solutions, and alginate was additionally included in the shell feed. For the core solutions, the total solids were 40% and the protein content was

fixed at 15% in the final capsule. Core feed solutions were prepared as previously described to produce monoaxial spray-dried capsules. The shell feed solutions were prepared at 30% wt. solids by adding either Arabic gum or an Arabic gum–alginate (1%) mix to distilled water and stirring for 2 h until complete dissolution. The marker 5(6)–carboxyfluorescein (25mM) was added at the moment of spray-drying in order to further confirm the formation of a core-shell structure. The formulations were dried using a 3–fluids nozzle with core and shell tip diameters of 0.7 and 2.0 mm, respectively (Büchi, Flawill, Switzerland). Inlet and outlet temperature of the drying air as well as air flow-rate were maintained the same as for the monoaxial spray-drying. The resulting microcapsules were stored at −20 °C in the dark until analysis.

Table 1. Composition of feed(s) formulations prepared for spray-drying encapsulation.

			Core (40% solids)		Shell (30% solids)
Substrate	**Code**	**Spray-drying configuration**	**Encapsulating material**	**Additives**	**Encapsulating material**
T. molitor meal	CT1	Monoaxial	Arabic gum	–	
	CT2		Arabic gum	Tween 20 (1%)	
	CT3		Arabic gum	Tween 20 (1%) + pullulan (1%)	
	CT4	Coaxial	Arabic gum	–	Arabic gum
	CT5		Arabic gum	–	Arabic gum + alginate (1%)
O. europaea seed meal	CO1	Monoaxial	Arabic gum	–	
	CO2		Arabic gum	Tween 20 (1%)	
	CO3		Arabic gum	Tween 20 (1%) + pullulan (1%)	
	CO4	Coaxial	Arabic gum	–	Arabic gum
	CO5		Arabic gum	–	Arabic gum + alginate (1%)

2.3. Characterization of the capsules

2.3.1. Morphology and particle size distribution

Scanning electron microscopy (SEM) was used to analyze the capsule morphology, employing a FESEM microscope (LEO 1500 GEMINI, Zeiss, Germany). Samples were prepared by mounting them on carbon tape and coating with carbon using a EMITECH K975X Turbo–Pumped Thermal Evaporator (Quorum Technologies, UK). SEM images were acquired at magnifications between 500X and 5KX, using a 3 kV accelerating voltage and a 30 μm aperture. The particle size distribution was determined by measuring 200 randomly selected particles with ImageJ software. The size distribution was represented and the average particle size calculated.

2.3.2. Core-shell structure of the coaxial microcapsules

The structure of the microcapsules was analyzed using confocal microscopy (Leica TCS SP5 I, Leica Microsystems Inc., IL, USA). A fluorescent dye, 5–carboxyfluorescein (0.5 mL, 25 mM), was incorporated into 300 g of the shell feed solution. The microparticles were mounted on a microscope slide and exposed to an excitation wavelength of 488 nm. The fluorescent signal was collected at 509–548 nm, and confocal images were obtained at a magnification of 3X.

2.3.3. Protein content

Nitrogen content in all samples (i.e., hydrolysates, encapsulates and digests) was determined in triplicate using the Dumas method(Liliana Krotz et al., n.d.) with a Flash 2000 CHNS/O elemental analyser (Thermo Scientific, Waltham, MA, USA). Protein content was subsequently calculated using nitrogen–to–protein conversion factors of 5.6 for *T. molitor* hydrolysate (Janssen et al., 2017) and 5.3 for olive seed hydrolysate (Maestri et al., 2019).

2.3.4. Surface nitrogen

X–ray photoelectron spectroscopy (XPS) was used to analyze the presence of protein hydrolysate on the surface of the microparticles. The microcapsule samples were mounted on a glass slide and examined using a Kratos Axis Ultra–DLD (Kratos Analytical, Manchester, UK) with Al–Kα radiation at 450 W. Wide–energy survey scans (0 – 1200 eV) were performed with a pass energy of 160 eV and a step size of 1.0 eV. Charge neutralization was activated, and the analysis was conducted with a penetration depth under 10 nm. Measurements were performed in triplicate, and the results are expressed as the nitrogen content relative to the total elemental composition on the capsule surface, presented as a percentage. It was observed that neither the encapsulating agents nor the additives exhibited any nitrogen when analyzed by XPS, indicating that all the detected nitrogen was attributed to the hydrolysate. To account for variations in nitrogen content among samples, the surface nitrogen detected by XPS was normalized to the total nitrogen content of the microcapsules, as determined by the Dumas method.

2.4. *In vitro* simulated gastrointestinal digestion (SGIC)

The digestion simulation was carried out following the INFOGEST Protocol (Brodkorb et al., 2019). The digestion process was conducted in duplicate for each sample using a temperature–controlled shaker (Heidolph, Germany) at 37°C with 250 rpm agitation. The hydrolysates were first dissolved in distilled water at a concentration of 50 mg protein/mL and then mixed with an equal volume of simulated salivary solution. After pH adjustment to 7, they were incubated for 2 min with salivary amylase (75 U/mL). Subsequently, the same volume of simulated gastric fluid was added, the pH was adjusted to 3, and the mixture was incubated for 2 h with pepsin (2000 U/mL). Finally, the simulated intestinal solution was added at the same ratio, the pH was adjusted to 7, and pancreatin (100 U/mL) was added, followed by a 2 h incubation. The digestion was terminated by heating the mixture at 85°C for 15 min to inactivate the enzymes (Gallo et al., 2022). The digested samples were then centrifuged at 5,000 g for 20 min and stored at –20°C until further analysis.

2.5. DPP-IV inhibitory activity

The DPP-IV inhibitory activity of the hydrolysates, the encapsulates, and the resulting digests was assessed using a modified method based on (Lacroix et al., 2017). Briefly, 100 µL of aqueous sample solutions at different concentrations (1.5–5 mg protein/mL) were incubated with 25 µL of DPP-IV enzyme (0.02 U/mL) at 37 °C for 10 min, followed by the addition of 50 µL of 1 mM Gly–Pro–p–nitroanilide. The reaction kinetic was measured at 405 nm (37 °C) over 2 hat 2 min intervals using a Multiskan FC microplate photometer (Thermo Scientific, Vantaa, Finland). All samples were tested in triplicate and a colour control was included. The activity was determined as the half–maximal inhibitory concentration (IC_{50}) by plotting the progress of the reactions compared to the blank (distilled water). Results are reported in mg protein/mL as mean ± standard deviation.

2.6. Size exclusion chromatography (SEC)

Size exclusion chromatography was employed to study the molecular weight distribution (MWD) of all samples. SEC analysis was conducted as described in (Ospina–Quiroga et al., 2022). The samples were solubilized in distilled water at a concentration of 5 mg/mL, and 500 µL aliquots were injected into an AKTA Purifier10 FLPC System with a Superdex Peptide 10/300 GL size-exclusion column (GE Health–care, Uppsala, Sweden), each sample was analysed in duplicate to ensure reproducibility. Elution was carried out using distilled

water as the mobile phase at a flow rate of 0.5 mL/min, and the absorbance of the eluted fractions was monitored at 280 nm. The molecular weight distribution of the samples was related to a calibration curve prepared with glycine (75.1 Da), peptide LPSDATPVLD (1027.1 Da), peptide VSKDSPETYEEALKR (1751.9 Da), peptide LLVQVGENLLKKPVSKDNPE (2220.6 Da), peptide GVKGIIPGTILEFLEGQLQKMDNNADAR (3028.44 Da), peptide SSQLGYNLLYCPVTSSSDDQFCSK (3810.08) and aprotinin (6511.5 Da) as standards.

2.7. Peptidomics analysis by LC–MS/MS

The detailed proteomics protocol has been previously described in the Materials and Methods section in the summary of this Ph.D thesis. Briefly, samples were solubilized, reduced, alkylated, and purified using C-18 StageTips. Peptides were resuspended in buffer of 2% acetonitrile (ACN) with 0.1% formic acid (FA) and analyzed via EASY-nLC 1200 system (Thermo Fisher Scientific, Waltham, MA, USA) with ESI coupled to a Q Exactive HF Orbitrap mass spectrometer (Thermo Fisher Scientific, Waltham, MA, USA). Peptides were first retained on a PepMap precolumn (C18, 100 Å, 100 µm x 2 cm), followed by a Pepmap analytical Column (C18, 100 Å, 74 µm x 50 cm). A 90-minute gradient was applied using mobile phase A (MPA, water) and mobile phase B (MPB, 95% acetonitrile). Mass spectrometry analysis was performed in full MS/ddMS2 data-dependent mode, as detailed earlier. Peptide match was preferred, and "exclude isotopes" was enabled.

2.8. LC-MS/MS data processing

Raw data processing was conducted as previously detailed in the Materials and Methods section in the summary of this Ph.D thesis. Briefly, data were analyzed using MaxQuant v.2.2.0.0 software and the Andromeda search engine against UniProt databases for *Tenebrio molitor* and *Olea europaea*. An unspecific *in silico* digestion approach was applied, with peptides filtered based on quality criteria: Andromeda score ≥40 and reproducibility in at least two out of three replicates. Peptide characteristics such as sequence length, molecular weight, hydrophobicity, key amino acid presence, and predicted bioactivity using StackDPPIV were assessed. Findings were validated against the BIOPEP database (Minkiewicz et al., 2019) and existing literature (Berraquero-García et al., 2023).

2.9. Statistical analysis

Statistical analysis was performed for experimental data in StatGraphics 5.1 (Statpoint Technologies, Inc., Warrenton, VA, USA) using multiple comparisons of means by multiple comparison analysis of variance (ANOVA) and Tukey's HSD test with a 95% confidence level.

3. Results and discussion

3.1. Characterization of the capsules

3.1.1. Morphology, structure and particle size distribution

The *T. molitor* (CT1–CT5) and olive seed (CO1–CO5) protein hydrolysates were microencapsulated using spray-drying, with Arabic gum serving as the main wall material. The SEM micrographs (Figure 1) depict the morphology of the hydrolysate-containing spray-dried powders, which exhibit a pseudo-spherical morphology with a wrinkled surface, small pores, and no apparent cracks. These heterogeneous shapes are typically observed for spray-dried particles in both monoaxial and coaxial configurations, obtained from aqueous solutions of Arabic gum (Bhujbal et al., 2021; Kim et al., 2009). This is due to the rapid evaporation of the solvent, leading to the formation of a crust of biopolymer on the surface that shrinks, resulting in dimpled shapes (Boel et al., 2020). Although the morphology was similar for all microcapsules, regardless of the substrate used, a few strands can be seen for samples CT3 and CO3, which correspond to those with added pullulan. This is normal for pullulan–containing samples, since pullulan tends to form this type of structures, although, due to the low concentration, it did not significantly affect the morphology.

The size distribution of microcapsules is illustrated in Figure 2, exhibiting significant variances across samples. Regarding capsules monoaxially spray-dried, those using Arabic gum with Tween 20 and pullulan (CT3 and CO3) exhibited the largest particle size (7.77 ± 5.26 μm and 8.55 ± 5.02 μm, respectively). This is consistent with previous reports on the encapsulation of *T. molitor* hydrolysates using monoaxial spray-drying (Berraquero-García, Martínez-Sánchez, et al., 2024) which associated the increased viscosity of the solution

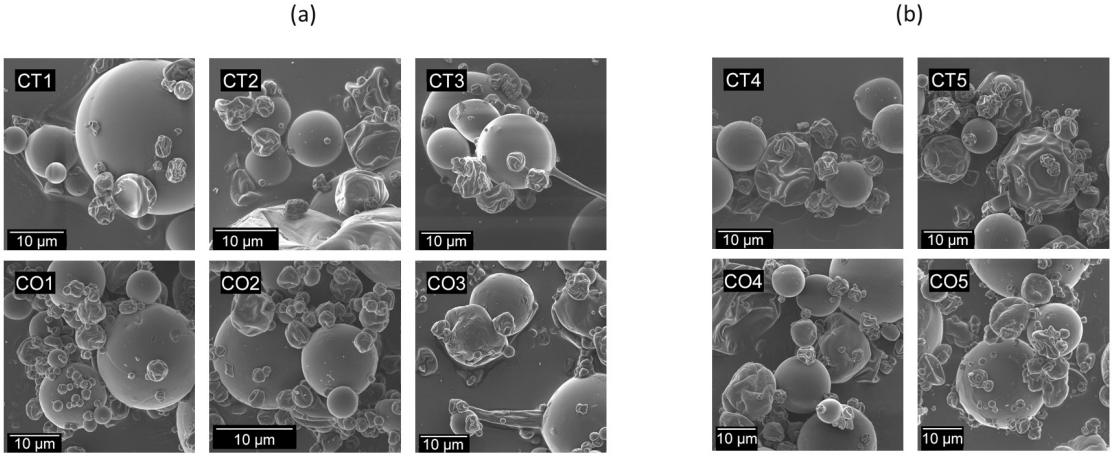

Figure 1. Scanning electron microscopy images of microcapsules loaded with *T. molitor* (CT) or *O. europaea* seed (CO) protein hydrolysate and obtained by (a) monoaxial or (b) coaxial spray-drying. Sample ID referring to Table 1.

provided by pullulan to the formation of larger droplets after atomization and, consequently, larger particles. Additionally, the incorporation of pullulan resulted in a greater size variability, suggesting that atomization and drying kinetics might have been less uniform.

Capsules produced using coaxial spray-drying, which incorporated an additional shell layer of Arabic gum, are generally larger and more robust due to the additional material surrounding the core. Notably, CT4 and CO4 demonstrated a marked increase in mean particle size compared to CT1 and CO2, reaching 8.71 ± 6.02 μm and 6.60 ± 5.68 μm, respectively. However, smaller particles were observed in CT5 (5.73 ± 5.87 μm) and CO5 (5.16 ± 4.38 μm), which included 1% alginate in the shell formulation. Given that alginate typically increases solution viscosity, it was expected to obtain larger particles (Permanadewi et al., 2022). Nonetheless, a similar trend was reported in the spray-drying of ranitidine-loaded capsules containing 1% alginate, where capsule size decreased(Szekalska et al., 2015).

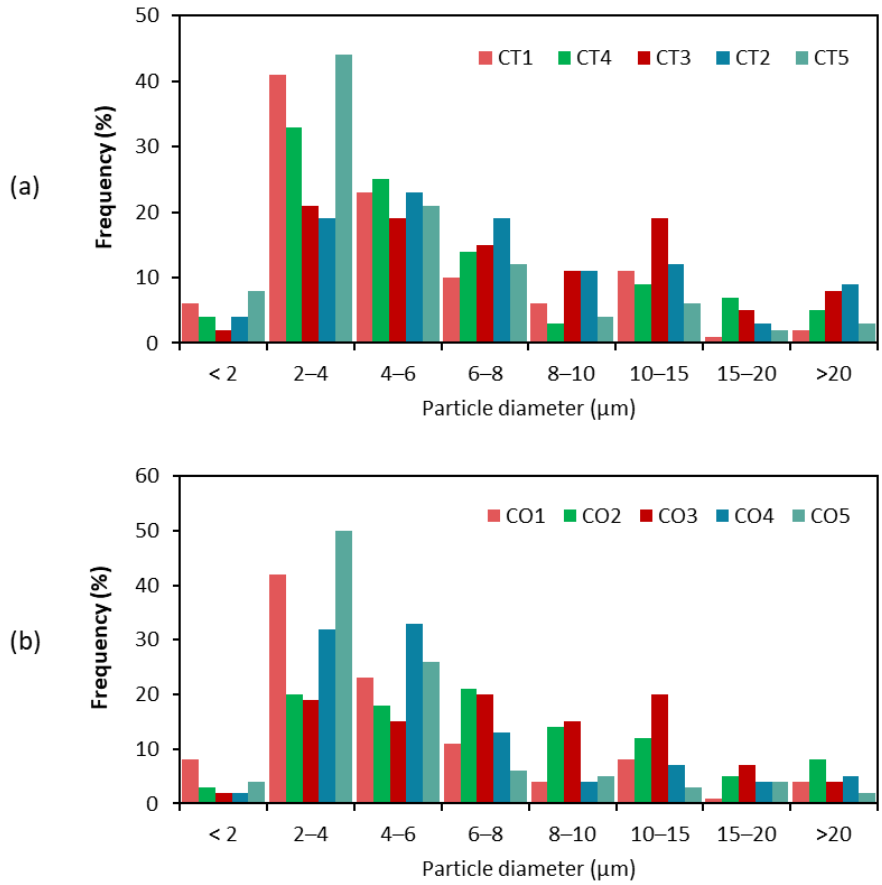

Figure 2. Size distribution of the microcapsules loaded with (a) *T. molitor* or (b) *O. europaea* seed protein hydrolysate. Sample ID referring to Table 1.

Confocal microscopy of the coaxially obtained microcapsules revealed green fluorescence from the 5-carboxyfluorescein present in the shell, while no fluorescence was observed in the core in any of the microcapsules (Figure 3). This indicated the formation of core-shell microcapsules for all the formulations and processing conditions evaluated in coaxial mode. This finding confirms the successful formation of core-shell microcapsules, which might help to prevent protein migration to the surface and protect the bioactive peptides from external stress (Maria Leena et al., 2020).

3.1.2. Yield, protein load and surface composition

The production yield of the spray-dried microcapsules is a critical parameter that directly impacts the efficiency and cost-effectiveness of the spray drying process. As presented in Table 2, the encapsulation yield ranged from 14.14% to 27.67% for *T. molitor* samples (CT1–CT5), and from 12.13% to 27.03% for olive seed samples (CO1–CO5). Generally, the monoaxial spray-drying method resulted in higher yields compared to the coaxial approach. This can be attributed to the challenges associated with coaxial spray-drying, such as the introduction of a second feed solution, which can potentially increase humidity levels within the drying

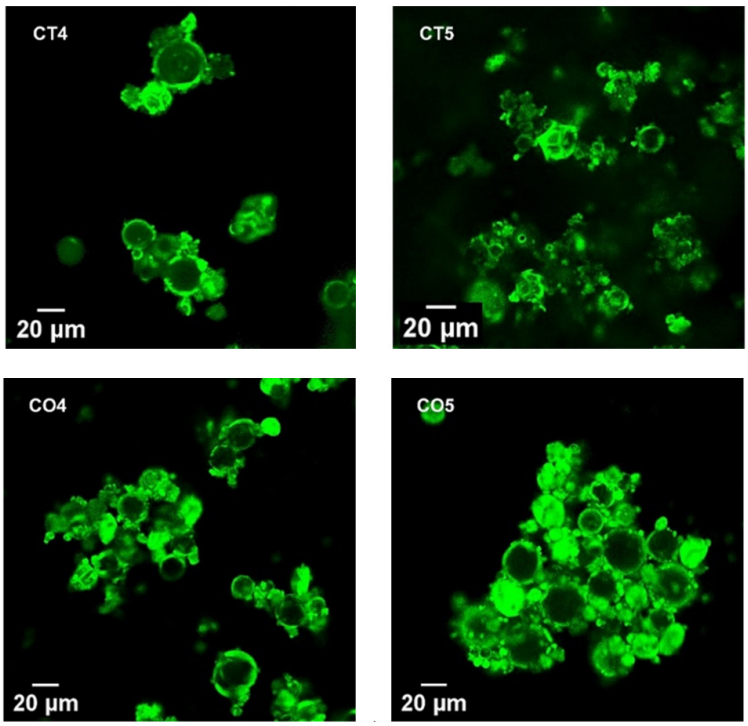

Figure 3. Confocal microscopy images of microcapsules loaded with *T. molitor* (CT) or *O. europaea* (CO) protein hydrolysate and obtained by coaxial spray-drying. Sample ID referring to Table 1.

chamber, leading to increased liquid deposits. These factors can contribute to powder stickiness and lower yields (Kauppinen et al., 2018). This effect was particularly evident in coaxial formulations containing alginate (CT5 and CO5), where yields were notably lower. The increased viscosity of alginate can hinder atomization and drying efficiency, leading to reduced powder recovery. Similar challenges were reported in the encapsulation of ascorbic acid using sodium alginate and Arabic gum, where viscosity alterations negatively affected the spray-drying performance (Barra et al., 2019).

Table 2 shows the surface nitrogen (N) of the capsules, which serves as an indicator of peptides encapsulation and peptides surface exposure. Among the *T. molitor* capsules, CT1 and CT5 exhibited the highest presence of surface N (6.44% and 5.56%, respectively), indicating notable peptides exposure on the surface. This increased exposure might lead to higher degradation of the encapsulated antidiabetic peptides during processing and storage.

Conversely, CT2 and CT3 exhibited remarkably lower surface N (4.52 and 4.18%, respectively), likely due to the stabilizing effects of Tween 20 on peptides and proteins in aqueous solutions. The presence of Tween 20 as a surfactant can compete with peptides for adsorption at the air-water interface during atomization and drying, potentially leading to a preferential migration of Tween 20 to the air/water interface over the peptides. This could result in reduced protein exposure at the surface (Adhikari et al., 2009; Rabe et al., 2020). This was also exhibited for the olive seed capsules CO2 and CO3 (4.46 % and 3.18%, respectively). It is worth noting the specially low values obtained for CT3 and CO3, which could be linked to the addition of pullulan, potentially contributing to peptide protection (Singh et al., 2009).

Interestingly, CT4 and CO4, despite having quite low protein loads (12.00% and 11.32%, respectively), displayed relatively high surface N at 4.26 and 3.12%, respectively, which suggest the incomplete formation of a shell layer during coaxial encapsulation. Additionally, the coaxial encapsulation with alginate resulted in a remarkably higher surface N, suggesting that the increased viscosity obtained from the alginate addition limited the efficiency of the encapsulation process (Weng et al., 2023).

It is worth noting that protein diffusion to the surface is a common occurrence during the drying process (Haque & Adhikari, 2014), as the surface activity of peptides can lead to their migration to the droplet surface, creating a diffusional flux towards it. Additionally, as the evaporating droplet diminishes in size, its receding surface also contributes to an increase in protein concentration on the surface.

3.2. Effect of gastrointestinal digestion on microcapsules properties

3.2.1. DPP-IV inhibitory activity

The DPP-IV inhibitory activity of all samples was evaluated *in vitro* before and after simulated gastric and intestinal digestion (Figure 4). In Figure 4a, results for the *T. molitor* hydrolysate, its encapsulated forms (CT1–CT5) and the respective digests (GD and ID) are expressed as IC_{50} (mg protein/mL), whereas for HO and its encapsulates (CO1–CO5), values are reported as IC_{30} (mg protein/mL) (Figure 4b). The distinction was partly attributed to the relatively lower inhibition exhibited by the HO samples, as well as the colorimetric nature of the assay used.

However, post-digestion analysis of HT and HO revealed a substantial loss of antidiabetic bioactivity in both cases. This was attributed to peptide degradation by the effect of digestive enzymes as well as the effect of the acidic digestive conditions, as similarly described for *T. molitor* antioxidant hydrolysates, where a reduction in bioactivity was observed after simulated digestion (Gonzalez-de la Rosa et al., 2024).

Table 2. Effect of encapsulation method and formulation on Yield (%), protein load (%), and surface nitrogen (%) of antidiabetic hydrolysates capsules. Samples with different letters are significantly different ($p < 0.05$). Lowercase used for *T. molitor* samples and uppercase used for olive seed.

Code	Yield (%)	Protein load (%)*	Surface Nitrogen (%)**
CT1	26.3	15.88 ± 0.28^{a}	6.44 ± 0.14^{a}
CT2	24.7	15.96 ± 0.08^{a}	4.52 ± 0.14^{b}
CT3	27.7	15.65 ± 0.04^{a}	4.18 ± 0.06^{bc}
CT4	20.6	12.00 ± 0.02^{b}	4.26 ± 0.13^{c}
CT5	14.1	12.73 ± 0.02^{c}	5.66 ± 0.10^{d}
CO1	27.0	15.90 ± 0.22^{A}	4.46 ± 0.04^{A}
CO2	23.5	15.24 ± 0.71^{AB}	3.18 ± 0.07^{B}
CO3	24.7	14.64 ± 0.09^{B}	1.75 ± 0.06^{C}
CO4	19.7	11.32 ± 0.04^{C}	3.12 ± 0.01^{B}
CO5	12.1	11.41 ± 0.02^{C}	3.03 ± 0.27^{B}

* Corresponds to the total protein content in the capsules

** Normalized to total protein content, represents the proportion of nitrogen detected on the capsule surface.

Before assessing the protective effect of encapsulation during digestion, it is crucial to consider its initial effect on hydrolysate activity. A clear variation in DPP-IV inhibition was observed depending not only on the encapsulation technique, but also on the encapsulating agents employed. Monoaxial spray-dried capsules (CT1, CT2, CO1 and CO2) exhibited the highest bioactivity loss, likely due to poor hydrolysate retention within the capsule and peptide migration to the surface, as represented by the surface N to protein ratio, exposing peptides to degradation during processing and posterior storage (Shrestha et al., 2007). Interestingly,

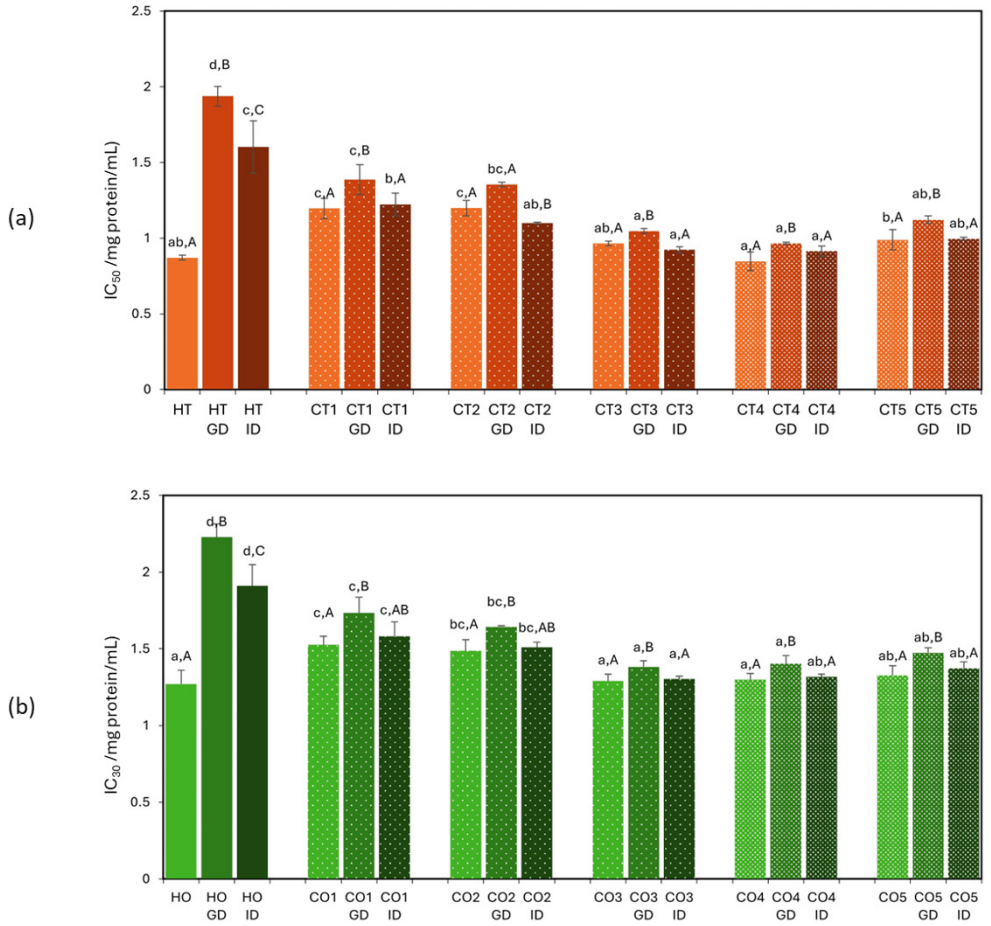

Figure 4. DPP-IV inhibitory activity of the (a) *T. molitor* and (b) olive seed protein hydrolysate, its encapsulates and digests. Samples ID referring to Table 1; GD indicates gastric digestion and ID indicates intestinal digestion. Results represent the mean ± SD (n = 3). Samples with different letters are significantly different ($p < 0.05$). Lowercase letters indicate differences within the same digestion level (non-digested, GD, or ID), while uppercase letters denote differences within the same encapsulation mechanism group (hydrolysate or capsules).

CT3 and CO3, despite being monoaxially encapsulated, retained more bioactivity comparable to coaxial formulations. This could be attributed to the inclusion of pullulan, which possesses excellent heat resistance, high mechanical strength and film-forming properties (Sun et al., 2020). Its addition increases the viscosity of the formulation, reducing peptide diffusion to the air-water interface and enhancing retention. Additionally, the combination of Arabic gum and pullulan has demonstrated synergistic effects in other encapsulation methods such as electrospinning, where strong hydrogen bond interactions improved matrix stability and thermal protection (Ma et al., 2021).

Regarding the protective effect of encapsulation against digestion, encapsulation significantly improved bioactivity retention compared to non-encapsulated hydrolysates. Particularly, coaxial spray-drying (CT4, CT5, CO4, CO5) generally outperformed monoaxial techniques (CT1–CT3, CO1–CO3). Nonetheless, the addition of pullulan enhanced activity retention after digestion, due to its role in maintaining capsule structural integrity as previously mentioned. The addition of Tween 20 (CT2 and CO2) did not result in a significant improvement, although previous studies reported enhanced protection of flaxseed peptides spray-dried capsules when using a similar surfactant, Tween 80. This was attributed to a reduction in the aggregation and localization of peptides at the interface during atomization and drying (Sarabandi & Jafari, 2020). Finally, among the selected coaxial encapsulating agents, 1% alginate led to a significant loss of bioactivity, particularly for *T. molitor* (CT5). This could be attributed to the increase in the formulation viscosity (Barra et al., 2019), which negatively impacted encapsulation efficiency and retention, as indicated as well by the reduced yield discussed in a previous section (3.1.2).

It is worth mentioning that a consistent trend was observed across both hydrolysates regarding the impact of either partial (GD- gastric) or complete (ID- intestinal) digestion. Gastric digestion (GD) led to a more pronounced bioactivity loss than intestinal digestion (ID), likely due to the pepsin broad specificity and a preference for cleaving peptide bonds adjacent to aromatic (Phe, Tyr and Trp) and hydrophobic residues (Ala, Val, Ile, Leu and Met) (Ahn et al., 2013). This specificity, distinct from the enzymes used to produce the original hydrolysates, results in higher degradation and bioactivity loss. Hence, considering the preferences of the enzymes is crucial for the design of bioactive peptides and their resistance to being further digested.

3.2.2. Peptide size distribution analysis

The molecular weight distribution (MWD) of the HO and HT hydrolysates, as well as the resulting encapsulates and their digests, was analysed using size-exclusion chromatography (Figure 5).

As established in Chapter VI, gastrointestinal stability of the hydrolysates correlates with MWD changes post-digestion. Comparative analysis of HT and HO samples during partial

and complete digestion revealed a significant decrease in peptide size, increasing the lower molecular weight fractions. Particularly for HT (Figure 4a), the 0.5–0.2 kDa fraction (32% of the peptides) was substantially degraded by intestinal pancreatin, with 51% of the peptides falling below 0.2 kDa post-digestion. In HO (Figure 4b), the > 7.0 kDa fraction, initially 59%, dropped to 24% after ID, with extensive digestion yielding 13% of peptides < 0.2 kDa. These drastic shifts coincide with the previously discussed loss of bioactivity.

Encapsulation influenced the MWD, resulting in distributions after digestion more similar to those of the original hydrolysate, though with varying degrees of efficiency. Monoaxial encapsulates (CT1, CT2, CO1 and CO2) presented the greatest peptide degradation

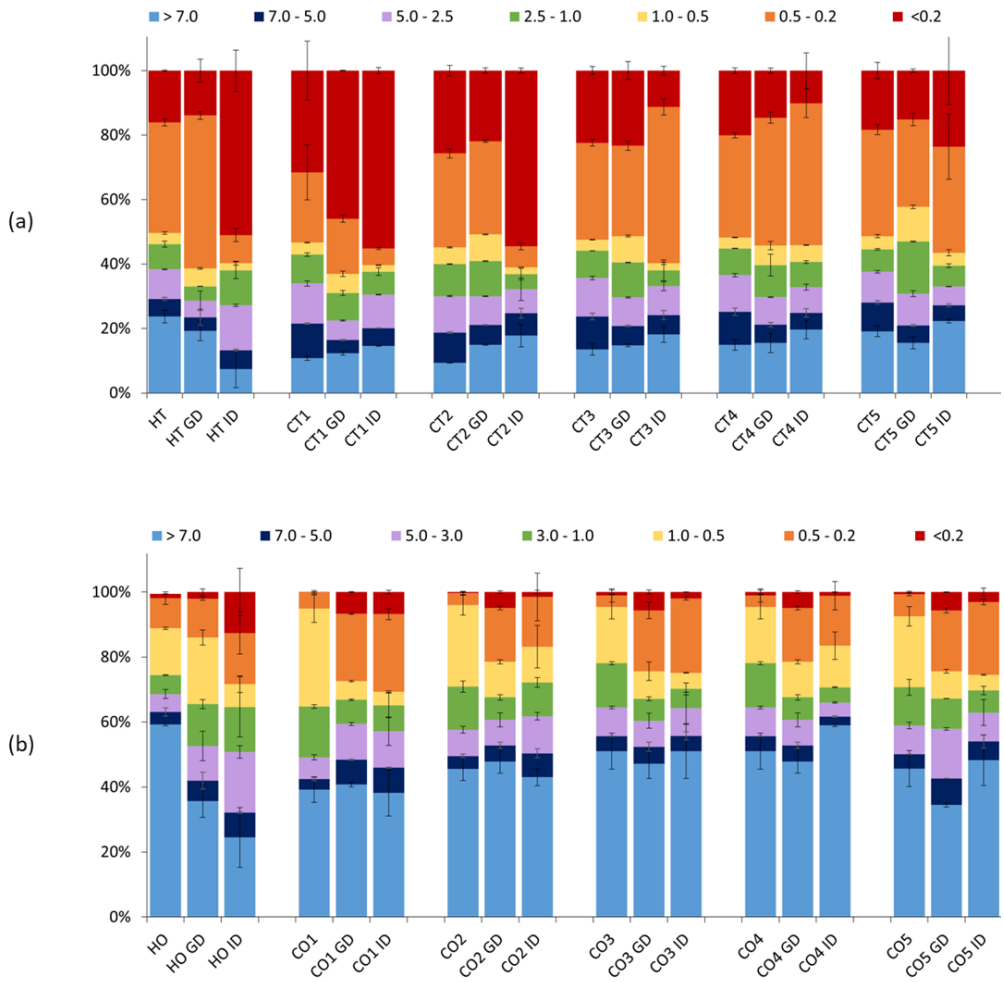

Figure 5. Molecular weight distribution of the *T. molitor* (a) and olive seed (b) hydrolysates, its capsules and their digests. Samples ID referring to Table 1; GD indicates gastric digestion and ID indicates intestinal digestion. Results represent the mean ± SD (n = 3).

and smaller molecular weight fragments, while pullulan-based formulations (CT3 and CO3) retained size distribution profiles resembling the original hydrolysates. Coaxial capsules (CT4-5 and CO4-5) also resulted in MWD similar to the free hydrolysates, suggesting that this encapsulation approach enhances the stability of the hydrolysates by retaining the peptides within the biopolymer matrix, thereby protecting them from degradation.

Regarding the protective effect of the encapsulation during partial (gastric - GD) and complete (intestinal - ID) digestion, a significant degradation during ID occurred in *T. molitor* capsules, especially in CT1 and CT2, which resulted in the generation of peptides in the <0.2 kDa range. In particular, CT1 exhibited moderate protection, reducing <0.2 kDa peptide content to 32% (vs. 51% in HT), while CT2 further improved stability (22% <0.2 kDa peptides), highlighting Tween 20's role in peptide preservation. CT3 behaved similarly to CT2, while coaxial encapsulation (CT4, CT5) improved resistance to digestion. CT4 was the most protective, suggesting its additional shell layer hindered peptide hydrolysis. CT5 also enhanced stability, though slightly less than CT4, likely due to its higher viscosity from alginate addition (Barra et al., 2019). This increased viscosity may have partially obstructed the nozzle, leading to an incomplete shell layer and affecting overall stability. It is worth noting an apparent increase in the >7.0 kDa fraction after digestion, which can be observed for all samples. This situation suggests peptide aggregation rather than new sequence formation, which has been previously reported and attributed to aggregates between peptides and other components by hydrophobic interactions and hydrogen bonds (Pérez-Gálvez et al., 2024).

Olive seed hydrolysate encapsulates exhibited similar trends as the ones containing *T. molitor*, with potential peptide aggregation increasing the >7.0 kDa fraction, most notably in CO4 and CO5. Additionally, the 1.0–0.5 kDa fraction was degraded to the greatest extent in CO1 and CO2, while there was also a notable increase in peptides <0.2 kDa. In comparison, the fraction > 7.0 kDa remained largely unaffected, which aligns with previous studies on plant-based proteins and their digestibility (Santos-Hernández et al., 2020).

In general, the consistent shift towards smaller peptides post-digestion across all samples indicated limited protection. Nonetheless, it can be concluded that coaxial encapsulation was more effective than monoaxial encapsulation in preserving the molecular size distribution of the hydrolysates, likely due to the additional protective layer, which would limit enzymatic access and peptide diffusion. Furthermore, Arabic gum, the main encapsulating agent in the shell, is known to resist digestion by enzymatic hydrolysis and gastric acid pH, as reported in multiple studies (Calame et al., 2008; Cherbut et al., 2003; Elnour et al., 2023; Rawi et al., 2021). This supports the idea that coaxial capsules would provide more protection, and the observed degradation could be attributed to incomplete shell formation.

Finally, it should be noted that some degree of degradation was expected to be found given the inherent challenges of achieving perfect encapsulation. Indeed, previous studies on bioactive peptide encapsulation via spray drying have reported variations in the size of the peptides even in samples where bioactivity was retained post-digestion (Cian et al., 2020; Garzón et al., 2023).

3.3. Peptidomics analysis

3.3.1. Impact of encapsulation on peptides retention

To further assess the impact of encapsulation and digestion on hydrolysates, two encapsulated formulations and their digests were selected alongside the original hydrolysates as references. Capsules CT3, CT4, CO3 and CO4 were chosen for their high yield, and superior bioactivity retention after simulated digestion. As previously described, these formulations were produced via monoaxial (CT3, CO3) and coaxial (CT4, CO4) spray drying, allowing comparison of the protective effects of additional additives (i.e., Tween 20 and pullulan) or an extra shell layer. Through peptide identification and characterization, we attempted to evaluate whether encapsulation preserved peptide sequences during digestion. The proteomic workflow employed LC-MS/MS to identify and compare peptide sequences across the free hydrolysates, their encapsulates, and the corresponding digested samples. Sequences were filtered based on quality criteria, as discussed in the methodology description, and those meeting the criteria were selected, with the complete dataset available in the Supplementary Material.

As can be seen in Table 3 peptide identification in *T. molitor* samples varied significantly depending on the sample type, with the hydrolysate containing the highest number of identifiable peptides, whereas the digested samples exhibited a substantial reduction in detectable sequences. This loss of identifiable peptides has been consistently reported in previous studies (Gonzalez-de la Rosa et al., 2024), where comparisons between hydrolysates and their corresponding digests revealed a significant decline in sequence detection. This reduction may be attributed to three main factors: (i) enzymatic cleavage during digestion generates smaller fragments, such as dipeptides and free amino acids, which cannot be easily identified and fall below the 3-30 aa stablished range; (ii) digestion also introduces additional background noise due to the reagents used, complicating even more peptide identification; and (iii) hydrophobic peptides may precipitate or adhere to container surfaces during digestion, reducing their presence in the soluble fraction (Ahrens et al., 2022).

Identification rates markedly differ between *T. molitor* and olive seed samples, which can be related to compositional differences. The greater complexity of olive seed hydrolysates, likely attributed to the presence of non-proteinaceous compounds (see Chapter III), may have contributed to increased background noise, making more difficult peptide detection across all samples. However, an important limitation to consider is the exclusive use of the seed, as it does

not fully represent the protein expression profile of the entire organism. This restricted scope may have led to an incomplete characterization of the samples. Indeed, previous studies on potato peptides reported that the variation in peptide identification could be primarily attributed to the influence of pepsin. The broad specificity of pepsin results in the exposition of additional sites for subsequent enzymatic action in the small intestine (Jiménez-Munoz et al., 2024). A similar reduction in detectable sequences was reported when encapsulating whey protein hydrolysate in micro-hydrogels subjected to simulated digestion (Gómez-Mascaraque et al., 2016).

Table 3. Number of peptide sequences identified in samples (ID referring to Table 1)

Original sequences			
Total *T. molitor*	223,239	Total *O. europaea*	184,251
Filtered sequences			
Total *T. molitor*	22,232	Total *O. europaea*	6,364
HT	7,565	HO	1,119
HT_ID	2,623	HO_ID	1,439
CT3	5,778	CO3	806
CT3_ID	3,237	CO3_ID	1,371
CT4	7,019	CO4	1,030
CT4_ID	3,104	CO4_ID	1,357

Peptide degradation is further evidenced by the distribution of peptides length (Figure 6). Notable differences can be observed across the samples, depending on the protein of origin. Nonetheless, encapsulated samples exhibit profiles closely resembling to the free hydrolysate (HT or HO), with this effect being more pronounced for *T. molitor* samples. Digestion was confirmed to shift peptide length distributions towards shorter sequences, which is also correlated to the differences presented in the SEC molecular weight distributions (Figure 5). This indicates partial peptide degradation and the generation of smaller fragments, likely due to enzymatic cleavage during gastrointestinal simulation. A similar trend was previously reported in the digestion of potato protein hydrolysate (Jiménez-Munoz et al., 2024). However, encapsulated digests displayed a comparatively lower amount of these smaller peptides, suggesting a partial protective effect against enzymatic hydrolysis, as can be seen in the density plots (Figure 6).

The impact of the encapsulation process on peptide preservation was analyzed using UpSet plots (Figure 7) and overlap calculations. These plots suppose a more informative alternative to Venn diagrams. The left bar chart represents the total number of peptides identified in each dataset, while the bottom matrix displays set interactions, where the dots indicate shared peptides across the sets. The top vertical bars quantify the number of peptides present in each intersection, allowing to assess peptide retention and loss across samples. Notably, a significant proportion of sequences were lost during encapsulation, suggesting that the

spray-drying configuration (monoaxial or coaxial) influences both peptide integrity and detectability. Interestingly, CT4 and CO4 retained more sequences (65.5% and 54.6%, respectively) compared to CT3 and CO3 (57.6% and 44.9%, respectively), indicating that the additional Arabic gum shell could enhance peptide stability during processing and storage, as previously observed in the analysis of the bioactivity and MWD. However, nearly half of the original sequences were not detected, which was unexpected given that degradation to this point should be minimal. This loss could be attributed to increased

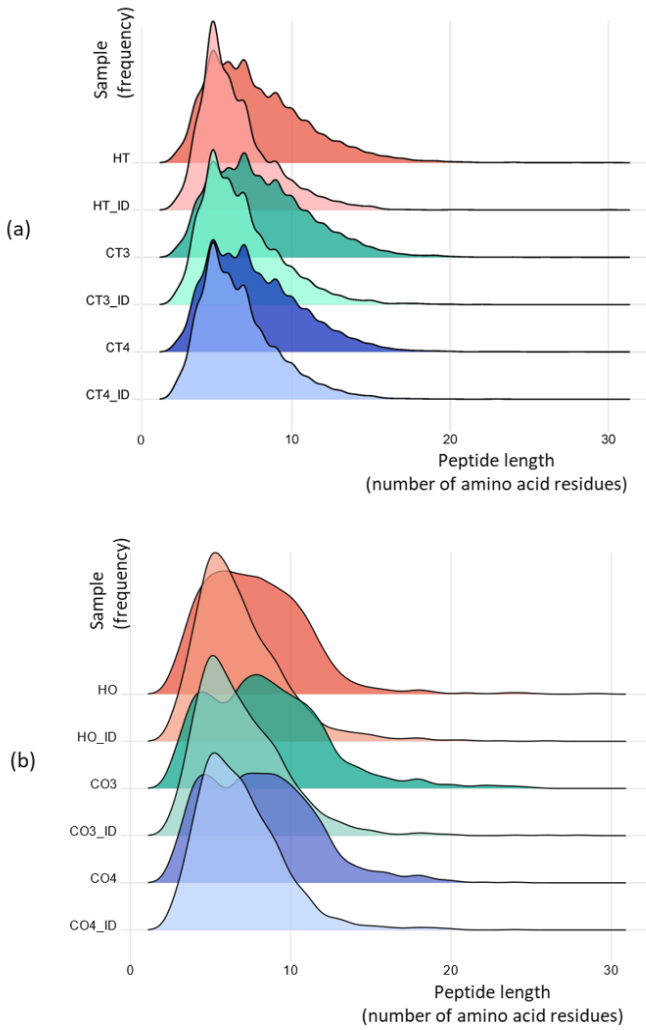

Figure 6. Density plot showing the distribution of peptide length of the different (a) *T. molitor* or (b) *O. europaea* seed samples obtained using http://www.bioinformatics.com.cn/srplot. Sample ID referring to Table 1.

interactions between peptides and the encapsulating matrix (Alvarado et al., 2019). Studies on whey protein have shown that at intermediate pH, when the proteins are not fully negative or positive, charge interactions can occur between proteins and Arabic gum, the main encapsulating agent employed in this study. This is due to the presence of positively charged peptide domains interacting with the negatively charged Arabic gum, forming weak complexes (Klein et al., 2010). Similar interactions have been reported in pea protein, particularly when Arabic gum is derived from *Acacia senegal* (Comunian et al., 2022). While these interactions contribute to encapsulation stability, they may also interfere with peptide identification by limiting their solubility in the analysis phase. This might explain why certain sequences detected in the free hydrolysates were not retrieved after dissolving the capsules. Similar interactions between the peptides from the hydrolysate and the encapsulation matrices have also been reported for encapsulating agents such as gelatin, chitosan, sodium alginate or collagen (Alvarado et al., 2019; Gómez-Mascaraque et al., 2016). Moreover, Gómez-Mascaraque et al. (2016) suggested that the spray-drying process used, involving the use of high temperature, might contribute to promoting crosslinking reactions between the matrix and the hydrolysate. It is important to emphasize that this remains a hypothesis, and further research is needed to confirm the extent to which encapsulation hinders peptide identification, employing different encapsulating agents, to better distinguish between true peptide loss and matrix-induced retention.

Regarding peptide preservation after digestion of the capsules, overlap calculations revealed that encapsulated samples retained a higher proportion of sequences that non-encapsulated hydrolysates, although not to a marked extent. For instance, 9.4% of sequences in CT3_ID persisted through encapsulation and digestion, a higher proportion than for CT4_ID (8.8%). On the other hand, better protection was reported when using coaxial spray-drying for olive seed hydrolysates (9.4% in CO4_ID vs 8.7% CO3_ID). Considering the previous results, these differences might be attributed to differences in peptides composition and their interactions with encapsulating agents. Understanding these variations is key for optimizing encapsulation strategies to improve peptide preservation and bioavailability. However, assessing encapsulation efficacy remains challenging due to multiple factors. Interactions between peptides and the

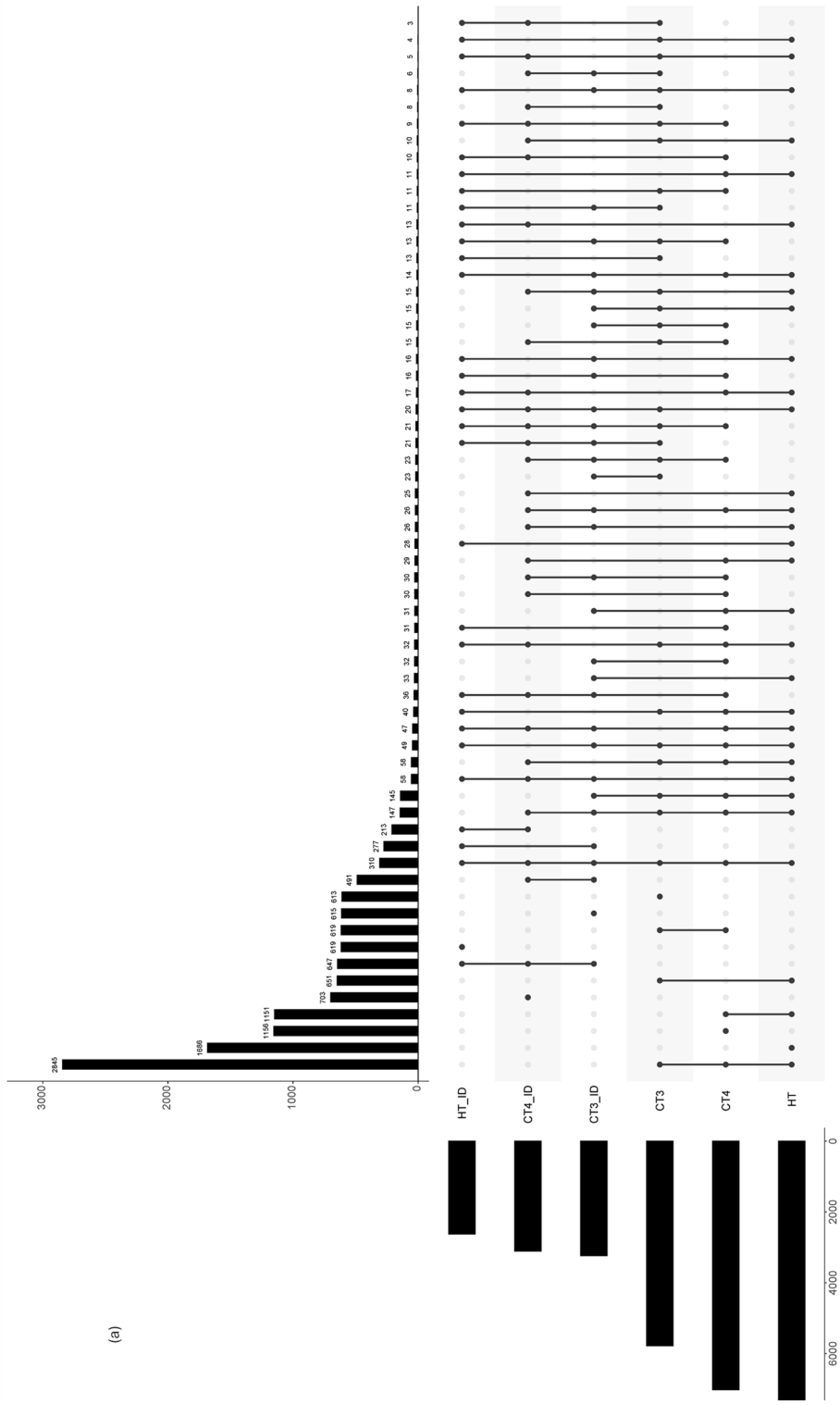

Figure 7a. UpSet plots showing intersections between the identified peptides in the different *T. molitor* samples obtained using https://www.bioinformatics.com.cn. Rows correspond to the sets, and columns to the intersections between these sets. Sample ID referring to Table 1.

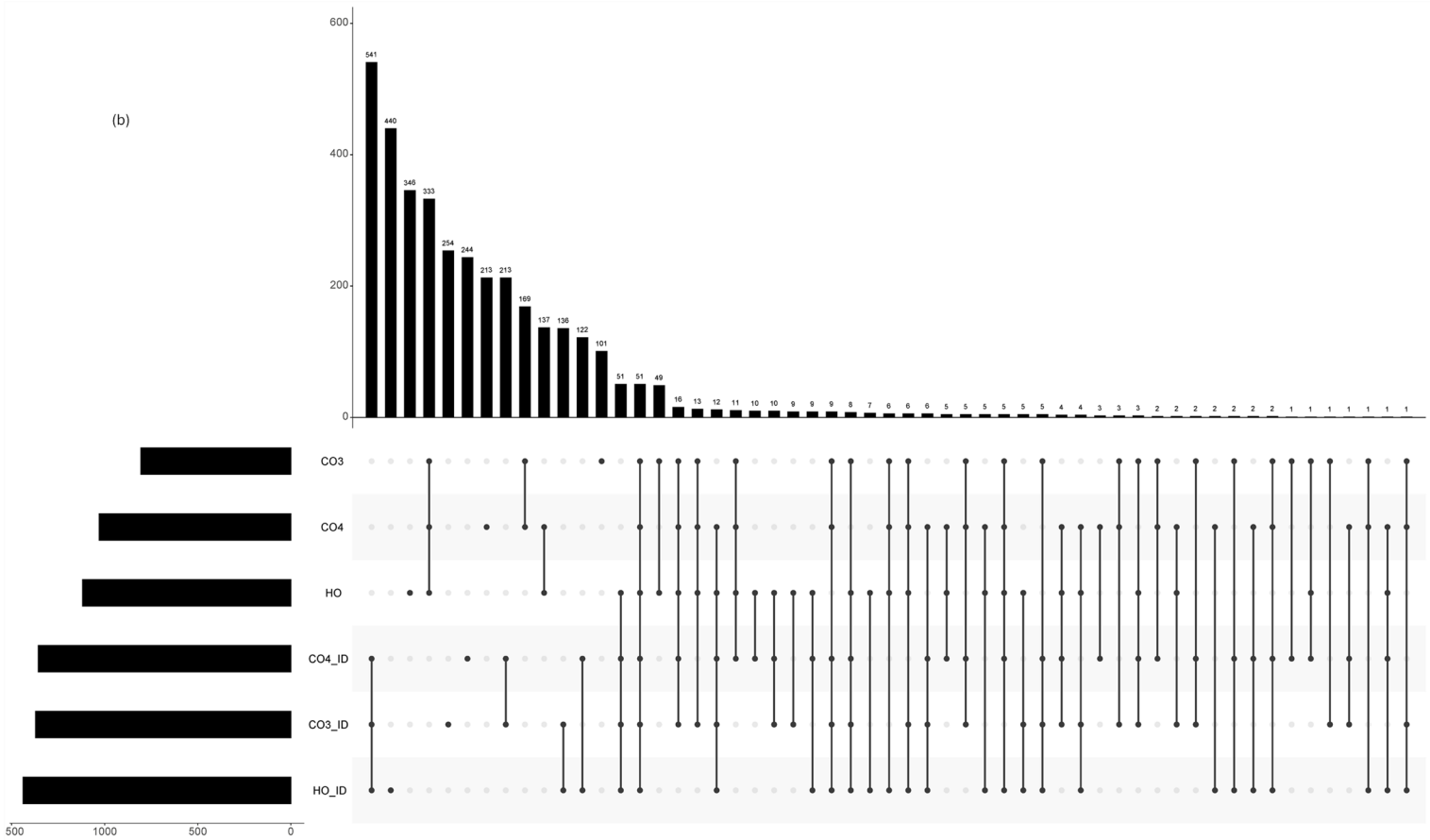

Figure 7b. UpSet plots showing intersections between the identified peptides in the different *O. europaea* seed samples obtained using https://www.bioinformatics.com.cn. Rows correspond to the sets, and columns to the intersections between these sets. Sample ID referring to Table 1.

encapsulating agents could potentially lead to amino acid modifications and cross-linking, affecting peptide identification. The complexity of the mixtures, particularly after digestion, introduces analytical challenges such as background noise. Additionally, it is most important to highlight that many peptides detected in the digests may not have been preserved by encapsulation but rather generated from the digestion of larger parent sequences. This complicates the differentiation between peptides genuinely retained by encapsulation and those newly formed during digestion. Given all these limitations, it is understandable that few studies have applied this approach to evaluate protein hydrolysate encapsulation. Literature on this topic has typically focused on a small set of longer peptides to minimize the confounding effect of peptide generation during gastrointestinal digestion (Alvarado et al., 2019; Jiménez-Munoz et al., 2024). Other studies have identified peptide sequences in the hydrolysate or its fractions but have not specifically assessed encapsulation success (Garzón et al., 2023).

3.3.2. Identification of bioactive peptides

Previous studies (Chapter VI) investigated the presence of bioactive peptides with DPP-IV inhibitory activity in the *T. molitor* and olive seed protein hydrolysates using databases such as BIOPEP (https://biochemia.uwm.edu.pl/biopep/peptide_data.php) and literature sources (Berraquero-García, Rivero-Pino, et al., 2023). While Chapter VI focused on identifying and characterizing the bioactive sequences in the free hydrolysates, this study examines their retention post-digestion. Consequently, we searched for these sequences across all samples and analysed their structural features associated with DPP-IV inhibition in *T. molitor* (Table 4) and *O. europaea* samples (Table 5).

Fewer sequences were identified in olive seed samples (Table 5) compared to *T. molitor* (Table 4). In our previous work, the longest peptide reported was 13 amino acids (Berraquero-García, Rivero-Pino, et al., 2023), suggesting that longer peptides, which may also contribute to DPP-IV inhibition, remain underexplored. Structurally, the presence of Pro in the N-terminus was the most conserved feature, consistent with the structural characteristics known for DPP-IV inhibitors (Nongonierma & Fitzgerald, 2016; Nongonierma & FitzGerald, 2019). *In silico* predicted bioactivity employing StackDPPIV assigned high inhibitory potential to nearly all sequences in both *T. molitor* and olive seed samples. However, APVAH (Table 4) received the lowest score (0.18), classifying it as non-inhibitory, despite its experimentally reported IC_{50} of 26 μM (Chapter II). These discrepancies highlight the limitations of predictive tools, which, while useful for screening, require experimental validation to confirm or deny functional activity.

Regarding peptide stability, encapsulation seemed to influence peptide preservation. Only a subset of sequences exhibited the expected protection pattern. LPR, present both in *T. molitor* and olive seed samples, followed the expected trend: present in the free hydrolysate, degraded post-digestion, but retained in encapsulated forms and their digests. VPF and LPVYD

(Table 4), appeared in all samples, suggesting at least some degree of natural resistance to enzymatic degradation rather than being actively protected by encapsulation. Additionally, LPLF and ELPF showed evidence of protection, possibly through monoaxial and coaxial encapsulation methods, respectively. Nonetheless, some peptides may not be protected per se but rather generated from the enzymatic degradation of larger parent sequences. Indeed, LPR is present in 567 identified sequences from *T. molitor*, suggesting that its continued detection may result from fragmentation rather than encapsulation protection, although this cannot be confirmed by this study. Another highly conserved peptide was DPF, which could only be identified in the digests; however, larger peptides containing this sequence were detected in the free hydrolysate up to 31 times. Similar results were reported for the encapsulation of whey protein in composite matrices of sodium alginate with Arabic gum, collagen, and gelatin (Alvarado et al., 2019), where digestion led to the degradation and formation of similar sequences. Moreover, inherent enzymatic resistance may contribute to peptide stability. Peptides containing Pro in positions P2–P3' can limit pepsin cleavage efficiency, while Pro in P1' restricts trypsin attack (Keil, 1992). Thus, this highly conserved characteristic may enhance peptide stability against digestive degradation.

Finally, the methodological limitations previously mentioned must be acknowledged, mainly the complex interaction between peptides, encapsulating agents and the additional complexity introduced by the digestive compounds. Additionally, only peptides within the 3–30 amino acid range were detected, excluding dipeptides. Given that the molecular weight of the identified peptides ranged from 0.3 to 3.2 kDa, this implies that for *T. molitor*-derived samples, over 20% of the peptides present in the hydrolysate, capsules, and digests (based on the previously presented MWD data) would not have been identified, representing a significant proportion. In contrast, for olive seed-derived samples, this percentage would be lower, with fewer than 10% of the peptides falling below 0.3 kDa. These constraints highlight the need for alternative purification and analytical techniques in future studies.

Table 4. Identification and characterization of bioactive peptides in *T. molitor* hydrolysates and encapsulated samples.

Sequence	Length	Mass (Da)	% Hydrophobic AA	P in Nt	A in Nt	F in Ct	W in Ct	Y in Ct	Predicted Bioactivity (StackDPPIV)	Biopep reported activity	IC_{50} reported in literature (μM)	Found in HT	Found in HT_ID	Found in CT3	Found in CT3_ID	Found in CT4	Found in CT4_ID
DPF	3	377.16	33.33%	Y		Y			0.95		1540.00	N	Y	N	Y	N	Y
GPF	3	319.15	66.67%	Y		Y			1.00	DPP-IV inhibitor		N	N	N	Y	N	Y
LPR	3	384.25	66.67%	Y					0.82		1430.00	Y	N	Y	Y	Y	Y
LPY	3	391.21	100.00%	Y				Y	0.83		87.15	Y	Y	N	N	N	Y
MPF	3	393.17	66.67%	Y		Y			0.97	DPP-IV inhibitor		Y	N	N	N	Y	N
VPF	3	361.20	66.67%	Y		Y			0.95		55.10	Y	Y	Y	Y	Y	Y
VPW	3	400.21	100.00%	Y			Y		0.93	Antioxidant	174.78	Y	Y	N	Y	Y	Y
WRA	3	431.23	66.67%						0.96	DPP-IV inhibitor		Y	N	N	N	N	Y
WRF	3	507.26	33.33%			Y			1.00	DPP-IV inhibitor		N	N	N	N	Y	N
ELPF	4	504.26	50.00%			Y			0.80		9920.00	Y	N	N	Y	Y	Y
LAVP	4	398.25	100.00%		Y				1.00		98.76	N	Y	N	Y	N	N
LLAP	4	412.27	100.00%						0.98	DPP-IV inhibitor	53.74	N	Y	N	Y	N	Y
LPLF	4	488.30	75.00%	Y		Y			1.00		463.60	Y	N	Y	Y	Y	N
LPVP	4	424.27	100.00%	Y					0.95		87.00	N	Y	Y	Y	Y	Y
APLP	4	396.24	100.00%	Y	Y				0.96		122.45	N	N	N	Y	N	N
TPGL	4	386.22	75.00%	Y					0.89		297.41	N	N	N	N	Y	N
APVAH	5	493.26	80.00%	Y	Y				0.18			Y	N	Y	N	Y	N
LPLPL	5	551.37	100.00%	Y					0.86	DPP-IV inhibitor		Y	N	N	N	Y	N

(Continued) **Table 4**. Identification and characterization of bioactive peptides in *T. molitor* hydrolysates and encapsulated samples.

Sequence	Length	Mass (Da)	% Hydrophobic AA	P in Nt	A in Nt	F in Ct	W in Ct	Y in Ct	Predicted Bioactivity (StackDP-PIV)	Biopep reported activity	IC_{50} reported in literature (μM)	Found in HT	Found in HT_ID	Found in CT3	Found in CT3_ID	Found in CT4	Found in CT4_ID
LPNYN	5	619.30	60.00%	Y					0.67	DPP-IV inhibitor		N	N	N	Y	N	Y
LPVYD	5	605.31	80.00%	Y					0.55	DPP-IV inhibitor	51.36	Y	Y	Y	Y	Y	Y
APVAH	5	493.26	80.00%	Y	Y				0.18			Y	N	Y	N	Y	N
FAGDDAPR	8	847.38	50.00%		Y				0.57		168.72	N	N	N	N	N	Y
FAGDDAPRA	9	918.42	55.56%		Y				0.51		393.30	Y	N	N	N	N	N

Table 5. Identification and characterization of bioactive peptides in *O. europaea* hydrolysates and encapsulated samples.

Sequence	Length	Mass (Da)	% Hydrophobic AA	P in Nt	A in Nt	F in Ct	W in Ct	Y in Ct	Predicted Bioactivity (StackDP-PIV)	Biopep reported activity	IC_{50} reported in literature (μM)	Found in HO	Found in HO_ID	Found in CO3	Found in CO3_ID	Found in CO4	Found in CO4_ID
LPQ	3	356.21	66.67%	Y					0.78	DPP-IV inhibitor	56.70	Y	N	Y	N	Y	N
LPR	3	384.25	66.67%	Y					0.82		1430.00	Y	Y	Y	Y	N	Y
LPLF	4	488.30	75.00%	Y		Y			1.00		463.60	Y	N	N	N	Y	N
VPW	3	400.21	100.00%	Y			Y		0.93		174.78	N	Y	N	Y	N	Y
VGL	3	287.18	100.00%						0.98	DPP-IV inhibitor		Y	N	Y	N	Y	N
LPGA	4	356.21	100.00%	Y					1.00		154.12	N	N	N	N	Y	N
LPVP	4	424.27	1	Y					0.95		87.00	Y	N	N	N	N	N

4. Conclusions

This study demonstrated that spray-drying encapsulation enhances the stability and bioactivity retention of *T. molitor* and *O. europaea* antidiabetic hydrolysates, with both monoaxial and coaxial techniques providing significant protection against enzymatic digestion. While coaxial spray-drying generally outperformed monoaxial techniques, the addition of Tween 20 and pullulan in monoaxial formulations led to comparable levels of bioactivity preservation, as determined by the *in vitro* activity values. Size-exclusion chromatography showed that encapsulation helped maintaining the molecular weight distribution of the hydrolysates after digestion, reducing the extent of peptide degradation observed in the free hydrolysates. Peptidomics analysis using LC-MS/MS highlighted the multiple challenges faced in the identification of bioactive peptides and validation of the encapsulation of complex samples such as hydrolysates. This was primarily due to the inability to confidently identify dipeptides in these matrices, as well as potential interactions with encapsulating agents, particularly Arabic gum, as well as the addition of reagents during the simulated digestion. Nonetheless, several peptide sequences, including LPR, VPF, LPLF, VPW, and ELPF, were successfully identified as resistant to digestion after encapsulation. Therefore, these findings underscore the importance of both the encapsulation technique and the formulation composition in preserving bioactivity. Notably, coaxial spray-drying exhibited a protective effect, by providing an additional shell layer without the need for additives. Ultimately, this study lays the groundwork for refining encapsulation strategies to enhance peptide stability and bioactivity retention in functional food applications.

5. References

Adhikari, B., Howes, T., Wood, B. J., & Bhandari, B. R. (2009). The effect of low molecular weight surfactants and proteins on surface stickiness of sucrose during powder formation through spray drying. *Journal of Food Engineering*, *94*(2), 135–143. https://doi.org/10.1016/J.JFOODENG.2009.01.022

Ahn, J., Cao, M. J., Yu, Y. Q., & Engen, J. R. (2013). Accessing the reproducibility and specificity of pepsin and other aspartic proteases. *Biochimica et Biophysica Acta (BBA) - Proteins and Proteomics*, *1834*(6), 1222–1229. https://doi.org/10.1016/J.BBAPAP.2012.10.003

Ahrens, C. H., Wade, J. T., Champion, M. M., & Langer, J. D. (2022). A Practical Guide to Small Protein Discovery and Characterization Using Mass Spectrometry. *Journal of Bacteriology*, *204*(1). https://doi.org/10.1128/JB.00353-21

Alvarado, Y., Muro, C., Illescas, J., Díaz, M. del C., & Riera, F. (2019). Encapsulation of Antihypertensive Peptides from Whey Proteins and Their Releasing in Gastrointestinal Conditions. *Biomolecules 2019, Vol. 9, Page 164*, *9*(5), 164. https://doi.org/10.3390/BIOM9050164

Alvarez, R., Robert, P., Quintriqueo, A., Oyarzún-Ampuero, F., Mackie, A., & Torcello-Gómez, A. (2024). Characterization and in vitro bioaccessability of optimized chia oil-Capsul-sodium alginate microparticles obtained by 3 nozzle spray-drying. *Food and Bioproducts Processing*, *148*, 240–246. https://doi.org/10.1016/J.FBP.2024.09.012

Amigo, L., & Hernández-Ledesma, B. (2020). Current Evidence on the Bioavailability of Food Bioactive Peptides. *Molecules 2020, Vol. 25, Page 4479*, *25*(19), 4479. https://doi.org/10.3390/MOLECULES25194479

Aquino, R. P., Auriemma, G., Conte, G. M., Esposito, T., Sommella, E., Campiglia, P., & Sansone, F. (2020). Development of Chitosan/Mannitol Microparticles as Delivery System for the Oral Administration of a Spirulina Bioactive Peptide Extract. *Molecules 2020, Vol. 25, Page 2086*, *25*(9), 2086. https://doi.org/10.3390/MOLECULES25092086

Atma, Y., Murray, B. S., Sadeghpour, A., & Goycoolea, F. M. (2024). Encapsulation of short-chain bioactive peptides (BAPs) for gastrointestinal delivery: a review. *Food & Function*, *15*(8), 3959–3979. https://doi.org/10.1039/D3FO04195F

Bagheri, L., Madadlou, A., Yarmand, M., & Mousavi, M. E. (2014). Spray-dried alginate microparticles carrying caffeine-loaded and potentially bioactive nanoparticles. *Food Research International*, *62*, 1113–1119. https://doi.org/10.1016/J.FOODRES.2014.05.040

Barra, P. A., Márquez, K., Gil-Castell, O., Mujica, J., Ribes-Greus, A., & Faccini, M. (2019). Spray-Drying Performance and Thermal Stability of L-ascorbic Acid Microencapsulated with Sodium Alginate and Gum Arabic. *Molecules 2019, Vol. 24, Page 2872*, *24*(16), 2872. https://doi.org/10.3390/MOLECULES24162872

Berraquero-García, C., Coronas-Lozano, C., Guadix, E. M., & García-Moreno, P. J. (2024). Optimization of Coaxial Spray-Drying for the Encapsulation of Tenebrio molitor Protein Hydrolysate Exhibiting DPP-IV Inhibitory Activity. *Food and Bioprocess Technology*. https://doi.org/10.1007/S11947-024-03695-4

Berraquero-García, C., Martínez-Sánchez, L., Guadix, E. M., & García-Moreno, P. J. (2024). Encapsulation of Tenebrio molitor Hydrolysate with DPP-IV Inhibitory Activity by Electrospraying and Spray-Drying. *Nanomaterials 2024, Vol. 14, Page 840*, *14*(10), 840. https://doi.org/10.3390/NANO14100840

Berraquero-García, C., Pérez-Gálvez, R., Espejo-Carpio, F. J., Guadix, A., Guadix, E. M., & García-Moreno, P. J. (2023). Encapsulation of Bioactive Peptides by Spray-Drying and Electrospraying. *Foods*, *12*(10), 2005. https://doi.org/10.3390/foods12102005

Berraquero-García, C., Rivero-Pino, F., Ospina, J. L., Pérez-Gálvez, R., Espejo-Carpio, F. J., Guadix, A., García-Moreno, P. J., & Guadix, E. M. (2023). Activity, structural features and in silico digestion of antidiabetic peptides. *Food Bioscience*, *55*, 102954. https://doi.org/10.1016/J.FBIO.2023.102954

Bhujbal, S. V., Su, Y., Pathak, V., Zemlyanov, D. Y., Cavallaro, A. A., Munson, E. J., Taylor, L. S., & Zhou, Q. (2021). Effect of storage humidity on physical stability of spray-dried naproxen amorphous solid dispersions with polyvinylpyrrolidone: Two fluid nozzle vs. three fluid nozzle. *Pharmaceutics*, *13*(7), 1074. https://doi.org/10.3390/PHARMACEUTICS13071074

Boel, E., Koekoekx, R., Dedroog, S., Babkin, I., Vetrano, M. R., Clasen, C., & Van den Mooter, G. (2020). Unraveling Particle Formation: From Single Droplet Drying to Spray Drying and Electrospraying. *Pharmaceutics 2020, Vol. 12, Page 625*, *12*(7), 625. https://doi.org/10.3390/PHARMACEUTICS12070625

Brodkorb, A., Egger, L., Alminger, M., Alvito, P., Assunção, R., Ballance, S., Bohn, T., Bourlieu-Lacanal, C., Boutrou, R., Carrière, F., Clemente, A., Corredig, M., Dupont, D., Dufour, C., Edwards, C., Golding, M., Karakaya, S., Kirkhus, B., Le Feunteun, S., … Recio, I. (2019). INFOGEST static in vitro simulation of gastrointestinal food digestion. *Nature Protocols 2019 14:4*, *14*(4), 991–1014. https://doi.org/10.1038/s41596-018-0119-1

Calame, W., Weseler, A. R., Viebke, C., Flynn, C., & Siemensma, A. D. (2008). Gum arabic establishes prebiotic functionality in healthy human volunteers in a dose-dependent manner. *British Journal of Nutrition*, *100*(6), 1269–1275. https://doi.org/10.1017/S0007114508981447

Camargo, T. R., Khelissa, S., Chihib, N. E., Dumas, E., Wang, J., Valenti, W. C., & Gharsallaoui, A. (2021). Preparation and Characterization of Microcapsules Containing Antioxidant Fish Protein Hydrolysates: a New Use of Bycatch in Brazil. *Marine Biotechnology*, *23*(2), 321–330. https://doi.org/10.1007/S10126-021-10026-7

Charoenkwan, P., Nantasenamat, C., Hasan, M. M., Moni, M. A., Lio', P., Manavalan, B., & Shoombuatong, W. (2022). StackDPPIV: A novel computational approach for accurate prediction of dipeptidyl peptidase IV (DPP-IV) inhibitory peptides. *Methods*, *204*, 189–198. https://doi.org/10.1016/J.YMETH.2021.12.001

Cherbut, C., Michel, C., Raison, V., Kravtchenko, T., & Severine, M. (2003). Acacia Gum is a Bifidogenic Dietary Fibre with High Digestive Tolerance in Healthy Humans. *Microbial Ecology in Health and Disease*, *15*(1), 43–50. https://doi.org/10.1080/08910600310014377

Cian, R. E., Campos-Soldini, A., Chel-Guerrero, L., Drago, S. R., & Betancur-Ancona, D. (2019). Bioactive Phaseolus lunatus peptides release from maltodextrin/gum arabic microcapsules obtained by spray drying after simulated gastrointestinal digestion. *International Journal of Food Science & Technology*, *54*(6), 2002–2009. https://doi.org/10.1111/IJFS.14031

Cian, R. E., Salgado, P. R., Mauri, A. N., & Drago, S. R. (2020). Pyropia columbina phycocolloids as microencapsulating material improve bioaccessibility of brewers' spent grain peptides with ACE-I inhibitory activity. *International Journal of Food Science & Technology*, *55*(3), 1311–1317. https://doi.org/10.1111/IJFS.14397

Comunian, T. A., Archut, A., Gomez-Mascaraque, L. G., Brodkorb, A., & Drusch, S. (2022). The type of gum arabic affects interactions with soluble pea protein in complex coacervation. *Carbohydrate Polymers*, *295*, 119851. https://doi.org/10.1016/J.CARBPOL.2022.119851

Consortium, T. U., Bateman, A., Martin, M.-J., Orchard, S., Magrane, M., Adesina, A., Ahmad, S., Bowler-Barnett, E. H., Bye-A-Jee, H., Carpentier, D., Denny, P., Fan, J., Garmiri, P., Gonzales, L. J. da C., Hussein, A., Ignatchenko, A., Insana, G., Ishtiaq, R., Joshi, V., … Zhang, J. (2025). UniProt: the Universal Protein Knowledgebase in 2025. *Nucleic Acids Research*, *53*(D1), D609–D617. https://doi.org/10.1093/NAR/GKAE1010

Consumer perceptions unwrapped: ultra-processed foods (UPF). (2024).

Cox, J., Neuhauser, N., Michalski, A., Scheltema, R. A., Olsen, J. V., & Mann, M. (2011). Andromeda: A peptide search engine integrated into the MaxQuant environment. *Journal of Proteome Research*, *10*(4), 1794–1805. https://doi.org/10.1021/PR101065J

Elnour, A. A. M., Abdurahman, N. H., Musa, K. H., & Rasheed, Z. (2023). Prebiotic potential of gum Arabic for gut health. *International Journal of Health Sciences*, *17*(6), 4. https://pmc.ncbi.nlm.nih.gov/articles/PMC10624802/

Gallo, V., Romano, A., Miralles, B., Ferranti, P., Masi, P., Santos-Hernández, M., & Recio, I. (2022). Physicochemical properties, structure and digestibility in simulated gastrointestinal environment of bread added with green lentil flour. *LWT*, *154*, 112713. https://doi.org/10.1016/J.LWT.2021.112713

García-Moreno, P. J., Gregersen, S., Nedamani, E. R., Olsen, T. H., Marcatili, P., Overgaard, M. T., Andersen, M. L., Hansen, E. B., & Jacobsen, C. (2020). Identification of emulsifier potato peptides by bioinformatics: application to omega-3 delivery emulsions and release from potato industry side streams. *Scientific Reports 2020 10:1*, *10*(1), 1–22. https://doi.org/10.1038/s41598-019-57229-6

Garzón, A. G., Cian, R. E., & Drago, S. R. (2023). Effects of agar-carrageenan wall materials and core-to-wall material ratio on physicochemical properties and in vitro bioaccessibility of microencapsulated bioactive peptides. *Food Hydrocolloids*, *139*, 108570. https://doi.org/10.1016/J.FOODHYD.2023.108570

Gómez-Mascaraque, L. G., Miralles, B., Recio, I., & López-Rubio, A. (2016). Microencapsulation of a whey protein hydrolysate within micro-hydrogels: Impact on gastrointestinal stability and potential for functional yoghurt development. *Journal of Functional Foods*, *26*, 290–300. https://doi.org/10.1016/J.JFF.2016.08.006

Gonzalez-de la Rosa, T., Montserrat-de la Paz, S., & Rivero-Pino, F. (2024). Production, characterisation, and biological properties of Tenebrio molitor-derived oligopeptides. *Food Chemistry*, *450*, 139400. https://doi.org/10.1016/J.FOODCHEM.2024.139400

Haque, M. A., & Adhikari, B. (2014). Drying and Denaturation of Proteins in Spray Drying Process. *Handbook of Industrial Drying*, 1001–1014. https://doi.org/10.1201/B17208-62

Jiménez-Munoz, L., Nielsen, S. D. H., & Corredig, M. (2024). Changes in potato peptide bioactivity after gastrointestinal digestion. An in silico and in vitro study of different patatin-rich potato protein isolate matrices. *Food Chemistry Advances*, *4*, 100679. https://doi.org/10.1016/J.FOCHA.2024.100679

Kauppinen, A., Broekhuis, J., Grasmeijer, N., Tonnis, W., Ketolainen, J., Frijlink, H. W., & Hinrichs, W. L. J. (2018). Efficient production of solid dispersions by spray drying solutions of high solid content

using a 3-fluid nozzle. *European Journal of Pharmaceutics and Biopharmaceutics*, *123*, 50–58. https://doi.org/10.1016/J.EJPB.2017.11.009

Keil, B. (1992). Specificity of Proteolysis. *Specificity of Proteolysis*. https://doi.org/10.1007/978-3-642-48380-6

Kim, E. H. J., Chen, X. D., & Pearce, D. (2009). Surface composition of industrial spray-dried milk powders. 2. Effects of spray drying conditions on the surface composition. *Journal of Food Engineering*, *94*(2), 169–181. https://doi.org/10.1016/J.JFOODENG.2008.10.020

Klein, M., Aserin, A., Ishai, P. Ben, & Garti, N. (2010). Interactions between whey protein isolate and gum Arabic. *Colloids and Surfaces B: Biointerfaces*, *79*(2), 377–383. https://doi.org/10.1016/J.COLSURFB.2010.04.021

Lacroix, I. M. E., Chen, X. M., Kitts, D. D., & Li-Chan, E. C. Y. (2017). Investigation into the bioavailability of milk protein-derived peptides with dipeptidyl-peptidase IV inhibitory activity using Caco-2 cell monolayers. *Food & Function*, *8*(2), 701–709. https://doi.org/10.1039/C6FO01411A

Lacroix, I. M. E., & Li-Chan, E. C. Y. (2012). Dipeptidyl peptidase-IV inhibitory activity of dairy protein hydrolysates. *International Dairy Journal*, *25*(2), 97–102. https://doi.org/10.1016/J.IDAIRYJ.2012.01.003

Liliana Krotz, A., Leone, F., & Giazzi Thermo Fisher Scientifi, G. (n.d.). *Application Note: Elemental Analysis: CHNS/O Determination in Coals*.

Liu, R., Cheng, J., & Wu, H. (2019). Discovery of Food-Derived Dipeptidyl Peptidase IV Inhibitory Peptides: A Review. *International Journal of Molecular Sciences 2019, Vol. 20, Page 463*, *20*(3), 463. https://doi.org/10.3390/IJMS20030463

Ma, J., Xu, C., Yu, H., Feng, Z., Yu, W., Gu, L., Liu, Z., Chen, L., Jiang, Z., & Hou, J. (2021). Electro-encapsulation of probiotics in gum Arabic-pullulan blend nanofibres using electrospinning technology. *Food Hydrocolloids*, *111*, 106381. https://doi.org/10.1016/J.FOODHYD.2020.106381

Maestri, D., Barrionuevo, D., Bodoira, R., Zafra, A., Jiménez-López, J., & Alché, J. de D. (2019). Nutritional profile and nutraceutical components of olive (Olea europaea L.) seeds. *Journal of Food Science and Technology*, *56*(9), 4359–4370. https://doi.org/10.1007/S13197-019-03904-5

Majura, J. J., Cao, W., Chen, Z., Htwe, K. K., Li, W., Du, R., Zhang, P., Zheng, H., & Gao, J. (2022). The current research status and strategies employed to modify food-derived bioactive peptides. *Frontiers in Nutrition*, *9*, 950823. https://doi.org/10.3389/FNUT.2022.950823

Maria Leena, M., Gover Antoniraj, M., Moses, J. A., & Anandharamakrishnan, C. (2020). Three fluid nozzle spray drying for co-encapsulation and controlled release of curcumin and resveratrol. *Journal of Drug Delivery Science and Technology*, *57*, 101678. https://doi.org/10.1016/J.JDDST.2020.101678

Minkiewicz, P., Iwaniak, A., & Darewicz, M. (2019). BIOPEP-UWM Database of Bioactive Peptides: Current Opportunities. *International Journal of Molecular Sciences*, *20*(23). https://doi.org/10.3390/IJMS20235978

Nongonierma, A. B., & Fitzgerald, R. J. (2016). Structure activity relationship modelling of milk protein-derived peptides with dipeptidyl peptidase IV (DPP-IV) inhibitory activity. *Peptides*, *79*, 1–7. https://doi.org/10.1016/J.PEPTIDES.2016.03.005

Nongonierma, A. B., & FitzGerald, R. J. (2019). Features of dipeptidyl peptidase IV (DPP-IV) inhibitory peptides from dietary proteins. *Journal of Food Biochemistry*, *43*(1), e12451. https://doi.org/10.1111/JFBC.12451

Ospina-Quiroga, J. L., García-Moreno, P. J., Guadix, A., Guadix, E. M., Almécija-Rodríguez, M. del C., & Pérez-Gálvez, R. (2022). Evaluation of Plant Protein Hydrolysates as Natural Antioxidants in Fish Oil-In-Water Emulsions. *Antioxidants*, *11*(8), 1612. https://doi.org/10.3390/ANTIOX11081612

Pérez-Gálvez, R., Berraquero-García, C., Ospina-Quiroga, J. L., Espejo-Carpio, F. J., Almécija, M. C., Guadix, A., García-Moreno, P. J., & Guadix, E. M. (2024). Influence of In Vitro Digestion on Dipeptidyl Peptidase-IV (DPP-IV) Inhibitory Activity of Plant-Protein Hydrolysates Obtained from Agro-Industrial By-Products. *Foods 2024, Vol. 13, Page 2691*, *13*(17), 2691. https://doi.org/10.3390/FOODS13172691

Permanadewi, I., Kumoro, A. C., Wardhani, D. H., & And Aryanti, N. (2022). Effect of viscosity on iron encapsulation using alginate as a carrying agent in a controlled spray drying process. *Food Research*,

6(5), 56–67. https://doi.org/10.26656/fr.2017.6(5).613

Phillips, G. O. (1998). Acacia gum (Gum Arabic): A nutritional fibre; metabolism and calorific value. *Food Additives & Contaminants*, *15*(3), 251–264. https://doi.org/10.1080/02652039809374639

Rabe, M., Kerth, A., Blume, A., & Garidel, P. (2020). Albumin displacement at the air-water interface by Tween (Polysorbate) surfactants. *European Biophysics Journal : EBJ*, *49*(7), 533–547. https://doi.org/10.1007/S00249-020-01459-4

Rawi, M. H., Abdullah, A., Ismail, A., & Sarbini, S. R. (2021). Manipulation of Gut Microbiota Using Acacia Gum Polysaccharide. *ACS Omega*, *6*(28), 17782–17797. https://doi.org/10.1021/ACSOMEGA.1C00302

Santos-Hernández, M., Alfieri, F., Gallo, V., Miralles, B., Masi, P., Romano, A., Ferranti, P., & Recio, I. (2020). Compared digestibility of plant protein isolates by using the INFOGEST digestion protocol. *Food Research International*, *137*, 109708. https://doi.org/10.1016/J.FOODRES.2020.109708

Sarabandi, K., & Jafari, S. M. (2020). Improving the antioxidant stability of flaxseed peptide fractions during spray drying encapsulation by surfactants: Physicochemical and morphological features. *Journal of Food Engineering*, *286*, 110131. https://doi.org/10.1016/J.JFOODENG.2020.110131

Shi, X., & Lee, Y. (2020). Encapsulation of tributyrin with whey protein isolate (WPI) by spray-drying with a three-fluid nozzle. *Journal of Food Engineering*, *281*, 109992. https://doi.org/10.1016/J.JFOODENG.2020.109992

Shrestha, A. K., Howes, T., Adhikari, B. P., Wood, B. J., & Bhandari, B. R. (2007). Effect of protein concentration on the surface composition, water sorption and glass transition temperature of spray-dried skim milk powders. *Food Chemistry*, *104*(4), 1436–1444. https://doi.org/10.1016/J.FOODCHEM.2007.02.015

Singh, R. S., Saini, G. K., & Kennedy, J. F. (2009). Downstream processing and characterization of pullulan from a novel colour variant strain of Aureobasidium pullulans FB-1. *Carbohydrate Polymers*, *78*(1), 89–94. https://doi.org/10.1016/J.CARBPOL.2009.03.040

Sobel, R., Versic, R., & Gaonkar, A. G. (2014). Introduction to Microencapsulation and Controlled Delivery in Foods. *Microencapsulation in the Food Industry: A Practical Implementation Guide*, 3–12. https://doi.org/10.1016/B978-0-12-404568-2.00001-7

Sun, H., Hua, X., Zhang, M., Wang, Y., Chen, Y., Zhang, J., Wang, C., & Wang, Y. (2020). Whey Protein Concentrate, Pullulan, and Trehalose as Thermal Protective Agents for Increasing Viability of Lactobacillus plantarum Starter by Spray Drying. *Food Science of Animal Resources*, *40*(1), 118–131. https://doi.org/10.5851/KOSFA.2019.E94

Szekalska, M., Amelian, A., & Winnicka, K. (2015). Alginate microspheres obtained by the spray drying technique as mucoadhesive carriers of ranitidine. *Acta Pharm.*, *65*, 15–27. https://intapi.sciendo.com/pdf/10.1515/acph-2015-0008

Tyanova, S., Temu, T., & Cox, J. (2016). The MaxQuant computational platform for mass spectrometry-based shotgun proteomics. *Nature Protocols 2016 11:12*, *11*(12), 2301–2319. https://doi.org/10.1038/nprot.2016.136

Wan, F., Maltesen, M. J., Andersen, S. K., Bjerregaard, S., Foged, C., Rantanen, J., & Yang, M. (2014). One-Step Production of Protein-Loaded PLGA Microparticles via Spray Drying Using 3-Fluid Nozzle. *Pharmaceutical Research*, *31*(8), 1967–1977. https://doi.org/10.1007/S11095-014-1299-1

Wang, B., Yu, Z., Yokoyama, W., Chiou, B. Sen, Chen, M., Liu, F., & Zhong, F. (2021). Collagen peptides with DPP-IV inhibitory activity from sheep skin and their stability to in vitro gastrointestinal digestion. *Food Bioscience*, *42*, 101161. https://doi.org/10.1016/J.FBIO.2021.101161

Weng, Y., Yang, G., Li, Y., Xu, L., Chen, X., Song, H., & Zhao, C. X. (2023). Alginate-based materials for enzyme encapsulation. *Advances in Colloid and Interface Science*, *318*, 102957. https://doi.org/10.1016/J.CIS.2023.102957

6. Supplementary material

- https://docs.google.com/spreadsheets/d/1qIyvIdnYoTmAoINHsM8NWeWqcvxur-Xp6/edit?usp=sharing&ouid=117129379747364115172&rtpof=true&sd=true

FINAL CONCLUSIONS

1. Bioinformatic approaches to identify potential dipeptidyl peptidase-IV (DPP-IV) inhibitory sequences from sustainable protein sources, using homology-based sequence alignment and targeted enzymatic hydrolysis, present significant challenges. Thus, trial-and-error hydrolysis remains necessary for optimizing the production of bioactive DPP-IV inhibitory peptides. Over 70% of the identified α-glucosidase and α-amylase inhibitors, and 35% of DPP-IV inhibitors, were extensively degraded during *in silico* digestion. Indeed, experimental validation of synthetic DPP-IV inhibitory peptides (i.e., ILAP and FLQP) resulted in fragments (i.e., IL, AP, FL and QP) with significantly reduced bioactivity after digestion

2. Enzymatic hydrolysis using Alcalase (subtilisin, EC 3.4.21.62), trypsin (EC 3.4.21.4) and Flavourzyme (endo- and exopeptidase mix, EC 3.4.11.1) allowed the successful production of DPP-IV inhibitory hydrolysates from sustainable protein sources (i.e., *Tenebrio molitor* and *Olea europaea* seed). The highest bioactivity was obtained when Alcalase and Flavourzyme were used in combination, with an optimal degree of hydrolysis of 20%, regardless of the protein substrate:

    2.1. DPP-IV inhibitory peptides derived from *T. molitor* had molecular weights primarily in the 2.5–1.0 kDa range, with a content of hydrophobic residues over 50% and 8% proline content, which correlated with the high inhibitory activity. The most bioactive hydrolysate had an IC_{50} of 0.87 mg protein/mL. Peptidomics analysis identified 7,565 peptides, 60% of which were classified as potential DPP-IV inhibitors based on the predictive model StackDPPIV. The presence of a hydrophobic residue at the N-terminal followed by proline was a common feature among the identified sequences.

    2.2. *O. europaea* seed-derived DPP-IV inhibitory peptides were predominantly larger, with over 50% being >7.0 kDa and a content of 45% hydrophobic amino acids. The most bioactive hydrolysate had an IC_{30} of 1.23 mg protein/mL. Peptidomics analysis was limited due to the complexity of this hydrolysate (only 22.6–26.8% protein content) and only 1,079 sequences were identified, 50% potentially bioactive according to StackDPPIV. This hydrolysate up-regulated GLP-1 gene expression in mouse intestinal organoids *ex vivo.*

3. *T. molitor* and *O. europaea* seed hydrolysates were significantly degraded after simulated gastrointestinal digestion, forming smaller fragments in the 1.0–0.2 kDa range. The DPP-IV inhibitory bioactivity of *T. molitor* hydrolysates decreased by up to 58% post-digestion, whereas *O. europaea* seed hydrolysates exhibited a reduction of up to 50%. This loss of activity was particularly pronounced in most of the bioactive hydrolysates, and the inclusion of trypsin during hydrolysis did not enhance resistance to digestion. Peptide degradation was primarily attributed to the gastric phase, specifically the action of pepsin, which preferentially cleaves peptide bonds containing amino acids such as tyrosine, phenylalanine, and tryptophan. These residues were present in concentrations ranging from 3.6% to 5.4% in *T. molitor* hydrolysates and from 2.6% to 5.2% in *O. europaea* seed hydrolysates, potentially contributing to their susceptibility to enzymatic breakdown.

4. Encapsulation of a *T. molitor* hydrolysate (IC_{50} of 0.87 ± 0.1 mg protein/mL), using Arabic gum as wall material, was significantly influenced by the encapsulation technology used (i.e., monoaxial electrospraying or spray-drying), as well as by the inclusion of stabilizing compounds (i.e., additives such as Tween 20 and pullulan) in the formulation. Electrospraying with Arabic gum as the encapsulating agent and additives produced small capsules with a narrow size distribution (1.2 ± 0.5 μm) and retained high bioactivity after processing (IC_{50}= 1.5 ± 0.1 mg protein/mL), but the low productivity of the setup used limited its application. The inclusion of additives in the monoaxial spray-drying formulation enhanced protein retention, compared to the formulation without Tween 20 and pullulan, due to the surface-active properties of Tween 20 limiting protein migration. This correlated with improved DPP-IV inhibitory activity *in vitro* (IC_{50}–without additives= 1.99 ± 0.03 mg protein/mL vs. IC_{50}–with additives= 1.61 ± 0.08 mg protein/mL).

5. The yield, morphology, particle size distribution, surface nitrogen content, and in vitro DPP-IV inhibitory activity of *T. molitor* hydrolysate encapsulates were significantly influenced by coaxial spray-drying processing conditions, including the solids content of the shell and core solutions and the shell/core feed flow-rate ratio. Optimization of processing variables led to maximum yield (31.32%), protein load (16.08%), minimal surface nitrogen content (4.63%), and an optimal IC_{50} value of 0.76 mg protein/mL. The optimized parameters included 40% solids in the core and 30% solids in the shell, highlighting the necessity of maintaining high solids content in both phases to ensure proper drying and prevent liquid deposits in the drying chamber. Additionally, a shell/core feed flow-rate ratio of 67% was optimized for the formation of a more complete and protective shell around the core encapsulated peptides, which in turn reduced

surface nitrogen content and enhanced bioactivity.

6. Encapsulation of *T. molitor* and *O. europaea* seed hydrolysates reduced peptide degradation during digestion, as confirmed by molecular weight distribution of hydrolysates, and bioactivity retention after gastrointestinal digestion. Encapsulation by coaxial and monoaxial spray-drying with additives (i.e., Tween 20 and pullulan) provided the highest stability and peptide protection. Bioactivity was highly retained after complete digestion, with the coaxial configuration outperforming monoaxial (*T. molitor* = 91% of bioactivity retention; *O. europaea* seed = 96% of bioactivity retention), indicating the favorable effect of forming core-shell structures to enhance protection. Partial degradation was observed independently of the encapsulation method after digestion, with the gastric phase degrading peptides < 7.0 kDa and the intestinal phase affecting peptides in the 1.0-0.2 kDa range.

7. The complexity in the composition of protein hydrolysates and potential peptide-encapsulant interactions, as well as the addition of numerous reagents during *in vitro* digestion, limited encapsulation validation employing peptidomics analysis. Coaxial spray-drying enhanced sequence retention (65%) compared to monoaxial spray-drying with additives (55%). Eleven DPP-IV inhibitory sequences with experimentally validated IC_{50} values were identified in the hydrolysates, with several (e.g., LPR, VPF, LPLF, VPW, and ELPF) resisting digestion after encapsulation but not after digestion of the non-encapsulated hydrolysates.